ADVANCES IN AGRONOMY



VOLUME ONE HUNDRED NINETEEN

ADVANCES IN AGRONOMY

Edited by

DONALD L. SPARKS
Department of Plant and Soil Sciences
University of Delaware
Newark, Delaware, USA



AMSTERDAM • BOSTON • HEIDELBERG • LONDON
NEW YORK • OXFORD • PARIS • SAN DIEGO
SAN FRANCISCO • SINGAPORE • SYDNEY • TOKYO
Academic Press is an imprint of Elsevier



Academic Press is an imprint of Elsevier
525 B Street, Suite 1900, San Diego, CA 92101-4495, USA
225 Wyman Street, Waltham, MA 02451, USA
32 Jamestown Road, London, NW1 7BY, UK
The Boulevard, Langford Lane, Kidlington, Oxford, OX51GB, UK
Radarweg 29, PO Box 211, 1000 AE Amsterdam, The Netherlands

First edition 2013

ISBN: 978-0-12-407247-3
ISSN: 0065-2113 (series)

For information on all Academic Press publications
visit our website at store.elsevier.com

Printed and bound in USA
13 14 15   10 9 8 7 6 5 4 3 2 1

CONTRIBUTORS

Barbara Amon
Leibniz Institute for Agricultural Engineering, Department of Technology Assessment and Substance Cycles Max-Eyth-Allee 100, D-14469 Potsdam, Germany

Melissa Arcand
Department of Soil Science, University of Saskatchewan, Saskatoon, Canada

Christel Baum
Soil Science, University of Rostock, Rostock, Germany

Nanthi S. Bolan
Centre for Environmental Risk Assessment and Remediation, University of South Australia, Mawson Lakes, Australia; Cooperative Research Centre for Contaminantion Assessment and Remediation of the Environment, Adelaide, Australia

Nathan S. Bryan
Brown Foundation Institute of Molecular Medicine, Department of Integrative Biology and Pharmacology, The University of Texas Health Science Center, Houston, TX, USA

Piotr Burczyk
Institute of Technology and Life Sciences (ITP), Westpomeranian Research Centre in Szczecin, Szczecin, Poland

Kai-Uwe Eckhardt
Soil Science, University of Rostock, Rostock, Germany

Richard Farrell
Department of Soil Science, University of Saskatchewan, Saskatchewan, Canada

Nicholas Hutchings
University of Aarhus, Dept. of Agroecology, Tjele, Denmark

M. P. Isaure
LCABIE (Laboratoire de Chimie Analytique BioInorganique et Environement), Institut des Sciences Analytique et de Physico-chimie pour l'Environnement et les Matériaux, Université de Pau et des Pays de l'Adour, Pau cedex 09, France

Satoru Ishikawa
Soil Environmental Division, National Institute for Agro-Environmental Sciences, Tsukuba, Japan

Gerald Jandl
Soil Science, University of Rostock, Rostock, Germany

Kristian Kiersch
Soil Science, University of Rostock, Rostock, Germany

Pil-Joo Kim
Institute of Agriculture and Life Sciences, Gyeongsang National University, Jinju, Republic of Korea

Mary B. Kirkham
Department of Agronomy, Throckmorton Plant Sciences Center, Kansas State University, Manhattan, KS, USA

J. Diane Knight
Department of Soil Science, University of Saskatchewan, Saskatchewan, Canada

Jens Kruse
Soil Science, University of Rostock, Rostock, Germany

Anitha Kunhikrishnan
Chemical Safety Division, Department of Agro-Food Safety, National Academy of Agricultural Science, Gyeonggi-do, Republic of Korea

Peter Leinweber
Soil Science, University of Rostock, Rostock, Germany

Tomoyuki Makino
Soil Environmental Division, National Institute for Agro-Environmental Sciences, Tsukuba, Japan

H. Castillo Michel
European Synchrotron Radiation Facility (ESRF), Grenoble Cedex, France

Masaharu Murakami
Soil Environmental Division, National Institute for Agro-Environmental Sciences, Tsukuba, Japan

Ravi Naidu
Centre for Environmental Risk Assessment and Remediation, University of South Australia, Mawson Lakes, Australia; Cooperative Research Centre for Contaminantion Assessment and Remediation of the Environment, Adelaide, Australia

Miriam Pinto
NEIKER, Derio (Bizkaia), Spain

Joanne Reid
Ricard-AEA, Didcot, UK

Lena Rodhe
Swedish Institute of Agricultural and Environmental Engineering (JTI), Uppsala, Sweden

Kenneth Sajwan
Department of Natural Science, Savannah State University, Savannah, GA, USA

Eva Salomon
Swedish Institute of Agricultural and Environmental Engineering (JTI), Uppsala, Sweden

G. Sarret
ISTerre, Institut des Sciences de la Terre, Université de Grenoble 1, CNRS, Grenoble, France

H. M. Selim
School of Plant, Environmental and Soil Science, Louisiana State University, Baton Rouge, Louisiana, USA

Balaji Seshadri
Centre for Environmental Risk Assessment and Remediation (CERAR), University of South Australia, South Australia, Australia; Cooperative Research Centre for Contaminants Assessment and Remediation of the Environment (CRC CARE), University of South Australia, South Australia, Australia

E.A.H. Pilon Smits
Biology Department, Colorado State University, Fort Collins, CO, USA

Peter Sørensen
University of Aarhus, Dept. of Agroecology, Tjele, Denmark

R. Tappero
Photon Sciences Department, NSLS, Brookhaven National Laboratory, Upton, NY, USA

Hans van Grinsven
PBL Netherlands Environmental Assessment Agency, Department of Water, Agriculture and Food, Bilthoven, The Netherlands

Gerard Velthof
Alterra, Wageningen, The Netherlands

Hailong Wang
School of Environmental and Resource Sciences, Zhejiang A & F University, Hangzhou, Zhejiang, China

J. Webb
Ricard-AEA, Didcot, UK

F. J. Zhao
College of Resources and Environmental Sciences, Nanjing Agricultural University, Nanjing, China; Rothamsted Research, Harpenden, Hertfordshire, UK

PREFACE

Volume 119 contains seven timely and thought provoking reviews that deal with three of the defining challenges of our time- environment, energy, and human health. The reviews not only contain cutting-edge science but provide insights into policy and technology applications. Chapter 1 is a comprehensive chapter on the use of novel synchrotron- based molecular scale techniques to understand metal uptake and metabolism in plants. Chapter 2 also provides advances in the use of synchrotron as well as other state-of-the-art tools to understand nitrogen chemistry in soils. Chapter 3 addresses the role of nitrate in human health. Chapters 4 and 5 and address various aspects of trace metal transport, contamination, and risk assessment. Chapter 4 covers cadmium contamination and risk assessment in rice ecosystems while Chapter 5 provides a thorough review on the competitive sorption effects on transport and retention of heavy metals in soils. Chapter 6 is a review on clean coal technology combustion products and aspects of their agricultural and environmental applications as well as risk assessment considerations. Chapter 7 discusses the variability of manure nitrogen efficiency in Europe and ways to increase efficiency.

I am grateful to the authors for their outstanding reviews.

Donald L. Sparks
Newark, Delaware, USA



CHAPTER ONE

Use of Synchrotron-Based Techniques to Elucidate Metal Uptake and Metabolism in Plants

G. Sarret[*,1], E. A. H. Pilon Smits[†], H. Castillo Michel[‡], M. P. Isaure[§], F. J. Zhao[¶,], R. Tappero[††]**

[*]ISTerre, Institut des Sciences de la Terre, Université de Grenoble 1, CNRS, Grenoble, France
[†]Biology Department, Colorado State University, Fort Collins, CO, USA
[‡]European Synchrotron Radiation Facility (ESRF), Grenoble Cedex, France
[§]LCABIE (Laboratoire de Chimie Analytique BioInorganique et Environement), Institut des Sciences Analytique et de Physico-chimie pour l'Environnement et les Matériaux, Université de Pau et des pays de l'Adour, CNRS, Pau cedex 09, France
[¶]College of Resources and Environmental Sciences, Nanjing Agricultural University, Nanjing, China
[**]Rothamsted Research, Harpenden, Hertfordshire, UK
[††]Photon Sciences Department, NSLS, Brookhaven National Laboratory, Upton, NY, USA
[1]Corresponding author: E-mail: geraldine.sarret@ujf-grenoble.fr

Contents

Advances in Agronomy, Volume 119
ISSN 0065-2113, http://dx.doi.org/10.1016/B978-0-12-407247-3.00001-9

Abstract

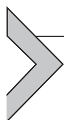
Synchrotron techniques have become key components of the toolbox for studying the mechanisms involved in metal(loid) uptake and metabolism in plants. Most widely used techniques in this field include micro-X-ray fluorescence (μXRF) for imaging the distribution of elements in plant tissues and cells and quantifying them, and X-ray absorption spectroscopy (XAS) for determining their chemical forms. Recent advances in terms of spatial resolution, sensitivity and versatility of the sample environment have opened new perspectives for the study of trace elements at the micro- and nanoscale with a minimal perturbation of the sample. Sample conditioning remains a key issue for the study of metals in plants. Cryogenic sample environments allow work on hydrated systems, with a limited risk of metal remobilization and changes in speciation. Still, radiation damage should be monitored carefully, especially for high-flux spectrometers. In addition, progress in software for data analysis has facilitated data mining and integration of results from various techniques. This chapter presents the principle and the basics of data analysis for μXRF imaging and tomography, XAS and micro-Fourier transform infrared spectromicroscopy (μFTIR). Major results obtained on Ni, Cd, Zn, Se, As, Cu, Mn and nanoparticles in hyperaccumulating and nonaccumulating plants are presented. Complementary approaches including histochemical techniques, micro and nanoscopic techniques using electron- or ion beams, and laser ablation coupled with inductively coupled plasma mass spectrometry (ICP-MS) are also presented, and key results reviewed. Finally, there is also great interest in coupling synchrotron techniques, which is possible on more and more beamlines, and also in coupling synchrotron techniques with other approaches such as the ones mentioned above; perspectives in this area are discussed.

1. INTRODUCTION

The status of metals in plants and the mechanisms controlling metal homeostasis in plants are still intensively studied as key processes for metal hyperaccumulation, detoxification, and prevention against nutrient deficiency. Applications of these research areas include phytoremediation and food safety in the case of metal-contaminated media, and biofortification of crops in the

case of low-nutrient soils. Key steps for metal homeostasis include mobilization from the soil, root uptake, xylem loading and unloading, storage/sequestration in the different plant parts, and, in some cases, exudation. Classical methods to assess gene functions and physiological processes in plants involve molecular biology and molecular genetics, and UV, visible light and electron microscopy. Synchrotron techniques have emerged as powerful and highly complementary techniques, particularly to study the distribution and the speciation of metals in plants. The major advantages of these techniques are their high sensitivity and lateral or spatial resolution, the limited sample preparation and nondestructive character, and the possibility to work on hydrated samples, in vivo in some cases. Another major advantage of this technology is the capacity to analyze several elements simultaneously and to combine different and complementary techniques, as discussed in this chapter.

The application of synchrotron techniques in plant sciences has been the subject of several reviews (Donner et al., 2012; Gardea-Torresdey et al., 2005; Lombi et al., 2011b; Lombi and Susini, 2009; Punshon et al., 2009; Salt et al., 2002). This chapter not only presents the principles of the techniques and data analysis but also emphasizes the results obtained for metals or metalloids of interest in plant sciences. Also, it compares synchrotron techniques with other imaging techniques that have undergone recent developments and can be combined with synchrotron techniques.



2. PRESENTATION OF THE TECHNIQUES

2.1. Introduction to X-ray Fluorescence Microprobe

X-ray fluorescence (XRF) as an elemental analysis technique, using characteristic X-rays emitted from atoms excited by an external source, is likely to be familiar to many scientists. X-ray tubes, scanning electron microscopes, proton and other particle beams have all been used as XRF sources. Utilizing synchrotron X-rays as the excitation source, materials can be analyzed with little or no pretreatment and with no requirement for analysis in vacuum. The low power deposition of the technique provides a practical means of analyzing materials in their natural state, even liquid, wet, or moist samples. The high-intensity photons that these facilities provide are up to 11 orders of magnitude brighter than can be generated using more conventional X-ray tube sources. It is the high brightness and brilliance of these sources, the extreme collimation of the synchrotron light, and the polarized nature of the X-ray beams, which makes them so amendable to building X-ray probes with high spatial resolution and sensitivity

(Lanzirotti et al., 2010). At an XRF microprobe, elemental imaging can be performed in two-dimensional and three-dimensional modes. A variety of major and trace elements can be analyzed and imaged simultaneously with detection sensitivities often as low as the femtogram (10^{-15}) to attogram (10^{-18}) level. By scanning the incident X-ray energy over the absorption edge of these elements, fine-scale speciation information can be obtained using microbeam X-ray absorption spectroscopy (XAS). In this section of the review, the practical application of XRF microprobe methods in the plant sciences will be discussed.

A basic XRF microprobe consists of a magnet source, crystal monochromator, slits and focusing optics, beam intensity monitor, motorized sample stage, and fluorescence detector. An inventory of the synchrotron-based X-ray probes, currently in operation worldwide, reveals notable differences in the magnet sources and focusing optics utilized, and these have consequences on the photon flux that can be delivered to the sample, the spatial resolution achievable, and in some cases, the types of techniques that can be effectively implemented. Some X-ray probes use synchrotron light emitted by bending magnet dipole sources, which are also responsible for steering the electron beam within the storage ring, while others rely on insertion devices such as wigglers and undulators. Bend magnets (dipole) and wigglers (multipole) produce a broadband energy spectrum in a wide fan such that the X-rays produced cover a broad spectral range, while undulators introduce harmonic peaks of greatly enhanced brightness, where the X-ray beam is highly collimated in both the horizontal and vertical directions. Thus, undulators boast a smaller source size and produce beam with less divergence (higher brightness) than do bend magnets or wigglers, but at the expense of a broadband spectrum. In general, the most spatially resolved X-ray probes utilize undulator-based sources, but imaging probes designed on broadband sources are easier to configure for scanning to extended energies, hundreds of eV above an absorption edge (i.e. extended X-ray absorption fine structure (EXAFS) spectroscopy).

There are differences in the performance capabilities of X-ray focusing optics that have consequences for the types of experiments one may wish to conduct. Beamlines that use diffractive focusing optics such as Fresnel zone plates and multilayer Laue lenses (MLLs) currently yield the highest spatial resolutions available (<30 nm); however, these optics suffer from low efficiencies (15–30%), chromaticity (energy-dependent focal length), and short working distances (limited space between sample and optic). Their short working distance limits both the type of analyses that are possible due to

space restrictions and the size and type of samples that can be analyzed. Their chromaticity can demand significant changes in the experimental setup (perhaps a change in the optic itself) for measurements at significantly different X-ray energies. Furthermore, it is important to recognize that the focal length is roughly proportional to the incident X-ray wavelength ($f \sim 1/\lambda$). Thus, absolute position of the focal spot changes significantly with energy, which can make their use difficult for energy-scanning experiments. Reflective X-ray optics include elliptically-bent mirrors, capillaries, and Bragg–Fresnel lenses. Of these, silicon mirrors coated with an X-ray reflective coating and arranged in a Kirkpatrick and Baez (KB) geometry (Kirkpatrick and Baez, 1948) are the most frequently used. Recent improvements in mirror flatness, bender designs, and nested mirror geometries have allowed these devices to routinely achieve spatial resolutions of a few hundred nanometers. Coupled with the smaller beam emittance provided by newer synchrotron facilities, it is expected that the next generation of KB-mirror-based probes could achieve spatial resolutions below 50 nm. Advantages of KB optics include their achromaticity, high efficiency (70–90%), and long working distances. Thus, KB-mirror-based probes are ideal for experiments that do not necessarily require submicrometer spatial resolutions but rather need the highest detection sensitivities, where microfocused XAS is a priority, and where sample requirements dictate the use of optics with longer working distances (e.g. reaction cells, large samples, crystal analyzers, tomography stages, etc.).

With any type of X-ray fluorescence microprobe, a factor that is often underappreciated is the large variation in detection sensitivity as a function of atomic number due to differences in fluorescence yield. If an inner-shell electron is ejected from an atom due to absorption of an X-ray photon, an electron from a higher shell fills the resultant core hole and releases an amount of energy equivalent to the difference between the energy levels involved in the transition. The energy released can be either emitted as a characteristic X-ray (fluorescence) or transferred to another atomic shell electron (Auger effect). Emissions of characteristic X-rays form the basis for detection of the chemical elements by XRF analysis. The probability of a characteristic X-ray resulting from this process is called the fluorescence yield (ω), and it depends on the shell, in which the core hole occurred, and the element's atomic number. The probability of a core hole in the L-shell being filled by a radiative process is considerably lower than for the K-shell. Thus, one would expect reduced detection sensitivity for elements excited from the L-shell (e.g. Pb) compared to elements excited from the K-shell (e.g. Zn). For a given shell, fluorescence yield increases with

increasing atomic number. For example, the fluorescence yield for calcium is approximately 0.2 (~20%); however, ω approaches unity for the K-shell of the heaviest elements. Thus, one can expect better sensitivity for elements with higher atomic number (e.g. Zn) than for elements with lower atomic number (e.g. Ca).

Differences in detection sensitivity for the chemical elements also arise from attenuation of the fluorescence signal by absorbers located between the sample and the detector. Less-energetic X-ray emissions are more easily absorbed by the sample itself, the air path, and the sample/detector filters. Instruments that operate in a helium atmosphere or vacuum to minimize absorption effects will have improved detection sensitivity for these low-energy emissions, but consider that absorption by the sample itself affects the depth within the sample from which fluorescence is being detected. One can demonstrate the potential effects graphically by modeling the fraction of Kα and Lα fluorescence photons that would be transmitted through a leaf sample of varying thickness and modeled as cellulose ($C_6H_{10}O_5$; $\varrho_{leaf} = 0.8$ g cm^{-3}) (Fig. 1.1). Taking a 300 μm thick "leaf" as an example, the sample will attenuate ~87% of the Ca Kα fluorescence and ~32% of the Fe Kα fluorescence from the entire leaf thickness. Furthermore, it will

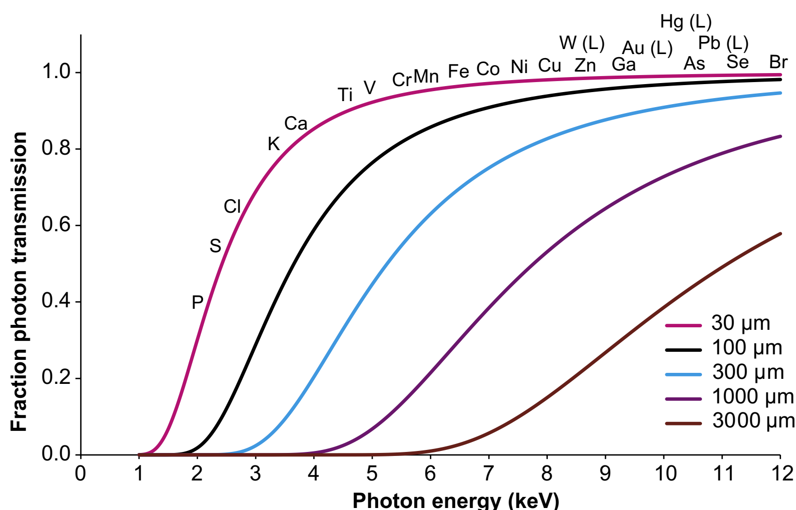


Figure 1.1 Plot of the fraction of transmitted X-rays through a "leaf" as a function of energy (leaf tissue modeled as cellulose, $C_6H_{12}O_5$, with density of 0.8 g cm^{-3}). Curves are shown for sample of 30, 100, 300, 1000, and 3000 μm thickness. Also shown are where the Kα and Lα emission energies of selected elements lie along the curve. For color version of this figure, the reader is referred to the online version of this book.

attenuate almost 99% of the P Kα fluorescence such that only the leaf surface is analyzable for P. This is an important consideration in analyzing samples that are rather thick or samples that are not flat. High-energy fluorescence lines in effect sample deeper into materials than low-energy emissions, and topographic features between the incident beam and detector can act to shadow low-energy fluorescence from the detector.

2.2. Micro X-ray Fluorescence Imaging

XRF data are recorded as an energy spectrum, which is a plot of the measured fluorescence counts or counts per second (Cps) as a function of energy (Fig. 1.2). For a particular element, the fluorescence intensity is proportional to the number of atoms. On the XRF spectrum in Fig. 1.2, one can see a number of Gaussian-shaped peaks appearing above background, each representing a different emission line (e.g. Ca Kα and Ca Kβ). With current detector technology, each emission "line" is resolved as a peak area not less than 140 eV wide at full-width at half maximum (FWHM). This present level of energy discrimination is insufficient to resolve K Kβ (3590 eV) from Ca Kα (3692 eV); however, it is adequate to resolve Ca Kα from Ca Kβ (4013 eV). It is helpful to recognize that the intensity ratio of Kα and Kβ emission is a fixed quantity for a particular element. For K, the $K\beta_{1,3}/K\alpha_1 = 0.11$, which indicates that the Kβ peak should have ~1/9 of the measured Cps for the Kα. This can be a useful diagnostic for evaluating

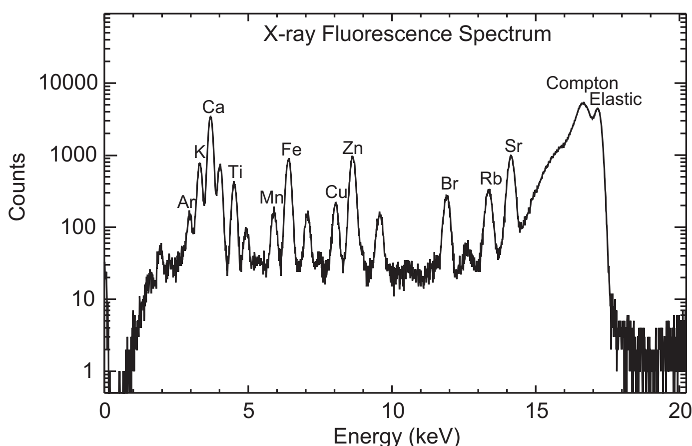


Figure 1.2 Log plot of a μXRF spectrum accumulated at 17.2 keV for a turmeric root showing the fluorescence intensities of major and trace elements, Compton and elastic scattering by the sample. For color version of this figure, the reader is referred to the online version of this book.

spectral overlaps (e.g. K Kβ with Ca Kα), and one can use peak fitting with a constraint on the Kα/Kβ ratio to remove the influence of a neighboring element's Kβ emission from another element's Kα (i.e. β-stripping). It is also true for the relative intensities of the L-line emissions, such as for Pb: $L\alpha_1 = 100$, $L\beta_1 = 66$, $L\beta_2 = 25$, $L\gamma_1 = 14$, $L\alpha_2 = 11$, $Ll = 6$.

Micro-X-ray fluorescence (μXRF) imaging proceeds by recording the emission of characteristic X-rays from many points on a sample. High-resolution optics focus X-rays into a small spot, and the sample is raster scanned through the focal spot. Rather than recording the signal only within a limited number of preset energy windows (i.e. spectral regions of interest, or ROIs), one can record the full energy spectrum at each scan point (i.e. pixel). A number of approaches can be used to extract elemental images from the set of XRF spectra. The most basic approach is the postcollection "ROI-cut," which amounts to collecting the signal within a discrete energy window (200–400 eV wide) centered on a particular emission line (e.g. Ca Kα) without applying corrections for spectral overlaps or background, and then recasting these per-pixel intensities as a 2-D image. Another approach is a "dedicated ROI," a discrete energy window typically set as an FWHM for each monitored emission line (e.g. Ca Kα), which employs some degree of background removal but does not account for spectral overlaps. As a first approximation, the convenient ROI-cuts and dedicated ROIs allow one a real-time view of the data, and can be very useful for decision-making at the beamline. Rather than manually defining the energy window for spectral ROIs, one can use nonlinear least squares fitting of the energy spectrum on a per-pixel basis, which has the advantage of removing spectral overlaps and background, but may suffer from the low count rate of single-pixel energy spectra. The background can be estimated using dedicated ROIs, and the influence of overlapping Kβ lines can be calculated or measured with standard reference material and then removed by fitting to known functions for XRF lines. One approach to reduce the complexity of the dataset and minimize the per-pixel noise level is to apply principle components analysis (PCA) as a filter (Vogt et al., 2003). By fitting the corresponding eigenspectra of the principle components, one can then generate maps of fitted elemental components with high accuracy, without the need to fit the spectra of single pixels (Vogt et al., 2005).

2.2.1. Visualization of μXRF Data

Once a set of μXRF images has been produced from the dataset, there are a number of visualization steps that can be taken to make sense of the large amount of data. The most obvious thing one can do is to plot a gray-scale

image for each element and compare them side by side. Such a set of images is presented in Fig. 1.3, which shows the elemental distributions for S, Ca, K, Mn, Fe, and Zn in a *Noccaea* seed (20 μm thick tissue cryosection) along with an optical image and the image of the Compton scatter (analog to backscattered electron image from a scanning electron microscope). The μXRF images are shown in negative contrast, so that high concentrations are shown as dark areas. Letting the eye roam around this figure, one can glean much information, for instance, both K and Ca appear to be abundant in all regions of the sample, whereas the other elements appear to be localized to specific tissues or cells. Sulfur is present in the endosperm and in the

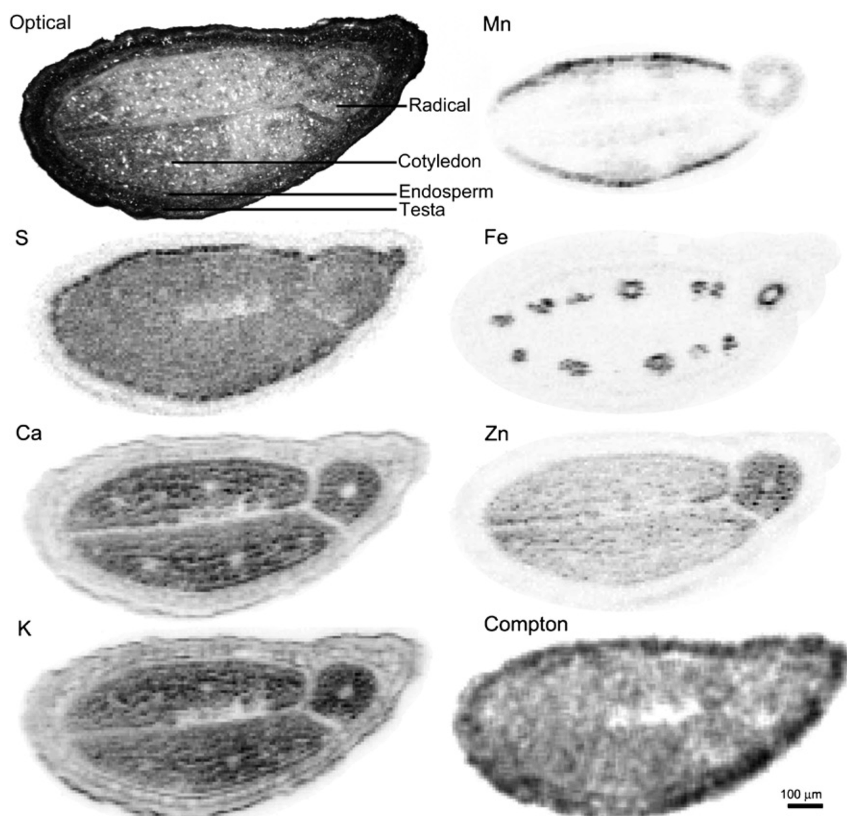


Figure 1.3 Grayscale synchrotron-based X-ray microfluorescence (μSXRF) images in negative contrast showing the distribution of S, Ca, K, Mn, Fe, and Zn in a *Noccaea* seed (20 μm thick tissue cryosection) along with an optical camera image and the image of the Compton scatter (analog to backscattered electron image). All μSXRF images were acquired at 12 keV.

embryo itself, but is not present in the seed coat as evident from an overlay of S Kα with the visible light image (data not shown). It can be very useful to overlay a μXRF image with a visible light image, and it is suggested to capture visible light images both before and after X-ray microanalysis to look for obvious signs of radiation damage, which is a greater concern with undulator-based X-ray probes. Another point to keep in mind, particularly when working with images derived from dedicated ROIs, is the potential for some signal from a neighboring element to bleed through into another element ROI. For example, consider the μXRF images of Mn and Fe in the seed. Some parts of the specimen show high Mn and low Fe, while other areas show high Fe and low Mn. In this case, the presence of Fe in the same vicinity of Mn enrichment should be suspected. When one extracts energy spectra from a small area for both conditions, one can see the influence of spectral overlap (Mn Kβ on Fe Kα) (Fig. 1.4). It should be noted that these

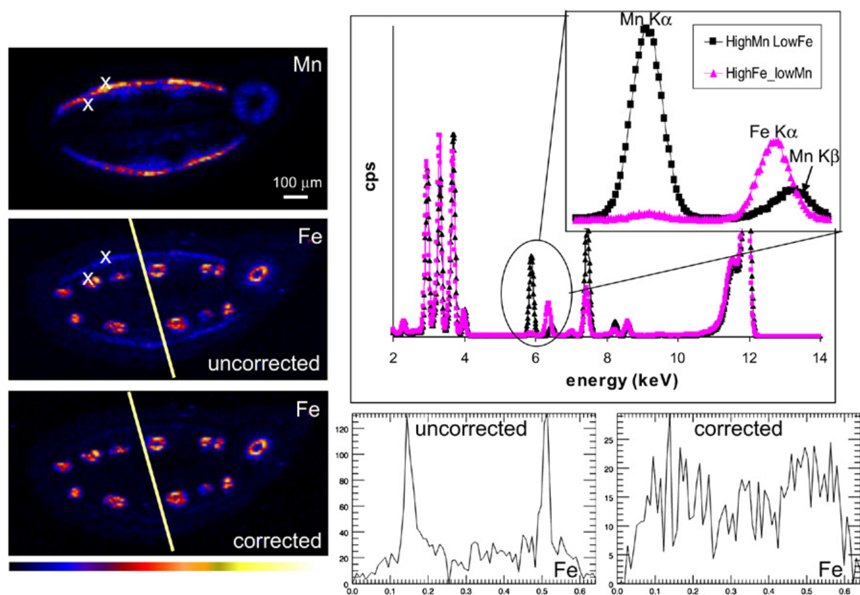


Figure 1.4 μXRF images of Mn and Fe in *Noccaea* seed generated from "dedicated ROIs" (uncorrected) and the Fe image resulting from spectral deconvolution via peak fitting of the energy spectra on a per-pixel basis (corrected); linear plot of the μXRF spectra extracted from a high Mn, low Fe region and a low Mn, high Fe region of the μSXRF image (denoted by "X") showing the effect of spectral overlap (Mn Kβ and Fe Kα); "line-out" spectra (fluorescence intensity versus distance in mm) extracted from the uncorrected and corrected Fe Kα image showing the result of image correction on a transect across the specimen (denoted by line). For color version of this figure, the reader is referred to the online version of this book.

spectra are presented as a linear plot to preserve the Kα/Kβ ratio, and that a log plot shows the more severe case of overlap. In Fig. 1.4, one can see the end result of spectral deconvolution via peak fitting of the energy spectra on a per-pixel basis. In the corrected image of Fe Kα, the region where Fe and Mn had appeared colocalized is no longer visible, but the regions with high Fe are unchanged. Effects of image correction are also apparent in the corresponding correlation plots (Mn vs Fe) and "line-out" spectra (Fe Kα), which can be produced from the μXRF images (Fig. 1.4). Another approach to resolve a spectral overlap is to repeat the image at multiple energies (above and below an absorption edge) and then isolate the signal by subtraction (difference mapping); a nice example of difference mapping used to image Pb and As in a soil ferromanganese nodule is presented in Manceau et al. (2002).

Adding another layer of sophistication to the mix is the μXRF overlay image. In this method, one makes an image in which the R (red), G (green), and/or B (blue) values of each pixel are proportional to the amounts of the elements they represent. An RGB image of K, Fe, and Mn in the seed specimen is shown in Fig. 1.5. If the elements are all the same, then R = G = B and one has a gray-scale image. If they are all different, one can get images that are informative and esthetically pleasing. The overall brightness of a region is related to the sum of the concentrations, and the hue is related to the difference (Manceau et al., 2002). A color triangle is very helpful for displaying the mixing of colors for RGB images. As an example, consider the bicolor image overlay of K (red) and Ca (blue) in the seed (Fig. 1.5). One clearly observes a magenta color for the embryo region and a predominance of red color in the seed coat region, but the color blue is not obvious anywhere on the overlay. The absence of pure blue suggests that Ca does not exist without K in any region of the sample; the relatively pure red suggests that K exists in the seed coat without much Ca, and the magenta color suggests that both Ca and K are present in similar proportions in the embryo. These trends are also reflected in the "line-out" spectra for K Kα and Ca Kα extracted from the bicolor image (Fig. 1.5).

Another useful technique for understanding trends in the data is the scatterplot, in which one plots the counts in one channel against the counts in another (Manceau et al., 2000). A nice discussion on cross-correlation analysis and the use of population-segmentation method for evaluation of corresponding scatterplots can be found in Manceau et al. (2002). A scatterplot for K Kα and Ca Kα in the seed image is shown in Fig. 1.5. One observes two distinct clouds of points with different

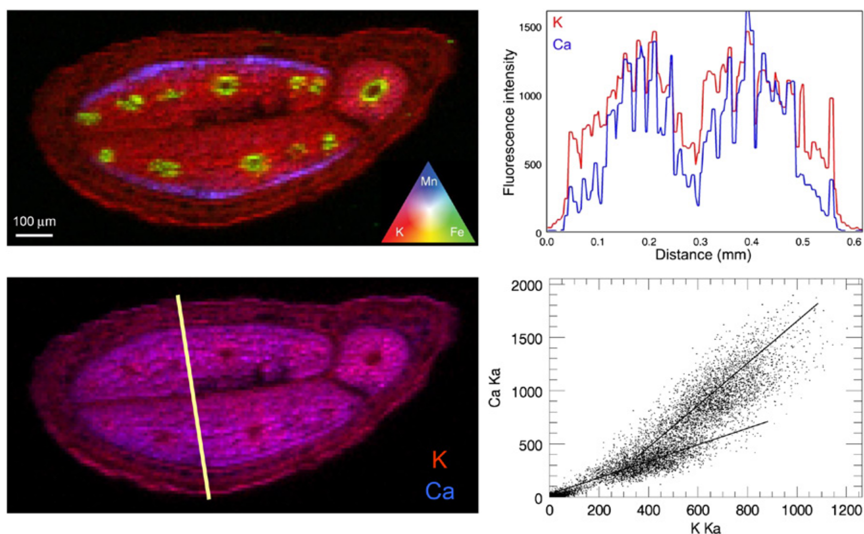


Figure 1.5 Tricolor (RGB) image of K, Fe, and Mn with color triangle and bicolor (RB) image of K and Ca in the *Noccaea* seed; "line-out" spectra for K Kα and Ca Kα showing the trend in their distribution between seed coat (testa) and embryo (denoted by line); correlation plot for counts in K Kα and Ca Kα channels of the bicolor image showing two distinct clouds of points with different [Ca]/[K] ratios in each population (population-segmentation method indicates the populations belong to the seed coat and embryo, respectively). See the color plate.

[Ca]/[K] ratios in each population. The low [Ca]/[K] points represent the seed coat region and the high [Ca]/[K] points represent the embryo region. One can mask the points in one region of the scatterplot using manual or automated methods and then backproject the images to observe where those particular points are located on the sample (i.e. population-segmentation method). By in large, these data-mining exercises are used to discover trends in the data that would otherwise be elusive. Ultimately, one would like to identify sample regions with similar trace-element fingerprints and compare spectra from these regions. An approach used to correlate elemental distributions in a µXRF dataset to reveal information about the number or composition of different major constituents in a sample is cluster analysis. In cluster analysis, a computer algorithm is applied to find clusters such that the Euclidian distance between cluster centers is minimized. For additional discussion on application of cluster analysis to spectromicroscopy data, the reader is directed to Vogt et al. (2003, 2005) and references therein.

μXRF images tend to reveal themselves over time. It may take more than one image of an element to show all the details that exist in the data, and it may take looking at the same images at several different times before certain details become evident. Furthermore, it may be necessary to apply other data-mining techniques (e.g. scatterplot and cross-correlation analysis, "line-out" analysis, cluster analysis, etc.) to gain a more complete understanding of the image data.

2.2.2. Quantification of μXRF Images

Methods for quantification of elemental abundance (i.e. conversion of fluorescence intensity to metal concentration on a per-weight or per-area basis) vary depending on the nature of the material being analyzed, thus a method appropriate for biological specimens may not be the most appropriate for geological samples. For more detailed discussions on quantitative interpretation of μXRF images, readers are directed to Lanzirotti et al. (2010), Punshon et al. (2009), Solé et al. (2007), Sutton et al. (2002) and Vogt et al. (2003, 2005). The basic procedure for obtaining quantitative compositional information from μXRF spectra is to fit the background spectrum, subtract the background, fit the remaining peaks to obtain net peak areas, and use these net areas to compute concentrations, where the concentration calculations include information on the analysis conditions and physical state and major element composition of the sample (Sutton et al., 2002). Two general approaches to solving the concentration to intensity relationship are to (1) use a standard for each element of interest or (2) use an internal standard element. A fundamental parameters (FPs) approach is very effective when coupled with standards analysis. Here, the relationship between concentration and intensity is determined with the standards, while FP algorithms are used to correct for absorption differences between the sample matrix and standard. This computation takes into account various parameters of the analysis conditions (absorption of X-rays by the Be windows, the air path between the sample and the detector, fluorescence yields, photoionization efficiencies, self-absorption, secondary fluorescence) and the matrix composition (thickness, density, major elemental composition). Various glass or organic standards from the National Institute of Standards and Technologies can be used for this standards-based FP approach. In the standardless FP approach, the FP algorithms compute both the intensity to concentrate relationship and the absorption effects based on the measured fluorescence from a single element in the sample of known concentration. This is an element whose abundance might be fixed by stoichiometry or known

based on another external analysis, such as electron microprobe analysis. In either approach, one is required to make reasonable assumptions of the bulk composition, sample density and thickness. Thus, quantification is relatively straightforward for thin samples with nearly uniform thickness and density (e.g. biological tissue section). One approach used for interrogating three-dimensional samples is tomography.

2.3. Computed Microtomography: Full-Field and Microfocused Beam Modes

Synchrotron-based computed microtomography (CMT) is an extension of conventional medical computed axial tomography (CAT) scans to high spatial resolution. By employing a nondestructive and in situ three-dimensional (3-D) imaging technique such as CMT, one can measure the internal structure or elemental distribution in a virtual cross-section of a biological specimen without the need for tissue preparation or sectioning that might cause loss of structural integrity or redistribution of the elements. Three-dimensional images and virtual cross-sections of the X-ray attenuation or individual elemental fluorescence within the specimen can be rendered, allowing visualization of the variability in microstructure or elemental distribution.

For detailed information on the principles, data collection and processing of microtomography data, including discussion of different types of CMT (e.g. transmission, edge, fluorescence, and diffraction), see Sutton et al. (2002). While X-ray diffraction techniques are not discussed in this review, examples of diffraction microtomography (DMT) can be found in Bleuet et al. (2008) and Lanzirotti et al. (2010). In recent years, there has been a growing interest in the use of phase-contrast imaging and phase-contrast tomography to obtain structural information, particularly for biological specimens which have low absorption-contrast yet decent phase-contrast because the X-ray phase-shift cross-section for light elements (e.g. C, H, O, N) is nearly a thousand times larger than their X-ray absorption cross-section (Momose et al., 1996). For additional information on phase-contrast imaging with hard X-rays, the reader is directed to Hornberger et al. (2008) and Holzner et al. (2010). The latter two references demonstrate the integration of phase-contrast detection with scanning XRF microprobe, thus detailed structural information can be collected simultaneously with μXRF images or fluorescence computed microtomography (fCMT) sinograms. The present discussion, however, will focus on transmission, edge and fCMT.

When elemental abundance is low, fCMT will be the method of choice. Synchrotron-based fCMT requires no sample pretreatment, allows

noninvasive examination of living materials, and can detect elemental abundances in the submicrogram per gram range with a resolution of 10 μm or less (Sutton et al., 2002). To use fCMT effectively, the absorption of emission lines of interest must be low enough through the sample to allow for their detection given the object's diameter (recall discussion from Section 2 concerning estimates for the fraction of X-rays transmitted through cellulose "leaf" material of 300 μm thickness). Thus, absorption effects generally make this imaging technique most applicable to samples of small diameter (typically <2–3 mm), the analysis of higher energy emission lines and/or materials of low density (e.g. biological tissues); however, some degree of correction for absorption effects can be made (Schroer, 2001).

In the fCMT measurement, the sample is translated and rotated under a microfocused beam while the fluorescence intensities for multiple elements are recorded with a solid-state detector and absorption contrast is recorded with a photodiode or ion chamber downstream of the sample. The conventional microprobe apparatus is used with the addition of a rotation stage upon whose axis the object is centered with a goniometer head. Once centered, fluorescence is measured as the object is translated through the X-ray beam. In effect, the resultant [X, theta] arrays of data can then be reconstructed as [X,Y] virtual slices through the object including "air" pixels on each side. At the end of each translation, the sample is rotated slightly, and the measurement is repeated in this manner until the sample has traversed 180°. The optimal number of projections (each line scan is a projection) is determined by the Nyquist limit for discrete sampling, and is $N\pi/2$, where N is the number of pixels per line (Dowd et al., 1999). The translation step size is chosen to be comparable to the beam size. Thus, high-resolution fCMT requires many projections to yield voxels (3-D pixels) at the target resolution; however, it is somewhat common practice to undersample in the interest of time, and Sutton et al. (2002) suggest a rotational step size (in radians) equal to π/N, which sets the number of projections needed for 180° rotation equal to the number of pixels per line. The raw dataset consists of a position-versus-angle image (or sinogram) for each emission line monitored. The resultant [X, theta] arrays of data can then be reconstructed as [X,Y] virtual slices through the object using backprojection or fast Fourier transform reconstruction algorithms. While, in some cases, it would be impractical to image a significant volume of sample using fCMT, it can be used to generate a full three-dimensional dataset (i.e. slice-by-slice), as done by Kim et al. (2006) (Fig. 1.6).

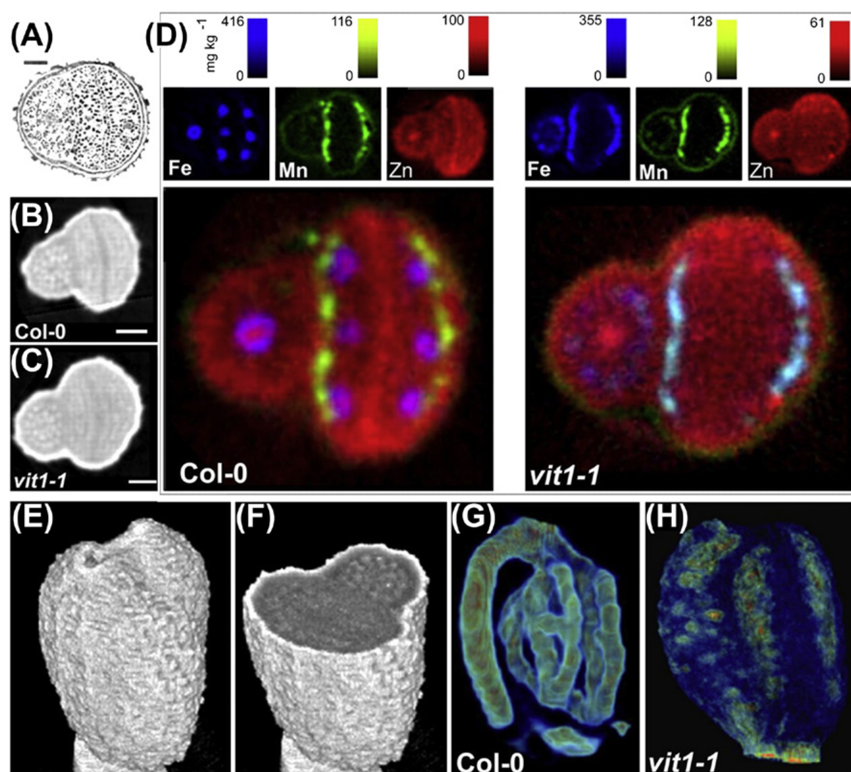


Figure 1.6 fCMT of *Arabidopsis* seed. (A) Light micrograph cross-section of a mature seed. (B, C) Total X-ray absorption tomographic slices of Columbia-0 (wild-type) and vit1-1 mutant seeds. (D) μXRF tomographic slices and composite images of Fe (blue), Mn (green) and Zn (red) Kα fluorescence lines from Columbia-0 and vit1-1. (E, F) Three-dimensional rendering of total X-ray absorption of a wild-type *Arabidopsis* seed. (G, H) Three-dimensional rendering of Fe Kα fluorescence in Columbia-0 and vit1-1, respectively. *(Reprinted with permission from Kim et al. (2006)).* See the color plate.

fCMT measurements require typically several hours to complete a single slice, thus the specimen must withstand a substantial X-ray dose without changing shape or dehydrating. Often, it is necessary to dry or freeze-dry plant material for fCMT (seeds are an exception). An early application of fCMT to plant biology was reported by Hansel et al. (2001, 2002) who used fCMT in combination with μXRF and XAS to study Fe plaques and associated metals on the roots of reed canary grass and cattail collected from a wetland receiving drainage from a century-old Ag mine. A similar study by Blute et al. (2004) used fCMT to record oxidation-state tomograms of As(III) and As(V) on root plaque of cattail. For detailed explanations of

oxidation-state μXRF mapping and tomography, readers are directed to Lanzirotti et al. (2010), Marcus (2010), and Sutton et al. (1995, 2002). The basic approach is to make multiple μXRF maps or fCMT sinograms of the specimen, where the monochromatic energy for each image is chosen to preferentially excite particular oxidation-state components of the element of interest (including an image at the edge-step for normalization), and then the distributions of individual oxidation states are determined by deconvolution of these images. Thus, the specimen receives three or more times the radiation dose than from a single measurement. It is worth mentioning that both of the root plaque studies were conducted with freeze-dried tissues, and the latter study acknowledged that wet roots dried and lost structural integrity during the required analysis time. However, recent advances in XRF detectors and fast detector electronics that allow scanning a sample "on-the-fly" have greatly reduced the overhead associated with sample positioning and detector readout, and these recent improvements have dramatically reduced the exposure time for fCMT and μXRF measurements.

When elemental abundance is high (*circa* >1 wt%), one can use a full-field mode of CMT for element-specific imaging. For full-field CMT, the sample is exposed to a wide-fan X-ray beam, and one measures the transmitted X-rays that are converted to visible light via a single-crystal scintillator and then projected with a microscope objective onto an area detector. Since a wide-fan X-ray beam is used, the sample is only rotated in the X-ray beam (i.e. no translation). Advantages are that sample dimensions can be large, the sample can be imaged in minutes and does not need to withstand a large radiation dose, and thus hydrated samples can be analyzed; however, one does not directly obtain element-specific images using this method (only structural information). For element sensitivity, it is necessary to record the image both above and below the absorption edge of the element of interest and then subtract the images, which is called edge or differential absorption computed microtomography (DA-CMT). While the subtracted image offers element specificity, the below-edge image provides a glimpse of the internal structure of the specimen, and can be useful to overlay with the elemental image to explore spatial associations. Tappero et al. (2007) used DA-CMT to image the internal distribution of Co in hydrated *Alyssum murale* leaves, and by registering the elemental and structural images, observed a distinct distribution of Co between cells (apoplastic) in the ground tissue and the localization of Co on the leaf surface near the tips and margins. Another advantage of the full-field mode for CMT is that more than a single slice is captured in the measurement, thus a full 3-D

volume of sample is recorded. For instance, the field of view in the vertical direction can be several millimeters with a pixel resolution on the order of 5 μm, thus a single measurement yields more than 500 tomographic slices. These slices can be arranged into a movie sequence to view the changes in elemental distribution as one traverses the sample in the X, Y, or Z direction. Additionally, these slices can be used to generate a full 3-D volume of the specimen that can be explored from every possible position and angle.

2.4. X-ray Absorption Spectroscopy (Bulk and Microanalyses)

XAS can be measured on the micron scale with focused X-ray beams, or measured on a "bulk" scale using an X-ray beam of several millimeter square. XAS, in general, is an element-specific, spectroscopic method that yields information about the chemical state and local atomic structure of the absorbing atom. XAS spectra are especially sensitive to the formal oxidation state, coordination chemistry, and the distances, coordination number and species of the atoms immediately surrounding the selected element. Detailed explanations of XAS principles, techniques, and applications in soil science can be found in a number of excellent reviews (Bertsch and Hunter, 2001; Brown and Sturchio, 2002; Fendorf et al., 1994; Kelly et al., 2008) while details on the physics of XAS appear in several books (Koningsberger and Prins, 1988; Stöhr, 1992; Teo, 1986).

In a standard XAS measurement, the absorption spectra are typically collected by scanning the monochromator energy through the absorption edge of the element of interest and then recording the incident (I_0) and absorbed (I) photon intensities with ion chambers placed before and after the sample. While this configuration directly measures the energy dependence of the absorption coefficient (μ), $\mu(E) = \log I_0/I$, these excited atoms decay within a few femtoseconds via XRF or Auger emission. As these emissions are proportional to X-ray absorption, either of these processes can be used to measure the absorption coefficient, and in an XRF configuration $\mu(E) \propto I_f/I_0$, where I_f is the monitored fluorescence intensity associated with the absorption process. A fluorescence detector with low-energy resolution and large-solid angle (e.g. a Lytle detector) is ideal for analysis of a single element that is the highest concentration detectable element in the sample, whereas analysis of a trace element in a chemically complex material typically requires a multi-element solid-state detector array. With an energy-discriminating detector, an XRF spectrum is recorded at each energy point in the XAS scan, and the fluorescence intensity for the element of interest is extracted, normalized to the incident beam intensity,

and plotted as a function of the incident energy. When full XRF spectra are preserved as a part of the scan at each energy step, Gaussian peak fitting of the fluorescence spectra can be used to mitigate effects of spectral overlap.

2.4.1. Anatomy of XAS Spectrum

An XAS spectrum is conventionally divided into two regimes: X-ray absorption near-edge structure (XANES) and EXAFS (Fig. 1.7). The energy region extending from 50 eV below the absorption edge to *circa* 200 eV above the absorption edge is the XANES portion of the spectrum. Fingerprint information can be rich in this region. XANES provides information on valence state of a selected element, the local symmetry of its unoccupied orbitals, and in some cases, the molecular species by comparison of measured spectroscopic data to a spectral library of known compounds. It is important to collect XANES data for the references on the same beamline, preferably during the same run, as used for the samples.

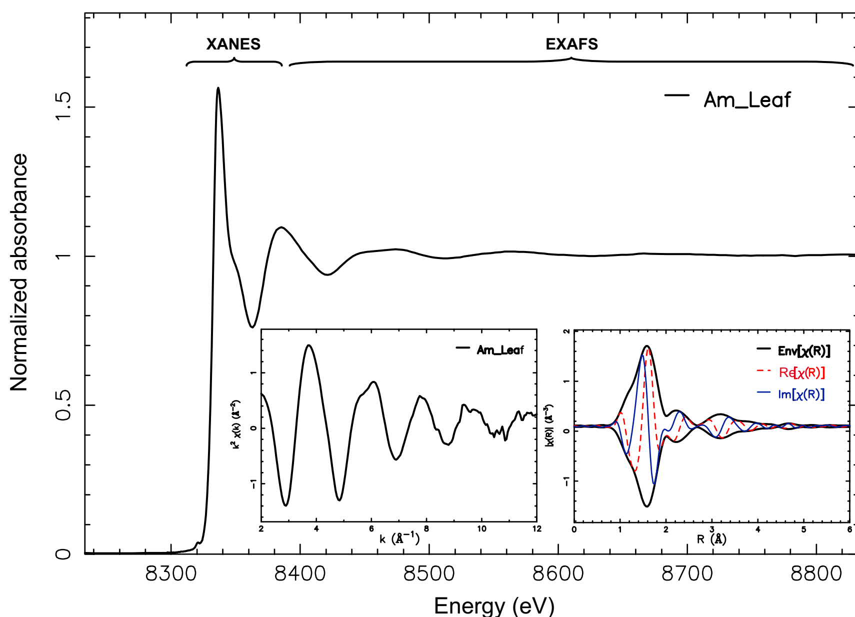


Figure 1.7 Ni K-edge µXAS spectrum of *Alyssum murale* leaf *(collected from the primary vein)* showing the region of the spectrum representing the XANES and EXAFS. Inset: k^2-weighted $\chi(k)$ EXAFS spectrum (left) and corresponding Fourier transform (including real and imaginary parts). For color version of this figure, the reader is referred to the online version of this book.

Since the binding energies of the valence orbitals are higher for more oxidized atoms, the energy position of the absorption edge and the pre-edge features are easily correlated with the valence state of the absorbing atom in the sample. The main step-like feature of the absorption spectrum is due to the excitation of the photoelectron into the continuum. The absorption edge is usually identified by the inflection point of this main absorption feature, and its position is dependent on the chemical environment of the absorbing atom. The position of the absorption edge generally increases by 1–3 eV for each electron removed from the valence shell due to the increasing binding energy of the core levels. However, the position of the absorption edge is also influenced by the bonding environment of the absorbing atom such that spectra of two reference compounds containing an element in the same formal valence state can have slightly different edge positions (typically <1 eV).

The EXAFS part of the spectrum is the normalized oscillatory part of the absorption coefficient above the absorption edge to *circa* 800 eV or higher, which contains the critical information required to determine the local coordination environment of the element of interest. Beyond the edge, oscillations are observed which arise from interference effects involving the photoelectron wave ejected from the absorbing atom and the fraction of the photoelectron wave backscattered by atoms surrounding the absorbing atom. The frequency of the oscillations is inversely related to the bond distance between the absorber and neighboring atoms, and the amplitude is related to the number and identity of the neighboring atoms in a particular shell (i.e. group of atoms at a unique radial distance from the absorber). Fourier transformation of the oscillatory fine structure (obtained after background subtraction) yields a radial structure function (RSF) in real space with peaks revealing the local environment of the target atom (Manceau et al., 2002). A plot of the oscillatory fine structure and corresponding Fourier transform for a Ni K-edge μXAS spectrum collected from an *Alyssum* leaf is shown as an inset in Fig. 1.7.

2.4.2. Data Analysis for Complex, Mixed-Component Systems

Traditional shell-by-shell XAS analysis, involving Fourier transforming, backtransforming and filtering, generally does not work well for multicomponent systems with a mixture of metal species. The atomic shells from the different species overlap, so that one cannot separate them out when there is a complex mixture (Manceau et al., 2002). One way to untangle

a complex mixture is to use a microprobe to examine multiple spots, and use PCA to determine how many independent components are needed to reproduce the spectral dataset. A primary goal of a μXAS experiment is to identify all the unique chemical forms for the element of interest. The PCA technique then determines if the dataset can be described as weighted sums of a smaller number of components (i.e. the principle components). Target transformation (TT) is used to identify the principle components by taking a spectrum of a candidate reference compound and mathematically removing from it anything that is not reconstructed by the set of principle components identified by PCA (Malinowski, 1978). One can compare various models by fitting the unknown spectrum with different combinations of reference spectra and tabulating the fit results to compare the goodness-of-fit. Once the best-fit components have been identified, their proportion can be determined in each sample by linear combination fitting. It is important to note that the accuracy of this fitting approach is dependent upon the data quality, the completeness and relevance of the standards dataset, and the range over which the data were fit. It should also be emphasized that consistent data treatment for both standards and sample spectra is required. Furthermore, this approach can be limited by the lack of unique spectral features for the candidate reference compounds, and it is well known that XAS techniques are inherently less sensitive to metals bound to lighter elements (Sarret et al., 2004). In such a case, it may not be possible to constrain the exact speciation without additional data from ancillary measurements. Linear combination fitting subroutines are available in XAS data analysis programs such as Athena (Ravel and Newville, 2005) and Sixpack (Webb, 2007). Additional discussions on XAS data analysis for heterogeneous systems can be found in Wasserman (1997, 1999), Manceau et al. (2002), and Kelly et al. (2008).

2.4.3. Self-Absorption

An important consideration for fluorescence XAS measurements is the potential for self-absorption to occur with thick samples or samples that are highly concentrated in the absorbing element. When samples are too thick or concentrated, the penetration depth of the incident beam will vary as a function of $\mu(E)$. As $\mu(E)$ increases above the absorption edge, the penetration depth decreases and, thus, attenuates the oscillatory structure of the XAS spectra. Some algorithms exist for calculating the magnitude of such effects but these rely on precise knowledge of the density of all atoms in the path of the X-rays which is rarely available (standards are an

exception), thus it is generally preferable to avoid self-absorption effects than to attempt mathematical corrections to the data. However, if one has a relevant reference spectrum that is free of self-absorption effects, then a straightforward correction to an experimental XANES spectrum can be made using the equation given by Sarret et al. (2007) [$y_{\text{corrected}} = y_{\text{experimental}}/(1 + a(1 - y_{\text{experimental}}))$], where the self-absorption parameter (*a*) equals 0 in the absence of a self-absorption effect and increases with this effect; as the precise composition of the sample is not known, "*a*" is adjusted iteratively to match the amplitude of the experimental spectrum with the standard. A detailed discussion of the origin of self-absorption (or "overabsorption") is presented in Manceau et al. (2002).

2.5. Synchrotron-Based μFTIR

Synchrotron radiation Fourier transform infrared spectromicroscopy (SR-μFTIR) is based on the absorption of light in the mid-IR region (700–4000 cm^{-1} or 14–2.5 μm) by vibrational transitions in functional groups present in the analyzed specimen. A particular bond in a molecule will absorb the incoming IR radiation if the frequency matches the frequency of the vibrational mode, and if the vibration causes an asymmetric change in the charge distribution in the molecule (dipole moment) (Martin and Holman, 2006). Hence, this technique is sensitive to many chemical functional groups from the molecules present in samples; each molecular configuration will have then a set of unique vibration modes. In complex biological samples such as plant tissues, the FTIR spectrum is the sum of contributions obtained from all the biomolecules. SR-μFTIR provides high-contrast 2-D images without the need for chemical staining and it does not induce any detectable side-effects even in live cells because it employs nonionizing radiation (Holman et al., 2002). Similar to X-ray microscopy methods where contrast is achieved from the absorption edges from elements present in the sample, SR-μFTIR achieves contrast from molecular vibration modes, but is not element-specific. Both techniques take advantage of the same characteristics of SR: brightness and energy tunability (Cotte et al., 2009a). The brightness is essential to obtain high-resolution 2-D images with small dwell time and high signal-to-noise ratio. Hence, SR-μFTIR provides interesting chemical information complimentary to other SR-based techniques such as μXRF, μXAS, and μXRD.

With respect to globar sources, SR provides an overall gain in brightness of at least two orders of magnitude that enhances lateral resolution

while still maintaining a high signal-to-noise ratio. An ideal synchrotron source for μFTIR is an ultrastable low-energy storage ring operating with the highest possible current (Levenson et al., 2008). The lateral resolution achieved with SR is at the diffraction limit and depends on the wavelength and the numerical aperture of the focusing optics. The lateral resolution is approximately 1.7 μm (at 4000 cm^{-1}) and 13 μm (at 500 cm^{-1}) (Cotte et al., 2009b). The IR signal is basically reduced when the aperture size is reduced. The globar source signal becomes hardly usable at apertures sizes below 15 × 15 μm^2. The IR signal from SR is usable at all aperture sizes although the signal-to-noise ratio also begins to decrease when the aperture size is reduced.

A typical μFTIR beamline is composed of a commercial manufacturer IR microscope and a Fourier transform spectrometer coupled to the SR source. The optical layout for IR radiation extraction from a storage ring generally consists of a combination of gold-coated mirrors (toroid/ellipsoid or spherical) that transport the beam of IR light into the spectrometer (Cotte et al., 2009b). The radiation modulated by the spectrometer goes then into the IR microscope that uses reflecting Schwarzschild objectives and a set of apertures to define the spot size that will illuminate the sample. The signal coming from the sample (in transmission or reflection) is detected by a liquid-N_2-cooled single-element detector. Depending on the size of the source, the characteristics of the extracted IR radiation and the peculiarities of each spectrometer and the objectives from the microscope, each beamline will have a unique performance. For a list of infrared beamlines worldwide, see Yousef et al. (2012).

Due to the low penetration depth of the IR radiation and the effects from water absorption, plant samples are usually prepared as thin sections with the use of a vibratome or a cryomicrotome. The required thickness of the sample will vary from one plant species to another and also within plant tissues (leaves, roots, etc.) but is normally in the range of 4–15 μm (Yu, 2004). The most used SR-μFTIR configurations are the transmission and the double transmission or reflectance mode. In the first configuration, two Schwarzschild objectives are used in a confocal mode and apertures before and after the sample are used to define the spot size illuminating the sample. This configuration provides better image contrast, spatial resolution (Cotte et al., 2009b) and allows studying slightly thicker samples (~20 μm). In the reflection-absorbance (or double transmission) mode, samples are deposited on IR-reflecting slides, only one objective is used to focus and collect the radiation on the sample. The IR radiation goes through the sample, gets

reflected on the slide, and goes through the sample once more and finally reaches the detector. In this case, the sample thickness has to be typically 4–10 μm. A great interest of μFTIR is the possibility to work on living cells in water (Holman et al., 2010; Tobin et al., 2010).

As previously mentioned, in a biological sample, the FTIR spectrum is given by the combination of the vibrations from the functional groups present in the sample. This makes data interpretation and analysis not so straightforward and normally chemometric methods such as PCA are used to reveal main spectral differences in the samples or between control and treated samples (Dokken et al., 2005). Some of the most representative absorption bands observed in plant samples are the Amide I band at around 1650 cm^{-1} from the (C═O) stretching vibrations of protein amide bonds; the Amide II band close to 1549 cm^{-1} from the (N–H) bending and (C–N) stretching vibrations of the amide bonds; the (C═O) stretching of lipids at about 1740 cm^{-1}; and the antisymmetric (PO_2^-) stretching of nucleic acids and phospholipids near 1225 cm^{-1}. In the spectral region between 2850 cm^{-1} and 3000 cm^{-1}, bands are observed resulting from symmetric (CH_2) and antisymmetric (CH_3) vibrations, while the (N–H) stretching absorption of proteins occurs at 3300 cm^{-1}. Lignin (C═C phenolic stretch at ≈1515 cm^{-1}) and cellulose (C–H bend of OCH_3 1445–1460 cm^{-1}) also present vibrations in the mid-IR region (Dokken and Davis, 2007). An image of the possible "lignin" distribution, for example, can be extracted by windowing the characteristic spectral band (C═C stretch) after proper background subtraction in a hyperspectral μFTIR map, in which each pixel corresponds to an FTIR spectrum, and then recasting these integrated intensities as a 2-D image. This can be done by OMNIC (Thermo) or PyMCA (Solé et al., 2007) software. SR-μFTIR in the study of metal uptake and metabolism by plants can be used to track changes in the distribution of biomolecules and induce changes in plant architecture (e.g. thickening of cell walls or membrane lipid peroxidation). Cell wall components play a major role in controlling apoplastic transport of trace metals; they are the first barrier against trace metals and offer protection to cell membranes (Krzeslowska, 2011). SR-μFTIR allows the direct analysis of plant cell wall architecture and it has been successfully used to study plant growth and development (Dokken and Davis, 2007; Dokken et al., 2005; Raab and Vogel, 2004). Studies that have relied on the bulk FTIR approach to study plant biopolymers (Bauer et al., 2006; Wei et al., 2009) and for the investigation of organic molecules involved in the transport of metals (McNear et al., 2010) could have benefited from the imaging capabilities

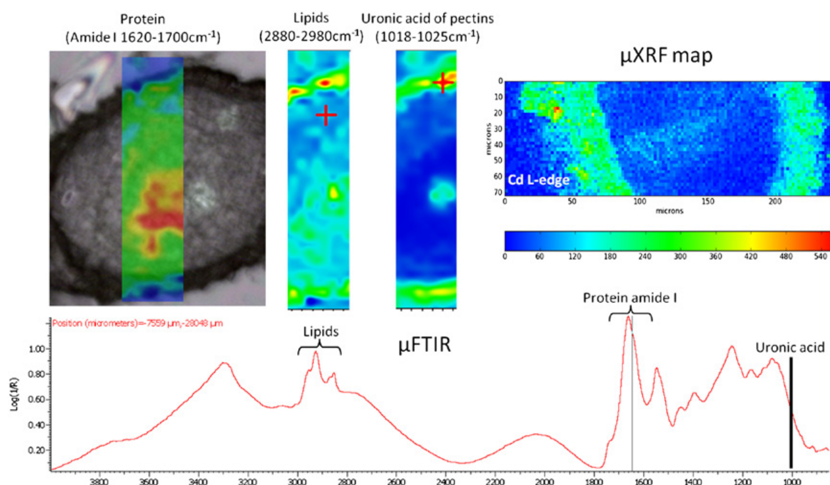


Figure 1.8 SR-μFTIR chemical distribution of lipids, protein and pectin from a root apex of sunflower plants exposed to Cd. The maps were acquired in transmission mode and the sample thickness was 10 μm. The infrared spectrum was obtained from the apical meristem of the sample. The μXRF map from the Cd L-edge shows the localization of Cd in the root surface. See the color plate.

of SR-μFTIR. Other groups that have used globar sources to study plant-architecture changes in the presence of toxic metals (Zhao et al., 2011) could benefit from the enhanced lateral resolution and signal-to-noise ratio of SR-μFTIR. As illustrated in Fig. 1.8, the synergy of SR-μFTIR and μXRF provide complimentary laterally resolved chemical (organic molecules) and elemental (metals) information, which is highly valuable to better understand the mechanisms of plant metal uptake and accumulation.

3. SAMPLE PREPARATION AND POSSIBLE ARTIFACTS

Since synchrotron techniques mainly deal with the location and chemical forms of metals, a crucial point and the main difficulty is to not disturb or disturb as less as possible the original species and their distribution. For that, sample preparation is a key step as previously highlighted by Donner et al. (2012), Lombi et al. (2011b), and Lombi and Susini (2009). It is also important to evaluate possible damage of the sample under the X-ray beam, which can alter the chemical species during analysis. While total deposited power on samples is less than what would be expected from an electron- or proton-beam instrument, it is well known that elements such as As (Foster et al., 1998), Se (Holton, 2007), Mn (Ross et al., 2001), and Cr (Tokunaga et al., 2003) can

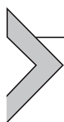
change oxidation state when exposed to high doses of ionizing radiations, effects which are exacerbated at high-brightness beamlines. It is also recognized that such effects are more pronounced in samples that are wet or moist or samples that are mounted with certain types of adhesives.

For XRF or XAS measurements, the first step of the plant preparation generally consists in cryofixation, and two techniques prevail, immersion in a cooled liquid and high-pressure freezing (McDonald, 2007). With the immersion technique, plant samples are rapidly plunged in melting nitrogen or cooled isopentane to minimize the formation of ice crystals, which can damage biological cells and membranes. The technique is easy to perform but large samples can be difficult to vitrify homogeneously. In high-pressure freezing, the cooling with liquid-nitrogen liquid occurs at high pressure, thus minimizing the formation of ice crystals. Thick samples are better vitrified than with the immersion technique.

Once it is frozen, three options are available. The simplest one is the freeze-drying. This technique is not adapted for studies on metal speciation since it was shown to induce artifacts in metal speciation because the most diffusive ions can move with water and aqueous complexes are affected by water extraction (Sarret et al., 2009; Tylko et al., 2007a). Freeze drying may be used for elemental localization at the tissue level. At the cellular level, element redistribution may be observed as well as shrinkage of the cell structures. Another alternative is the freeze substitution, which consists in exchanging the vitrified water by an organic solvent, generally acetone, at low temperature. When the substitution is achieved, the sample is warmed up to room temperature. In this case, sample structures are fixed by the solvent, but redistributions and changes in chemical species cannot be excluded especially for soluble elements and aqueous complexes. Finally, the sample may remain in hydrated frozen state, which causes a minimum perturbation. Bulk samples are then ground and homogenized in liquid nitrogen before being prepared as frozen pressed pellets and transferred into the analysis chambers in frozen state (Sarret et al., 2009). The measurements are then performed using a cryostage, and thus the beamlines need to be equipped consequently. When one wants to investigate specific tissues or cell layers, it is required to work with thin sections because when using a whole organ (leaf for instance), the depth of penetration of X-rays is higher than a cell layer and signal of various tissues are summed up. Cryo thin sections are also prepared from frozen hydrated samples embedded in a frozen cryoprotector using a cryomicrotome and kept at low temperature until the analysis using the cryostage (Roschzttardtz et al., 2011). These cryopreparations appear as

the less disturbing and limit the redistribution on metals and change in speciation. Dried thin or ultrathin sections can be also prepared, after removing water and warming up, but in this case, it is necessary to embed the samples in resin such as epoxy resin. The elemental distribution and speciation can also be altered by this preparation.

Finally, some experiments were performed in vivo (Bulska et al., 2007; Fernando et al., 2006b; Hokura et al., 2006; Lombi et al., 2011a; Pickering et al., 2000a, 2003, 2006; Scheckel et al., 2004; Takahashi et al., 2009). In this case, exposure time under the beam should be reduced as much as possible and radiation damage should be monitored carefully. Multipoint data acquisition can be used for the acquisition of XAS spectra, where one assumes that the speciation over a small area is homogeneous such that successive scans are offset in the X or Y position by a distance slightly larger than the footprint of the beam. These multipoint scans from a given region are then averaged to produce a good-quality spectrum. In some situations, it may be necessary to reduce the integration time per energy point and/or increase the energy step size to capture the speciation before significant beam damage occurs, even at the expense of good-quality spectra (Scheckel et al., 2004). Recent development in detector technologies allowing measurements in the sub-millisecond can significantly decrease the radiation dose (Lombi et al., 2011c).



4. RESULTS OBTAINED

4.1. Nickel

Nickel is an essential plant nutrient. Nickel requirements for crop plants are very low, and deficiencies in soil-grown plants are not observed. In most plants, the Ni content in the vegetative organs is in the range 1–10 μg g^{-1} DW (Marschner, 1995). Anthropogenic activities such as mining, smelting, electroplating, waste disposal, and intensive agriculture have resulted in Ni contamination of surface soils. Application of sewage sludge, which is often high in Ni, can elevate the level of Ni in agricultural soils. Symptoms of Ni toxicity are closely linked to Fe deficiency, and include interveinal chlorosis, bleaching of younger leaves, and stunted growth. Critical toxicity levels in crop species are in the range of >10 μg g^{-1} DW in sensitive species, and >50 μg g^{-1} DW in moderately tolerant species (Marschner, 1995).

Serpentine soils are rich in ultramafic minerals and contain high abundance of Ni, Mn, Fe, Cr, and Co. The flora on these soils includes many species exhibiting Ni hyperaccumulation, where the Ni content in leaves can exceed 30,000 μg g^{-1} DW. For Ni, the threshold for hyperaccumulation is

a concentration >1000 μg g^{-1} DW in aerial parts of plants growing in their natural environment (McGrath et al., 2002). By far, the greatest volume of work and general interest in Ni hyperaccumulators has been focused on the genus *Alyssum* (*Brassicaceae*), which followed from the original discovery of 1% Ni in *Alyssum bertolonii* growing over ultramafic rocks in Tuscany (Minguzzi and Vergnano, 1984). The only other genus with such a large number of Ni hyperaccumulators is *Noccaea* (formerly *Thlaspi*), a plant that seems to occupy the same ecological niches in Southern Europe as does *Alyssum* (Brooks, 1998). Presently, more than 300 Ni hyperaccumulators have been reported, and more than 50 of the genus *Alyssum*. Analysis of the phytochemistry of *Alyssum* Ni hyperaccumulators has implicated an involvement of organic acids in metal chelation and xylem transport. Malic, malonic, and citric acids have consistently appeared as the principle organic acids in Mediterranean *Alyssum* species such as *A. bertolonii* (Gabbrielli et al., 1991; Pelosi et al., 1976), *Alyssum serpyllifolium* subspecies (Alves et al., 2011; Brooks et al., 1981; Lee et al., 1978) and *A. murale* (Tappero, 2008; Wei et al., 2010). Nickel speciation in hyperaccumulator plants of the genus *Alyssum* has been assessed using bulk and microbeam XAS (Broadhurst et al., 2009; Kramer et al., 1996; McNear et al., 2010; Montarges-Pelletier et al., 2008). Kramer et al. (1996) investigated xylem fluid composition in *Alyssum* species exposed to different Ni concentrations and observed a linear correlation between the concentration of metal and free histidine (His) in the xylem of *A. murale*, *A. bertolonii*, and *Alyssum lesbiacum* (i.e. His response). In addition, these authors measured organic acids in root-pressure exudates from *A. lesbiacum*, and reported that citrate (0.3 mM) and malate (0.15 mM) were present at constitutively high concentrations. At xylem pH (pH ≥ 6.5), the stability of the Ni–His complex is higher than for any other amino or organic acid; however, at vacuolar pH (pH ≤ 5.0), amino acids form less-stable complexes with nickel. XAS data collected for xylem sap of *A. lesbiacum* plants grown for 18 d in 0.3 mM Ni (leaf containing >1% Ni) suggests complexation of Ni with free His. Conversely, in *A. murale* plants grown for 5 months in soils containing buried bags of Ni-bearing minerals and with leaf concentrations <0.05% Ni (i.e. below threshold for hyperaccumulation), bulk XAS analysis of frozen, ground leaf tissue indicated that the predominant Ni ligands were citrate (stems) and malate (leaves) (Montarges-Pelletier et al., 2008). In a study on the simultaneous hyperaccumulation of Ni and Co by *A. murale*, (Tappero, 2008) used bulk and microbeam XAS to elucidate the metal speciation, and found that the bulk Ni speciation in ground leaf tissue of 6-week-old plants was a mixture of Ni–His (70%) and Ni-citrate/malate (30%). Fortunately, Ni–His has unique spectral features that allow its identification from Ni-citrate/malate;

however, it is challenging to distinguish different carboxylate ligands (e.g. Ni-citrate and Ni-malate) using XAS, thus no attempt was made to uniquely identify citrate and malate, which were both present at millimolar levels in naturally bleeding xylem sap. Broadhurst et al. (2009) used XRF microprobe to investigate the interaction of Ni and Mn in *Alyssum corsicum* and *A. murale*, and identified Mn(II) as the predominant oxidation state in the trichome base where Mn was colocalized with Ni(II). Following the work of Küpper et al. (2001), they had used electron microprobe to investigate Ni compartmentalization in *Alyssum*, and found the trichome pedicle, trichome basal compartment, and epidermal cells adjacent to the trichome attachment were primary Ni-storage locations in *A. murale*, and also observed simultaneous hyperaccumulation of Ni and Mn in the trichome basal compartment (Broadhurst et al., 2004a, 2004b). Using a variety of techniques, McNear et al. (2010) examined the transport and storage of Ni in *A. murale*. For plants grown on the contaminated Quarry muck soil, the bulk leaf speciation was a mixture of Ni-succinate (67%) and Ni-tartrate (30%), and for plants grown on the contaminated Welland loam soil, the bulk leaf speciation was Ni-tartrate (50%) and Ni-succinate (44%). They also used XAS and FTIR to interrogate the composition of xylem sap extracted by a pressure-bomb apparatus, and found Ni-His (23%), free Ni(aq) (34%), and Ni-tartrate (43%) in the xylem exudates. In addition, they used microbeam XAS to explore the speciation *in planta*, and reported a variety of metal–ligand complexes including Ni-aconitate, Ni-malate, Ni-succinate, Ni-His, and Ni-tartrate along with Ni(aq), and concluded that *A. murale* uses complexation with nitrogen- and oxygen-donor ligands for Ni transport and storage. In a study of Ni speciation in hyperaccumulator *Stackhousia tryonii* using XRF microprobe, Ionescu et al. (2008) found that the majority of leaf, stem, and root Ni was chelated by citrate. A small fraction of Ni was chelated by His and phosphate (leaves), or by His and phytate (stems and roots).

Nickel-localization patterns have been determined for 12 *Alyssum* Ni hyperaccumulator species/ecotypes (Asemaneh et al., 2006; Broadhurst et al., 2004a, 2004b; De La Fuente et al., 2007; Kerkeb and Kramer, 2003; Kramer et al., 1997; Küpper et al., 2001; Marmiroli et al., 2004; McNear et al., 2005; Psaras et al., 2000; Smart et al., 2007, 2010; Tappero et al., 2007) using electron-, proton-, X-ray-, and particle-beam probes (i.e. SEM, PIXE, μXRF, and nano-SIMS, respectively). Nickel is mainly stored in the leaves, and is particularly concentrated in epidermal cells, trichome bases, and the lower parts of the trichome pedicle. Several of these studies have identified leaf epidermal cell vacuoles as the primary storage compartment for nickel in *Alyssum*. Vacuolar sequestration has been recognized as a key component of the (hyper)

tolerance mechanism common to many hyperaccumulator plants (Küpper and Kroneck, 2005).

One exception to the (hyper)tolerance mechanism was reported by Tappero et al. (2007) who investigated Ni and Co hyperaccumulation by *A. murale* using µXRF, XAS, and microtomography. µXRF images revealed a uniform distribution of Ni in leaves, consistent with the notion of epidermal compartmentalization, but showed preferential localization of Co at leaf tips and margins (Fig. 1.9). Using DA-CMT to image the distribution of Ni and Co in fresh, hydrated leaves, they observed a Co-rich material on the leaf exterior near tips/margins, which was identified as hydrous Co-silicate mineral precipitate via microbeam XAS. They concluded that *A. murale* relies on a different metal storage mechanism for Co (exocellular sequestration) than for Ni (vacuolar sequestration).

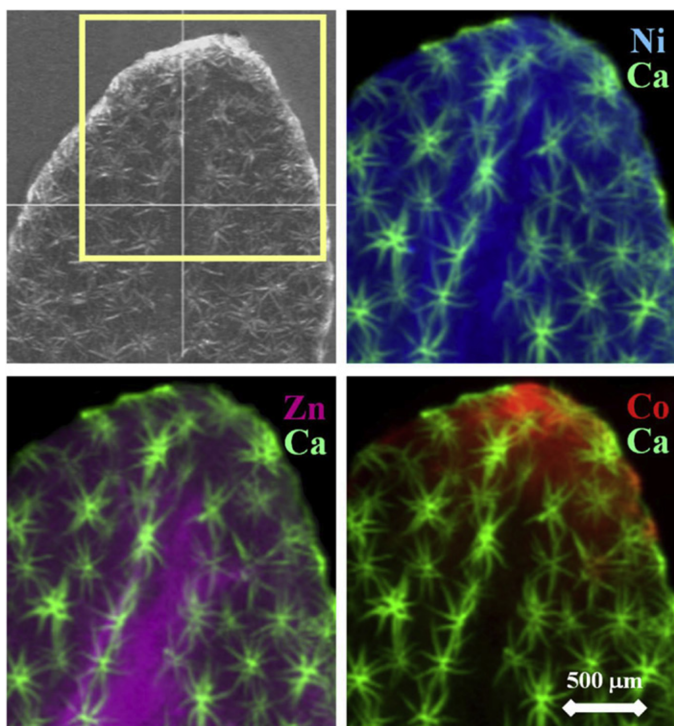


Figure 1.9 µXRF images of the nickel (Ni), cobalt (Co), and zinc (Zn) distributions in a hydrated *Alyssum murale* leaf. Leaf trichomes are depicted in the Ca channel. The optical microscope image shows the leaf region selected for SXRF imaging. *(Reprinted with permission from Tappero et al. (2007)).* See the color plate.

XRF microprobe has been used to investigate Ni localization and speciation in growth rings of black willow (*Salix nigra* L.) trees impacted by influx of contaminated sediment during historical storm breaches at the Savannah River Site (Punshon et al., 2003, 2005). Nickel abundance was elevated within distinct regions of tree cores collected from the Steep pond and Tims branch corridor only, and not from the unaffected location upstream (Boggy gut). The geochemical signature of contaminants recorded in annual rings reflected the sediment remobilization events consistent with the detailed history of the site, and at concentrations relative to their proximity to the source. Based on XANES data for a steep-pond specimen (annual ring from 1996) and for candidate reference compounds selected from an understanding of vascular system chemistry, Ni in the vasculature of black willow was most similar to Ni–pectic acid complex or Ni–His complex.

In an effort to demonstrate fast XRF imaging of metals in hydrated tissue of a nonaccumulator plant, Lombi et al. (2011a) recorded fCMT tomograms for roots of 3-days-old cowpea seedlings treated for 24 h with Ni (5 μM) or Zn (40 μM). Using a sample environment similar to Tappero et al. (2007) for imaging hydrated leaves by DA-CMT, roots were sealed in a polyimide capillary (860 μm i.d.) and maintained at high humidity but not submerged. In order to minimize exposure time and hence beam damage, the number of projections (n = 200) was reduced well below the Nyquist limit (n = 675 for 860 μm translation in 2 μm steps) at the expense of image resolution. Despite these efforts, only 2-D (single-slice) fCMT data of hydrated roots could be collected before the onset of observable beam damage, which likely resulted from the generation of hydrated electrons (e_{aq}^-) and hydroxyl radicals (OH•) due to interaction of the X-ray beam with water (radiolysis) (Klassen, 1987). fCMT images collected at 2.5 mm from the root apex showed that Ni was localized predominantly in the root cortex of cowpea while Zn was localized in the stele and root epidermis.

With an elegant use of quantitative fCMT, McNear et al. (2005) explored the localization and abundance of Ni in roots, stems, and leaves of *A. murale* grown on soils collected from a historic Ni refinery in Port Colborne, Ontario, Canada. Since these plant structures are relatively large diameter for fCMT measurements, and because the Ni Kα fluorescence energy is easily absorbed by the sample itself, absorption corrections were necessary. In agreement with previous work by other groups using electron and proton probes, their results showed localization of Ni in leaf epidermis and colocalization of Ni and Mn at the base of leaf trichomes.

4.2. Zinc

Zinc is an essential element for all living organisms, and is the second most abundant transition metal in organisms after iron. High Zn concentrations are found in soils impacted by mining and smelting activities, and diffuse Zn contaminations in soils result from the application of fertilizers, pesticides and sewage sludge. On the contrary, Zn deficiency in soils is observed in numerous regions. It concerns 50% of cultivated soils in India and Turkey, one-third of cultivated soils in China, and most soils in Western Australia. The critical deficiency levels in leaves of crop plants are below 15–20 μg Zn g^{-1} DW, whereas toxicity levels are from <100 to 300 μg Zn g^{-1} DW (Marschner, 1995), and toxicity thresholds can be highly variable even within the same species. Some plants are hypertolerant to Zn, and some hypertolerant plants are also hyperaccumulators (Zn content in the aerial parts of plants growing in their natural environment >10,000 μg Zn g^{-1} DW).

The metal is mostly stored in the vacuoles of epidermal cells in the leaves of *Noccaea caerulescens*, and in the vacuoles of mesophyll cells in the leaves of *Arabidopsis halleri* (Verbruggen et al., 2009). A first study on Zn speciation in *N. caerulescens* was done by Salt et al. (1999). In the roots, the majority of intracellular Zn was bound to His. In the xylem sap, Zn was present as free Zn^{2+} with a smaller proportion coordinated with organic acids. In the shoots, Zn was mainly bound to organic acids, with a smaller proportion of free Zn^{2+}, Zn–His and Zn–cell wall complexes. Later, the speciation of Zn in the stem and in leaves of *N. caerulescens* at different stages of development was studied by Küpper et al. (2004). Zn was bound to O and His ligands, and the proportion of His was higher in the stems and in dead leaves than in young and mature leaves. In the leaves of *A. halleri*, Zn was bound to a mixture of Zn–organic acid complexes (Zn–OAs) and free Zn^{2+} (both species being in octahedral coordination) and as Zn–cell wall and/or Zn-phosphate as minor species (20–27%, both being in tetrahedral coordination) (Sarret et al., 2009). In the nontolerant and nonaccumulating *Arabidopsis lyrata sp. petrea*, Zn–cell wall and Zn–OAs + free Zn^{2+} represented 49 and 41%, respectively, and the rest was present as Zn-phosphate. In the F2 progeny from the interspecific cross between *A. halleri* and *A. lyrata* segregating for Zn accumulation, a correlation was observed between the proportion of Zn–OAs + free Zn^{2+} and Zn content in the leaves. This is consistent with a vacuolar sequestration in the leaf cells in the stronger accumulators. In the same study, μXRF was used to map the distribution

of Zn in leaf portions. A negative correlation was found between the vein:tissue fluorescence ratio and Zn accumulation, which was interpreted as a higher xylem unloading in the leaves for the stronger accumulators (Sarret et al., 2009).

Two studies were done on nonaccumulating plants. The distribution and speciation of Zn in rocket plants (*Eruca vesicaria* L. Cavalieri) grown in untreated soil and compost-treated soils were studied by fCMT and μXANES spectroscopy (Terzano et al., 2008). Differences in Zn distribution and speciation were observed. Roots of plants grown in the presence of compost showed high Zn concentrations outside the root endodermis, while a higher transfer to the xylem was observed in the control plant. In the leaves, Zn was mostly present in the veins for both treatments. Concerning Zn speciation, linear combination fits of the spectra showed that Zn was present as Zn-phosphate (66%) and Zn-oxalate (34%) in roots of the plants grown in the untreated soil, and as Zn-phytate (76%) and Zn-citrate (24%) in those grown in compost-treated soils. In leaves, Zn-phosphate (57%) and Zn-oxalate (43%) were found in the plants grown without amendment, and Zn-phosphate (54%), Zn-cysteine (25%) and Zn-His (21%) in the plants grown on the compost-treated soil. Kopittke et al. (2011) studied roots of cowpea exposed to 40 μM Zn for 3 and 24 h by 2-D and 3-D μXRF, and by Zn K-edge bulk XANES and EXAFS. Roots showed Zn accumulations mostly in the meristematic region, and 60–85% of the total Zn was stored as Zn phytate. Based on the observations, the authors suggested that much of the Zn was taken up close to the root apex (where the Casparian strip is not fully formed), stored as Zn-phytate, with some Zn moving into the stele and presumably into the shoot.

Thus, organic acids seem to be predominant ligands in Zn-hyperaccumulating species, whereas phosphate ligands, either from inorganic phosphate or from phytate, seem to be predominant ligands in nonaccumulators. Sulfur ligands, which are present in the coordination sphere of Zn in some metalloproteins, are generally not detected as Zn ligands in plant tissues. In contrast, Wellenreuther et al. (2009) found that Zn present in Zn-storage vesicles of murine macrophage cells was bound to S, His and O ligands.

Accumulation of Zn and other metals in the trichomes of plant species has been the subject of several synchrotron studies. The trichomes of *A. halleri* show a strong metal enrichment at their base, as shown by electron microscopy (Küpper et al., 2000; Zhao et al., 2000) and μXRF (Sarret et al., 2002, 2009). Similar enrichments are observed in the hyperaccumulator *A. halleri* sp. *gemmifera* (Fukuda et al., 2008; Hokura et al., 2006) and in the

nontolerant nonaccumulators *Arabidopsis thaliana* (Ager et al., 2003; Isaure et al., 2006b) and *A. lyrata* (Sarret et al., 2009). Thus, metal enrichments in these specialized cells are not related to the tolerance or hyperaccumulation traits. The trichomes of *Arabidopsis* species and of other species were found to be enriched in other metals, such as Cd in *A. thaliana* (Isaure et al., 2006b), and Ni in *Alyssum* (Broadhurst et al., 2004b; Smart et al., 2007). The significance and the mechanism responsible for this enrichment are still debated. The trichomes of *Arabidopsis* and of *Alyssum* are nonglandular, and no excretion of metals was observed. On the contrary, tobacco leaves are covered by glandular trichomes which excrete various types of compounds including various alkaloids such as nicotine, terpenoids (resins) and defensive proteins. When tobacco plants are exposed to elevated Zn or Cd levels (250 and 25 μM, respectively), they excrete Zn, Ca or Cd, Ca-containing grains. This process is enhanced when plants receive a Ca supplement (3.28 mM instead of 0.28 mM). This excretion of metals through the trichomes partly alleviates metal toxicity. However, the major part of accumulated Zn and Cd is present in the leaf tissue. A combination of techniques including SEM-EDX, μXRD and μXAS spectroscopy (Zn K-edge μEXAFS, Cd L_{III}-edge μXANES and Ca K-edge μXANES) was used to image the morphology of the grains, identify the crystallized mineral phases, and speciate the metals, respectively (Isaure et al., 2010; Sarret et al., 2006, 2007). Grains were mostly composed of $CaCO_3$ in the form of microcrystalline calcite (major phase), vaterite, aragonite and amorphous $CaCO_3$. Metals were present as Ca substituents in calcite and vaterite, and as other minor phases. The authors suggest that these grains likely result from the progressive precipitation of Ca, Zn, and the other elements excreted by trichomes in a liquid form, in contact with air.

4.3. Cadmium

Cadmium is a nonessential element, highly toxic for plants, and high concentrations in soils are related to mining/industrial activity or addition of phosphates fertilizers. It has only been identified as a micronutrient in a marine alga, *Thalassiosira weissflogii* (Lane and Morel, 2000). Interestingly, some hyperaccumulators can accumulate up to 100 μg Cd g^{-1}, which is toxic for "normal" plants (Baker, 2000). These hyperaccumulators include the Brassicaceae *N. caerulescens*, *Noccaea praecox*, *A. halleri*, and a Crassulaceae *Sedum alfredii*. The quest to understand this phenomenon has generated much research, and hyperaccumulators have been preferentially investigated in comparison to nonaccumulators.

The localization of Cd in plants has been investigated by µXRF as well as by TEM-EDX, µPIXE and Laser ablation coupled with inductively coupled plasma mass spectrometry (LA-ICP-MS), and the chemical forms of Cd by Cd K-edge EXAFS spectroscopy, Cd L-edge XANES spectroscopy and ^{113}Cd-NMR spectroscopy. XAS techniques enable the identification and quantification of O/N ligands from S ligands (Isaure et al., 2006a; Pickering et al., 1999), but the distinction between various species containing S ligands such as Cd-PC, Cd-GSH and Cd-cysteine is challenging (Huguet et al., 2012).

Concerning its localization, Cd was found to be mainly accumulated in mesophyll cells of the hyperaccumulator *A. halleri* (Küpper et al., 2000). In the Japanese *A. halleri* sp. *gemmifera,* the metal is concentrated in the main vein and in the mesophyll/epidermis (Fukuda et al., 2008; Hokura et al., 2006). In this study, leaves were investigated as whole in vivo samples, and thus, high beam penetration did not allow the distinction between epidermis and mesophyll. Cd was also found in trichomes in hyperaccumulators (Fukuda et al., 2008; Hokura et al., 2006; Huguet et al., 2012) but also in nontolerant plants such as *A. thaliana* (Isaure et al., 2006a) indicating that this mechanism is not related to hyperaccumulation. Elimination of Cd via calcium carbonates exuded from tobacco trichomes was also evidenced using a combination of µXRD, µXRF and µXANES (Isaure et al., 2010). Recently, Tian et al. (2011) compared a Cd hyperaccumulating and a nonaccumulator ecotype of *S. alfredii* by µXRF and LA-ICP-MS. In the stem of the nonaccumulator ecotype, Cd is located in the vascular bundles while it is distributed in the parenchyma tissues of the cortex and pith in the hyperaccumulator. In the leaves, the metal is located in both the vascular bundles and the mesophyll.

At the leaf cell level, highest Cd accumulation was found in the vacuole as shown for Ni (Broadhurst et al., 2009) and Zn (Küpper et al., 2000; Sarret et al., 2009). Fluorescence microscopy showed that Cd was accumulated in vesicles in the cytoplasm before entering the vacuole (Leitenmaier and Küpper, 2011). The authors also evidenced an enhanced transport of Cd in protoplast extracted from the epidermis compared to the mesophyll. Although a high concentration of Cd was found in the epidermis leaves of *N. praecox* by µPIXE (Pongrac et al., 2010), the mesophyll remains the main compartment of storage due to its larger volume as previously shown by Ma et al. (2005) for *N. caerulescens*.

Cd localization was also investigated in some nonaccumulators. Two species of Japanese willows were studied using µXRF with a 1 µm beam lateral resolution and serrations of leaves were found to accumulate high level of metal (Harada et al., 2010). The authors suggest that it could be a mechanism of Cd extrudation. In stems, the metal is preferentially accumulated in

bark. In all these compartments enriched with Cd, Cd K-edge μXANES indicated that the metal is coordinated by oxygen/nitrogen atoms.

Concerning Cd speciation in plant tissues, the formation of strong complexes with thiol-containing ligands such as metallothioneins and phytochelatins (PCs) was suggested as a mechanism of detoxification (Clemens, 2006). Studies on Cd hyperaccumulators have shown that Cd detoxification is realized by sequestration in the vacuole and complexation to oxygen ligands.

Küpper et al. (2004) showed by Cd K-edge EXAFS spectroscopy that in *N. caerulescens*, O/N ligands were predominant, and a minor proportion sulfhydryl ligands was found. This proportion was higher in young and mature leaves in comparison with senescent ones. Authors suggested that young tissues required strong ligands for metal detoxification or that the storage in the vacuoles of the epidermis was less important in the young leaves. In *N. praecox* and *A. halleri* leaves, EXAFS showed that Cd was also mainly coordinated by oxygen atoms (Huguet et al., 2012; Vogel-Mikus et al., 2010). Using the same technique, Tian et al. (2011) found that in the leaves and stems of the hyperaccumulator *S. alfredii*, Cd was sixfold coordinated by oxygen ligands, possibly provided by malic acid, which was the major organic acid in the shoots of the plants. In the roots, sulfhydryl groups accounted for 24% of the Cd ligands. Using ^{113}Cd-NMR spectroscopy, Ueno et al. (2005) identified malate as major ligand for Cd in the leaves of *N. caerulescens*.

In the nonhyperaccumulator *Brassica juncea*, Salt et al. (1995) showed that Cd was coordinated by N/O atoms in the xylem sap, while in roots, it was mainly bound by S ligands. They also showed that the metal was mainly associated to S ligands (60%) in the whole plants after 20 h of 1 μM Cd exposure, while this proportion was <40% in the first hours of exposure (Salt et al., 1997).

4.4. Selenium

Selenium is chemically similar to sulfur (S), and therefore, thought to be taken up and metabolized by the same transporters and enzymes. Selenium is taken up mainly as selenate (SeO_4^{2-}) by means of sulfate transporters, and subsequently reduced and incorporated into selenoaminoacids by the sulfur assimilation pathway (for reviews, see Pilon-Smits and Quinn, 2010; Sors et al., 2005). Selenate is first reduced to selenite (SeO_3^{2-}), then to selenide (Se^{2-}), which is assimilated into selenocysteine (SeCys) and selenomethionine (SeMet). While all plants take up Se to some extent, most

do not reach levels higher than 100 mg Se kg^{-1} DW when growing in the field. A select group of ~30 plant species typically accumulate Se to levels above 1000 mg Se kg^{-1} DW in the field, up to 15,000 mg Se kg^{-1} DW (1.5%). These are termed Se hyperaccumulators (Beath et al., 1993a, 1993b). Well-studied examples are *Astragalus bisulcatus* and *Stanleya pinnata* (Galeas et al., 2007). Better knowledge of the mechanisms and the limiting factors of plant Se uptake and metabolism will have not only intrinsic scientific significance but also broader medical and environmental impacts. Both Se toxicity and Se deficiency are serious problems worldwide; both cost hundreds of millions of dollars annually in the United States alone.

Se is not considered essential for higher plants, in contrast to some green algae (Zhang and Gladyshev, 2010). Nevertheless, Se can have beneficial effects on plant growth and antioxidant activity (for a review, see Pilon-Smits et al., 2009). This positive effect of Se on plant growth is particularly pronounced for Se-hyperaccumulator species (El Mehdawi and Pilon-Smits, 2012).

Microfocused X-ray fluorescence (μXRF) mapping and selenium (Se) K-edge μXANES have proven very useful to investigate the spatial distribution and chemical speciation of Se in plants and their ecological partners. There are many organic and inorganic selenocompounds in organisms and in the environment. The Se in these compounds can exist in different oxidation states (+6, +4, 0, −2), and can be bound to different neighboring atoms. Because of this variation, different selenocompounds yield different XANES spectra (Fig. 1.10A). Bulk XANES on frozen, ground material or μXANES on intact frozen material can be used to obtain Se K-edge spectra from samples. Comparison of these sampled spectra with those of standard selenocompounds using least-square linear combination fitting can give information about the chemical composition of the Se in any location in a sample. Some organic C–Se–C forms cannot be distinguished by XANES (Fig. 1.10A) and require further biochemical analysis, e.g. via liquid chromatography mass spectrometry (LC-MS). Using μXRF, information can be obtained about the spatial distribution of Se in an intact frozen sample, by mapping a selected area of the sample with an incident beam at an energy above the Se K-edge (>12.658 keV). Other elements can be mapped simultaneously as long as they can be detected with the same incident beam. The use of a Peltier stage at −33 °C to study frozen hydrated samples appeared sufficient to reduce radiation damage (Freeman et al., 2006b).

XANES and μXRF have shown that Se hyperaccumulators differ markedly from Se accumulators and nonaccumulators in terms of Se localization

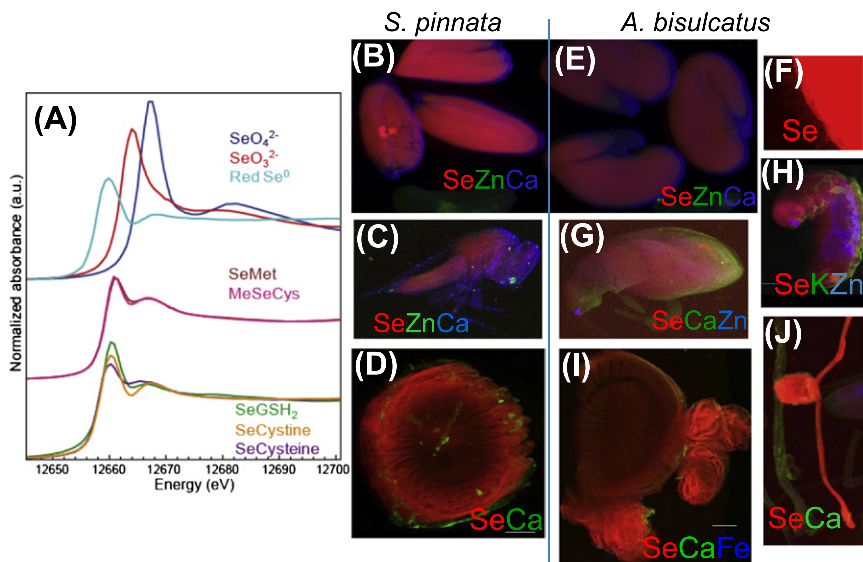


Figure 1.10 (A) Se K-edge XANES spectra from different selenocompounds. SeMet: Selenomethionine; MeSeCys: methyl-selenocysteine; $SeGSH_2$: Selenodiglutathione. (B–J) m X-ray fluorescence maps of Se (in red) and other elements in two hyperaccumulator plant species and their Se-resistant ecological partners. B: *S. pinnata* seed, including one with frass left behind by seed wasp larva; C: adult seed wasp from *S. pinnata*; D: root cross-section of *S. pinnata* colonized by fungus; E: *A. bisulcatus* seeds; F: seed coat fungus growing on *A. bisulcatus* seed; G: seed weevil from *A. bisulcatus* seed; H: *Apamea sordens* moth larva found feeding on *A. bisulcatus* leaves; I,J: root of *A. bisulcatus* with root nodules containing *Rhizobia* bacteria. See the color plate.

and speciation. The nonhyperaccumulator species *B. juncea* and *A. thaliana* were found to accumulate Se primarily in the form of selenate, both in their leaves and roots (De Souza et al., 1998; Pilon-Smits et al., 1999; Van Hoewyk et al., 2005). Selenium hyperaccumulators *A. bisulcatus*, *Astragalus racemosus* and *S. pinnata*, on the other hand, accumulated predominantly organic selenocompounds with a C–Se–C configuration, both in their leaves and roots (Freeman et al., 2006b, 2010; Lindblom et al., in press). Further chemical analysis using LC-MS showed the C–Se–C fraction to be composed of 50% methyl-SeCys and 50% γ-glutamyl-methyl-SeCys in *A. bisulcatus* while in *S. pinnata*, it consisted of 88% methyl-SeCys and 12% seleno-cystathionine (Freeman et al., 2006b, 2010). Thus, the reduction of selenate to selenite appears to be a limiting step for Se assimilation in nonhyperaccumulator species. Indeed, overexpression of the enzyme ATP-sulfurylase, which is involved in the conversion of selenate to selenite, was shown by XANES to

result in a metabolic shift in *B. juncea* toward the accumulation of predominantly C–Se–C compounds (Pilon-Smits et al., 1999). The finding that Se hyperaccumulators contain predominantly methyl-SeCys may explain their extreme Se tolerance. By methylating SeCys to methyl-SeCys, they avoid the misincorporation of SeCys into protein; the proposed enzyme responsible for this methylation is SeCys methyltransferase (SMT) (Neuhierl and Böck, 1996). Overexpression of SMT in *B. juncea* was indeed shown to enhance Se tolerance and to 10-fold enhance methyl-SeCys levels (LeDuc et al., 2004).

The patterns of Se localization in the leaf differ between Se hyperaccumulators and other species. Hyperaccumulator *A. bisulcatus* was shown to accumulate ~90% of its Se in the leaf hairs, and *S. pinnata* accumulated Se primarily in its epidermis, particularly in specialized cells along the leaf edges (Freeman et al., 2006b). In contrast, in *B. juncea* and *A. thaliana* leaves, most Se was present in the vasculature (Freeman et al., 2006b; Van Hoewyk et al., 2005). Thus, sequestration of Se in specialized cells along the leaf periphery appears to be a specific trait for Se hyperaccumulators, and may further contribute to their Se tolerance.

Plant Se accumulation varies between different organs and throughout the growing season, and both are different between hyperaccumulators and nonhyperaccumulators. The flowers of hyperaccumulators are particularly Se-rich, with the highest levels found in pollen and ovules; the form of Se in the flowers was C–Se–C, the same as in the leaf and root (Quinn et al., 2011). In *B. juncea*, the flowers were not higher in Se than the leaves, and interestingly, the flowers were the only organ that contained substantial levels of C–Se–C (58%) in this nonhyperaccumulator species (Quinn et al., 2011). A 2-year field study revealed seasonal fluctuations in Se accumulation, with the highest leaf Se levels occurring in the early spring in Se hyperaccumulators, but in mid-summer, in nonhyperaccumulators (Galeas et al., 2007). In the course of the growing season, Se appeared to be redistributed from the leaves of hyperaccumulators to the reproductive organs and the roots (Galeas et al., 2007). The form of Se that is remobilized may be organic, as *A. bisulcatus* was shown by XANES to accumulate mostly organic Se in young leaves and roots, while older leaves hyperaccumulated mainly inorganic selenate and at much lower concentrations (Pickering et al., 2000a).

The functional significance of Se hyperaccumulation and the ecological implications of the extreme plant Se levels have received much interest in the past years. Selenium hyperaccumulation may have evolved as a defense

mechanism against herbivory since Se can protect plants from a wide variety of Se-sensitive invertebrate and vertebrate herbivores, both due to deterrence and toxicity (for reviews, see Boyd, 2007, 2010; El Mehdawi and Pilon-Smits, 2012). While deterring Se-sensitive herbivores, hyperaccumulators may host Se-tolerant herbivores. Larvae from a Se-tolerant *Plutellidae* closely resembling the diamondback moth (*Plutella xylostella*), an important agricultural pest, were collected from *S. pinnata* growing in a seleniferous area (Fort Collins, CO, USA). The larvae were shown to be completely tolerant to 2000 mg Se kg^{-1} DW in *S. pinnata* leaves, and were not deterred by high-Se plants (Freeman et al., 2006a). In contrast, a diamondback moth population from a nonseleniferous area in the Eastern USA. was deterred by high-Se *S. pinnata* plants and quickly died after feeding on high-Se leaves (Freeman et al., 2006a). The mechanism for the difference in Se tolerance between the two moth populations was revealed by Se μXANES and LCMS. The Se-tolerant moth accumulated nontoxic methyl-SeCys, while the Se-sensitive population accumulated SeCys, which is toxic when it gets nonspecifically incorporated into proteins (Freeman et al., 2006a). Interestingly, the Se-tolerant moth larvae were parasitized by a Se-tolerant wasp, *Diadegma insulare*, which was shown by μXANES and LC-MS to also accumulate C–Se–C, mainly as MeSeCys (Freeman et al., 2006a). Similarly, leaves of *A. bisulcatus* are used as a food source by the moth *Apamea sordens*, which is in turn parasitized by a wasp (Fig. 1.10H, unpublished results). In addition, seeds of *A. bisulcatus* and *S. pinnata* were found to be consumed by various Se-resistant herbivores (Fig. 1.10B,C,E,G, unpublished results). Thus, hyperaccumulators may be a portal for Se into the local food chain via a range of Se-tolerant herbivores.

A variety of Se-tolerant microbes were found to live in association with hyperaccumulators, in the rhizosphere, in tissues as endophytes, or as litter decomposers (Wangeline and Reeves, 2007; Wangeline et al., 2011; Fig. 1.10F). XANES showed several of these rhizosphere and endophytic fungi to produce predominantly elemental Se, which was an interesting finding in view of the fact that roots of *A. bisulcatus* and *S. pinnata* collected in the field also contained up to 35% elemental Se, while greenhouse-grown plants of the same species accumulated exclusively C–Se–C (Lindblom et al., in press; Fig. 1.10D). Also, root nodules of the legume hyperaccumulator *A. racemosus* were found to contain substantial fractions of elemental Se, while the root proper contained only C–Se–C (Lindblom et al., in press; Fig. 1.10I,J). Thus, microbial partners may affect plant Se speciation, and with that, perhaps, Se accumulation and tolerance.

There is no indication that high-Se plants deter insect pollinators: honey bees foraged to equal extent on high- and low-Se *B. juncea* or *S. pinnata* plants (Quinn et al., 2011). Honey bees and bumble bees collected from Se hyperaccumulators in the field contained Se levels around 15 and 275 mg kg^{-1} DW, respectively. μXRF showed that the Se was present throughout the bee tissues, as well as in the pollen baskets on their legs. The bumble bees mainly accumulated C–Se–C (96%) while the honey bees contained 58% C–Se–C. It will be interesting in future studies to determine the effect of the accumulated Se on bee health, which may be positive or negative.

The overall picture that emerges from these studies is that Se hyperaccumulators have a profound effect on the local ecology of seleniferous areas. Hyperaccumulators tend to negatively affect Se-sensitive ecological partners while favoring Se-resistant partners. Via these combined effects, hyperaccumulators may influence species composition at different trophic levels, as well as Se cycling in seleniferous ecosystems. These findings provide insight into the ecology of seleniferous areas and the functional significance of plant-Se hyperaccumulation, and have broader impacts for the further development and implementation of Se phytoremediation and Se biofortification.

4.5. Arsenic

Arsenic (As), a class-one carcinogen, is ubiquitous in the environment. Recent studies have shown that foods, especially rice, are a major source of inorganic As to human's As intake (Meharg and Zhao, 2012). It is therefore important to understand the pathways and mechanisms of As uptake, metabolism and translocation in plants in order to develop strategies to minimize the transfer of As from the soil to food crops. Over the years 2001–2010, there has been a great deal of interest in the phenomenon of As hyperaccumulation, which occurs in a small number of fern species (Ma et al., 2001; Zhao et al., 2002). The As hyperaccumulators are able to accumulate and tolerate over 1000 mg As kg^{-1} in the aboveground tissues, a feature that has attracted much attention for the purpose of phytoremediation. Synchrotron-based XAS has played an important role in revealing As localization and speciation in both As hyperaccumulators and nonaccumulators; this is reviewed briefly here.

Because As is redox-sensitive and can also undergo biomethylation, a number of As forms may be present in the environment (Zhao et al., 2010). The biogeochemical cycle of As is influenced profoundly by the environmental conditions, particularly the redox potential. This is exemplified by

the dynamics of As speciation in the rhizosphere of aquatic/semiaquatic plants. Such plants typically form iron plaque on the root surfaces as a result of the oxidation of ferrous iron (Fe^{2+}) by O_2 released by the aerenchyma of the roots. XAS analysis reveals that the iron plaque on the root surfaces of *Phalaris arundinacea* and rice (*Oryza sativa*) consists mainly of ferrihydrite with goethite and siderite as minor components (Frommer et al., 2011; Hansel et al., 2001; Liu et al., 2006). Iron plaque is a strong sink for As, especially arsenate; this is confirmed by μ-XRF imaging showing a strong colocalization of Fe and As (Blute et al., 2004; Seyfferth et al., 2010), and by XANES analysis and fCMT showing the dominance of arsenate adsorbed on the iron plaque (Blute et al., 2004; Frommer et al., 2011; Liu et al., 2006; Seyfferth et al., 2010) (Fig. 1.11). Iron plaque may present a barrier to the entry of As into the root cells. On the other hand, iron plaque is likely to enrich As locally, particularly around the mature root zone (Seyfferth et al., 2010). In contrast, young and fine roots, which are important for solute uptake, have little iron plaque. Seyfferth et al. (2010) argued that iron plaque may not directly intercept and, hence, restrict As supply to and uptake by rice roots but rather serves as a bulk scavenger of As predominantly near the root base.

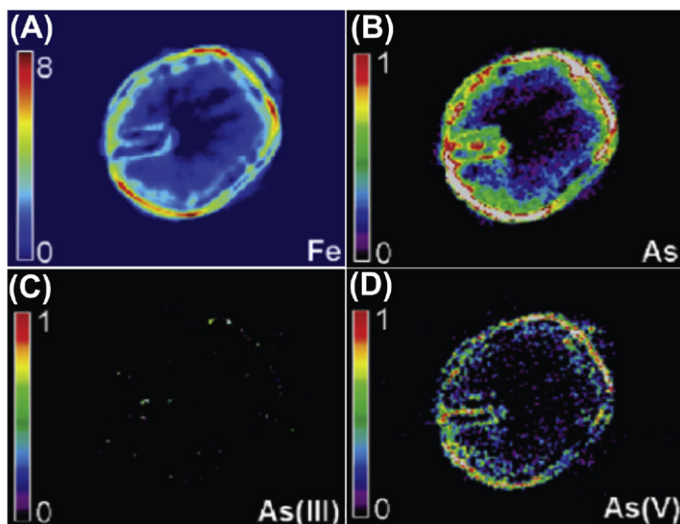


Figure 1.11 Cross-sectional fCMT of a rice root coated with iron plaque showing spatial distribution of total Fe (a), total As (b), arsenite (c) and arsenate (d). *(Adapted with permission from Seyfferth et al. (2010); Copyright (2010) American Chemical Society)*. For color version of this figure, the reader is referred to the online version of this book.

Different As species enter root cells via different membrane transporters. Arsenate, being a chemical analog of phosphate, is taken up via the phosphate transporters (Zhao et al., 2009). Arsenite has a high pK_a and, therefore, is present mostly as undissociated neutral molecules under the normal pH ranges observed in the environment and inside the plant cells. Arsenite permeates through a group of aquaporin channels called Nodulin 26-like Intrinsic Proteins (NIPs) (Ma et al., 2008; Zhao et al., 2010). Undissociated methylated As species (monomethylarsonic acid (MMA) and dimethylarsinic acid (DMA)) can also permeate through the rice NIP2;1 channel (Li et al., 2009).

Once inside the plant cells, arsenate is readily reduced to arsenite. Both the in situ XANES analysis (Aldrich et al., 2007; Dhankher et al., 2002; Pickering et al., 2000b; Smith et al., 2008) and the ex situ analysis using HPLC-ICP-MS (e.g. Xu et al., 2007) have shown that As is present predominantly as As(III). In the As hyperaccumulator *Pteris vittata*, XANES analysis reveals the dominance of As(III) in the fronds and in the gametophyte, whereas the roots appear to contain proportionally more As(V) than As(III) (Ellis et al., 2006; Huang et al., 2008; Lombi et al., 2002; Pickering et al., 2006; Webb et al., 2003). The smaller proportion of As(III) in the roots of *P. vittata* than nonhyperaccumulators may be a result of a much faster uptake of As(V) exceeding the arsenate reduction capacity and/or a highly efficient root-to-shoot translocation of As(III) in the former (Su et al., 2008). In contrast to the findings of Su et al. (2008) who analyzed the As speciation in the xylem sap using HPLC-ICP-MS, Pickering et al. (2006) showed that arsenate is the main form of As in the vein based on the μXANES and μXRF data, suggesting that As transport in the vascular tissue from the roots to the fronds involves mainly arsenate. Recently, Lei et al. (2012) used μXANES and observed a transition of As speciation from As(V) in the epidermis and cortex to As(III) in the vascular bundle in the rhizoid of *P. vittata* exposed to As(V), supporting the notion that arsenite is the main form loaded into the xylem.

A crucial difference between the As hyperaccumulators and nonhyperaccumulators lies in the vastly different degrees of As(III)–thiol complexation. Arsenite has a high affinity for thiol groups with a coordination stoichiometry of one As(III) to three –SH groups. There is strong evidence from XANES analysis that the majority of As(III) in nonhyperaccumulators is complexed with thiol groups, presumably PCs and/or glutathione (GSH) (Aldrich et al., 2007; De la Rosa et al., 2006; Pickering et al., 2000b; Smith et al., 2008). Using HPLC-ICP-MS and ESI-MS, a number

of As(III)–PC and As(III)–GS complexes have been identified (Liu et al., 2010; Raab et al., 2005). Bluemlein et al. (2008) conducted a comparison on As speciation analysis in *Thunbergia alata* between the in situ XANES and the ex situ HPLC-ICP-MS/ESI-MS measurements. According to the XANES measurements, 53% of the As in the roots freshly exposed to arsenate was As(III) bound to S, with 38% and 9% as free arsenite and arsenate, respectively. Similarly, the ex situ measurements revealed that 55–64% of the As was complexed with thiol peptides, mainly as As(III)–$(PC_2)(_2)$, As(III)–(PC_3) and As(III)–(PC_4). Thus, the two methods corroborate each other. In As hyperaccumulators, however, very little of As(III) is complexed with thiol compounds. Based on the analysis of As and PC concentrations, Zhao et al. (2003) estimated that only a small proportion (1–3%) of the As in *P. vittata* may be complexed with PCs, suggesting that the majority of As(III) was present in the uncomplexed form. This was later confirmed by XANES and EXAFS analysis (Ellis et al., 2006; Huang et al., 2004; Pickering et al., 2006; Webb et al., 2003). Pickering et al. (2006) further observed the presence of As(III)-thiolate species only in the region surrounding the vein in *P. vittata*. Complexation of As(III) with PCs results in a decreased mobility of As(III) in the translocation from roots to shoots in *A. thaliana* (Liu et al., 2010). Conversely, limited As(III)–PC complexation in hyperaccumulators probably explains the high translocation efficiency of arsenite from roots to fronds (Su et al., 2008). It is clear that *P. vittata* does not rely on PCs for As detoxification, at least not to the same extent as in nonhyperaccumulators.

Cellular and subcellular compartmentation is an important mechanism for As detoxification. In *P. vittata*, free arsenite is stored in the vacuoles (Lombi et al., 2002; Pickering et al., 2006); transport of arsenite into the vacuoles is probably mediated by the tonoplast transporter PvACR3 (Indriolo et al., 2010). In contrast, As(III)–PCs are the main storage forms of As in nonhyperaccumulators. Transport of As(III)–PCs into the vacuole is carried out by the ATP-binding cassette transporters ABCC1 and ABCC2 in *A. thaliana* (Song et al., 2010). Subcellular localization using nano-SIMS reveals a strong colocalization of As and S in the vacuoles of the pericycle and the endodermal cells of rice roots, consistent with As(III)–PCs being stored in the vacuoles (Moore et al., 2011). This study clearly shows that As is not distributed uniformly in all cells but is sequestered mainly in some specific types of cells.

Apart from As hyperaccumulators, most plant species have limited root-to-shoot translocation of inorganic As (Zhao et al., 2009). However, methylation of As significantly increases its mobility during both xylem and

phloem transport (Raab et al., 2007; Ye et al., 2010). MMA and DMA are efficiently translocated from roots and other vegetative tissues to rice grain (Carey et al., 2010, 2011). The reason for this difference remains unclear. Inorganic As is delivered to the rice grain mainly through the phloem (Carey et al., 2010; Zhao et al., 2012), whereas both the phloem and xylem pathways contribute to DMA loading/unloading into the grain (Carey et al., 2010). The different mobility of inorganic As versus methylated As species is also apparent from their distribution patterns in rice grain. When arsenite or DMA was fed to a cut panicle of rice and As distribution in the rice grain subsequently observed with μXRF, arsenite was found to be retained in the ovular vascular trace (OVT) (Fig. 1.12), whereas DMA dispersed throughout the external grain parts and into the endosperm (Carey et al., 2010, 2011). For inorganic As, there appears to be a transport barrier between the maternal tissue OVT and the filial tissues (e.g. aleurone and endosperm); this barrier may be due to the discontinuity in the symplast, so that As species (and other solutes) have to exit the OVT into the apoplast before being loaded into the symplast of the nucellar tissue for distribution to the aleurone and endosperm (Lombi et al., 2009). In contrast, DMA can permeate through this barrier efficiently via as-yet unknown mechanisms.

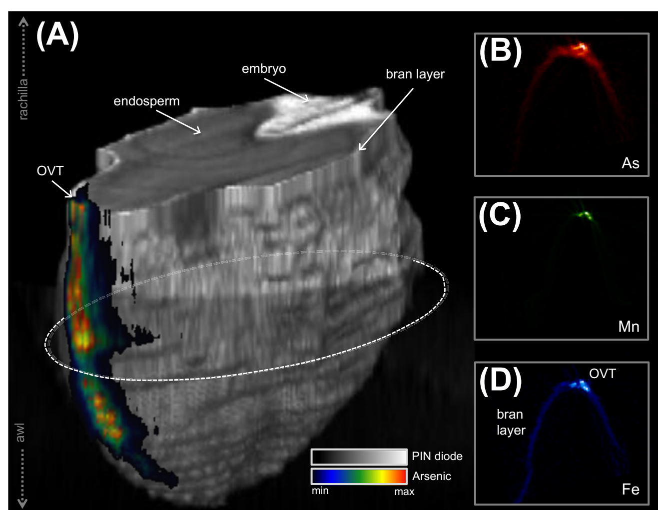


Figure 1.12 Three-dimensional rendering of total X-ray absorption (gray-scale color bar) and arsenic (As) (rainbow color bar) fluorescence of an immature rice grain pulsed with 133 μM arsenite (a). (b–d) Individual tomograms of As, manganese (Mn) and iron (Fe) in the ovular vascular trace. *(Redrawn with permission from Carey et al. (2011)).* See the color plate.

Consequently, the rice endosperm (i.e. polished white rice) generally contains a lower total concentration of As but a higher percentage of methylated As species (mainly DMA) than the bran fraction, which includes the OVT (Lombi et al., 2009; Meharg et al., 2008; Sun et al., 2008). XANES analysis shows that the majority of As(III) in rice grain is bound to thiol groups (Lombi et al., 2009).

4.6. Copper

Copper is an essential element for all living organisms and is involved in a number of essential processes of plant cell metabolism such as photosynthesis and defense against pathogens. Unlike Cd and Zn, there are only a few studies on Cu speciation in plants. These studies are critically reviewed by Mijovilovich et al. (2009). Previous works were conducted on the Cu-resistant Cu indicator plant *Larrea tridentata* (creosote bush) (Polette et al., 2000). The authors found that Cu was absorbed and transported in *L. tridentata* (creosote bush) as Cu(II), but was present as Cu(I) and Cu(II) in the leaves. The authors suggested that Cu was complexed to PCs in roots and stem, and present as crystalline material possibly transferred through stomata in the shoots. In the leaves of the Cu hyperaccumulator and amphibious water plant *Crassula helmsii*, Kupper et al. (2009) found that Cu was bound almost exclusively by oxygen ligands, likely organic acids, and not any sulfur ligands. On the contrary, in the leaves of the Cd/Zn hyperaccumulator *N. caerulescens* which is sensitive to Cu toxicity, Mijovilovich et al. (2009) found that a large proportion of Cu was bound by sulfur ligands. The authors interpreted these differences by different strategies for Cu detoxification in the leaves of hyperaccumulators and nonaccumulators. Moreover, in some specimens of *N. caerulescens* which were more resistant to Cu, Cu-containing crystalline phases, possibly Cu(II) oxalate and Cu(II) oxides, were found in the leaves.

Several studies were conducted on roots of nonaccumulators. The distribution of Cu in roots of the Cu-tolerant plant *Commelina communis* was studied by μXRF (Shi et al., 2011). Higher Cu concentrations were found in the vascular cylinder compared to the endodermis, related to the root-to-shoot transport of Cu. Moreover, the comparison of Fe and Cu distribution suggested a competition between the two elements for Cu transmembrane transport and cell wall binding.

Kopittke et al. (2011) studied the localization and speciation of Cu in the roots of the nonaccumulator cowpea (*Vigna unguiculata*) after short exposure to 1.5 μM Cu. After 24 h of exposure, most Cu was bound to

polygalacturonic acid of the rhizodermis and outer cortex, and authors suggested that binding of Cu to the cell walls in the rhizodermis possibly contributed to the toxic effects of Cu. Manceau et al. (2008) found by μXRF, μXRD and Cu K-edge EXAFS and μEXAFS that the wetland plants *Phragmites australis* and *Iris pseudoacorus* could transform copper into metallic nanoparticles (NPs) in and near roots.

4.7. Manganese

Manganese is an essential element for all living organisms. It exists as various oxidation states from 0 to VII. In biological systems, Mn is present as Mn(II), Mn(III) and Mn(IV). Mn(II) is the dominant form in plants but it can be easily oxidized into Mn(III) and Mn(IV). Mn concentrations in plants range between 20 and 500 mg kg^{-1} DW, and higher than 1000 mg kg^{-1} DW for some species (Baker and Brooks, 1989; Kabata-Pendias and Pendias, 2001). Mn-deficiency threshold for plants is around 15 and 25 mg kg^{-1} DW, and toxicity threshold is around 500 mg kg^{-1} DW but varies strongly between species and as a function of culture conditions. Mn toxicity may be expressed by chlorosis, necroses on leaves, accumulation of Mn oxide particles in epidermal cells, and strong decrease of root growth (Kabata-Pendias and Pendias, 2001).

The distribution of Mn has been studied in several Mn-hyperaccumulating species. For a number of species including Chengiopanax *sciadophylloides* (Memon et al., 1980), *Phytolacca acinosa* Roxb (Xu et al., 2006), *Maytenus fournieri* (Panch. and Sebert) Loesn. (Celastraceae) and *Grevillea exul Lindley* (Proteaceae) (Fernando et al., 2008), highest Mn concentrations were found in the epidermis of the leaves. However, different distribution patterns were observed for other species. In *Gonocalyx amplexicaulis*, Mn was relatively evenly distributed throughout the leaf photosynthetic (mesophyll) and nonphotosynthetic (epidermis) tissues. In the Mn-hyperaccumulating trees *Gossia bidwillii*, *Virotia neurophylla*, *Macadamia integrifolia* and *Macadamia tetraphylla*, Mn was found in the photosynthetic tissues (Fernando et al., 2006a). Moreover, in *G. bidwillii*, the highest vacuolar Mn concentration was found in the upper-layer palisade mesophyll, and the lowest concentration in the spongy mesophyll, and Mn was mostly sequestered in the vacuoles (Fernando et al., 2006b). High Mn concentrations were also found at the base of the trichomes of the Zn hyperaccumulator *A. halleri* and nonaccumulator *A. lyrata*, which concentrate Zn as well (Sarret et al., 2009). Similarly, Mn was colocalized with Ni in trichome bases and in cells adjacent

to trichomes and of the Ni hyperaccumulator *A. corsicum* and *A. murale* (Broadhurst et al., 2004b, 2009).

Concerning the speciation of Mn in leaf tissues, several studies using chemical extractions and analytical techniques suggested a complexation of Mn by organic acids including oxalic, succinic, malic, and malonic acids (Bidwell et al., 2002; Do et al., 2009). X-ray absorption studies confirmed these findings in the Mn-hyperaccumulator *P. acinosa* Roxb. Mn in leaves was bivalent and almost 90% of the total Mn was Mn-oxalate (Xu et al., 2009). The oxalate concentration in the leaves of *P. acinosa* was not affected by increasing Mn concentration in the solution. In Mn-hyperaccumulating woody species from Australia, New Caledonia and Japan, Fernando et al. (2010) found that Mn was present as Mn(II) and complexed to organic acids such as malate or citrate.

Synchrotron techniques were also used to study Mn localization and speciation in plant roots. Lanson et al. (2008) identified Zn-rich phyllomanganate found on the roots of the graminaceous plant *Festuca rubra* grown on a Zn-contaminated sediment. μXRD and μEXAFS analysis showed that crystallites consisted in single Mn(IV) octahedral layers, with Zn sorbed above and below vacant sites, probably formed by Mn–Zn coprecipitation. Naftel et al. (2007) showed by XANES spectroscopy that Cu and Mn were present in the reduced states Mn(II) and Cu(I) near and in the roots of *Populus tremuloides* collected from forested soils in northern Quebec.

4.8. Other Elements

Chromium (Cr) is a common contaminant in air, soil, and water in industrialized regions. Cr industrial uses include leather tanning, chrome plating, paints, and catalysts. Industry is one of the main anthropogenic sources of Cr contamination and its presence in the environment represents a risk to humans and other species. Thus, Cr accumulation in plants may represent potential health hazards to animals and humans. Cr is found mostly in the environment as Cr metal, trivalent Cr (Cr[III]), and hexavalent Cr (Cr[VI]). The most toxic is the highly oxidizing agent Cr(VI), which also is soluble in water and absorbed through the skin. Cr(VI) uptake and biotransformation by plants has been studied by bulk XAS in several crop and desert plant species (Aldrich et al., 2003; Montes-Holguin et al., 2006; Zayed et al., 1998). Overall, the results have shown that plants exposed to Cr(VI) reduce it to Cr(III) in the roots as no presence of Cr(VI) in the tissues has been reported. However, the mechanism of Cr reduction in plants is not clearly understood. In Aldrich et al. (2003), bulk XANES identified Cr-phosphate, Cr-acetate

and Cr-nitrate as species present in the tissues of the plants. The hypothesized mechanism of uptake and reduction of Cr(VI) is through the complexation of Cr by organic acids from root exudates. Transport of Cr(III) to the root vascular tissues would depend on its complexation to organic acids and/or amino acids that will increase Cr(III) solubility at plant physiological pH (4.5–7.0). This has been clearly shown by Howe et al. (2003) in subterranean clover plants. The authors studied the uptake of Cr(VI) and Cr(III)-citrate in order to compare the mobility of both species in the plant tissues. The concentration of Cr in the leaves was significantly higher in the plants exposed to Cr(III)-citrate compared to Cr(VI). A combined approach of electron paramagnetic resonance and bulk XANES enabled to determine the oxidation state of Cr in the tissues of clover plants was Cr(III) and that Cr(III)-citrate was translocated unchanged to the leaves. μXRF mapping from leaf tissues showed that Cr was distributed in the veins and leaf margins of the subterranean clover plants. The reduction, uptake and transport of Cr in plants are far from being well understood. More studies are required in order to locate the sites for reduction (extracellular or intracellular) and the role of complexation to organic acids and amino acids in Cr translocation. The use of synchrotron techniques like μXRF, μXAS and μFTIR should help to advance our understanding of Cr plant metabolism.

Cesium (Cs) occurs naturally in the environment from erosion and weathering of Cs containing rocks and minerals. It can be released into the air, water and soil through mining and milling activities. Moreover, Cs radioactive isotopes might be released into the air by nuclear power plants and during nuclear accidents. Cs is particularly available for plants due to its chemical similarities with potassium (K). The uptake mechanism of Cs and its interaction with K was studied by Isaure et al. (2006b) and Le Lay et al. (2006). In the first report, the uptake of Cs in the absence and presence of K was studied in *A. thaliana* plants, and later in cell suspensions of the same plant. Images from μXRF evidenced the colocalization of Cs and K in veins, mesophyll/epidermis, stems and trichomes (Fig. 1.13). The content of Cs decreased in all the abovementioned compartments with high K application. The authors also used particle-induced X-ray emission (PIXE) and Rutherford backscattering spectrometry (RBS) for elemental mapping; these methods offer good elemental detection limits and are quantitative, but μXRF still offered highest lateral resolution for this study. Results from cell suspensions showed that Cs uptake was faster in K-depleted medium. μXRF analysis

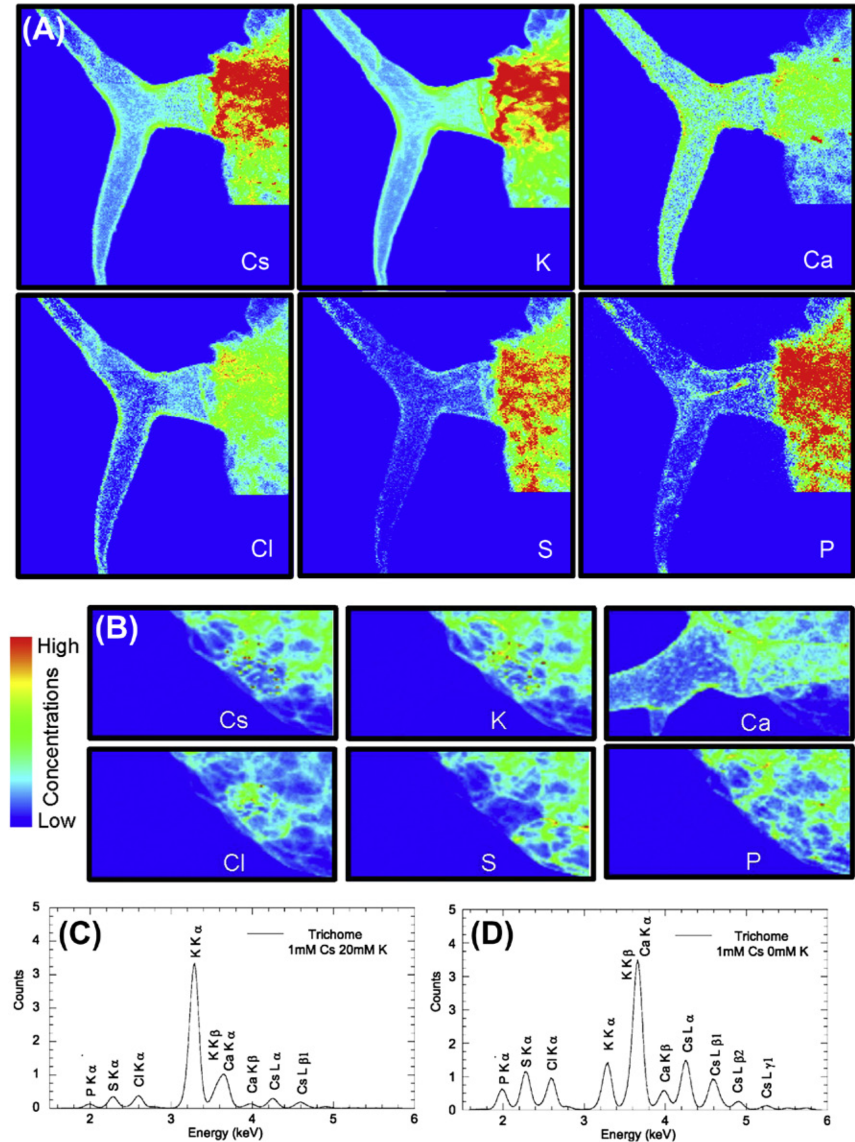


Figure 1.13 False-color elemental µXRF maps of trichomes recorded on plants treated for 4 days with 1 mM Cs, 20 mM K (A), and with 1 mM Cs, 0 mM K (B), and X-ray fluorescence spectra (arbitrary units) collected on the basis of the trichome treated for 4 days with 1 mM Cs, 20 mM K (C) and 1 mM Cs, 0 mM K (D). *(Reprinted with permission from Isaure et al. (2006b)).* See the color plate.

of individual cells showed that Cs accumulated in structures of micrometer dimensions that could be chloroplasts. Subcellular localization was possible, thanks to the submicron size beam, obtained from the use of Fresnel zone plates, and analyses were done in cryogenic conditions on frozen hydrated state. This work was complemented by Matrix-assisted laser desorption ionization (MALDI-ToF) mass spectrometry for metabolic profiling and proteomic analyses that underlined the chloroplast target by showing a decrease in Rubisco amount and a perturbation of chlorophyll metabolism. This study shows the interest of coupling state-of-the-art physical and analytical techniques to investigate the metabolism of trace elements in biological samples.

Thallium (Tl) is an extremely toxic metal to mammals. Ingestion of vegetables grown in Tl-contaminated soils is the main route of exposure to humans. However, its hyperaccumulation in plant species such as *Iberis intermedia* suggests there is potential for successful phytoremediation of Tl-contaminated environments. Scheckel et al. (2004) reported first on the distribution and speciation of this element in leaves of *I. intermedia* using an interesting in vivo approach. They evidenced the presence of Tl as aqueous Tl(I) inside whole leaves from living plants. In a follow-up study, the distribution and compartmentalization of Tl in *I. intermedia* was assessed by DA-CMT (Scheckel et al., 2007). The authors also studied the effects of freeze drying as sample preparation method in the distribution of Tl in *I. intermedia*. The results confirmed the compartmentalization of Tl within the vascular system of cotyledons and leaves, similar to K distribution. The authors also concluded that in their study, freeze drying (with prior LN2 plunging) as a sample preparation step did not result in redistribution artifacts.

4.9. Nanoparticles

Nanotechnology is a profitable, rapidly growing industry that promises a revolution in our world. The unique properties of nanomaterials (NMs) (at least one dimension below 100 nm) and NPs (at least two dimensions below 100 nm) such as enhanced magnetic, catalytic, optical, electrical or mechanical properties compared to their bulk analogs supports the daily quest for novel applications to develop present technologies. Particularly, metallic NPs (metal oxides and elemental) are widely used in commodities, pharmaceutics, cosmetics, and biomedical products (Nel et al., 2006).

However, these same unique properties of NMs raise a concern about the possible adverse environmental and human health effects. Plants play a fundamental ecological and economic role in our society; it is therefore of paramount importance to investigate the interactions of NPs with plants as it represents a potential entry into the food chain. The results from studies in the field of plant nanotoxicology have been recently reviewed (Rico et al., 2011). The uptake, translocation, and accumulation of NPs in plants depend on chemical composition, functionalization, and stability of the NPs. Hence, fundamental questions about the speciation and localization of metallic NPs in plants can be answered with the use of synchrotron-based methods.

4.9.1. Metal-Oxide NPs

The most studied metal-oxide NPs are CeO_2, ZnO, and TiO_2. These NPs are used in many commercial products and being produced in high tonnage (Xia et al., 2008). CeO_2 NPs are used in engineering processes involving catalysts, polishing agents, fuel additives, and microelectronics. The effects of 7 nm cubic CeO_2 NPs in the edible plants—cucumber, tomato, alfalfa, corn, and soy bean—grown in hydroponics were investigated by Lopez-Moreno et al. (2010a, 2010b). Seed germination was reduced in corn, tomato and cucumber. However, the treatments promoted root growth in cucumber, corn and soybean plants. The authors used Ce L_{III}-edge bulk XAS to determine the speciation of Ce in the roots tissues from the four studied plant species. The roots from all species showed a spectral signature consistent with the CeO_2 NP spectrum. The authors conclude that unchanged CeO_2 NPs are accumulated in the roots of the studied edible plants (Ce chemical form in shoots was not investigated). In both studies, no microscopic confirmation is presented and the specific localization of the NPs in the roots is unknown. The uptake of 7 nm CeO_2 NPs in cucumber plants was also studied by Zhang et al. (2011). The specific localization of Ce in the tissues was studied by TEM and autoradiography. The Ce NPs adsorbed to the root surface and were not observed inside the root cells.

ZnO NPs are widely used as polymer fillers, UV absorbers and antibiotics. The speciation of ZnO NPs in soybean plants as well as in desert plant species (*Prosopis juliflora*, *Salsola tragus*, and *Parkinsonia florida*) has been studied by bulk XAS (de la Rosa et al., 2011; Lopez-Moreno et al., 2010a). The plants were exposed to 8 nm ZnO NPs at germination stage and the XAS studies were performed on 7-day old seedlings exposed to 4000 mg L^{-1}. The LC-XANES results from root tissues showed that ZnO NPs were transformed into Zn-citrate, Zn-nitrate, and Zn-phosphate species.

Germination was not significantly affected in any of the studied plant species but the root growth was decreased in all species. Hernandez-Viezcas et al. (2011) used μXRF and μXANES to study ZnO NPs uptake in plants. Mesquite plants exposed to ZnO NPs (8 nm) in hydroponic culture showed increased uptake of Zn compared to control plants. μXRF maps of Zn from root thin sections (30 μm) showed Zn accumulated mainly in the vascular region (Fig. 1.14a). The μXRF maps from leaves showed Zn is concentrated in the leaf veins but also has diffused signal all across the leaf tissues (Fig. 1.14b). The combination of bulk and μXANES confirmed that ZnO NPs were transformed on/in root surface and transported as Zn(II) from roots to leaves. The results from μXANES and bulk-XANES showed that Zn has a different coordination environment compared to the ZnO NPs. Exposure to ZnO NPs increased the specific activity of stress enzymes catalase in root, stem and leaves and ascorbate peroxidase only in stem and

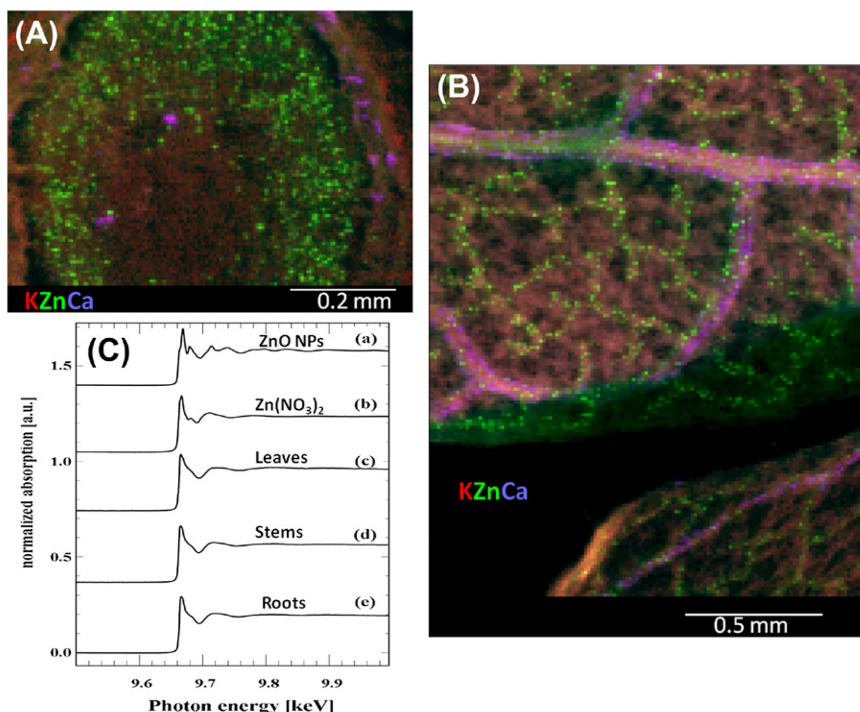


Figure 1.14 Tricolor micro-XRF images from mesquite tissues exposed to ZnO NPs. (A) Mesquite root thin sections (30 μm thickness). (B) Freeze-dried leaves. (C) XANES spectra from mesquite tissues and the ZnO NPs reference. *(Reprinted and adapted with permission from Hernandez-Viezcas et al. (2011)).* See the color plate.

leaves. These effects can be a result of the increased pool of Zn ions coming from the dissolution of ZnO NPs. However, it has been shown in another plant species (*Allium cepa*) that ZnO NPs can induce cytogenetic and genotoxic effects that are not observed in plants exposed only to dissolved Zn ions (Kumari et al., 2011).

TiO_2 NPs are used in a large variety of products (paints, paper, concrete, glasses, sunscreens) for their photocatalytic properties which confer to the materials some self-cleaning or anti-UV properties. In vivo and in vitro toxicological studies have focused in pulmonary and dermal hazards of TiO_2 NPs (Johnston et al., 2009). However, reports on the toxicological effects on the environment, i.e. destabilization of ecosystems and trophic transfer, are scarce. The literature on the impact of TiO_2 NPs on plants is limited (Rico et al., 2011), and only one report is found in the literature using synchrotron techniques on nano TiO_2 plant uptake. Wheat plants were exposed to anatase TiO_2 NPs (12 and 25 nm) dispersed in Hoagland's nutrient solution. Results from μXRF and μXANES on wheat plants exposed to anatase TiO_2 NPs showed that NPs penetrated inside the root tissues and were transferred unchanged in the parenchyma and vascular tissue of leaves (Larue et al., 2011, accepted for publication). Pre-edge analysis from laterally resolved μXANES showed no significant modifications of anatase TiO_2 NPs after plant internalization. The germination and root elongation were not significantly affected by the exposure to TiO_2 NPs in the wheat plants.

Applications of iron oxide nanoparticles include magnetic storage devices, catalysis, sensors, and magnetic resonance imaging in medical diagnosis and therapeutics. The magnetic properties of these NPs allow its detection in tissues with the use of a vibrating sample magnetometer (VSM). The uptake and accumulation of Fe_2O_3 (magnetite) NPs in plants has been studied in pumpkin by VSM (Zhu et al., 2008) and in pumpkin and rye grass by VSM and Fe K-edge bulk-XANES and EXAFS (Wang et al., 2011a). The presence of Fe_2O_3 NPs in the roots was confirmed in both studies. Zhu et al. (2008) reported that Fe_2O_3 NPs were translocated to the shoots of pumpkin plants. On the contrary, Wang et al. (2011a) found Fe in a coordination environment similar to Fe-citrate in the shoots of pumpkin and rye grass. These contrasting results might result from different experimental conditions. The properties of NPs and solution conditions largely determine the degree of agglomeration, which may influence the stability and availability of NPs. Results from EXAFS and VSM of Fe_2O_3 NPs in rye grass plants showed that NPs were detected in the roots but not in the shoots (Wang et al., 2011a). The exposure to Fe_2O_3 NPs caused oxidative stress in roots

and shoots of pumpkin and rye grass plants, as shown by increased superoxide dismutase and catalase enzyme activities, and lipid peroxidation (Wang et al., 2011a).

Rare-earth oxide NPs, such as La_2O_3 and Yb_2O_3, are used as catalysts, painting coatings, polishing powder, and luminescent materials. The distribution and speciation of La_2O_3 NPs (65 nm) were studied in the roots of cucumber plants by TEM-EDS, STXM and NEXAFS (Ma et al., 2011). The formation of La needle-like nanoclusters in the intercellular regions of the cucumber roots was observed by TEM-EDS. The chemical composition ($LaPO_4$) of the observed nanoclusters was determined by STXM and NEXAFS. The formation of the nanoclusters could reduce the available pool of inorganic P contributing to the phytotoxicity of La_2O_3 NPs in the cucumber plants. Zhang et al. (2012) studied the uptake of Yb_2O_3 NPs also in cucumber plants using a similar electron microscopy and synchrotron STXM/NEXAFS approach. The Yb_2O_3 NPs formed $YbPO_4$ nanoclusters in the cell walls but also in the cytoplasm. The presence of nanoclusters in the cytoplasm was not observed in treatments with bulk and $YbCl_3$ solutions.

4.9.2. Elemental Nanoparticles

The production of metal NPs (Au, Ag, and Cu) by plants and at the root–soil interface has been reported in several plant species (Bali et al., 2010; Haverkamp and Marshall, 2009; Manceau et al., 2008; Marshall et al., 2007). Moreover, the use of plant tissues, plant extracts, and living plants has been suggested as a green chemistry alternative for the production of metal NPs (Parsons et al., 2007). Au NPs are being used in a variety of applications including the detection and imaging of cancer cells, pharmaceuticals, and as catalysts in fuel cells. Ag NPs are used for their antimicrobial properties in detergents, plastics, and textiles. Studies regarding the toxicity of these NPs in plants have relied on synchrotron techniques for the localization and speciation of the metals.

A combined approach of electron and X-ray microscopy was used to study the distribution and speciation of Au NPs in the tissues of tobacco plants (Sabo-Attwood et al., 2011). The authors compared the uptake of citrate-capped Au NPs of different sizes (3.5 and 18 nm). The 3.5 nm NPs were observed inside the cell cytoplasm, whereas the 18 nm NPs remained aggregated in the cell wall and cell membrane. Necrosis was observed only in the plant tissues from plants exposed to the 3.5 nm NPs. Synchrotron X-ray microspectroscopy provided confirmation of the Au oxidation state, which remained as Au^0 in both roots and leaves of tobacco plants. Contrasting

results were obtained for Ag NPs in roots from common grass (Yin et al., 2011). X-ray microspectroscopy showed that Ag NPs were oxidized within plant tissues. Ag NPs toxicity was influenced by total NP surface area with smaller Ag NPs (6 nm), more strongly affecting growth than did similar concentrations of larger (25 nm) NPs for a given mass.

5. COMPLEMENTARY TECHNIQUES

5.1. Histochemical Techniques

The principle of histochemical techniques is the use of dyes which are supposed to specifically chelate a free or labile metal, and the observation of the stained samples by microscopy. The use of these techniques to detect trace metals in biological media dates back more than 140 years, and is reviewed in detail in the case of animal cells and tissues by McRae et al. (2009). Imaging of metals in plant tissues is challenging for several reasons. First, the cell-wall barriers can pose significant challenges for the dye to penetrate inside the plant tissue. Second, for aerial parts, the cuticle represents an additional barrier, and the strong autofluorescence signal arising mainly from the chlorophyll (excitation range: 420–460 nm and emission range: 600–750 nm), but also from carotene, and xanthophyll is a big constraint. Probes have to be cell permeable to penetrate inside cells, but must be able to cross the cell wall as well. The autofluorescence problem may be overcome by the choice of appropriate dyes in terms of excitation and emission bands, and of proper excitation and emission bands. These limitations may explain why histological techniques have been (and still are) more widely used for animal cells and tissues than for plant samples, and in the case of plants, more often used on roots than on aerial parts. Other intrinsic limitations of histochemical techniques is the fact that chelating dyes react with the fraction of metal ions that is loosely bound or labile, and generally with a single valence state for a given metal (e.g. Fe(II) for iron). This redox-state specificity may be an advantage, but chemical treatments prior to staining may be necessary if one want to visualize the distribution of a metal regardless of the oxidation state.

Classical techniques use chromogenic ligands and visible light microscopy. Details on most widely used chromophores and sample preparation protocols are detailed in McRae et al. (2009). These techniques have some limitations including a relatively limited sensitivity and the lack of specificity in some cases. However, they still provide very reliable results for metals in relatively high concentrations in cells such as iron or hyperaccumulated metals. Roschzttardtz et al.

(2011) used ferrocyanide and diaminobenzidine (Perls/diaminobenzidine) and DAPI to study iron vs DNA distribution in cells of Pea (*Pisum sativum*) embryo. With the help of μXRF and μPIXE, they evidenced a hot spot of iron in the nucleolus, a subcompartment of the nucleus. Richau et al. (2009) studied the distribution of nickel (Ni) over root segments and tissues in the hyperaccumulator *N. caerulescens* and the nonhyperaccumulator *Noccaea arvense* using dimethylglyoxime staining and light microscopy. They evidenced strongly decreased ability to accumulate Ni in root cell vacuoles for the hyperaccumulator.

Chromogenic ligands have been progressively replaced by fluorescent dyes. Observations can be made with an epifluorescence microscope or a confocal laser scanning microscopy (CLSM). Main improvements include a high sensitivity and specificity, and the versatility of CLSM; the use of laser excitation and filters allows the selection of a specific wavelength for excitation and specific channels for the emitted light. In addition, the confocal mode provides 3-D images without sectioning the samples. Fluorescent dyes used in recent studies include, for example, Zinpyr (Hanikenne et al., 2008; Sinclair et al., 2007) and Zinquin (Sarret et al., 2006) for Zn, and BTC-5N (Lu et al., 2008) and Leadmium Green (Lu et al., 2008; Tian et al., 2011) for Cd. In parallel to the localization of metals, fluorescence tagging is used to study the expression of proteins and peptides involved in metal homeostasis or detoxification by using GFP or GUS reporter gene fusion (Hanikenne et al., 2008; Morel et al., 2009; Oomen et al., 2011). Hanikenne et al. (2008) nicely combined GUS reporter gene and Zinpyr staining on roots of *A. halleri* and of *A. thaliana* mutant expressing AhHMA4 to study the role of this heavy metal transporter gene in Zn root-to-shoot transfer.

Finally, fluorescent polystyrene nanoparticles of different diameters were used as a probe to evaluate the size of cuticular and stomatal pores present on plant leaves, which are supposed to act as an entry point for particles inside the leaf tissue using CLSM (Eichert et al., 2008) (Fig. 1.15). Another study used SiO_2 nanoparticles labeled with FITC to study the fate of these NPs after their uptake by rice seedlings using an epifluorescence microscope (Nair et al., 2011). Quantum dots, which are autofluorescent, may be used in a similar way (Al-Salim et al., 2011; Navarro et al., 2012).

5.2. Electron Microscopy

The use of electron microscopy allows researchers to obtain highly detailed images of plant structure and cells useful in the study of metal uptake and metabolism in plants. The imaging and analytical capabilities of electron microscopy are over 1000 times better than light microscopy since

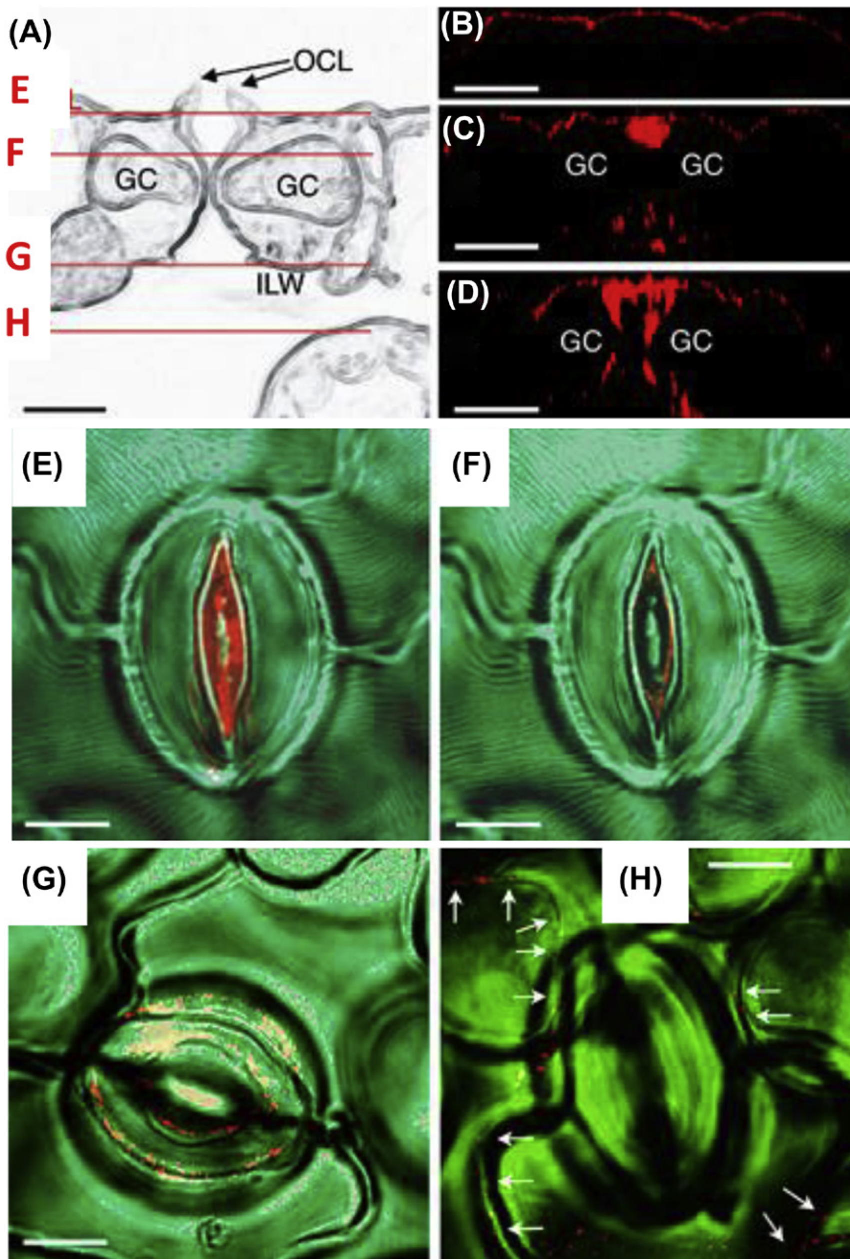


Figure 1.15 (A) Vertical section of *Vicia faba* stomata. Red lines indicate the approximate position of the respective image planes of Fig. 1.1E–H. GC, guard cell; OCL, outer cuticular ledges; ILW, inner lateral guard cell wall. The CLSM images (B–H) show the distribution of fluorescent particles of 43 nm diameter in *V. faba* leaves in optical vertical sections (B–D) and in optical paradermal sections in different depths below the leaf surface (E–H). Fluorescence is detectable on the cuticle, between the pair of guard cells and below in the substomatal cavity. The focal planes in (E–H) are in depths of 3.6, 14.5, 41 and 63 mm below the leaf surface, respectively. Bars ¼ 10 mm. *(Modified after Eichert et al. (2008))*. See the color plate.

electrons have wavelengths about 100,000 times shorter than visible light and are easily focused with electromagnetic fields. The two basic types of electron microscopy are scanning electron microscopy (SEM) and transmission electron microscopy (TEM). Modern instruments are capable of imaging frozen-hydrated specimens and the use of energy-dispersive X-ray (EDX) detectors allows elemental mapping of specimens in both TEM and SEM microscopes. With the environmental scanning electron microscope (ESEM), it is possible to examine hydrated, unfixed, nonfrozen, uncoated vegetal specimens under partial pressure in the specimen chamber.

The TEM microscope uses a high-voltage electron beam produced by an electron gun composed of a filament cathode. The produced electron beam is accelerated by an anode (40–400 keV) and it is focused with the use of electromagnetic lenses. The sample thickness is critical in this microscope as the sample should be relatively transparent to electrons (~100 nm). The images are generated by sending the electron beam through the sample and the emerging electron beam carrying information about the sample is then magnified by an electromagnetic lens system. The magnified electron image is projected to a scintillator coupled to a CCD camera. Sample preparation requires chemical fixation, dehydration and polymer embedding to stabilize them for ultramicrotomy. Sectioned specimens also need staining with heavy atom (U, Pb) in order to achieve the required image contrast. TEMs are useful to study the interior of sliced cells and subcellular entities where metals can be stored. This technique is nicely paired up with synchrotron μXRF, μEXAFS and STXM in studies of uptake of nanoparticles in plants (Ma et al., 2011; Sabo-Attwood et al., 2011; Zhang et al., 2012). The TEM offers the spatial resolution required for observing the NPs in the plant tissues and cells, whereas synchrotron X-rays techniques provide trace element localization and more importantly speciation of the element of interest in the tissues.

In contrast, SEMs are used to study the three-dimensional features of intact specimens (leaves, roots, trichomes, etc.). The SEM produces images by scanning the specimen with a focused electron beam. From the electron interactions with the sample, secondary electrons, backscattered electrons, and X-ray emission are the main detection probes used to obtain information from the sample such as its topography and composition. Sample preparation requires mainly dehydration to prevent distortions induced from water removal under the high vacuum operating conditions of the microscopes. However, no universal method for SEM sample preparation exists so the specific technique to employ will vary according to the surface features

to be preserved, availability of processing equipment and the characteristics of the available microscope. Interesting reviews on sample preparation for the study of plant surface are found in Pathan et al. (2008, 2010). The use of SEM in combination with synchrotron techniques has been used in the study of Cd accumulation in trichomes of *A. thaliana* (Isaure et al., 2006a) and Cd elimination in tobacco plants (Isaure et al., 2010).

5.3. Techniques Using Ion Beams (PIXE, SIMS)

Among ion beams, PIXE and secondary ion mass spectrometry (SIMS) are the most popular, may be because they are quantitative to measure elemental concentrations. In PIXE, an inner-shell electron is ejected from the atom by the incident beam, and the rearrangement of the electronic shells by an outer-shell electron filling the vacancy generates the emission of characteristic X-rays, which are detected for quantification. PIXE generally uses a proton beam because of the higher ionization cross-section compared to heavier particles such as alpha particles. All elements with $Z > 10$ can be detected, which is attractive for plant studies where light elements (Mg, P, S…) are of interest, and detection limit is in the range of 1–10 $\mu g\ g^{-1}$. The quantification is achieved thanks to a combination with RBS or scanning transmission ion spectrometry (Deves et al., 2005) to quantify the mass of the analyzed volume. Most of the microprobes have a lateral resolution around the micrometer, which is generally sufficient to image plant tissues. The depth penetration of the beam is higher than with electrons, in the range of 10–100 μm, which can be a drawback since it is not restricted to the cell layer and can probe a superimposition of several tissues. PIXE and micro-PIXE have been largely applied to localize and quantify metals in plants (Mesjasz Przybylowicz and Przybylowicz, 2002). To cite the most recent studies, Co was imaged in wheat and tomato (Collins et al., 2010), As in rice (Lombi et al., 2009), U in wheat, sunflower and oilseed rape (Laurette et al., 2012), Cd and Ni in soybean seeds (Malan et al., 2012), Ni in the hyperaccumulator *Berkheya coddii Roessler* (Orłowska et al., 2011), Cd in the hyperaccumulator *N. praecox* (Pongrac et al., 2010; Vogel-Mikus et al., 2008). At the cell level, Cs was imaged in *A. thaliana* cells (Deves et al., 2005; Isaure et al., 2006b) and more recently, Fe in the nucleus of pea embryos cells (Roschzttardtz et al., 2011). In all these studies, samples were analyzed as freeze-dried samples or embedded samples. Interestingly, the development of cryostages has started for a few years to study frozen hydrated

samples. Sakai et al. (2005) imaged onion skins using a cryojet, and recently, Tylko et al. (2007a, 2007b) adapted a cryosystem to image and quantify elements in leaves of the Ni-hyperaccumulator S*enecio anomalochrous Hilliard*. PIXE nano imaging with lateral resolution of 200–300 mm has also been used in the past few years (Barberet et al., 2009; Ortega et al., 2009; Reinert et al., 2007). Although not yet applied to plants, it opens new possibilities in plant imaging at the cell level, which appears promising in combination with cryoanalysis.

SIMS uses a primary beam of ions (Cs^+, O^-, ...) to sputter the surface of a sample (a few nanometers), where atoms are ionized and secondary ions are detected by a mass spectrometer. Isotope differentiation is thus possible, and the detection limit is in the range of 0.1 μg g^{-1}. It has been applied for 30 years to minerals but the investigation of plants is scarce. All elements from hydrogen to uranium can be studied. The spatial resolution depends on the ion source used, for instance, 50 nm for Cs^+ and 150 nm for O^-. SIMS using ions with low current density (static SIMS) minimizes molecule fragmentation, thus providing molecular information from the surface sample. Using higher current density (dynamic SIMS) generally destroys the molecules, thus leading to elemental and isotopic distribution. It is a destructive technique, giving information on the surface (the first atomic layers) but as the sample is sputtered, in-depth information can be obtained by eroding successive layers. Development of probes below the micrometer leads to nano-SIMS opening new possibilities (Moore et al., 2012). Stable isotopic spiking, especially for light elements (^{13}C, ^{15}N, ^{34}S, ^{44}Ca or 41K) has been successfully applied to plant samples to follow the uptake and compartmentalization of elements. However, the quantification of elements can be arduous for biological samples due to the variations of ionization yield related to the elements and noncalibrated matrix (Moore et al., 2012). The sample preparation is of particular importance for nano-SIMS since the surface must be as flat as possible to avoid artifacts from inhomogeneity and roughness, and since water needs to be removed as the techniques operates in high vacuum. As a result, measurements require either embedding in resins, thus possibly introducing redistribution of the most mobile elements, or the combination of high-pressure freezing and freeze substitution, which is the most applied procedure. The choice of preparation must be done depending on the objectives of the experiment (Grovenor et al., 2006). CryoNanoSIMS and preparation of cryosections remains unambiguously as a Holy Grail to limit sample artifacts. CryoSIMS has been applied

to follow chemical elements in xylem and stem tissues of beans (Metzner et al., 2008, 2010). Imaging of light elements such as N, C, Mg, P, K, Ca and their isotopes was reported in the plant–soil system (Clode et al., 2009; Kilburn et al., 2010), as well as metalloids and metals. For instance, As and Se were imaged in cereal grains (Moore et al., 2010) and Ni in the hyper-accumulator *A. lesbiacum* (Smart et al., 2007, 2010). However, some metals generally of interest in contaminated environments such as Zn and Cd are difficult to analyze due to their low relative sensitivity factor (Moore et al., 2012; Wilson, 1995).

5.4. Laser Ablation Coupled with ICP-MS

Laser ablation coupled with inductively coupled plasma mass spectrometry emerged more than 25 years ago (Gray, 1985) and has been mainly applied to geological samples (Durrant and Ward, 2005). For a decade, it has gained interest in biological samples and plant studies (Becker et al., 2010). Briefly, a laser beam (in most of the cases, a Nd:Yag laser) is focused on the sample and laser pulses ablate material, which is transported to an ICP-MS by a carrier gas, ionized and quantified. The most common MS is a quadrupole-based inductively coupled plasma mass spectrometer (ICP-QMS) but more rarely, LA can be coupled to double-focusing sector field ICP-MS with single-ion collection (ICP-SFMS) or multiple-ion collector ICP-MS (MC-ICP-MS), which allow higher sensitivity (Becker et al., 2010). A review of the existing systems is described in Mokgalaka and Gardea-Torresdey (2006). The rasterring of samples provides spatially resolved elemental or isotopic maps. Lateral resolution ranging from 5 to 50 μm is generally enough to map the plant tissue, but is too large to investigate the distribution at the cellular level. However, it benefits from high sensitivity associated with unrivaled detection limits in the 0.01 $\mu g\ g^{-1}$ range. It is also quantitative, using external and/or internal calibration, and several strategies of calibration are available (Durrant, 1992; Mokgalaka and Gardea-Torresdey, 2006; Punshon et al., 2004; Wu et al., 1999). Samples are analyzed at ambient pressure and temperature, thus they can be analyzed as fresh samples; in this case, the quantification can be more difficult and requires that C is measured as an internal standard (Wu et al., 2009). For plant studies, pioneer work emerged around 2000, with investigations of tree rings (Prohaska et al., 1998; Watmough et al., 1998), bark (Narewski et al., 2000) and leaves of oak (Hoffmann et al., 2000). Quantitative imaging of Cd and Pb was performed on tobacco root and shoot thin sections (Becker et al., 2008), while relative distribution of Pb was reported in sunflower (Galiová et al., 2008; Kaiser

et al., 2009) and *Capsicum annuum* leaves (Galiová et al., 2011). Cu was imaged and quantified in leaves of the Cu tolerant plant *Elsholtzia splendens* (Becker et al., 2010). Al and Ni profiles were determined in root sections of buckwheat (Klug et al., 2011), and roots of the hyperaccumulator *B. coddii* (Moradi et al., 2010), respectively while Cu and Zn profiles have been recorded on roots of cucumber (Shi et al., 2009). P has been investigated in the rhizosphere of *Brassica napus* (Santner et al., 2012). Profiles of U and Ni were studied in *Andropogon elliottii* plants (Punshon et al., 2004), and As in rice (Meharg et al., 2008). Recently, LA-ICP-MS was used to localize and quantify Cd in fresh and freeze-dried thin sections of the hyperaccumulator *S. alfredii* (Tian et al., 2010). Wang et al. (2011b) combined ^{70}Zn spiking and LA-ICP-MS to elucidate Zn transport and storage in wheat grain. LA-ICP-MS has also been applied to detect metals in proteins extracted by gel electrophoresis (Lobinski et al., 2006). For instance, Polatajko et al. (2007) identified Cd in proteins from spinach, and Wu et al. (2011) screened metals in proteins extracted from the Cu-tolerant plant *E. splendens*. New developments now involve a lower lateral resolution and a nanoscale (Zoriy et al., 2008, 2009). Some preliminary tests were performed on biological samples (Becker et al., 2006) but the nano-LA-ICP-MS has not yet been applied to image plant samples. Certainly, it opens new challenging opportunities in cellular and subcellular investigations.



6. CONCLUSIONS AND PERSPECTIVES

Synchrotron beamlines are continuously improving and new beamlines are designed which offer breakthrough capabilities. Progress is being made with respect to the source intensity and focusing, with fluxes in the range of 10^{12}–10^{13} photons/s and beam size smaller than 100 × 100 nm like on ID22 beamline at the ESRF (Martinez-Criado et al., 2012), and fast detectors/electronics which allow beam exposure in the submilliseconds. These improvements have strongly decreased the acquisition time. High-resolution μXRF mapping of trace elements over millimeter-sized regions can be done in a few hours (Lombi et al., 2011c), and fCMT becomes feasible. Also, it is possible to study nonhyperaccumulating species exposed to realistic conditions in terms of metal exposure, and even in nutrient deficiency conditions.

Sample preparation remains a key issue for the study of metals in plants since the localization and the chemical form of metals should not be altered. The structure and composition of plant leaves, with more than 90% water

and the presence of a large vacuole representing more than 90% of the cell volume, make it difficult to section and to avoid the formation of ice crystals. Thus, the presence of a cooling system on the beamline is essential, at least for plant tissues containing a large percentage of water such as plant leaves or roots, and particularly for speciation studies.

Beside the technical improvements in terms of flux, resolution and detection efficiency discussed above, the integration of different techniques on the same beamline, as done on beamlines 10.3.2 (ALS), 2–3 (SSRL), 13-ID (APS) and X26A/X27A (NSLS) for μXRF, fCMT, μXRD and μXAS and ID21 at the ESRF for μXRF, μXANES, and μFTIR is highly beneficial. Scanning transmission X-ray microscopy (STXM) has been used successfully to study metals in microorganisms and inorganic colloids (Benzerara et al., 2008; Couradeau et al., 2012; Dynes et al., 2006; Miot et al., 2009). It is a promising technique for plant samples as well, thanks to its high resolution, possibility to work on hydrated samples, and to combine the mapping of organic compounds and metal species.

Besides technical improvements of the beamlines, data treatment is continuously evolving as well, for example, with the implementation of statistical treatment for XAS data or quantification modules for μXRF data. The development of user-friendly software adapted to researchers who are not pure physicists is particularly important to allow them to derive the most benefit from their experiments. Also, the integration of data obtained by different techniques in the same software, as it is the case for PyMCA (Solé et al., 2007), which can allow a full analysis of XRF data and do basic operations for XAS, XRD and FTIR data, is particularly profitable. Another current and future challenge is the handling of increasing amounts of data generated due to the improved spatial resolution and fast acquisition.

Finally, combination of synchrotron techniques with other approaches may be highly beneficial. For example, Kim et al. (2006) used μXRF and fCMT in combination with established genomic techniques to characterize the function of the gene VIT1 (vacuolar iron transporter 1) in *A. thaliana* seed. Histochemical techniques are highly complementary to μXRF since they allow the colabeling of metals and other structures or molecules (cell wall, DNA, Roschzttardtz et al., 2011) or of gene expression using GFP tagging. Nano-SIMS is another very promising technique that may provide additional information, e.g. on the isotopic composition of elements (Moore et al., 2012).

To conclude, there is a growing interest of the community of plant physiologists and biogeochemists for synchrotron-based techniques. Progress in instrumentation, sample preparation and data analysis opens new perspectives for research on several "hot topics" such as the uptake of nanoparticles by plants or the biofortification of crops.

ACKNOWLEDGMENTS

Portions of this work were performed at Beamline X27A, National Synchrotron Light Source (NSLS), Brookhaven National Laboratory. X27A is supported in part by the U.S. Department of Energy-Geosciences (DE-FG02-92ER14244 to The University of Chicago-CARS) and Brookhaven National Laboratory-Department of Environmental Sciences. Use of the NSLS was supported by the U.S. Department of Energy, Office of Science, Office of Basic Energy Sciences, under Contract No. DE-AC02-98CH10886. Funding for Elizabeth A. H. Pilon-Smits was provided by U.S. National Science Foundation grant # IOS-0817748. Research in Fang-Jie Zhao's lab is financially supported by the Priority Academic Program Development of Jiangsu Higher Education Institutions (PAPD). Funding was provided by PHYMET ANR project no. 2010 JCJC 605 01 for Marie Pierre Isaure and Géraldine Sarret, and by NanoHouse EU FP7 project no. 247810 for Géraldine Sarret. They also acknowledge SOLEIL and ESRF synchrotrons (France) for the provision of beamtime, and the staff of the beamlines Lucia at SOLEIL, and ID21 and FAME at the ESRF.

REFERENCES

Ager, F.J., Ynsa, M.D., Dominguez Solis, J.R., Lopez Martin, M.C., Gotor, C., Romero, L.C., 2003. Nuclear micro-probe analysis of *Arabidopsis thaliana* leaves. Nucl. Inst. Meth. Phys. Res. B 210, 401–406.

Al-Salim, N., Barraclough, E., Burgess, E., Clothier, B., Deurer, M., Green, S., Malone, L., Weir, G., 2011. Quantum dot transport in soil, plants, and insects. Sci. Total Environ. 409, 3237–3248.

Aldrich, M., Gardea-Torresdey, J., Peralta-Videa, J., Parsons, J., 2003. Uptake and reduction of Cr(VI) to Cr(III) by mesquite (*Prosopis* spp.): chromate-plant interaction in hydroponics and solid media studied using XAS. Environ. Sci. Technol. 37, 1859–1864.

Aldrich, M.V., Peralta-Videa, J.R., Parsons, J.G., Gardea-Torresdey, J.L., 2007. Examination of arsenic(III) and (V) uptake by the desert plant species mesquite (*Prosopis* spp.) using X-ray absorption spectroscopy. Sci. Total Environ. 379, 249–255.

Alves, S., Nabais, C., de Lurdes Simoes Goncalves, M., Correia dos Santos, M., 2011. Nickel speciation in the xylem sap of the hyperaccumulator *Alyssum serpyllifolium* ssp. lusitanicum growing on serpentine soils of northeast Portugal. J. Plant Physiol. 168, 1715–1722.

Asemaneh, T., Ghaderian, S., Crawford, S., Marshall, A., Baker, A., 2006. Cellular and subcellular compartmentation of Ni in the Eurasian serpentine plants Alyssum bracteatum, *Alyssum murale* (Brassicaceae) and *Cleome heratensis* (Capparaceae). Planta 225, 193–202.

Baker, A.J.M., 2000. Metal Hyperaccumulator Plants: A Review of the Ecology and Physiology of a Biochemical Resource for Phytoremediation of Metal-polluted Soils. Lewis publishers, Boca Raton, FL, USA.

Baker, A.J.M., Brooks, R.R., 1989. Terrestrial higher plants which hyperaccumulate metallic elements-A review of their distribution, ecology and phytochemistry. Biorecovery 1, 81–126.

Bali, R., Siegele, R., Harris, A.T., 2010. Phytoextraction of Au: uptake, accumulation and cellular distribution in Medicago sativa and Brassica juncea. Chem. Eng. J. 156, 286–297.

Barberet, P., Incerti, S., Andersson, F., Delalee, F., Serani, L., Moretto, P., 2009. Technical description of the CENBG nanobeam line. Nucl. Inst. Meth. Phys. Res. B 267, 2003–2007.

Bauer, S., Vasu, P., Persson, S., Mort, A.J., Somerville, C.R., 2006. Development and application of a suite of polysaccharide-degrading enzymes for analyzing plant cell walls. PNAS 103, 11417–11422.

Beath, O.A., Gilbert, C.S., Eppson, H.F., 1993a. The use of indicator plants in locating seleniferous areas in Western United States. I. General. Am. J. Bot. 26, 257–269.

Beath, O.A., Gilbert, C.S., Eppson, H.F., 1993b. The use of indicator plants in locating seleniferous areas in Western United States. II. Correlation studies by states. Am. J. Bot. 26, 296–315.

Becker, J.S., Dietrich, R.C., Matusch, A., Pozebon, D., Dressler, V.L., 2008. Quantitative images of metals in plant tissues measured by laser ablation inductively coupled plasma mass spectrometry. Spectrochim. Acta Part B At. Spectrosc. 63, 1248–1252.

Becker, J.S., Gorbunoff, A., Zoriy, M., Izmer, A., Kayser, M., 2006. Evidence of near-field laser ablation inductively coupled plasma mass spectrometry (NF-LA-ICP-MS) at nanometre scale for elemental and isotopic analysis on gels and biological samples. J. Anal. At. Spectrom. 21, 19–25.

Becker, J.S., Zoriy, M., Matusch, A., Wu, B., Salber, D., Palm, C., Becker, J.S., 2010. Bioimaging of metals by laser ablation inductively coupled plasma mass spectrometry (LA-ICP-MS). Mass. Spectrom. Rev. 29, 156–175.

Benzerara, K., Morin, G., Yoon, T., Miot, J., Tyliszczak, T., Casiot, C., Bruneel, O., Farges, F., Brown, G., 2008. Nanoscale study of as biomineralization in an acid mine drainage system. Geochim. Cosmochim. Acta 72, 3949–3963.

Bertsch, P.M., Hunter, D., 2001. Applications of synchrotron-based X-ray microprobes. Chem. Rev. 101, 1809–1842.

Bidwell, S.D., Woodrow, I.E., Batianoff, G.N., Sommer-Knudsen, J., 2002. Hyperaccumulation of manganese in the rainforest tree Austromyrtus bidwillii (Myrtaceae) from Queensland, Australia. Funct. Plant Biol. 29, 899–905.

Bleuet, P.E., Welcomme, E., Dooryhee, E., Susini, J.H., Hodeau, J.-L., Walter, P., 2008. Probing the structure of heterogeneous diluted materials by diffraction tomography. Nat. Mater. 7, 468–475.

Bluemlein, K., Raab, A., Meharg, A.A., Charnock, J.M., Feldmann, J., 2008. Can we trust mass spectrometry for determination of arsenic peptides in plants: comparison of LC-ICP-MS and LC-ES-MS/ICP-MS with XANES/EXAFS in analysis of Thunbergia alata. Anal. Bioanal. Chem. 390, 1739–1751.

Blute, N.K., Brabander, D.J., Hemond, H.F., Sutton, S.R., Newville, M.G., Rivers, M.L., 2004. Arsenic sequestration by ferric iron plaque on cattail roots. Environ. Sci. Technol. 38, 6074–6077.

Boyd, R.S., 2007. The defense hypothesis of elemental hyperaccumulation: status, challenges and new directions. Plant Soil 293, 153–176.

Boyd, R.S., 2010. Heavy metal pollutants and chemical ecology: exploring new frontiers. J. Chem. Ecol. 36, 46–58.

Broadhurst, C.L., Chaney, R.L., Angle, J.S., Erbe, E.F., Maugel, T.K., 2004a. Nickel localization and response to increasing Ni soil levels in leaves of the Ni hyperaccumulator *Alyssum murale*. Plant Soil 265, 225–242.

Broadhurst, C.L., Chaney, R.L., Angle, J.S., Maugel, T.K., Erbe, E.F., Murphy, C.A., 2004b. Simultaneous hyperaccumulation of nickel, manganese, and calcium in Alyssum leaf trichomes. Environ. Sci. Technol. 38, 5797–5802.

Broadhurst, C.L., Tappero, R., Maugel, T., Erbe, E., Sparks, D., Chaney, R., 2009. Interaction of nickel and manganese in accumulation and localization in leaves of the Ni hyperaccumulators *Alyssum murale* and *Alyssum corsicum*. Plant Soil 314, 35–48.
Brooks, R.R., 1998. Plants that Hyperaccumulate Heavy Metals. CAB International, New York.
Brooks, R.R., Shaw, S., Asensi Marfil, A., 1981. The chemical form and physiological function of nickel in some Iberian Alyssum species. Physiol. Plant 51, 167–170.
Brown, G.E., Sturchio, N.C., 2002. An overview of synchrotron radiation applications to low temperature geochemistry and environmental science. In: Fenter, P.A., Rivers, M.L., Sturchio, N.C., Sutton, S. (Eds.), Applications of Synchrotron Radiation in Low-temperature Geochemistry and Environmental Sciences, vol. 49, pp. 1–115.
Bulska, E., Wysocka, I., Wierzbicka, M., Proost, K., Janssens, K., Falkenberg, G., 2007. In vivo investigation of the distribution and the local speciation of selenium in Allium cepa L. by means of microscopic absorption near-edge structure spectroscopy and confocal microscopic X-ray fluorescence analysis. Anal. Chem.
Carey, A.M., Norton, G.J., Deacon, C., Scheckel, K.G., Lombi, E., Punshon, T., Guerinot, M.L., Lanzirotti, A., Newville, M., Choi, Y., Price, A.H., Meharg, A.A., 2011. Phloem transport of arsenic species from flag leaf to grain during grain filling. New Phytol. 192, 87–98.
Carey, A.M., Scheckel, K.G., Lombi, E., Newville, M., Choi, Y., Norton, G.J., Charnock, J.M., Feldmann, J., Price, A.H., Meharg, A.A., 2010. Grain unloading of arsenic species in rice. Plant Physiol. 152, 309–319.
Clemens, S., 2006. Toxic metal accumulation, responses to exposure and mechanisms of tolerance in plants. Biochimie 88, 1707–1719.
Clode, P.L., Kilburn, M.R., Jones, D.L., Stockdale, E.A., Cliff, J.B., Herrmann, A.M., Murphy, D.V., 2009. In situ mapping of nutrient uptake in the rhizosphere using nanoscale secondary ion mass spectrometry. Plant Physiol. 151, 1751–1757.
Collins, R., Bakkaus, E., Carriere, M., Khodja, H., Proux, O., Morel, J., Gouget, B., 2010. Uptake, localization, and speciation of cobalt in *Triticum aestivum* L. (Wheat) and Lycopersicon esculentum m. (Tomato). Environ. Sci. Technol. 44, 2904–2910.
Cotte, M., Checroun, E., Mazel, V., Sole, V.A., Richardin, P., Taniguchi, Y., Walter, P., Susini, J., 2009a. Combination of FTIR and X-rays synchrotron based micro-imaging techniques for the study of ancient paintings. A practical point of view. Preservation Sci. 6, 1–9.
Cotte, M., Dumas, P., Taniguchi, Y., Checroun, E., Walter, P., Susini, J., 2009b. Recent applications and current trends in cultural heritage science using synchrotron-based Fourier transform infrared micro-spectroscopy. C.R. Physique 10, 590–600.
Couradeau, E., Benzerara, K., Gérard, E., Moreira, D., Bernard, S., Brown Jr., G.E., López-García, P., 2012. An early-branching microbialite cyanobacterium forms intracellular carbonates. Science 336, 549–562.
De La Fuente, V., Rodríguez, N., Díez-Garretas, B., Rufo, L., Asensi, A., Amils, R., 2007. Nickel distribution in the hyperaccumulator *Alyssum serpyllifolium* Desf. spp. from the Iberian Peninsula. Plant Biosystems 141, 170–180.
de la Rosa, G., Lopez-Moreno, M.L., Hernandez-Viezcas, J., Montes, M.O., Peralta-Videa, J.R., Gardea-Torresdey, J.L., 2011. Toxicity and biotransformation of ZnO nanoparticles in the desert plants Prosopis juliflora-velutina, Salsola tragus and Parkinsonia florida. Int. J. Nanotechnol. 8, 492–506.
De la Rosa, G., Parsons, J.G., Martinez-Martinez, A., Peralta-Videa, J.R., Gardea-Torresdey, J.L., 2006. Spectroscopic study of the impact of arsenic speciation on arsenic/phosphorus uptake and plant growth in tumbleweed (Salsola kali). Environ. Sci. Technol. 40, 1991–1996.

De Souza, M.P., Pilon-Smits, E.A.H., Lytle, C.M., Hwang, S., Tai, J., Honma, T.S.U., Yeh, L., Terry, N., 1998. Rate-limiting steps in selenium assimilation and volatilization by Indian mustard. Plant Physiol. 117, 1487–1494.
Deves, G., Isaure, M.P., Le Lay, P., Bourguignon, J., Ortega, R., 2005. Fully quantitative imaging of chemical elements in *Arabidopsis thaliana* tissues using STIM, PIXE and RBS. Nucl. Instrum. Methods Phys. Res. B 231, 117–122 Special Iss. SI.
Dhankher, O.P., Li, Y.J., Rosen, B.P., Shi, J., Salt, D., Senecoff, J.F., Sashti, N.A., Meagher, R.B., 2002. Engineering tolerance and hyperaccumulation of arsenic in plants by combining arsenate reductase and gamma-glutamylcysteine synthetase expression. Nat. Biotechnol. 20, 1140–1145.
Do u, C.-M., Fu, X.-P., Chen, X.-C., Shi, J.-Y., Chen, Y.-X., 2009. Accumulation and detoxification of manganese in hyperaccumulator *Phytolacca americana*. Plant Biol. 11, 664–670.
Dokken, K.M., Davis, L.W., 2007. Infrared imaging of sunflower and maize root anatomy. J. Agric. Food Chem. 55, 10517–10530.
Dokken, K.M., Davis, L.W., Marinkovic, N.S., 2005. Use of infrared microspectroscopy in plant growth and development. Appl. Spectros. Rev. 40, 301–326.
Donner, E., Punshon, T., Guerinot, M., Lombi, E., 2012. Functional characterisation of metal(loid) processes in planta through the integration of synchrotron techniques and plant molecular biology. Anal. Bioanal. Chem. 402, 3287–3298.
Dowd, B.A., Campbell, G., Marr, R., Nagarkar, V., Tipnis, S., Axe, L., Siddons, D., 1999. Developments in synchrotron X-ray computed microtomography at the national synchrotron light source.. Proceedings of SPIE, Developments in X-ray Tomography II. 3772, 224–236.
Durrant, S.F., 1992. Multi-elemental analysis of environmental matrices by laser ablation inductively coupled plasma mass spectrometry. Analyst 117, 1585–1592.
Durrant, S.F., Ward, N.I., 2005. Recent biological and environmental applications of laser ablation inductively coupled plasma mass spectrometry (LA-ICP-MS). J. Anal. At. Spectrom. 20, 821–829.
Dynes, J., Tyliszczak, T., Araki, T., Lawrence, J., Swerhone, G., Leppard, G., Hitchcock, A., 2006. Speciation and quantitative mapping of metal species in microbial biofilms using scanning transmission X-ray microscopy. Environ. Sci. Technol. (asap).
Eichert, T., Kurtz, A., Steiner, U., Goldbach, H.E., 2008. Size exclusion limits and lateral heterogeneity of the stomatal foliar uptake pathway for aqueous solutes and water-suspended nanoparticles. Physiol. Plant 134, 151–160.
El Mehdawi, A.F., Pilon-Smits, E.A.H., 2012. Ecological aspects of plant selenium hyperaccumulation. Plant Biol. 14, 1–10.
Ellis, D.R., Gumaelius, L., Indriolo, E., Pickering, I.J., Banks, J.A., Salt, D.E., 2006. A novel arsenate reductase from the arsenic hyperaccumulating fern Pteris vittata. Plant Physiol. 141, 1544–1554.
Fendorf, S.E., Sparks, D., Lamble, G., Kelley, M.J., 1994. Applications of X-ray absorption fine structure spectroscopy to soils. Soil. Sci. Soc. Am. J. 58, 1583–1595.
Fernando, D.R., Bakkaus, E.J., Perrier, N., Baker, A.J.M., Woodrow, I.E., Batianoff, G.N., Collins, R.N., 2006a. Manganese accumulation in the leaf mesophyll of four tree species: a PIXE/EDAX localization study. New Phytol. 171 (4), 751–758.
Fernando, D.R., Batianoff, G.N., Baker, A.J., Woodrow, I.E., 2006b. In vivo localization of manganese in the hyperaccumulator Gossia bidwillii (Benth.) N. Snow & Guymer (Myrtaceae) by cryo-SEM/EDAX. Plant Cell. Environ. 29, 1012–1020.
Fernando, D.R., Marshall, A.T., Gouget, B., Carriere, M., Collins, R.N., Woodrow, I.E., Baker, A.J., 2008. Novel pattern of foliar metal distribution in a manganese hyperaccumulator. Funct. Plant Biol. 35, 193–200.

Fernando, D.R., Mizuno, T., Woodrow, I.E., Baker, A.J.M., Collins, R.N., 2010. Characterization of foliar manganese (Mn) in Mn (hyper)accumulators using X-ray absorption spectroscopy. New Phytol. 188, 1014–1027.

Foster, A.L., Brown, G.E., Tingle, T.N., Parks, G.A., 1998. Quantitative arsenic speciation in mine tailings using X-ray absorption spectroscopy. Am. Mineral. 83, 553.

Freeman, J.L., Quinn, C.F., Marcus, M.A., Fakra, S., Pilon-Smits, E.A.H., 2006a. Selenium-tolerant diamondback moth disarms hyperaccumulator plant defense. Curr. Biol. 16, 2181–2192.

Freeman, J.L., Tamaoki, M., Stushnoff, C., Quinn, C.F., Cappa, J.J., Devonshire, J., Fakra, S.C., Marcus, M.A., McGrath, S.P., Van Hoewyk, D., Pilon-Smits, E.A.H., 2010. Molecular mechanisms of selenium tolerance and hyperaccumulation in *Stanleya pinnata*. Plant Physiol. 153, 1630–1652.

Freeman, J.L., Zhang, L.H., Marcus, M.A., Fakra, S., McGrath, S.P., Pilon-Smits, E.A.H., 2006b. Spatial imaging, speciation, and quantification of selenium in the hyperaccumulator plants *Astragalus bisulcatus* and *Stanleya pinnata*. Plant Physiol. 142, 124–134.

Frommer, J., Voegelin, A., Dittmar, J., Marcus, M.A., Kretzschmar, R., 2011. Biogeochemical processes and arsenic enrichment around rice roots in paddy soil: results from micro-focused X-ray spectroscopy. Eur. J. Soil Sci. 62, 305–317.

Fukuda, N., Hokura, A., Kitajima, N., Terada, Y., Saito, H., Abed, T., Nakai, A., 2008. Micro X-ray fluorescence imaging and micro X-ray absorption spectroscopy of cadmium hyper-accumulating plant, *Arabidopsis halleri* ssp. *gemmifera*, using high-energy synchrotron radiation. J. Anal. At. Spectrom. 23, 1068–1075.

Gabbrielli, R., Mattioni, C., Vergnano, O., 1991. Accumulation mechanisms and heavy metal tolerance of a nickel hyperaccumulator. J. Plant Nutr. 14, 1067–1080.

Galeas, M.L., Zhang, L.H., Freeman, J.L., Wegner, M., Pilon-Smits, E.A.H., 2007. Seasonal fluctuations of selenium and sulfur accumulation in selenium hyperaccumulators and related non-accumulators. New Phytol. 173, 517–525.

Galiová, M., Kaiser, J., Novotný, K., Hartl, M., Kizek, R., Babula, P., 2011. Utilization of laser-assisted analytical methods for monitoring of lead and nutrition elements distribution in fresh and dried Capsicum annuum l. leaves. Microsc. Res. Tech. 74, 845–852.

Galiová, M., Kaiser, J., Novotný, K., Novotný, J., Vaculovič, T., Liška, M., Malina, R., Stejskal, K., Adam, V., Kizek, R., 2008. Investigation of heavy-metal accumulation in selected plant samples using laser induced breakdown spectroscopy and laser ablation inductively coupled plasma mass spectrometry. Appl. Phys. A Mater. Sci. Process. 93, 917–922.

Gardea-Torresdey, J.L., Peralta-Videa, J.R., de la Rosa, G., Parsons, J.G., 2005. Phytoremediation of heavy metals and study of the metal coordination by X-ray absorption spectroscopy. Coord. Chem. Rev. 249, 1797.

Gray, A.L., 1985. Solid sample introduction by laser ablation for inductively coupled plasma source mass spectrometry. Analyst 110, 551–556.

Grovenor, C.R.M., Smart, K.E., Kilburn, M.R., Shore, B., Dilworth, J.R., Martin, B., Hawes, C., Rickaby, R.E.M., 2006. Specimen preparation for NanoSIMS analysis of biological materials. Appl. Surf. Sci. 252 (19), 6917–6924 Special Iss. SI.

Hanikenne, M., Talke, I.N., Haydon, M.J., Lanz, C., Nolte, A., Motte, P., Kroymann, J., Weigel, D., Kramer, U., 2008. Evolution of metal hyperaccumulation required cis-regulatory changes and triplication of HMA4. Nature 453, 391–395.

Hansel, C.M., Fendorf, S., Sutton, S., Newville, M., 2001. Characterization of Fe plaque and associated metals on the roots of mine-waste impacted aquatic plants. Environ. Sci. Technol. 35, 3863–3868.

Hansel, C.M., LaForce, M., Fendorf, S., Sutton, S., 2002. Spatial and temporal association of as and Fe species on aquatic plant roots. Environ. Sci. Technol. 36, 1988–1994.

Harada, E., Hokura, A., Takada, S., Baba, K., Terada, Y., Nakai, I., Yazaki, K., 2010. Characterization of cadmium accumulation in willow as a woody metal accumulator using synchrotron radiation-based X-ray microanalyses. Plant Cell Physiol. 51, 848–853.

Haverkamp, R., Marshall, A., 2009. The mechanism of metal nanoparticle formation in plants: limits on accumulation. J. Nanopart. Res. 11, 1453–1463.

Hernandez-Viezcas, J.A., Castillo-Michel, H., Servin, A.D., Peralta-Videa, J.R., Gardea-Torresdey, J.L., 2011. Spectroscopic verification of zinc absorption and distribution in the desert plant Prosopis juliflora-velutina (velvet mesquite) treated with ZnO nanoparticles. Chem. Eng. J. 170, 346–352.

Hoffmann, E., Lüdke, C., Skole, J., Stephanowitz, H., Ullrich, E., Colditz, D., 2000. Spatial determination of elements in green leaves of oak trees (Quercus robur) by laser ablation-ICP-MS. Fresenius J. Anal. Chem. 367, 579–585.

Hokura, A., Onuma, R., Kitajima, N., Terada, Y., Saito, H., Abe, T., Yoshida, S., Nakai, I., 2006. 2-D X-ray fluorescence imaging of cadmium hyperaccumulating plants by using high-energy synchrotron radiation X-ray microbeam. Chem. Lett. 35, 1246–1247.

Holman, H., Bechtel, H., Hao, Z., Martin, M., 2010. Synchrotron IR spectromicroscopy: chemistry of living cells. Anal. Chem. 82, 8757–8765.

Holman, H.Y.N., Bjornstad, K.A., McNamara, M.P., Martin, M.C., McKinney, W.R., Blakely, E.A., 2002. Synchrotron infrared spectromicroscopy as a novel bioanalytical microprobe for individual living cells: cytotoxicity considerations. J. Biomed. Opt. 7, 417–424.

Holton, J., 2007. XANES measurements of the rate of radiation damage to selenomethionine side chains. J. Synchrotron Radiat. 14, 51–72.

Holzner, C.M., Feser, M., Vogt, S., Hornberger, B., Baines, S., Jacobsen, C., 2010. Zernike phase contrast in scanning microscopy with X-rays. Nat. Phys. 6, 883–887.

Hornberger, B., de Jonge, M.D., Feser, M., Holl, P., Holzner, C., Jacobsen, C., Legnini, D.P.D., Rehak, P., Strüder, L., Vogt, S., 2008. Differential phase contrast with a segmented detector in a scanning X-ray microprobe. J. Synchrotron Radiat. 15, 355–362.

Howe, J.A., Loeppert, R.H., Derose, V.J., Hunter, D.B., Bertsch, P.M., 2003. Localization and speciation of chromium in subterranean clover using XRF, XANES, and EPR spectroscopy. Environ. Sci. Technol. 37, 4091–4097.

Huang, Z.C., Chen, T.B., Lei, M., Hu, T.D., 2004. Direct determination of arsenic species in arsenic hyperaccumulator Pteris vittata by EXAFS. Acta Botanica Sinica 46, 46–50.

Huang, Z.C., Chen, T.B., Lei, M., Liu, Y.R., Hu, T.D., 2008. Difference of toxicity and accumulation of methylated and inorganic arsenic in arsenic-hyperaccumulating and -hypertolerant plants. Environ. Sci. Technol. 42, 5106–5111.

Huguet, S., Bert, V., Laboudigue, A., Barthès, V., Isaure, M., Llorens, I.H.S., Sarret, G., 2012. Cd speciation and localization in the hyperaccumulator *Arabidopsis halleri*. Environ. Exp. Bot. 82, 54–65.

Indriolo, E., Na, G., Ellis, D., Salt, D.E., Banks, J.A., 2010. A vacuolar arsenite transporter necessary for arsenic tolerance in the arsenic hyperaccumulating fern Pteris vittata is missing in flowering plants. Plant Cell 22, 2045–2057.

Ionescu, M.N.P., Bhatia, N., Cohen, D., Kachenko, A., Siegele, R., Marcus, M., Fakra, S., Foran, G., 2008. X-ray absorption spectroscopy at the Ni-K edge in Stackhousia tryonii Bailey hyperaccumulator. X-ray Spectrom. 37, 629–634.

Isaure, M., Sarret, G., Harada, E., Choi, Y., Marcus, M., Fakra, S., Geoffroy, N., Pairis, S., Susini, J., Clemens, S., Manceau, A., 2010. Calcium promotes cadmium elimination as vaterite grains by tobacco trichomes. Geochim. Cosmochim. Acta 74, 5817–5834.

Isaure, M.P., Fayard, B., Sarret, G., Pairis, S., Bourguignon, J., 2006a. Localization and chemical forms of cadmium in *Arabidopsis thaliana*. Spectrochim. Acta B 61, 1242–1252.

Isaure, M.P., Fraysse, A., Deves, G., Le Lay, P., Fayard, B., Susini, J., Bourguignon, J., Ortega, R., 2006b. Micro-chemical imaging of cesium distribution in *Arabidopsis thaliana* plant and its interaction with potassium and essential trace elements. Biochimie 88, 1583–1590.

Johnston, H.J., Hutchison, G.R., Christensen, F.M., Peters, S., Hankin, S., Stone, V., 2009. Identification of the mechanisms that drive the toxicity of TiO_2 particulates: the contribution of physicochemical characteristics. Part. Fibre Toxicol. 6, 33–60.
Kabata-Pendias, A., Pendias, H., 2001. Trace Elements in Soils and Plants, third ed. Boca Raton, Florida.
Kaiser, J., Galiová, M., Novotný, K., Červenka, R., Reale, L., Novotný, J., Liška, M., Samek, O., Kanický, V., Hrdlička, A., Stejskal, K., Adam, V., Kizek, R., 2009. Mapping of lead, magnesium and copper accumulation in plant tissues by laser-induced breakdown spectroscopy and laser-ablation inductively coupled plasma mass spectrometry. Spectrochim. Acta Part B At. Spectrosc. 64, 67–73.
Kelly, S.D., Hesterberg, D., Ravel, B., 2008. Analysis of soils and minerals using X-ray absorption spectroscopy. In: Ulery, A.L., Drees, L.R. (Eds.), Methods of Soil Analysis, Part 5 – Mineralogical Methods, Soil Science Society of America, Madison, WI, USA.
Kerkeb, L., Kramer, U., 2003. The role of free histidine in xylem loading of nickel in *Alyssum lesbiacum* and *Brassica juncea*. Plant Physiol. 131, 716–724.
Kilburn, M.R., Jones, D.L., Clode, P.L., Cliff, J.B., Stockdale, E.A., Herrmann, A.M., Murphy, D.V., 2010. Application of nanoscale secondary ion mass spectrometry to plant cell research. Plant Signal. Behav. 5, 1–3.
Kim, S.A., Punshon, T., Lanzirotti, A., Li, L.T., Alonso, J.M., Ecker, J.R., Kaplan, J., Guerinot, M.L., 2006. Localization of iron in Arabidopsis seed requires the vacuolar membrane transporter VIT1. Science 314, 1295–1298.
Kirkpatrick, P., Baez, A.V., 1948. Formation of optical images by X-rays. J. Opt. Soc. Am. 38, 766–773.
Klassen, N.V., 1987. Primary products in radiation chemistry. In: Farhatazis, I., Rodgers, M. (Eds.), Radiation Chemistry Principles & Applications, VCH, pp. 29–61.
Klug, B., Specht, A., Horst, W.J., 2011. Aluminium localization in root tips of the aluminium-accumulating plant species buckwheat (Fagopyrum esculentum Moench). J. Exp. Bot. 62, 5453–5462.
Koningsberger, D., Prins, R., 1988. X-ray Absorption: Principles, Applications, Techniques of EXAFS, SEXAFS, and XANES. Wiley, New York.
Kopittke, P., Menzies, N., de Jonge, M., McKenna, B., Donner, E., Webb, R., Paterson, D., Howard, D., Ryan, C., Glover, C., Scheckel, K., Lombi, E., 2011. In situ distribution and speciation of toxic copper, nickel, and zinc in hydrated roots of cowpea. Plant Physiol. 156, 663–673.
Kramer, U., Cotter-Howells, J.D., Charnock, J.M., Baker, A.J.M., Andrew, C., Smith, J., 1996. Free histidine as a metal chelator in plants that accumulate nickel. Nature 379, 635–638.
Kramer, U., Grime, G., Smith, J., Hawes, C., Baker, A., 1997. Micro-PIXE as a technique for studying nickel localization in leaves of the hyperaccumulator plant *Alyssum lesbiacum*. Nucl. Instrum. Methods Phys. Res. B 130, 346–350.
Krzeslowska, M., 2011. The cell wall in plant cell response to trace metals: polysaccharide remodelling and its role in defense strategy. Acta Physiol. Planta. 33, 35–51.
Kumari, M., Khan, S.S., Pakrashi, S., Mukherjee, A., Chandrasekaran, N., 2011. Cytogenetic and genotoxic effects of zinc oxide nanoparticles on root cells of Allium cepa. J. Hazard. Mat. 190, 613–621.
Küpper, H., Gotz, B., Mijovilovich, A., Kupper, F., Meyer-Klaucke, W., 2009. Complexation and toxicity of copper in higher plants. I. Characterization of copper accumulation, speciation, and toxicity in Crassula helmsii as a new copper accumulator. Plant Physiol. 151, 702–714.
Küpper, H., Kroneck, P.M.H., 2005. Heavy metal uptake by plants and cyanobacteria. In: Sigel, A., Sigel, H., Sigel, R. (Eds.), Metal Ions in Biological Systems, vol. 44. Marcel Dekker, New York, pp. 97–142.

Küpper, H., Lombi, E., Zhao, F.J., McGrath, S.P., 2000. Cellular compartmentation of cadmium and zinc in relation to other elements in the hyperaccumulator *Arabidopsis halleri*. Planta 212, 75–84.

Küpper, H., Lombi, E., Zhao, F.J., Wieshammer, G., McGrath, S.P., 2001. Cellular compartmentation of nickel in the hyperaccumulators *Alyssum lesbiacum*, *Alyssum bertolonii* and *Thlaspi goesingense*. J. Exp. Bot. 52, 2291–2300.

Küpper, H., Mijovilovich, A., Meyer-Klaucke, W., Kroneck, P.M.H., 2004. Tissue- and age-dependent differences in the complexation of cadmium and zinc in the cadmium/zinc hyperaccumulator Thlaspi caerulescens (Ganges ecotype) revealed by X-ray absorption spectroscopy. Plant Physiol. 134, 748.

Lane, T.W., Morel, F.M.M., 2000. A biological function for cadmium in marine diatoms. Proc. Natl. Acad. Sci. U S A 97, 4627–4631.

Lanson, B., Marcus, M.A., Fakra, S., Panfili, F., Geoffroy, N., Manceau, A., 2008. Formation of Zn–Ca phyllomanganate nanoparticles in grass roots. Geochim. Cosmochim. Acta 72, 2478–2490.

Lanzirotti, A., Tappero, R., Schulze, D.G., 2010. Practical application of synchrotron-based hard X-ray microprobes in soil sciences. In: Singh, B., Gräfe, M. (Eds.), Developments in Soil Science, vol. 34. Elsevier, pp. 27–72.

Larue, C., Khodja, H., Herlin-Boime, N., Brisset, F., Flank, A.M., Fayard, B., Chaillou, S., Carriere, M., 2011. Investigation of titanium dioxide nanoparticles toxicity and uptake by plants. J. Phys. Conf. 304, 1–7.

Larue, C., Laurette, J., Herlin-Boime, N., Khodja, H., Fayard, B., Flank, A., Brisset, F., Carriere, M. Accumulation, translocation and impact of TiO2 nanoparticles in wheat (*Triticum aestivum* spp.): influence of diameter and crystal phase. Sci. Total. Environ. accepted for publication.

Laurette, J., Larue, C., Mariet, C., Brisset, F., Khodja, H., Bourguignon, J., Carrière, M., 2012. Influence of uranium speciation on its accumulation and translocation in three plant species: oilseed rape, sunflower and wheat. Environ. Exp. Bot. 77, 96–107.

Le Lay, P., Isaure, M.P., Sarry, J.E., Kuhn, L., Fayard, B., Le Bail, J.L., Bastien, O., Garin, J., Roby, C., Bourguignon, J., 2006. Metabolomic, proteomic and biophysical analyses of *Arabidopsis thaliana* cells exposed to a caesium stress. Influence of potassium supply. Biochimie 88, 1533–1547.

LeDuc, D.L., Tarun, A.S., Montes-Bayón, M., Meija, J., Malit, M.F., Wu, C.P., AbdelSamie, M., Chiang, C.-Y., Tagmount, A., de Souza, M.P., Neuhierl, B., Böck, A., Caruso, J., Terry, N., 2004. Overexpression of selenocysteine methyltransferase in Arabidopsis and Indian mustard increases selenium tolerance and accumulation. Plant Physiol. 135, 377–383.

Lee, J., Reeves, R., Brooks, R., Jaffré, T., 1978. The relation between nickel and citric acid in some nickel-accumulating plants. Phytochem 17, 1033–1035.

Lei, M., Wan, X.M., Huang, Z.C., Chen, T.B., Li, X.W., Liu, Y.R., 2012. First evidence on different transportation modes of arsenic and phosphorus in arsenic hyperaccumulator Pteris vittata. Environ. Pollut. 161, 1–7.

Leitenmaier, B., Küpper, H., 2011. Cadmium uptake and sequestration kinetics in individual leaf cell protoplasts of the Cd/Zn hyperaccumulator Thlaspi caerulescens. Plant Cell Environ. 34, 208–219.

Levenson, E., Lerch, P., Martin, M.C., 2008. Spatial resolution limits for synchrotron-based spectromicroscopy in the mid- and near-infrared. J. Synchrotron. Radiat. 15, 323–328.

Li, R.Y., Ago, Y., Liu, W.J., Mitani, N., Feldmann, J., McGrath, S.P., Ma, J.F., Zhao, F.J., 2009. The rice aquaporin Lsi1 mediates uptake of methylated arsenic species. Plant Physiol. 150, 2071–2080.

Lindblom, S.D., Valdez-Barillas, J.R., Fakra, S. C., Marcus, M.A., Wangeline, A.L., Pilon-Smits, E.A.H. Influence of microbial associations on selenium localization and speciation in roots of Astragalus and Stanleya hyperaccumulators. Exp. Environ. Bot. in press. http://dx.doi.org/10.1016/j.envexpbot.2011.12.011.

Liu, W.J., Wood, B.A., Raab, A., McGrath, S.P., Zhao, F.J., Feldmann, J., 2010. Complexation of arsenite with phytochelatins reduces arsenite efflux and translocation from roots to shoots in Arabidopsis. Plant Physiol. 152, 2211–2221.

Liu, W.J., Zhu, Y.G., Hu, Y., Williams, P.N., Gault, A.G., Meharg, A.A., Charnock, J.M., Smith, F.A., 2006. Arsenic sequestration in iron plaque, its accumulation and speciation in mature rice plants (Oryza sativa L.). Environ. Sci. Technol. 40, 5730–5736.

Lobinski, R., Moulin, C., Ortega, R., 2006. Imaging and speciation of trace elements in biological environment. Biochimie 88, 1591–1604.

Lombi, E., de Jonge, M.D., Donner, E., Kopittke, P.M., Howard, D.L., Kirkham, R., Ryan, C.G., Paterson, D., 2011a. Fast x-ray fluorescence microtomography of hydrated biological samples. Plos One 6.

Lombi, E., Scheckel, K., Kempson, I., 2011b. In situ analysis of metal(loid)s in plants: state of the art and artefacts. Environ. Exp. Bot. 72, 3–17.

Lombi, E., Scheckel, K.G., Pallon, J., Carey, A.M., Zhu, Y.G., Meharg, A.A., 2009. Speciation and distribution of arsenic and localization of nutrients in rice grains. New Phytol. 184, 193–201.

Lombi, E., Smith, E., Hansen, T.H., Paterson, D., de Jonge, M.D., Howard, D.L., Persson, D.P., Husted, S., Ryan, C., Schjoerring, J.K., 2011c. Megapixel imaging of (micro)nutrients in mature barley grains. J. Exp. Bot. 62, 273–282.

Lombi, E., Susini, J., 2009. Synchrotron-based techniques for plant and soil science: opportunities, challenges and future perspectives. Plant Soil 320, 1–35.

Lombi, E., Zhao, F.J., Fuhrmann, M., Ma, L.Q., McGrath, S.P., 2002. Arsenic distribution and speciation in the fronds of the hyperaccumulator Pteris vittata. New Phytol. 156, 195–203.

Lopez-Moreno, M.L., de la Rosa, G., Hernandez-Viezcas, J.A., Castillo-Michel, H., Botez, C.E., Peralta-Videa, J.R., Gardea-Torresdey, J.L., 2010a. Evidence of the differential biotransformation and genotoxicity of ZnO and CeO_2 nanoparticles on soybean (Glycine max) plants. Environ. Sci. Technol. 44, 7315–7320.

Lopez-Moreno, M.L., de la Rosa, G., Hernandez-Viezcas, J.A., Peralta-Videa, J.R., Gardea-Torresdey, J.L., 2010b. X-ray absorption spectroscopy (XAS) corroboration of the uptake and storage of CeO_2 nanoparticles and assessment of their differential toxicity in four edible plant species. J. Agric. Food Chem. 58, 3689–3693.

Lu, L.L., Tian, S.K., Yang, X.E., Wang, X.C., Brown, P., Li, T.Q., He, Z.L., 2008. Enhanced root-to-shoot translocation of cadmium in the hyperaccumulating ecotype of Sedum alfredii. J. Exp. Bot. 59, 3203–3213.

Ma, J.F., Ueno, D., Zhao, F.J., McGrath, S.P., 2005. Subcellular localisation of Cd and Zn in the leaves of a Cd-hyperaccumulating ecotype of Thlaspi caerulescens. Planta 220, 731–736.

Ma, J.F., Yamaji, N., Mitani, N., Xu, X.Y., Su, Y.H., McGrath, S.P., Zhao, F.J., 2008. Transporters of arsenite in rice and their role in arsenic accumulation in rice grain. Proc. Natl. Acad. Sci. U S A 105, 9931–9935.

Ma, L.Q., Komar, K.M., Tu, C., Zhang, W.H., Cai, Y., Kennelley, E.D., 2001. A fern that hyperaccumulates arsenic. Nature 409, 579.

Ma, Y., He, X., Zhang, P., Zhang, Z., Guo, Z., Tai, R., Xu, Z., Zhang, L., Ding, Y., Zhao, Y., Chai, Z., 2011. Phytoxicity and biotransformation of La_2O_3 nanoparticles in a terrestrial plant cucumber (Cucumis sativus). Nanotoxicology 5, 743–753.

Malan, H.L., Mesjasz-Przybylowicz, J., Przybylowicz, W.J., Farrant, J.M., Linder, P.W., 2012. Distribution patterns of the metal pollutants Cd and Ni in soybean seeds. Nucl. Instrum. Methods Phys. Res. B 273, 157–160.

Malinowski, E., 1978. Theory of error for target factor analysis with applications to mass spectrometry and nuclear magnetic resonance spectrometry. Anal. Chim. Acta 103, 359–363.

Manceau, A., Lanson, B., Schlegel, M.L., Hargé, J.C., Musso, M., Eybert-Bérard, L., Hazemann, J.L., Chateigner, D., Lamble, G.M., 2000. Quantitative Zn speciation in smelter-contaminated soils by EXAFS spectroscopy. Am. J. Sci. 300, 289–343.
Manceau, A., Marcus, M.A., Tamura, N., 2002. Quantitative speciation of heavy metals in soils and sediments by synchrotron X-ray techniques. In: Fenter, P., Rivers, M., Sturchio, N., Sutton, S. (Eds.), Applications of Synchrotron Radiation in Low-temperature Geochemistry and Environmental Science, Reviews in Mineralogy and Geochemistry, vol. 49. Mineralogical Society of America, Washington, DC, pp. 341–428.
Manceau, A., Nagy, K.L., Marcus, M.A., Lanson, M., Geoffroy, N., Jacquet, T., Kirpichtchikova, T., 2008. Formation of metallic copper nanoparticles at the soil-root interface. Environ. Sci. Technol. 42, 1766–1772.
Marcus, M.A., 2010. X-ray photon-in/phton-out methods for chemical imaging. Trends Anal. Chem. 29, 508–517.
Marmiroli, M., Gonnelli, C., Maestri, E., Gabbrielli, R., Marmiroli, N., 2004. Localisation of nickel and mineral nutrients Ca, K, Fe, Mg by scanning electron microscopy microanalysis in tissues of the nickel-hyperaccumulator Alyssum bertolonii desv. and the non-accumulator Alyssum montanum L. Plant Biosyst. 138, 231–243.
Marschner, H., 1995. Mineral Nutrition of Higher Plants, second ed. Academic press, London.
Marshall, A.T., Haverkamp, R.G., Davies, C.E., Parsons, J.G., Gardea-Torresdey, J.L., Agterveld, D.V., 2007. Accumulation of gold nanoparticles in Brassica juncea. Int. J. Phytoremed. 9, 197–206.
Martin, M.C., Holman, H.Y.N., 2006. Synchrotron radiation infrared spectromicroscopy: a non invasive chemical probe for monitoring biogeochemical processes. Adv. Agron. 90, 79–127.
Martinez-Criado, G., Tucoulou, R., Cloetens, P., Bleuet, P., Bohic, S., Cauzid, J., Kieffer, I., Kosior, E., Laboure, S., Petitgirard, S., Rack, A., Sans, J.A., Segura-Ruiz, J., Suhonen, H., Susini, J., Villanova, J., 2012. Status of the hard X-ray microprobe beamline ID22 of the European synchrotron radiation facility. J. Synchrotron. Radiat. 19, 10–18.
McDonald, K., 2007. Cryopreparation methods for electron microscopy of selected model systems. Meth. Cell Biol. 79, 23–56.
McGrath, S., Zhao, F., Lombi, E., 2002. Phytoremediation of metals, metalloids, and radionuclides. Adv. Agron. 75, 1–56.
McNear, D., Peltier, E., Everhart, J., Chaney, R., Sutton, S., Newville, S., Rivers, M., Sparks, D.L., 2005. Application of quantitative fluorescence and absorption-edge computed microtomography to image metal compartmentalization in *Alyssum murale*. Environ. Sci. Technol. 39, 2210–2218.
McNear, D.H., Chaney, R.L., Sparks, D., 2010. The hyperaccumulator *Alyssum murale* uses complexation with nitrogen and oxygen donor ligands for Ni transport and storage. Phytochem 71, 188–200.
McRae, R., Bagchi, P., Sumalekshmy, S., Fahrni, C.J., 2009. In situ imaging of metals in cells and tissues. Chem. Rev. 109, 4780–4827.
Meharg, A.A., Lombi, E., Williams, P.N., Scheckel, K.G., Feldmann, J., Raab, A., Zhu, Y.G., Islam, R., 2008. Speciation and localization of arsenic in white and brown rice grains. Environ. Sci. Technol. 42, 1051–1057.
Meharg, A.A., Zhao, F.J., 2012. Arsenic & Rice. Springer, Dordrecht.
Memon, A.R., Chino, M., Takeoka, Y., Hara, K., Yatazawa, M., 1980. Distribution of manganese in leaf tissues of manganese accumulator – Acanthopanax Sciadophylloides as revealed by electronprobe X-ray microanalyzer. J. Plant Nutr. 2, 457–476.
Mesjasz Przybylowicz, J., Przybylowicz, W.J., 2002. Micro-PIXE in plant sciences: present status and perspectives. Nucl. Instrum. Methods Phys. Res. B 189, 470–481.

Metzner, R., Schneider, H.U., Breuer, U., Schroeder, W.H., 2008. Imaging nutrient distributions in plant tissue using time-of-flight secondary ion mass spectrometry and scanning electron microscopy. Plant Physiol. 147, 1774–1787.
Metzner, R., Schneider, H.U., Breuer, U., Thorpe, M.R., Schurr, U., Schroeder, W.H., 2010. Tracing cationic nutrients from xylem into stem tissue of French bean by stable isotope tracers and cryo-secondary ion mass spectrometry. Plant Physiol. 152, 1030–1043.
Mijovilovich, A., Leitenmaier, B., Meyer-Klaucke, W., Kroneck, P.M.H., Gotz, B., Kupper, H., 2009. Complexation and toxicity of copper in higher plants. II. Different mechanisms for copper versus cadmium detoxification in the copper-sensitive Cadmium/Zinc hyperaccumulator Thlaspi caerulescens (Ganges ecotype). Plant Physiol. 151, 715–731.
Minguzzi, C., Vergnano, O., 1984. Il contenuto di nichel nell ceneri di Alyssum bertolonii Desv. Mem. Soc. Tosc. Sci. Nat. A 55, 49–77.
Miot, J., Benzerara, K., Obst, M., Kappler, A., Hegler, F., Schadler, S., Bouchez, C., Guyot, F., Morin, G., 2009. Extracellular iron biomineralization by Photoautotrophic iron-oxidizing bacteria. Appl. Environ. Microbiol. 75, 5586–5591.
Mokgalaka, N., Gardea-Torresdey, J.L., 2006. Laser ablation inductively coupled plasma mass spectrometry: principles and applications. Appl. Spectros. Rev. 41, 131–150.
Momose, A., Takeda, T., Itai, Y., Hirano, K., 1996. Phase-contrast X-ray computed tomography for observing biological soft tissues. Nat. Med. 2, 473–475.
Montarges-Pelletier, E.V., Chardot, V., Echevarria, G., Michot, L., Bauer, A., Morel, J., 2008. Identification of nickel chelators in three hyperaccumulating plants: an X-ray spectroscopic study. Phytochemistry 69, 1695–1709.
Montes-Holguin, M.O., Peralta-Videa, J.R., Meitzner, G., Martinez-Martinez, A., De la Rosa, G., Castillo-Michel, H.A., Gardea-Torresdey, J.L., 2006. Biochemical and spectroscopic studies of the responses of Convolvulus arvensis L. to chromium(III) and chromium (VI) stress. Environ. Toxicol. Chem. 25, 220–226.
Moore, K.L., Lombi, E., Zhao, F.J., Grovenor, C.R.M., 2012. Elemental imaging at the nanoscale: NanoSIMS and complementary techniques for element localisation in plants. Anal. Bioanal. Chem. 402, 3263–3273.
Moore, K.L., Schroder, M., Lombi, E., Zhao, F.J., McGrath, S.P., Hawkesford, M.J., Shewry, P.R., Grovenor, C.R.M., 2010. NanoSIMS analysis of arsenic and selenium in cereal grain. New Phytol. 185, 434–445.
Moore, K.L., Schröder, M., Wu, Z.C., Martin, B.G.H., Hawes, C.R., McGrath, S.P., Hawkesford, M.J., Ma, J.F., Zhao, F.J., Grovenor, C.R.M., 2011. NanoSIMS analysis reveals contrasting patterns of arsenic and silicon localization in rice roots. Plant Physiol. 156, 913–924.
Moradi, A.B., Swoboda, S., Robinson, B., Prohaska, T., Kaestner, A., Oswald, S.E., Wenzel, W.W., Schulin, R., 2010. Mapping of nickel in root cross-sections of the hyperaccumulator plant Berkheya coddii using laser ablation ICP-MS. Environ. Exp. Bot. 69, 24–31.
Morel, M., Crouzet, J., Gravot, A., Auroy, P., Leonhardt, N., Vavasseur, A., Richaud, P., 2009. AtHMA3, a P-1b-ATPase allowing Cd/Zn/Co/Pb vacuolar storage in Arabidopsis. Plant Physiol. 149, 894–904.
Naftel, S.J., Martin, R.R., Macfie, S.M., Courchesne, F., Seguin, V., 2007. An investigation of metals at the soil/root interface using synchrotron radiation analysis. Can. J. Anal. Sci. Spectros. 52, 18–24.
Nair, R., Poulose, A.C., Nagaoka, Y., Yoshida, Y., Maekawa, T., Kumar, D.S., 2011. Uptake of FITC Labeled Silica nanoparticles and quantum dots by rice seedlings: effects on seed germination and their potential as biolabels for plants. J. Fluoresc. 21, 2057–2068.
Narewski, U., Werner, G., Schulz, H., Vogt, C., 2000. Application of laser ablation inductively coupled mass spectrometry (LA-ICP-MS) for the determination of major, minor, and trace elements in bark samples. Fresenius J. Anal. Chem. 366, 167–170.

Navarro, D., Bisson, M., Aga, D., 2012. Investigating uptake of water-dispersible CdSe/ZnS quantum dot nanoparticles by *Arabidopsis thaliana* plants. J. Hazard. Mater. 211–212, 427–435.
Nel, A., Xia, T., Madler, L., Li, N., 2006. Toxic potential of materials at the nanolevel. Science 311, 622–627.
Neuhierl, B., Böck, A., 1996. On the mechanism of selenium tolerance in selenium-accumulating plants: purification and characterization of a specific selenocysteine methyltransferase from cultured cells of *Astragalus bisulcatus*. Eur. J. Biochem. 239, 235–238.
Oomen, R., Seveno-Carpentier, E., Ricodeau, N., Bournaud, C., Conejero, G., Paris, N., Berthomieu, P., Marques, L., 2011. Plant defensin AhPDF1.1 is not secreted in leaves but it accumulates in intracellular compartments. New Phytol. 192, 140–150.
Orłowska, E., Przybyłowicz, W., Orlowski, D., Turnau, K., Mesjasz-Przybyłowicz, J., 2011. The effect of mycorrhiza on the growth and elemental composition of Ni-hyperaccumulating plant Berkheya coddii Roessler. Environ. Pollut. 159, 3730–3738.
Ortega, R., Devès, G., Carmona, A., 2009. Bio-metals imaging and speciation in cells using proton and synchrotron radiation X-ray microspectroscopy. J. R. Soc. Interface 6, S649–S658.
Parsons, J.G., Peralta-Videa, J.R., Gardea-Torresdey, J.L., 2007. Chapter 21 Use of plants in biotechnology: synthesis of metal nanoparticles by inactivated plant tissues, plant extracts, and living plants. Concepts Appl. Environ. Geochem. 5, 463–485.
Pathan, A.K., Bond, J., Gaskin, R.E., 2008. Sample preparation for scanning electron microscopy of plant surfaces-Horses for courses. Micron 39, 1049–1061.
Pathan, A.K., Bond, J., Gaskin, R.E., 2010. Sample preparation for SEM of plant surfaces. Mater. Today 12, 32–43.
Pelosi, P., Fiorentini, R., Galoppini, C., 1976. On the nature of nickel compound in Alyssum bertolonii Desv. II. Agric. Biol. Chem. 40, 1641–1642.
Pickering, I., Hirsch, G., Prince, R., Sneeden, E., Salt, D., George, G., 2003. Imaging of selenium in plants using tapered metal monocapillary optics. J. Synchrotron. Radiat. 10, 289–290.
Pickering, I., Prince, R., Salt, D., George, G., 2000a. Quantitative, chemically specific imaging of selenium transformation in plants. Proc. Natl. Acad. Sci. U S A 97, 10717–10722.
Pickering, I.J., Gumaelius, L., Harris, H.H., Prince, R.C., Hirsch, G., Banks, J.A., Salt, D.E., George, G.N., 2006. Localizing the biochemical transformations of arsenate in a hyperaccumulating fern. Environ. Sci. Technol. 40, 5010–5014.
Pickering, I.J., Prince, R.C., George, G.N., Rauser, W.E., Wickramasinghe, W.A., Watson, A.A., Dameron, C.T., Dance, I.G., Fairlie, D.P., Salt, D.E., 1999. X-ray absorption spectroscopy of cadmium phytochelatin and model systems. Biochim. Biophys. Acta 1429, 351–364.
Pickering, I.J., Prince, R.C., George, M.J., Smith, R.D., George, G.N., Salt, D.E., 2000b. Reduction and coordination of arsenic in Indian mustard. Plant Physiol. 122, 1171–1177.
Pilon-Smits, E.A.H., Hwang, S.B., Lytle, C.M., Zhu, Y.L., Tai, J.C., Bravo, R.C., Chen, Y.C., Leustek, T., Terry, N., 1999. Overexpression of ATP sulfurylase in Indian mustard leads to increased selenate uptake, reduction, and tolerance. Plant Physiol. 119, 123–132.
Pilon-Smits, E.A.H., Quinn, C.F., 2010. Selenium metabolism in plants. In: Hell, R., Mendel, R. (Eds.), Cell Biology of Metals and Nutrients, vol. 17. Springer, Heidelberg, pp. 225–241.
Pilon-Smits, E.A.H., Quinn, C.F., Tapken, W., Malagoli, M., Schiavon, M., 2009. Physiological functions of beneficial elements. Curr. Opin. Plant Biol. 12, 267–274.
Polatajko, A., Azzolini, M., Feldmann, I., Stuezel, T., Jakubowski, N., 2007. Laser ablation-ICP-MS assay development for detecting Cd- and Zn-binding proteins in Cd-exposed Spinacia oleracea L. J. Anal. At. Spectrom. 22, 878–887.

Polette, L., Gardea-Torresdey, J.L., Chianelli, R., George, G.N., Pickering, I.J., Arenas, J., 2000. XAS and microscopy studies of the uptake and bio-transformation of copper in Larrea tridentata (creosote bush). Microchem. J. 65, 227.

Pongrac, P., Vogel-Mikus, K., Vavpetic, P., Tratnik, J., Regvar, M., Simsic, J., Grlj, N., Pelicon, P., 2010. Cd induced redistribution of elements within leaves of the Cd/Zn hyperaccumulator Thlaspi praecox as revealed by micro-PIXE. Nucl. Instrum. Methods Phys. Res. B.

Prohaska, T., Stadlbauer, C., Wimmer, R., Stingeder, G., Latkoczy, C., Hoffmann, E., Stephanowitz, H., 1998. Investigation of element variability in tree rings of young Norway spruce by laser-ablation-ICPMS. Sci. Total. Environ. 219, 29–39.

Psaras, G., Constantinidis, T., Cotsopoulos, B., Manetas, Y., 2000. Relative abundance of nickel in the leaf epidermis of eight hyperaccumulators: evidence that the metal is excluded from both guard cells and trichomes. Ann. Bot. 86 (1), 73–78.

Punshon, T., Bertsch, P.M., Lanzirotti, A., McLeod, K., Burger, J., 2003. Geochemical signature of contaminated sediment remohilization revealed by spatially resolved X-ray microanalysis of annual rings of Salix nigra. Environ. Sci. Technol. 37, 1766–1774.

Punshon, T., Guerinot, M., Lanzirotti, A., 2009. Using synchrotron X-ray fluorescence microprobes in the study of metal homeostasis in plants. Ann. Bot. 103, 665–672.

Punshon, T., Jackson, B.P., Bertsch, P.M., Burger, J., 2004. Mass loading of nickel and uranium on plant surfaces: application of laser ablation-ICP-MS. J. Environ. Monit. 6, 153–159.

Punshon, T., Lanzirotti, A., Harper, S., Bertsch, P.M., Burger, J., 2005. Distribution and speciation of metals in annual rings of black willow. J. Environ. Qual. 34, 1165–1173.

Quinn, C.F., Prins, C.N., Freeman, J.L., Gross, A.M., Hantzis, L.J., Reynolds, R.J.B., Yang, S.I., Covey, P.A., Banuelos, G.S., Pickering, I.J., Fakra, S.C., Marcus, M.A., Arathi, H.S., Pilon-Smits, E.A.H., 2011. Selenium accumulation in flowers and its effects on pollination. New Phytol. 192, 727–737.

Raab, A., Schat, H., Meharg, A.A., Feldmann, J., 2005. Uptake, translocation and transformation of arsenate and arsenite in sunflower (*Helianthus annuus*): formation of arsenic-phytochelatin complexes during exposure to high arsenic concentrations. New Phytol. 168, 551–558.

Raab, A., Williams, P.N., Meharg, A., Feldmann, J., 2007. Uptake and translocation of inorganic and methylated arsenic species by plants. Environ. Chem. 4, 197–203.

Raab, T.K., Vogel, J.P., 2004. Ecological and agricultural applications of synchrotron IR microscopy. Infrared Phys. Tech. 45, 393–402.

Ravel, B., Newville, M., 2005. ATHENA and ARTEMIS: interactive graphical data analysis using IFEFFIT. J. Synchrotron. Radiat. 12, 537–541.

Reinert, T., Fiedler, A., Morawski, M., Arendt, T., 2007. High resolution quantitative element mapping of neuromelanin-containing neurons. Nuclear Instrum. Methods Phys. Res. B 260, 227–230.

Richau, K., Kozhevnikova, A., Seregin, I., Vooijs, R., Koevoets, P.L.M., Smith, A., Ivanov, V., Schat, H., 2009. Chelation by histidine inhibits the vacuolar sequestration of nickel in roots of the hyperaccumulator Thlaspi caerulescens. New Phytol.10.1111/j.1469-8137.2009.02826.x.

Rico, C.M., Majumdar, S., Duarte-Gardea, M., Peralta-Videa, J.R., Gardea-Torresdey, J.L., 2011. Interaction of nanoparticles with edible plants and their possible implications in the food chain. J. Agric. Food Chem. 59, 3485–3498.

Roschzttardtz, H., Grillet, L., Isaure, M.P., Conejero, G., Ortega, R., Curie, C., Mari, S., 2011. Plant cell nucleolus as a hot spot for iron. J. Biol. Chem. 286, 27863–27866.

Ross, D.S., Hales, H., Shea-McCarthy, G., Lanzirotti, A., 2001. Sensitivity of soil manganese oxides: XANES spectroscopy may cause reduction. Soil Sci. Soc. Am. J. 65, 744–752.

Sabo-Attwood, T., Unrine, J., Stone, J., Murphy, C., Ghoshroy, S., Blom, D., Bertsch, P.M., Newman, L.A., 2011. Uptake, distribution and toxicity of gold nanoparticles in tobacco (*Nicotiana xanth*) seedlings. Nanotoxicology 5, 1–8.

Sakai, T., Oikawa, M., Sato, T., Nagamine, T., Moon, H.D., Nakazato, K., Suzuki, K., 2005. New in-air micro-PIXE system for biological applications. Nucl. Instrum. Methods Phys. Res. B 231, 112–116.

Salt, D.E., Pickering, I.J., Prince, R.C., Gleba, D., Dushenkov, S., Smith, R.D., Raskin, I., 1997. Metal accumulation by aquacultured seedlings of Indian mustard. Environ. Sci. Technol. 31, 1636–1644.

Salt, D.E., Prince, R.C., Baker, A.M., Raskin, I., Pickering, I.J., 1999. Zinc ligands in the metal hyperaccumulator Thlaspi caerulescens as determined using X-ray absorption absorption spectroscopy. Environ. Sci. Technol. 33, 713–717.

Salt, D.E., Prince, R.C., Pickering, I.J., 1995. Mechanisms of cadmium mobility and accumulation in Indian mustard. Plant Physiol. 109, 1427–1433.

Salt, D.E., Prince, R.C., Pickering, I.J., 2002. Chemical speciation of accumulated metals in plants: evidence from X-ray absorption spectroscopy. Microchem. J. 71, 255–259.

Santner, J., Zhang, H., Leitner, D., Schnepf, A., Prohaska, T., Puschenreiter, M., Wenzel, W.W., 2012. High-resolution chemical imaging of labile phosphorus in the rhizosphere of Brassica napus L. cultivars. Environ. Exp. Bot. 77, 219–226.

Sarret, G., Balesdent, J., Bouziri, L., Garnier, J.M., Marcus, M.A., Geoffroy, N., Panfili, F., Manceau, A., 2004. Zn speciation in the organic horizon of a contaminated soil by micro X-ray fluorescence, micro and powder EXAFS spectroscopy and isotopic dilution. Environ. Sci. Technol. 38, 2792–2801.

Sarret, G., Harada, E., Choi, Y.E., Isaure, M.P., Geoffroy, N., Birschwilks, M., Clemens, S., Fakra, S., Marcus, M.A., Manceau, A., 2006. Trichomes of tobacco excrete zinc as Zn-substituted calcium carbonate and other Zn-containing compounds. Plant Physiol. 141, 1021–1034.

Sarret, G., Isaure, M., Marcus, M., Harada, E., Choi, Y., Pairis, S., Fakra, S., Manceau, A., 2007. Chemical forms of calcium in Ca, Zn- and Ca, Cd-containing grains excreted by tobacco trichomes. Can. J. Chem. 85, 738–746.

Sarret, G., Saumitou-Laprade, P., Bert, V., Proux, O., Hazemann, J.L., Traverse, A., Marcus, M.A., Manceau, A., 2002. Forms of zinc accumulated in the hyperaccumulator *Arabidopsis halleri*. Plant Physiol. 130, 1815–1826.

Sarret, G., Willems, G., Isaure, M.P., Marcus, M.A., Fakra, S., Frérot, H., Pairis, S., Geoffroy, N., Manceau, A., Saumitou-Laprade, P., 2009. Zn localization and speciation in *Arabidopsis halleri* x *Arabidopsis lyrata* progenies presenting various Zn accumulation capacities. New Phytol. 184, 581–595.

Scheckel, K.G., Hamon, R., Jassogne, L., Rivers, M., Lombi, E., 2007. Synchrotron X-ray absorption-edge computed microtomography imaging of thallium compartmentalization in Iberis intermedia. Plant Soil 290, 51–60.

Scheckel, K.G., Lombi, E., Rock, S.A., McLaughlin, N.J., 2004. In vivo synchrotron study of thallium speciation and compartmentation in lberis intermedia. Environ. Sci. Technol. 38, 5095–5100.

Schroer, C.G. 2001. Reconstructing X-ray fluorescence microtomograms. Appl. Phys. Lett. 79, 1912–1914.

Seyfferth, A.L., Webb, S.M., Andrews, J.C., Fendorf, S., 2010. Arsenic localization, speciation, and co-occurrence with iron on rice (*Oryza sativa* L.) roots having variable Fe coatings. Environ. Sci. Technol. 44, 8108–8113.

Shi, J., Gras, M.A., Silk, W.K., 2009. Laser ablation ICP-MS reveals patterns of copper differing from zinc in growth zones of cucumber roots. Planta 229, 945–954.

Shi, J.Y., Yuan, X.F., Chen, X.C., Wu, B., Huang, Y.Y., Chen, Y.X., 2011. Copper uptake and its effect on metal distribution in root growth zones of Commelina communis revealed by SRXRF. Biol. Trace. Elem. Res. 141, 294–304.

Sinclair, S.A., Sherson, S.M., Jarvis, R., Camakaris, J., Cobbett, C.S., 2007. The use of the zinc-fluorophore, Zinpyr-1, in the study of zinc homeostasis in Arabidopsis roots. New Phytol. 174, 39–45.

Smart, K.E., Kilburn, M.R., Salter, C.J., Smith, J.A.C., Grovenor, C.R.M., 2007. NanoSIMS and EPMA analysis of nickel localisation in leaves of the hyperaccumulator plant *Alyssum lesbiacum*. Int. J. Mass Spectrom. 260, 107–114.
Smart, K.E., Smith, J.A.C., Kilburn, M.R., Martin, B.G.H., Hawes, C., Grovenor, C.R.M., 2010. High-resolution elemental localization in vacuolate plant cells by nanoscale secondary ion mass spectrometry. Plant J. 63, 870–879.
Smith, P.G., Koch, I., Reimer, K.J., 2008. Uptake, transport and transformation of arsenate in radishes (*Raphanus sativus*). Sci. Total Environ. 390, 188–197.
Solé, V., Papillon, E., Cotte, M., Walter, P., Susini, J., 2007. PyMCA: a multiplatform code for the analysis of energy-dispersive X-ray fluorescence spectra. Spectrochim. Acta B 62, 63–68.
Song, W.Y., Park, J., Mendoza-Cozatl, D.G., Suter-Grotemeyer, M., Shim, D., Hortensteiner, S., Geisler, M., Weder, B., Rea, P.A., Rentsch, D., Schroeder, J.I., Lee, Y., Martinoia, E., 2010. Arsenic tolerance in Arabidopsis is mediated by two ABCC-type phytochelatin transporters. Proc. Natl. Acad. Sci. U S A 107, 21187–21192.
Sors, T.G., Ellis, D.R., Salt, D.E., 2005. Selenium uptake, translocation, assimilation and metabolic fate in plants. Photosyn. Res. 86, 373–389.
Stöhr, J., 1992. NEXAFS Spectroscopy. Springer-Verlag, New York.
Su, Y.H., McGrath, S.P., Zhu, Y.G., Zhao, F.J., 2008. Highly efficient xylem transport of arsenite in the arsenic hyperaccumulator Pteris vittata. New Phytol. 180, 434–441.
Sun, G.X., Williams, P.N., Carey, A.M., Zhu, Y.G., Deacon, C., Raab, A., Feldmann, J., Islam, R.M., Meharg, A.A., 2008. Inorganic arsenic in rice bran and its products are an order of magnitude higher than in bulk grain. Environ. Sci. Technol. 42, 7542–7546.
Sutton, S., Bajt, S., Delaney, J., Schulze, D., Tokunaga, T., 1995. Synchrotron X-ray fluorescence microprobe: quantification and mapping of mixed valence state samples using micro-XANES. Rev. Sci. Instrum. 66, 1464–1467.
Sutton, S.R., Bertsch, P.M., Newville, M., Rivers, M., Lanzirotti, A., Eng, P., 2002. Microfluorescence and microtomography analysis of heterogeneous earth and environmental materials. Rev. Mineral. Geochem. 49, 429–483.
Takahashi, M., Nozoye, T., Kitajima, N., Fukuda, N., Hokura, A., Terada, Y., Nakai, I., Ishimaru, Y., Kobayashi, T., Nakanishi, H., Nishizawa, N.K., 2009. In vivo analysis of metal distribution and expression of metal transporters in rice seed during germination process by microarray and X-ray fluorescence imaging of Fe, Zn, Mn, and Cu. Plant Soil 325, 39–51.
Tappero, R., 2008. Microspectroscopic Study of Cobalt Speciation and Localization in Hyperaccumulator *Alyssum murale*. University of Delaware, Newark, DE.
Tappero, R., Peltier, E., Grafe, M., Heidel, K., Ginder-Vogel, M., Livi, K., Rivers, M., Marcus, M., Chaney, R., Sparks, D., 2007. Hyperaccumulator *Alyssum murale* relies on a different metal storage mechanism for cobalt than for nickel. New Phytol. 175, 641–654.
Teo, B.K., 1986. EXAFS: Basic Principles and Data Analysis. Springer-Verlag, Berlin.
Terzano, R., Al Chami, Z., Vekemans, B., Janssens, K., Miano, T., Ruggiero, P., 2008. Zinc distribution and speciation within rocket plants (Eruca vesicaria L. Cavalieri) grown on a polluted soil amended with compost as determined by XRF microtomography and Micro-XANES. J. Agric. Food Chem. 56, 3222–3231.
Tian, S., Lu, L.J.L., Yang, X., He, Z., Hu, H., Sarangi, R., Newville, M., Commisso, J., Brown, P., 2011. Cellular sequestration of cadmium in the hyperaccumulator plant species Sedum alfredii. Plant Physiol. 157, 1914–1925.
Tian, S., Lu, L., Yang, X., Webb, S., Du, Y., Brown, P., 2010. Spatial imaging and speciation of lead in the accumulator plant Sedum alfredii by microscopically focused synchrotron X-ray investigation. Environ. Sci. Technol. 44, 5920–5926.
Tobin, M.J., Puskar, L., Barber, R.L., Harvey, E.C., Heraud, P., Wood, B.R., Bambery, K.R., Dillon, C.T., Munro, K.L., 2010. FTIR spectroscopy of single live cells in aqueous media by synchrotron IR microscopy using microfabricated sample holders. Vib. Spectros. 53, 34–38.

Tokunaga, T.K., Wan, J.M., Firestone, M.K., Hazen, T.C., Olson, K.R., Herman, D.J., Sutton, S.R., Lanzirotti, A., 2003. In situ reduction of chromium(VI) in heavily contaminated soils through organic carbon amendment. J. Environ. Qual. 32, 1641–1649.
Tylko, G., Mesjasz-Przybylowicz, J., Przybylowicz, W.J., 2007a. In-vacuum micro-PIXE analysis of biological specimens in frozen-hydrated state. Nucl. Instrum. Meth. Phys. Res. B 260, 141–148.
Tylko, G., Mesjasz-Przybylowicz, J., Przybylowicz, W.J., 2007b. X-ray microanalysis of biological material in the frozen-hydrated state by PIXE. Microsc. Res. Tech. 70, 55–68.
Ueno, D., Ma, J.F., Iwashita, T., Zhao, F.J., McGrath, S.P., 2005. Identification of the form of Cd in the leaves of a superior Cd-accumulating ecotype of Thlaspi caerulescens using Cd-113-NMR. Planta 221, 928–936.
Van Hoewyk, D., Garifullina, G.F., Ackley, A.R., Abdel Ghany, S.E., Marcus, M.A., Fakra, S., Ishiyama, K., Inoue, E., Pilon, M., Takahashi, H., Pilon Smits, E.A.H., 2005. Overexpression of AtCpNifS enhances selenium tolerance and accumulation in Arabidopsis. Plant Physiol 139, 1518–1528.
Verbruggen, N., Hermans, C., Schat, H., 2009. Molecular mechanisms of metal hyperaccumulation in plants. New Phytol. 181, 759–776.
Vogel-Mikus, K., Arcon, I., Kodre, A., 2010. Complexation of cadmium in seeds and vegetative tissues of the cadmium hyperaccumulator Thlaspi praecox as studied by X-ray absorption spectroscopy. Plant Soil 331, 439–451.
Vogel-Mikus, K., Regvar, M., Mesjasz-Przybylowicz, J., Przybylowicz, W.J., Simcic, J., Pelicon, P., Budnar, M., 2008. Spatial distribution of cadmium in leaves of metal hyperaccumulating Thlaspi praecox using micro-PIXE. New Phytol. 179, 712–721.
Vogt, S., Jacobsen, C., LeFurgey, A., Kopf, D., Lai, B., Ingram, P., Maser, J., 2005. Mapping 3D X-ray fluorescence datasets to elemental distributions using principle component analysis and fitting. Microsc. Microanal. 11, 430–431.
Vogt, S., Maser, J., Jacobsen, C., 2003. Data analysis for X-ray fluorescence imaging. J. Phys. IV France 104, 617–622.
Wang, H.H., Kou, X.M., Pei, Z.G., Xiao, J.Q., Shan, X.Q., Xing, B.S., 2011a. Physiological effects of magnetite (Fe(3)O(4)) nanoparticles on perennial ryegrass (*Lolium perenne* L.) and pumpkin (*Cucurbita mixta*) plants. Nanotoxicology 5, 30–42.
Wang, Y.X., Specht, A., Horst, W.J., 2011b. Stable isotope labelling and zinc distribution in grains studied by laser ablation ICP-MS in an ear culture system reveals zinc transport barriers during grain filling in wheat. New Phytol. 189, 428–437.
Wangeline, A.L., Reeves, F.B., 2007. Two new Alternaria species from selenium-rich habitats in the Rocky Mountain Front Range. Mycotaxon 99, 83–89.
Wangeline, A.L., Valdez, J.R., Lindblom, S.D., Bowling, K.L., Reeves, F.B., Pilon-Smits, E.A.H., 2011. Selenium tolerance in rhizosphere fungi from Se hyperaccumulator and non-hyperaccumulator plants. Am. J. Bot. 98, 1139–1147.
Wasserman, S.R., 1997. The analysis of mixtures: application of principal component analysis to XAS spectra. J. Phys. IV 7, 203–205.
Wasserman, S.R., Allen, P.G., Shuh, D.K., Bucher, J.J., Edelstein, N.M., 1999. EXAFS and principal component analysis: a new shell game. J. Synchrotron. Radiat. 6, 284–286.
Watmough, S.A., Hutchinson, T.C., Evans, R.D., 1998. Development of solid calibration standards for trace elemental analyses of tree rings by laser ablation inductively coupled plasma-mass spectrometry. Environ. Sci. Technol. 32, 2185–2190.
Webb, S., 2007. SixPACK (Sam's Interface for XAS Package). Available at Stanford Synchrotron Radiation Source, Stanford, CA (accessed 20.03.12.). http://sixpack.sams-xrays.com/.
Webb, S.M., Gaillard, J.F., Ma, L.Q., Tu, C., 2003. XAS speciation of arsenic in a hyperaccumulating fern. Environ. Sci. Technol. 37, 754–760.
Wei, W.Z., Wei, Z., Wang, Y., Baker, A., Zhao, H., Li, H., Hu, F., 2010. Simultaneous determination of organic acids and nitrate in xylem saps of the hyperaccumulator *Alyssum*

murale by RP-HPLC after solid-phase extraction with nanosized hydroxyapatite. J. Chromatogr. Sci. 48, 840–847.
Wei, Z.L., Dong, L., Tian, Z.H., 2009. Fourier transform infrared spectrometry study on early stage of cadmium stress in clover leaves. Pak. J. Bot. 41, 1743–1750.
Wellenreuther, G., Cianci, M., Tucoulou, R., Meyer-Klaucke, W., Haase, H., 2009. The ligand environment of zinc stored in vesicles. Biochem. Biophys. Res. Commun. 380, 198–203.
Wilson, R.G., 1995. SIMS quantification in Si, GaAs, and diamond – an update. Int. J. Mass. Spectrom. Ion. Process. 143, 43–49.
Wu, B., Susnea, I., Chen, Y., Przybylski, M., Becker, J.S., 2011. Study of metal-containing proteins in the roots of Elsholtzia splendens using LA-ICP-MS and LC-tandem mass spectrometry. Int. J. Mass Spectrom. 307, 85–91.
Wu, B., Zoriy, M., Chen, Y., Becker, J.S., 2009. Imaging of nutrient elements in the leaves of Elsholtzia splendens by laser ablation inductively coupled plasma mass spectrometry (LA-ICP-MS). Talanta 78, 132–137.
Wu, J., Hsu, F., Cunningham, S., 1999. Chelate-assisted Pb phytoextraction: Pb availability, uptake, and translocation constraints. Environ. Sci. Technol. 33 (11), 1898–1904.
Xia, T., Kovochich, M., Liong, M., Madler, L., Gilbert, B., Shi, H.B., Yeh, J.I., Zink, J.I., Nel, A.E., 2008. Comparison of the mechanism of toxicity of zinc oxide and cerium oxide nanoparticles based on dissolution and oxidative stress properties. Acs Nano 2, 2121–2134.
Xu, X., Shi, J., Chen, X., Chen, Y., Hu, T., 2009. Chemical forms of manganese in the leaves of manganese hyperaccumulator Phytolacca acinosa Roxb. (Phytolaccaceae). Plant Soil 318, 197–204.
Xu, X.H., Shi, J.Y., Chen, Y.X., Xue, S.G., Wu, B., Huang, Y.Y., 2006. An investigation of cellular distribution of manganese in hyperaccumlator plant Phytolacca acinosa Roxb. using SRXRF analysis. J. Environ. Sci. (China) 18, 746–751.
Xu, X.Y., McGrath, S.P., Zhao, F.J., 2007. Rapid reduction of arsenate in the medium mediated by plant roots. New Phytol. 176, 590–599.
Ye, W.L., Wood, B.A., Stroud, J.L., Andralojc, P.J., Raab, A., McGrath, S.P., Feldmann, J., Zhao, F.J., 2010. Arsenic speciation in phloem and xylem exudates of castor bean. Plant Physiol. 154, 1505–1513.
Yin, L., Cheng, Y., Espinasse, B., Colman, B.P., Auffan, M., Wiesner, M., Rose, J., Liu, J., Bernhardt, E., 2011. More than ions: the effects of silver nanoparticles on Lolium multiflorum. Environ. Sci. Technol. 45, 2360–2367.
Yousef, I., Lefrancois, S., Moreno, T., Hoorani, H., Makahleh, F., Nadji, A., Dumas, P., 2012. Simulation and design of an infrared beamline for SESAME (Synchrotron-light for experimental science and applications in the Middle East). Nucl. Inst. Met. A 673, 73–81.
Yu, P., 2004. Applications of advanced synchrotron radiation-based Fourier transform infrared (SR-FTIR) microspectroscopy to animal nutrition and feed science: a novel approach. Br. J. Nutr. 92, 869–885.
Zayed, A., Lytle, C.M., Qian, J.H., Terry, N., 1998. Chromium accumulation, translocation and chemical speciation in vegetable crops. Planta 206, 293–299.
Zhang, P., Ma, Y., Zhang, Z., He, X., Guo, Z., Tai, R., Ding, Y., Zhao, Y., Chai, Z., 2012. Comparative toxicity of nanoparticulate/bulk Yb_2O_3 and $YbCl_3$ to cucumber (*Cucumis sativus*). Environ. Sci. Technol. 46, 1834–1841.
Zhang, Y., Gladyshev, V.N., 2010. General trends in trace element utilization revealed by comparative genomic analyses of Co, Cu, Mo, Ni, and Se. J. Biol. Chem. 285, 3393–3405.
Zhang, Z., He, X., Zhang, H., Ma, Y., Ding, Y., Zhao, Y., 2011. Uptake and distribution of ceria nanoparticles in cucumber plants. Metallomics 3, 816–822.
Zhao, F., Lombi, E., Breedon, T., McGrath, S., 2000. Zinc hyperaccumulation and cellular distribution in *Arabidopsis halleri*. Plant Cell Environ. 23, 507–514.
Zhao, F.J., Dunham, S.J., McGrath, S.P., 2002. Arsenic hyperaccumulation by different fern species. New Phytol. 156, 27–31.

Zhao, F.J., Ma, J.F., Meharg, A.A., McGrath, S.P., 2009. Arsenic uptake and metabolism in plants. New Phytol. 181, 777–794.
Zhao, F.J., McGrath, S.P., Meharg, A.A., 2010. Arsenic as a food-chain contaminant: mechanisms of plant uptake and metabolism and mitigation strategies. Ann. Rev. Plant Biol. 61, 535–559.
Zhao, F.J., Stroud, J.L., Khan, M.A., McGrath, S.P., 2012. Arsenic translocation in rice investigated using radioactive ^{73}As tracer. Plant Soil 350, 413–420.
Zhao, F.J., Wang, J.R., Barker, J.H.A., Schat, H., Bleeker, P.M., McGrath, S.P., 2003. The role of phytochelatins in arsenic tolerance in the hyperaccumulator Pteris vittata. New Phytol. 159, 403–410.
Zhao, Y., Peralta-Videa, J.R., Lopez-Moreno, M.L., Saupe, G.B., Gardea-Torresdey, J.L., 2011. Use of plasma-based spectroscopy and infrared microspectroscopy to determine the uptake and effects of chromium(III) and chromium(VI) on Parkinsonia aculeata. Int. J. Phytoremed. 13, 17–33.
Zhu, H., Han, J., Xiao, J.Q., Jin, Y., 2008. Uptake, translocation, and accumulation of manufactured iron oxide nanoparticles by pumpkin plants. J. Environ. Monit. 10, 713–717.
Zoriy, M.V., Kayser, M., Becker, J.S., 2008. Possibility of nano-local element analysis by near-field laser ablation inductively coupled plasma mass spectrometry (LA-ICP-MS): new experimental arrangement and first application. Int. J. Mass Spectrom. 273, 151–155.
Zoriy, M.V., Mayer, D., Becker, J.S., 2009. Metal imaging on surface of micro- and nanoelectronic devices by laser ablation inductively coupled plasma mass spectrometry and possibility to measure at nanometer range. J. Am. Soc. Mass Spectrom. 20, 883–890.



CHAPTER TWO

Advances in Understanding Organic Nitrogen Chemistry in Soils Using State-of-the-art Analytical Techniques

Peter Leinweber*,#, Jens Kruse*, Christel Baum*, Melissa Arcand†, J. Diane Knight†, Richard Farrell†, Kai-Uwe Eckhardt*, Kristian Kiersch*, Gerald Jandl*

*Soil Science, University of Rostock, Rostock, Germany
†Department of Soil Science, University of Saskatchewan, Saskatoon, Canada
#Corresponding author: E-mail: peter.leinweber@uni-rostock.de

Contents

Advances in Agronomy, Volume 119
ISSN 0065-2113, http://dx.doi.org/10.1016/B978-0-12-407247-3.00002-0

Abstract

During the past decade, soil and geochemists have adopted a variety of novel chemical–analytical methods to explore the chemistry of soil organic N (N_{org}). This chapter summarizes some of the more recent developments in the use of wet-chemical and instrumental methods to determine total N_{org} concentrations as well as to speciate the N_{org} in soils. A critical evaluation of ^{15}N nuclear magnetic resonance (NMR) spectroscopy found the technique to be wanting, in terms of its sensitivity and ability to identify classes of N_{org} compounds in soils. Complementary mass spectrometric techniques are described briefly, and improved data evaluations based on broad applications of high-resolution pyrolysis-field ionization mass spectrometry are presented and discussed. A reassessment of older data sets using the new spectral evaluation algorithms provides strong evidence of fire- and management-induced changes in N_{org} speciation. Isotope-ratio mass spectrometry, Fourier transform ion cyclotron resonance mass spectrometry, and nanoscale secondary ion mass spectrometry (Nano-SIMS) also are discussed, with the latter two techniques having potential to (1) identify N_{org} compounds and (2) provide spatially resolved information on the molecular, elemental and isotopic composition of soil N_{org}. The use of ^{15}N labeling techniques is discussed both from a methodological standpoint and in terms of tracking the fate of plant-derived (residue or rhizodeposit) N in the soil. Indeed, coupling ^{15}N labeling with analytical techniques such as ^{15}N NMR, Nano-SIMS and high- or ultrahigh-resolution mass spectrometry can provide information on how N is incorporated into soil organic matter. Analytical and instrumental innovations have resulted in new insights into the chemistry of N_{org}—together with a revised summary of the relative amounts of the different N_{org} compound classes present in soils (e.g. aliphatic amine and amide N, aromatic heterocyclic N), as well as their ecophysiological functions. Particular emphasis is given to the use of multitechnique analyses and the outstanding molecular–chemical diversity of biogenic heterocyclic N_{org} compounds. Examples are given of the new insights obtained using multi-analytical research approaches to explore microbial utilization of heterocyclic N and organic–mineral interactions, as well as the ability of human and environmental intervention to alter the composition of soil N_{org}. Finally, we examine future challenges and propose analytical approaches to tackle open questions regarding the basic chemistry and cycling of N_{org} in soils, as well as the agronomic and environmental consequences associated with N transformations in agro-ecosystems.

1. INTRODUCTION

Organic nitrogen (N_{org}) is an important constituent of soil organic matter (SOM) and, as such, plays a key role in soil N cycling and crop production. Indeed, the mineralization of N_{org} produces microbe- and plant-available forms of N which, in turn, participate in reactions that yield N compounds of concern in the environment (e.g. nitrification → NO_3^-; denitrification → N_2O). Thus, a detailed, molecular-scale understanding of N_{org} compounds will enhance our ability to quantify and elucidate the fate of these compounds, or

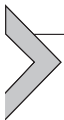
compound classes, in soil. This will support the development of best management practices that improve the N supply in agricultural production systems—while minimizing or avoiding adverse environmental effects.

Earlier overview papers and reviews on this topic were published by Greenfield (1972), Kelley and Stevenson (1995), Mengel (1996), Nannipieri and Eldor (2009), Olk (2008), Schulten and Schnitzer (1998) and Stevenson (1994). Greenfield (1972) compiled wet-chemical N fractionation data for proteins, litters and soil samples and concluded that 70–80% of the total N_{org} in litter and soil was in the form of amino acids and proteins. Stevenson (1994) compiled a wealth of information regarding the analytical techniques and methodological difficulties associated with N_{org} determinations, as well as classical wet-chemical N_{org} fractionations and identifiable N compounds in soils from different climate zones around the world and how these N_{org} pools were affected by soil management. As such, the review by Stevenson (1994) remains an important source of information. Kelley and Stevenson (1995) summarized the proportions and turnover processes of N fractions derived from hydrolysis and wet-chemical N fractionation; i.e. acid-insoluble N, NH_3–N, amino acid N, amino sugar N, and hydrolyzable unidentified N. They suggested five different forms for the unidentified N fraction and state that all N forms—including the acid-insoluble fraction—appeared to be biodegradable. Furthermore, they provided the first overview of evidence for N_{org} compounds obtained from newly emerging "solid state techniques," including nuclear magnetic resonance (NMR) spectroscopy and pyrolysis-mass spectrometry (Py-MS). At almost the same time, Mengel (1996), referring to the derivatization-gas chromatography-mass spectrometry work of Schnitzer and Spiteller (1986), emphasized the importance of heterocyclic N (present in purine and pyrimidine derivatives, indols, chinolin, piperidine and pyrrolidine compounds) entering the soil in the form of plant-derived pyrrole rings from chlorophylls and cytochromes and the N bases of nucleic acids. Mengel (1996) described N heterocycles as very resistant to biodegradation and thus enriched in soil—contrary to the view of Kelley and Stevenson (1995). In his discussion of N_{org} mineralization, however, Mengel (1996) refers only to amino sugars (e.g. N-acetylglucosamine) and polypeptides/proteins (e.g. muropeptide)—reflecting the prevailing views of N_{org}. That is, at this point in time, N_{org} research was focused on chemically identifiable amino acids/amino sugars and relevant polymers, as well as on their transformations in soil. The nonidentified N forms were considered to be structural components of humic substances. Also during this period, the identification of defined chemical compounds in both

the hydrolyzable, but unidentified, and the nonhydrolyzable N fractions (referred to as "unknown N"; see Iverson and Schnitzer, 1979) was in its infancy. Schulten and Schnitzer (1998) significantly advanced our understanding of this "unknown N" by identifying "new" N compounds in both humic and nonhumic substances. Based mainly on Py-MS results, they discussed 27 groups of molecular structures for N_{org} compounds occurring in extracted humic substances and nonextracted bulk soil samples. Cited nearly 300 times, this review is one of the most popular and important reviews in SOM research.

More recently, Olk (2008) published an outstanding review emphasizing analytical–technical advances in N speciation techniques and the occurrence of N_{org} compounds in physical fractions of soil (i.e. density, size and aggregate fractions). Nannipieri and Eldor (2009) added newer results of mass- and X-ray absorption spectroscopies, as well as detailed information on links between N_{org} compounds and the enzymatic and microbial processes driving their turnover. How selected scenarios of global change affect the abundance, diversity and activity of microorganisms involved in soil N turnover was reviewed by Ollivier et al. (2011), but without particular emphasis to N_{org} compounds.

Other important reviews discuss specific N compounds [e.g. amino sugars and amino acid enantiomers as markers for microbial residues and/or SOM aging; see Amelung (2003)], environmental situations [e.g. N turnover following wildfires; see González-Pérez et al. (2004) and Knicker (2007)] and agricultural systems [e.g. paddy soils; see Kögel-Knabner et al. (2010)]. Most recently, particular attention has been focused on links between the N and C cycles (e.g. Gärdenäs et al., 2011; Knicker, 2011a; Macdonald et al., 2011). However, without more detailed knowledge of the chemistry of N_{org} compounds, the scientific community's understanding of these linked cycles remains fragmentary. Therefore, the objective of the this chapter is to summarize recent advances in soil N_{org} research with particular emphasis on new developments in the instrumental-analytical techniques and examples of multimethodological approaches to disclose the chemistry of N_{org} and its transformations in soil.



2. OVERVIEW OF ANALYTICAL METHODS

2.1. Total N_{org} Concentrations and Wet-Chemical Fractionations and Speciation Techniques

Bremner (1996), Mulvaney (1996) and Stevenson (1996) described the basic methodologies, including discussions of errors and uncertainties, that remain

the basis for soil N_{org} studies. Total N_{org} concentrations are frequently determined using the Kjeldahl method. This involves heat- and catalyst-supported digestion in concentrated H_2SO_4 (to convert the N_{org} into NH_4^+), followed by distillation of the digest with NaOH, and analysis of the distillate NH_4^+–N by titration. Principal modifications to the method involve digestion with HF to include mineral-fixed-NH_4^+, and the salicylic acid-thiosulfate or alkaline reduction methods to include NO_3^-–N and NO_2^-–N. Although still widely used, the Kjeldahl N_{org} method has been gradually supplanted by the Dumas (dry combustion) method. In general, this involves high-temperature combustion of the soil in a pure-O_2 atmosphere (converting N_{org} into NO_x), followed by reduction of the NO_x to N_2, and detection/quantification of the N_2 using a thermal conductivity detector. Several types of Dumas systems that employ elemental analyzers (EAs) are commercially available and offer the simplicity of modern automated instruments capable of the simultaneous determination of C, N, S (and/or H and/or O) together with high sample throughput. These systems also offer the benefit of eliminating the need for sample pretreatment and avoiding the use of hazardous reagents (Craft et al., 1991; Pérez et al., 2001; Rutherford et al., 2008; Yeomans and Bremner, 1991). However, dry combustion methods determine total soil N (N_t), with N_{org} determined by subtraction, i.e. $N_{org} = N_t - (NH_4^+ + NO_3^- + NO_2^-)$. This requires a separate determination of the exchangeable and soluble NH_4^+, NO_2^-, and NO_3^-, which generally account for <2% of N_t in surface soils. If required (e.g. after mineral fertilizer application), N-ions in solution and those easily desorbed can be separated using mild extractions (e.g. with K_2SO_4 or $CaCl_2$ solution) and quantified using ion chromatography. The determination of nonexchangeable, or fixed, NH_4^+ is more time-consuming—requiring extraction of the sample with KOBr to remove exchangeable NH_4^+ and labile organic N compounds, followed by digestion with HF–HCl solution (Mulvaney, 1996). Though time-consuming, these steps are necessary to avoid the significant errors that can arise when N_t is used as a proxy for N_{org}, for example, when using the calculated $C:N_t$ ratio (as opposed to the $C:N_{org}$ ratio) as an indicator of SOM quality. Indeed, data compiled by Stevenson (1986) show that the presence of fixed-NH_4^+ causes $C:N_t$ ratios in surface and subsurface soils to deviate systematically (6–37%, respectively) from the corresponding $C:N_{org}$ ratios. Not surprisingly, the effects of fixed-NH_4^+ can be pronounced in investigations of N_{org} in different particle-size fractions of SOM (Olk, 2008; Schulten and Leinweber, 2000). As seen in Fig. 2.1, N_t values determined by dry combustion strongly reflect the contribution of fixed-NH_4^+, whereas

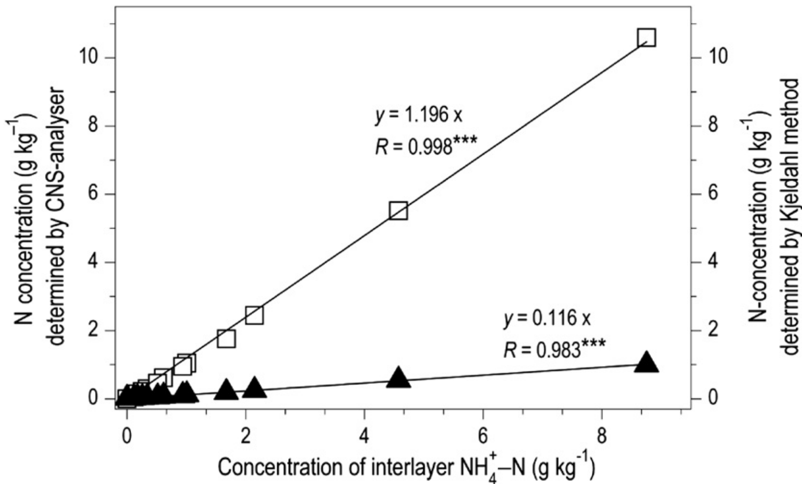


Figure 2.1 Impact of interlayer NH_4^+ on N concentrations as determined by (□) dry combustion (CNS-analyzer) and (▲) the Kjeldahl method. NH_4^+ smectites and vermiculites with determined concentrations of sorbed NH_4^+–N were kindly provided by Dr. S. Dultz, Institute of Soil Science, Leibniz University, Hannover, Germany.

the corresponding total-Kjeldahl N (N_{org}) values were essentially unaffected by the presence of fixed-NH_4^+. Likewise, in a comparison of the N_t and N_{org} in organic-mineral clay fractions from a long-term (34-yr) humus formation study (Leinweber and Reuter, 1992), N_t concentrations determined by dry combustion (4.5–23.4 g kg^{-1}) exceeded the corresponding Kjeldahl N_{org} concentrations (0.40–20.4 g kg^{-1}) by 4–17% (Leinweber, unpublished). Clearly, there is a need to exercise great care in determining N_{org} concentrations, and when using C:N ratios to evaluate SOM quality. Surprisingly, however, there is little evidence in the recent literature to suggest that potential contributions from fixed-NH_4^+ are often taken into account when making C and N determinations for SOM characterization.

Stevenson (1994, 1996) compiled data on the various organic forms of N obtained by liberating N_{org} constituents from organic and inorganic colloids using hot, 6 *M* HCl followed by direct distillation and separate determination of NH_3–N, or Kjeldahl N digestion, distillation and titration of the 6 *M* HCl extract. In this relatively simple way, three different N_{org} fractions were obtained (Table 2.1). Comparisons of the N_{org} fractions determined in this way show a great similarity among samples—irrespective of soil type, management or particle-size fractions.

Table 2.1 Distribution of N_{org} Fractions (%) in Different Reference Soil Groups and Organic-mineral Particle-size Fractions from Unfertilized and Fertilized Experimental Soils (uh–N = unidentified hydrolyzable N)

References	Soil units	Amino-N + uh–N	NH_3–N	Nonhydrolyzed N
Sulçe et al. (1996)	Arenosol	43	19	37
	Cambisol	37	29	34
	Fluvisols	50–54	27–29	20–22
	Vertisols	43–48	27–33	19–29
Zhang et al. (2006)	Anthrosols	30–39	14–17	24–39
Leinweber et al. (1999)	Vertisols	43–53	32–54	15–20
Leinweber and Schulten (1998a, 1998b)	Cambisols	51–54	26–29	13–17
	Luvisols	41–53	21–26	8–13
	Phaeozems	42–51	28–31	20–27
	Chernozems	48–50	28–30	21
	Clay, unfertilized	88–95	46–58	13–18
	Fine silt, unfertilized	80–97	40–50	15–27
	Medium silt, unfertilized	76–94	40–45	14–27
	Coarse silt, unfertilized	42–97	46–68	11–28
	Sand, unfertilized	43–94	20–59	13–31
	Clay, fertilized	81–97	43–53	14–18
	Fine silt, fertilized	72–88	31–44	18–25
	Medium silt, fertilized	73–82	33–39	19–27
	Coarse silt, fertilized	69–97	41–50	15–25
	Sand, fertilized	58–95	14–47	10–25

Bulk α-amino-N concentrations in the HCl extracts can be determined colorimetrically using the ninhydrin method. However, Stevenson (1996) emphasized that this method can be applied exclusively for amino acids with $-NH_2$ adjacent to –COOH or with NH–CH_2 group—thus underestimating the amino-acid-N content of the sample. Amino acids in soil hydrolyzates can be determined by ion exchange-, liquid- (High pressure liquid chromatography (HPLC)) and gas chromatography—the latter two

often in combination with mass spectrometric detection. A review of 46 research articles published between 2000 and 2012[1] indicates the prevalence of HPLC methods. Olk (2008) summarized advances in the extraction of amino acids using 4 *M* methanesulfonic acid and quantification by anion chromatography. Using this approach, Martens and Loeffelmann (2003) and Martens et al. (2006) determined that amino acid N (consisting of 17 amino acids) accounted for 51–52% of soil N, with NH_4–N and nonamide N_{org} accounting for 34% and 14–15%, respectively. Warren (2008) developed a capillary electrophoresis with laser-induced fluorescence (CE-LIF) detection method as a more rapid alternative to GC and LC methods for measuring individual amino acids in soil KCl extracts. The CE-LIF method separated 17 common amino acids in crude 1 *M* KCl extracts, with detection limits between 7 and 250 *nM* and a run time of only 12 min. The relative standard deviation of migration times for replicate analyses was <0.2% and relative standard deviations for peak areas was <5%. Hou et al. (2009) proposed an HPLC-MS method based on a 6-aminoquinolyl-N-hydroxysuccinimidyl carbamate (AQC) derivatization; baseline separation of 17 amino acid–AQC-derivatives on an XTerraR MS C_{18} column, using ammonium formate as a mobile-phase modifier; and optimized MS detection. Detection limits were 0.20–0.60 pmol μL^{-1} on column (i.e. 0.07–0.24 mg kg^{-1} soil) under the optimized conditions.

Amelung (2003) used amino acid enantiomers—especially the D:L ratios of alanine, aspartic acid, lysine and proline—as biomarkers to assess the mechanisms of N_{org} transformations and aging in soil. He also discussed the relevant analytical methods needed to reliably determine amino sugars and amino acid enantiomers in soil. Furthermore, Zhang et al. (2007) published a GC/MS method for the assessment of ^{15}N and ^{13}C incorporation into soil amino acid enantiomers using labeled $^{15}NH_4^+$ or ^{13}C-glucose substrates. In the mass spectra, ^{15}N-enrichment of the amino acids was estimated by calculating the atom percentage excess from intensity increases of fragment peaks [F + 1 for neutral (alanine, proline) and acidic (aspartic acid) and F + 2 for basic amino acids (lysine)].

Although they do not occur in significant amounts in plant residues, amino sugars—such as glucosamine, galactosamine, mannosamine, and muramic acid, as well as more than 20 other minor amino sugars—account for about 5–10% of the N_{org} in soil (Amelung, 2003) and can be used as biomarkers for soil N_{org} transformations affected by natural and anthropogenic influences. The

[1] Obtained by searching Science Direct (http://www.sciencedirect.com/) for "amino acid soil".

method for amino sugar determinations in 6 *M* HCl hydrolyzates was based on derivatization with acetonitrile–acetate, purification, GC separation and flame ionization detection (Zhang and Amelung, 1996).

Various mild extractants are used to isolate available N from soil. In addition to inorganic N (i.e. NO_3^- and NH_4^+), however, these extracts contain dissolved N_{org} (Kuzyakov and Siniakina, 2001; Landgraf et al., 2006). Concentrations of N_{org} in these extracts are usually obtained by subtracting the available N (NO_3^- + NH_4^+; determined independently) from the N_t determined using either the Kjeldahl method or thermal–catalytical oxidation (C, N EA). Various forms of N_{org} in these extracts can be qualitatively examined using the above-described N_{org} fractionations and/or amino acid and amino sugar determinations, though more detailed information can be gained using the different spectrometric and spectroscopic methods described in Sections 2.2, 2.3, and 2.4.

2.2. NMR Spectroscopy

NMR spectroscopy is based on the magnetic properties of atomic nuclei (such as ^{13}C and ^{15}N) and has been widely applied in soil and organic geochemistry (e.g. Knicker, 2011b). Discussion of the theory behind NMR techniques is beyond the scope of this review, but can be found in Simpson and Simpson (2009). In NMR, chemical shifts (i.e. resonant frequency of a nucleus relative to a standard) are easily measured and carry important structural information. Chemical shifts for environmentally relevant N compounds, used to interpret solid-state, cross-polarization magic angle spinning (CP/MAS) ^{15}N NMR spectra, are compiled in Fig. 2.2. Overlap of chemical shifts for some N compounds (e.g. between the N in Maillard products/melanoidins or pyrroles with amide, and in pyridine N-oxides with nitriles) may be problematic in soil N_{org} research.

Early applications of CP/MAS ^{15}N NMR spectroscopy to labeled compounds of known composition and their reaction products indicate the formation of nonamide N through the Maillard reaction (Benzing-Purdie et al., 1983; 1986; 1992). More recently, Knicker (2011b) reviewed applications of CP/MAS ^{15}N NMR in organic geochemistry which indicate that amides are the major form of N in humic substances, soils and similar samples. Heterocyclic N, on the other hand, was present in measurable quantities only in some aquatic humic substances (Thorn and Cox, 2009), samples from reduced soils (Mahieu et al., 2000; Maie et al., 2006) and samples from fire-impacted sites (Almendros et al., 2003; González-Pérez et al., 2004; Hilscher and Knicker, 2011; Knicker et al., 2005). Heterocyclic N also was present in

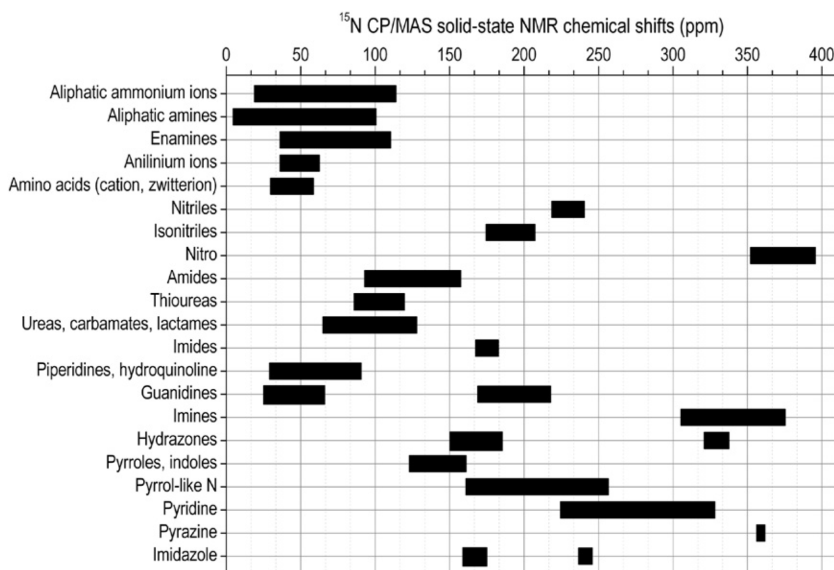


Figure 2.2 Ranges of chemical shifts of various soil-relevant N moieties in solid-state ^{15}N nuclear magnetic resonance spectroscopy (chemical shift referenced to liquid ammonia at 25 °C = 0 ppm). *(Data compiled from Levy and Lichter (1979); Solum et al. (1997)).*

various ^{15}N-enriched below- and aboveground plant materials (*Triticum aestivum*, *Pisum sativum*, *Pennisetum clandestinum*, *Eucalyptus globulus*)—accounting for 3–7% of the total ^{15}N NMR signal (Smernik and Baldock, 2005a).

A critical evaluation of the literature describing the use of CP/MAS ^{15}N NMR spectroscopy to determine soil N_{org} (e.g. Knicker, 2011b and references therein) led us to the following conclusions:

(1) Based on the natural abundance of ^{15}N in materials (0.3663 atom%), the ^{15}N NMR spectra represents only about 0.37% of all N atoms in the sample, and even less after HF treatment. In addition, data interpretations appear to be strongly affected by instrumental parameters (Knicker, 2011b). Thus, the technique does not appear to have the sensitivity required for investigating N_{org} compounds in bulk soil samples at the molecular scale. Bosshard et al. (2011) used ^{15}N NMR and Curie-point pyrolysis coupled to gas chromatography electron impact mass spectrometry (Cp Py-GC/MS) to characterize the N forms in feces of sheep fed a diet of ^{15}N-labeled ryegrass. Whereas the ^{15}N NMR spectra showed only one broad peak assigned to amide N, the Cp Py-GC/MS technique detected 10 different molecular structures with individual ^{15}N-enrichments above the background level.

(2) Another weakness of the ^{15}N NMR technique in soil and geochemical applications is the infrequent use of reference compounds; e.g. to evaluate signal recovery and method sensitivity. Spectra of nonprotonated pyridine and protonated pyrrole were reported by Kelemen et al. (2002), as well as spectra of gliadin, caffeine and glycine by Smernik and Baldock (2005b). Furthermore, Smernik and Baldock (2005b) stated that when they used reference compounds and optimized instrumental parameters, N heterocyclic structures, which may contribute to 26–56% of N_t, were insensitive to ^{15}N NMR detection in HF-treated clay fractions of four soils. Systematic studies investigating how N functionalities are detected in the presence of a soil-mineral matrix are missing in the literature, as are studies investigating exactly how pretreatments, e.g. with HF, affect the sample.

(3) Although CP/MAS NMR is frequently referred to as a nondestructive technique, most recently published ^{15}N NMR spectra of soil materials were obtained from samples with some destructive pretreatment applied. Four of the five ^{15}N NMR spectra shown in Fig. 2.3 (Knicker, 2011a) were obtained after (i) ultrasonic disaggregation (which may redistribute sonically destroyed particulate organic matter (Amelung and Zech, 1999)), (ii) particle-size fractionation by repeated sedimentation/decantation cycles (which may lead to losses of dissolved organic matter (DOM) or its concentration in the finest size fractions), (iii) drying, and (iv) repeated treatment with 10% HF (which destroys silicate minerals and organo–clay complexes). Based on C:N ratios and CP/MAS NMR spectra, it is frequently claimed that HF-treatments do not alter the composition of the organic matter under study (e.g. Hilscher and Knicker, 2011; Knicker et al., 2000). Schmidt and Gleixner (2005), however, reported that HF treatment removed 13–46% of the N_{org} and that the material removed was enriched in ^{15}N (by 1–4‰). Furthermore, using Py-FIMS, Sleutel et al. (2009) demonstrated that significant changes in SOM composition resulted from the conventional HF treatment.

(4) Replicates or standard errors are never reported with CP/MAS NMR results, limiting the value of the data especially in "noisy" spectra from bulk soils and particle-size fractions, such as the spectra shown in Fig. 2.3.

A new NMR development is the saturation-pulse-induced dipolar exchange with recoupling technique, in which the chemical forms of C bonded to N are selectively observed (Schmidt-Rohr and Mao, 2002). Using this technique, Olk et al. (2002) showed that a labile mobile humic acid in a

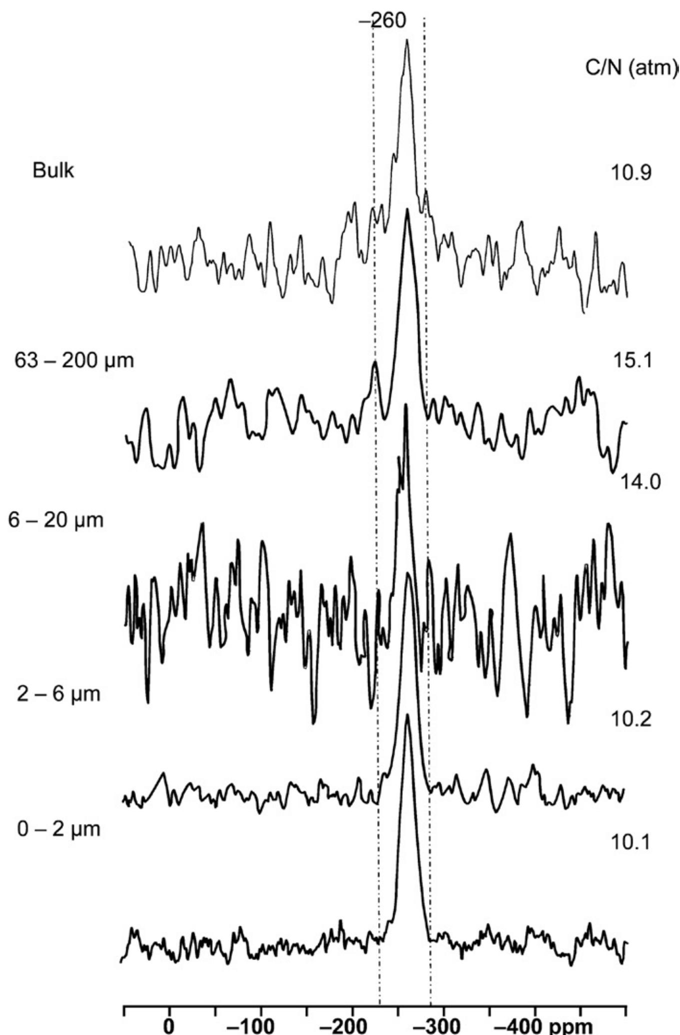


Figure 2.3 Solid-state ^{15}N nuclear magnetic resonance spectra of the HF-treated bulk material and the fine particle-size fractions from a Luvisol topsoil. *(Reproduced from Knicker (2011a) with permission from Elsevier).*

submerged lowland rice soil was enriched in both N and phenolic compounds. They also detected heteroaromatic N in pyridine and found that amide N was covalently bound in an anilide structure of lignin-derived polyphenols. Such N covalently bound to a phenolic structure also was detected in the mobile humic acid of an aerobic upland rice soil (Olk, 2008). The author concluded that, in the past, conventional ^{15}N NMR

detected this anilide N as secondary amide N. Furthermore, removal of the mineral components from a submerged lowland rice soil using HF made a small signal for N bound to aromatic ether rings visible in the whole soil sample (Schmidt-Rohr et al., 2004).

2.3. Mass Spectrometry Techniques

2.3.1. Pyrolysis-Gas Chromatography/Mass Spectrometry

Pyrolysis-gas chromatography/electron impact mass spectrometry (Py-GC/MS) can be used to investigate constituents of complex organic structures, such as SOM and its fractions. Two fast-heating (flash) pyrolysis techniques are used: (1) Curie-point pyrolysis (Cp Py) (Leinweber and Schulten, 1998a; Schulten, 1987; Schulten et al., 2002) and (2) "double-shot" pyrolysis (González-Pérez et al., 2007; Quénéa et al., 2006). Both methods rely on pyrolysis at a specific temperature, which depends on the Curie-point of the ferromagnetic sample carrier (300–800 °C). Double-shot pyrolysis uses two temperature steps to distinguish thermally labile from stable or tightly trapped compounds. Both techniques employ on-line chromatographic capillary column gas chromatography coupled with mass spectrometry to detect the pyrolyzed and volatilized compounds. For MS detection, the compounds are ionized by hard electron impact (EI) ionization at 70 eV, which generates a molecule ion and fragment ions with different masses for each volatilized compound. The continuous recording of mass spectra results in chromatograms where the corresponding mass spectrum of each peak can be compared with mass spectral libraries for assignment. Bosshard et al. (2011), using Cp Py-GC/MS, successfully detected the ^{15}N label in individual molecules of ryegrass and feces that were labeled up to 14.6 atom% ^{15}N. The ^{15}N-enriched, substituted, pyrroles, pyridines and pyrimidines were disclosed by their isotope peak [M+1] whose intensity was significantly increased in comparison to the corresponding mole peak in the library spectra.

Although it is assumed that the assigned compounds are characteristic of the original structure (Galletti and Bocchini, 1995; Schulten, 1996), the utility of the technique is often thought to be constrained by the formation of so-called "artifacts" induced by secondary reactions and fragmentation during the high energy impact of the pyrolysis (Hatcher et al., 2001; Zang and Hatcher, 2002). Known formations include furans from carbohydrates, alkylaromatics from cycled fatty acids (Saiz-Jimenez, 1994; Saiz-Jimenez et al., 1994), aromatic N heterocyclic compounds and nitriles from amino

acids and peptides (Chiavari and Galletti, 1992; Patterson et al., 1973; Schulten and Schnitzer, 1998; Schulten et al., 1995; Sorge, 1995; Tsuge and Matsubara, 1985), and nitriles from the reaction of carboxylic acids and mineral-bound NH_4^+ (Evans et al., 1985). The described formation of artifacts does not preclude the genuine occurrence of such compounds in SOM. A recent example for this is the detection of aromatic N heterocyclic compounds in humic substances from a Latosol (Pereira de Assis et al., 2012), using a pyrolysis temperature of 280 °C—i.e. below the temperature required for the thermal decomposition of peptides.

2.3.2. Pyrolysis-Field Ionization Mass Spectrometry

Pyrolysis-field ionization mass spectrometry (Py-FIMS) combines the temperature-resolved pyrolysis inside the ion source with a "soft", less-fragmenting (compared to EI) ionization. Py-FIMS is described in detail by Leinweber et al. (2009), Schulten (1996) and Schulten et al. (1998). Briefly, ~5 mg sample is heated from 110 to 700 °C in steps of 10 °C in the FI ion source of a double-focusing mass spectrometer. During progressive heating, 60 spectra are recorded in the mass-to-charge ratio (m/z) range of 15–900 and, in routine applications, three to five replicate samples are measured and the data averaged. Nitrogenous compounds most often have odd-numbered nominal m/z and, based on the PhD work of Sorge (1995)—who investigated the mass spectra of 26 essential amino acids by Cp Py-GC/MS and Py-FIMS (Sorge et al., 1993)—are assigned to two classes of N_{org} compounds: "peptides" (based on the marker signals of the amino acids) and "N-containing compounds" (based on odd-numbered m/z that were complementarily identified by Py-GC/MS). The latter compound class was interpreted as containing mostly non-peptide-derived molecules such as aromatic N heterocyclic compounds and nitriles. Py-FIMS and the analytical-pyrolysis methods, in general, sometimes, were criticized as producing and detecting aromatic N heterocyclic compounds as artifacts that are not abundant in the original SOM structures (e.g. Knicker, 2004).

The following points shed light on this controversial discussion:

(1) When discussing the different analytical-pyrolysis methods, nondifferentiation is misleading because the two most applied methods, Cp Py-GC/MS and Py-FIMS, fundamentally differ in their energetic impacts on the SOM; thus, confounding the identification of genuine N_{org} compounds. For example, Cp Py-GC/MS occurs in a gaseous atmosphere and the flash pyrolysis (occurring over milliseconds) transfers a tremendous

amount of energy into the sample by heating to the Cp of the metal sample holder, almost exclusively forming aromatic N heterocyclic compounds and nitriles from any N_{org} (including amino acids, sugars and peptides). However, in temperature-resolved Py-FIMS, the stepwise heating of the sample in the high vacuum of the ion source transfers less energy into the sample, reducing consecutive cyclization reactions and producing mainly molecular ions. Furthermore, amino acids are detected by their characteristic molecular masses in the protonated form or after water elimination. Whereas Cp Py-GC/MS of N_{org} clearly produces exclusively aromatic N heterocyclic compounds and nitrile artifacts—thereby complicating conclusions about the genuine occurrence of these compounds in SOM—claiming the same for Py-FIMS is misleading.

(2) The production of aromatic N heterocyclic compounds and nitriles as artifacts by one of the two most commonly applied Py-MS methods does not necessarily preclude their natural occurrence in soils. Indeed, many biological inputs to the soil naturally contain aromatic N heterocyclic compounds, such as nucleobases in DNA/RNA, pyrrole in chlorophyll porphyrin rings and many others secondary metabolites (see Section 3), as well as pyromorphic pyrrole-type N formed under fire (González-Pérez et al., 2004).

(3) Using Py-FIMS marker signals for peptides, single free amino acids were identified in day-time rhizodeposits (Melnitchouck et al., 2005). Moreover, proportions of amino acids/peptides assigned by Py-FIMS were in agreement with the results of α-amino N in freshwater DOM (Leinweber et al., 2009), HPLC of rhizodeposits (Fischer et al., 2010) and, GC/MS of plant material extracts (Schlichting and Leinweber, unpublished data). Thus, assignments of odd-numbered *m/z* to aromatic N heterocyclic compounds and nitriles are quantitatively reliable—a conclusion that is supported by X-ray absorption spectroscopy (see Section 2.4).

Nonetheless, there is a possibility that Py-FIMS can produce aromatic N heterocyclic compounds and nitriles. To address this issue, we recently undertook efforts to improve data evaluation and *m/z* assignment, and to quantify the thermal formation and recording of artificial N-compounds. This work was based largely on high-resolution MS with an MAT 95 (Finnigan MAT, 28197 Bremen, Germany) as described in the following:

The accuracy of mass determinations was investigated using ^{15}N-labeled ryegrass from Bosshard et al. (2011) and high-resolution Py-EIMS (at 70 eV

and a resolution of 13,000). The mass spectrum (Fig. 2.4) shows ^{13}C and protonated mass peaks of propionitrile (C_3H_5N) as typical pyrolysis products of plant material and bacteria. Furthermore, the mass of the $^{13}CC_2H_5N$ (1.07 atom% ^{13}C) was in close agreement with the natural ^{13}C abundance of the isotopologue (1.1 atom%). Such high resolution of isotope ratios can be achieved only using sector-field mass spectrometers. Mass spectrometers with a lower resolution cannot separate the mass of an isotope ion of a compound from its protonated form [M+H]. Moreover, the ^{15}N-enrichment in propionitrile ($C_3H_5{}^{15}N$) contained in the ryegrass tissue was greater (22.3 atom% ^{15}N) than the bulk ^{15}N-labeled ryegrass (14.6 atom% ^{15}N), indicating that the N compounds in the plant were not uniformly labeled. Furthermore, the excellent agreement of the theoretical masses with analyzed masses supports the high accuracy of this method: C_3H_5N 55.0422 vs 55.0427, $C_3H_5{}^{15}N$ 56.0392 vs 56.0389, $^{13}CC_2H_5N$ 56.0456 vs 56.0455, $C_3H_5N + H$ 56.0500 vs 56.0512.

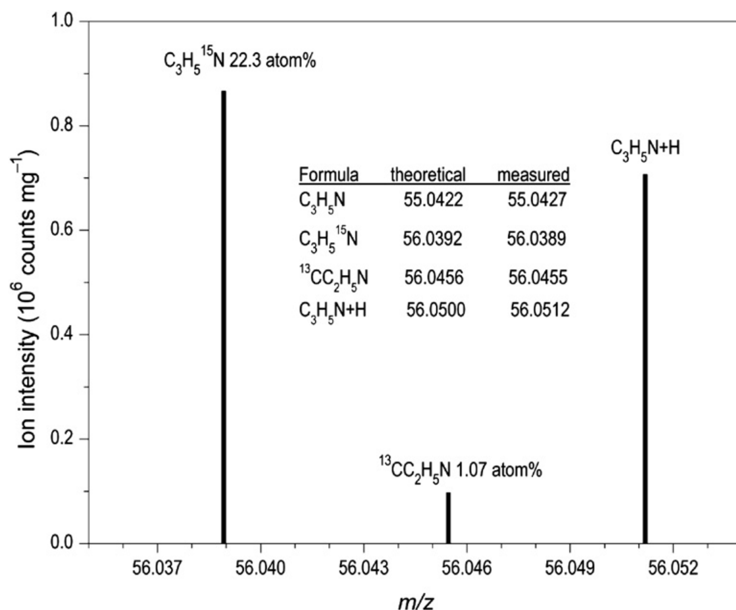


Figure 2.4 Zoomed view of a high-resolution, pyrolysis (electron impact)-mass spectrum of ^{15}N-labeled rye grass (14.6 atom%) showing the isotope and protonated peaks of propionitrile (C_3H_5N), a typical pyrolysis product of plant materials and bacteria. The enrichment of ^{15}N in propionitrile ($C_3H_5{}^{15}N$) with 22.3 atom%, the natural abundance of ^{13}C in propionitrile $^{13}CC_2H_5N$ with 1.07 atom% and the protonated propionitrile ($C_3H_5N + H$), formed by the pyrolytic conditions, are displayed. Note that the signal of C_3H_5N is not shown for a better visualization.

In the past, evaluation of Py-FIMS data was hampered by interferences due to more than one substance being assigned to one nominal mass. The application of high-resolution MS, however, provides higher accuracy of the detected masses and supports a revision of the marker signals for compound classes derived from Sorge (1995). We propose *m/z* 58, 59, 70, 73, 74, 75, 84, 87, 91, 97, 99, 115, 120, 125, 129, 135, 167, 185, 203, 243, and 276 for nonaromatic amides (peptides, amino sugars) and free amino acids and *m/z* 67, 79, 80, 81, 93, 95, 103, 109, 111, 117, 123, 137, 139, 153, and 161 for the aromatic N heterocyclic compounds and nitriles.

The advantage of high-resolution Py-FIMS in detecting genuine aromatic N heterocyclic compounds is demonstrated by the analysis of chlorophyll a (Fig. 2.5). The most intense signal (at *m/z* 278) originates from the phytyl side chain (substituted phytadiene) (Fig. 2.5(a)). Expanding the y-axis to focus on

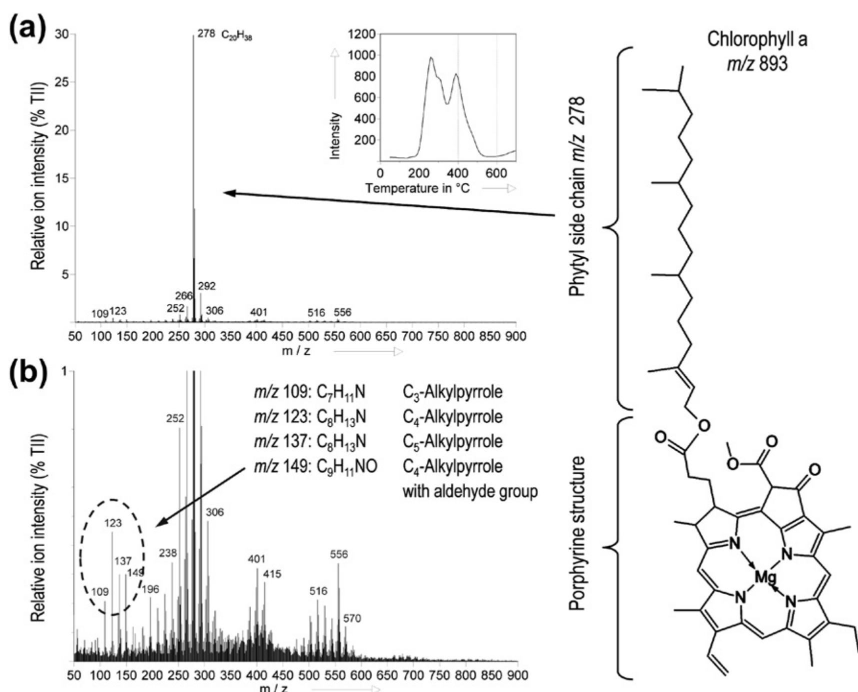


Figure 2.5 Chemical structure of chlorophyll a (a), and the recorded pyrolysis-field ionization mass spectrum of chlorophyll a from spinach (CAS: 479-61-8) showing the most intensive *m/z* 278 of phytyl side chain (a) and a zoom-in highlighting *m/z* 109, 123, 137, 149 of different alkylpyrroles (b). The high-resolved masses determined are shown as nominal masses for simplification.

the remaining spectrum reveals that, in addition to the alkenes and isoprenes from the phytyl side chain (*m/z* 252, 266, 280, 292 and 306), there are several odd-numbered signals in the lower mass range (*m/z* 109, 123, 137 and 149) that represent the four pyrrole derivatives constituting the porphyrin structure (Fig. 2.5(b)). The molecular formulas determined by high-resolution MS revealed correspondence of the *m/z* 109.0892 ($C_7H_{11}N$) to C_3-alkylpyrrole, *m/z* 123.1048 ($C_8H_{13}N$) to C_4-alkylpyrrole and *m/z* 137.1205 ($C_9H_{15}N$) to C_5-alkylpyrrole as typical pyrolysis fragments which appear in every kind of chlorophyll. The exclusive feature of chlorophyll a is the aldehyde group at the second pyrrole ring, detected as *m/z* 149.0841 ($C_9H_{11}NO$). Differentiation of the two main pyrolysis products of chlorophyll corresponds to the two main peaks in the TII-thermogram at 260 °C (phytyl side chain) and 390 °C (pyrrole derivatives). Since these pyrrole derivatives were not recorded in Py-FIMS of pure amino acids (Sorge, 1995), their detection in plant and SOM samples points to their genuine occurrence in natural materials.

Formation and MS detection of aromatic N heterocyclic compounds and nitriles as artifacts was investigated in more detail in spiking experiments with pure peptides. Kruse et al. (2011) proposed thermal decomposition schemes for a dipeptide (glycyl-L-aspartic acid, Gly-Asp) heated stepwise in a matrix consisting of a largely SOM-free soil substrate. Glycyl-L-aspartic acid was selected as a worst-case example because its structure promotes various cyclization reactions. Detailed investigations of volatile and nonvolatile thermal reaction products by Infrared spectroscopy, Py-FIMS, LC/MS and C- and N-XANES spectroscopy revealed that the majority of aromatic N heterocyclic compounds formed by pyrolysis remained in the char, and thus, did not dramatically contradict the results of Py-FIMS measurements. Based on the assignment of all volatilized N-containing reaction products, a correction factor of 0.4 (nonaromatic amides and free amino acids/aromatic N heterocyclic compounds and nitriles) was derived for the temperature-resolved pyrolytic formation and subsequent FIMS detection for the aromatic N heterocyclic compounds and nitriles. Application of this correction factor to the proportions of compound classes in an overview of world soils analyzed by Py-FIMS (Leinweber et al., 2009) indicated that 14–30% of N_{org} could be assigned to aromatic N heterocyclic compounds and nitriles.

In another spiking experiment, albumin was added to a soil sample to enrich the N_{org} pool by factors of 2, 5 and 10. The N_{org} concentration of the samples was highly correlated with the intensity of the marker signals for amides and free amino acids ($R = 0.9998^{***}$) and for the aromatic N heterocyclic compounds and nitriles ($R = 0.9996^{***}$) (Fig. 2.6). This

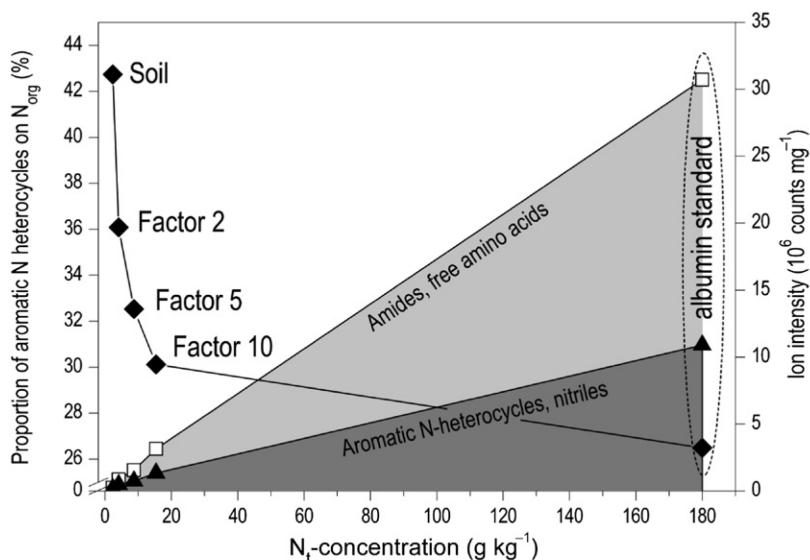


Figure 2.6 Correlation of the ion intensity (counts mg^{-1}) of the marker signals obtained by Py-FIMS for the compound classes (□) amides, free amino acids, and (▲) aromatic N heterocycles, nitriles, and of (◆) the proportion of aromatic N heterocycles, nitriles on total N_{org} (%), respectively, with the concentrations of total N (g kg^{-1}). Sample set consisted of an arable topsoil, the same soil spiked with albumin (from chicken egg white, CAS: 9006-59-1) to yield factors of N_{org} enrichment of 2, 5 and 10 and (encircled) the standard substance albumin alone.

confirms the validity of the selected marker signals for the nonaromatic amides/free amino acids and the aromatic N heterocyclic compounds and nitriles over a range of N_{org} concentrations relevant for soil and related samples. Furthermore, plotting the intensity ratio of aromatic N heterocyclic compounds and nitriles to the amides/free amino acids against the N concentration reveals that the soil itself originally contained more aromatic N heterocyclic compounds and nitriles than were pyrolytically formed from the added albumin. The decrease in intensity ratio with increasing amounts of albumin (up to 20 g kg^{-1}) provides further evidence that any artificial formation of aromatic N heterocyclic compounds and nitrile compounds from peptides cannot explain the measured proportions of nonproteinaceous N in the soil. Nevertheless, for the pure albumin, aromatic N heterocyclic compounds and nitriles were formed and detected in proportions up to 35% of the amide intensity. Accounting for this overestimation reveals a corrected proportion of aromatic N heterocyclic compounds and nitriles in the original (nonspiked) soil of 20% of the N_{org}. This is well within the

range derived from the spiking experiment described above (Kruse et al., 2011). The same experiment conducted with N-acetylglucosamine (chitin), an amide, resulted in a pyrolytic formation and Py-FIMS detection of aromatic N heterocyclic compounds and nitriles of about 17% of the amide intensity (not shown).

In summary, evaluation of the Py-FIMS data was improved by (1) developing a new set of marker signals for amides (peptides, amino sugars), free amino acids, aromatic N heterocyclic compounds and nitriles, and (2) developing correction factors to account for the pyrolytic formation of cyclic N_{org} compounds from noncyclic N_{org} compounds. Correction factors vary from 0.35 (for albumin) to 0.17 (for glucosamine); however, because proteins and amino sugars represent the major noncyclic N_{org} compounds, an average value of 0.25 was used to calculate corrected TII proportions for aromatic N heterocyclic compounds and nitriles [Eqn (1)] and amides and free amino acids [Eqn (2)]:

$$TII_{cycl\text{-}N\text{-}c} = 1 - (0.25 \times TII_{amide\text{-}N\text{-}u}) \quad (1)$$

$$TII_{amide\text{-}N\text{-}c} = 1.25 \times TII_{amide\text{-}N\text{-}u} \quad (2)$$

where $TII_{cycl\text{-}N\text{-}c}$ is the corrected proportion of cyclic N_{org} compounds in percentage of total ion intensity (TII); 0.25 is the correction factor derived from spiking experiments with albumin and glucosamine; $TII_{amide\text{-}N\text{-}u}$ is the uncorrected proportion of amides and free amino acids in percentage of TII; and $TII_{amide\text{-}N\text{-}c}$ is the corrected proportion of amides and free amino acids in percentage of TII.

Leinweber and Eckhardt (unpublished data) used the new *m/z* marker signals and correction factor to re-analyze a large Py-FIMS data set obtained from microbial biomass, plant, bulk soil and DOM samples. This revealed a wide range of values for the TII-proportions of amides + free amino acids and aromatic N heterocyclic compounds + nitriles (Table 2.2). Primary organic matter entering the soil—such as plant material, litter, and soil biota—seem to contain amides and free amino acids (5–11% of TII) in amounts not very different from those of soils (5–13%) and DOM (3–10%). However, some soils appear to be enriched in aromatic N heterocyclic compounds and nitriles, relative to the primary organic matter and DOM. Indeed, based on the amounts of N heterocyclics + nitriles expressed as percentage of all signals assigned to N_{org}, the reference soil groups were grouped as follows: relatively young, less-developed soils (Anthrosols, Andosols, Podzols and Regosols) with <10% N_{org}; soils influenced by groundwater

Table 2.2 Composition of N_{org} as Revealed by Py-FIMS in Parent Materials of Soil Organic Matter, Bulk Samples from Reference Soil Groups and Dissolved Organic Matter of Different Origin (Leinweber and Eckhardt, 2012, unpublished data); Soils are Arranged According to the Rationalized Key to The WRB Reference Soil Groups (IUSS Working Group WRB, 2006)

Sample origin	Sample number	Amides, free amino acids (% TII)	Aromatic N heterocyclic compounds and nitriles (% TII)	Aromatic N heterocyclic compounds and nitriles (% N_{org})
Soil microbes and plant litter				
Bacteria	4	10.7 ± 1.2	2.1 ± 0.5	16.2 ± 4.1
Fungi	4	8.3 ± 3.8	1.3 ± 1.1	13.6 ± 7.8
Plant residues	7	8.2 ± 1.2	0.7 ± 0.7	7.9 ± 6.0
Litter layers	8	4.6 ± 0.4	0.8 ± 0.1	14.0 ± 0.6
Soils				
Histosols	20	5.9 ± 1.5	0.9 ± 0.8	13.0 ± 8.4
Anthrosols*	8	5.3 ± 0.6	0.6 ± 0.2	9.4 ± 1.6
Vertisols	5	12.2 ± 0.1	5.5 ± 4.5	30.9 ± 5.8
Fluvisols	4	10.3 ± 0.1	4.0 ± 1.9	26.9 ± 6.1
Gleysols†	6	7.8 ± 0.7	1.4 ± 0.2	15.0 ± 2.3
Andosols	4	7.9 ± 0.9	0.5 ± 0.4	6.4 ± 3.9
Podzols‡	9	2.6 ± 1.7	0.5 ± 0.9	3.9 ± 19.1
Stagnosols	3	12.9 ± 0.1	6.2 ± 0.7	32.3 ± 1.7
Chernozems	29	9.6 ± 4.4	3.8 ± 3.1	23.9 ± 8.6
Kastanozems	2	7.6 ± 0.1	2.2 ± 0.3	23.4 ± 4.1
Phaeozems	85	6.6 ± 1.2	1.9 ± 0.8	21.4 ± 5.8
Luvisols	35	11.4 ± 0.1	4.9 ± 2.1	30.1 ± 4.8
Regosols	9	5.2 ± 1.2	0.6 ± 0.3	8.7 ± 4.4
Dissolved organic matter				
Rhizodeposits	44	8.9 ± 3.9	0.7 ± 0.5	7.4 ± 4.4
CW§ extracts	6	4.4 ± 0.3	0.6 ± 0.1	12.0 ± 0.9
HW§ extracts	6	8.6 ± 1.9	1.8 ± 0.7	16.5 ± 3.4
Groundwater	6	3.3 ± 0.2	0.3 ± 0.1	6.8 ± 3.5

*Plaggic anthrosols.
†Colluvic gleysols.
‡Only illuvic subsoil horizons with humus enrichments.
§CW = cold-water, HW = hot-water.

(Histosols, Fluvisols, Gleysols) with 15–27% N_{org}; zonal soils from steppe climates likely influenced by fire (Chernozems, Kastanozems and Phaeozems) with 21–24% N_{org}; and soils with high clay contents and fluctuating redox conditions (Vertisols, Stagnosols and Luvisols) with 30–32% N_{org}. These data, together with the groupings, indicate that soil processes affect

the partitioning of N_{org} into nonaromatic and aromatic compounds. In Section 4, we will explain how two of the above soil-forming factors—fire and organic–mineral interactions—promote the formation of aromatic N heterocyclic compounds and nitriles.

2.3.3. Isotope-Ratio Mass Spectrometry

Isotope-ratio mass spectrometry (IRMS) measures the relative abundance of stable isotopes in a sample. However, for a given element, the abundances of the various stable isotopes vary according to physical, physiological, and biochemical isotopic fractionation processes. Consequently, variations in the isotopic ratio of N (i.e. $^{15}N/^{14}N$) can be used both as fingerprints of the N source and to track the fate and transformation of N-containing compounds (Elsner, 2010). The acronym "IRMS" encompasses several MS techniques, which differ in the type of mass separation, ionization and inlet system. Elemental analyzers are the most commonly used inlet systems in environmental studies of light elements such as N. Nonvolatile liquid or solid samples are combusted under a continuous oxygen flow producing N_2 and NO_x (which are then converted to N_2) and after chromatographic separation of the N_2 from other gases, the effluent is analyzed by the IRMS (Fry et al., 1992). Isotopic results are presented relative to a reference standard analyzed in conjunction with the sample. Because EA-IRMS involves the total combustion of a sample, the elemental isotopic information is for the bulk soil sample. In contrast, compound-specific N-isotope analyses require hyphenated gas chromatography (GC/C/IRMS; Isobe et al., 2011), liquid chromatography (LC/IRMS; Krummen et al., 2004), or ultrahigh-resolution Fourier transform-ion cyclotron resonance mass spectrometry (FT-ICR MS; see Section 2.3.4). Spatial information can be obtained using laser ablation inductively coupled plasma mass spectrometry (Böhme et al., 2010)—though this has a relatively high detection limit (5 g N kg^{-1})—or by using nanoscale secondary ion mass spectrometry (Nano-SIMS; see Section 2.3.5).

2.3.4. Fourier Transform-Ion Cyclotron Resonance Mass Spectrometry

FT-ICR MS is one of the most sensitive MS techniques—capable of detecting molecular masses with both ultrahigh mass resolution ($>10^6$) and mass accuracy. Ions are most often generated via atmospheric pressure ionization techniques such as electron spray ionization or matrix-assisted laser desorption ionization. These ions are guided into the ICR cell and forced as an ion cloud in a circular motion via the magnetic field of a superconducting magnet (typically 4.7–13 T). The ions are excited to a larger orbit radius

by an oscillating electric field through two opposite excitation electrodes perpendicular to the magnetic field. After excitation, the increased orbit radius induces an oscillating current in two opposite detection plates, whose frequency is a function of the *m*/*z* of the single ions. Using an oscillating electric field impulse enables the detection of ions with varying *m*/*z*. The resulting superimposition of many signal frequencies is deconvoluted into single frequencies and, hence, *m*/*z* signals by applying Fourier transformation. Mass resolution increases linearly with magnetic field strength and ongoing technical developments have resulted in the application of superconducting magnets with up to 20 T. On-line coupling of the FT-ICR MS with chromatographic interfaces such as LC may further enhance the analytical power of this technique (Wang et al., 2010). To date, however, organic N compounds have been studied most intensively in crude oils (e.g. Mapolelo et al., 2011; Marshall and Rodgers, 2004; Rodgers et al., 2009) and there are only a few investigations of N_{org} compounds in environmental samples by FT-ICR MS—e.g. the characterization of DOM from lake water and corresponding watershed N (Minor et al., 2012) and groundwater (Longnecker and Kujawinski, 2011). Furthermore, $CHON^+$ compounds formed the largest class in DOM of continental precipitation with the majority containing only one N atom. The elemental ratios of these compounds and their detection in the positive-ion mode suggested compounds with reduced N functionality (Altieri et al., 2009). Schmidt et al. (2009) progress in the characterization of N_{org} in DOM for pore water samples from continental shelf sediments, and recently concluded from FT-ICR MS measurements (Schmidt et al., 2011) that organic-matter quality and contrasting redox conditions had no effect on the protein diagenesis in the subsea floor. Furthermore, Podgorski et al. (2010) used atmospheric pressure photoionization for FT-ICR MS to efficiently ionize N-containing DOM species; their results indicated that N may have been incorporated into ring structures. Clearly, these techniques have great potential to identify N_{org} compounds in environmentally relevant samples—especially the soil DOM fraction.

2.3.5. Nanoscale Secondary Ion Mass Spectrometry

Secondary ion mass spectrometry (SIMS) is a destructive desorption MS technique linking high-resolution microscopy with isotopic analysis, which provides spatially resolved information on the molecular, elemental and isotopic composition of a sample. The SIMS technique involves continuous bombardment of the sample surface with a focused high-energy beam of

primary ions. This results in sputtering of the upper surface of the sample and release of neutral particles and positively or negatively charged “secondary ions”. The system is maintained under ultrahigh vacuum (~1.3 × 10^{-11} kPa) to prevent atmospheric interference with the primary and secondary ions. Using cesium (Cs^+) or oxygen (O^-) as the primary ion beam enhances the yield of secondary ions compared to nonreactive ions (Heister et al., 2012). Secondary ions produced can be mono-atomic or polyatomic (e.g. $^{12}C^-$, $^{13}C^-$, $^{12}C^{14}N^-$ using a Cs^+ beam or C^+, $^{23}Na^+$, $^{39}K^+$, $^{40}Ca^+$ using an O^- beam). Polyatomic ions result from recombination reactions of reactive mono-atomic ions (Legent et al., 2008; McMahon et al., 2006). For example, N is detectable as the recombined secondary ion species CN^- only because the yield of secondary N^- ions is too low for detection. The secondary ions are then separated in the magnetic field of a mass spectrometer according to their m/z. By recording a series of spatially resolved mass spectra through raster-scanning, line- or map-scans of the sample can be produced for selected m/z signals.

There are two classes of SIMS instruments: static SIMS (time-of-flight secondary ion mass spectrometry: ToF-SIMS), which uses a pulsed primary ion beam with limited dose (<10^{12} ions cm^{-2}) to reveal the molecular composition of the top surface, and dynamic SIMS (Nano-SIMS) using an unlimited primary ion dose for in-depth elemental distribution analysis. The main advantage of the latest generation of Nano-SIMS spectrometers (e.g. Cameca, Nano-SIMS 50L) over ToF-SIMS is very high mass resolution. This enables isotopic differentiation between $^{13}C^{14}N$ (m/z 27.016) and $^{12}C^{15}N^-$ (m/z 27.009), while maintaining both excellent signal transmission and high spatial resolution. Spatial resolution depends on the primary ion—equaling ~150 nm for O^- and ~50 nm for Cs^+ (Müller et al., 2012). However, high spatial resolutions can be achieved only by focusing the ion beam, which results in a dramatic decrease in beam intensity. For applications to SOM, the beam is usually defocused to maintain a sufficient ion yield at the expense of spatial resolution (~200 nm) (Heister et al., 2012). The latest generation of Nano-SIMS can record up to seven m/z signals simultaneously. Due to the high dose of the primary ion beam, almost all molecules at the sample surface are completely fragmented resulting in rapid surface erosion (several tens of micrometers). However, this enables 3-D mapping of the sample using computational 3-D reconstruction of the images obtained from the subsequent scanning cycles. Such 3-D reconstructions are affected by element-, isotope- and matrix-dependent sputtering rates as well as ion yields and charging effects (Ghosal et al., 2008; Winterholler et al., 2008).

Furthermore, topographical unevenness of the sample can distort subsequent 3D reconstruction. Attempts to overcome such difficulties combine topographical information from atomic force microscopy with Nano-SIMS analysis (Fleming et al., 2011) together with the analysis of standard materials of known composition and matrix to determine matrix-specific mass and ion yield fractionation. Figure 2.7(a) shows the uneven distribution of $^{12}C^{14}N^{-}$ at the surface of organic-mineral soil particles. Figure 2.7(b) indicates how the secondary organic ions were sputtered from the surface in three regions of interest—reaching a minimum after 80 scanning cycles. Theoretically, this enables estimation of the thickness of organic matter at mineral surfaces, provided sputter rates and the thickness of one layer can be determined exactly. A potential application of the method lies in determination and visualization of a ^{15}N label incorporated into the soil architecture (Müller et al., 2012). The application of this technique to soil N research, however, is still in its infancy.

2.4. X-ray Absorption Spectroscopy

2.4.1. X-ray Photoelectron Spectroscopy

X-ray photoelectron spectroscopy (XPS), also called electron spectroscopy for chemical analysis, is based on the use of energy from a fixed X-ray to excite core electrons from a sample. Whereas conventional XPS uses a monochromatic X-ray source (e.g. Al Kα: $h\nu$ = 1486.6 eV, or Mg Kα:

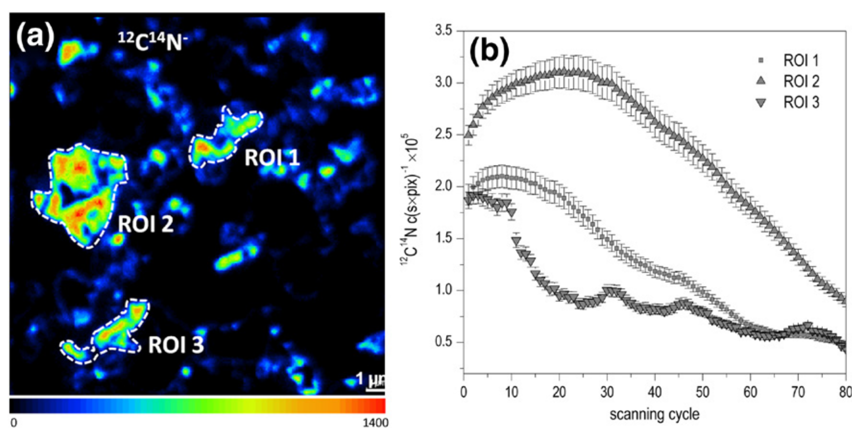


Figure 2.7 Image (15 µm × 15 µm) of $^{12}C^{14}N^{-}$ distribution (a) on fine silt/clay particles on Si-wafer. The graph (b) shows the depth distribution of $^{12}C^{14}N^{-}$ for 80 subsequent drift corrected measuring cycles. *(Reproduced from Müller et al. (2012) with permission from Elsevier)*. For color version of this figure, the reader is referred to the online version of this book.

$h\nu$ = 1253.6 eV), the use of synchrotron radiation as an X-ray source has increased dramatically over the past 15 years. The kinetic energies of emitted electrons are measured via an electron analyzer. The binding energy (BE) for an electron ($BE = h\nu - KE - \Phi$; where KE is the measured kinetic energy and Φ is the spectrometer work function) is characteristic of a given element and its chemical environment. Thus, variations in the elemental binding energy (i.e. chemical shifts) indicate the local coordination of the N atoms in the sample (Fig. 2.8).

By deconvoluting the XPS spectra into sub-peaks using additively linked Gaussian–Lorentzian functions, peak areas of individual species can be calculated. These peak areas are then converted into atomic concentrations (>~0.1 atom%) using atomic sensitivity factors (Yeh and Lindau, 1985). Alternatively, proportions of individual N species can be calculated to gain quantitative information.

Due to the small penetration depth (small mean free path) of the emitted photoelectron, only electrons from the near surface can be captured by the detector. Therefore, qualitative or quantitative information gained from an XPS experiment is always limited to the upper 10 nm of the surface. Because of this high surface sensitivity, XPS experiments usually require ultrahigh vacuum conditions to avoid any contamination of the surface by adsorbates from the ambient atmosphere. However, recent advances in

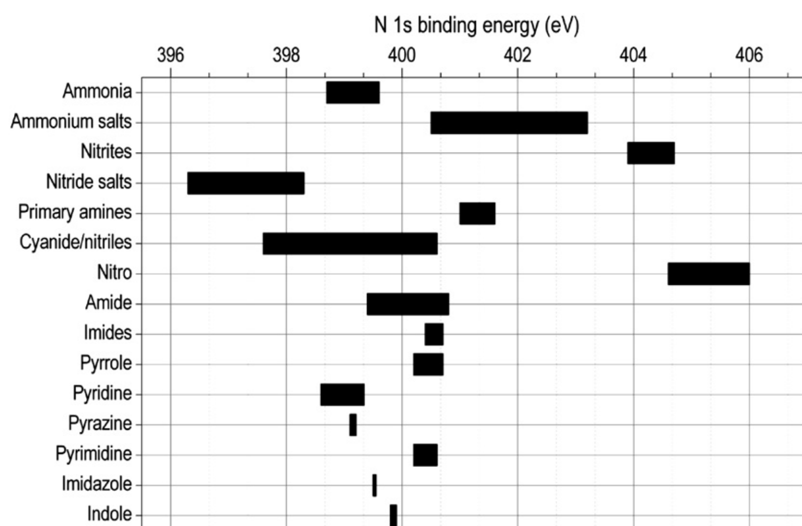


Figure 2.8 Ranges of N 1s binding energies of various soil-relevant N moieties in XPS spectra (Moulder et al., 1992).

synchrotron-based XPS also allow measurements at ambient pressure and in hydrated samples (Ghosal et al., 2005; Salmeron and Schlögl, 2008). The use of intense third-generation synchrotron radiation as the X-ray source ameliorates the risk of radiation-induced chemical changes in the sample (e.g. Zubavichus et al., 2005). The combination of a reasonably short exposure time (e.g. <5 min at 3×10^{11} photons s^{-1} for histidine) and cryogenic cooling of the sample eliminates spectral changes (Zubavichus et al., 2005).

Using XPS, Abe and Watanabe (2004) demonstrated that the N_{org} in purified humic substances was composed of aromatic (3–19%), peptide-bound (67–90%) and primary amine N (7–17%), and that the proportions of aromatic N were positively correlated with the degree of humification. This general composition of humic substances was confirmed by CP/MAS ^{15}N NMR spectra, and the comparison of the two methods revealed significant positive correlations for the proportions of peptide N (i.e. 70–85% of N_{org}) and proportions of heterocyclic N (i.e. 5–20% of N_{org}) (Abe et al., 2005).

Another fast growing technique is lateral resolved XPS. The lateral resolution is on the order of several micrometers and enables the study of heterogeneous sample surfaces and determination of spatial distributions and relationships between chemical species (e.g. Escher et al., 2010; Walton and Fairley, 2005).

2.4.2. XANES Spectroscopy

The use of synchrotron radiation has enabled development of several spectroscopic and microscopic analytical techniques to investigate chemical processes at the molecular-scale. XANES spectroscopy, also known as near-edge X-ray absorption fine structure, is an element specific spectroscopic technique that yields electronic and structural information about the element of interest. An XANES spectrum is usually characterized by intense resonance features, arising from the transition of a core electron to an unoccupied orbital and continuum level, and from multiple scattering of the emitted photoelectrons by the geometrical arrangement of neighboring atoms around the absorbing atom. The energy position of the resonance features is related to the chemical environment of the absorber, such as oxidation state (Fendorf and Sparks, 1996). An N-XANES spectrum is typically recorded in the energy range from 380 to 420 eV, and is characterized by more or less sharp $1s \rightarrow \pi^{\star}$ resonances (<405 eV) and considerably broader $1s \rightarrow \sigma^{\star}$ resonances. An N-XANES spectrum represents the weighted sum of all spectra of all N-containing compounds in a sample. There are two basic ways to estimate

N composition in an unknown sample from an N-XANES spectrum. The "fingerprint" approach directly compares the sample spectrum with spectra from known reference compounds, enabling the assignment of spectral features characteristic of the respective N moieties. A wide range of reference spectra have been published; e.g. Leinweber et al. (2007; 2010a) published comprehensive spectral libraries of environmentally relevant N-containing compounds and moieties (see Fig. 2.9). The XANES regions of different N species often overlap significantly over the entire spectra region. Therefore, in complex matrices or samples such as whole soil, generally only three groups of N moieties can be distinguished: (1) C=N aliphatic and/or aromatic imine at ~398.9 eV, (2) nitrilic N and/or aromatic C=N in pyrazoles or imidazoles at ~400 eV and (3) amidic N with some contribution of pyrrolic N at ~401.4 eV. A few studies also showed nitro-N-compounds at 405 eV (Gillespie et al., 2011a). When published reference spectra are used for comparison and feature assignment, it is important that the experimental setup, including energy step size and scan resolution, is in the same range—a correct energy alignment of all spectra is crucial (Gillespie et al., 2008).

Whereas feature assignment by comparison with reference spectra yields qualitative information, quantitative information on sample composition can be obtained if spectra deconvolution into sub-peaks—using Gaussian or additively linked Gaussian–Lorentzian functions—occurs. Calculated peak area as a proportion of the total peak area indicates the proportion of

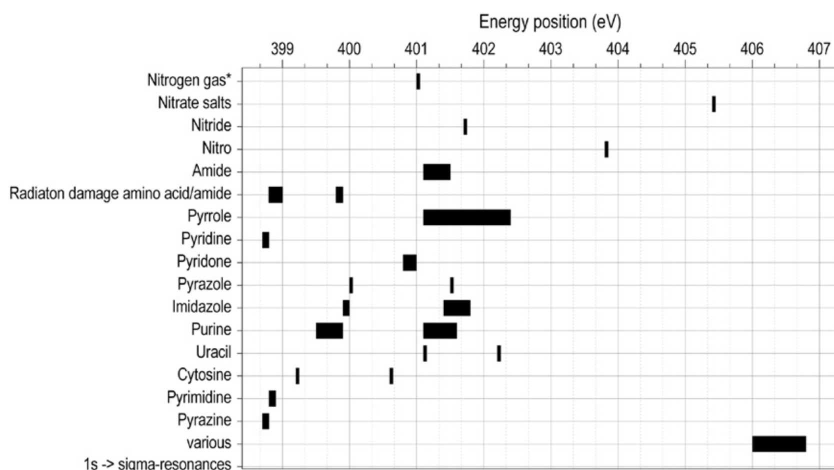


Figure 2.9 Ranges of the energy positions of main features of various soil relevant N moieties in K-edge X-ray absorption near edge structure spectra. *(Data compiled from Leinweber et al. (2007)).*

individual N moieties. Compared to other elements in SOM (e.g. S or C), there are only a few publications that applied this approach to N-XANES spectra from environmental samples (Kiersch et al., 2012a; Leinweber et al., 2010a; Vairavamurthy and Wang, 2002). More research is required to derive sensitivity factors for N moieties relevant to SOM, like those published for S-compounds of different oxidation state (Huffman et al., 1991; Xia et al., 1998). Another approach to reducing spectral complexity involves combining bulk XANES (with relatively large sample spots: ~1 mm^2) with spatially resolved techniques such as μ-XRF and μ-XANES (with relatively small sample spots: ~50 nm^2) to investigate hot spots with a more uniform SOM composition than is found in the bulk sample. An even more advanced approach is the application of submicroscopically resolved techniques for N speciation; i.e. scanning transmission X-ray microscopy (STXM).

2.4.3. Scanning Transmission X-ray Microscopy

The term STXM applies to microscopes operating in the soft X-ray range (<2000 eV). The STXM image is formed by scanning the sample through the focal spot of a Fresnel zone plate in the X- and Y-directions. A series of images is collected by recording the total transmitted X-ray intensity for each scanned pixel as a function of sample position and energy. The series of images can then be aligned (stacked) to enable the extraction of whole spectral information of a specific point of interest. These spatially aligned stacks can be further processed and statistically evaluated to extract spatial distribution patterns or maps (Jacobsen et al., 2000; Lerotic et al., 2005). Quantitative composition maps can be derived by converting the transmitting signal to an optical density. All measurements with STXM require undisturbed samples that must be partly transparent at the X-ray energy of interest, which means a sample thickness of about 100–400 nm for studies of N_{org}. Such thin sections can be prepared by drop coating (Covelli et al., 2009; Schumacher et al., 2005) or embedding in elemental S and subsequent cutting (Kinyangi et al., 2006; Lehmann et al., 2008). Particular care must be taken to ensure that the sample is representative because only a small area of the sample is mapped with a high spatial resolution (~40 nm), and complementary investigations such as digital image analysis of thin sections and scanning electron microscopy are recommended to identify regions of interest within the sample. The first STXM applications to soil particles indicated larger abundance of features at 399.1 eV (pyridine, pyrazine) and 400.1 eV (imidazole) in a pyrogenic microenvironment compared to the amide-N feature at 401.4 eV, which predominated in a section with enrichment of

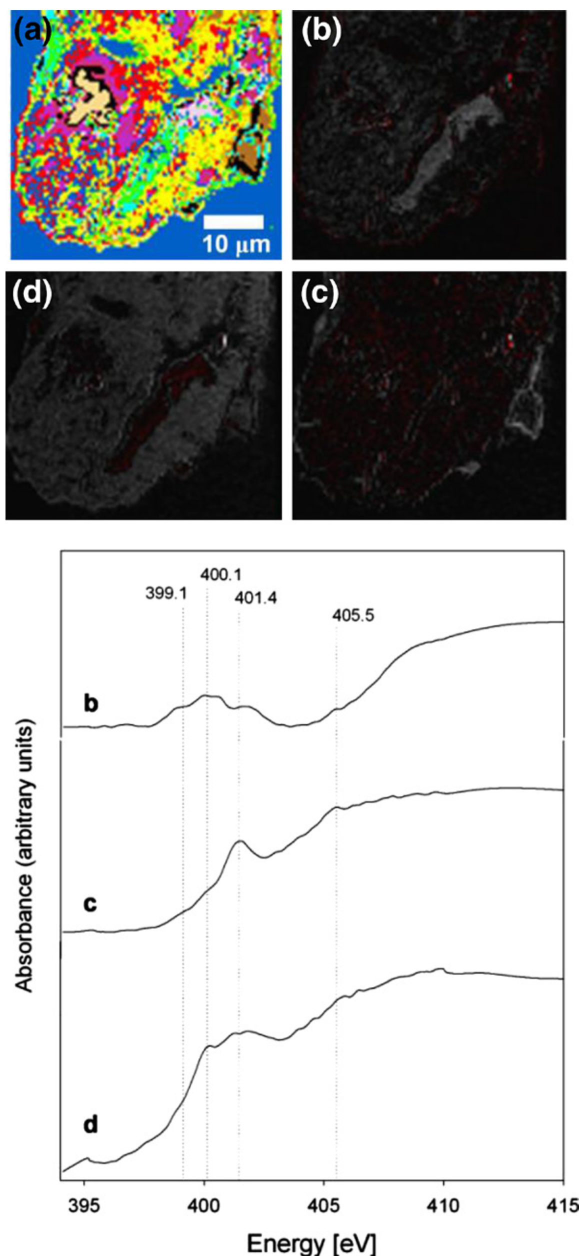


Figure 2.10 N K-edge X-ray absorption near edge structure cluster image (a) and target maps with associated target spectra of a thin section obtained from a soil microaggregate, (b) black carbon region, (c) regions with organic matter of microbial origin and (d) the remainder of the aggregate section (Lehmann and Solomon, 2008). *(Reproduced with permission from the authors)*. For color version of this figure, the reader is referred to the online version of this book.

microbial matter (Lehmann and Solomon, 2008) (Fig. 2.10). A similar, but more detailed study reported slight differences among various nanoregions of microbial structures and a general predominance of amino acids/peptides (401.4 eV) (Solomon et al., 2012). The N-XANES features at a nearby (<1 μm distance) organic–mineral interface showed more intensive features at 400.0 and 402 eV (assigned to N heterocyclic compounds and amino sugars), although there were also differences among the outer, intermediate and inner interface (Solomon et al., 2012).

2.5. ^{15}N Isotope Techniques

Nitrogen exists as two stable isotopes, ^{14}N and ^{15}N, the latter of which naturally occurs at 0.3663 atom% in atmospheric N_2. Stable isotope techniques enable the investigator to measure changes in the abundance of ^{15}N relative to ^{14}N in various N pools caused by natural isotopic fractionation (^{15}N natural abundance techniques) or by exogenous additions of simple and complex ^{15}N-enriched materials (^{15}N-enrichment techniques). Natural abundance techniques can provide mechanistic insight into the N cycle and are often used for exploratory purposes and hypothesis generation. Enrichment techniques are more appropriate for quantifying the transfer of N from source to sink and tracing the fate of N through the N cycle (Bedard-Haughn et al., 2003). The following discussion briefly highlights ^{15}N tracer techniques, with a focus on ^{15}N labeling of plants for organic residue decomposition and rhizodeposition studies. For extensive reviews on ^{15}N isotopic dilution, refer to Hart et al. (1994) and Murphy et al. (2003). More detailed information on the technical and theoretical applications of ^{15}N natural abundance and enrichment techniques can be found in books edited by Boutton and Yamasaki (1996), Knowles and Blackburn (1993), and Unkovich et al. (2001).

Classical ^{15}N tracer techniques have been used in agronomic research for the past 70 years to directly assess biochemical pathways in the N cycle (Hauck and Bremner, 1976). Nitrogen-15 is added into a substrate pool of interest and the ^{15}N traced into various product pools. In their simplest application, tracer techniques can be used to qualitatively identify processes within the N cycle (e.g. N_2 fixation, plant uptake of amino acids) (Powlson and Barraclough, 1993). Mass balance approaches—based on quantitative ^{15}N recovery of added ^{15}N fertilizer in soil and crops—have been used extensively for determining losses of N from agricultural systems via gaseous loss (volatilization and denitrification) or N leaching (Gardner and Drinkwater, 2009). Provided the substrate pool is uniformly enriched with ^{15}N, changes in ^{15}N abundance in the substrate

and product pools over time can be measured and used to quantify rates of various N transformations, such as plant uptake and metabolism of N fertilizer, N_2 fixation, microbial assimilation of NH_4^+ and NO_3^-, and nitrification and denitrification (Hart and Myrold, 1996; Powlson and Barraclough, 1993). Commercial availability of $^{15}NH_4^+$, $^{15}NO_3^-$ and ^{15}N-amino acids (available at enrichments of 5–99 atom% ^{15}N) and access to commercial IRMS laboratories led to the widespread use of ^{15}N tracer techniques. Tracer approaches have been used to challenge classic paradigms of the N cycle, including plant uptake of organic N and successful plant competition with microorganisms for soil N (Schimel and Bennett, 2004). Dual ^{15}N isotope labeling with ^{13}C, ^{14}C, or ^{18}O has extended the utility of tracer techniques to further understand processes within the N cycle including organic N uptake by plants (Jones et al., 2005b); the contribution of belowground plant N and C to soil pools and processes (Wichern et al., 2007a; Yasmin et al., 2010); and, source partitioning of N_2O emissions from soils (Baggs, 2008).

Complex ^{15}N-enriched organic materials, such as plant residues and animal manures, are not commercially available and must be prepared by the researcher. Experiments investigating the decomposition of plant residues and their influence on soil N processes generally take a two-step approach: first, plants are grown in soil or solution culture supplied with repeat pulses of ^{15}N-enriched fertilizer to obtain a target ^{15}N-enrichment in the plant; likewise, manures can be prepared by feeding an animal ^{15}N-enriched feed (Bosshard et al., 2011). The ^{15}N enrichment of the harvested residues or manure is then determined using IRMS and the ^{15}N-enriched materials are applied to the soil at known ^{15}N rates in laboratory incubation, pot or field studies. Homogeneity of ^{15}N within the labeled organic material is necessary when tracing the fate of the residue-derived N in soil to avoid underestimations of the whole-residue contribution to processes or soil N pools (Fillery and Recous, 2001). Uneven enrichment of symbiotically fixing legumes can occur due to dilution of fertilizer-derived ^{15}N by fixed atmospheric ^{14}N (Fillery and Recous, 2001), unless N fixation is suppressed (Frimpong and Baggs, 2010). Application of ^{15}N-enriched organic materials to soil has been instrumental in determining the fate of N from decomposition of organic residues to soil inorganic and organic N pools, soil microbial biomass (Jensen, 1994), the production of N_2O (Millar and Baggs, 2004), and recently within specific microbial communities using ^{15}N-DNA stable isotope probing (^{15}N-DNA-SIP) (España et al., 2011).

Nitrogen-15 labeling techniques of plant and soil have been developed primarily for investigations of N rhizodeposition, with the ^{15}N label being used to differentiate the small input of N from roots against the large background of soil N (Schmidtke, 2005a). Interest in developing methods to determine N-rhizodeposition has increased between the years 2001 and 2010 as scientists seek to understand the contribution of belowground N to total N budgets, particularly in legume-based crop rotation and intercropping systems (Fustec et al., 2010), and the fate of rhizodeposits from legumes and cereals in the various soil N pools (De Graaff et al., 2007; Janzen, 1990; Jensen, 1996; Mayer et al., 2004; Wichern et al., 2007a; zu Schweinsberg-Mickan et al., 2010). Despite our limited understanding of the ecological significance of N rhizodeposition (Wichern et al., 2008), few ^{15}N studies have investigated the chemical composition of the organic N compounds released to the soil from plant roots (Hertenberger and Wanek, 2004; Merbach et al., 1999). While there are clear conceptual definitions of rhizodeposition, elucidating differences in processes through experimentation remains difficult (Jones et al., 2009). Due to methodological challenges, even relatively recent studies on N rhizodeposition have focused on improvement and comparison of ^{15}N stable isotope techniques (Hertenberger and Wanek, 2004; Khan et al., 2002a; Mahieu et al., 2007, 2009; Schmidtke, 2005a; Yasmin et al., 2006). Indeed, the methods developed to determine C and, particularly, N rhizodeposition are fraught with uncertainty, primarily due to difficulties in achieving label uniformity within the plant and thus difficulties satisfying the assumptions of the calculations involved (Rasmussen, 2011).

Most ^{15}N isotope methods take the approach of supplying the tracer directly to the plant without labeling the soil and include shoot labeling (Mayer et al., 2003; Russell and Fillery, 1996; Wichern et al., 2007a, 2007b); leaf immersion (De Graaff et al., 2007; Khan et al., 2002a); and atmospheric labeling using NH_3 (Janzen and Bruinsma, 1989; Schulze and Merbach, 2008) or N_2 (Mohr et al., 1998; Russelle et al., 1994). Only split-root labeling introduces the ^{15}N label to the plant through the soil (Jensen 1996; Mahieu et al., 2007). Of these methods, the atmospheric labeling of N_2 and NH_3 and the split-root technique assimilate ^{15}N into the plant via natural mechanisms. Comprehensive reviews of the labeling techniques used to investigate N rhizodeposition have been published by Fustec et al. (2010) and Wichern et al. (2008).

Nitrogen rhizodeposits are often quantified by calculating the percentage of soil N derived from rhizodeposition (% NdfR) using the equation developed by Janzen and Bruinsma (1989):

$$\% \text{ NdfR} = \frac{\left(\text{atom } \% \, {}^{15}\text{N soil} - \text{atom } \% \, {}^{15}\text{N background A}\right)}{\left(\text{atom } \% \, {}^{15}\text{N roots} - \text{atom } \% \, {}^{15}\text{N background B}\right)} \times 100$$

where A is the background ^{15}N in the soil in which unlabeled plants are grown and B is the background ^{15}N in the roots of unlabeled plants (Schmidtke, 2005b). Quantities of NdfR are calculated by multiplying %NdfR by the total N in the particular soil pool of interest (Jensen, 1996; López-Bellido et al., 2011; Mahieu et al., 2007; Mayer et al., 2003; Wichern et al., 2007b; Yasmin et al., 2010; zu Schweinsberg-Mickan et al., 2010). These calculations represent net rhizodeposition since re-absorption of N by the plant is not determined. The precision of the calculation can be improved by increasing the ^{15}N-enrichment of the roots and the rhizodeposits, and by increasing the number of plants grown per pot (Schmidtke, 2005b). Use of the Janzen and Bruinsma equation involves several assumptions; for example, that ^{15}N enrichment of the roots is the same as the ^{15}N enrichment of the rhizodeposits; distribution of ^{15}N within the root system is uniform; and ^{15}N enrichment of roots is constant over the growth period of the plants (Mayer et al., 2003). However, variation in ^{15}N enrichment along the root has been observed (Khan et al., 2002a), and ^{15}N enrichment can differ among nodulated roots, non-nodulated roots, and nodules due to dilution by atmospheric ^{14}N (Khan et al., 2002b; Russell and Fillery, 1996). In addition, the longer the duration of the experiment, the more likely that changes in root ^{15}N content may occur without a concomitant loss to the soil, thus resulting in violation of assumptions and erroneous interpretation of results (Rasmussen, 2011). For example, the Janzen and Bruinsma equation will overestimate N rhizodeposition when root ^{15}N enrichment is diluted with ^{14}N incorporated from the soil during root growth following ^{15}N labeling, or when ^{15}N is redistributed from roots to shoots during regrowth of perennial forages following cutting (Rasmussen, 2011). To avoid these issues, some researchers report the ^{15}N recovered in the soil as a percentage of total ^{15}N (De Graaff et al., 2007; Yasmin et al., 2006), which allows for comparison among treatments (Wichern et al., 2008) without relying on the Janzen and Bruinsma equation. Nevertheless, when these isotope techniques are applied to plants grown in the field, or in intact soil cores, researchers must take care to separate roots of ^{15}N-labeled plants from recoverable unlabeled roots of previous crops or weeds.

Rasmussen (2011) suggests that using a ^{15}N mass balance approach in conjunction with total plant N yields to quantify N rhizodeposition will ameliorate problems of heterogeneous ^{15}N enrichment compared to relying on specific ^{15}N abundance of roots and soil. However, where the ratio of ^{15}N enrichment of shoots to roots is high, mass-balance calculations may underestimate the contribution of N rhizodeposition to total plant N. Nonuniform distribution of ^{15}N among roots and aboveground plant parts is inherent to most shoot-labeling approaches (Mahieu et al., 2007; Mayer et al., 2003; Russell and Fillery, 1996; Yasmin et al., 2006) and may lessen the utility of using a simple ^{15}N mass balance approach to estimate belowground N (Khan et al., 2002a).

Estimates of N-rhizodeposition as a percentage of total plant N vary between 4% and 71% using in situ labeling methods, even within a single plant species (*Pisum sativum* L.) (see review by Wichern et al., 2008). This is partially due to differences in how the ^{15}N labeling is performed. Application of ^{15}N-enriched solutions to the aerial parts of the plant is the most common method used to label roots and ultimately the soil through rhizodeposition. These methods are technically simple to implement for a variety of crop species and do not require complicated or expensive equipment. Leaf and petiole labeling involves cutting the leaf and immersing the cut leaf or petiole in a vial containing the ^{15}N-labeled solution. Alternatively, the ^{15}N solution can be supplied to the plant via a cotton wick, threaded into the stem, and immersed in ^{15}N-enriched solution contained in a vial, and is often referred to as the stem- or cotton-wick technique (Fig. 2.11). The transpiration stream drives the ^{15}N uptake using stem-wick feeding, whereas active and passive transport mechanisms are involved in transfer of ^{15}N using leaf-immersion techniques (Russell and Fillery, 1996). Solution uptake efficiency generally follows the order: cut leaf feeding > petiole feeding > stem-wick feeding (McNeill et al., 1997; Yasmin et al., 2006). Khan et al. (2002b) suggested that whereas leaf and petiole feeding may be suitable for short-duration ^{15}N labeling in the field, the stem-wick feeding apparatus is more robust and is suitable for long-duration labeling in the field (Mahieu et al., 2007; Wichern et al., 2007b)—though labeling frequency may be limited if field sites are relatively remote.

Labeling method, frequency of ^{15}N labeling, and type and concentration of labeling solution used in leaf- and shoot-labeling experiments influences ^{15}N-enrichment of roots and soil, thus influencing calculations of N-rhizodeposition. Leaf- and shoot-labeling studies most often use highly enriched (99 atom% ^{15}N) urea as a carrier for the ^{15}N label (Khan et al.,

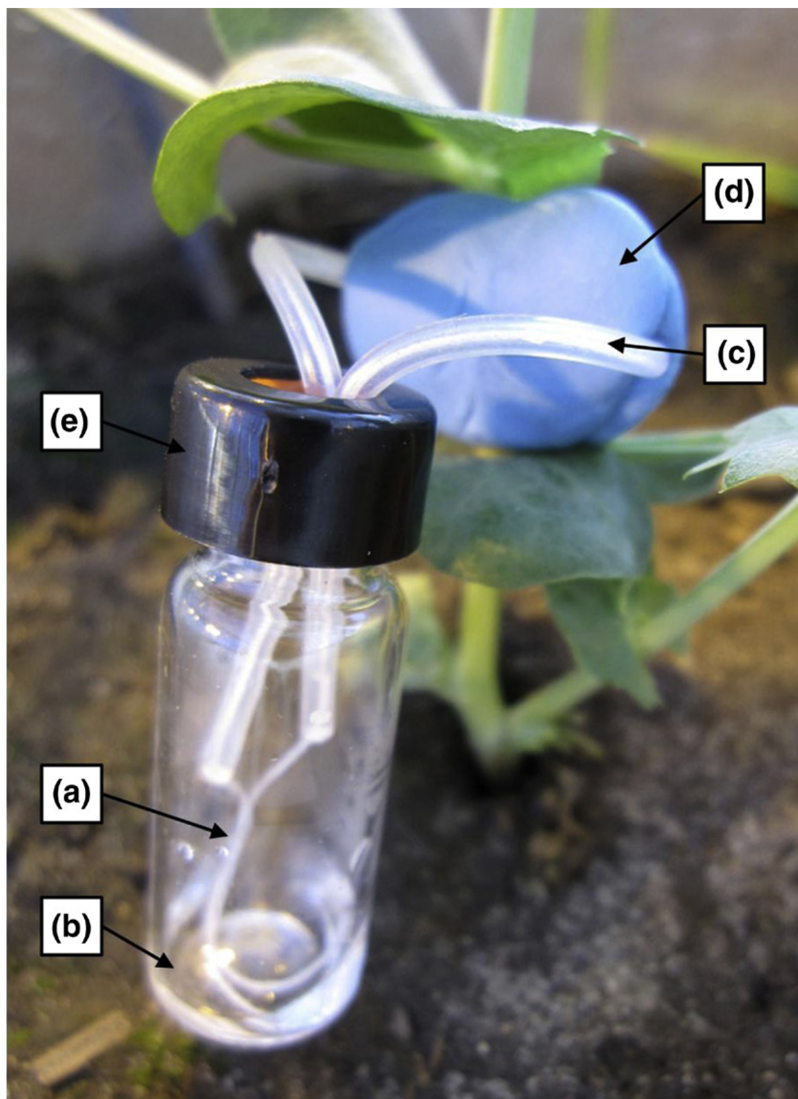


Figure 2.11 Photograph of the stem-wick ^{15}N labeling technique applied to field pea. A piece of cotton string (a) is threaded through the stem of the plant and immersed in a highly ^{15}N-enriched solution of urea (b). The string is protected by silicon tubing (c), which is held in place against the stem using putty (d). The cap (e) of the vial contains a septum for easy application of multiple urea pulses using a needle and syringe. For color version of this figure, the reader is referred to the online version of this book.

2002b; Russell and Fillery, 1996) because it is nonpolar, has a high N-to-mass ratio, and may be readily metabolized by urease within the plant (McNeill, 2001). However, solutions of NH_4Cl (Götz and Herzog, 2000) and KNO_3 (De Graaff et al., 2007) also have been used. Mahieu et al. (2009) observed a linear relationship between the atom% ^{15}N of roots and soil when pea was supplied with urea at concentrations of 0.2–0.6%. However, this relationship did not hold, and ^{15}N soil enrichment was higher and more variable, when the urea concentration was 0.8%. The authors suggested that since plant urease may not be responsive to high exogenous additions of urea, temporary buildup of the urea in plant organs can occur. This will affect the composition and distribution of the ^{15}N within the plant if the urea is not metabolized by urease, and will have consequences for the assessment of N rhizodeposition (Mahieu et al., 2009). In addition, high concentrations of urea can cause necrosis though the concentration threshold 0.5–2.0% (w/v) depends on plant species (Khan et al., 2002b; Mahieu et al., 2009; Russell and Fillery, 1996).

Labeling frequency can vary from a single application of ^{15}N (Khan et al., 2002b; Yasmin et al., 2006) to fortnightly or weekly ^{15}N pulses (Mahieu et al., 2007; Mayer et al., 2003; Russell and Fillery, 1996), or ^{15}N pulses at specific growth stages (Mahieu et al., 2007; Wichern et al., 2007b); to continuous application (Mahieu et al., 2009). Mahieu et al. (2007) reported that fortnightly pulses of urea resulted in higher soil ^{15}N enrichment than pulses applied at specific growth stages. In a subsequent study, labeling frequency did not influence root ^{15}N enrichment; though, more frequent labeling (continuous vs fortnightly pulses) increased soil ^{15}N enrichment in field pea through rhizodeposition—indicating that continuous labeling resulted in higher and more reliable estimates of N rhizodeposition (Mahieu et al., 2009). Regardless of ^{15}N-labeling frequency, the root distribution ratios (distribution of ^{15}N in roots to distribution of total N in roots) were always <1 (Mahieu et al., 2009), indicating that labeling frequency does not always improve the distribution of ^{15}N within the whole plant. Using continuous ^{15}N urea stem-wick labeling, we found that root distribution ratios averaged 0.66 in mature field pea (Arcand et al., unpublished data). Therefore, more frequent application of ^{15}N-labeled urea can increase ^{15}N enrichment of the soil—improving quantification of N rhizodeposition—even though distribution of the ^{15}N may still favor aboveground components. In some studies, application rates of ^{15}N have been matched with plant N demand in an attempt to improve label uniformity (Mahieu et al., 2007; Mayer et al., 2003; Russell and Fillery, 1996). A preliminary experiment

is necessary to generate N uptake curves to estimate rates of ^{15}N urea required to match plant demand (usually 2.5 atom% ^{15}N in excess of plant N) in the ^{15}N-labeling experiment. This prolongs the study and provides only an approximation when extrapolating from greenhouse to field (and vice versa) or between different seasons. Despite best efforts to improve ^{15}N homogeneity by applying a continuous supply of ^{15}N in concert with whole-plant demand, variations in the N sink strength within the plant that occur throughout the growth cycle can potentially result in heterogeneous distribution of ^{15}N (Mahieu et al., 2009).

The split-root technique involves splitting the root system of a single plant or plants into two compartments: one that is supplied with ^{15}N fertilizer and the other, which is sampled and analyzed for ^{15}N-enrichment in the roots and rhizodepositional transfer to the soil (Sawatsky and Soper, 1991). This technique enables continuous labeling through a natural uptake mechanism and provides relatively homogeneous root enrichment (Wichern et al., 2008). Root ^{15}N enrichment is greater when labeled with split-root techniques compared to shoot-labeling techniques (Schmidtke, 2005b), but ^{15}N recoveries tend to be lower (Mahieu et al., 2007). Schmidtke (2005a) suggests that N rhizodeposition as a proportion of total plant N is underestimated using split-root techniques because only half of the root system is considered; however, the results of Mahieu et al. (2007) indicate that the converse may be true. They determined that the ratio of NdfR to total plant N was 10% higher in split-root compared to stem-wicked pea plants. However, because the relationship between root and soil ^{15}N-enrichment differed between methods, they could not resolve which of the two labeling techniques produced the most "correct" estimate of rhizodeposition. They did observe that for any given root ^{15}N enrichment, soil ^{15}N enrichment was greater using stem-wicked versus the split-root labeling. However, for an equal increase in root ^{15}N enrichment, split-root labeling yielded a greater increase in ^{15}N enrichment of the soil than the stem-wick technique (Mahieu et al., 2007).

Atmospheric labeling of $^{15}N_2$ can be used to assess the proportion of symbiotically or nonsymbiotically fixed N to soil by legumes (Mohr et al., 1998; Russell and Fillery, 1996) and nonlegumes (Bremer et al., 1995), respectively. Plants may be labeled with ^{15}N by exposing the root system to an atmosphere enriched in $^{15}N_2$, either continuously or as one or a series of short-duration labeling periods to determine symbiotic or associative N_2 fixation. A greater proportion of fixed ^{15}N will be recovered in soil N pools under continuous labeling and this technique yields results that are

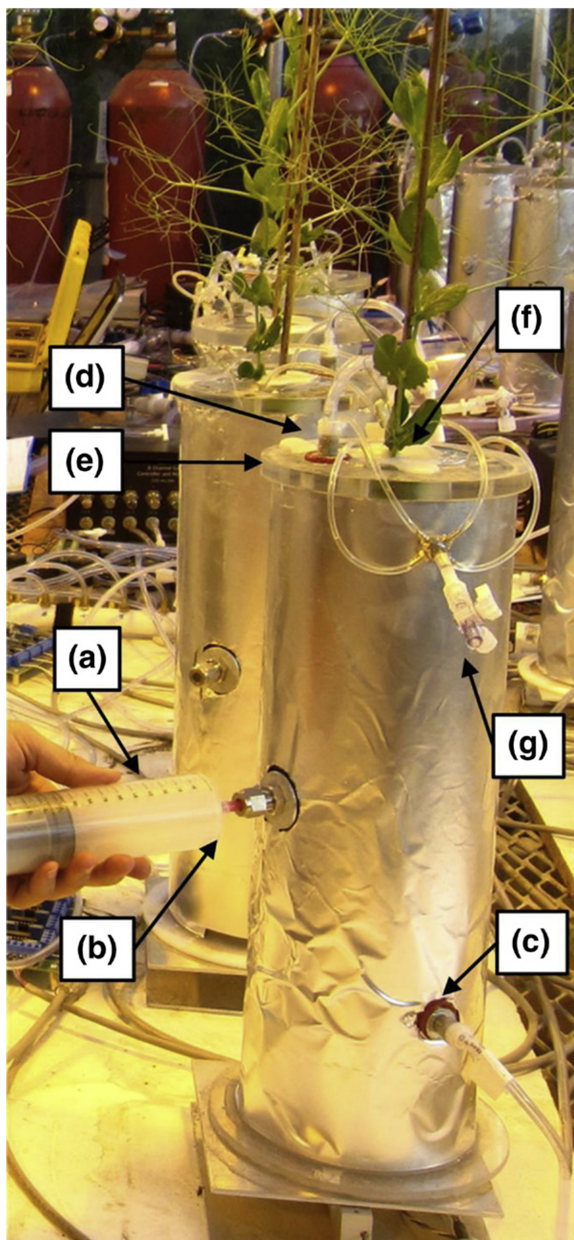


Figure 2.12 Photograph of a $^{15}N_2$ gas-labeling system designed to continuously label 24 plants simultaneously. A syringe (a) is used to manually inject $^{15}N_2$ into the injection port (b). The soil atmosphere is circulated among the 24 pots to replenish O_2, remove CO_2, and circulate $^{15}N_2$ via an inlet (c) and outlet (d) port. The plant stem is fed through a hole in an acrylic cap (e), which is sealed with medical grade silicone and paraffin/lanolin wax (f). Plants are watered manually via a two-way luer lock stopcock (g). For color version of this figure, the reader is referred to the online version of this book.

more representative of the N fixed during the lifecycle of the plant (Mohr et al., 1998) compared to short-duration pulses (Russelle et al., 1994). However, the equipment required to simultaneously regulate $^{15}N_2$, O_2, and CO_2 concentrations is both expensive and technically complicated, which limits widespread adoption of this method and restricts it to controlled environment experiments. We recently were able to maintain a relatively steady $^{15}N_2$ enrichment (3.1308 atom% ^{15}N) in the atmosphere of soil cores growing field pea with daily manual injections of $^{15}N_2$ (99 atom% ^{15}N) and pure O_2 over an 8-week period (Arcand et al., unpublished data). The aerial parts of the plant were exposed to ambient atmosphere, while the soil was exposed to a ^{15}N-enriched atmosphere that was separated from the ambient atmosphere. The plant stem was fed through a hole in the cap on the soil cores, which was then sealed with silicone and wax (Fig. 2.12). Continuous labeling of 24 soil cores required approximately 16 L of pure $^{15}N_2$ (99 atom% ^{15}N) to counteract losses in this complex system. Despite the high cost and technical difficulty, direct labeling of legumes by root and nodule exposure to $^{15}N_2$ gas is the most accurate measure of N_2 fixation compared to other methods (Warembourg, 1993), and therefore, provides a true representation of the contribution of fixed N to soil through N rhizodeposition of legumes.

3. OCCURRENCE AND ECOLOGICAL FUNCTION OF NON-CYCLIC AND CYCLIC N_{ORG} COMPOUNDS IN SOIL

This section provides an overview of the chemically defined N_{org} compounds identified using the analytical methods described in Section 2, as well as a discussion of their ecological significance in soil. Classes of N_{org} compounds that are important constituents of SOM, and the analytical methods used for their detection, are highlighted in Table 2.3.

Noncyclic compounds comprise the majority (60–90%) of the N_{org} with amides—including peptides, proteins and amino sugars—being the predominate compounds. Peptides and proteins are usually combinations of the 20 most common amino acids, which form oligo-, poly- and macropeptides.

Ecologically, soil proteins can be subdivided into (1) detrital proteins released upon cell death and (2) functional proteins actively released into the soil for specific functions (Rillig, 2004). Detrital proteins originate mainly from vascular plants (>95%), but also from animals and microorganisms

Table 2.3 An Overview of Important Classes of N_{org} Compounds in Soils, Ranges of their Proportions in Mineral Top Soils, and Indications of The Analytical Methods by Which these Ranges of Proportions Were Determined

		Research methods					
Class of N_{org} compounds	**Proportions (% N_{org})**	**Wet-chemical**	**Chromatography**	**NMR**	**Py-MS**	**XPS**	**XANES**
Noncyclic							
Amides	60–90	X	X	X	X	X	X
Peptides/proteins	50–80	X	X		X		
Amino sugars	5–10		X		X		
Amines							
Free amino acids	1–5	X	X		X		
Aliphatic nitriles	1–5		X		X		X*
Cyclic							
Aromatics	5–35		X	X	X	X	X
Heterocyclics	5–25		X	X	X	X	X
Nitriles	1–5		X		X		X*
Anilides	<10–25†		X	X	X		
Nonaromatic							
Nitriles	<1		X		X		X*

*No analytical separation of aliphatic and aromatic nitriles.
†Schmidt-Rohr et al. (2004).

(Stevenson, 1994). Functional proteins include extracellular enzymes and surface-active proteins of microbial origin (e.g. glomalin, hydrophobins) (Rillig, 2004). Among functional proteins, the extracellular enzymes are the most extensively investigated. Caldwell (2005) compiled soil enzyme data that could be used to distinguish inter- and extra-cellular enzyme sources and substrate specificity of single enzymes within (e.g. N cycle) and between (e.g. N and P or N and C cycles) major nutrient cycles. The functional diversity of soil enzymes links resource availability, microbial community structure and nutrient turnover in soils. Extracellular enzymes contribute to the stabilization of soil aggregates, decomposition of organic matter, formation of humified SOM, and nutrient cycling (Bakshi and Varma, 2011). Their activities are often used as indices of microbial growth and activity in soils, though quantitative information regarding which enzymes are associated with a particular microbial process is generally lacking (Bakshi and Varma, 2011). The same type of enzyme can be found in multiple locations including both intracellular (e.g. in the cytoplasm, periplasm, or attached to the outer surface of active cells, resting cells, dead cells or cell debris) and extracellular (in the soil solution, or adsorbed on substrates or soil colloids) locations (Nannipieri, 2006). Mass spectrometric protein analysis from DOM can distinguish the phylogenetic origin of proteins in soil leachates. Schulze (2004) suggested that a proteomics approach could be taken to obtain a "proteomic fingerprint" of the presence and activity of soil organisms. Nannipieri (2006) suggested two approaches: (1) functional proteomics (which considers the ca 4% of soil N occurring in microbial biomass) and (2) structural proteomics (which considers the ca 30–45% of soil N occurring in extracellular proteins stabilized by soil colloids).

Recently, Gillespie et al. (2011b) used structural proteomics to investigate the extracellular protein glomalin. Glomalin is a glycoprotein associated with carbohydrates, contains 30–40% (w/w) C (González-Chávez et al., 2004), is assumed to be stable and persistent in soil, and is thought to be produced in copious quantities by arbuscular mycorrhizal fungi (Glomeromycota). Glomalin-related soil protein (GRSP) is operationally defined by the extraction method (high-temperature sodium citrate extraction followed by either trichloroacetic acid or hydrochloric acid precipitation). Synchrotron-based N-XANES spectroscopy and Py-FIMS revealed that GRSP extracts contain a consortium of proteins along with many impurities (i.e. phenolics, lipids and humic substances) (Gillespie et al., 2011b). Taking a proteomics approach, the authors found that glomalin itself may be a thioredoxin-containing chaperone, but that no homologies with proteins or DNA of

mycorrhizal origin were detected. Proteomics also revealed that the extracts contained large amounts of soil-related, heat-stable proteins and proteins of nonmycorrhizal origin. Despite its obvious advantages, the applicability of proteomics to soil systems suffers, in part, from poor protein extraction efficiency caused by the impact of clay minerals and SOM (Giagnoni et al., 2011). For this reason, research progress will depend greatly on improved extraction methods (e.g. Chourey et al., 2010; Taylor and Williams, 2010).

Hydrophobins constitute another group of structural proteins and are similar to glomalin in their suspected functionality (Nichols, 2003). They are small (ca 100 amino acids), cysteine-rich proteins unique to filamentous fungi (Linder et al., 2005; Wessels, 1997) and are thought to contribute to SOM stability and contribute to the water repellency of soils (Rillig, 2005). For this reason, structural proteins were suspected to reside longer in soil than the majority of other proteins. However, all proteins in soil can be digested by proteolytic enzymes and taken up as ammonium or nitrate by plants and microorganisms; taken up directly by plants into root cells, most likely via endocytosis; or taken up directly by microorganisms (Näsholm et al., 2009). Plants colonized by mycorrhizal fungi are predicted to have greater access to N_{org} than noncolonized plants (Schimel and Bennett, 2004).

Amino sugars, which account for 5–10% of the soil N_{org} (Table 2.3), are mainly of microbial origin (Amelung, 2003). The most important amino sugars in the soil are glucosamine, galactosamine, muramic acid and mannosamine (Appuhn et al., 2004). However, free amino sugars and amino acids comprise only a small proportion of the dissolved N_{org} in soils (Roberts et al., 2007). For example, Roberts et al. (2007) showed that glucosamine had a half-life of only 1–3 h in soil solution—its removal from solution being a predominantly biotic process—and that glucosamine was only weakly sorbed to the solid phase of the soil ($K_d = 6.4 \pm 1.0$). Based on these results, Roberts et al. (2007) suggested that free amino sugars turn over rapidly in soil. Glucosinolates are another group of amino sugars that enter the soil through plant litter. These compounds, which are secondary metabolites produced mainly by plants of the order Brassicales, can have diverse fungicidal, bacteriocidal, nematocidal and allelopathic effects on soil ecological functioning (Fahey et al., 2001). To date, more than 120 different glucosinolate structures have been described.

Several thousands of amines originating from plants, animals and microorganisms can be detected in soil. Ecologically they can exert antimicrobial and allelopathic effects and can be toxic to both invertebrates and vertebrates

(Vranova et al., 2011). Some amines are toxic, odorous, volatile compounds that contribute to soil fungistasis (Fekete et al., 2010; Zou et al., 2007). Free amino acids constitute a very diverse group of amines in the soil and occur in smaller quantities than amino acids bound in peptides and proteins. Plants release free amino acids (e.g. arginine, asparagine, aspartate, cysteine, cystine, glutamine) via diffusion into the rhizosphere. However, exudation of amino acids is a function of plant genotype and environmental conditions, and is enhanced under stress (Bertin et al., 2003). Free amino acids represent a significant source of available N for soil microorganisms and some plants. Plant uptake of free amino acids is maximized when soil amino acid concentrations are high; a condition caused by a slow microbial utilization (Jones et al., 2005a).

Cyclic N_{org} compounds in soil consist of aromatic heterocyclics, nitriles and anilides, and nonaromatic nitriles (Table 2.3). Quantitatively, this group of compounds accounts for about 5–35% of the soil N_{org} and originates from a variety of biological sources, including chromatophores (porphyrin structures in chlorophyll) from microorganisms and plants; purine and pyrimidine bases of RNA and DNA; and secondary metabolites such as alkaloids from most organisms. Inputs of chlorophyll at the surface of the soil are significant during primary succession—reflecting high densities of cyanobacteria, algae and mosses (Castle et al., 2011). DNA and RNA are present in all habitats occupied by prokaryotic and eukaryotic organisms, and contribute to the soil N_{org} pool in the form of both living and dead cells. DNA also can exist extracellularly upon its release from organisms into the soil (Wackernagel, 2006). Extracellular DNA in the soil can be protected against DNase degradation by interactions with clay minerals and soil colloidal particles (Cai et al., 2006).

A tremendous diversity of cyclic N_{org} compounds originate from secondary metabolites produced by plants, animals, and microorganisms. An evaluation of *Natural Product Reports* (RSC publishing) indicates that more than 25,000 cyclic N compounds from the biogeosphere were newly detected and reported during the period from 2000 to 2011 (Fig. 2.13). Evidence for these structures was provided by isolation, purification and analysis, as well as through synthesis.

The majority of alkaloids are N heterocyclics and, at present, about 10,000 alkaloid structures have been described (Hesse, 2002; Joosten and van Veen, 2011). Alkaloids are produced mainly by plants, but also by bacteria, fungi and animals. They are often toxic, and many (e.g. berberine) exhibit antibiotic effects to soil microorganisms. Alkaloids can also affect the litter feeding preferences of soil fauna because of their generally bitter taste (Hesse, 2002).

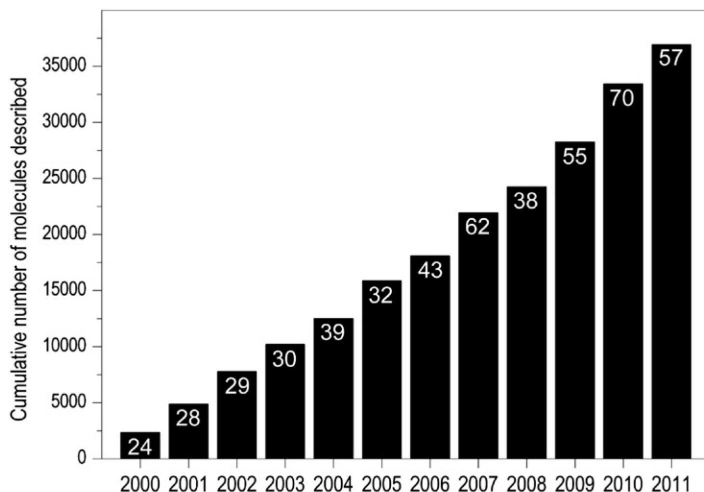


Figure 2.13 Cumulative number of described natural occurring cyclic N_{org} compounds in the journal "Natural Products Reports" (RSC publishing) within the period 2000–2011. Numbers within the bars indicate the total number of publications in the year describing at least one cyclic organic N compound. On average, 76 new compounds were described per publication with a maximum number of 791 in a single publication.

Although the ecological importance of N heterocycles in general remains controversial, the ecological effects of a variety of specific cyclic N_{org} compounds in the soil have been described. These include antibiotics (e.g. calvulinic acid and β-lactam calvam from streptomycetes and pyridone harzianopyridone from *Trichoderma* spp.) and metal-chelating agents (e.g. the siderophore desferrioxamine from streptomycetes) (Hanson, 2008; Tarkka and Hampp, 2008). Furthermore, a diverse group of fungal pigments (e.g. azaquinone agaricone from *Agaricus* spp.), toxins (e.g. amanitins from *Amanita* spp.) and volatile compounds (e.g. methyl pyrazine from *Paecilomyces* spp.) found in the soil contain N heterocyclic compounds (Hanson, 2008). Yet, due to their high specificity (often strain-specific), low concentration, and heterogeneous distribution—and despite their considerable ecological significance—these N_{org} compounds are only rarely quantified in soils. Nevertheless, cyclic N_{org} compounds have been identified as soil fungicides (Chuankun et al., 2004), biocontrol agents against soil-borne pathogens (e.g. Paula and Hau, 2007) and as controls on feeding preferences of soil animals (e.g. Böllmann et al., 2010).

A final group of cyclic aromatic N_{org} compounds are the anilides. Schmidt-Rohr et al. (2004) reported finding significant amounts of amide N bound directly to aromatic rings in a humic acid fraction from a submerged rice soil. They also reported that most of aromatic-bound-N was

anilide N and suggested that this represented an agronomically significant fraction of the soil N. Indeed, the large amount of anilide N in the continually submerged soil was thought to contribute to a decline in yield, relative to a comparable aerobic rice soil.

The cyclic nonaromatic nitrile N compounds, including cyanogenic glucosides, comprise a minor (<1%) class of N_{org} in soil (Table 2.2). They are toxic compounds, which can affect the feeding preference of the soil fauna and the microbial colonization of the rhizosphere (Ubalua, 2010). These compounds are produced by plants, arthropods and microorganisms. At present, about 60 cyanogenic glycosides have been described in the literature (Ubalua, 2010).

In addition to biological sources, N_{org} compounds can enter soils as xenobiotics; e.g. through the application of pesticides or as contaminants from dyes, pharmaceuticals and petroleum products. The primary N-containing xenobiotic species that undergo biological degradation in soils are nitroaromatics, nitrate esters, and compounds containing N-ring heterocycles (Ye et al., 2004). Most herbicides that target photosynthesis or amino acid or lipid biosynthesis are biodegradable N heterocycles. For example, the herbicide atrazine can be biodegraded in the soil via a series of biochemical processes including N-dealkylation, dechlorination and ring cleavage (Ye et al., 2004). Regardless of the processes involved, the use of xenobiotic N by soil microorganisms as an N source is controlled by the general availability of N in the soil, and increases in times of N starvation (Sims, 2006).

In summary, soils contain an incredible diversity of biogenic, pyrogenic and xenobiotic cyclic N_{org} compounds. A particular challenge for investigators originates from similarities in the molecular structures of N_{org} compounds, which are often present only in low concentrations and are heterogeneous in distribution, but vary fundamentally in their ecological effects. The method overview in Table 2.3 illustrates the toolbox of analytical methods that can be applied to detect and quantify the N_{org} species or compound classes. Moreover, it illustrates the versatility and limitations of methods which, at best, are applied in combination to provide insights into the composition and turnover of soil N_{org}.

4. EXAMPLES FOR RECENT MULTIMETHODOLOGICAL STUDIES OF SOIL N_{ORG} CHEMISTRY

This section presents examples of how complementary analytical methods have been applied to advance our knowledge of the chemistry of soil N_{org} with particular emphasis on the less intensively studied cyclic N_{org} compounds.

4.1. Microbial Turnover of N Heterocycles

Recently, Baum (unpublished data) used state-of-the-art analytical techniques to determine the extent to which aromatic N heterocycles are utilized by soil microorganisms. An incubation experiment was carried out in which a soil was enriched in aromatic heterocyclic N by the addition of uracil to yield N-enrichment factors of 2-, 5- and 10-fold of the original N concentration. The soils were incubated under aerobic conditions at 60% water holding capacity and 20 °C for 3 weeks, after which the enzyme activities in the soil were measured and changes in the uracil concentration assessed using N-XANES spectroscopy and Py-FIMS. N-XANES spectra obtained before and after incubation showed that diagnostic features present prior to incubation (i.e. feature "d" at 402.2 eV and feature "e" at 405.1 eV) were absent in the incubated sample (Fig. 2.14, left panel).

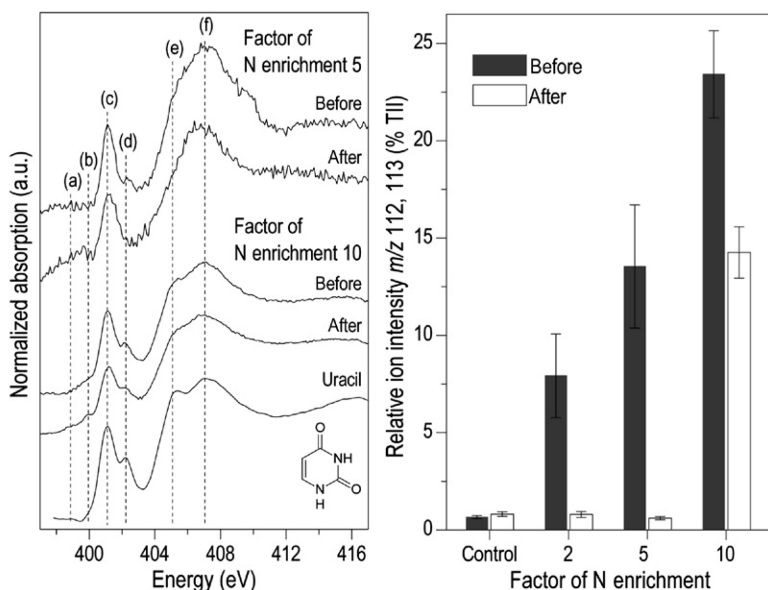


Figure 2.14 The decomposition of uracil (CAS: 66-22-8) spiked into a soil to yield various factors of N enrichment (2, 5 and 10 relative to the initial total N concentration) after 3 weeks of incubation. The left panel shows spectral changes in the N K-edge X-ray absorption near edge structure spectra due to incubation and a spectrum of the uracil standard; (a) 398.9 eV, (b) 399.9 eV, (c) 401.1 eV, (d) 402.2 eV, (e) 405.1 eV, (f) 407 eV. Changes in the relative ion intensity (% TII) of marker signals of uracil (*m/z* 112, 113) determined by Py-FIMS (right) (means and standard deviations of 3–4 replicate measurements).

Likewise, Py-FIMS analysis of the incubated samples revealed that almost all of the added uracil disappeared from the samples with two- and five-fold enrichments and that about 53% of the original uracil spike remained in the sample enriched 10-fold (Fig. 2.14, right panel). However, the fate of the added uracil was not clear. Whereas there are reports of direct incorporation of uracil into RNA (e.g. Cornelius et al., 2012), increases in dehydrogenase activity from 10 units in the control to ca 44, 125 and 184 units in the 2× -, 5× -, and 10× -fold enrichments treatments, respectively, suggest that at least some of the added uracil was metabolized by soil microorganisms. Although this study provides a good proof-of-concept for the analytical approach, more detailed studies are required to provide insights into the fate of the major cyclic N_{org} compounds—not to mention the myriad of minor or trace compounds—in soil.

Driven by the high nutrient supply resulting from root exudation, the rhizosphere is a "hot-spot" of microbial turnover processes in soil. Many studies investigating root exudation and turnover in the rhizosphere are based on artificial liquid culture systems, leachates or ^{15}N-labeling techniques combined with traditional methods of measuring soil organic N. However, few studies have examined compound-specific differences in N_{org} chemistry between rhizosphere and bulk soil samples. Rhizosphere and nonrhizosphere soil samples from pea (*Pisum sativum* L.) grown in different soils were studied using C- and N K-edge XANES spectroscopy and Py-FIMS (Gillespie et al., 2009). The C- and N-XANES revealed that in a clay soil, heterocyclic N compounds, proteins, and carboxylates were enriched in the rhizosphere compared to the bulk soil. In contrast, the rhizosphere of pea grown in a sandy clay loam soil was enriched in nitro-aromatic and reduced-aromatic compounds relative to the bulk soil. Proteins, carbohydrates, and carboxylic compounds, on the other hand, remained unchanged. The presence of nitro-aromatic and alkyl-amide compounds in the rhizosphere indicates a unique cycling of N in this soil compartment. These two studies provide evidence—obtained using complementary spectroscopic and spectrometric methods—for novel turnover processes of cyclic N_{org} compounds in soil.

4.2. Organic–Mineral Interactions

In mineral surface soils, about 70–>95% of the N_{org} is associated with minerals, indicating that binding to, or stabilization by minerals is an important feature of N_{org} chemistry. Indeed, Leinweber and Schulten (2000) attributed the nonhydrolyzability of 25–52% of N_{org} to stabilization by pedogenic Fe

oxides. Mineral phases not only stabilize the N_{org} as a whole but may also be involved in chemical reactions of N_{org} compounds, thus altering the quality of the N_{org}. Manganese (IV) oxides were shown to catalyze the Maillard reaction (sugar–amino acid condensation) under ambient conditions (Jokic et al., 2004). Using an array of complementary methods—including optical (FTIR) and NMR ($^1H/^{13}C$-NMR) spectroscopy, atomic force microscopy, mass spectrometry and XANES spectroscopy—the authors determined this reaction to be a humification pathway. Moreover, the latter two methods provided compelling evidence for the abiotic formation of heteroaromatic N compounds. Fine and coarse clay fractions from a clay-rich Cryoboroll in Canada were initially investigated using wet-chemical methods (Schnitzer and Kodama, 1992) and more recently by Py-GC/MS, Py-FIMS and N-XANES (Leinweber et al., 2010a). Py-GC/MS revealed the presence of various substituted N heteroaromatic compounds such as pyrazoles, pyrazines, pyridines and pyrroles. The presence of the latter two classes of compounds was confirmed by Py-FIMS, which also revealed aliphatic nitriles suspected of originating from thermally induced reactions of aliphatics with NH_3. At the same time, N-XANES spectroscopy, which is nondestructive, supported the presence of genuine nitrilic and heteroaromatic N compounds that together accounted for 30–40% of the total N_{org} (Fig. 2.15).

Somewhat lower proportions of aromatic N_{org} (18–34%) were derived from XPS studies of mineral-bound (density fraction >1.6 g cm^{-3}) organic matter along a weathering and chronosequence in Hawaii (Mikutta et al.,

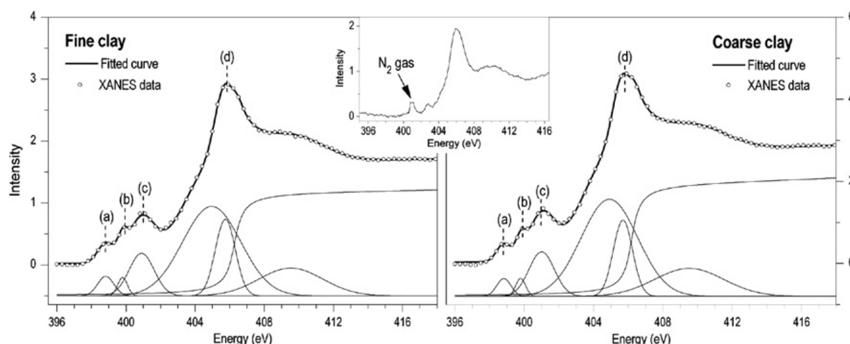


Figure 2.15 N K-edge X-ray absorption near edge structure spectra of the fine clay (left) and coarse clay (right) fractions of a Cryoboroll from Melfort (Canada). The insert in center shows the N X-ray absorption near edge structure spectrum of a bentonite from Wyoming (USA) loaded with interlayer NH_4^+; (a) 398.8 eV, (b) 399.9 eV, (c) 401.1 eV, (d) 405.5 eV. *(Reproduced from Leinweber et al. (2010b) with permission from the Agriculture Institute of Canada).*

2010). The youngest (300-year-old) soils contained only small amounts of mineral-associated N_{org} but large amounts of hydrolyzable amino sugars and amino acids of mainly microbial origin. Soils in the intermediate weathering stage (20,000–400,000 years) contained mainly poorly crystalline minerals and had more mineral-associated N_{org} and significantly smaller proportions of hydrolyzable amino sugars and amino acids. The oldest soils (1.4–4.1 Myr) contained mostly crystalline secondary Fe- and Al-(hydr)oxides and kaolinite, and smaller amounts of total N_{org} that were depleted of hydrolyzable amino sugars and amino acids and enriched in lignin phenols. N-XANES and XPS spectroscopy assigned 59–78% of the mineral-bound N_{org} to peptide structures. The proportion of nonhydrolyzable N_{org} increased with ^{14}C-dated-age of the mineral-associated organic matter (Mikutta et al., 2010). These examples show that application of an array of complementary methods is fundamental to detect small molecular–chemical changes in soil N_{org} as a result of pedo–mineral interactions.

4.3. Impact of Fire and Soil Cultivation

Fire is an important environmental factor that alters soil properties and causes changes in SOM composition (González-Pérez et al., 2004). Heat-induced formation of pyrroles (major) and pyridines (minor) from peptides was observed in ^{15}N-NMR studies of HF-treated soils and extracted humic substances (Knicker, 2009). The term "black nitrogen" was coined for the heterocyclic N in pyrogenic organic material (PyOM), and it was hypothesized that this fraction contributes to the recalcitrance of charcoal (Knicker, 2010). However, methodological limitations led to unsatisfactory quantification and understanding of the processes occurring at the molecular level.

N-XANES spectra for a soil heated under aerobic conditions exhibited a predominant diagnostic feature for amide-N (feature (d) in Fig. 2.16) in the original soil and in soil heated to 100 °C or 200 °C (Kiersch et al., 2012b). This agreed with previous N-XANES spectra of soil and soil-related materials (Gillespie et al., 2009, 2011a; Leinweber et al., 2010a, 2010b; Vairavamurthy and Wang, 2002). However, in soils heated to 300 °C, diagnostic features for non-peptide C=N (feature (a); as in aliphatic imines and/or aromatic pyridines or pyrazines) and nitriles and/or C–NH–C (feature (b); as in aromatic purines, pyrazoles and/or imidazoles) became more prominent—reaching a maximum in the range 400–500 °C. As well, in all soils heated above 200 °C, feature (b) exceeded feature (a). These spectral changes suggest the formation of unsaturated and/or heteroaromatic N compounds from other N species at temperatures >200 °C. The overlap of feature (c) by (d) in all spectra for soil heated

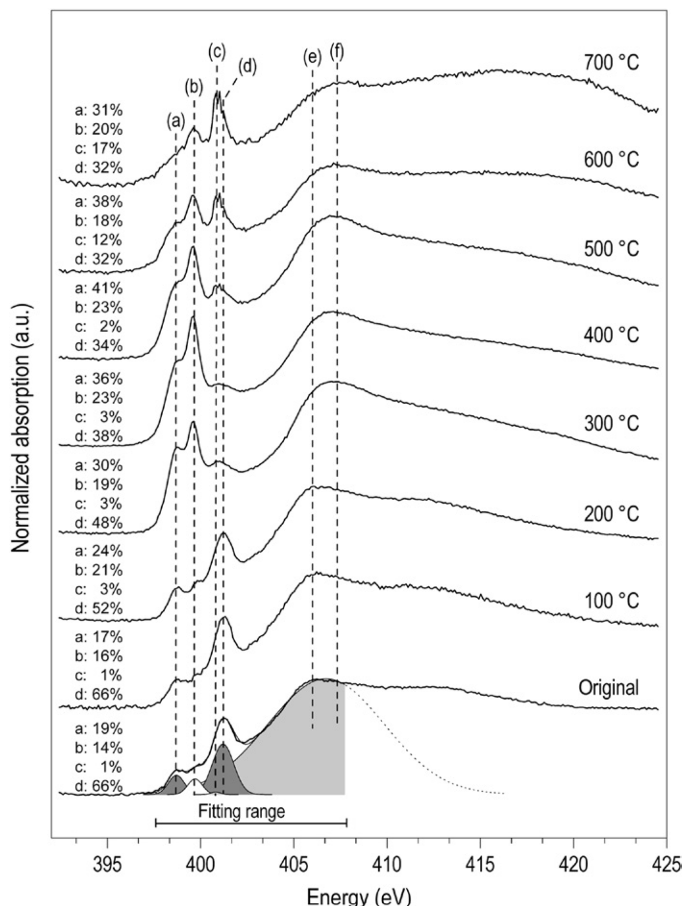


Figure 2.16 Stacked N K-edge X-ray absorption near edge structure spectra of the original and the heated samples; (a) 398.7 eV, (b) 399.6 eV, (c) 400.8 eV, (d) 401.2 eV, (e) 406.0 eV, (f) 407.4 eV. Values at the left side indicate proportions of peak areas. *(Reproduced from Kiersch et al. (2012b) with permission from Elsevier).*

to <500 °C indicates an increasing contribution of pyrrolic N, which can interfere with the high energy side of the amidic N feature in the N-XANES spectra (Abe and Watanabe, 2004; Kelemen et al., 2002). This interference complicates compound differentiation in mixtures of amidic and pyrrolic N at the present spectral resolution of N-XANES. Finally, at 600–700 °C, a large amount of N_{org} was lost and the vibrational manifold at 400.8 eV indicated the release of N_2 gas from the remaining interlayer NH_4^+ (Leinweber et al., 2010b). The predominance of nitrilic and heteroaromatic N compounds at 300–500 °C agreed with enrichments in C=C and substituted aromatic C in

the corresponding C-XANES spectra, and with further confirmation obtained using Py-FIMS (Kiersch et al., 2012b). Although the temperature range of intensive alterations in N_{org} compounds (300–600 °C) agreed with an evolved gas analysis performed by coupling thermal analysis (thermogravimetry and differential scanning calorimetry) with a fast quadruple mass spectrometer, De la Rosa et al. (2008) did not detect N_{org} compounds released from the control (unburned) and burned (340 °C) soils.

Fire impacts on natural soils are generally much less pronounced than those produced in high-temperature laboratory experiments. Nevertheless, N-XANES spectra of samples from two long-term field experiments showed that peak areas of the diagnostic features assigned to N in aromatic compounds and nitriles increased as a result of burning at both sites (Kiersch et al., 2012a). Textural differences between the two sites were reflected in the alterations in N_{org} compounds observed due to burning, and were more pronounced at the sandy clay loam site than the silty clay site. This was thought to be a reflection of the greater water holding- and heat capacities of the silty clay soil. Furthermore, alterations in compound classes were accompanied by increases in thermal stability, as revealed by Py-FIMS. Decreases in the abundance of low-molecular-weight compounds due to the release of functional groups and/or formation of higher molecular weight compounds were detected by Py-FIMS and pyrolysis-single photon ionization-time-of-flight mass spectrometry (Py-SPI-ToF-MS).

Soil from a wheat field near Rostock, Germany showed dark-colored aggregates at the surface a few days after an accidental fire. Stratified sampling followed by N-XANES analyses revealed larger peak areas corresponding to pyridinic N (29%) and nitrilic N (20%) at the surface, as opposed to the interior (19% pyridinic N and 17% nitrilic N), of a fire-affected aggregate (Table 2.4). These results were confirmed by C-XANES spectroscopy and, at least partly, by Py-FIMS.

Data compiled in Table 2.4 show that in the abovementioned sample sets and another laboratory-scale experiment (Lab experiment SL-2N), burning increased the proportions of the peaks corresponding to pyridinic N (398.9 eV) and nitrilic N (399.9 eV) in the N-XANES spectra at the expense of the peak corresponding to amide N (401.4 eV). In the laboratory and plot experiments, this corresponded to an increase in heteroaromatic N at the expense of proteinaceous (aliphatic) N in the Py-FIM spectra. In summary, combining N- and C-XANES with pyrolysis-mass spectrometry revealed that burning produced a multitude of nonpeptidic

Table 2.4 Proportions of Integrated Peak Areas in N-XANES Spectra and the Corresponding Compound Classes (% TII assigned to N_{org}) Obtained from Py-FI Mass Spectra of Control Samples and the Corresponding Samples Affected by Heat from Burning. The Samples Originate from Two Laboratory-scale Heating Experiments (Lab experiment LS-6N: Kiersch et al., 2012b; Lab experiment SL-2N: Kiersch, unpublished data), a Plot-scale Field Experiment with Periodic Vegetation Burning (Kiersch et al., 2012a) and an Accidentally Burned Wheat Field (Kiersch, unpublished data)

	Peak position for binding energy in N K-edge XANES spectra					
	398.9 eV		399.9 eV		401.4 eV	
Sample origin	**Control**	**Burned**	**Control**	**Burned**	**Control**	**Burned**
Lab experiment LS-6N*	18‡	33§	15‡	21§	66‡	43§
Lab experiment SL-2N†	13	21	10	15	77	64
Plot: periodic burning	18	20	11	13	71	67
Wheat field	19	29	17	20	64	51

	Proportions of compound classes in Py-FIMS			
	Aromatic N heterocyclic compounds and nitriles		Amides, free amino acids	
	Control	**Burned**	**Control**	**Burned**
Lab experiment LS-6N*	15‡	66§	85‡	34§
Lab experiment SL-2N†	31	42	69	58
Plot: periodic burning	16	18	84	82
Wheat field	23	15	77	85

*LS-6N means texture loamy sand and N_t concentration 6.5 g kg^{-1} soil.
†SL-2N means texture sandy loam and N_t concentration 1.6 g kg^{-1} soil.
‡Averaged for temperature ranges 20–100 °C.
§300–400 °C.

N compounds in soil. Whereas this involved formation of pyridines and nitriles, there were no strong indications for the formation of substituted pyrroles. In this respect, our results differ considerably from those reported for ^{15}N-NMR-based studies (e.g. Knicker, 2009).

Cultivation of the Canadian prairies has resulted in depleted levels of N_{org} in the soil (Monreal and Janzen, 1993). We investigated this impact

of cultivation by examining three native vs cultivated sample pairs along a pedoclimatic gradient in Saskatchewan (Leinweber et al., 2007). N-XANES and Py-FIMS revealed that cultivation altered the composition of the N_{org} and that susceptibility to cultivation-induced losses varied among the different compound classes. Py-FIMS analysis revealed that thermally labile peptides and, to a lesser extent, other labile N-containing compounds were preferentially lost from the cultivated sites. The magnitude of these losses decreased in the order: Lethbridge (80-year cultivation) > Macklin (85-year cultivation) > St. Denis (57+ year cultivation). Relative gains in thermally stable N-containing compounds (all sites) and peptides (Macklin only) followed the same order. The weaker cultivation effect at St. Denis could be explained by a greater inherent stability of the N_{org} compounds in the native soil—as indicated by the thermal volatilization curves of the peptides. N-XANES confirmed enrichment of nitriles and N heterocycles, at the expense of amide N, in the cultivated Lethbridge soil.

In the hummocky landscape of Saskatchewan, Canada, variations in SOM characteristics at different topographic positions have been linked to tillage-induced translocation of soil (Pennock et al., 1994) and to water redistribution toward downslope positions (Verity and Anderson, 1990). Using a novel application of nonmetric multidimensional scaling ordination to XANES data, Gillespie et al. (2011a) observed more heteroaromatic N in cultivated vs uncultivated soils, thus confirming the results of Leinweber et al. (2007). However, the XANES data also showed the presence of unique oxidized N-bonded aromatics, which predominated at calcareous divergent slope positions. These types of N_{org} compounds are rarely reported in the literature, except in samples obtained from acidic or anaerobic environments (e.g. Olk, 2008; Schmidt-Rohr et al., 2004). These examples show that C- and N-XANES and Py-MS techniques complement one another very well, allowing detection of even small differences in the composition of N_{org} in whole (nonextracted) bulk soil samples and providing new insights into how the chemistry of soil N_{org} is impacted by changes in environment and management.

5. CONCLUSIONS AND OUTLOOK

Developments in the instrumentation and analytical techniques used to speciate N_{org} in bulk or fractionated soil samples have yielded new information regarding the chemistry of N_{org} and its transformations in soil. Moreover, as no single method can cover the whole range of N_{org} compounds that

occur in soils, it is clear that multimethodological approaches are required to gain new insights into the quality of soil N_{org} and further our understanding of N_{org} chemistry in soils. For example, combining the sensitivity of a high-resolution mass spectrometric method with the bulk probing of an X-ray absorption method provides a good overview of the major cyclic and noncyclic N_{org} compounds in soil.

It is generally accepted that amides and amines account for the majority of the N_{org} in soils; however, recent advances in the analytical techniques used to examine soils have enabled more detailed analyses into both the quality and quantity of aromatic N compounds. For example, using synchrotron-based N-XANES spectroscopy, this class of N_{org} compounds—previously described as "unknown N"—could be subdivided into pyridinic-, nitrilic- and pyrrolic N. Moreover, when used to analyze intact (bulk) soil samples, N-XANES provided evidence for environmental (e.g. fire) and management-induced (e.g. cropping system, erosion) alterations in N_{org} speciation. This was later confirmed using Py-FIMS analyses. For the evaluation of Py-FIMS datasets, we propose a modified set of *m/z*-signals (based on high-resolution mass spectrometry) for two classes of N_{org} compounds; i.e. the nonaromatic amides (peptides, amino sugars) and free amino acids, and the aromatic N heterocyclic compounds and nitriles (Section 2.3.2).

For the first time, we have the analytical tools to assess the extreme chemical diversity of biogenic, cyclic N_{org} compounds in soil—several thousands of which enter the soil via the incorporation of biomass residues or as microbial metabolites having very specific (down to strain-level) functions. The richness and importance of cyclic N_{org} compounds of biogenic origin in soils contradict previous simple differentiations of biogenic (i.e. amides and amines) versus pyrogenic (i.e. aromatic) N_{org} compounds. Furthermore, the designation of aromatic N_{org} compounds arising from thermal (e.g. fire-induced) alterations of the soil as "black nitrogen" is misleading. That is, N-XANES and Py-FIMS analyses of sample pairs (with and without burning) revealed that pyridinic- and nitrilic N, rather than pyrrolic N compounds were thermally formed from amides and amino acids.

Improper management of the soil N for crop production is often wasteful and has negative environmental consequences. Hence, to increase efficiencies and minimize environmental consequences, more research is needed to better understand the role of non cyclic and cyclic N_{org} compounds in ecosystem-level N cycling—especially contributions to plant N uptake, nitrate leaching and gaseous N loss. The issue of N_{org} cycling also addresses the question of why biologically derived, easily mineralizable N_{org} compounds such as

amides and amines form the largest N pool. There is good evidence to suggest that significant proportions of the soil N_{org} (e.g. 2–11 % in bulk soils and 12–25% in soil clays fractions) are bound to pedogenic oxides—explaining 18–49% (bulk soils) and 39–61% (soil clay fractions) of the nonhydrolyzable N_{org} (Leinweber and Schulten, 1998b, 2000) and the resistance of amide- and amine N against microbial attack and metabolism. On the other hand, the persistence of amide- and amine N in soils can be explained simply as a consequence of the ubiquitous presence of microbial biomass (with a ratio of noncyclic N_{org}:cyclic N_{org} of 6:1–7:1). Therefore, it appears necessary to investigate how the chemically different N_{org} pools are utilized by microorganisms; i.e. at the genomic, transcriptomic and metabolomic levels.

This review has shown that the complementary use of state-of-the-art analytical techniques enables researchers to take innovative approaches to tracing the fate of N_{org} in soils. For instance, ^{15}N-labeling techniques combined with soil compartment sampling and high- or ultrahigh-resolution mass spectrometry, provide opportunities to trace the ^{15}N label in individual molecules. Furthermore, visualization techniques such as Nano-SIMS and synchrotron-based STXM methods can uncover the heterogeneous distribution of functionally different N_{org} fractions at the micro- or nanoscale; e.g. in the rhizosphere or in association with mineral surfaces. However, the heterogeneity of N_{org} in soils, combined with very small sampling spots, means that special care must be exercised when choosing representative regions of interest of the bulk or fractionated sample to examine, selecting proper upscaling methods and formulating an appropriate research question. Therefore, it is recommended that detailed, spatially resolved analyses always be complemented by state-of-the-art bulk analyses (e.g. N-XANES, MS) of the soil or soil compartment under study. The tremendous progress made in developing new analytical chemistry techniques also bears a risk of producing more technique-driven investigations at the expense of research topic or hypothesis-driven investigations. Future challenges requiring a collaborative application of different chemical–analytical techniques include (1) tracing fluxes among the chemically different N_{org} pools that depend on site (e.g. soil, climate, land-use) and management (e.g. cropping system, fertilization) conditions and the consequences of these fluxes in terms of environmentally relevant N losses from soils; (2) linking N_{org} cycling with that of the other major nutrient elements (such as C, P and S) and their compounds in SOM; and (3) assessing the response of particularly vulnerable, extremely N-limited sites and ecosystems to a changing climate in an effort to develop effective mitigation strategies.

ACKNOWLEDGMENTS

Research conducted by the authors was funded by various organizations. Kristian Kiersch received a PhD scholarship from the Department Life, Light and Matter of the Faculty of Interdisciplinary Research at the University of Rostock. Melissa Arcand's PhD research was supported by a Natural Sciences and Engineering Research Council of Canada, Canada Graduate Scholarship; the Agricultural Bioproducts Innovation Program–Pulse Research Network (PURENet); and the Saskatchewan Pulse Growers. Technical and logistical support were provided by the Saskatchewan Ministry of Agriculture Strategic Research Project–Soil Biological Processes (Drs Knight and Farrell, co-PIs).

The Mass Spectrometry Laboratory of the Rostock Soil Science group was supported by the "Exzellenzförderprogramm" of the Ministerium für Bildung, Wissenschaft und Kultur Mecklenburg-Western Pomerania, project UR 07 079, and initial FT-ICR-MS measurements were funded by the German Research Council (INST 264/56-1). Almost all of the author's XANES measurements were performed at the Canadian Light Source (CLS), which is supported by Natural Sciences and Engineering Research Council of Canada (NSERC), National Research Council Canada (NRC), Canadian Institutes of Health Research (CIHR) and the University of Saskatchewan. Measurements of the German Researchers at the CLS were supported by a travel grant of the German Academic Exchange Service (D/05/50492). Furthermore, we thank our technical staff (E. Heilmann, R. Beese: University of Rostock), (M. Sather, D. Richman, M. Cooke, Dw. Richman and F. Krijnen: University of Saskatchewan). Finally, many thanks to Dr. Stefan Dultz (Institute of Soil Science, Leibniz-University Hannover, Germany) for providing NH_4^+-interlayered smectite and vermiculite.

REFERENCES

Abe, T., Watanabe, A., 2004. X-ray photoelectron spectroscopy of nitrogen functional groups in soil humic acids. Soil Sci. 169, 35–43.

Abe, T., Maie, N., Watanabe, A., 2005. Investigation of humic acid N with X-ray photoelectron spectroscopy: effect of acid hydrolysis and comparison with ^{15}N cross polarization/magic angle spinning nuclear magnetic resonance spectroscopy. Org. Geochem. 36, 1490–1497.

Almendros, G., Knicker, H., González-Vila, F.J., 2003. Rearrangement of carbon and nitrogen forms in peat after progressive thermal oxidation as determined by solid-state ^{13}C- and ^{15}N-NMR spectroscopy. Org. Geochem. 34, 1559–1568.

Altieri, K.E., Turpin, B.J., Seitzinger, S.P., 2009. Composition of dissolved organic nitrogen in continental precipitation investigated by ultra-high resolution FT-ICR mass spectrometry. Environ. Sci. Technol. 43, 6950–6955.

Amelung, W., 2003. Nitrogen biomarkers and their fate in soil. J. Plant Nutr. Soil Sci. 166, 677–686.

Amelung, W., Zech, W., 1999. Minimisation of organic matter disruption during particle-size fractionation of grassland epipedons. Geoderma 92, 73–85.

Appuhn, A., Joergensen, R.G., Raubuch, M., Scheller, E., Wilke, B., 2004. The automated determination of glucosamine, galactosamine, muramic acid, and mannosamine in soil and root hydrolysates by HPLC. J. Plant Nutr. Soil Sci. 167, 17–21.

Baggs, E.M., 2008. A review of stable isotope techniques for N_2O source partitioning in soils: recent progress, remaining challenges and future considerations. Rapid Commun. Mass. Spectrom. 22, 1664–1672.

Bakshi, M., Varma, A., 2011. Soil enzymes: the state-of-art. In: Shukla, S., Varma, A. (Eds.), Soil Enzymology, Soil Biology 22, Springer Verlag, Berlin, Heidelberg, pp. 1–23.

Bedard-Haughn, A., van Groenigen, J.W., van Kessel, C., 2003. Tracing ^{15}N through landscapes: potential uses and precautions. J. Hydrol. 272, 175–190.
Benzing-Purdie, L., Ripmeester, J.A., Preston, C.M., 1983. Elucidation of the nitrogen forms in melanoidins and humic acid by nitrogen-15 cross polarization-magic angle spinning nuclear magnetic resonance spectroscopy. J. Agric. Food Chem. 31, 913–915.
Benzing-Purdie, L.M., Cheshire, M.V., Williams, B.L., Sparling, G.P., Ratcliffe, C.I., Ripmeester, J.A., 1986. Fate of [^{15}N] glycine in peat as determined by ^{13}C and ^{15}N CP-MAS NMR spectroscopy. J. Agric. Food Chem. 34, 170–176.
Benzing-Purdie, L., Cheshire, M.V., Williams, B.L., Ratcliffe, C.I., Ripmeester, J.A., Goodman, B.A., 1992. Interactions between peat and sodium acetate, ammonium sulphate, urea or wheat straw during incubation studied by ^{13}C and ^{15}N NMR spectroscopy. J. Soil Sci. 43, 113–125.
Bertin, C., Yang, X., Weston, L.A., 2003. The role of root exudates and allelochemicals in the rhizosphere. Plant Soil. 67, 67–83.
Böhme, M., Höhn, P., Günther, D., Kniep, R., Auffermann, G., 2010. Quantitative determination of nitrogen by LA-ICP-MS using ^{15}N enriched binary calcium nitrides. J. Anal. Spectrom. 25, 856–860.
Böllmann, J., Elmer, M., Wöllecke, J., Raidl, S., Hüttl, R.F., 2010. Defensive strategies of soil fungi to prevent grazing by *Folsomia candida* (Collembola). Pedobiologia 53, 107–114.
Bosshard, C., Oberson, A., Leinweber, P., Jandl, G., Knicker, H., Kreuzer, M., Wettstein, H.-R., Frossard, E., 2011. Characterization of fecal nitrogen forms produced by a sheep fed with ^{15}N labeled ryegrass. Nutr. Cycl. Agroecosyst. 90, 355–368.
Boutton, T.W., Yamasaki, S., 1996. Mass Spectrometry of Soils. Marcel Dekker, New York.
Bremer, E., Janzen, H., Gilbertson, C., 1995. Evidence against associative N2 fixation as a significant N source in long-term wheat plots. Plant Soil. 175, 13–19.
Bremner, J.M., 1996. Nitrogen–Total. In: Sparks, D.L. (Ed.), Methods of Soil Analysis. Part. 3. Chemical Methods, Soil Science Society of America, Madison, WI, pp. 1085–1121.
Cai, P., Huang, Q.-Y., Zhang, X.-W., 2006. Interactions of DNA with clay minerals and soil colloidal particles and protection against degradation by DNase. Environ. Sci. Technol. 40, 2971–2976.
Caldwell, B.A., 2005. Enzyme activities as a component of soil biodiversity: a review. Pedobiologia 49, 637–644.
Castle, S.C., Morrisson, C.D., Barger, N.N., 2011. Extraction of chlorophyll a from biological crusts: a comparison of solvents for spectrophotometric determination. Soil Biol. Biochem. 43, 853–856.
Chiavari, G., Galletti, G.C., 1992. Pyrolysis-gas chromatography mass spectrometry of amino acids. J. Anal. Appl. Pyrol. 24, 123–137.
Chourey, K., Jansson, J., VerBerkmoes, N., Shah, M., Chavarria, K.L., Tom, L.M., Brodie, E.L., Hettich, R.L., 2010. Direct cellular lysis/protein extraction protocol for soil metaproteomics. J. Proteome Res. 9, 6615–6622.
Chuankun, X., Minghe, M., Leming, Z., Keqin, Z., 2004. Soil volatile fungistasis and volatile fungstatic compounds. Soil Biol. Biochem. 36, 1997–2004.
Cornelius, S., Traub, M., Bernard, C., Salzig, C., Lang, P., Möhlmann, T., 2012. Nucleoside transport across the plasma membrane mediated by equilibrative nucleoside transporter 3 influences metabolism of Arabidopsis seedlings. Plant Biol.10.1111/j.1438-8677.2012.00562.x.
Covelli, D., Hernández-Cruz, D., Haines, B.M., Munoz, V., Omotoso, O., Mikula, R., Urquhart, S., 2009. NEXAFS microscopy studies of the association of hydrocarbon thin films with fine clay particles. J. Electron. Spectrosc. Relat. Phenom. 173, 1–6.
Craft, C.B., Seneca, E.D., Broome, S.W., 1991. Loss on ignition and Kjeldahl digestion for estimating organic carbon and total nitrogen in estuarine marsh soils: calibration with dry combustion. Estuaries. 14, 175–179.

De Graaff, M.-A., Six, J., Van Kessel, C., 2007. Elevated CO_2 increases nitrogen rhizodeposition and microbial immobilization of root-derived nitrogen. New Phytol. 173, 778–786.
De la Rosa, J.M., González-Pérez, J.A., González-Vázquez, R., Knicker, H., López-Capel, E., Manning, D.A.C., González-Vila, F.J., 2008. Use of pyrolysis/GC-MS combined with thermal analysis to monitor C and N changes in soil organic matter from a Mediterranean fire affected forest soil. Catena. 74, 296–303.
Elsner, M., 2010. Stable isotope fractionation to investigate natural transformation mechanisms of organic contaminants: principles, prospects and limitations. J. Environ. Monitor. 12, 2005–2031.
Escher, M., Winkler, K., Renault, O., Barrett, N., 2010. Applications of high lateral and energy resolution imaging XPS with a double hemispherical analyser based spectromicroscope. J. Electron. Spectrosc. Relat. Phenom. 178–179 (C), 303–316.
España, M., Rasche, F., Kandeler, E., Brune, T., Rodriguez, B., Bending, G.D., Cadisch, G., 2011. Identification of active bacteria involved in decompostion of complex maize and soybean residues in a tropical Vertisol using ^{15}N-DNA stable isotope probing. Pedobiologia 54, 187–193.
Evans, E.J., Batts, B.D., Cant, N.W., Smith, J.W., 1985. The origin of nitriles in shale oil. Org. Geochem. 8, 367–374.
Fahey, J.W., Zalcmann, A.T., Talalay, P., 2001. The chemical diversity and distribution of glucosinolates and isothiocyanates among plants. Phytochemistry 56, 5–51.
Fekete, A., Malik, A.K., Kumar, A., Schmitt-Kopplin, P., 2010. Amines in the environment. Crit. Rev. Anal. Chem. 40, 102–121.
Fendorf, S.E., Sparks, D.L., 1996. X-ray absorption fine structure spectroscopy. In: Bigham, J.M. (Ed.), Methods of Soil Analysis: Chemical Methods, ASA, Madison, WI, pp. 377–416.
Fillery, I.R.P., Recous, S., 2001. Use of enriched ^{15}N sources to study soil N transformations. In: Unkovich, M., Pate, J., McNeill, A., Gibbs, D.J. (Eds.), Stable Isotope Techniques in the Study of Biological Processes and Functioning of Ecosystems, Kluwer Academic Publishers, Dordrecht, pp. 167–194.
Fischer, H., Eckhardt, K.-U., Meyer, A., Neumann, G., Leinweber, P., Fischer, K., Kuzyakov, Y., 2010. Rhizodeposition of maize: short-term carbon budget and composition. J. Plant Nutr. Soil Sci. 173, 67–79.
Fleming, Y., Wirtz, T., Gysin, U., Glatzel, T., Wegmann, U., Meyer, E., Maier, U., Rychen, J., 2011. Three dimensional imaging using secondary ion mass spectrometry and atomic force microscopy. Appl. Surf. Sci. 258, 1322–1327.
Frimpong, K.A., Baggs, E.M., 2010. Do combined applications of crop residues and inorganic fertilizer lower emission of N_2O from soil? Soil Use Manage. 26, 412–424.
Fry, B., Brand, W., Mersch, F.J., Tholke, K., Garritt, R., 1992. Automated analysis system for coupled δ^{13}C and δ^{15}N measurements. Anal. Chem. 64, 288–291.
Fustec, J., Lesuffleur, F., Mahieu, S., Cliquet, J.-B., 2010. Nitrogen rhizodeposition of legumes: a review. Agron. Sust. Dev. 30, 57–66.
Galletti, G.C., Bocchini, P., 1995. Pyrolysis/gas chromatography/mass spectrometry of lignocellulose. Rapid Comm. Mass. Spectrom. 9, 815–826.
Gärdenäs, A.I., Ågren, G.I., Bird, J.A., Clarholm, M., Hallin, S., Ineson, P., Kätterer, T., Knicker, H., Nilsson, S.I., Näsholm, T., Ogle, S., Paustian, K., Persson, T., Stendahl, J., 2011. Knowledge gaps in soil carbon and nitrogen interactions – from molecular to global scale. Soil Biol. Biochem. 43, 702–717.
Gardner, J.B., Drinkwater, L.E., 2009. The fate of nitrogen in grain cropping systems: a meta-analysis of ^{15}N field experiments. Ecol. Appl. 19, 2167–2184.
Ghosal, S., Fallon, S.J., Leighton, T.J., Wheeler, K.E., Kristo, M.J., Hutcheon, I.D., Weber, P.K., 2008. Imaging and 3D elemental characterization of intact bacterial spores by high-resolution secondary ion mass spectrometry. Anal. Chem. 80, 5986–5992.

Ghosal, S., Hemminger, J.C., Bluhm, H., Mun, B.S., Hebenstreit, E.L.D., Ketteler, G., Ogletree, D.F., Requejo, F.G., Salmeron, M., 2005. Electron spectroscopy of aqueous solution interfaces reveals surface enhancement of halides. Science 307, 563–566.

Giagnoni, L., Magherini, F., Landi, L., Taghavi, S., Modesti, A., Bini, L., Nannipieri, P., Van der lelie, D., Renella, G., 2011. Extraction of microbial proteome from soil: potential and limitations assessed through a model study. Eur. J. Soil Sci. 62, 74–81.

Gillespie, A.W., Walley, F.L., Farrell, R.E., Regier, T.Z., Blyth, R.I.R., 2008. Calibration method at the N K-edge using interstitial nitrogen gas in solid-state nitrogen-containing inorganic compounds. J. Synchrotron Radiat. 15, 532–534.

Gillespie, A.W., Walley, F.L., Farrell, R.E., Leinweber, P., Schlichting, A., Eckhardt, K.-U., Regier, T.Z., Blyth, R.I.R., 2009. Profiling rhizosphere chemistry: evidence from C & N K-edge XANES and Py-FIMS. Soil Sci. Soc. Am. J. 73, 2002–2012.

Gillespie, A.W., Walley, F.L., Farrell, R.E., Leinweber, P., Eckhardt, K.-U., Regier, T.Z., Blyth, R.I.R., 2011a. XANES and Py-FIMS evidence for variations in molecular composition of soil organic matter in a hummocky landscape. Soil Sci. Soc. Am. J. 75, 1741–1755.

Gillespie, A.W., Farrell, R.E., Walley, F.L., Ross, A.R.S., Leinweber, P., Eckhardt, K.-U., Regier, T.Z., Blyth, R.I.R., 2011b. Glomalin-related soil protein contains thioredoxin, non-mycorrhizal-related heat-stable proteins, lipids & humic materials: evidence from XANES, Py-FIMS and proteomics. Soil Biol. Biochem. 43, 766–777.

González-Chávez, M.C., Carrillo-González, R., Wright, S.F., Nichols, K.A., 2004. The role of glomalin, a protein produced by arbuscular mycorrhizal fungi, in sequestering potentially toxic elements. Environ. Pollut. 130, 317–323.

González-Pérez, J.A., González-Vila, F.J., Almendros, G., Knicker, H., 2004. The effect of fire on soil organic matter—a review. Environ. Int. 30, 855–870.

González-Pérez, J.A., Arbelo, C.D., González-Vila, F.J., Rodríguez, A.R., Almendros, G., Armas, C.M., Polvillo, O., 2007. Molecular features of organic matter in diagnostic horizons from andosols as seen by analytical pyrolysis. J. Anal. Appl. Pyrol. 80, 369–382.

Götz, K.P., Herzog, H., 2000. Distribution and utilization of ^{15}N in cowpeas injected into the stem under influence of water deficit. Isotope. Environ. Health Stud. 36, 111–121.

Greenfield, L.G., 1972. The nature of organic nitrogen in soil. Plant Soil. 36, 191–198.

Hanson, J.R., 2008. The Chemistry of Fungi. RSC Publishing, Cambridge, UK.

Hart, S.C., Myrold, D.D., 1996. ^{15}N tracer studies of soil nitrogen transformations. In: Boutton, T.W., Yamasaki, S. (Eds.), Mass Spectrometry of Soils, Marcel Dekker, Inc., New York, pp. 225–245.

Hart, S.C., Stark, J.M., Davidson, E.A., Firestone, M.K., 1994. Nitrogen mineralization, immobilization, and nitrification. In Methods of Soil Analysis, Part 2. Microbiological and Biochemical Properties, Soil Science Society of America, ASA, Madison, Wisconsin, USA, pp. 985–1018.

Hatcher, P.G., Dria, K.J., Kim, S., Frazier, S.W., 2001. Modern analytical studies of humic substances. Soil Sci. 166, 770–794.

Hauck, R.D., Bremner, J.M., 1976. Use of tracers for soil and fertilizer nitrogen research. Adv. Agron. 28, 219–266.

Heister, K., Höschen, C., Pronk, G.J., Mueller, C.W., Kögel-Knabner, I., 2012. NanoSIMS as a tool for characterizing soil model compounds and organomineral associations in artificial soils. J. Soil Sediment. 12, 35–47.

Hertenberger, G., Wanek, W., 2004. Evaluation of methods to measure differential ^{15}N labeling of soil and root N pools for studies of root exudation. Rapid Commun. Mass. Spectrom. 18, 2415–2425.

Hesse, M., 2002. Alkaloids: Nature's Curse or Blessing? Wiley-VCH.

Hilscher, A., Knicker, H., 2011. Carbon and nitrogen degradation on molecular scale of grass-derived pyrogenic organic material during 28 months of incubation in soil. Soil Biol. Biochem. 43, 261–270.

Hou, S., Hea, H., Zhanga, W., Xiea, H., Zhang, X., 2009. Determination of soil amino acids by high performance liquid chromatography-electro spray ionization-mass spectrometry derivatized with 6-aminoquinolyl-N-hydroxysuccinimidyl carbamate. Talanta 80, 440–447.

Huffman, G.P., Mitra, S., Huggins, F.E., Shah, N., Vaidya, S., Lu, F., 1991. Quantitative analysis of all major forms of sulfur in coal by X-ray absorption fine structure spectroscopy. Energ. Fuel. 5, 574–581.

Isobe, K., Suwa, Y., Ikutani, J., Kuroiwa, M., Makita, T., Takebayashi, Y., Yoh, M., Otsuka, S., Senoo, K., Ohmori, M., Koba, K., 2011. Analytical techniques for quantifying (15) N/(14)N of nitrate, nitrite, total dissolved nitrogen and ammonium in environmental samples using a gas chromatograph equipped with a quadrupole mass spectrometer. Microbe. Environ. 26, 46–53.

IUSS Working Group WRB, 2006. World Reference Base for Soil Resources. World Soil Resources Reports No. 103. FAO, Rome.

Iverson, K.C., Schnitzer, M., 1979. The biodegradability of the "unknown" soil nitrogen. Can. J. Soil Sci. 59, 277–286.

Jacobsen, C., Wirick, S., Flynn, G., Zimba, C., 2000. Soft X-ray spectroscopy from image sequences with sub-100 nm spatial resolution. J. Microsc. 197, 173–184.

Janzen, H.H., 1990. Deposition of nitrogen into the rhizosphere by wheat roots. Soil Biol. Biochem. 22, 1155–1160.

Janzen, H.H., Bruinsma, Y., 1989. Methodology for the quantification of root and rhizosphere nitrogen dynamics by exposure of shoots to ^{15}N-labelled ammonia. Soil Biol. Biochem. 21, 189–196.

Jensen, E.S., 1994. Dynamics of mature pea residue nitrogen turnover in unplanted soil under field conditions. Soil Biol. Biochem. 26, 455–464.

Jensen, E.S., 1996. Rhizodeposition of N by pea and barley and its effect on soil N dynamics. Soil Biol. Biochem. 28, 65–71.

Jokic, A., Cutler, J.N., Anderson, D.W., Walley, F.L., 2004. Detection of heterocyclic N compounds in whole soils using N-XANES spectroscopy. Can. J. Soil Sci. 84, 291–293.

Jones, D., Nguyen, C., Finlay, R., 2009. Carbon flow in the rhizosphere: carbon trading at the soil–root interface. Plant Soil. 321, 5–33.

Jones, D.J., Shannon, D., Junvee-Fortune, T., Farrar, J.F., 2005a. Plant capture of free amino acids is maximized under high soil amino acid concentrations. Soil Biol. Biochem. 37, 179–181.

Jones, D.L., Healey, J.R., Willett, V.B., Farrar, J.F., Hodge, A., 2005b. Dissolved organic nitrogen uptake by plants–an important N uptake pathway? Soil Biol. Biochem. 37, 413–423.

Joosten, L., van Veen, J.A., 2011. Defensive properties of pyrrolizidine alkaloids against microorganisms. Phytochem. Rev. 10, 127–136.

Kelemen, S.R., Afeworki, M., Gorbaty, M.L., Kwiatek, P.J., Solum, M.S., Hu, J.Z., Pugmire, R.J., 2002. XPS and ^{15}N NMR study of nitrogen forms in carbonaceous solids. Energ. Fuel. 16, 1507–1515.

Kelley, K.R., Stevenson, F.J., 1995. Forms and nature of organic N in soil. Fert. Res. 42, 1–11.

Khan, W.D.F., Peoples, M.B., Herridge, D.F., 2002a. Quantifying below-ground nitrogen of legumes. 2. A comparison of ^{15}N and nonisotopic methods. Plant Soil. 239, 277–289.

Khan, W.D.F., Peoples, M.B., Herridge, D.F., 2002b. Quantifying below-ground nitrogen of legumes. 1. Optimising procedures for ^{15}N shoot-labelling. Plant Soil. 245, 327–334.

Kiersch, K., Kruse, J., Eckhardt, K.-U., Fendt, A., Streibel, T., Zimmermann, R., Broll, G., Leinweber, P., 2012a. Impact of grassland burning on soil organic matter as revealed by a synchrotron- and pyrolysis–mass spectrometry-based multi-methodological approach. Org. Geochem. 44, 8–20.

Kiersch, K., Kruse, J., Regier, T.Z., Leinweber, P. 2012b. Temperature resolved alteration of soil organic matter composition during laboratory heating as revealed by C and N XANES spectroscopy and Py-FIMS. Thermochim. Acta 537, 36–43.
Kinyangi, J., Solomon, D., Liang, B., Lerotic, M., Wirick, S., Lehmann, J., 2006. Nanoscale biogeocomplexity of the organomineral assemblage in soil: application of STXM microscopy and C 1s-NEXAFS spectroscopy. Soil Sci. Soc. Am. J. 70, 1708–1718.
Knicker, H., 2004. Stabilization of N-compounds in soil and organic matter rich sediments – what is the difference? Mar. Chem. 92, 167–195.
Knicker, H., 2007. How does fire affect the nature and stability of soil organic nitrogen and carbon? A review. Biogeochemistry 85, 91–118.
Knicker, H., 2009. Black carbon and thermally altered (pyrogenic) organic matter: chemical characteristics and the role in the environment. In: Senesi, N., Xing, B., Huang, P.M. (Eds.), Biophysico-chemical Processes Involving Natural Nonliving Organic Matter in Environmental Systems, John Wiley & Sons, Inc, Chichester, England, pp. 273–303.
Knicker, H., 2010. "Black nitrogen"—an important fraction in determining the recalcitrance of charcoal. Organ. Geochem. 41, 947–950.
Knicker, H., 2011a. Soil organic N—an under-rated player for C sequestration in soils? Soil Biol. Biochem. 43, 1118–1129.
Knicker, H., 2011b. Solid state CPMAS ^{13}C and ^{15}N NMR spectroscopy in organic geochemistry and how spin dynamics can either aggravate or improve spectra interpretation. Org. Geochem. 42, 867–890.
Knicker, H., Schmidt, M.W.I., Kögel-Knabner, I., 2000. Nature of organic nitrogen in fine particle size separates of sandy soils of highly industrialized areas as revealed by NMR spectroscopy. Soil Biol. Biochem. 32, 241–252.
Knicker, H., González-Vila, F.J., Polvillo, O., González, J.A., Almendros, G., 2005. Fire-induced transformation of C- and N-forms in different organic soil fractions from a Dystric Cambisol under a Mediterranean pine forest (Pinus pinaster). Soil Biol. Biochem. 37, 701–718.
Knowles, R., Blackburn, T.H., 1993. Nitrogen Isotope Techniques. Academic Press, Inc., San Diego.
Kögel-Knabner, I., Amelung, W., Cao, Z., Fiedler, S., Frenzel, P., Jahn, R., Kalbitz, K., Kölbl, A., Schloter, M., 2010. Biogeochemistry of paddy soils. Geoderma. 157, 1–14.
Krummen, M., Hilkert, A.W., Juchelka, D., Duhr, A., Schlüter, H.-J., Pesch, R., 2004. A new concept for isotope ratio monitoring liquid chromatography/mass spectrometry. Rapid Commun. Mass. Spectrom. 18, 2260–2266.
Kruse, J., Eckhardt, K.-U., Regier, T., Leinweber, P., 2011. TG-FTIR, LC/MS, XANES and Py-FIMS to disclose the thermal decomposition pathways and aromatic N formation during dipeptide pyrolysis in a soil matrix. J. Anal. Appl. Pyrol. 90, 164–173.
Kuzyakov, Y., Siniakina, S., 2001. A novel method for separating root derived organic compounds from root respiration in non sterilized soils. J. Plant Nutr. Soil Sci. 164, 511–517.
Landgraf, D., Leinweber, P., Makeschin, F., 2006. Cold and hot water extractable organic matter as indicators of litter decomposition in forest soils. J. Plant Nutr. Soil Sci. 169, 76–82.
Legent, G., Delaune, A., Norris, V., Delcorte, A., Gibouin, D., Lefebvre, F., Misevic, G., Thellier, M., Ripoll, C., 2008. Method for macromolecular colocalization using atomic recombination in dynamic SIMS. J. Phys. Chem. B 112, 5534–5546.
Lehmann, J., Solomon, D., 2008. Nitrogen Speciation in Soils by Near-edge X-ray Absorption Fine Structure (NEXAFS) Spectroscopy and Scanning Transition X-ray Microscopy (STXM). Activity Report 2007. Canadian Light Source, Saskatoon, Canada 84–85.
Lehmann, J., Solomon, D., Kinyangi, J., Dathe, L., Wirick, S., Jacobsen, C., 2008. Spatial complexity of soil organic matter forms at nanometre scales. Nat. Geosci. 1, 238–242.

Leinweber, P., Reuter, G., 1992. The influence of different organic fertilization practices on concentrations of organic carbon and total nitrogen in particle-size fractions during 34 years of a soil formation experiment in loamy marl. Biol. Fert. Soils. 13, 119–124.
Leinweber, P., Schulten, H.-R., 1998a. Advances in analytical pyrolysis of soil organic matter. J. Anal. Appl. Pyrol. 47, 165–189.
Leinweber, P., Schulten, H.-R., 1998b. Nonhydrolyzable organic nitrogen in soil size separates from long-term agricultural experiments. Soil Sci. Soc. Am. J. 62, 383–393.
Leinweber, P., Schulten, H.-R., 2000. Nonhydrolyzable forms of soil organic nitrogen: extractability and composition. J. Plant Nutr. Soil Sci. 163, 433–439.
Leinweber, P., Schulten, H.-R., Jancke, H., 1999. New evidence for the molecular composition of soil organic matter in vertisols. Soil Sci. 64, 857–870.
Leinweber, P., Kruse, J., Walley, F.L., Gillespie, A., Eckhardt, K.-U., Blyth, R.I.R., Regier, T., 2007. Nitrogen K-edge XANES—an overview of reference compounds used to identify 'unknown' organic nitrogen in environmental samples. J. Synchrotron Rad. 14, 500–511.
Leinweber, P., Jandl, G., Eckhardt, K.-U., Schlichting, A., Hofmann, D., Schulten, H.-R., 2009. Analytical pyrolysis and soft-ionization mass spectrometry. In: Senesi, N., Xing, B., Huang, P.M. (Eds.), Biophysico-chemical Processes Involving Natural Nonliving Organic Matter in Environmental Systems, John Wiley & Sons, Inc, Chichester, England, pp. 539–588.
Leinweber, P., Jandl, G., Eckhardt, K.-U., Kruse, J., Walley, F.L., Khan, M.J., Blyth, R.I.R., Regier, T., 2010a. Nitrogen speciation in fine and coarse clay fractions of a cryoboroll—new evidence from pyrolysis-mass spectrometry and nitrogen K-edge XANES. Can. J. Soil Sci. 90, 309–318.
Leinweber, P., Kruse, J., Gillespie, A., Walley, F.L., Eckhardt, K.-U., Blyth, R.I.R., Regier, T., 2010b. Nitrogen compounds in dissolved and solid environmental samples. In: Singh, B., Gräfe, M. (Eds.), Advances in Understanding Soil Environments by Application of Synchrotron-based Techniques. Developments in Soil Science 34, Elsevier, pp. 255–288.
Lerotic, M., Jacobsen, C., Gillow, J.B., Francis, A.J., Wirick, S., Vogt, S., Maser, J., 2005. Cluster analysis in soft X-ray spectromicroscopy: finding the patterns in complex specimens. J. Electron. Spectrosc. Relat. Phenom. 144-147, 1137–1143.
Levy, G.C., Lichter, R.L., 1979. Nitrogen-15 Nuclear Magnetic Resonance Spectroscopy. Wiley & Sons, New York.
Linder, M.B., Szilvay, G.R., Nakari-Setälä, T., Penttilä, M.E., 2005. Hydrophobins: the protein-amphiphiles of filamentous fungi. FEMS Microbiol. Rev. 29, 877–896.
Longnecker, K., Kujawinski, E.B., 2011. Composition of dissolved organic matter in groundwater. Geochim. Cosmochim. Acta 75, 2752–2761.
López-Bellido, L., Benítez-Vega, J., García, P., Redondo, R., López-Bellido, R.J., 2011. Tillage system effect on nitrogen rhizodeposited by faba bean and chickpea. Field Crop Res. 120, 189–195.
Macdonald, C.A., Anderson, I.A., Bardgett, R.D., Singh, B.K., 2011. Role of nitrogen in carbon mitigation in forest ecosystems. Curr. Opin. Environ. Sustainability 3, 303–310.
Mahieu, N., Olk, D.C., Randall, E.W., 2000. Accumulation of heterocyclic nitrogen in humified organic matter: a ^{15}N-NMR study of lowland rice soils. Eur. J. Soil Sci. 51, 379–389.
Mahieu, S., Fustec, J., Faure, M.L., Corre-Hellou, G., Crozat, Y., 2007. Comparison of two ^{15}N labelling methods for assessing nitrogen rhizodeposition of pea. Plant Soil. 295, 193–205.
Mahieu, S., Fustec, J., Jensen, E.S., Crozat, Y., 2009. Does labelling frequency affect N rhizodeposition assessment using the cotton-wick method? Soil Biol. Biochem. 41, 2236–2243.
Maie, N., Knicker, H., Watanabe, A., Kimura, M., 2006. Heterocyclic N in the highly humified humic acids extracted from the subsoil of paddy fields and surface ando soils. Org. Geochem. 37, 12–19.

Mapolelo, M.M., Rodgers, R.P., Blakney, G.T., Yen, A.T., Asomaning, S., Marshall, A.G., 2011. Characterization of naphthenic acids in crude oils and naphthenates by electrospray ionization FT-ICR mass spectrometry. Int. J. Mass. Spectrom. 300, 149–157.
Marshall, A.G., Rodgers, R.P., 2004. Petroleomics: the next grand challenge for chemical analysis. Acc. Chem. Res. 37, 53–59.
Martens, D.A., Loeffelmann, K.L., 2003. Soil amino acid composition quantified by acid hydrolysis and anion chromatography-pulsed amperometry. J. Agric. Food Chem. 51, 6521–6529.
Martens, D.A., Jaynes, D.B., Colvin, T.S., Kaspar, T.C., Karlen, D.L., 2006. Soil organic nitrogen enrichment following soybean in an Iowa corn-soybean rotation. Soil Sci. Soc. Am. J. 70, 382–392.
Mayer, J., Buegger, F., Jensen, E.S., Schloter, M., Heβ, J., 2003. Estimating N rhizodeposition of grain legumes using a ^{15}N in situ stem labelling method. Soil Biol. Biochem. 35, 21–28.
Mayer, J., Buegger, F., Jensen, E.S., Schloter, M., Heβ, J., 2004. Turnover of grain legume N rhizodeposits and effect of rhizodeposition on the turnover of crop residues. Biol. Fert. Soils. 39, 153–164.
McMahon, G., Saint-Cyr, H.F., Lechene, C., Unkefer, C.J., 2006. CN- secondary ions form by recombination as demonstrated using multi-isotope mass spectrometry of ^{13}C- and ^{15}N-labeled polyglycine. J. Am. Soc. Mass. Spectrom. 17, 1181–1187.
McNeill, A., 2001. Stable isotope techniques using enriched ^{15}N and ^{13}C for studies of soil organic matter accumulation and decomposition in agricultural systems. In: Unkovich, M., Pate, J., McNeill, A., Gibbs, D.J. (Eds.), Stable Isotope Techniques in the Study of Biological Processes and Functioning of Ecosystems, Kluwer Academic Publishers, Dordrecht, pp. 195–218.
McNeill, A.M., Zhu, C.Y., Fillery, I.R.P., 1997. Use of in situ ^{15}N-labeling to estimate the total below-ground nitrogen of pasture legumes in intact soil-plant systems. Aust. J. Agr. Res. 48, 295–304.
Melnitchouck, A., Leinweber, P., Eckhardt, K.-U., Beese, R., 2005. Qualitative differences between day- and nighttime rhizodeposition in maize (Zea mays L.) as investigated by pyrolysis-field ionization mass spectrometry. Soil Biol. Biochem. 37, 155–162.
Mengel, K., 1996. Turnover of organic nitrogen in soils and its availability to crops. Plant Soil. 181, 83–93.
Merbach, W., Mirus, E., Knof, G., Remus, R., Ruppel, S., Russow, R., Gransee, A., Schulze, J., 1999. Release of carbon and nitrogen compounds by plant roots and their possible ecological importance. J. Plant Nutr. Soil Sci. 162, 373–383.
Mikutta, R., Kaiser, K., Dörr, N., Vollmer, A., Chadwick, O.A., Chorover, J., Kramer, M.G., Guggenberger, G., 2010. Mineralogical impact on organic nitrogen across a long-term soil chronosequence (0.3–4100 kyr). Geochim. Cosmochim Acta 74, 2142–2164.
Millar, N., Baggs, E.M., 2004. Chemical composition, or quality, of agroforestry residues influences N_2O emissions after their addition to soil. Soil Biol. Biochem. 36, 935–943.
Minor, E.C., Steinbring, C.J., Longnecker, K., Kujawinski, E.B., 2012. Characterization of dissolved organic matter in Lake Superior and its watershed using ultrahigh resolution mass spectrometry. Org. Geochem. 43, 1–11.
Mohr, R.M., Janzen, H.H., Bremer, E., Entz, M.H., 1998. Fate of symbiotically-fixed $^{15}N_2$ as influenced by method of alfalfa termination. Soil Biol. Biochem. 30, 1359–1367.
Monreal, C.M., Janzen, H.H., 1993. Soil organic-carbon dynamics after 80 years of cropping a Dark Brown Chernozem. Can. J. Soil Sci. 73, 133–136.
Moulder, J.F., Stickle, W.F., Sobol, P.E., Bomben, K.D., 1992. In: Moulder, J.F., Stickle, W.F., Sobol, P.E. (Eds.), Handbook of X-ray Photoelectron Spectroscopy: A Reference Book of Standard Spectra for Identification and Interpretation of XPS Data, Perkin-Elmer Corp., Physical Electronics Division, USA.

Müller, C.W., Kölbl, A., Hoeschen, C., Hillion, F., Heister, K., Herrmann, A.M., Kögel-Knabner, I., 2012. Submicron scale imaging of soil organic matter dynamics using NanoSIMS—from single particles to intact aggregates. Org. Geochem. 42, 1476–1488.
Mulvaney, R.L., 1996. Nitrogen—inorganic forms. In: Bigham, J.M. (Ed.), Methods of Soil Analysis Part 3: Chemical Methods, Soil Science Society of America, Inc, Madison, WI, pp. 1123–1184.
Murphy, D.V., Recous, S., Stockdale, E.A., Fillery, I.R.P., Jensen, L.S., Hatch, D.J., Goulding, K.W.T., 2003. Gross nitrogen fluxes in soil: theory, measurement and application of ^{15}N pool dilution techniques. Adv. Agron. 79, 69–118.
Nannipieri, P., 2006. Role of stabilised enzymes in microbial ecology and enzyme extraction from soil with potential applications in soil proteomics. In: Nannipieri, P., Smalla, K. (Eds.), Soil Biology Volume 8 Nucleic Acids and Proteins in Soil, Springer Verlag, Berlin, Heidelberg, pp. 75–94.
Nannipieri, P., Eldor, P., 2009. The chemical and functional characterization of soil N and its biotic components. Soil Biol. Biochem. 41, 2357–2369.
Näsholm, T., Kielland, K., Ganeteg, U., 2009. Uptake of organic nitrogen by plants. New Phytol. 182, 31–48.
Nichols, K.A., 2003. Characterization of Glomalin: A Glycoprotein Produced by Arbuscular Mycorrhizal Fungi. PhD Dissertation. University of Maryland, College Park, MD.
Olk, D.C., 2008. Organic forms of soil nitrogen. In: Schepers, J.S., Raun, W.R. (Eds.), Nitrogen in Agricultural Systems, American Society of Agronomy, pp. 57–100.
Olk, D.C., Dancel, M.C., Moscoso, E., Jimenez, R.R., Dayrit, F.M., 2002. Accumulation of lignin residues in organic matter fractions of lowland rice soils: a pyrolysis-GC-MS study. Soil Sci. 167, 590–606.
Ollivier, J., Töwe, S., Bannert, A., Hai, B., Kastl, E.-M., Meyer, A., Su, M.X., Kleineidam, K., Schloter, M., 2011. Nitrogen turnover in soil and global change. FEMS Microbiol. Ecol. 78, 3–16.
Patterson, J.M., Haidar, N.F., Papadopoulos, E.P., Smith, W.T., 1973. Pyrolysis of phenylalanine, 3,6-dibenzyl-2,5-piperazinedione, and phenetylamine. J. Org. Chem. 4, 663–666.
Paula, T.J., Hau, B., 2007. Effect of soil moisture on activity and dynamics of *Rhizoctonia solani* and *Trichoderma harzianum*. J. Plant Dis. Protect. 114, 126–132.
Pennock, D.J., Anderson, D.W., de Jong, E., 1994. Landscape-scale changes in indicators of soil quality due to cultivation in Saskatchewan, Canada. Geoderma. 64, 1–19.
Pereira de Assis, C., González-Pérez, J.A., de la Rosa, J.M., Jucksch, I., de Sá Mendoça, E., González-Vila, F.J., 2012. Analytical pyrolysis of humic substances from a Latosol (Typic Hapludox) under different land uses in Minas Gerais, Brazil. J. Anal. Appl. Pyrol. 93, 120–128.
Pérez, D.V., De Alcantara, S., Arruda, R.J., Meneghelli, N.D.A., 2001. Comparing two methods for soil carbon and nitrogen determination using selected Brazilian soils. Commun. Soil Sci. Plan. 32, 295–309.
Podgorski, D.C., Osborne, D.M., McKenna, A.M., Rodgers, R.P., Marshall, A.G., Cooper, W.T., 2010. The molecular characterization of dissolved organic nitrogen by APPI FT-ICR MS Goldschmidt Conference Abstracts. p. A 821.
Powlson, D.S., Barraclough, D., 1993. Mineralization and assimilation in soil-plant systems. In: Knowles, R., Blackburn, T.H. (Eds.), Nitrogen Isotope Techniques, Academic Press, Inc., San Diego, pp. 209–242.
Quénéa, K., Derenne, S., González-Vila, F.J., González-Pérez, J.A., Mariotti, A., Largeau, C., 2006. Double-shot pyrolysis of the non-hydrolysable organic fraction isolated from a sandy forest soils (Landes de Gascogne, South-West France) – comparison with classical Curie-point pyrolysis. J. Anal. Appl. Pyrol. 76, 271–279.
Rasmussen, J., 2011. Why we need to restrict the use of "rhizodeposition" and the Janzen and Bruinsma equation. Soil Biol. Biochem. 43, 2213–2214.

Rillig, M.C., 2004. Arbuscular mycorrhizae, glomalin and soil quality. Can. J. Soil Sci. 84, 355–363.
Rillig, M.C., 2005. A connection between fungal hydrophobins and soil water repellency? Pedobiologia 49, 395–399.
Roberts, P., Bol, R., Jones, D.L., 2007. Free amino sugar reactions in soil in relation to soil carbon and nitrogen cycling. Soil Biol. Biochem. 39, 3081–3092.
Rodgers, R.P., McKenna, A.M., Marshall, A.G., 2009. Compositional analysis of heavy conventional crude oils: the definition of asphaltenes and maltenes by high resolution mass spectrometry. ACS Natl. Meet. Book Abstr. 1p.
Russell, C.A., Fillery, I.R.P., 1996. In situ ^{15}N labelling of lupin below-ground biomass. Aust. J. Agr. Res. 47, 1035–1046.
Russelle, M.P., Allan, D.L., Gourley, C.J.P., 1994. Direct assessment of symbiotically fixed nitrogen in the rhizosphere of alfalfa. Plant Soil. 159, 233–243.
Rutherford, P.M., McGill, W.B., Arocena, J.M., Figueiredo, C.T., 2008. Total nitrogen. In: Carter, M.R., Gregorich, E.G. (Eds.), Soil Sampling and Methods of Analysis, CRC Press, Taylor & Francis Group, Boca Raton, FL, pp. 239–256.
Saiz-Jimenez, C., 1994. Analytical pyrolysis of humic substances: pitfalls, limitations, and possible solutions. Environ. Sci. Tech. 28, 1773–1780.
Saiz-Jimenez, C., Ortega-Calvo, J.J., Hermosin, B., 1994. Conventional pyrolysis: a biased technique for providing structural informations on humic substances? Naturwissenschaften. 81, 28–29.
Salmeron, M., Schlögl, R., 2008. Ambient pressure photoelectron spectroscopy: a new tool for surface science and nanotechnology. Surf. Sci. Rep. 63, 169–199.
Sawatsky, N., Soper, R.J., 1991. A quantitative measurement of the nitrogen loss from the root system of field peas (*Pisum avense* L.) grown in the soil. Soil Biol. Biochem. 23, 255–259.
Schimel, J.P., Bennett, J., 2004. Nitrogen mineralization: challenges of a changing paradigm. Ecology. 85, 591–602.
Schmidt, M.W.I., Gleixner, G., 2005. Carbon and nitrogen isotope composition of bulk soils, particle-size fractions and organicmaterial after treatment with hydrofluoric acid. Eur. J. Soil Sci. 56, 407–416.
Schmidt, F., Elvert, M., Koch, B.P., Witt, M., Hinrichs, K.-U., 2009. Molecular characterization of dissolved organic matter in pore water of continental shelf sediments. Geochim. Cosmochim. Acta 73, 3337–3358.
Schmidt, F., Koch, B.P., Elvert, M., Schmidt, G., Witt, M., Hinrichs, K.-U., 2011. Diagenetic transformation of dissolved organic nitrogen compounds under contrasting sedimentary redox conditions in the Black Sea. Environ. Sci. Technol. 45, 5223–5229.
Schmidtke, K., 2005a. How to calculate nitrogen rhizodeposition: a case study in estimating N rhizodeposition in the pea (*Pisum sativum* L.) and grasspea (*Lathyrus sativus* L.) using a continuous ^{15}N labelling split-root technique. Soil Biol. Biochem. 37, 1893–1897.
Schmidtke, K., 2005b. A model to predict the accuracy of measurements of legume N rhizodeposition using a split-root technique. Soil Biol. Biochem. 37, 829–836.
Schmidt-Rohr, K., Mao, J.-D., 2002. Selective observation of nitrogen-bonded carbons in solid-state NMR by saturation-pulse induced dipolar exchange with recoupling. Chem. Phys. Lett. 359, 403–411.
Schmidt-Rohr, K., Mao, J.-D., Olk, D.C., 2004. Nitrogen-bonded aromatics in soil organic matter and their implications for a yield decline in intensive rice cropping. Proc. Natl. Acad. Sci. U.S.A. 101, 6351–6354.
Schnitzer, M., Kodama, H., 1992. Interactions between organic and inorganic compounds in particle-size fractions separated from four soils. Soil Sci. Am. J. 56, 1099–1105.
Schnitzer, M., Spiteller, M. 1986. The chemistry of the "unknown" soil nitrogen. Trans. Int. Congr. Soil Sci. vol. 3. Hamburg, pp. 473–474.

Schulten, H.-R., 1987. Pyrolysis and soft ionization mass spectrometry of aquatic/terrestrial humic substances and soils. J. Appl. Anal. Pyrolysis. 12, 149–186.
Schulten, H.-R., 1996. Direct pyrolysis-mass spectrometry of soils: a novel tool in agriculture, ecology, forestry, and soil science. In: Boutton, T.W., Yamasaki, S.I. (Eds.), Mass Spectrometry of Soils, Marcel Dekker, New York, pp. 373–436.
Schulten, H.-R., Leinweber, P., 2000. New insights into organic-mineral particles: composition, properties and models of molecular structure. Biol. Fert. Soils. 30, 399–432.
Schulten, H.-R., Schnitzer, M., 1998. The chemistry of soil organic nitrogen: a review. Biol. Fert. Soils. 26, 1–15.
Schulten, H.-R., Leinweber, P., Jandl, G., 2002. Analytical pyrolysis of humic substances and dissolved organic matter in water. In: Frimmel, F.H., Abbt-Braun, G., Heumann, K.G., Hock, B., Lüdemann, H.-D., Spiteller, M. (Eds.), Refractory Organic Substances in the Environment, Wiley-VCH, Heidelberg, pp. 163–187.
Schulten, H.-R., Leinweber, P., Schnitzer, M., 1998. Analytical pyrolysis and computer modelling of humic and soil particles. In: Huang, P.M., Senesi, N., Buffle, J. (Eds.), IUPAC Environmental Analytical and Physical Chemistry Series, Environmental Particles: Structure and Surface Reactions of Soil Particles., vol. 4. Wiley, Chichester, England, pp. 281–324.
Schulten, H.-R., Sorge, C., Schnitzer, M., 1995. Structural studies on soil nitrogen by Curie-point pyrolysis-gas chromatography/mass spectrometry with nitrogen-selective detection. Biol. Fertil. Soils. 20, 174–184.
Schulze, W., 2004. Protein analysis in dissolved organic matter: what free proteins from soil leachate and surface water can tell us – a perspective. Biogeosciences Discuss. 1, 825–853.
Schulze, J., Merbach, W., 2008. Nitrogen rhizodeposition of young wheat plants under elevated CO_2 and drought stress. Biol. Fert. Soils. 44, 417–423.
Schumacher, M., Christl, I., Scheinost, A.C., Jacobsen, C., Kretzschmar, R., 2005. Chemical heterogeneity of organic soil colloids investigated by scanning transmission X-ray microscopy and C-1s NEXAFS microspectroscopy. Environ. Sci. Technol. 39, 9094–9100.
Simpson, A.J., Simpson, M.J., 2009. Nuclear magnetic resonance analysis of natural organic matter. In: Senesi, N., Xing, B., Huang, P.M. (Eds.), Biophysico-chemical Processes Involving Natural Nonliving Organic Matter in Environmental Systems, John Wiley & Sons, Inc, Chichester, England, pp. 589–650.
Sims, G.K., 2006. Nitrogen starvation promotes biodegradation of N-heterocyclic compounds in soil. Soil Biol. Biochem. 38, 2478–2480.
Sleutel, S., Leinweber, P., Begum, S.A., Abdul Kader, M., De Neve, S., 2009. Shifts in soil organic matter composition following treatment with sodium hypochlorite (NaOCl) and hydrofluoric acid (HF). Geoderma. 149, 257–266.
Smernik, R.J., Baldock, J.A., 2005a. Solid-state ^{15}N NMR analysis of highly ^{15}N-enriched plant materials. Plant Soil. 275, 271–283.
Smernik, R.J., Baldock, J.A., 2005b. Does solid-state ^{15}N NMR detect all soil organic nitrogen. Biogeochem. 75, 507–528.
Solomon, D., Lehmann, J., Har, J., Wang, J., Kinyani, J., Heymann, K., Karunakaran, C., Lu, Y., Wirick, S., Jacobsen, C., 2012. Micro- and nano-environments of carbon species: multi-element STXM-NEXAFS spectromicroscopic assessment of microbial carbon and mineral associations. Chem. Geol. 329, 53–73.
Solum, M.S., Altmann, K.L., Strohmeier, M., Berges, D.A., Zhang, Y., Facelli, J.C., Pugmire, R.J., Grant, D.M., 1997. ^{15}N-chemical shift principal values in nitrogen heterocycles. J. Am. Chem. Soc. 119, 9804–9809.
Sorge, C., 1995. Struktur der organischen Substanz in Böden und Partikelgrößenfraktionen: Pyrolyse-Gaschomatographie/Massenspektrometrie und Pyrolyse-Feldionisation Massenspektrometrie. PhD thesis, University of Kiel, Institute for Plant Nutrition and Soil Science, pp. 177.

Sorge, C., Schnitzer, M., Schulten, H.-R., 1993. In-source pyrolysis-field ionization mass spectrometry and Curie-point pyrolysis-gas chromatography/mass spectrometry of amino acids in humic substances and soils. Biol. Fert. Soils. 16, 100–110.
Stevenson, F.J., 1986. Cycles of Soil. Carbon, Nitrogen, Phosphorus, Sulphur and Micronutrients. pp. 176–177. John Wiley & Sons, Inc, New York.
Stevenson, F.J., 1994. Organic forms of soil nitrogen. Humus Chemistry, Genesis, Composition, Reactions, John Wiley & Sons, Inc, New York, pp. 59–95.
Stevenson, F.J., 1996. Nitrogen–organic forms. In: Sparks, D.L. (Ed.), Methods of Soil Analysis. Part 3-chemical Methods, Soil Science Society of America, ASA, Madison, Wisconsin, USA, pp. 1185–1200.
Sulçe, S., Palma-Lopez, D., Jacquin, F., Vong, P.C., Guiraud, G., 1996. Study of immobilization and remobilization of nitrogen fertilizer in cultivated soils by hydrolytic fractionation. Europ. J. Soil Sci. 47, 249–255.
Tarkka, M., Hampp, R., 2008. Secondary metabolites of soil streptomycetes in biotic interactions. In: Karlovski, P. (Ed.), Secondary Metabolites in Soil Ecology. Soil Biology 14, Springer Verlag, Berlin, Heidelberg, pp. 107–126.
Taylor, E.B., Williams, M.A., 2010. Microbial protein in soil: influence of extraction method and C amendment on extraction and recovery. Microb. Ecol. 59, 390–399.
Thorn, K.A., Cox, L.G., 2009. N-15 NMR spectra of naturally abundant nitrogen in soil and aquatic natural organic matter samples of the International Humic Substances Society. Org. Geochem. 40, 484–499.
Tsuge, S., Matsubara, H., 1985. High-resolution pyrolysis-gas chromatography of proteins and related materials. J. Anal. App. Pyrolysis. 8, 49–64.
Ubalua, A.O., 2010. Cyanogenic glycosides and the fate of cyanide in soil. Aust. J. Crop Sci. 4, 223–237.
Unkovich, M., Pate, J., McNeill, A., Gibbs, D.J., 2001. Stable Isotope Techniques in the Study of Biological Processes and Functioning of Ecosystems. Kluwer Academic Publishers, Dordrecht.
Vairavamurthy, A., Wang, S., 2002. Organic nitrogen in geomacromolecules: insights on speciation and transformation with K-edge XANES spectroscopy. Environ. Sci. Technol. 36, 3050–3056.
Verity, G.E., Anderson, D.W., 1990. Soil erosion effects on soil quality and yield. Can. J. Soil Sci. 70, 471–484.
Vranova, V., Rejsek, K., Skene, K.R., Formanek, P., 2011. Non-protein amino acids: plant, soil and ecosystem interactions. Plant Soil. 342, 31–48.
Wackernagel, W., 2006. The various sources and the fate of nucleic acids in soils. In: Nannipieri, P., Smalla, K. (Eds.), Soil Biology Volume 8 Nucleic Acids and Proteins in Soil, Springer-Verlag, Berlin, Heidelberg, pp. 117–139.
Walton, J., Fairley, N., 2005. Noise reduction in X-ray photoelectron spectromicroscopy by a singular value decomposition sorting procedure. J. Electron. Spectrosc. Relat. Phenom. 148, 29–40.
Wang, X., Emmett, M.R., Marshall, A.G., 2010. Liquid chromatography electrospray ionization Fourier transform ion cyclotron resonance mass spectrometric characterization of N-linked glycans and glycopeptides. Anal. Chem. 82, 6542–6548.
Warembourg, F.R., 1993. Nitrogen fixation in soil and plant systems. In: Knowles, R., Blackburn, T.H. (Eds.), Nitrogen Isotope Techniques, Academic Press, Inc., San Diego, pp. 127–156.
Warren, C.R., 2008. Rapid and sensitive quantification of amino acids in soil extracts by capillary electrophoresis with laser-induced fluorescence. Soil Biol. Biochem. 40, 916–923.
Wessels, J., 1997. Hydrophobins: proteins that change the nature of a fungal surface. Adv. Microb. Physiol. 38, 1–45.

Wichern, F., Mayer, J., Joergensen, R.G., Müller, T., 2007a. Release of C and N from roots of peas and oats and their availability to soil microorganisms. Soil Biol. Biochem. 39, 2829–2839.

Wichern, F., Mayer, J., Joergensen, R.G., Müller, T., 2007b. Rhizodeposition of C and N in peas and oats after ^{13}C-^{15}N double labelling under field conditions. Soil Biol. Biochem. 39, 2527–2537.

Wichern, F., Eberhardt, E., Mayer, J., Joergensen, R.G., Müller, T., 2008. Nitrogen rhizodeposition in agricultural crops: methods, estimates and future prospects. Soil Biol. Biochem. 40, 30–48.

Winterholler, B., Hoppe, P., Foley, S., Andrea, M.O., 2008. Sulfur isotope ratio measurements of individual sulfate particles by NanoSIMS. Int. J. Mass. Spectrom. 272, 63–77.

Xia, K., Weesner, F., Bleam, W.F., Bloom, P.R., Skyllberg, U.L., Helmke, P.A., 1998. XANES studies of oxidation states of sulfur in aquatic and soil humic substances. Soil Sci. Soc. Am. J. 62, 1240–1246.

Yasmin, K., Cadisch, G., Baggs, E.M., 2006. Comparing ^{15}N-labelling techniques for enriching above- and below-ground components of the plant-soil system. Soil Biol. Biochem. 38, 397–400.

Yasmin, K., Cadisch, G., Baggs, E.M., 2010. The significance of below-ground fractions when considering N and C partitioning within chickpea (*Cicer arietinum* L.). Plant Soil. 327, 247–259.

Ye, J., Singh, A., Ward, O.P., 2004. Biodegradation of N-containing xenobiotics. In: Singh, A., Ward, O.P. (Eds.), Soil Biology vol. 2, Biodegradation and Bioremediation, Springer-Verlag, Berlin, Heidelberg, pp. 149–173.

Yeh, J.J., Lindau, L., 1985. Atomic subshell photoionization cross sections and asymmetry parameters: $1 \leq Z \geq 103$. Data Nucl. Data Tables. 32, 1–155.

Yeomans, J.C., Bremner, J.M., 1991. Carbon and nitrogen analysis of soils by automated combustion techniques. Comm. Soil Sci. Plant Anal. 22, 843–850.

Zang, X., Hatcher, P.G., 2002. A Py-GC-MS and NMR spectroscopy study of organic nitrogen in Mangrove Lake sediments. Org. Geochem. 33, 201–211.

Zhang, X., Amelung, W., 1996. Gas chromatographic determination of muramic acid, glucosamine, mannosamine, and galactosamine in soils. Soil Biol. Biochem. 28, 1201–1206.

Zhang, X., He, H., Amelung, W., 2007. A GC/MS method for the assessment of ^{15}N and ^{13}C incorporation into soil amino acid enantiomers. Soil Biol. Biochem. 39, 2785–2796.

Zhang, Q.C., Wang, G.-H., Xie, W.-X., 2006. Soil organic N forms and N supply as affected by fertilization under intensive rice cropping system. Pedosphere. 16, 345–353.

Zou, C.-S., Mo, M.-H., Gu, Y.-Q., Zhou, J.-P., Zhang, K.-Q., 2007. Possible contributions of volatile-producing bacteria to soil fungistasis. Soil Biol. Biochem. 39, 2371–2379.

Zubavichus, Y., Zharnikov, M., Yang, Y., Fuchs, O., Heske, C., Umbach, E., Tzvetkov, G., Netzer, F.P., Grunze, M., 2005. Surface chemistry of ultrathin films of histidine on gold as probed by high-resolution synchrotron photoemission. J. Phys. Chem. B. 109, 884–891.

zu Schweinsberg-Mickan, M.S., Joergensen, R.G., Müller, T., 2010. Fate of ^{13}C- and ^{15}N-labelled rhizodeposition of Lolium perenne as function of the distance to the root surface. Soil Biol. Biochem. 42, 910–918.



CHAPTER THREE

The Role of Nitrate in Human Health

Nathan S. Bryan[*,**], **Hans van Grinsven**[†]
*Brown Foundation Institute of Molecular Medicine, Department of Integrative Biology and Pharmacology, The University of Texas Health Science Center, Houston, TX, USA
†PBL Netherlands Environmental Assessment Agency, Department of Water, Agriculture and Food, Bilthoven, The Netherlands
**Corresponding author: E-mail: Nathan.Bryan@uth.tmc.edu

Contents

Abstract

The enrichment of the biosphere with reactive nitrogen from anthropogenic origin, in combination with increased consumption of vegetables and (preserved) animal products, has led to increased intake by humans of nitrite and nitrate. Nitrate and nitrate-forming salts are among the key components of fertilizers and the increased dependency of farming practices on such fertilizers over several decades has led to increasing levels of human exposure. This arises from consumption of crops and from nitrate-contaminated drinking water due to agricultural land runoff. For years, people have viewed dietary sources of nitrate as harmful to humans causing methemoglobinemia and cancers. However, methemoglobinemia is rare and evidence suggests a relation with infective enteritis rather than with nitrate alone. Also, epidemiological evidence for an association between cancers of the digestive tract and nitrate intake is inconclusive in terms of increased risks of cancer although the International Agency for Research on Cancer concluded "ingested nitrite or nitrate under conditions that result in endogenous nitrosation is probably carcinogenic to humans (Group 2A)". The discovery of the nitric oxide pathway in the early 1980s revealed that nitrate is produced endogenously in the body changing our perception of nitrate safety. Recently benefits of dietary sources of nitrate for cardiovascular health and protection against infections

Advances in Agronomy, Volume 119
ISSN 0065-2113, http://dx.doi.org/10.1016/B978-0-12-407247-3.00003-2

have been unveiled, calling for an assessment of the risk and benefits associated with nitrate in our food and water supply. The scope of this article is to review the current state of the science on nitrate in human health and disease.

1. INTRODUCTION

Since 1950, global fertilizer use per hectare has increased by a factor of five and meat consumption has doubled (Erisman et al., 2008). Erisman et al. attribute the presence of about half of the current global population to the availability to nitrogen fertilizer. The doubling of meat consumption (Smil, 2002) and fertilizer intensities (Dobermann and Cassman, 2005) in the developed world has also doubled the human intake of nitrogen through food; now protein intake is almost twice the intake recommended by World Health Organization (WHO) (FAO, 2009). The increase of fertilizer intensity has been most pronounced for high-value vegetable crops, increasing nitrate levels and human intake for some vegetables (lettuce, spinach) over the past century up to fourfold.

Despite historical use of nitrate and nitrite as medicinal agents, the fact that these anions are produced naturally in the body from the oxidation of nitric oxide (NO), and recent demonstration of physiological roles for nitrate and nitrite in vascular and immune function, public perception is that these are harmful substances in our food and water supply (L'Hirondel, 2001; Lundberg et al., 2009). Ironically, most people would not argue that a diet rich in fruits and vegetables is healthy. In an assessment of nitrate, nitrite and N-nitroso compounds in the human diet, it was concluded that vegetables contribute over 85% of the daily dietary intake of nitrate and that endogenous synthesis is an important contributor to human's overall exposure of nitrate (Gangolli et al., 1994). Hord et al. (2009) estimated that approximately 80% of dietary nitrate is derived from vegetable consumption. Since approximately 80% of dietary nitrate is derived from vegetable consumption, the primary source of exposure to nitrate by humans is through eating vegetables. Recent reports have shown that <5% of the ingested nitrite and nitrate are derived from cured meat sources with the remainder coming from vegetables and saliva (Archer, 2002; Cassens, 1997; Milkowski et al. 2010). Relative intake of nitrate from drinking water in Europe typically ranges from 10 to 20% but may amount to 30–40% Asia and Africa in view of lower intake from food sources (Fig. 3.1; Santamaria, 2006). However, some populations, such as those living in rural agricultural areas using shallow wells, may have much higher exposure to nitrate from drinking water. The

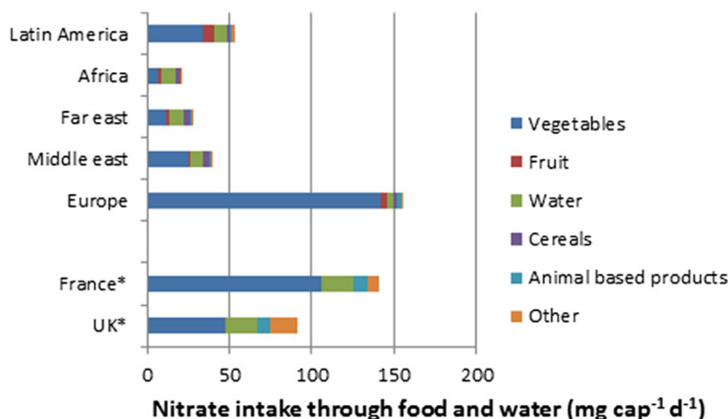


Figure 3.1 Relative intake contribution for sources of nitrate in world regions and the UK and France. *(Santamaria, 2006; European Food Safety Authority. Nitrates in vegetables.* EFSA Journal *2008, 689:1–79).* For color version of this figure, the reader is referred to the online version of this book.

primary sources of nitrate that contaminate groundwater and surface water are fertilizers and manures applied to soil, including waste from farm animals, but locally human waste from septic tanks and waste water treatment systems (discharge) can also be a dominant source (Harter, 2009). In the Southwestern U.S. and other agricultural areas, inorganic fertilizer and animal manure are the most common nitrate source while urban areas without proper sewer containment contribute to the nitrate levels in groundwater. Further, ammonia will volatilize from manures and fertilizers to be transported through the atmosphere to be deposited and nitrified by microbial action, and to become an additional source of nitrate pollution of waters.

Regulatory standards and monitoring measures for nitrate in water supply and food sources have been established due to potential toxicity of nitrate at high levels and unknown effects from chronic exposure. The two main concerns are methemoglobinemia and potential for harmful nitrosation of low-molecular-weight amines that can occur in the stomach forming N-nitrosamines, some of which have been shown to cause a wide range of tumors in more than 40 animal species (Tricker and Preussmann, 1991). With nitrate at extremely high levels, acute toxicity can arise such as methemoglobinemia (Marcus and Joffe, 1949). However, in moderation, emerging evidence indicates that nitrate can play an important and beneficial role in human physiology (Lundberg et al., 2008). Paraphrasing Paracelsus, "the dose makes the poison;" however, with respect to nitrate, one could add the

duration, location and context of exposure. The purpose of this review is to highlight the risk–benefit evaluation of nitrate in the proper context of human nutrition and how this may be affected by modern fertilizer practices.

Intake of excess nitrate and nitrite can be, in specific contexts, associated with increased risk of negative health outcomes as mentioned above. Dietary reference intake (DRI) categories are set by the Food and Nutrition Board of the National Academy of Sciences for essential nutrients in order to clearly define, where possible, the contexts in which intakes are deficient, safe or potentially excessive. These DRI categories include the Recommended Dietary Allowance, Adequate Intake, Tolerable Upper Level Intake and Estimated Average Intake (Otten et al., 2006). The process of setting DRIs for nutrients considers a broad range of physiological factors, including nutritional status and potential toxicities. It is important to note that nitrate exposure limits are set on the basis of nitrate in drinking water, the route of exposure associated with nitrate toxicities, although accidental toxic exposures of nitrate and nitrite have occurred through other means (2002).

The U.S. Environmental Protection Agency (EPA) maximum contaminant level (MCL) for nitrate in drinking water of 10 mg/L nitrate–nitrogen (nitrate–N) (equivalent to 45 mg/L as nitrate) and the WHO guideline and European Union (EU) Council Directive 98/83/EC of 50 mg/L as nitrate (equivalent to 11 mg/L as nitrate–N) were promulgated to protect against methemoglobinemia or "blue baby syndrome," to which infants are especially susceptible (2004). The U.S. and the E.U. MCL for nitrate were promulgated (US: 1962–EU: 1980) without scientific explanation. In 1993, the WHO recognized that the epidemiological evidence for an association between dietary nitrate and cancer was not sufficient for action and that the guideline value should be established solely to prevent methemoglobinemia (WHO, 1998). As a result, the U.S. EPA limits human exposure to inorganic nitrate to >10 mg/L or 10 ppm nitrate–N, and nitrite to 1 ppm nitrite–N (Agency, 1991). The Joint Food and Agricultural Organization/WHO has set the Acceptable Daily Intake (ADI) for the nitrate ion at 3.7 mg/kg body weight and for the nitrite ion at 0.06 mg/kg body weight (Authority, 2008). This translates into an exposure limit of 222 mg nitrate and 3.6 mg nitrite for a 60 kg adult. Likewise, EPA has set a Reference Dose for nitrate of 1.6 mg nitrate–N/kg body weight per day (equivalent to about 7 mg nitrate ion/kg body weight per day). The regulatory level is usually met for public water supplies, which are routinely monitored. In the EU, noncompliance to the nitrate or nitrite standards in large public supplies is reported regularly but rarely exceeds 4% of the sample population (Fig. 3.2).

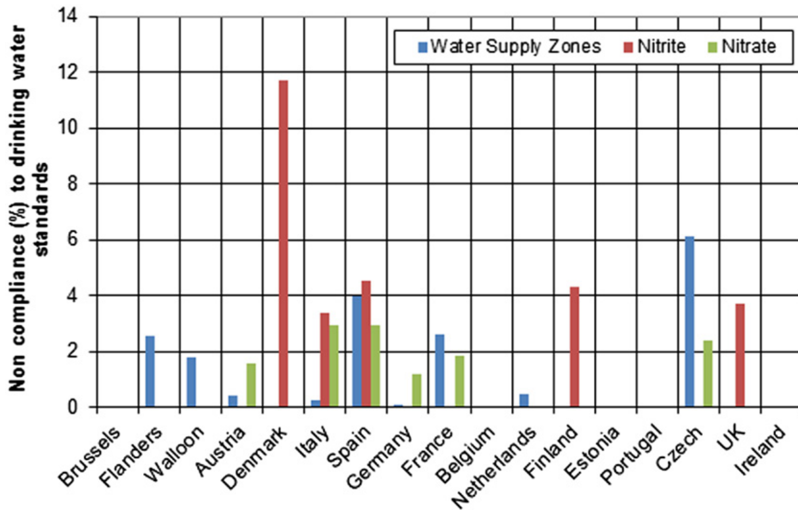
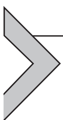


Figure 3.2 Noncompliance for EU legal standards for nitrite and nitrate in drinking water (exceedance in more than 1% of all samples taken) between 2000 and 2004 and the associated proportion of Water Supply Zones (WSZ). *European Commission: the quality of drinking water in the European Union, 2002–2004. Synthesis report for EU Directives 80/778/EEC and 98/83/EC; 2007. [*http://circa.europa.eu/Public/irc/env/drinking_water_rev/library?l=/drinking_synthesis/report_2002-2004pdf/_EN_1.0_&a=d*].* For color version of this figure, the reader is referred to the online version of this book.

Much less is known about private wells, which in the United States are usually required to be tested only when the well is constructed or when the property is sold. Due to their very high solubility, nitrate can enter groundwater. Tentative estimates for Western Europe and the United States are that 2–3% of the population is potentially exposed to drinking water exceeding 50 mg nitrate/L (van Grinsven et al., 2006).



2. IMPACTS ON HUMAN HEALTH

2.1. Nitrate Metabolism in Humans

The risk–benefit spectrum from nitrate may very well depend on the specific metabolism and the presence of other components that may be concomitantly ingested. The stepwise reduction to nitrite and NO may account for the benefits while pathways leading to nitrosation of low-molecular-weight amines or amides may account for the health risks of nitrate exposure. Understanding and affecting those pathways will certainly help in mitigating the risks. The discussion below will describe these two pathways.

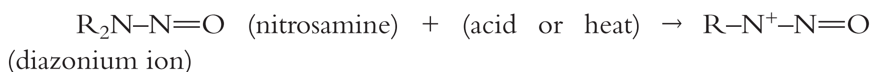
The exposure to nitrate by humans is dependent on an individual's intake of vegetables and the local concentration of nitrate in drinking water as well as the total amount of NO produced in the body. Nitrate ingested from the diet is rapidly absorbed in the small intestine, mixes with the endogenous nitrate from oxidation of NO and is readily distributed throughout the body (Walker, 1996). About 25% of an oral nitrate load is concentrated and excreted by salivary glands (Spiegelhalder et al., 1976), so that salivary nitrate concentration is approximately 10 times higher than plasma nitrate. Approximately 20% of salivary nitrate is reduced to nitrite in the mouth by facultative anaerobic bacteria which are found on the surface of the tongue (Bjorne et al., 2004; Doel et al., 2005; Lundberg et al., 2004) resulting in about a 5% reduction of total ingested nitrate to nitrite. As a result, nitrate ingestion is the main source of nitrite exposure. This biochemistry has been demonstrated stoichiometrically in mice fed 20 times higher nitrate than nitrite (Bryan et al., 2007). Humans, unlike prokaryotes, are thought to lack the enzymatic machinery to reduce nitrate back to nitrite. However, recent discoveries reveal a functional mammalian nitrate reductase (Jansson et al., 2008). Nitrate, when consumed orally, reaches a peak plasma concentration in about 1 h (McKnight et al., 1997). The half-life of plasma nitrate is approximately 5 h (McKnight et al., 1997). Since nitrate is a relatively small anion and is not protein-bound, its pharmacokinetics and half-life suggest that it is reabsorbed in the renal tubules. Nitrate is excreted in the urine directly or after conversion to urea (Green et al., 1981). Clearance of nitrate from blood to urine approximates 20 mL/min in adults (Wennmalm et al., 1993) indicating considerable renal tubular reabsorption of the ion. It is estimated that 96% of the filtered nitrite and nitrate is reabsorbed in the renal tubules (Rahma et al., 2001). Other studies in dogs suggest that approximately 80% of filtered nitrate is reabsorbed (Godfrey and Majid, 1998). The high concentration of nitrate in saliva, continuous production from NO and the reabsorption from renal tubules strongly suggest that nitrate has a definite role in normal human physiology and is not just an unwanted toxin.

Nitrate itself is generally considered to be harmless at low concentrations. Nitrite, on the other hand, is reactive especially in the acid environment of the stomach where it can nitrosate other molecules including proteins, amines and amides. Nitrite is occasionally found in the environment but most human exposure occurs through ingested nitrate that can be broken down to nitrite by the reaction with commensal bacteria often

found in saliva (Lundberg et al., 2004). The specter of a cancer risk posed by nitrite and nitrate is invariably accompanied by concern about exposure to preformed N-nitrosamines or N-nitrosamines formed in the stomach from ingesting foods enriched in nitrite and nitrate. This is because some low-molecular-weight amines can be converted (nitrosated) to their carcinogenic N-nitroso derivatives by reaction with nitrite (see reaction below) (Spiegelhalder et al., 1976). Nitrosamines are a class of chemical compounds that were first described in the chemical literature over 100 years ago, but not until 1956 did they receive much attention. In that year, two British scientists, John Barnes and Peter Magee, reported that dimethylnitrosamine produced liver tumors in rats (Magee and Barnes, 1956). This discovery was made during a routine screening of chemicals that were being proposed for use as solvents in the dry cleaning industry. Magee and Barnes' landmark discovery caused scientists around the world to investigate the carcinogenic properties of other nitrosamines. Approximately 300 of these compounds have been tested, and 90% of them have been found to be carcinogenic in a wide variety of experimental animals. Most nitrosamines are mutagens and a number of them are transplacental carcinogens. Most are organ-specific. For instance, dimethylnitrosamine causes liver cancer in experimental animals, whereas some of the tobacco-specific nitrosamines cause lung cancer. Since nitrosamines are metabolized the same in human and animal tissues, it seems highly likely that humans are susceptible to the carcinogenic properties of nitrosamines. Amines can occur commonly, and nitrite is derived from nitrate. Nitrosamines can occur because their chemical precursors—amines and nitrosating agents—occur commonly, and the chemical reaction for nitrosamine formation is quite facile. The reactions below illustrate the nitrosation reactions:


$$R_2NH \text{ (amines)} + NaNO_2 \text{ (sodium nitrite)} \rightarrow R_2N{-}N{=}O \text{ (nitrosamine)}$$

In the presence of acid (such as in the stomach) or heat (such as via cooking), nitrosamines are converted to diazonium ions.


$$R_2N{-}N{=}O \text{ (nitrosamine)} + \text{(acid or heat)} \rightarrow R{-}N^+{-}N{=}O \text{ (diazonium ion)}$$

Certain nitrosamines such as dimethylnitrosamine and N-nitrosopyrrolidine form carbocations that react with biological nucleophiles (such as DNA or an enzyme) in the cell.

R–N^+–N═O (diazonium ion) → R^+ (carbocation) + N_2 (leaving group) + :Nu (biological nucleophiles) → R–Nu

If this reaction occurs at a crucial site in a biomolecule, it can disrupt normal cell function leading to cancer or cell death.

About 1970, it was discovered that ascorbic acid very potently inhibits nitrosamine formation (Mirvish, 1975). Another antioxidant, alpha-tocopherol (vitamin E), has also been shown to inhibit nitrosamine formation (Mirvish, 1996). Ascorbic acid, erythorbic acid, and alpha-tocopherol inhibit nitrosamine formation due to their oxidation–reduction properties. For example, when ascorbic acid is oxidized to dehydroascorbic acid, nitrous anhydride, a potent nitrosating agent formed from sodium nitrite, is reduced to NO, which is not a nitrosating agent. Most vegetables which are enriched in nitrate are also rich in antioxidants such as vitamins C and E that can act to prevent the unwanted nitrosation chemistry. Nitrate in drinking water, on the other hand, has no such protective molecules present and may be cause for concern. Controlling the metabolic fate of nitrate and nitrite away from amine nitrosation and toward reduction to NO may provide a strategy to promote health benefits while mitigating the health risks. Adverse health effects may be the result of a complex interaction of the amount of nitrate ingested, the concomitant ingestion of nitrosation cofactors and precursors, and specific medical conditions that increase nitrosation such as chronic inflammation.

2.2. Cardiovascular Effects of Nitrate

Most of the emerging science on the benefits of inorganic nitrate is in the realm of NO biochemistry, which has a very large number of effects which are thought to be beneficial in mammals. NO is the most important molecule in regulating blood pressure and maintaining vascular homeostasis. It rapidly reacts with oxyhemoproteins, such as oxyhemoglobin to form nitrate and methemoglobin (Yoshida and Kasama, 1987). As a result, nitrate is formed within the body as a result of NO production. In 1994, two groups independently presented evidence for generation of NO in the stomach resulting from the acidic reduction of inorganic nitrite (Benjamin et al., 1994; Lundberg et al., 1994) demonstrating a recycling pathway whereby nitrate could be reduced back to NO. Benjamin et al. demonstrated that the antibacterial effects of acid alone was markedly enhanced by addition of nitrite which is present in saliva, whereas Lundberg et al. could measure high levels of NO in expelled air from the stomach in humans. These levels

were abolished after pretreatment with a proton-pump inhibitor and markedly increased after ingestion of nitrate, showing the importance of both luminal pH and the conversion of nitrate to nitrite for stomach NO generation. These were the first reports of nitric oxide synthase (NOS)-independent formation of NO *in vivo*. In the classical NOS pathway, NO is formed by oxidation of the guanidino-N of L-arginine with molecular oxygen as the electron acceptor (Moncada and Higgs, 1993). This complex reaction is catalyzed by specific heme-containing enzymes: the NOSs, and several cofactors. The alternative pathway was fundamentally different; instead of L-arginine, it used the simple inorganic anions nitrate (NO_3^-) and nitrite (NO_2^-) as substrates in a stepwise reduction process that did not require NOS or multiple cofactors. The biochemical pathway and biological effects of nitrate reduction to nitrite and further on to NO in the gastrointestinal tract have now been further characterized (Lundberg et al., 2004). Oral commensal bacteria are essential for the first step in the nitrate–nitrite–NO pathway since they are responsible for the reduction of the higher nitrogen oxide nitrate to form nitrite. It was known from the literature that the salivary glands extract nitrate from plasma but the reason for this active process was not explained. Oral facultative anaerobic bacteria residing mainly in the crypts of the tongue then reduce nitrate to nitrite by the action of nitrate reductase enzymes (Duncan et al., 1995; Spiegelhalder et al., 1976). These bacteria use nitrate as an alternative electron acceptor to gain adenosine triphosphate in the absence of oxygen. This relatively effective bacterial nitrate reduction results in salivary levels of nitrite that are 1000-fold higher than those found in plasma (Lundberg and Govoni, 2004). When nitrite-rich saliva meets the acidic gastric juice, nitrite (pKa 3.6) is protonated to form nitrous acid (HNO_2), which then decomposes to NO and a variety of other nitrogen oxides (Benjamin et al., 1994; Lundberg et al., 1994). It is now established that oral commensal bacteria are pivotal in gastric NO formation, and gastric NO levels are consistently low in animals reared under complete germ-free conditions (Sobko et al., 2004). If the oral bacteria are selectively removed with an antiseptic mouthwash, the gastric NO levels decrease drastically (Petersson, 2008). This NO, generated as a result of nitrate, promotes a number of beneficial health effects. NO, along with prostaglandins, is known to modulate a number of mechanisms involved from increasing gastric blood flow and mucus production to regulation of the epithelial barrier. Increased dietary nitrate and the application of nitrite have both been shown to increase gastric blood flow and gastric mucosal thickness in a NO-dependent manner (Bjorne et al., 2004; Petersson et al.,

2007, 2009). This has been shown to confer protection against ulceration induced by nonsteroidal anti-inflammatory drugs (NSAIDs) (Jansson et al., 2007). Thus, when endogenous production of one of the major determinants of gastric protection, prostaglandins, is depressed by cyclo-oxygenase inhibition by NSAIDs, the integrity of the gastric mucosa can be preserved by nitrate.

It is known that a diet rich in fruits and vegetables has a positive influence on blood pressure (Appel et al., 1997). It has been speculated that the blood-pressure-lowering effects of certain diets may be due to the nitrate content (Lundberg et al., 2006). In fact, a recent food sample survey indicated that a Dietary Approach to Stop Hypertension (DASH) diet exceeds the ADI for nitrate by >500% and may account for the modest blood pressure effects (Hord et al., 2009). Webb et al. (2008) demonstrated a significant decrease in systolic and diastolic blood pressure within 3 h of ingestion of 0.5 L of beetroot juice (a rich source of nitrate). These data were consistent with earlier results from Lundberg's group showing a significant blood-pressure-lowering effect from 3 days supplementation with sodium nitrate (Larsen et al., 2006). The maximal effect in Webb's study coincided with peak plasma levels of nitrite and was abolished if the study participants did not swallow their saliva suggesting that bacterial reduction of nitrate to nitrite and nitrite entering the acid stomach to produce NO is necessary in order for it to have biological activity. This concept was confirmed in a study showing treating with antimicrobial mouthwashes is sufficient to abolish any beneficial effect in animals given supplementary nitrate (Petersson et al., 2009). The stepwise reduction of nitrate to nitrite to NO is, by necessity, an inefficient process by which each step yields a 3-log lower concentration of product than substrate (Jansson et al., 2008). Although the reduction efficacy from nitrate to NO is very inefficient, it is clear that a diet rich in nitrate can provide a source of bioactive NO due to this human nitrogen cycle. This pathway is illustrated in Fig. 3.3.

Recent data are also emerging implicating nitrate and nitrite on endothelial function. NO synthesized by endothelial nitric oxide synthase (eNOS) plays a key role in vascular homeostasis by maintaining vessels in their relaxed state. Experimental and clinical studies provide evidence that defects of endothelial NO function, referred to as endothelial dysfunction, not only is associated with all major cardiovascular risk factors such as hyperlipidemia, diabetes, hypertension, smoking and severity of atherosclerosis, but also has a profound predictive value for future atherosclerotic disease progression (Bugiardini et al., 2004; Halcox et al., 2002; Lerman

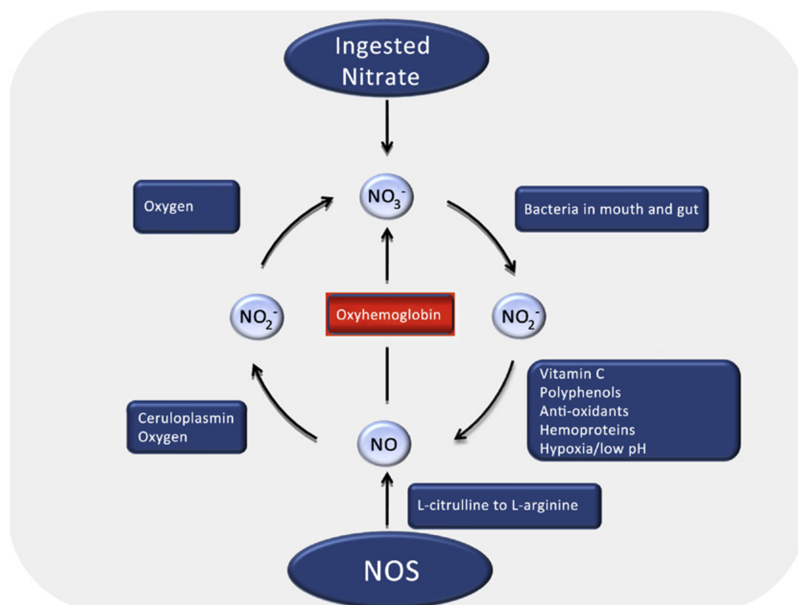


Figure 3.3 The human nitrogen cycle: dietary nitrate is rapidly absorbed into the bloodstream through the proximal gut, where it mixes with endogenous nitrate from the NOS/NO pathway. A large portion of nitrate is taken up by the salivary glands, secreted with saliva and reduced to nitrite by symbiotic bacteria in the oral cavity. Salivary-derived nitrite is further reduced to NO and other biologically active nitrogen oxides in the acidic stomach. Remaining nitrite is rapidly absorbed and accumulates in tissues, where it serves to regulate cellular functions via reduction to NO or possibly by direct reactions with protein and lipids. NO and nitrite are ultimately oxidized to nitrate, which again enters the enterosalivary circulation or metabolized and excreted in urine, sweat and feces. For color version of this figure, the reader is referred to the online version of this book.

and Zeiher, 2005; Schachinger et al., 2000). Increasing numbers of risk factors results in a stepwise reduction in plasma nitrite, a surrogate for eNOS activity (Kleinbongard et al., 2006). In conventional and eNOS knockout mice, dietary nitrate and nitrite supplementation restores NO homeostasis and protects against ischemia reperfusion injury (Bryan et al., 2007, 2008). Nitrite supplementation ameliorates the microvascular inflammation and endothelial dysfunction in mice subject to a high-cholesterol diet (Stokes et al., 2009). Research has also shown a biological activity of nitrate on platelet function (Webb et al., 2008). The role of platelet adhesion, activation, and aggregation in atherosclerosis and thrombosis is well known (Davi and Patrono, 2007). Platelet adhesion and aggregation are inhibited

by NO, either from within the platelet itself or produced by the vascular endothelium (Radomski et al., 1987, 1990). Dietary supplementation with either potassium nitrate in the range 0.5–2 mmol (Richardson et al., 2002) or using beetroot juice (Webb et al., 2008) results in a significant inhibition of platelet aggregation. In fact, an all-natural dietary supplement containing nitrite and nitrate has been shown to improve cardiovascular risks in 30 days (Zand et al., 2011).

Exercise performance is a direct reflection of our body's ability to accommodate increased blood flow to working muscle. Endothelial production of NO provides vessel dilation in response to exercise. Plasma nitrite levels increase in response to exercise in healthy individuals, whereby in aged patients with endothelial dysfunction, there is no increase in nitrite from exercise (Lauer et al., 2008). Nitrite has also been shown to predict exercise capacity in humans (Rassaf et al., 2007). Short-term (3-day) dietary supplementation with sodium nitrate results in improved muscular efficiency and a reduction in oxygen consumption during submaximal exercise in healthy subjects and enhance tolerance to high-intensity exercise in humans (Bailey et al., 2009; Larsen et al., 2007). The amount of nitrate used in these studies was 8.5 mg/kg for the Larsen study and 6.8 mg/kg for the Bailey study, exceeding the ADI for nitrate in both studies.

Nitrate is also found naturally in mother's breast milk demonstrating that it is not just a contaminant but in the right context, an essential nutrient provided to the nursing infant. Human breast milk is recommended to serve as the exclusive food for the first 6 months of life and continue, along with safe, nutritious complementary foods, up to 2 years (Gartner et al., 2005; Heinig, 1998). Breast milk is nature's most perfect food. In fact, the U.S. Centers for Disease Controls in 2010 acknowledged "Breast milk is widely acknowledged as the most complete form of nutrition for infants, with a range of benefits for infants' health, growth, immunity and development". Breast milk is a unique nutritional source for infants that cannot adequately be replaced by any other food, including infant formula. Human milk is known to confer significant nutritional and immunological benefits for the infant (Hoddinott et al., 2008; Ip et al., 2007; James and Lessen, 2009). Several research studies have previously demonstrated relatively high concentrations of nitrite and nitrate in human breast milk. Ohta et al. (2004) found high concentrations of nitrite and nitrate (166–1246 μM or 10–70 mg/L) in the breast milk of Japanese mothers from days 1–8. Cekmen et al. (2004) found high concentrations >50 μM of nitrite in breast milk of healthy mothers that was reduced in pre-eclampsia patients. The origins of nitrate

and nitrite in human milk are not known. Maternal nitrate and nitrite intakes are not reflected in nitrate and nitrite composition of human milk (Greer and Shannon, 2005). The data supporting this conclusion are sparse. One study published on this topic demonstrated that women who consumed water with a nitrate concentrations up to 100 mg/L did not produce milk with elevated nitrate levels (Dusdieker et al., 1996). Hord et al. (2011) recently demonstrated that nitrite and nitrate are found at high levels in human breast milk and the ratio of these anions change over time to meet the changing metabolic demands of the infant. The presence of nitrate and nitrite in human milk provides evidence for a physiologic benefit for the protection of the gastrointestinal tract in the neonate. Based on exposure rates of infants from breast milk nitrite and nitrate, the most reasonable conclusion that can be made is that humans are adapted to receive dietary nitrite and nitrate from birth and, therefore, may not pose significant risks at levels naturally found in certain foods (Hord et al., 2011).

2.3. Nitrate Effects on Host Defense

Dietary nitrate also plays a very important role in the host defense of mammals through the conversion to nitrite and NO, both precursors for potent antimicrobial substances. Reduction of nitrate to nitrite in the mouth provides a first site for exerting protective effects. Nitrite produced on the dorsal surface of the tongue by bacterial reduction is further reduced to NO under acidic conditions (Duncan et al., 1995) and results in the destruction of acid-producing organisms. NO from acidic reduction of nitrite, along with other reactive nitrogen species, is produced in the stomach following a nitrate-rich meal in quantities far greater than that required to produce vasodilatation suggesting a role other than modulation of gastric blood flow (McKnight et al., 1997). A number of important human pathogens (*Candida albicans*, *Escherichia coli* H7:O157, *Salmonella*, *Shigella*) are resistant to a low pH found in the stomach that enable them to survive passage through the human stomach (Duncan et al., 1997). The addition of nitrite in concentrations found in human saliva results in much more effective killing of these pathogens than in acid alone (Benjamin et al., 1994; Dykhuizen et al., 1996). Indeed even *Helicobacter pylori*, a bacteria well adapted to colonize the human stomach, is susceptible to acidified nitrite (Dykhuizen et al., 1998). The acidification of nitrite derived from dietary nitrate appears to play a pivotal role in protection against ingested pathogens. Further support for this can be found in the reduced levels of post-prandial salivary nitrite found

in subjects treated with the broad-spectrum antibiotic amoxicillin (Dougall et al., 1995). Patients on broad-spectrum antibiotics are at increased risk of opportunistic gastrointestinal tract infections from species such as *C. albicans* and *Clostridium difficile*. It may be that the killing of commensal bacteria by the overuse of antibiotics is responsible disruption of salivary nitrate reduction and subsequent suppression of salivary nitrite that allows these organisms to establish themselves in the gastrointestinal tract.

It appears that nature has also designed an effective strategy for wound healing. Both man and animals will lick their wounds upon sustaining injury, an action which promotes wound healing (Bodner, 1991). This effect is likely to be due in part to saliva's antimicrobicidal properties, which can substantially reduce bacterial contamination of the wound (Hart and Powell, 1990). Licking of human skin results in production of NO as salivary nitrite is reduced on the acidic skin surface (Benjamin et al., 1997). A number of common skin pathogens are effectively killed by acidified nitrite (Weller et al., 2001). It seems likely that the beneficial effect of saliva on wound healing is due in part to acidification of nitrite that results from dietary sources of nitrate.

2.4. Nitrate and Methemoglobinemia or (Blue Baby Syndrome)

The most recent health benefits of nitrate are still shadowed by the more well-known health risks that dictated regulation. Formula-fed infants younger than 6 months of age may be exposed to excess nitrate in bacterially contaminated well water that reduces nitrate to nitrite (Johnson and Kross, 1990). Infants consuming excess nitrite experience blue baby syndrome due to nitrite-mediated oxidation of ferric (Fe^{2+}) iron in oxyhemoglobin that leads to hypoxia and cyanosis and the resulting blue color (Fan and Steinberg, 1996; McKnight et al., 1999). Nitrate itself is unreactive. Under physiological conditions, methemoglobin reduction is accomplished primarily by red cell reduced nicotinamide adenine dinucleotide reductase so efficiently that there is <1% of methemoglobin in the circulating blood of healthy adults. Infants younger than 6 months are particularly susceptible to nitrate-induced methemoglobinemia because of their low stomach acid production, large numbers of nitrite-reducing bacteria, the relatively easy oxidation of fetal hemoglobin, and immaturity of the methemoglobin reductase system (Dusdieker et al., 1994; Kross et al., 1992). As such, an American Academy of Pediatrics consensus panel concluded that all prenatal and well-infant visits should include questions

about the home water supply; if the water source is a private well, the water should be tested for nitrate (Greer and Shannon, 2005). The panel concluded that infants fed commercially prepared infant foods are generally not at risk of nitrate poisoning, but that home-prepared infant foods from vegetables (e.g. spinach, beets, green beans, squash, carrots) should be avoided until infants are 3 months or older. Breast-fed infants are not at risk of excessive nitrate exposure from mothers, who ingest water with high-nitrate content (up to 100 ppm nitrate nitrogen) as nitrate concentration is thought not to increase significantly in the breast milk under these circumstances (Greer and Shannon, 2005). However, breast milk does contain nitrite and nitrate at levels that can still exceed the ADI (Hord et al., 2011).

It is noteworthy that the few human nitrate and nitrite exposure studies, including children and adults, have not produced methemoglobinemia. Infants exposed to 175–700 mg nitrate per day did not experience methemoglobin levels above 7.5%, suggesting that nitrate alone is not causative for methemoglobinemia (Cornblath and Hartmann, 1948). However, some reports of methemoglobinemia were observed in infants with nitrate-contaminated well water with as little as 22–27 mg/L (Knobeloch et al., 2000). A more recent randomized three-way crossover study exposed healthy volunteer adults to single doses of sodium nitrite that ranged from 150 to 190 mg per volunteer to 290–380 mg per volunteer (Kortboyer et al., 1997). Observed methemoglobin concentrations were 12.2% for volunteers receiving the higher dose of nitrite ion and 4.5% for those receiving the lower dose. Recent nitrite infusion studies of up to 110 μg/kg body wt/min for 5 min induced methemoglobin concentrations of only 3.2% (Dejam et al., 2007). These data have led scientists to propose alternative explanations for the observed methemoglobinemia in infants, including gastroenteritis and associated upregulation of inducible isoform of nitric oxide synthase overproduction of NO induced by bacteria-contaminated water (L'Hirondel et al., 2006; Powlson et al., 2008). These studies call into question the mechanistic basis for exposure regulations for nitrate and nitrite. At best, these findings highlight a serious, but context-specific, risk associated with nitrite and nitrate overexposure in infants. Experts have questioned the veracity of the evidence supporting the hypothesis that nitrates and nitrites are toxic for healthy postinfant populations (Authority, 2008; L'Hirondel, 2001; McKnight et al., 1999). There may, however, be at-risk populations such as infants <3 months that are more susceptible to methemoglobinemia at lower levels of nitrate exposure than others.

2.5. Chronic Effects of Nitrate: Cancers and Reproductive Outcomes

NO and NOS are known to be involved in cancer-related events (angiogenesis, apoptosis, cell cycle, invasion, and metastasis) and are linked to increased oxidative stress and DNA damage (Ying and Hofseth, 2007). There is evidence that dietary patterns, foods, nutrients, and other dietary constituents are closely associated with the risk for several types of cancer. And while it is not yet possible to provide quantitative estimates of the overall risks, it has been estimated that up to 35% of cancer deaths may be related to dietary factors (Doll and Petro, 1981). Nitrate exposure through formation of N-nitrosamines has been associated with negative health effects due to increased risk for certain cancers, primarily gastric and colon cancers. In 1976, Spiegelhalder in Germany and Tannenbaum in the USA showed that nitrate could theoretically be transformed into N-nitrosamines by the reaction of salivary nitrite with secondary amines in the diet (Spiegelhalder et al., 1976; Tannenbaum et al., 1976). Since then, when the formation of potentially carcinogenic N-nitrosamines from the reaction of HNO_2 with secondary amines was recognized, the use of nitrate and nitrite salts as food preservatives has come under intense scrutiny. It has been known since 1956 that N-nitrosamines could cause hepatic tumors in laboratory animals by reacting with nucleic acids (Magee and Barnes, 1956). This reached a crisis in 1979 when Newberne published a report that dietary nitrite caused lymphomas in rats although not thought to occur through the formation of N-nitrosamines (Newberne, 1979). Nitrite has been used for centuries to protect from food-borne illnesses. There is no other effective way to kill botulinum spores which are resistant even to boiling (Pierson and Smoot, 1982). Although further analysis of Newberne's results and further work carried out by the Food and Drug Administration failed to confirm that nitrite causes cancer, this initial report along with the clear association with N-nitrosamines and cancer created the public perception that nitrite and nitrate are harmful and should be avoided. Public policy also intervened during this time to quantify and limit exposure to nitrite and nitrate. A large number of studies were undertaken, many of which purported to show a positive link between nitrate intake and cancer. Experimental evidence does indicate that co-administering a low-molecular-weight amine with nitrite can cause N-nitrosamine formation (Sen et al., 1969). Nitrosamines have been shown to cause a wide range of tumors in more than 40 animal species and may be specifically involved in the etiology of gastric cancer and esophageal cancer (Tricker and Preussmann, 1991) although so far, there is

no conclusive epidemiologic evidence that these compounds are related to cancer risk in humans.

Numerous case–control studies have been conducted worldwide to determine if there is a link between gastric cancer and nitrate intake (Blot et al., 1999; Eichholzer and Gutzwiller, 1998; Moller, 1995). It is well known that elevated dietary nitrate intake leads to elevated salivary nitrate levels and, after reduction by oral bacteria, higher levels of ingested nitrite. Studies in Canada, Italy, Sweden and Germany involving thousands of study subjects have failed to show an association or have demonstrated an inverse association between estimated nitrate intake and gastric cancer, perhaps because much of the nitrate was from vegetables (Moller, 1995). Occupational exposure to very high levels of nitrate occurs in nitrate fertilizer workers, who have elevated body burdens of nitrate and elevated salivary nitrate and nitrite levels, but no increase in gastric cancers has been observed (Moller, 1995). Case–control studies attempting to link nitrate and nitrite consumption to brain, esophageal, and nasopharyngeal cancers have also been inconclusive (Eichholzer and Gutzwiller, 1998). In other studies published over two decades, the relationship between the consumption of cured meats during pregnancy and the risk of brain and other tumors in offspring was examined (Blot et al., 1999). In this review of 14 epidemiological studies, 13 of which were case–control studies, Blot et al. (1999) could not conclude that there was a relationship between cured meat consumption during pregnancy and brain or any other cancers. It may be that in the limited number of epidemiological studies linking nitrate, nitrite or cured meat to a specific cancer site, other as-yet uncharacterized dietary or environmental factors may be involved. Most if not all of the epidemiological studies showing a relationship between nitrate exposure and cancer are very weak, and in 2003, the Joint FAO/WHO Expert Committee on Food Additives pronounced "Overall, the epidemiological studies showed no consistently increased risk for cancer with increasing consumption of nitrate. These data, combined with the results of the epidemiological studies considered by the Committee at its 44th meeting, do not provide evidence that nitrate is carcinogenic to humans" (Speijers and Brandt, 2003). Subsequent epidemiological studies have similarly failed to show a convincing link between nitrate intake and cancer. In fact, many experts suggest that any epidemiological study with a relative risk index of <2.0 should not be used for public policy recommendations (Anderson, 1994; Rosenberg, 1994) due to chance, statistical bias or effects of confounding factors that are sometimes not evident. Many epidemiologic studies have shown that

populations that eat diets high in vegetables and fruits and low in animal fat, meat, and/or calories have reduced risk of some of the most common cancers. Coincidently, fruits and vegetables are enriched with nitrite and nitrate from the soil. The presence of numerous classes of antioxidants is generally accepted as the explanation for the preventive effect of vegetables consumption, which may prevent oxidative stress and nitrosative DNA damage (Nishino et al., 2005). Despite this, it is entirely possible that certain subgroups of patients may have a higher risk of cancer when exposed to high levels of dietary nitrate. These at-risk populations will have to be identified. It is possible that future research will show that there are some groups, in whom it may be advisable to reduce nitrate exposure similar to groups that should avoid coffee or other otherwise safe products.

In view of the complex context and multiple cofactors of nitrate in diet-related carcinogenesis, it is not surprising that epidemiological studies into the relation between nitrate in drinking water and cancers (or other health effects) often provide weak associations, and both positive and negative (Ward et al., 2005). Ward et al. (2005) conclude that "the few studies that have evaluated intake of nitrosation precursors or inhibitors have observed elevated risks for colon cancer and neural tube effects associated with drinking-water nitrate concentrations below the regulatory limit." For example, De Roos et al. (2003) found that the odds ratio for colon cancer (which is equivalent to the relative incidence) almost doubled (95% CI) for the subgroup with above-median meat intake and exposed for more than 10 years to nitrate concentrations in drinking water exceeding 5 mg N/L (22 mg NO_3/L, which is half the legal US limit) as compared to the reference group that was not exposed (Fig. 3.4). This study did not find an association between colon cancer and nitrate for the total population. However, the European Food Safety Authority (Authority, 2008) concluded from a review of recent epidemiological studies, "these were mostly studies with a weak study design and limited strength of evidence; other case–control studies and cohort studies (which provide stronger evidence) find no increased risk with increasing nitrate intake after multivariate adjustment."

Many, if not most, of the early studies on nitrate and cancer were conducted before it was realized that nitrate is actually produced endogenously in the body. Endogenous NO activity leads to an increase in blood and tissue nitrate. In fact, it has been estimated that at least half of human nitrate exposure comes from endogenous production of NO and the other half from what we eat. A report from the National Research Council (*The Health Effects of Nitrate, Nitrite, and N-Nitroso Compounds*, NRC, 1981)

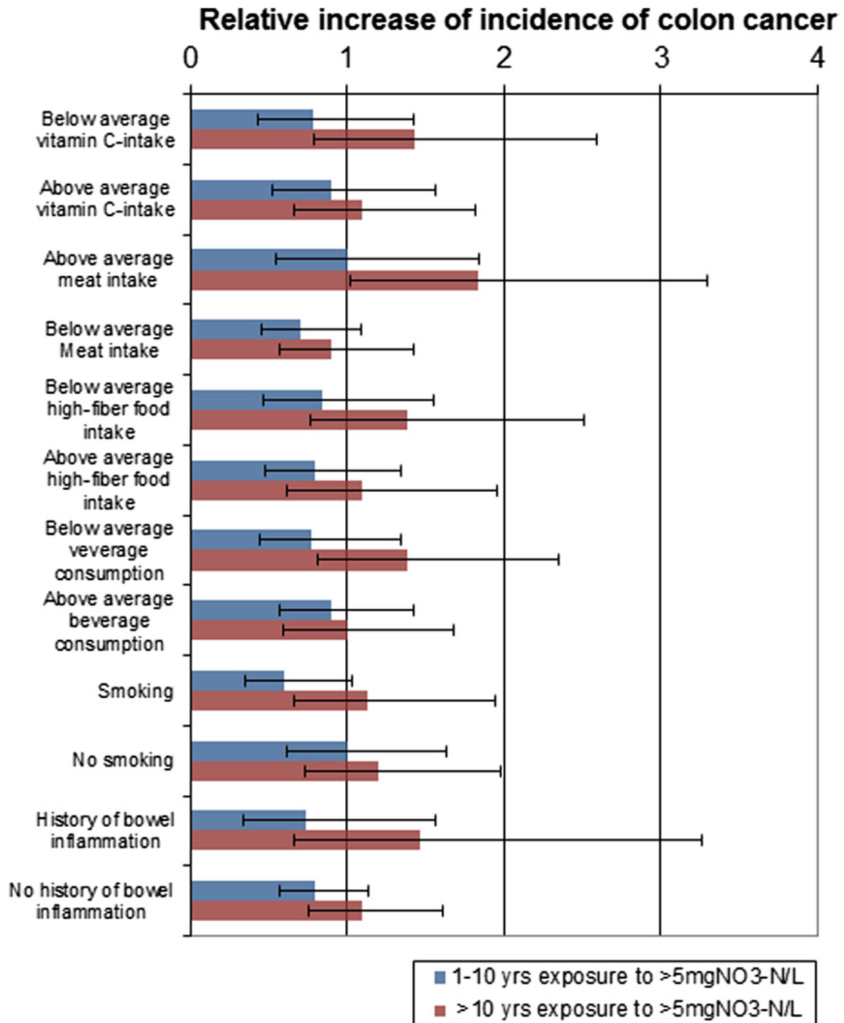


Figure 3.4 Increase of colon cancer incidence by drinking water nitrate in Iowa public water supply (and 95% confidence intervals) for subgroups with above and below median dietary and medical risk factors, and with 1–10 years of exposure and more than 10 years of exposure to drinking water exceeding 5 mg NO_3-N/L, relative to the subgroup with no exposure *(van Grinsven et al., 2010, inferred from De Roos et al., 2003)*. For color version of this figure, the reader is referred to the online version of this book.

(Pennington, 1998) estimated based on food-consumption tables that the average total nitrite and nitrate intake in the United States was 0.77 mg and 76 mg, respectively. If we assume our body (70 kg) produces 1.68 mmol NO per day (based on 1 μmol/kg/h NO production). An average daily

intake of 0.77 mg of nitrite would equate to 11.1 μmol per day and 76 mg nitrate would equate to 894 μmol per day or roughly 1 mmol nitrite and nitrate per day from diet. This almost matches what our body makes from NO if we assume most of the NO goes to stepwise oxidation to nitrite and nitrate. The dietary exposure of nitrate is even higher in vegetarians and in the populations in the Mediterranean region. Furthermore, physical activity enhances NO output and leads to a concomitant increase in nitrate. Therefore, our steady-state level of nitrate is derived almost 50% from diet and lifestyle. We now know that increasing endogenous exposure of nitrate is a natural and adaptive physiological response. In comparison to humans living at sea level, high-altitude residents of Tibet (4200 m above seal level) have >10-fold-higher circulating concentrations of bioactive NO, including nitrite and nitrate (Erzurum et al., 2007). There does not appear to be any adverse consequences to this population as a result of their increased nitrate exposure from endogenous synthesis of NO despite decades of exposure to these high concentrations of nitrate.

Early reports indicated dietary nitrate may affect iodine metabolism and thyroid function (Bloomfield, et al., 1961). More recent data indicate that relatively low doses exceeding the ADI for nitrate by three times have no effect on thyroid function (Hunault et al., 2007). However, emerging epidemiological data suggest that dietary nitrate exposure may be associated with thyroid cancer (Kilfoy et al., 2011). Additional research is needed to determine the role of nitrate and thyroid function and cancer.

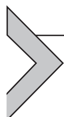
In 2006, a review of ingested nitrate and nitrite carcinogenicity was conducted by an expert working group convened by the International Agency for Research on Cancer (IARC), a United Nations/WHO headquartered in Lyon, France. The agency is involved in both epidemiological and laboratory research and disseminates scientific information through publications, meetings, courses, and fellowships. The IARC working group, whose report is not yet publicly available except in summary form IARC (2010) (http://monographs.iarc.fr/ENG/Monographs/vol94/mono94.pdf), classified nitrate and nitrite as a probable carcinogenic agent to humans:

> *"Ingested nitrate or nitrite under conditions that result in endogenous nitrosation is probably carcinogenic to humans (Group 2A)."*

This category is used when there is *limited evidence of carcinogenicity* in humans and *sufficient evidence of carcinogenicity* in experimental animals. In some cases, an agent may be classified in this category when there is *inadequate evidence of carcinogenicity* in humans and *sufficient evidence of*

carcinogenicity in experimental animals and strong evidence that the carcinogenesis is mediated by a mechanism that also operates in humans. Exceptionally, an agent may be classified in this category solely on the basis of *limited evidence of carcinogenicity* in humans. An agent may be assigned to this category if it clearly belongs, based on mechanistic considerations, to a class of agents for which one or more members have been classified in Group 1 or Group 2A.

The expert group found that nitrate/nitrite was only weakly associated with human stomach cancer and no other cancers. In simple terms, this overall evaluation means that the ingestion of food and water that contain nitrate or nitrite (e.g. spinach and other green leafy vegetables, root vegetables, bread, beer, cured meats), in combination with amines and amides commonly found in food, can react in the stomach to form N-nitrosamines and N-nitrosamides, which are known animal carcinogens already classified by IARC. However, the classification of nitrite and nitrate as Group 2A appears unwarranted and unjustified since there is no evidence based on new data demonstrating no association between nitrite and nitrate and gastric or esophageal cancer (Cross et al., 2010) combined with limited evidence in experimental animals.



3. RISK–BENEFIT ANALYSIS

The WHO ADI level for nitrate (0–3.7 mg/kg) translates into an equivalent of 222 mg nitrate for a 60 kg adult. Hord et al. (2009) recently reported that an individual following a DASH dietary pattern with high-nitrate vegetable and fruit choices would exceed this ADI by 500%. In fact, as has been observed previously, a portion of spinach commonly consumed in one serving of salad can exceed the ADI for nitrate (Lundberg and Govoni, 2004). Infants consuming breast milk and some commercial formula can exceed the ADI for nitrite and nitrate (Hord et al. 2011). The fact that typical consumption patterns of vegetables and fruit exceed the current WHO ADIs of nitrate should be one of the factors considered in any analysis of risks and benefits. The long standing and recognized health benefits of diets rich in fruits and vegetables (which are naturally high in nitrate) suggests that at levels found in our foods, nitrate exposure through vegetables or fruits should be considered safe (Authority, 2008). Part of the health benefits of vegetable sources of nitrate may be in context with the high antioxidant capacity of vegetables. Vitamin C and other antioxidants are very potent inhibitors of nitrosation reactions (Mirvish, 1975; Wilms

et al., 2005) and many vegetables are rich in antioxidants. The nitrate and nitrite content of cured and processed meats presents a completely separate context, in which the reactions and metabolism of nitrate may be different than in a vegetable food matrix. Part of the context may be the heme iron content in meats that may facilitate nitrosation reactions (Cross et al., 2003), which then changes the chemical fate of metabolized nitrate. This may, in part, explain the epidemiological studies demonstrating increased risk of cancers with high-meat intake. Other confounding factors may also provide context for adverse effects of nitrate. The association between the risk of gastric cancer and total meat intake is especially large in *H. pylori*-infected subjects (odds ratio per 100 g/day increase = 5.32; 95% CI = 2.10–13.4) (Gonzalez et al., 2006). It is known that nitrosating agents are overproduced under chronic inflammatory conditions (Grisham et al., 1992; Li et al., 2001), a common step in the gastric precancerous process. The necessity to address the potential protective and carcinogenic roles of dietary nitrate and nitrite are possible only through understanding particular at-risk populations, i.e. *H. pylori*-positive subjects or patients with undiagnosed precancerous lesions. Dietary factors have different effects on different stages of carcinogenesis (Fenton and Hord, 2006). Fenton and Hord, (2006) have demonstrated that preneoplastic colon epithelial cells, but not normal cells, respond with different cell phenotypes in response to curcumin, various flavonoids and adipokines. It may be a very similar scenario with nitrate and nitrite. Under normal healthy conditions, nitrate and nitrite may prevent the early inflammatory cascade protecting from cancer. On the other hand, in the precancerous lesion stage of carcinogenesis, nitrate and nitrite may be sequentially reduced to nitrite and NO to provide an angiogenic signal to fuel tumor growth (Harris, 1995; Kumar et al., 2008). Most recent data reveal that physiological amounts of nitrite inhibits stage 1-3 colon cancer proliferation and metastatic potential (Jiang et al., 2012). These findings necessitate the design of appropriate experiments *in vitro* and *in vivo* which address the stage at which dietary nitrate and nitrite may exert protective or promotional influences on carcinogenesis and also a more accurate patient assessment in epidemiological studies. In practical terms, this means that certain at-risk populations may respond differently to dietary sources of nitrate than otherwise healthy subjects and may account for the slight risk in epidemiological studies. These considerations may assist in the identification of molecular signatures that provide evidence of the protective effects of dietary nitrate and nitrite to prevent cancer while highlighting

potential promotional effects of dietary nitrate and nitrite in the face of preneoplastic, proinflammatory conditions.



4. CONCLUSIONS

The causal inference with regard to the etiologic roles of dietary nitrate and nitrite in methemoglobinemia and cancer may have exerted a detrimental effect on the recognition of the health benefits of nitrate- and nitrite-containing fruits and vegetables. This has occurred in spite of the historically observed (acute) benefits of nitrate and nitrite in medical therapeutics (Butler and Feelisch, 2008) and the undisputed health benefits recently discovered (Bryan et al., 2007, 2008; Webb et al., 2008). Results from a report from the National Research Council (*The Health Effects of Nitrate, Nitrite, and N-Nitroso Compounds*, NRC, 1981) show that the amount of nitrite and nitrate consumed through our diet matches what our body makes from NO if we assume most of the endogenous NO goes to stepwise oxidation to nitrite and nitrate. Therefore, steady-state levels of nitrite and nitrate, which are routinely used as clinical biomarkers of NO activity, come almost 50% from diet. In fact, swallowing saliva alone is a primary source of exposure to nitrite and nitrate. The enterosalivary concentration and circulation of nitrate and ultimately nitrite provides an essential pathway for health and host defense (Erzurum et al., 2007; Petersson et al., 2007). These positive health impacts need to be weighted against the more uncertain negative health impacts of chronic exposure to high nitrate in drinking water for susceptible subpopulations (e.g. with low-vitamin C intake, high-meat intake and a history of bowel inflammation) (Powlson et al., 2008; Ward et al., 2005).

There will very likely be considerable debate about the need for reviews by regulatory agencies and potential action on nitrite and nitrate in our food and water supply. It is hard to conceive that the ingestion of nitrate from fruits and vegetables could have any impact on potential adverse toxic outcomes. The food additive use of nitrite in, e.g. processed meats is a reason of some concern as it may contribute to increased risk on gastric cancer (Gonzalez et al., 2006). In general, intake of nitrate from water impacted by runoff from fertilizer and manure represents only a small addition to the body burden of endogenously produced nitrogen oxides, but at high-nitrate concentrations and for above-average ingestion can contribute the majority of the intake. Although health risks and social cost of nitrate in drinking water are small, they may justify adjustment of agricultural practices

as there is quite some scope for cost-efficient reduction of nitrate runoff (van Grinsven et al., 2010). We must also recognize potentially susceptible populations may exist that put them (either genetically or environmentally due to lifestyle and/or dietary habits) at particular risk that otherwise healthy individuals may not be susceptible, i.e. people with a history of bowel inflammation. Furthermore, although epidemiological studies are designed to reveal associations and not causal evidence, it is important to also consider whether those populations that eat primarily a high meat may concomitantly eat too few vegetables and fruits. It may be this insufficient vegetable intake along with high-meat diet that is the root of the problem and not meat intake itself.

Due to the intense social and governmental desire to identify causes of cardiovascular disease and cancer, we, as a society, have come to a point where some mechanistic/physiological observations and weak epidemiological associations can mislead us, even when the totality of evidence shows such findings to be biologically implausible. The risk/benefit balance should be a strong consideration before there are any suggestions for new regulatory or public health guidelines for nitrite and nitrate exposures.

REFERENCES

Methemoglobinemia following unintentional ingestion of sodium nitrite–New York, 2002. MMWR Morb. Mortal. Wkly. Rep. 51 (29), 639–642.

Recommendations: Nitrate and Nitrite. World Health Organization, 2004. Geneva, Switzerland.

Agency, U.E.P., 1991. National primary drinking water regulations: final rule, 40. Fed. Regist. 56 (20), 3526–3597 CFR Parts 141–143.

Anderson, L., 1994. Abortion and Possible Risk for Breast Cancer: Analysis and Inconsistencies. National Cancer Institute, Bethesda, MD.

Appel, L.J., Moore, T.J., et al., 1997. A clinical trial of the effects of dietary patterns on blood pressure. DASH Collaborative Research Group. N. Engl. J. Med. 336 (16), 1117–1124.

Archer, D.L., 2002. Evidence that ingested nitrate and nitrite are beneficial to health. J. Food Prot. 65 (5), 872–875.

Authority, E.F.S., 2008. Nitrate in vegetables: scientific opinion of the panel on contaminants in the food chain. EFSA J. 289, 1–79.

Bailey, S.J., Winyard, P., et al., 2009. Dietary nitrate supplementation reduces the O_2 cost of low-intensity exercise and enhances tolerance to high-intensity exercise in humans. J. Appl. Physiol.

Benjamin, N., O'Driscoll, F., et al., 1994. Stomach NO synthesis. Nature 368 (6471), 502.

Benjamin, N., Pattullo, S., et al., 1997. Wound licking and nitric oxide. Lancet 349 (9067), 1776.

Bjorne, H.H., Petersson, J., et al., 2004. Nitrite in saliva increases gastric mucosal blood flow and mucus thickness. J. Clin. Invest. 113 (1), 106–114.

Bloomfield, R.A., Welsch, C.W., et al., 1961. Effect of dietary nitrate on thyroid function. Science 134, 1690.

Blot, W.J., Henderson, B.E., et al., 1999. Childhood cancer in relation to cured meat intake: review of the epidemiological evidence. Nutr. Cancer 34 (1), 111–118.
Bodner, L., 1991. Effect of parotid submandibular and sublingual saliva on wound healing in rats. Comp. Biochem. Physiol. A Comp. Physiol. 100 (4), 887–890.
Bryan, N.S., Calvert, J.W., et al., 2007. Dietary nitrite supplementation protects against myocardial ischemia-reperfusion injury. Proc. Natl. Acad. Sci. U. S. A. 104 (48), 19144–19149.
Bryan, N.S., Calvert, J.W., et al., 2008. Dietary nitrite restores NO homeostasis and is cardioprotective in endothelial nitric oxide synthase-deficient mice. Free Radic. Biol. Med. 45 (4), 468–474.
Bugiardini, R., Manfrini, O., et al., 2004. Endothelial function predicts future development of coronary artery disease: a study of women with chest pain and normal coronary angiograms. Circulation 109 (21), 2518–2523.
Butler, A.R., Feelisch, M., 2008. Therapeutic uses of inorganic nitrite and nitrate: from the past to the future. Circulation 117 (16), 2151–2159.
Cassens, R.G., 1997. Residual nitrite in cured meat. Food Technol. 51, 53–55.
Cekmen, M.B., Balat, A., et al., 2004. Decreased adrenomedullin and total nitrite levels in breast milk of preeclamptic women. Clin. Biochem. 37 (2), 146–148.
Cornblath, M., Hartmann, A.F., 1948. Methemoglobinaemia in young infants. J. Pediatr. 33, 421–425.
Cross, A.J., Freedman, N.D., et al., 2010. Meat consumption and risk of esophageal and gastric cancer in a large prospective study. Am. J. Gastroenterol.
Cross, A.J., Pollock, J.R., et al., 2003. Haem, not protein or inorganic iron, is responsible for endogenous intestinal N-nitrosation arising from red meat. Cancer Res. 63 (10), 2358–2360.
Davi, G., Patrono, C., 2007. Platelet activation and atherothrombosis. N. Engl. J. Med. 357 (24), 2482–2494.
De Roos, A.J., Ward, M.H., et al., 2003. Nitrate in public water supplies and the risk of colon and rectum cancers. Epidemiology 14 (6), 640–649.
Dejam, A., Hunter, C.J., et al., 2007. Nitrite infusion in humans and nonhuman primates: endocrine effects, pharmacokinetics, and tolerance formation. Circulation 116 (16), 1821–1831.
Dobermann, A., Cassman, K.G., 2005. Cereal area and nitrogen use efficiency are drivers of future nitrogen fertilizer consumption. Sci. China. Ser. C, Life Sciences/Chinese Acad. Sci. 48 Spec No, 745–758.
Doel, J.J., Benjamin, N., et al., 2005. "Evaluation of bacterial nitrate reduction in the human oral cavity." Eur. J. Oral Sci. 113 (1), 14–19.
Doll, R., Petro, R., 1981. The causes of cancer: quantitative estimates of avoidable risks of cancer in the United States today. J. Natl. Cancer Inst. 66, 1191–1308.
Dougall, H.T., Smith, L., et al., 1995. The effect of amoxycillin on salivary nitrite concentrations: an important mechanism of adverse reactions? Br. J. Clin. Pharmacol. 39 (4), 460–462.
Duncan, C., Dougall, H., et al., 1995. Chemical generation of nitric oxide in the mouth from the enterosalivary circulation of dietary nitrate. Nat. Med. 1 (6), 546–551.
Duncan, C., Li, H., et al., 1997. Protection against oral and gastrointestinal diseases: importance of dietary nitrate intake, oral nitrate reduction and enterosalivary nitrate circulation. Comp. Biochem. Physiol. A Physiol. 118 (4), 939–948.
Dusdieker, L.B., Getchell, J.P., et al., 1994. Nitrate in baby foods. Adding to the nitrate mosaic. Arch. Pediatr. Adolesc. Med. 148 (5), 490–494.
Dusdieker, L.B., Stumbo, P.J., et al., 1996. Does increased nitrate ingestion elevate nitrate levels in human milk? Arch. Pediatr. Adolesc. Med. 150 (3), 311–314.

Dykhuizen, R.S., Fraser, A., et al., 1998. *Helicobacter pylori* is killed by nitrite under acidic conditions. Gut 42 (3), 334–337.
Dykhuizen, R.S., Frazer, R., et al., 1996. Antimicrobial effect of acidified nitrite on gut pathogens: importance of dietary nitrate in host defense. Antimicrob. Agents Chemother. 40 (6), 1422–1425.
Eichholzer, M., Gutzwiller, F., 1998. Dietary nitrates, nitrites, and N-nitroso compounds and cancer risk: a review of the epidemiologic evidence. Nutr. Rev. 56 (4 Pt 1), 95–105.
Erisman, J.W., Galloway, J.N., et al., 2008. How a century of ammonia synthesis changed the world. Nat. Geosci. 1, 636–639.
Erzurum, S.C., Ghosh, S., et al., 2007. Higher blood flow and circulating NO products offset high-altitude hypoxia among Tibetans. Proc. Natl. Acad. Sci. U. S. A. 104 (45), 17593–17598.
Fan, A.M., Steinberg, V.E., 1996. Health implications of nitrate and nitrite in drinking water: an update on methemoglobinemia occurrence and reproductive and developmental toxicity. Regul. Toxicol. Pharmacol. 23 (1 Pt 1), 35–43.
Fenton, J.I., Hord, N.G., 2006. Stage matters: choosing relevant model systems to address hypotheses in diet and cancer chemoprevention research. Carcinogenesis 27 (5), 893–902.
Gangolli, S.D., van den Brandt, P.A., et al., 1994. Nitrate, nitrite and N-nitroso compounds. Eur. J. Pharmacol. 292 (1), 1–38.
Gartner, L.M., Morton, J., et al., 2005. Breastfeeding and the use of human milk. Pediatrics 115 (2), 496–506.
Godfrey, M., Majid, D.S., 1998. Renal handling of circulating nitrates in anesthetized dogs. Am. J. Physiol. 275 (1 Pt 2), F68–F73.
Gonzalez, C.A., Jakszyn, P., et al., 2006. Meat intake and risk of stomach and esophageal adenocarcinoma within the European Prospective Investigation into Cancer and Nutrition (EPIC). J. Natl. Cancer Inst. 98 (5), 345–354.
Green, L.C., Ruiz de Luzuriaga, K., et al., 1981. Nitrate biosynthesis in man. Proc. Natl. Acad. Sci. U. S. A. 78 (12), 7764–7768.
Greer, F.R., Shannon, M., 2005. Infant methemoglobinemia: the role of dietary nitrate in food and water. Pediatrics 116 (3), 784–786.
Grisham, M.B., Ware, K., et al., 1992. Neutrophil-mediated nitrosamine formation: role of nitric oxide in rats. Gastroenterology 103 (4), 1260–1266.
Halcox, J.P., Schenke, W.H., et al., 2002. Prognostic value of coronary vascular endothelial dysfunction. Circulation 106 (6), 653–658.
Harris, C.C., 1995. 1995 Deichmann lecture–p53 tumor suppressor gene: at the crossroads of molecular carcinogenesis, molecular epidemiology and cancer risk assessment. Toxicol. Lett. 82–83, 1–7.
Hart, B.L., Powell, K.L., 1990. Antibacterial properties of saliva: role in maternal periparturient grooming and in licking wounds. Physiol. Behav. 48 (3), 383–386.
Harter, T., 2009. Agricultural impacts on groundwater nitrate. Hydrology 8 (4), 22–23.
Heinig, M.J., 1998. The American Academy of Pediatrics recommendations on breastfeeding and the use of human milk. J. Hum. Lact. 14 (1), 2–3.
Hoddinott, P., Tappin, D., et al., 2008. Breast feeding. BMJ 336 (7649), 881–887.
Hord, N.G., Ghannam, J.S., et al., 2011. Nitrate and nitrite content of human, formula, bovine and soy milks: implications for dietary nitrite and nitrate recommendations. Breastfeeding Med. Dec 6(6), 393–399.
Hord, N.G., Tang, Y., et al., 2009. Food sources of nitrates and nitrites: the physiologic context for potential health benefits. Am. J. Clin. Nutr. 90 (1), 1–10.
Hunault, C.C., Lambers, A.C., et al., 2007. Effects of sub-chronic nitrate exposure on the thyroidal function in humans. Toxicol. Lett. 175 (1–3), 64–70.

Ip, S., Chung, M., et al., 2007. Breastfeeding and Maternal and Infant Health Outcomes in Developed Countries. Evidence Report/Technology Assessment. A. Publication. Rockville, MD, Tufts-New England Medical Center Evidence-based Practice center, under Contract NO. 290-02-0022.

James, D.C., Lessen, R., 2009. Position of the American Dietetic Association: promoting and supporting breastfeeding. J. Am. Diet. Assoc. 109 (11), 1926–1942.

Jansson, E.A., Huang, L., et al., 2008. A mammalian functional nitrate reductase that regulates nitrite and nitric oxide homeostasis. Nat. Chem. Biol. 4 (7), 411–417.

Jansson, E.A., Petersson, J., et al., 2007. Protection from nonsteroidal anti-inflammatory drug (NSAID)-induced gastric ulcers by dietary nitrate. Free Radic. Biol. Med. 42 (4), 510–518.

Jiang, H., Tang, Y., Garg, H.K., Parthasarathy, D.K., Torregrossa, A.C., Hord, N.G., Bryan, N.S., 2012. Concentration-and Stage-specfic effects of nitrite on colon cancer cell lines. Nitric oxide 26 (4) May 15, 267–273.

Johnson, C.J., Kross, B.C., 1990. Continuing importance of nitrate contamination of groundwater and wells in rural areas. Am. J. Ind. Med. 18 (4), 449–456.

Kilfoy, B.A., Zhang, Y., et al., 2011. Dietary nitrate and nitrite and the risk of thyroid cancer in the NIH-AARP diet and health study. Int. J. Cancer. 129 (1) Jul 1, 160–72.

Kleinbongard, P., Dejam, A., et al., 2006. Plasma nitrite concentrations reflect the degree of endothelial dysfunction in humans. Free Radic. Biol. Med. 40 (2), 295–302.

Knobeloch, L., Salna, B., et al., 2000. Blue babies and nitrate-contaminated well water. Environ. Health Perspect. 108 (7), 675–678.

Kortboyer, J., Olling, M., Zeilmaker, M.J., 1997. The Oral Bioavailability of Sodium Nitrite Investigated in Healthy Adult Volunteers. National Institute of Public Health and the Environment, Bilthoven, Netherlands.

Kross, B.C., Ayebo, A.D., et al., 1992. Methemoglobinemia: nitrate toxicity in rural America. Am. Fam. Physician 46 (1), 183–188.

Kumar, D., Branch, B.G., et al., 2008. Chronic sodium nitrite therapy augments ischemia-induced angiogenesis and arteriogenesis. Proc. Natl. Acad. Sci. U. S. A. 105 (21), 7540–7545.

L'Hirondel, J.,L., Avery, A.A., et al., 2006. Dietary nitrate: where is the risk? Environ. Health Perspect. 114 (8), A458–A459 author reply A459–461.

L'Hirondel, J.L., 2001. Nitrate and Man: Toxic, Harmless or Beneficial? CABI Publishing, Wallingford, UK.

Larsen, F.J., Ekblom, B., et al., 2006. Effects of dietary nitrate on blood pressure in healthy volunteers. N. Engl. J. Med. 355 (26), 2792–2793.

Larsen, F.J., Weitzberg, E., et al., 2007. Effects of dietary nitrate on oxygen cost during exercise. Acta Physiol. (Oxf) 191 (1), 59–66.

Lauer, T., Heiss, C., et al., 2008. Age-dependent endothelial dysfunction is associated with failure to increase plasma nitrite in response to exercise. Basic Res. Cardiol. 103 (3), 291–297.

Lerman, A., Zeiher, A.M., 2005. Endothelial function: cardiac events. Circulation 111 (3), 363–368.

Li, C.Q., Pignatelli, B., et al., 2001. Increased oxidative and nitrative stress in human stomach associated with cagA+ *Helicobacter pylori* infection and inflammation. Dig. Dis. Sci. 46 (4), 836–844.

Lundberg, J.O., Feelisch, M., et al., 2006. Cardioprotective effects of vegetables: is nitrate the answer? Nitric Oxide 15 (4), 359–362.

Lundberg, J.O., Gladwin, M.T., et al., 2009. Nitrate and nitrite in biology, nutrition and therapeutics. Nat. Chem. Biol. 5 (12), 865–869.

Lundberg, J.O., Govoni, M., 2004. Inorganic nitrate is a possible source for systemic generation of nitric oxide. Free Radic. Biol. Med. 37 (3), 395–400.

Lundberg, J.O., Weitzberg, E., et al., 2004. Nitrate, bacteria and human health. Nat. Rev. Microbiol. 2 (7), 593–602.
Lundberg, J.O., Weitzberg, E., et al., 2008. The nitrate–nitrite–nitric oxide pathway in physiology and therapeutics. Nat. Rev. Drug Discov. 7 (8), 156–167.
Lundberg, J.O., Weitzberg, E., et al., 1994. Intragastric nitric oxide production in humans: measurements in expelled air. Gut 35 (11), 1543–1546.
Magee, P.N., Barnes, J.M., 1956. The production of malignant primary hepatic tumours in the rat by feeding dimethylnitrosamine. Br. J. Cancer 10 (1), 114–122.
Marcus, H., Joffe, J.R., 1949. Nitrate methemoglobinemia. N. Engl. J. Med. 240 (15), 599–602.
McKnight, G.M., Duncan, C.W., et al., 1999. Dietary nitrate in man: friend or foe? Br. J. Nutr. 81 (5), 349–358.
McKnight, G.M., Smith, L.M., et al., 1997. Chemical synthesis of nitric oxide in the stomach from dietary nitrate in humans. Gut 40 (2), 211–214.
Milkowski, A., Garg, H.K., et al., 2010. Nutritional epidemiology in the context of nitric oxide biology: a risk-benefit evaluation for dietary nitrite and nitrate. Nitric Oxide 22 (2), 110–119.
Mirvish, S.S., 1975. Blocking the formation of N-nitroso compounds with ascorbic acid in vitro and in vivo. Ann. N.Y Acad. Sci. 258, 175–180.
Mirvish, S.S., 1996. Inhibition by vitamins C and E of in vivo nitrosation and vitamin C occurrence in the stomach. Eur. J. Cancer Prev. 5 (Suppl. 1), 131–136.
Moller, H., 1995. Adverse Health Effects of Nitrate and Its Metabolites: Epidemiological Studies in Humans. Health Aspects of Nitrates and Its Metabolites Pparticularly Nitrite. Council of Europe Press, Strasbourg Cedex, France.
Moncada, S., Higgs, A., 1993. The L-arginine–nitric oxide pathway. N. Engl. J. Med. 329 (27), 2002–2012.
Newberne, P.M., 1979. Nitrite promotes lymphoma incidence in rats. Science 204 (4397), 1079–1081.
Nishino, H., Murakoshi, M., et al., 2005. Cancer prevention by phytochemicals. Oncology 69 (Suppl. 1), 38–40.
Ohta, N., Tsukahara, H., et al., 2004. Nitric oxide metabolites and adrenomedullin in human breast milk. Early Hum. Dev. 78 (1), 61–65.
Otten, J.J., Hellwig, J.P., Meyers, L.D. (Eds.), 2006. Dietary Reference Intakes: The Essential Guide to Nutrient Requirements, National Academy Press, Food and Nutrition Board, Institute of Medicine, National Academy of Sciences.
Pennington, J.A.T., 1998. Dietary exposure models for nitrates and nitrites. Food Control 9 (6), 385–395.
Petersson, J., 2008. Nitrate, Nitrite and Nitric Oxide in Gastric Mucosal Defense. Uppsala University, Uppsala.
Petersson, J., Carlstrom, M., et al., 2009. Gastroprotective and blood pressure lowering effects of dietary nitrate are abolished by an antiseptic mouthwash. Free Radic. Biol. Med. 46 (8), 1068–1075.
Petersson, J., Phillipson, M., et al., 2007. Dietary nitrate increases gastric mucosal blood flow and mucosal defense. Am. J. Physiol. Gastrointest. Liver Physiol. 292 (3), G718–G724.
Pierson, M.D., Smoot, L.A., 1982. Nitrite, nitrite alternatives, and the control of *Clostridium botulinum* in cured meats. Crit. Rev. Food Sci. Nutr. 17 (2), 141–187.
Powlson, D.S., Addiscott, T.M., et al., 2008. When does nitrate become a risk for humans? J. Environ. Qual. 37 (2), 291–295.
Radomski, M.W., Palmer, R.M., et al., 1987. The anti-aggregating properties of vascular endothelium: interactions between prostacyclin and nitric oxide. Br. J. Pharmacol. 92 (3), 639–646.

Radomski, M.W., Palmer, R.M., et al., 1990. An L-arginine/nitric oxide pathway present in human platelets regulates aggregation. Proc. Natl. Acad. Sci. U. S. A. 87 (13), 5193–5197.

Rahma, M., Kimura, S., et al., 2001. Effects of furosemide on the tubular reabsorption of nitrates in anesthetized dogs. Eur. J. Pharmacol. 428 (1), 113–119.

Rassaf, T., Lauer, T., et al., 2007. Nitric oxide synthase-derived plasma nitrite predicts exercise capacity. Br. J. Sports Med. 41 (10), 669–673 discussion 673.

Richardson, G., Hicks, S.L., et al., 2002. The ingestion of inorganic nitrate increases gastric S-nitrosothiol levels and inhibits platelet function in humans. Nitric Oxide 7 (1), 24–29.

Rosenberg, L., 1994. Induced abortion and breast cancer: more scientific data are needed. J. Natl. Cancer Inst. 86 (21), 1569–1570.

Santamaria, P., 2006. Nitrate in vegetables: toxicity, content, intake and EC regulation. J. Sci. Food Agric. 86, 10–17.

Schachinger, V., Britten, M.B., et al., 2000. Prognostic impact of coronary vasodilator dysfunction on adverse long-term outcome of coronary heart disease. Circulation 101 (16), 1899–1906.

Sen, N.P., Smith, D.C., et al., 1969. Formation of N-nitrosamines from secondary amines and nitrite in human and animal gastric juice. Food Cosmet. Toxicol. 7 (4), 301–307.

Smil, V., 2002. Eating meat: evolution, patterns and consequences. Popul. Dev. Rev. 28 (4), 599–640.

Sobko, T., Reinders, C., et al., 2004. Gastrointestinal nitric oxide generation in germ-free and conventional rats. Am. J. Physiol. Gastrointest. Liver Physiol. 287 (5), G993–G997.

Speijers, G., Brandt, P.A. d. e. n., 2003. Nitrate. Food Additive Series, Joint FAO/WHO Expert Committee on Food Additives, Geneva.

Spiegelhalder, B., Eisenbrand, G., et al., 1976. Influence of dietary nitrate on nitrite content of human saliva: possible relevance to in vivo formation of N-nitroso compounds. Food Cosmet. Toxicol. 14, 545–548.

Stokes, K.Y., Dugas, T.R., et al., 2009. Dietary nitrite prevents hypercholesterolemic microvascular inflammation and reverses endothelial dysfunction. Am. J. Physiol. Heart Circ. Physiol. 296 (5), H1281–H1288.

Tannenbaum, S.R., Weisman, M., et al., 1976. The effect of nitrate intake on nitrite formation in human saliva. Food Cosmet. Toxicol. 14 (6), 549–552.

Tricker, A.R., Preussmann, R., 1991. Carcinogenic N-nitrosamines in the diet: occurrence, formation, mechanisms and carcinogenic potential. Mutat. Res. 259 (3–4), 277–289.

van Grinsven, H., Rabl, A., et al., 2010. Estimation of incidence and social cost of colon cancer due to nitrate in drinking water in the EU: a tentative cost-benefit assessment cost–benefit assessment. Environ. Health 9, 58. (doi:10.1186/1476-069X-9-58).

van Grinsven, H.J., Ward, M.H., et al., 2006. Does the evidence about health risks associated with nitrate ingestion warrant an increase of the nitrate standard for drinking water? Environ. Health 5, 26.

Walker, R., 1996. The metabolism of dietary nitrites and nitrates. Biochem. Soc. Trans. 24 (3), 780–785.

Ward, M.H., deKok, T.M., et al., 2005. Workgroup report: drinking-water nitrate and health–recent findings and research needs. Environ. Health Perspect. 113 (11), 1607–1614.

Webb, A.J., Patel, N., et al., 2008. Acute blood pressure lowering, vasoprotective, and antiplatelet properties of dietary nitrate via bioconversion to nitrite. Hypertension 51 (3), 784–790.

Weller, R., Price, R.J., et al., 2001. Antimicrobial effect of acidified nitrite on dermatophyte fungi, Candida and bacterial skin pathogens. J. Appl. Microbiol. 90 (4), 648–652.

Wennmalm, A., Benthin, G., et al., 1993. Metabolism and excretion of nitric oxide in humans. An experimental and clinical study. Circ. Res. 73 (6), 1121–1127.
WHO, 1998. Guidelines for Drinking-water Quality. Health Criteria and Other Supporting Information. World Health Organization, Geneva, 2
Wilms, L.C., Hollman, P.C., et al., 2005. Protection by quercetin and quercetin-rich fruit juice against induction of oxidative DNA damage and formation of BPDE-DNA adducts in human lymphocytes. Mutat. Res. 582 (1–2), 155–162.
Ying, L., Hofseth, L.J., 2007. An emerging role for endothelial nitric oxide synthase in chronic inflammation and cancer. Cancer Res. 67 (4), 1407–1410.
Yoshida, K., Kasama, K., 1987. Biotransformation of nitric oxide. Environ. Health Perspect. 73, 201–205.
Zand, J., Lanza, F., et al., 2011. All-natural nitrite and nitrate containing dietary supplement promotes nitric oxide production and reduces triglycerides in humans. Nutr. Res. 31 (4), 262–269.



CHAPTER FOUR

Cadmium Contamination and Its Risk Management in Rice Ecosystems

Nanthi S. Bolan*,†,#, Tomoyuki Makino‡, Anitha Kunhikrishnan§, Pil-Joo Kim¶, Satoru Ishikawa‡, Masaharu Murakami‡, Ravi Naidu*,†, Mary B. Kirkham**

*Centre for Environmental Risk Assessment and Remediation, University of South Australia, Mawson Lakes, Australia
†Cooperative Research Centre for Contamination Assessment and Remediation of the Environment, Adelaide, Australia
‡Soil Environmental Division, National Institute for Agro-Environmental Sciences, Tsukuba, Japan
§Chemical Safety Division, Department of Agro-Food Safety, National Academy of Agricultural Science, Gyeonggi-do, Republic of Korea
¶Institute of Agriculture and Life Sciences, Gyeongsang National University, Jinju, Republic of Korea
**Department of Agronomy, Throckmorton Plant Sciences Center, Kansas State University, Manhattan, KS, USA
#Corresponding author: E-mail: Nanthi.Bolan@unisa.edu.au

Contents

Advances in Agronomy, Volume 119
ISSN 0065-2113, http://dx.doi.org/10.1016/B978-0-12-407247-3.00004-4

Abstract

Cadmium (Cd) has been identified as one of the major heavy metals reaching the food chain through various geogenic and anthropogenic activities. In many East and South Asian countries including Japan, Bangladesh, Indonesia, and Korea, Cd accumulation in rice (*Oryza sativa* L.) ecosystems and its subsequent transfer to the human food chain is a major environmental issue. Rice soils in these countries have been affected by Cd accumulation derived from fertilizer and manure application, mine tailings, and refining plants. Excessive intake of Cd into the human body is detrimental to human health, causing serious illnesses such as itai-itai disease. To ensure the safety of foods, the concentrations of Cd in staple crops should be below a standard value; this applies particularly to rice because 34–50% of the Cd intake by people in many Asian countries has been derived from rice. Therefore, development of remediation methods for Cd-contaminated rice soils has become an urgent task to ensure food safety. This chapter provides an overview of the various sources of Cd in rice ecosystems and the biogeochemical processes that regulate Cd bioavailability to organisms, including microbes, plants, animals, and humans. Because of the complexity involved in dealing with Cd in rice ecosystems, exacerbated by the Cd source, site characteristics, and the nature of water management strategies, we have attempted to describe an "integrated" approach that employs a combination of remediation technologies, with the aim of securing methods that are economically and technologically viable.

1. INTRODUCTION

Heavy metals reach soils through natural pedogenic (or geogenic) processes and anthropogenic activities. Often the concentrations of heavy metals released into the soil system by pedogenic processes are low and are largely related to the origin and nature of the parent material. Anthropogenic activities primarily associated with agricultural and mining activities, industrial processes, manufacturing, and the disposal of domestic and

industrial waste materials are the major sources of metal enrichment in soils. Unlike pedogenic input, metals added through anthropogenic activities often have high bioavailability (Adriano, 2001; Naidu and Bolan, 2008).

Cadmium (Cd) has been identified as one of the major heavy metals reaching the food chain through various activities (Kirkham, 2006; Loganathan et al., 2012; Naidu et al., 1997). For example, in New Zealand and Australia, Cd has been identified as the most common heavy metal reaching the food chain mainly through animal transfer in pastoral agriculture (Loganathan et al., 2012; McLaughlin et al., 1996). Similarly, in many East and South Asian countries including Japan, Bangladesh, Indonesia, and Korea, Cd accumulation in rice ecosystems and its subsequent transfer to the human food chain is a major environmental issue (Kawada and Suzuki, 1998; Simmons et al., 2008) (Tables 4.1 and 4.2). In Australia (Mann et al., 2002; McLaughlin et al., 1996; Williams and David, 1976) and New Zealand (Longhurst et al., 2004; Roberts et al., 1994), most of the Cd that has accumulated in the topsoil has been derived from impurities in phosphate (P) fertilizers added during normal farming practice. The paddy soils in many countries have been affected by Cd derived from not only fertilizer application but also mine tailings and refining plants (Luo et al., 2009; Zarcinas et al., 2004).

Rice is one of the most widely consumed staple cereal foods in the world constituting about 89% of the diet of people in Asian countries (Chandler and Colo, 1979; Papademetriou, 2000). In these countries, rice is a major source of Cd intake by humans. Excessive intake of Cd into the human body is detrimental to human health, causing serious illnesses such as itai-itai

Table 4.1 Selected References on Cadmium Content in Paddy Soils

Country	Soil Type	Concentration (mg kg^{-1})	References
Japan	Fluvisols	0.40	Herawati et al. (2000)
Japan	Cambisol	0.60	Herawati et al. (2000)
Japan	Andosols	0.40	Herawati et al. (2000)
Indonesia	Histosols	0.04	Herawati et al. (2000)
Indonesia	Luvisols	0.09	Herawati et al. (2000)
Indonesia	Acrisols	0.15	Herawati et al. (2000)
China	Gleysols	0.09	Herawati et al. (2000)
Macedonia	Acidic soil	0.1–6.4	Rogan et al. (2009)
Thailand	–	0.5–284	Simmons et al. (2005)
China	Red soil	2.01–29.68	Yang et al. (2006)
Italy	Aquept	0.96	Cattani et al. (2008)
Korea	Long-term fertilized soils	1.08–1.16	Jung et al. (2004)

Table 4.2 Selected References on Cadmium Content in Various Parts of the Rice Plant

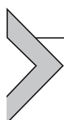
Country	Element Location	Concentration (mg kg^{-1})	References
Macedonia	Grain	0.005–0.31	Rogan et al. (2009)
19 countries	Grain	0.0008–0.21	Watanabe et al. (1989)
Malaysia	Grain	0.18 ± 0.028	Yap et al. (2009)
	Husk	0.183 ± 0.022	
	Leaf	0.203 ± 0.023	
	Stem	0.239 ± 0.386	
	Root	0.19 ± 0.028	
Thailand	Stem	0.38–22.0	Simmons et al. (2005)
	Leaf	0.05–13.5	
	Grain	0.02–5.0	
China	Root	1.79–23.47	Yang et al. (2006)
	Straw	0.50–6.24	
	Stalk	0.95–5.86	
	Hull	0.55–0.81	
	Grain with hull	0.35–1.15	
	Grain without hull	0.03–0.46	
Japan	Grain	0.15–0.16	Nogawa et al. (1983)
Taiwan	Grain	0.01 ± 0.04	Lin et al. (2004)
Iran	Grain	0.12–0.18	Khaniki and Zazoli (2005); Zazoli et al. (2006)
Korea	Grain	0.013 ± 0.003	Jung et al. (2004)
	Stem and straw	0.139 ± 0.001	
	Root	1.627 ± 0.0.04	

disease (Nogawa and Kido, 1996; Ogawa et al., 2004). Current Japanese regulations have designated certain paddy fields, which have produced rice grains containing more than 0.4 mg kg^{-1} of Cd as "contaminated paddy fields." Furthermore, the Codex Alimentarius Commission of the United Nations Food and Agriculture Organization (FAO) and the World Health Organization (WHO) recently proposed a new international standard for Cd concentrations in polished rice, 0.4 mg Cd kg^{-1} (Codex Alimentarius Commission (Codex); Codex, 2005). Therefore, development of remediation methods for Cd-contaminated soils has become an urgent task to ensure food safety.

Unlike organic contaminants, most metals do not undergo microbial or chemical degradation, and the total concentration of these metals in soils persists for a long time after their introduction (Adriano, 2001). With greater public awareness of the implications of contaminated soils on human and animal health, there has been increasing interest in the development of technologies

to remediate contaminated sites. For diffused distribution of metals such as fertilizer-derived Cd input on soils, remediation options generally include amelioration of soils to minimize the metal bioavailability. Bioavailability can be minimized through chemical and biological immobilization of metals using a range of inorganic compounds including lime, P compounds and organic amendments (Bolan and Duraisamy, 2003; Kumpiene et al., 2007; Park et al., 2011). Reducing metal availability and maximizing plant growth through inactivation may also prove to be an effective method of *in situ* soil remediation on industrial, urban, smelting, and mining sites. The more localized metal contamination found in urban environments, such as chromium (Cr) contamination in timber treatment plants, is remediated by mobilization processes that include phytoremediation and chemical washing.

This chapter focuses on the various sources of Cd in rice ecosystems and the biogeochemical processes that regulate Cd bioavailability to organisms, including microbes, plants, animals, and humans. After laying down the fundamental mechanisms and factors regulating Cd bioavailability, we then assemble the various physical, chemical, and biological mitigative methods that have been demonstrated, highlighting their special strengths and potential for more effective and economical widespread applications in rice fields. Because of the complexity involved in dealing with Cd in rice ecosystems, exacerbated by the Cd source, site characteristics, and the nature of water management strategies, no one remedial technology might suffice. Therefore, we have attempted to describe an "integrated" approach of employing a combination of technologies depending on extenuating circumstance, with the aim of securing methods that are, economically and technologically viable. Future research needs, especially in the area of Cd bioavailability and remediation strategies, are identified.



2. ORIGIN AND SOURCES OF CADMIUM IN PADDY SOILS

Trace elements include both biologically essential [e.g. copper (Cu), Cr, and zinc (Zn)] and nonessential [e.g. Cd, lead (Pb) and mercury (Hg)] elements (Sparks, 2003). The essential elements (for plant, animal or human nutrition) are required in low concentrations and hence are known as "micro nutrients." The nonessential trace elements are phytotoxic and/or zootoxic even at low concentration and are widely known as "toxic elements" or "heavy metals." Both groups are toxic to plants, animals and/or humans at excessive concentrations (Adriano, 2001; Alloway, 1990).

Most trace elements reach the soil environment through both pedogenic and anthropogenic processes. Some of them occur naturally in soil parent materials, chiefly in forms that are not readily bioavailable for plant uptake. Anthropogenic sources include mining and manufacturing activities, and the disposal of domestic and industrial waste materials (Adriano, 2001). Phosphate fertilizers and organic amendments including manures and biosolids are considered to be the major sources of certain trace elements [e.g. Cd, Cu, Zn and fluorine (F)] input to soils (Bolan et al., 2003a; Loganathan et al., 2008; Park et al., 2011).

2.1. Geogenic

In nature, Cd occurs mainly in association with Zn ores, of which sphalerite (zinc sulfide) forms the main commercial source of Cd. Although Cd occurs in most soil parent materials, its concentration in the common soil-forming rocks such as igneous rocks, sandstones, and limestone is generally low (Bramley, 1990; Loganathan et al., 2012; MacDonald et al., 2005). However, the concentration of Cd in rocks derived from lake sediments and marine black shales is considered to be high. Although none of these rocks occurs to any great extent in most agricultural soils, they can contribute to Cd accumulation, especially in paddy soils derived from these rocks.

The presence of black shales containing high concentrations of trace elements including Cd is significant in environmental geochemistry. For instance, the Okchon black shale, which is underlain by the black slates in the central part of the southern Korean Peninsula, provides a typical example of natural geological materials enriched with potentially toxic elements (Kim, 1989). The Okchon Zone of the central part of Korea with an area of about 5100 km^2 covers about 5.5% of the total territory of the entire country. Soils derived from these parent materials tend to reflect their extreme geochemical composition (Bowie and Thornton, 1984) and may influence human health by affecting the elemental composition of crop plants (Foth, 1978). In particular, barium (Ba), Cd, molybdenum (Mo), vanadium (V), and uranium (U) in Okchon black shale are highly enriched, and their mean concentrations are significantly higher than those in black slates (Chon et al., 1996; Kim and Thornton, 1993, Table 4.3). Cadmium occurs predominantly as an exchangeable phase in these soils, thereby influencing the high Cd uptake of crop plants.

Black shales act as a source of these elements in the rock–soil–plant–human system. Cd concentrations in surface soils are higher in most of the examined

areas (Chung-Joo, Duk-Pyung, Geum-Kwan, I-Won, Bo-Eun and Chu-Bu) than the world average of 0.4 mg kg^{-1} Cd quoted by Berrow and Reaves (1984) (Table 4.4; Lee et al., 1998). In the black shale areas, high Cd concentrations are found in residual soils developed from bedrock with high Cd concentrations. High Cd concentrations are also found in alluvial soils in the black slate, black shale, or gray chlorite schist areas. Cadmium concentrations in rice grains are higher in the black shale areas than in the black slate or gray chlorite schist areas. Mean Cd concentrations of rice cultivated in these areas were significantly higher than those in normal rice grown on uncontaminated soils (Masironi et al., 1977; Watanabe et al., 1989; Yoo et al., 1992). Among the six examined areas, the highest mean concentrations

Table 4.3 Ranges and Mean Concentrations of Cadmium in Black Shales and Slates from Different Areas in the Okchon Zone, Korea

	Cd Concentration (mg kg^{-1})	
Area	**Range**	**Arithmetic Mean**
Chung-Joo (N = 7)	0.5–6.5	1.4
Duk-Pyung (N = 9)	1.0–36.0	10.9
Geum-Kwan (N = 4)	0.4–0.6	0.5
I-Won (N = 5)	0.5–1.0	0.6
Bo-Eun (N = 5)	2.3–3.8	3.0
Chu-Bu (N = 10)	0.5–3.9	1.1
Average shale*		0.3
Average black shale†		1.0

*Turekian and Wedepohl (1961).
†Vine and Tourtelot (1970).
Modified from Lee et al. (1998)

Table 4.4 Cadmium Concentrations (mg kg^{-1}) of Rock, Soil and Rice (Dried Weight Base) Samples in the Duk-Pyung Area in the Okchon Zone, Korea

	Black Shale Area			Gray Chlorite Schist, or Black Slate Area		
Sample Type	**Range**	**Arithmetic Mean**	**Geometric Mean**	**Range**	**Arithmetic Mean**	**Geometric Mean**
Rock	0.4–46	6.3	2.4	0.4–1.7	0.8	0.8
Residual soil	0.3–3.9	1.3	1.0	0.5–1.2	0.8	0.7
Alluvial soil	0.3–8.3	1.2	0.9	0.3–11	1.1	0.8
Rice shoot	0.1–2.7	0.6	0.3	0.1–0.2	0.2	0.2
Rice stalk	1.0–6.6	1.7	1.0	0.1–1.7	0.5	0.3
Rice grain	0.1–3.5	0.6	0.4	0.2–0.3	0.2	0.2

Modified from Lee et al. (1998)

of 0.61 and 1.74 mg kg^{-1} Cd were found in rice grains and stalks from the Duk-Pyung area, respectively (Table 4.4; Lee et al., 1998).

2.2. Anthropogenic

Prior to the industrial revolution, Cd entered agriculture systems at a slow rate as a result of the weathering of rocks and volcanic activity. Now Cd is released into the environment through various industrial processes that include smelting of metals, combustion of coal, oil and wood, and incineration of wastes. The use of P fertilizers and the disposal of sewage sludges and mine tailings directly add Cd to soil.

Phosphate compounds contain a suite of trace elements (Bolan et al., 2003a; Loganathan et al., 2008; McLaughlin et al., 1996; Mortvedt, 1996; Syers et al., 1986). Addition of P compounds to soils not only helps to overcome the deficiency of some of the essential trace elements, such as Mo, but may also introduce toxic trace elements, such as Cd and F (Loganathan et al., 2008; McLaughlin et al., 1996; Naidu et al., 1997, Table 4.5). In this context, Cd contamination of agricultural soils is of particular concern because this trace element reaches the food chain through regular and frequent use of Cd-containing P fertilizer materials, such as single superphosphate (SSP), triple superphosphate (TSP), and phosphate rocks (PRs) (Loganathan et al., 2008). Moreover, presence of Cd in amounts exceeding food guidelines has implications on both local and international trade.

Accumulation of Cd in soils through regular fertilizer use has been observed in many countries. For example, in New Zealand and Australia, most of the Cd and F accumulation in pasture soils has been attributed to the use of P fertilizers containing these trace elements (Loganathan et al., 2008). The Cd and F in most P fertilizers originate mainly from the PRs used for manufacturing P fertilizers. It is important to stress that, depending on the source, the PR deposits vary in their Cd content (Bolan et al., 2003a). Thus, manufactured P fertilizers also vary accordingly in their Cd content. The Cd in superphosphates is water soluble and high-analysis P fertilizers, such as TSP and ammonium phosphates, generally contain lower Cd content relative to P (Loganathan et al., 2003). However, depending on the calcium (Ca) content of P fertilizers, the bioavailability of Cd is likely to vary among the P fertilizers. The Ca ion, in addition to competing with Cd for sorption sites, will also reduce the surface negative charge density of soil colloid particles, thereby influencing the bioavailability of Cd (Naidu et al., 1997).

Positive relationships between total P and total Cd or F in soils that have received accumulative P fertilizers have often been observed

Table 4.5 Selected References on Sources of Cadmium Input (as a Cocontaminant) to Soils

P Compound*	P Loading (kg P ha^{-1})	Farming System	Observation	References
SSP	188, 376 for 44 years	Pasture	Increased total soil Cd in the 0–75 mm depth from 0.055 to 0.219 mg Cd kg^{-1} (low P rate) and 0.049–0.432 mg Cd kg^{-1} (high rates); the rate of Cd accumulation in the topsoil for the high P rate was estimated at 7.8 g Cd ha^{-1} $year^{-1}$.	Gray et al. (1999a)
PR, $Ca(H_2PO_4)_2$	30	Pasture	Cd-containing NPK fertilizers increased Cd concentration in ryegrass, carrot and spinach; Cd uptake decreased with increasing pH; low recovery of Cd from PR.	He and Singh (1994)
P	0–780	Mine tailing soil	Significantly increased radish Cd uptake.	Hong et al. (2005)
NC-SSP, NC-PR, Togo-PR, Togo PAPR, Togo-SSP	126–320	P amended upland paddy soil	Cd uptake by rice grains followed the order of NC-SSP > NC-PR and Togo SSP > Togo PAPR > Togo PR.	Iretskaya et al. (1998)
DAP, SSP	450	Horticulture	The soils had 4–>100 years of fertilizer history, but the increase in soil Cd was more closely related to Cd input through poultry manure than through fertilizers.	Jinadasa et al. (1997)
Phosphate ($Na_4P_2O_7 \cdot 10H_2O$)	250	Sewage sludge (SS) and P-treated soil	Cd decreased with incubation time and was reduced by the SS and P additions.	Karaca et al. (2002)

Continued

Table 4.5 Selected References on Sources of Cadmium Input (as a Cocontaminant) to Soils—cont'd

P Compound*	P Loading (kg P ha^{-1})	Farming System	Observation	References
SSP	0–400	P-treated paddy soil	Grain Cd affected but did not exceed the permissible concentration.	Lavres et al. (2011)
SSP	0, 113, 765	Pasture	Total Cd increased from 0.10 to 0.4 mg kg^{-1}; linear relationship between total P and total Cd in soils.	Loganathan et al. (1995)
DAP, JPR, NCPR, SSP	0–60 for 10 years	Pasture	Total Cd concentration increased in the top 120 mm depth; total and plant available Cd was higher in soils treated with high Cd-containing fertilizers.	Loganathan et al. (1996); Loganathan and Hedley (1997)
HRP, NCPR, PAPR	40–320	Pasture	No effect of fertilizer addition on F concentration in clover; whereas fertilizer addition increased Cd concentration in clover.	McLaughlin et al. (1997)
TSP, K_2SO_4	250	Biosolid and P-treated soil	Maximum grain Cd in 20 t ha^{-1} biosolid + 1/2 P fertilizer treatment.	Mousavi et al. (2010)
SSP	188, 376 for 39 years	Pasture	Total Cd in soil ranged from 0.024 to 0.14 mg kg^{-1} in the unfertilized soils and from 0.085 to 0.34 Cd kg^{-1} in the P-fertilized soils; obtained a significant correlation between total soil P and Cd.	Roberts et al. (1994)

NPK fertilizers, PR	0–188	NPK-fertilized soil	DTPA extractable Cd increased with increasing level of Cd addition; there was no effect of Cd addition on plant uptake.	Singh and Myhr (1998)
DSP, TSP	0–240	Horticulture	Potato tuber Cd concentration increased with increasing amount of Cd applied in P fertilizers; liming did not affect tuber Cd concentration.	Sparrow et al. (1993)
SSP	185–4000	Pasture	Both soil and plant Cd levels were higher in the fertilized plots than the control plots; Cd uptake decreased with increasing pH	Williams and David (1976)

*DAP—diammonium phosphate, DSP—double superphosphate, FSP—fused superphosphate; JPR—Jordan phosphate rock, NCPR—North Carolina phosphate rock, NCSSP—North Carolina single superphosphate; HRP—Hamrawein phosphate rock; SSP—single superphosphate, TSP—triple superphosphate; PR—phosphate rock; PAPR—partially acidulated phosphate rock.

(Fig. 4.1; Loganathan et al., 2003). Comparison between unfertilized native and fertilized agricultural soils has often been employed to scrutinize the link between soil contamination and agricultural practices. For example, Roberts et al. (1994), Gray et al. (1999a) and Loganathan et al. (1995) obtained significant positive correlations between total P and total Cd in pasture soils in New Zealand receiving long-term inputs of superphosphates. Similar results were also obtained for a range of Australian soils (McLaughlin et al., 1996). This is not surprising considering the long history of use in both New Zealand and Australia of superphosphates manufactured from PRs containing high levels of Cd (Rothbaum et al., 1986; Schipper et al., 2011).

A number of studies have reported that Cd is derived primarily from P fertilizers used in paddy soils. The application of Mussoorie PR to cultivated paddy areas in India caused an increase in Cd content of the rice grain (Ramachandran et al., 1998), and in Malaysia, small amounts of Cd in the bioavailable form were found to be present in paddy soils (Khairiah et al., 2009). Iretskaya et al. (1998) found that Cd in PR was not readily

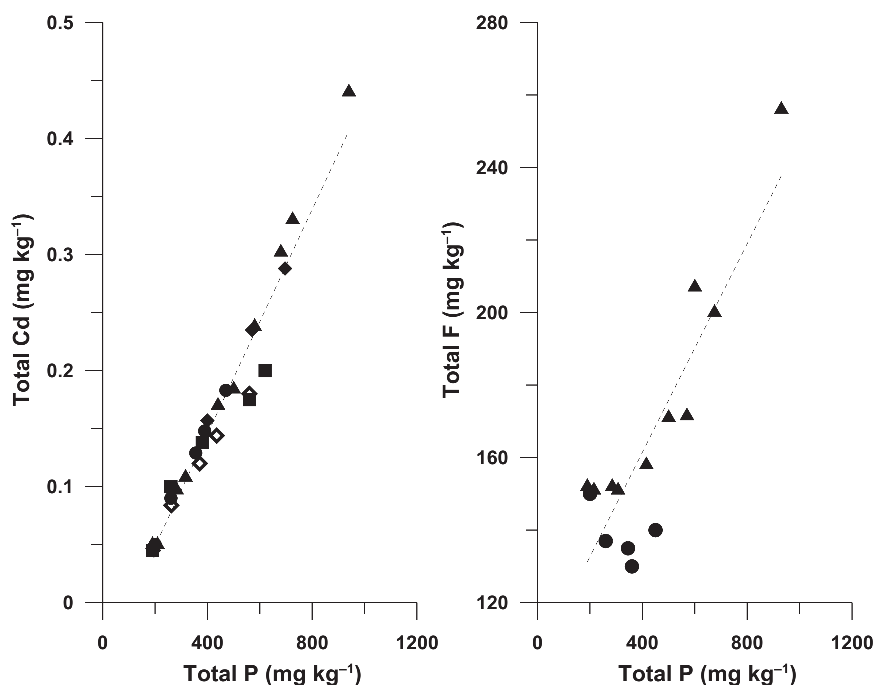


Figure 4.1 Relationship between total P and total Cd or F in soils [●, control; ▲, SSP (single superphosphate); ◆, JPR (Jordan phosphate rock); ■, NCPR (North Carolina phosphate rock); ◇, DAP (Diammonium phosphate)] (Loganathan et al., 1999).

available to rice within few months following its addition to limed soils. However, they noticed that the availability increased markedly in the second year. While the exact mechanism was unclear, they presumed that an increased dissolution of PR, particularly in the acidic soil environments, occurred. Jiaka et al. (2009) studied the effects of different P fertilizers on yields and Cd uptake by paddy rice. Among the three P fertilizer treatments, they observed that amounts of Cd uptake by paddy rice were closely correlated with the amounts of ammonium (NH_4) contained in the P fertilizers. The two NH_4-bearing P fertilizers [$(NH_4)_2HPO_4$ and $NH_4H_2PO_4$] significantly promoted Cd uptake by rice compared to $Ca(H_2PO_4)_2$; also, $(NH_4)_2HPO_4$ increased Cd uptake by rice more than $NH_4H_2PO_4$. This may be attributed to the acidification caused by NH_4 fertilizers, thereby resulting in the enhanced mobilization and bioavailability of Cd.

In another study, Jamil et al. (2011) evaluated the heavy metal contamination including Cd in slightly acidic cultivated paddy areas, exposed to fluctuating redox conditions. Their results revealed that high amounts of bioavailable Cd in paddy soils might be attributed to the soil type, redox condition, and repeated application of fertilizers in the study areas. The study found that all of the fertilizers commonly used for rice cultivation contained a certain amount of Cd. Although present in small quantities, the investigators warned that Cd could accumulate in soils after several years of application of fertilizers. Recently, Lavres et al. (2011) investigated the P uptake by upland rice and subsequent accumulation in grains from superphosphate fertilizers produced with sulfuric acid treatments of Brazilian PRs. Another objective of their study was to determine the translocation of Cd from P fertilizers to rice grains. Their results revealed that although the grain Cd concentration was significantly affected by P rates, it did not exceed the permissible concentration for human consumption, according to Brazilian food legislation.

Conventionally, the term, biosolids (also called "sewage sludge"), refers to the final product derived from the biological treatment of municipal sewage wastewaters. However, recently, the terminology connotates a more inclusive definition to include also livestock manure and other organic wastes, especially when they are composted in the presence of sewage sludge (e.g. greenwaste compost). Most metals, including Cd in biosolids, originate primarily from the contamination of these wastes with industrial wastewater. Traditionally, biosolids are viewed as one of the major sources of metal accumulation in soils, and a large volume of work has been carried to examine the mobilization and bioavailability of biosolids-borne metals in

soil (Bolan et al., 2003b; Haynes et al., 2009; Park et al., 2011). Advances in the treatment of sewage water and isolation of industrial wastewater in the sewage treatment plants have resulted in a steady decline in the metal content of biosolids (Esmaeily, 2002). Furthermore, stabilization using alkaline materials has resulted in the immobilization of metals in biosolids (Basta et al., 2001; Bolan et al., 2003b). Composted alkaline-stabilized biosolids that are low in total and/or bioavailable metal content (known in the USA as "exceptional quality" biosolids; Basta and Sloan, 1999) can be used as an effective sink for reducing the bioavailability of metals in contaminated soils and sediments (Park et al., 2011). However, in most developing countries, biosolids are still considered as a major source of heavy metal input to soils (Haynes et al., 2009).

Although many countries have formulated threshold levels for Cd and other heavy metal accumulation in soils due to the use of municipal sewage sludge, such limits have not been established for fertilizer use. Based on the regulatory threshold level for sewage application (3 mg Cd kg^{-1} soil), the number of years required that would exceed this threshold limit in soil through addition of various sources of Cd including P fertilizer and biosolids is presented in Table 4.6. This indicates that although fertilizer addition represents the major source of Cd input to soils, at the normal annual rate of fertilizer input (20–40 kg P ha^{-1}) to soils, the rate of Cd

Table 4.6 Phosphorus (P) and Cadmium (Cd) Contents in Various Phosphate Fertilizers and Organic Amendments, and the Estimated Number of Years Required to Exceed the Threshold Concentration of Cd (3 mg Cd kg^{-1}) in Rice Soils due to their Application

Phosphate Fertilizer	Concentration: P (g kg^{-1})	Concentration: Cd (mg kg^{-1})	Years Required to Exceed the Threshold Limit*
Single superphosphate	98	32	149–298
Triple superphosphate	190	70	132–264
Diammonium phosphate	200	10	975–1950
North Carolina phosphate rock	132	54	119–238
Sechura phosphate rock	131	12	532–1064
Egyptian phosphate rock	130	10	633–1267
Gafsa phosphate rock	134	70	93–186
Farm yard manure	7.5	7.6	48–96
Biosolid	8.5	32	12–25
Poultry manure	17.8	7.5	115–231
Mushroom compost	5.3	3.1	84–166

*At an annual phosphorus application rate of 20–40 kg P ha^{-1} for rice soils (bulk density of rice soil = 1300 kg m^{-3} to a depth of 5 cm)

accumulation appears to be very slow; however, continuous addition of biosolids as a carbon and nutrient source could accelerate the accumulation of Cd in soils.

Anthropogenic activities such as mining and smelting of metal ores have increased the occurrence of heavy metal contamination of soil and water sources. Specifically, opencast mining activities have a serious environmental impact on soils and water streams and have generated millions of tons of sulfide-rich tailings (Bhattacharya et al., 2006). Moreover, acidic drainage resulting from the oxidation of sulfides from metalliferous mine spoils leads to the leaching of large quantities of metals including iron (Fe^{2+}), manganese (Mn^{2+}), Pb^{2+}, Cu^{2+}, Zn^{2+}, etc. (Vega et al., 2006). Thus, metal contamination and acid-mine drainage are major environmental concerns where waste materials containing metal-rich sulfides from mining activity have been stored or abandoned (Concas et al., 2006).

In general, Cd concentrations in rice and vegetables in the dense mining areas were found to be remarkably higher than those in areas with less mining (Ok et al., 2011; Zhai et al., 2008). Long-term Cd exposure by regular consumption of rice and vegetables posed potential health problems to residents in the vicinity of mines. For example, despite the restoration schemes currently in operation, over 1000 abandoned metal mines are still present in South Korea, posing a potential risk to humans and to the ecosystems (Kim et al., 2005). Large amounts of mine wastes including tailings have been left without proper environmental treatment, thus becoming an important point source of toxic elements such as arsenic (As), Cd, Cu, Pb, and Zn in the environment. These materials are dispersed down slope by surface erosion, wind action, and effluent draining from the mine wastes contaminating the low-lying arable lands. In South Korea, 21% of arable soil near mining and industrial areas was found to be contaminated by heavy metals (NIAST, 1997).

For example, the Daduk gold (Au)–silver (Ag)–Pb–Zn mine, which is located in the middle part of Korea, is a major source of heavy metal contamination of arable soils. This mine was one of the largest Au–Ag–Pb–Zn mines in Korea. The mine ceased production in 1984 and large amounts of mine wastes have been left without proper environmental treatment. The mine tailings contained high concentration of heavy metals, and they were dispersed down slope by erosion and effluent draining into low-lying land, mainly used for paddy cultivation. Elevated levels of Cd were found in soils sampled in paddy fields and the forest area (Table 4.7). According to the Korean Soil Environmental Conservation Act, soils containing more than

Table 4.7 Concentration of Cadmium in Mine Tailings and Surface Soils Collected from the Abandoned Daduk Au–Ag–Pb–Zn Mining Area

Sample Type		Total Cd (mg kg^{-1})		0.1 N HCl Extractable Cd (mg kg^{-1})	
		Arithmetic Mean	Range	Arithmetic Mean	Range
Tailings and soils	*Contaminated area*				
	Tailing (n = 12)	8.57	1.56–36.0	5.67	0.05–38.4
	Paddy (n = 34)	1.78	0.40–4.76	0.78	0.10–2.49
	Forest (n = 8)	1.30	0.80–2.20	0.38	0.13–1.21
	Control area				
	Paddy (n = 24)	1.18	0.48–4.24	0.35	0.07–2.5
	Forest (n = 4)	0.77	0.64–0.96	0.09	0.07–0.09
Rice plants	*Contaminated area*				
	Grain (n = 8)	0.15	0.03–0.65		
	Stalks and leaves (n = 20)	0.80	0.11–5.85		
	Control area				
	Grain (n = 6)	0.09	0.01–0.24		
	Stalks and leaves (n = 10)	0.64	0.12–2.95		

Modified from Lee et al. (2001)

1.5 kg^{-1} Cd extracted by 0.1 N HCl solution and 4.0 mg kg^{-1} Cd in total need to be continuously monitored and not used for agricultural purposes, respectively.

In urban and semiurban areas throughout Asia, paddy fields for rice production are often close to industrial sites that discharge part of their chemical waste into irrigation channels used for flooding paddy fields (Lin, 2002; Wang et al., 2007; Plate 4.1). Wastewater discharged from metal plating factories (Higurashi et al., 1976), coating and paint factories (Masui et al., 1971), and electronics and home appliance manufacturing plants (Asami, 1974; Asami et al., 1984; Matsuzaki et al., 1987) is also an important source of Cd contamination. This wastewater often becomes mixed with irrigation water and, thus, contaminates paddy fields.

In particular, the metal-smelting process is regarded as the most important Cd contamination source to paddy soils. For example, Cu and Zn mining was the main activity at many nonferrous metal mines in Asian countries like China, Japan, and Korea. At these sites, Cd present in Cu and Zn ores was removed during the concentration or smelting processes and released into the environment with the wastewater and smoke. This



Plate 4.1 Paddy fields in front of electric factory, leading to heavy-metal contamination. For color version of this figure, the reader is referred to the online version of this book.

discharged Cd was then carried to agricultural land by water and wind, causing soil contamination (Asami, 1972; Fujimoto and Yamashita, 1976). A Zn smelting factory located in the eastern part of the Korean peninsula is a typical example of Cd contamination resulting from the smelting process. This is the third largest Zn smelting facility in the world. This factory, founded in the 1970s, produces 280,000 tons of Zn, 450,000 tons of sulfuric acid, 1700 tons of Cu, and 900 tons of Cd per year. However, there have been issues reported previously concerning the ill-health effects of heavy metals on exposed workers, living communities, and the environment. Specifically, about 20 ha of arable land near the factory cultivated with different crops were reported to be contaminated by Cd and Zn. The average values for 0.1 N HCl extractable Cd and Zn concentration were 1.7 ± 0.7 and 407 ± 143 mg kg^{-1}, respectively. About 65% (Cd) and 80% (Zn) of the total sampling sites gave values higher than the warning level (0.1 N HCl extractable Cd 1.5 mg kg^{-1}; Hong et al., 2009).

Recently there has been an exponential increase in the production of nickel (Ni)–Cd batteries, especially after the introduction of hybrid car production. For example, in Japan, the domestic production of Cd was over 2000 tons while about 4000 tons of Cd were imported in 2000. Of this amount, the production of Ni–Cd batteries accounted for more than 90% at about 5400–5500 tons. Large numbers of Ni–Cd batteries were distributed domestically and were also exported. Because the recycling rate for batteries is low, it is estimated that more than 1000 tons of Cd may pollute the Japanese environment every year. However, there is no quantitative investigative data on Cd contamination of arable soil by Ni–Cd battery production. In addition,

the illegal dumping of home electronics products is increasing every year and has become a social problem. Although the number of dumped Ni–Cd batteries and the products using them have not been investigated, it is thought that a considerable amount has been dumped in wooded areas and deserted fields near agricultural land, so that there is the risk of Cd leaking out from illegally dumped Ni–Cd batteries and contaminating agricultural soil.



3. BIOGEOCHEMISTRY OF CADMIUM IN THE ENVIRONMENT

3.1. Distribution and Speciation

In soils, Cd occurs in various forms which include free ions in solution, soluble and insoluble inorganic and organometallic complexes, ions absorbed onto Fe, aluminum (Al) and Mn hydrous oxides, precipitates such as sulfides, phosphates, and carbonates, and minerals, primarily biotite and riebeckite (Adriano, 2001; Peterson and Alloway, 1979). Understanding the factors controlling Cd speciation and bioavailability in flooded, drained, and alternately flooded/drained paddy soil will be crucial to developing and implementing best management practices needed for productive agricultural areas. Unlike upland soil, lowland rice paddy soil undergoes a flooding and draining cycle, which can change soil conditions into anaerobic and aerobic states and modify the biological and chemical properties of the soil, especially pH and redox potential (Eh) (Kögel-Knabner et al., 2010). These modifications of soil properties may affect Cd speciation present in the Cd-contaminated paddy soils.

Waterlogging of paddy soils contributes to an increased pH of acid soils and a decrease in pH of alkaline soils. Therefore, the pH tends to converge to neutral, whether the initial soil was acidic or alkaline. Increased pH in acid soils may result in more negative charges on soil clay colloids and organic matter (OM) surfaces, and, therefore, decreases the exchangeable heavy metals by immobilization (Yuan and Lavkulich, 1997). Lim et al. (2002) investigated the changes of speciation of Cd in a tropical coastal clay soil at various pH values at different times and found that the changes of Cd in the exchangeable fraction were pH-dependent. Generally, the change was small under acidic conditions and larger decreases occurred at pH 7. By monitoring the process of heavy metals on iron oxide (α-FeOOH), Martínez and McBride (2001) found that either adsorption or coprecipitation of heavy metals with ferrihydrite was pH-dependent. They also found that an increasing pH and incubation time resulted in an increase of

adsorption and coprecipitation of heavy metals. Zheng and Zhang (2011) suggested that increased concentrations of an OM-bound Cd fraction in flooded soil was probably due to metal–organic complex formation, which has a higher magnitude in waterlogged soils, because lower values of Eh and higher values of pH favored the formation of metal–organic complexes (Gambrell, 1994) and microbial immobilization (Haldar and Mandal, 1979).

In waterlogged paddy soils, biological and microbiological activities combined with limited oxygen diffusion causes oxygen depletion, thus resulting in reducing conditions (Kögel-Knabner et al., 2010). In this situation, there is an observable change where a decrement of Eh is followed by an associated increase of pH toward neutrality (Narteh and Sahrawat, 1999). Moreover, the intensity of reduction is higher in the presence of OM due to its oxidizability, and soil components are reduced by anaerobic microbial respiration (Conrad and Frenzel, 2002; Ponnamperuma, 1972). In waterlogged soils, reducing conditions would cause the oxides of Fe and Mn in soil solid phases to be reduced and dissolved (Iu et al., 1981; Ma and Dong, 2004). Chuan et al. (1996) pointed that the pH-dependent metal adsorption reaction and the dissolution of Fe–Mn oxyhydroxides under reducing conditions were the mechanisms controlling heavy-metal mobility in acidic soils. Reduced Fe and Mn via hydrolysis and oxidation precipitate as highly amorphous hydrous oxides that have a strong sorption capacity for trace elements (Shuman, 1976). Kashem and Singh (2004) also observed that the breakdown of Fe and Mn oxides caused by waterlogging provided, on one hand, surfaces with high adsorbing capacity for Cd and Zn but, on the other hand, increased concentrations of Fe and Mn in the mobile fraction. Kashem and Singh (2001) suggested that adsorption of trace metals on Fe–Mn oxyhydroxide fractions was the major mechanism of their solubility reduction in submerged conditions. Zheng and Zhang (2011) demonstrated that Cd added to paddy soil in a soluble form under flooding moisture regimes was transformed slowly and consistently from the exchangeable fraction to more stable fractions (Fe–Mn oxide- and OM-bound), leading to the decrease of metal mobility in paddy soil. They suggested that the paddy soil under a flooding regime had higher metal reactivity resulting in more complete transformation of metals to stable fractions, which might be related to increased pH, precipitation of the metals with sulfides, and higher concentrations of amorphous Fe oxides under submerged condition.

Cadmium is associated with several mineral phases during flooding periods in paddy soils, including carbonates, humic acid, ferrihydrite, kaolinite, and cadmium sulfide (CdS) (Khaokaew et al., 2011). In general,

Cd carbonates ($CdCO_3$) and Cd–humic complexes are the major species in lowland paddy soils, while a small amount of CdS was found after the soils were flooded for longer periods (Khaokaew et al., 2011). Insoluble sulfide forms of metals would be generated in reductive conditions driven by flooding, which could be one of the reasons why heavy metals exhibit low mobility in waterlogged soil. Most metal sulfides are highly insoluble (Sposito, 1994), and under the indirect effects of flooding conditions (low Eh), sulfate ions are reduced to the sulfide form, which might form a complex with heavy metals and immobilize them as sulfide salts (de Livera et al., 2011; Gambrell and Patrick, 1988). Calmano et al. (1993) reported that generally the easily and moderately reducible fractions increase during oxidation while the sulfidic fraction decreases.

Humic acids enhance Cd sorption to hematite, goethite, or kaolinite (Arias et al., 2002; Davis and Bhatnagar, 1995; Lai et al., 2002). Humic acids can directly bind metals via their functional groups, and sorb to oxides and clay minerals, allowing the formation of ternary surface complexes (Arias et al., 2002; Weber et al., 2006). Cadmium bound to humic acids is not stable, especially at lower pH values (Candelaria and Chang, 1997; Kunhikrishnan et al., 2012; Zachara et al., 1994). In addition, Cd and Ca can compete for adsorption sites on calcite in alkaline soils since Cd^{2+} and Ca^{2+} have similar hydrated ionic radii (Garin et al., 2003; McBride, 1980; Pickering, 1983; Zachara et al., 1994). Therefore, a mixture of (Cd, Ca)CO_3 precipitates can occur at calcite surfaces (Stipp et al., 1992). Mononuclear Cd^{2+} can chemisorb to the calcite surface at low-Cd concentrations, and/or precipitate to form $CdCO_3$ at high Cd loadings (McBride, 1980; Prieto et al., 2003). Liming causes precipitation of Cd as $CdCO_3$ and a significant decrease of the exchangeable fraction of Cd in contaminated soil (Knox et al., 2001). The formation of Cd carbonates, Cd-kaolinite, and CdS species in paddy soils could limit the release of Cd from soil and Cd uptake by the rice plant.

After entering the soil, Cd may be distributed among soil components and associated with them in various forms, which have often been referred to as speciation (Onyatta and Huang, 1999). To characterize the activities of Cd in soil, information about both total concentration and chemical speciation is necessary. However, in order to measure Cd activity in soil and to determine how readily Cd uptake by plants occurs, it is necessary to evaluate the chemical speciation rather than the total Cd content as the former determines the mobility and bioavailability of Cd (Huang et al., 1988; Kazi et al., 2005). Generally, most speciation studies are carried out using single or sequential extractions using diverse reagents with different

chemical properties (Arain et al., 2008; Rauret, 1998). Sequential extraction techniques provide a powerful tool for evaluating metal forms (Grzebisz et al., 1997; Shuman, 1985).

There are many methods for classifying heavy metal fractionations (Ahnstrom and Parker, 1999; Krishnamurti and Naidu, 2002; Qiao et al., 2003; Silveira et al., 2006; Tessier et al., 1979). Widely used is Tessier's five-step sequential extraction procedure (Tessier et al., 1979), in which heavy metals in soils were categorized in five chemical fractionations including the exchangeable fractionation (F1), carbonate-bound fractionation (F2), Fe–Mn-oxide-bound fractionation (F3), OM-bound fractionation (F4), and residual fractionation (F5) (Silveira et al., 2006; Tessier et al., 1979). F1 is the bioavailable fractionation; F2, F3, and F4 are potentially bioavailable fractionations and F5 is the nonbioavailable fractionation (He et al., 2005; Ma and Rao, 1997). The scheme was developed for sediments but it can also be applied to soils.

3.2. Biogeochemistry of Cadmium

The important factors that affect the activity of Cd in soils and its availability for plant uptake include soil pH, soil OM content, the metal sorption capacity of the soils, the presence of other micro elements (e.g. Zn) and macro elements (e.g. P), and soil temperature, moisture, and aeration (Bolan et al., 2003a; Chaney and Hornick, 1977; Loganathan et al., 2012). The affinity of Cd for soil surfaces is dependent on the pH and the type of surfaces. The affinity of Cd increases with pH and decreases with concentration of Cd added (Loganathan et al., 2012; Naidu et al., 1994).

Adsorption of metals almost invariably decreases with increasing soil acidity (Basta and Tabatabai, 1992; Bolan et al., 1999a; Naidu et al., 1994; Tiller, 1988). Three possible reasons have been advanced for this phenomenon (Naidu et al., 1994). First, in variable-charge soils, a decrease in pH causes a decrease in surface negative charge, lowering cation adsorption. The amount of surface charge acquired through an increase in pH depends on the amount and nature of variable-charge components (Bolan et al., 1999b). However, Bolan et al. (2003c) noticed that although there was a positive relationship between increases in pH-induced surface charge through liming and Cd^{2+} adsorption, only a small fraction of the surface charge was occupied by Cd^{2+}. Second, a decrease in soil pH is likely to decrease hydroxy species of metal cations (MOH^{n+}), which are adsorbed preferentially over mere metal cations (Hodgson et al., 1964). For example, Naidu et al. (1994) observed that $CdOH^{+}$ species dominate at above pH 8,

which have greater affinity for adsorption sites than just Cd^{2+}. And third, acidification causes the dissolution of metal compounds, increasing the concentration of metals in soil solution.

Liming, as part of normal cultural practices, has often been shown to reduce the concentration of Cd and other metals in the edible parts of a number of crops (Bolan et al., 2003c; Hong et al., 2010a; Lee et al., 2004) (Table 4.8). Addition of other alkaline waste materials such as coal fly ash has also been shown to decrease Cd content of plants (Pourrut et al., 2011). In these cases, the effect of liming materials in decreasing Cd uptake has been attributed to both decreased mobility of Cd in soils and to competition between Ca^{2+} and Cd^{2+} ions on the root surface. In general, Cd uptake by plants decreases with increasing pH. For example, higher Cd concentrations were obtained for lettuce (*Lactuca sativa* L.) and Swiss chard (*Beta vulgaris* L.) on acid soils (pH 4.8–5.7) than on calcareous soils (pH 7.4–7.8) (Mahler et al., 1978; Szomolányi and Lehoczky, 2002). Consequently, it is recommended that soil pH be maintained at pH 6.5 or greater in land receiving biosolids containing Cd (Adriano, 2001; Evanylo, 2009). However, it is also possible that in alkaline soils, solubility of Cd can be enhanced due to facilitated complexation of Cd with humic or organic acids (Bolan et al., 2011; Harter and Naidu, 1995). Thus, the resultant effect of liming on Cd (im)mobilization and subsequent phytoavailability depends on the relative changes in pH and Ca^{2+} concentration in the soil solution.

Ok et al. (2011) conducted laboratory and greenhouse experiments to assess the effects of contaminated rice paddy soils amended with several ameliorants including lime to immobilize Cd and inhibit Cd translocation to rice grain. Sequential extraction analysis revealed that treatment with the ameliorants induced a 50–90% decrease in the bioavailable Cd fractions when compared to the untreated control soil. Their results showed that Cd uptake by rice was decreased by 65% in soils treated with lime compared to the control. But they noticed that ameliorants did not influence rice yield when compared to that of the control. In another pot study, Li et al. (2008) studied the effect of several amendments including limestone on rice growth and uptake of Cd from a Cd-contaminated paddy soil. Their results demonstrated that application of limestone increased grain yield by 12.5–16.5-fold, and decreased Cd concentrations in grain by 50.4%. They suggested that concentrations of Cd in grain and straw were dependent on the available Cd in the soils, and soil-available Cd was significantly affected by the soil pH.

Table 4.8 Selected References on the Immobilization and Phytoavailability of Cadmium by Various Soil Amendments

Soil Amendments	Cadmium Source	Observation	References
Palygorskite; Sepiolite	Highly polluted mine soil	Maximum Cd sorption capacity at pH 5–6; soluble and readily extractable Cd fraction decreased; 66% and 59% reduction in Cd leaching with palygorskite and sepiolite, respectively.	Álvarez-Ayuso and García-Sánchez (2003a; 2003b)
$Ca(OH)_2$ (8, 15 and 22 Mg ha^{-1})	Limed biosolids (spiked with $Cd(NO_3)_2$)	Decreased soil solution Cd and plant uptake of Cd	Basta and Sloan (1999)
PR (NCPR)	Smelter-contaminated soil	PR decreased the gastrointestinal bioavailability of Cd by 23 and 92% in gastric and intestinal solution, respectively.	Basta et al. (2001)
$CaCO_3$ (10 g kg^{-1})	Cd-enriched sewage sludge	Decreased Cd phytotoxicity in wheat	Bingham et al. (1979)
KH_2PO_4, $Ca(H_2PO_4)_2$	Variable-charge soil	Cd adsorption increased with increasing level of P, which was attributed to increased negative charge; Cd adsorption was less in the presence of $Ca(H_2PO_4)_2$ than KH_2PO_4, which was attributed to increased competition from Ca.	Bolan et al. (1999a; 2003d)
$Ca(OH)_2$ (8, 15 and 22 Mg ha^{-1})	Sewage sludge	Decreased the solution Cd; increased residual fraction and plant uptake of Cd	Brallier et al. (1996)
$Ca(OH)_2$ and $CaCO_3$ (0–1120 kg ha^{-1})	Sand	Reduced Cd phytotoxicity	Chaney et al. (1977)
PR waste clay	Sewage sludge	DTPA extractable soil Cd and Cd uptake by alfalfa grown on a sludge-amended soil was suppressed by the addition of PR waste clay.	Gonzalez et al. (1992)

Continued

Table 4.8 Selected References on the Immobilization and Phytoavailability of Cadmium by Various Soil Amendments—cont'd

Soil Amendments	Cadmium Source	Observation	References
$Ca(OH)_2$	Arable soil-fertilizer Cd	Decreased Cd in chemical extractants and plant tissue	Gray et al. (1999b)
$CaCO_3$ (to pH 7.4)	Arable soil/sewage sludge	Decreased Cd^{2+} adsorption	Hooda and Alloway (1996)
$CaCO_3$, $Ca(OH)_2$, $CaSO_4.2H_2O$, Oyster shell meal	Heavy-metal-contaminated soil	$Ca(OH)_2$ was found to be more efficient on reducing soil NH_4OAc extractable Cd and plant-Cd concentrations, due to increased net-negative charge of soil induced by pH increase.	Hong et al. (2007)
$CaCO_3$ (17.92 Mg ha^{-1})	Sewage sludge and milorganite	Decreased uptake of Cd by plants resulting in Cd attenuation	John and Van Laerhoven (1976)
$CaMgCO_3$ (4 Mg ha^{-1})	Forest soil	Decreased Cd concentration in soil solution	Kreutzer (1995)
$CaCO_3$ (0–20 Mg ha^{-1})	Arable soil	Increased Cd concentration in potato tuber	Maier et al. (1997)
Hydroxyapatite (HA)	Cd solution (spiked with $Cd(NO_3)_2$)	HA removed Cd from aqueous solutions with efficiency higher than 99.5% at pH 5–6. XRD and SEM indicated that Cd is incorporated into the hydroxyapatite structure via diffusion and ion exchange.	Mandjiny et al. (1998)
$(NH_4)_2HPO_4$	Smelter-contaminated soil	P decreased the leaching of Cd through precipitation as metal phosphate; solubility diagram provided evidence for $Cd_3(PO_4)_2$.	McGowen et al. (2001)

Natural oyster shell powder (NOSP) and calcined oyster shell powder (COSP)	Mine tailings soil	After 30 days of incubation, 0.1 N HCl extractable Cd in soil decreased significantly as a result of an increase in soil pH and the formation of metal hydroxides. COSP was more effective in immobilizing Cd than NOSP.	Ok et al. (2010)
Zerovalent iron (ZVI), lime, humus, compost	Metal-contaminated paddy soil	Compared to the control Cd uptake by rice was decreased by: ZVI + humus (69%), lime (65%), ZVI + compost (61%), compost (46%), ZVI (42%), and humus (14%).	Ok et al. (2011)
$CaCO_3$ (0–2.5 Mg ha^{-1})	Arable soil	Decreased Cd concentration in barley grain	Oliver et al. (1996)
K_2HPO_4	Cd-amended artificial soil	Decreased the solubility and bioavailability of Cd to earthworms. XRD indicated $Cd_3(PO_4)_2$ formation.	Pearson et al. (2000)
Hydroxyapatite (HA)	Contaminated soil	Decreased solution concentration through secondary precipitates rather than sorption by weathered hydroxyapatite grains.	Seaman et al. (2001)
Aqueous palygorskite, sepiolite and calcite	Cd-amended soil	Average amount of Cd released after five desorption steps was 13.8%, 2.2% and 3.6% for the palygorskite, sepiolite and calcite, respectively, indicating that a large portion of Cd was irreversibly retained by the minerals.	Shirvani et al. (2006)

Continued

Table 4.8 Selected References on the Immobilization and Phytoavailability of Cadmium by Various Soil Amendments—cont'd

Soil Amendments	Cadmium Source	Observation	References
$CaCO_3$	NPK fertilizer	Decreased DTPA and NH_4NO_3 extractable Cd; increased plant-tissue Cd	Singh and Myhr (1998)
$CaCO_3$ (1–5 g kg^{-1})	Arable soil	Decreased DTPA and NH_4NO_3 extractable Cd, and plant-tissue Cd	Singh et al. (1995)
P-rich biosolid	Cd-spiked soil (spiked with $Cd(NO_3)_2$)	Cd adsorption increased with increasing pH; about 82–92% of adsorbed Cd was retained by cation exchange and complexing sites; adsorption by cation exchange became more dominant as the amount of Cd in the soil was increased.	Soon (1981)
$CaCO_3$	Pasture soil	Decreased Cd concentration in plant tissue	Tyler and Olsson (2001)
$Ca(OH)_2$, Sepiolite	Cd-contaminated paddy field	Application of $Ca(OH)_2$ and sepiolite increased soil pH; $NaNO_3$ and $CaCl_2$ extracted Cd reduced by 61–100% and 52–98%; Cd in rice reduced significantly; sepiolite or sepiolite-lime more effective than lime alone.	Zhu et al. (2010)

SEM–scanning electron microscope; XRD–X-ray diffraction.

Liu et al. (2011) examined the effects of lime and other alkaline substances on remediation of Cd-contaminated paddy soil using a pot experiment. The results showed that a single application (2 g kg^{-1}) of lime and other alkaline substances increased soil pH and soil-exchangeable Ca content. The soil-available Cd content was decreased by 37.4% and 33.2% at 30 and 60 days after rice transplantation, respectively. Their study revealed that Cd content in rice root and brown rice was decreased by 24.0% and 26.3%, respectively. Cattani et al. (2008) conducted a field trial during 2003 and 2004 in Italy to study reduction of the uptake of Cd by rice using lime as an amendment. They found that submersion was the main factor decreasing Cd concentration in rice grain, producing maximum concentrations of 0.14 and 0.06 mg kg^{-1} in 2003 and 2004, respectively. They observed that Cd concentrations were at least two times higher for rice cultivated by irrigation only than under submerged conditions. The addition of lime decreased the Cd concentration of rice by about 25% compared with control under dry conditions. They suggested that lime addition appeared to be a promising technique to reduce the bioavailability of soil Cd and minimize Cd concentrations in the rice. Differences in uptake over the years, with concentrations up to 40% lower in 2004, were explained by differences in transpiration. Their results also demonstrated that the influence of climatic conditions on Cd uptake in plants should not be underestimated.

Metals form both inorganic and organic complexes with a range of solutes in soils. For example, a number of studies have indicated that chloride (Cl^-) forms a soluble complex with Cd as $CdCl^+$, thereby decreasing the adsorption of Cd onto soil particles (McLaughlin et al., 1996; Naidu et al., 1994, 1997; Weggler-Beaton et al., 2000). Similarly, the formation of aqueous complexes with dissolved organic carbon (DOC) and low-molecular weight organic acids from root exudates is expected to dominate the solution chemistry of certain metals, such as Cd and Cu in the rhizosphere (Bolan et al., 2011; Fotovat and Naidu, 1997; Krishnamurti et al., 1996; Kunhikrishnan et al., 2012). Although the effect of organic amendments such as composted biosolids on Cd^{2+} adsorption is not consistent, the phytoavailability of Cd has been shown to be greatly inhibited (Bolan et al., 2003b; Park et al., 2011). Addition of composted biosolids increases surface charge, which may be one of the reasons for increasing Cd adsorption, thereby decreasing phytoavailability.

Plants exhibit greater tolerance to metals introduced through sewage sludge addition than when they are added as inorganic salts. For example, Chang et al. (1992) and Logan et al. (1997) presented data for maize

(*Zea mays* L.) and other crops grown on metal-contaminated sludge-amended soils, which revealed an inconsequential change in crop tissue Cd concentrations in response to substantial increases in total Cd loading in soils. The decrease in the phytoavailability of metals in the presence of organic amendments is often attributed to increased complexation of the metal by the organic constituents (Adriano, 2001). However, the presence of phosphates, Al and Fe compounds, and other inorganic minerals in typical municipal sewage sludge is also believed to be responsible for inducing the "plateau effect" in Cd uptake by crops, thereby preventing the increased Cd availability suggested in the "time bomb" hypothesis (Brown et al., 1998).

In soils containing large amounts of OM, such as pasture soils and organic manure-amended soils, only a small proportion of the Cd in soil solution remains as free Cd^{2+} and a large portion is complexed with soluble organic carbon (del Castilho et al., 1993; Sauve et al., 2000). Addition of manure and composted biosolids has been found to increase the complexation of Cd in soils, the extent of which is related to the amount of DOC. Although a wide variety of organic compounds in DOC are involved in the formation of soluble complexes with metals, Zhou and Wong (2001) and del Castilho et al. (1993) observed that low-molecular fractions, such as hydrophilic bases, have a strong affinity to form soluble Cd complexes. Similarly Riffaldi et al. (1983) obtained significant correlations between Cd sorption and phenolic hydroxyl groups and carboxyl groups of fulvic acids. Fulvic acid, although representing an average 9% of the total organic C content in sludges, plays an essential role in metal retention (Bolan et al., 2011; Senesi and Loffredo, 1999; Senesi and Plaza, 2007).

Farmyard manure (FYM), including cow or pig manure, decreases bioavailability of heavy metals in soil and crop plants (Pichtel and Bradway, 2008; Ram and Veerloo, 1985). FYM positively influences crop production (Kaihura et al., 1999), improves soil physical properties (Chen et al., 1996), and can be used to reduce heavy metal hazards in plants (Yassen et al., 2007). Li et al. (2009a) investigated the effects of pig manure on the distribution and accumulation of Cd in a soil–rice system using a pot experiment. Results showed that application of pig manure decreased the concentrations of Cd in rice roots by 35.6%. They observed that pig manure not only decreased uptake of Cd by rice but also restrained the transfer of Cd from the rice root to the stem and grain. The application of amendments increased soil pH and resulted in the reduction of Cd concentrations in soil solutions, which were significantly correlated to the uptake of Cd by the rice stem and grain. In a

similar study, Kibria et al. (2011) also noticed a significant reduction in the grain Cd content of rice by 27% by FYM.

Han et al. (2011) conducted a glasshouse experiment to examine the Cd concentrations in the aboveground parts of rice after application of pig manure in three soils differing in pH, texture, OM, and CEC. The results demonstrated that soil pH increased with increasing rates of pig manure from 1% to 3%, and the highest rate of manure produced lower Cd concentrations in the grain, husk, and straw on all three soils. They noticed that grain Cd concentrations were lower in soil with the highest pH, but in other soils, it exceeded the guideline value of 0.2 mg kg^{-1}. In another pot study, Li et al. (2009b) applied composted pig manure to soils at rates of 0%, 0.5%, 1.5%, 3.0%, and 5.0% which were equivalent to 0, 0.1, 0.3, 0.6, and 1.0 mg kg^{-1} of Cd to assess the Cd accumulation by rice plants. Results indicated that Cd concentrations in rice grains were more than the limit of 0.2 mg kg^{-1} when 0.14 mg kg^{-1} or more Cd was loaded to Ferralsols by manure application, but it was not more than the limit in Calcaric Cambisols (Table 4.9). They also found that in all treatments, Cd accumulations in rice straw and roots were significantly greater than those in rice grains and only a small portion of Cd absorbed by rice plants was transferred into the grains.

With composted biosolids, one of the main concerns about its long-term metal-immobilization efficiency is the potential for metals to mobilize if and when the OM undergoes significant oxidation. Stacey et al. (2001) observed that the release of Cd and Zn from composted biosolids, as the OM in the compost decomposed, depended to a large extent on the composition of the composted biosolids. However, Hyun et al. (1998) obtained no evidence for increased phytoavailability of Cd with the breakdown of

Table 4.9 Cadmium Contents in Rice and Soil from Various Soil Types (Herawati et al., 2000)

Soil type	In Rice (mg kg^{-1})	In Soil* (mg kg^{-1})	In Soil† (mg kg^{-1})
Andosols	0.0667	0.0603	0.4034
Cambisols	0.0494	0.1484	0.6018
Fluvisols	0.1640	0.0737	0.4037
Gleysols	0.0122	0.0447	0.0995
Histosols	0.0182	0.0122	0.0366
Luvisols	0.0245	0.0271	0.0900
Acrisols	0.0404	0.0300	0.1484
Mixed soils	0.0366	0.0814	0.4034

*Metals extracted by hydrochloric acid.
†Metals ashed by nitric acid.

OM in sludge-treated soils. Furthermore, Hettiarachchi et al. (2006) and Li et al. (2001) observed evidence for greater affinity for Cd adsorption by the inorganic components of the composted biosolids-amended soils indicating that the increased adsorption of Cd is independent of the added OM and of a persistent nature.

Although the formation of soluble metal–organic complex reduces the phytoavailability of metals, the mobility of the metal may be facilitated greatly in soils receiving alkaline-stabilized composted biosolids because of an increased concentration of soluble metal–organic complexes in solution (Brown et al., 1997; Dinel et al., 2000; Gove et al., 2001). Soluble complexing ligands in biosolids cause certain trace elements to be more mobile than they would be in the absence of organics (Ashworth and Alloway, 2008; Camobreco et al., 1996; Frenkel et al., 1997). Camobreco et al. (1996) found that soluble complexing ligands in biosolids enabled metals with low (Cd, Zn) and high (Cu, Pb) organic affinities to move through undisturbed soil columns. Lamy et al. (1993) also observed DOC facilitation of Cd mobility following sludge application. The behavior of Cd in a mixed sludge–soil system showed that the addition of sludge-soluble OM to the soil led to a decrease of Cd sorption across the pH range between 5 and 7.

Antoniadis and Alloway (2002) investigated the leaching of Cd, Ni, and Zn down the profile of sewage sludge-treated soil from packed columns and found that the metals moved significantly down the soil profile to a depth of at least 8 cm at 50 t ha^{-1}. They suggested that DOC increased the mobility of these heavy metals by acting as a ligand in the soil with sewage sludge application. They cautioned that the depth of metal movement could increase at high sludge-application rates and in areas with high precipitation, even where the soil pH does not necessarily encourage metal solubility.

For most heavy metals and sludge types, the highest dissolved metal concentrations appear in leachates during or shortly after the sewage sludge amendments (Richards et al., 2000). However, McBride et al. (1999) observed that trace metals including Cd, Zn, Ni, and Cu continued a gradual process of leaching from contaminated subsoil and through the shallow subsoil more than 15 years after sewage sludge application. McBride et al. (1999) observed that 82% of the Cd in percolates collected at the 60 cm depth from a long-term study was largely in complexed form with DOC. In another similar study, Schaecke et al. (2002) investigated the fate of heavy metal concentrations in soil fractions including Cd after biosolid application at 0–0.25 m depth. They observed that 11 years after the last application, metals supplied with the sludge had moved as far as 50 cm in

depth. Concentrations of metals in the saturation extract of the sampled soil layers were closely correlated to the concentrations of DOC. Zubillaga and Lavado (2008) examined the accumulation of Cd, Cu, Pb, and Zn in soils throughout 5 years, during and after biosolid application and their movement with depth in a Typic Argiudoll and a Typic Hapludoll. They noticed that only total Cd in the Typic Argiudoll moved with depth, which they attributed to the metal complexation by DOC released from the biosolids.

Data from laboratory and glasshouse experiments have clearly demonstrated that P addition enhances the immobilization of Cd in soils, thereby alleviating its phytotoxicity (Bolan et al., 2003d; Kumpiene et al., 2007) (Table 4.8). Two reasons could be attributed to P-induced immobilization of Cd in soils: (1) P-induced Cd^{2+} adsorption; and (2) precipitation of Cd as $Cd(OH)_2$ and $Cd_3(PO_4)_2$. Several mechanisms can be advanced for P-induced Cd^{2+} adsorption. These include: (1) increase in pH; (2) increase in surface charge, (3) co-adsorption of P and Cd as an ion pair, and (4) surface complex formation of Cd on the P compound (Bolan et al., 2003d).

The effect of P addition on soil pH depends on the buffering capacity of the soil, the nature of P compounds, and the extent of P adsorption (Havlin et al., 1999). While the addition of nitrogen (N)- and Ca-containing P fertilizers generally decreases soil pH due to acidification reactions, addition of other P fertilizers increases soil pH mainly due to the ligand-exchange (i.e. OH^- ions) P adsorption reaction. Levi-Minzi and Petruzzelli (1984) observed that P-induced variation in soil pH influenced the solubility of Cd in soils. They noticed that while the effect of P on pH and Cd solubility was less evident in an organic soil with high pH-buffering capacity, the addition of diammonium phosphate (DAP) increased soil pH, thereby reducing the solubility of Cd in a mineral soil with less pH-buffering capacity.

A number of studies have shown that specific adsorption of anions increases the net negative charge of variable charge surfaces (Bolan et al., 2003d; Bolland et al., 1977; Kuo, 1986; Lackovic et al., 2003; Naidu et al., 1994, 1997). The amount of surface charge acquired through specific adsorption depends on the nature of anion adsorbed and the pH and electrolyte concentration of the solute. Naidu et al. (1994) and Bolan et al. (1999a; 2003d) showed that increasing P addition caused a significant increase in Cd^{2+} adsorption by soils dominated by variable-charge components. It has been shown that Zn^{2+}, Cd^{2+}, or Cu^{2+} adsorption by variable-charge components, such as Al and Fe hydrous oxides, can be increased by low or moderate enrichment of oxides with P (Bolland et al., 1977; Hong et al.,

2008, 2010b; Kuo, 1986), which has been attributed to increases in surface negative charge after P adsorption.

While surface complex formation has also been offered for the increased adsorption of Ca^{2+} or Zn^{2+} onto P-enriched gibbsite and goethite by Helyar et al. (1976) and Bolland et al. (1977), Xu et al. (1994) concluded that coprecipitation was the dominant process in the adsorption of Cd^{2+} (Eqn (1)) and Zn^{2+} by hydroxyapatite:



$$Ca_{10}(PO_4)_6(OH)_2 + xCd^{2+} \rightarrow (Cd_{x,}Ca_{10-x})(PO_4)_6(OH)_2 + xCa^{2+} \quad (1)$$

Precipitation as metal phosphates has also been proved to be a main mechanism in immobilizing metals, such as Cd, Pb, and Zn, by P compounds (Table 4.8). McGowen et al. (2001) have examined the immobilization of As, Cd, Pb, and Zn in a smelter-contaminated soil using DAP. Application of high levels of DAP at a rate of 2300 mg P kg^{-1} was effective in immobilizing Cd, Pb, and Zn in the contaminated soil. Others have also shown that $Cd_3(PO_4)_2$ can control Cd solubility in P-sufficient soils or soils amended with P (Hong et al., 2010b; Santillan-Medrano and Jurinak, 1975; Street et al., 1978). However, because the solubility of $Cd_3(PO_4)_2$ is too high to control the concentration of Cd in soils, it is unlikely this solid phase can play a significant role in the immobilization of Cd (Bolland et al., 1977; Soon, 1981; Xiong, 1995, Table 4.8).

4. BIOAVAILABILITY AND TOXICITY OF CADMIUM

The bioavailability of a chemical in the soil environment has been defined as the fraction of the total element in the interstitial pore water (i.e. soil solution) and soil particles that are available to the receptor organism (Naidu et al., 2008). Considerable controversy exists in the literature relating to bioavailable fraction, including the definition itself and the methods used for its measurement. A more generic definition of *bioavailability* is the potential for living organisms to take up chemicals from food (i.e. oral) or from the abiotic environment (i.e. external) to the extent that the chemicals may become involved in the metabolism of the organism. More specifically, it refers to the biologically available chemical fraction (or pool) that can be taken up by an organism and can react with its metabolic machinery (Campbell, 1995); or it refers to the fraction of the total chemical that can interact with a biological target (Vangronsveld and Cunningham, 1998). In order to be bioavailable, the trace elements have to come in contact with

the organism (i.e. physical accessibility). Moreover, trace elements need to be in a particular form (i.e. chemical accessibility) to be able to enter biota. In essence, for a trace element to be bioavailable, it will have to be mobile and transported and be in an accessible form to the biota concerned.

4.1. Toxicity to Plants and Microorganisms

Although Cd is a nonessential element for both plants and animals, increasing Cd concentration in soil leads to an increase in Cd uptake below the phytotoxicity threshold concentrations. Plant species differ in their ability to extract soil Cd and, in general, weed species are shown to accumulate more Cd. For example, a nationwide survey by Roberts et al. (1994) indicated significantly higher Cd concentration in weeds (0.28 mg Cd kg^{-1}) than grasses and legumes (0.06–0.1 mg Cd kg^{-1}). Similarly, in Australia, the highest Cd concentration is obtained in cape weed (1.57 mg Cd kg^{-1}), which is a common component of pastures in Australia and New Zealand. Loganathan et al. (2003), McLaughlin et al. (1997), and Williams and David (1973) have shown that the concentration of Cd in legumes is several times higher (0.155 mg Cd kg^{-1}) than the associated grass (0.031 mg Cd kg^{-1}). The increased concentration of Cd in legumes may be related to the acidifying effect of legumes (Tang et al., 1998).

It is well known that Cd concentration in plants vary with plant species (Adriano, 1986; Alloway, 1995; Almas et al., 2006; Black et al., 2011). In general, leafy plants tend to accumulate higher metal concentrations than root, grain, or fruit crops (Alloway, 1995). Cadmium accumulation in rice grains cropped on Cd-contaminated soils could increase 6- to 10-fold depending on the genotype of the cultivar used (Arao and Ishikawa, 2006; Yu et al., 2006). Both soil properties which control Cd availability and differences between cultivars are relevant in order to assess risks of Cd in soil in relation to the quality of rice. Although numerous factors contribute to final Cd levels in rice grains, the increase in Cd uptake by rice coincides with an increase in the available Cd pool in soil.

Cadmium uptake levels of rice grains could be quite different among cultivars under similar soil conditions (Table 4.10). In general, Cd accumulation in rice grains of *Indica* species proved to be high compared to *Japonica* species (Römkens et al., 2009). Hence, *Japonica* species are more suitable for cropping on soils affected by Cd pollution (He et al., 2006). Irrespective of rice cultivars, the combination of elevated total Cd concentrations in soil, a low pH, and low soil OM content results in an increased availability of Cd in soil, which results in a high uptake of Cd by rice plants (Römkens et al., 2009).

Table 4.10 Overview of Cadmium Concentrations in Roots and Grains of *Indica* and *Japonica* Rice Cultivars

		Total Cd in Soils (mg kg^{-1})		Cd in Roots (mg kg^{-1})		Cd in Grains (mg kg^{-1})		Ratio Cd-Rice
Family	**Cultivar Name**	**Median**	**Range**	**Median**	**Range**	**Median**	**Range**	**Grains/Roots**
Japonica	Tainung no. 70	0.60	0.13–27.8	8.0	0.8–373.4	0.21	0.02–4.6	0.029
Japonica	Taiken no. 8	0.61	0.09–18.8	6.6	0.5–181.3	0.23	0.11–6.0	0.037
Japonica	Tainung no. 72	0.65	0.11–18.2	9.7	0.4–403.9	0.19	0.02–3.0	0.026
Japonica	Kaohsiung no. 143	0.64	0.07–17.4	8.0	0.5–198.5	0.19	0.01–4.5	0.029
Japonica	Taitung no. 30	0.59	0.06–23.9	8.8	0.7–213.6	0.18	0.02–3.3	0.025
Japonica	Tainung Sen no. 20	0.71	0.08–21.2	6.5	0.6–247.7	0.43	0.02–12.6	0.096
Japonica	Tainung no. 71	0.60	0.13–25.9	7.2	0.6–175.7	0.20	0.10–3.7	0.030
Japonica	Tainung no. 67	0.66	0.08–26.6	5.4	0.6–139.2	0.19	0.09–3.4	0.032
Indica	Kaohsiung Sen Yu no. 1151	0.57	0.09–25.9	6.2	0.5–107.0	0.44	0.23–7.6	0.075
Indica	Taichung Sen Waxy no. 1	0.71	0.14–25.8	6.4	0.5–161.8	0.60	0.25–25.3	0.092
Indica	Taichung Sen no. 10	0.70	0.14–22.7	9.6	0.7–266.6	0.37	0.19–29.1	0.061
Indica	Kaohsiung no. 144	0.59	0.13–16.8	4.6	0.6–107.7	0.16	0.08–3.7	0.032

Modified from Römkens et al. (2009)

Despite observed differences in Cd levels in grains of *Indica* versus *Japonica* cultivars (Table 4.10), no significant differences in Cd-root levels were observed (Liu et al., 2003; Römkens et al., 2009). This finding suggests that *Indica* and *Japonica* cultivars mainly differ in their ability to transfer Cd from the root into the shoot. Indeed, the ratio of Cd in rice grains to that in the root differs substantially between *Japonica* (0.03) and *Indica* (0.08), which explains the higher Cd levels in rice grains of *Indica* cultivars.

In general, Cd uptake by rice roots is known to be affected by competitive cations having similar electronic properties such as Ca, magnesium (Mg), and Zn. For example, the effect of Zn on uptake of Cd by roots and rice grain has often been reported (Girling and Peterson, 1981; Hassan et al., 2006), although contrasting effects have been demonstrated depending on the levels of Zn and Cd in the soil and the soil Cd-to-Zn ratio (Dunbar, 2004; Kukier and Chaney, 2002). Liu et al. (2007) found that Zn in solution suppressed Cd uptake by roots but increased the transfer of Cd from root to rice grains.

4.2. Risk to Animals and Humans

The tolerable intake for Cd as proposed by FAO/WHO (1972) is 400–500 μg $week^{-1}$ $person^{-1}$ or 57–71 μg day^{-1} $person^{-1}$ weighing 70 kg. Despite the difference in the amount of dietary Cd intake, however, rice is the leading source of Cd common to many populations in Asia, e.g. approximately ranging from 20% of total dietary Cd intake in the Philippines (Zhang et al., 1998), to 30–40% in Japan (Ikeda et al., 1999; Watanabe et al., 2000a), many parts in mainland China (Zhang et al., 1997), Taiwan (Ikeda et al., 1996), and Thailand (Zhang et al., 1999), and with a much higher level (53%) in Malaysia (Moon et al., 1996). It may be of interest to stress that wheat (*Triticum aestivum* L.) and other cereals are additional sources of dietary Cd when people consume such cereals more than rice, as observed in northern China (Watanabe et al., 1998, 2000b). It is, however, worth noting that while rice is the major component of food among the Asian community, many of them (especially females and children) weigh <70 kg. Thus FAO/WHO tolerable limit for Cd and indeed other potentially toxic substances may not be appropriate for Asian communities.

In comparison, dietary Cd intake levels in the 1990s in Europe have been made available in recent years. The levels reported (mostly geometric mean or medians for adult people, unless otherwise specified) include 6.3 μg $week^{-1}$ $person^{-1}$ for 1.5–5.3-year-old children in a remote island in the North Sea, Germany (Schrey et al., 2000), approximately 7 μg day^{-1}

in Duisburg, Germany (Wilhelm et al., 1995), 9–22 μg day^{-1} in Sweden (Järup et al., 1998), 11.1 μg day^{-1} for students in Spain (Barbera et al., 1993), 14 μg day^{-1} in the UK (Ysart et al., 1999), 17.5 μg day^{-1} in Croatia (Sapunar-Postruznik et al., 1996), 19–27 μg day^{-1} in Belgium (Van Cauwenbergh et al., 2000), and 28 μg day^{-1} in the Ruhr district, Germany (Wilhelm et al., 2002). The value reported for Canadians (Dabeka and McKenzie, 1995), 13 μg day^{-1}, was also close to these values observed in Europe. The levels as a whole appear to be close to or slightly higher than the levels in Asia (5–15 μg day^{-1}; Ikeda et al., 2000) excluding Japan where the exposure level is much higher (i.e. ~30 μg day^{-1}).

In particular, background exposure of general populations in Japan to Cd has been relatively high (Watanabe et al., 2000a). According to Watanabe et al. (1996), there is a significant difference in geometric mean Cd content in rice samples (1546) collected in 17 areas in the world, but it was the highest in Japan (0.0557 mg kg^{-1}) and Colombia (0.13320 mg kg^{-1}) (Table 4.11). Analysis of data from food duplicate surveys in the mid 1990s on some 600 women throughout the country coupled with air pollution data disclosed that foods were the almost exclusive source of Cd exposure for the general population, whereas the exposures through the respiration route was essentially negligible; rice (paddy rice), the staple cereal for most Japanese, was in fact the leading source of Cd intake via daily foods, accounting for 30–40% in the 1980s and 1990s (Ikeda et al., 1999; Watanabe et al., 2000a), although a substantial decrease in total dietary intake occurred in the mid 1990s as compared with the levels 10–15 years ago (Watanabe et al., 1996, 2000a).

The Japanese people used to take in approximately 8.2 and 1.8 μg Cd day^{-1} from rice and wheat, respectively (Shimbo et al., 2001) (Table 4.12). It is worth noting that the dietary route is responsible for 99% of

Table 4.11 Cadmium Contents in Rice Grain from Various Areas (Watanabe et al., 1996)

Areas	Mean Cd (mg kg^{-1})	Areas	Mean Cd (mg kg^{-1})
Australia	0.00267	Vietnam	0.01850
China	0.01554	Canada	0.02902
Taiwan	0.03955	Colombia	0.13320
Indonesia	0.02177	Finland	0.02580
Japan	0.05570	France	0.01741
Korea	0.01570	Italy	0.03392
Thailand	0.01570	South Africa	0.02582
Malaysia	0.02774	Spain	0.00085
Philippines	0.02014	USA	0.00743

total Cd intake in Japan because Cd concentration in general atmospheric air is low compared to food (Ikeda et al., 2000). The dietary Cd intake by middle-aged Japanese women in the late 1990s was 25.5 μg day^{-1} (Watanabe et al., 2000a) (Table 4.13). This amount of Cd intake in Japan appeared to be 2–3 times higher than the levels among other women populations in east and south-east Asia (Ikeda et al., 2000), possibly because Cd contents in the rice are lower there, even though in these places people depend even more heavily on rice as a major source of energy for daily life.

Cadmium reaches the food chain also through uptake by grazing animals. For example, in New Zealand, most of the Cd accumulated in grazing animals is derived mainly from the pasture intake (Loganathan et al., 2008). Bramley (1990) has estimated that annually ~55 and 275 mg Cd is ingested per sheep and cow, respectively, through the intake of herbage. Work in New Zealand has indicated that cattle and sheep may ingest 1–10% and >30%, respectively, of their dry matter intake in the form of soil. In areas where soils contain high Cd, for example, as a result of sewage sludge and fertilizer application, soil ingestion is expected to play a significant role in Cd uptake by farm animals (Loganathan et al., 2003; Wilkinson et al., 2001). Roberts et al. (1994) have shown that even though sheep ingest 36–46 kg soil per year, this only contributes 5–8% of the total Cd intake for the lax and hard grazed flocks, respectively.

Ruminants do not have a homeostatic control mechanism for regulating Cd absorption or excretion which is affected by the level of dietary Cd content (Lee et al., 1996; Loganathan et al., 2008). Although intestinal uptake of Cd has been estimated to account for over 90% of the

Table 4.12 Intake of Cadmium by Japanese via Rice and Wheat in 1998–2000

	Rice		Wheat	
Item	**Average**	**Ranges**	**Average**	**Ranges**
Daily cereal consumption (g day^{-1})	165	158–178	91	67–104
Cadmium content (mg kg^{-1})*	0.0497	0.0430–0.0701	0.0193	0.0170–0.0212
Daily Cd intake (μg day^{-1})	8.2	7.409–12.506	1.754	1.297–1.993

*Cited from Ministry of Health and Welfare (2000)
Revised from Shimbo et al. (2001)

Table 4.13 Dietary Exposure to Cadmium (Cd), and Cd Concentration in Blood and Urine among Nonsmoking Adult Women in the Cities in Asia

	Cadmium in			
Location	**Food ($\mu g\ day^{-1}$)**	**Blood ($\mu g\ L^{-1}$)**	**Urine ($mg\ kg^{-1}$ Creatinine)**	**References**
Japan (A group of 27 sites)				
1977–1981	37.5	3.47	–	Watanabe et al. (2000a)
1991–1997	25.5	1.90	4.39	Watanabe et al. (2000a)
Bangkok	7.1	0.41	1.40	Zhang et al. (1999)
China (A group of 4 sites)	9.9	1.07	2.30	Zhang et al. (1997)
Korea (A group of 4 sites)	21.2	1.39	2.26	Moon et al. (1998)
Kuala Lumpur	9.0	0.74	1.51	Moon et al. (1996)
Manila	14.2	0.47	1.21	Zhang et al. (1998)
Tainan	9.7	0.83	1.59	Ikeda et al. (1996)

Revised from Watanabe et al. (2000a)

total Cd absorbed, about 80–90% and 0.05% of the total ingested Cd is excreted in the faeces and urine, respectively. Most dietary Cd is bound to metallothionein and is absorbed intact into the circulation, and, in animals, kidney and liver Cd accounts for 50–70% of the total Cd with kidney having a higher Cd concentration than the liver. Other organs such as the pancreas, spleen, heart, brain, and testis, together with muscle and fat accumulate small amounts of Cd. In blood, Cd is associated with albumin-like protein, which is transported to the kidney where it is filtered through the glomerulus and reabsorbed by the proximal tubules (Friberg et al., 1985).

In animals, the effects of prolonged exposure to abnormal levels of Cd include testicular necrosis, placenta destruction, abortion, teratogenic malformations, renal damage, osteomalacia, immunosuppression, pulmonary edema, and emphysema. In humans, severe Cd exposure can result in emphysema, bronchitis, ulceration of nasal mucosa, renal dysfunction, liver necrosis and anemia, hypertension, skeletal deformities, prostrate and lung cancer, and teratogenesis (Chowdhury and Chandra, 1987).

Different countries have set guidelines on the maximum permissible levels for Cd in various meat products. In a survey of cattle, pigs, and sheep in New Zealand, the mean Cd concentration in kidney cortex, liver, and muscle was <0.4, 0.1, and 0.05 mg Cd kg^{-1} wet weight, respectively (Solly et al., 1981). These values are well below both the concentration measured in other countries and the maximum permissible concentration stipulated by many countries. However, Roberts et al. (1994) indicated that between 1988 and 1991, some 22–28% of sheep and 14–20% of cattle had kidney Cd contents greater than the permissible level of 1 mg Cd kg^{-1}. In general, older animals had higher kidney Cd contents as these animals had longer exposure to Cd in their environment and, hence, greater opportunity to consume and retain Cd (Petterson et al., 1991). However, the rate of Cd increase decreases with age (Lee et al., 1996); for example, at 6 months of age, sheep retain about 0.1% of the Cd intake in the kidneys, with this value decreasing to 0.04% or less with increasing age (Loganathan et al., 2008). Feral deer and sheep isolated from human intervention also showed age-related retention of Cd in kidney tissue as a result of exposure to naturally occurring Cd in the environment.

Cadmium in cow and goat milk (0.002–0.006 μg kg^{-1}) (Rayment, 1988) and sheep and cattle muscle (0.01–0.03 mg kg^{-1} wet weight) were reported to be very low. Cadmium measured in carcass meat in New Zealand (0.02–0.03 mg kg^{-1} wet weight) (Roberts and Longhurst, 2002) and Australia (median, 0.01 mg kg^{-1} wet weight) (Langlands et al., 1988) were also significantly lower than the permissible level of 0.05 mg kg^{-1} fresh tissue (kidneys, liver, muscle) in these countries (Loganathan et al., 2008). Because the accumulation of Cd in kidneys was high, whereas the amounts in milk and meat were low, Loganathan et al. (2008) suggested that the grazing animal can be viewed as a "filter" capable of ensuring that the amounts of Cd entering the food chain are low. They also conveyed that this was similar to the case, in which Cd-rich bran and roots were removed from processed grains and edible parts of plants, respectively, and then less Cd entered the food chain (Sauerbeck, 1992).

The average annual consumption of red meat per New Zealander (70 kg adult) is estimated to be 80 kg. Based on a median Cd content of 0.01 mg kg^{-1} wet weight, the annual intake of Cd is expected to be 0.8 mg, which is equivalent to a daily intake of 2.19 μg Cd. This is considerably less than the maximum safe level of 70 μg Cd day^{-1} (Ledgard et al., 2010; Loganathan et al., 2008) from all sources in the diet. Although offal, such as liver and kidney, contains more Cd than the other meat, the small quantity

of offal consumed by the New Zealand population is unlikely to contribute significantly to the total Cd intake. Also, as most meat-producing animals are slaughtered at a young age, this ensures that Cd concentrations of their edible offal products are within permissible limits (Loganathan et al., 2008). However, in sections of population and in pets where offal forms a larger portion of the diet, Cd intake from this source could be a major concern (Loganathan et al., 1999).

The "population critical concentration" of Cd at which 10% of the human population would exhibit signs of renal impairment on the kidney is about 160 mg Cd kg^{-1} wet weight (Friberg, 1984). From the above calculations, it can be shown that it is unlikely that Cd input from meat exceeds the critical concentration in the life time of a New Zealander. However, Loganathan et al. (2008) proposed that computer-based models are required to identify farming systems that present a high risk of Cd concentrations in edible offal exceeding the permissible levels and livestock at risk of chronic toxicity. They recommended that a decision support model of this kind may be useful in developing management strategies capable of reducing Cd accumulation in animals. They stated that although preliminary empirical models have been developed for Cd accumulation in sheep grazing on New Zealand pastures (Loganathan et al., 1999), further development of these models is required for their wider applicability.



5. RISK MANAGEMENT OF CADMIUM IN RICE ECOSYSTEMS

Among heavy metals, Cd has been recognized as one of the most detrimental because Cd uptake is known to have caused itai-itai disease. The Codex Alimentarius Commission, set up by the UN Food and Agriculture Organization and the World Health Organization, has set standards 0.4 mg Cd kg^{-1} as the maximum permissible concentration of Cd in polished rice (Codex, 2006). Therefore, evaluation of the risk of Cd uptake is needed, as well as minimization of that risk by either decreasing soil Cd contamination or reducing Cd bioavailability to plants, which will improve food safety and safeguard human health. In this section, we describe appropriate methods to minimize Cd contamination in rice grains, including (1) decreasing Cd inputs to rice soils through the use of low Cd-containing P fertilizers, (2) water management to reduce bioavailability of soil Cd to rice plants, (3) replacement of contaminated soil with nonpolluted soil, (4) selection and breeding of low Cd-accumulating rice cultivar,

(5) phytoremediation of the polluted soil by rice and other promising crops, and (6) chemical remediation of Cd-contaminated soil by soil washing with chemicals such as iron salts.

5.1. Decreasing Cd Inputs to Rice Soils

The main sources of Cd inputs to rice soil include P fertilizers, biosolids, and mine tailings (Table 4.5). Cadmium input through P fertilizers can be reduced by either selective use of PRs with low Cd or treating the PRs to remove Cd. Superphosphate fertilizer manufacturers in many countries including New Zealand and Australia are introducing voluntary controls on the Cd content of P fertilizers. For example, the fertilizer industry in New Zealand achieved its objective of lowering the Cd content in P fertilizers from 340 mg Cd kg^{-1} P in the 1990s to 280 mg Cd kg^{-1} P by the year 2000 (Bolan et al., 2003a; Rys, 2011). The Cd content as determined by the PR source is the most difficult to control because supplies of PRs with low Cd contents are limited and sources with higher Cd contents continue to be used in many countries for practical reasons. A number of PRs (e.g. Jordan (El Hassa) PR and Morocco (Khouribga) PR) are low in Cd, and these can be used for the manufacture of superphosphates. Alternatively, since Cd has a low boiling point (BP = 767 °C), it can be removed by calcining the PRs. Phosphoric acid used in the food industry is manufactured mostly only after the removal of Cd through calcination of the PRs. Calcination of PRs may not be a likely option in the fertilizer industry because it is expensive and calcination decreases the reactivity of PRs making them unsuitable for direct application as a source of P (Ando, 1987).

Chien et al. (2009) mentioned in a recent review that if a water-soluble P (WSP) fertilizer contains a high Cd content, granulation of WSP fertilizer with potassium chloride (KCl) may result in a higher Cd uptake by crops compared to the same, but bulk-blended PK fertilizer. They suggested that a possible explanation would be that in granulated PK fertilizers, KCl- and Cd-containing P fertilizers are in the same granule and thus are in close contact, thereby increasing the possibility of forming readily bioavailable $CdCl_2^0$ and $CdCl^{1+}$ complexes. They also added that it would be less likely that the complexes would form when KCl- and Cd-containing P granules are physically separated in bulk-blended PK fertilizers.

The above hypothesis was tested and confirmed by Chien et al. (2003) in a preliminary greenhouse study using upland rice and soybean (*Glycine max* (L.) Merr.). In their study, all P and K sources produced by either granulation or bulk blending had the same granule size (1.68–3.36 mm diameter).

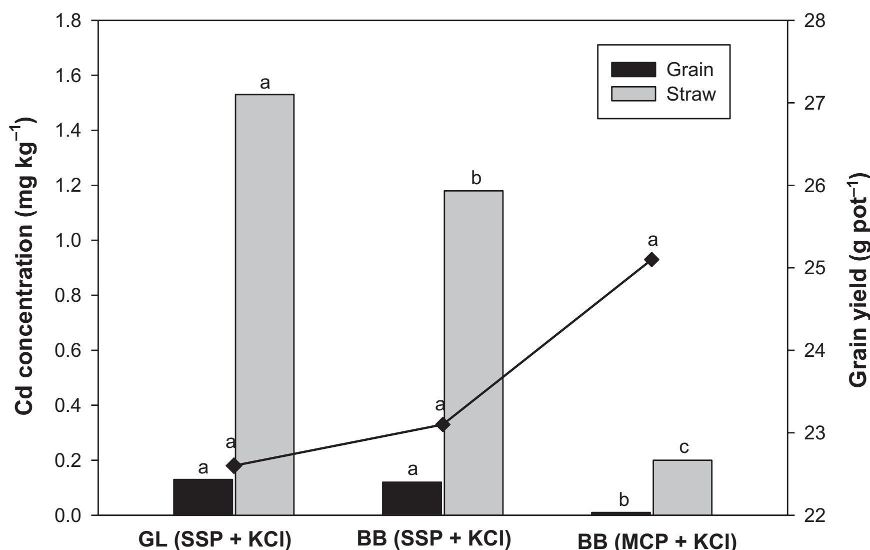


Figure 4.2 Grain yield of upland rice and Cd concentrations in rice grain and straw. GL, granulated; SSP, single super phosphate; BB, bulk-blended; MCP, mono calcium phosphate (Chien et al., 2003). Means followed by the same letter within the treatments are not significantly different at $p < 0.05$.

The results showed that the agronomic effectiveness in increasing crop yield was the same with Cd-containing SSP and the reagent-grade monocalcium phosphate [(MCP) (0% Cd)], whether granulated or bulk blended with KCl. However, they noticed that concentrations of Cd in plant-tissue samples of all crops were much lower for MCP than for SSP. In all the plant-tissue samples, Cd concentrations obtained with granulated (SSP + KCl) fertilizers were higher than that with bulk-blended (SSP) + (KCl) fertilizers. Their results demonstrated that bulk blending of Cd-containing P fertilizers with KCl can reduce Cd uptake by crops compared to the same, but granulated, PK fertilizers (Fig. 4.2). Although PK sources, instead of NPK sources, were used in their study, they expected that inclusion of N will not affect the results, and, if proven true, the process of bulk blending, compared to granulation in decreasing Cd uptake, would also apply to NPK compound fertilizers.

5.2. Water Management to Reduce Cd Bioavailability

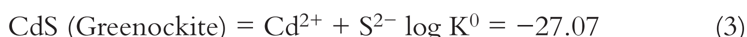
Water management is a popular and cost-effective cultural practice for alleviating rice Cd contamination in Japan. Heavy-metal uptake by paddy rice, in particular, uptake of Cd, is considerably influenced by water management,

hence, the redox state of the paddy soil. Table 4.14 shows the effect of water management on Cd content in rice grains. Cadmium absorption by rice was decreased drastically by continuous submergence of the paddy field after heading time.

It is most likely that a considerable decrease in Cd absorption by rice under submerged conditions is due to a decrease in the Cd solubility because of the formation of carbonates (Khaokaew et al., 2011) and/or CdS (de Livera et al., 2011; Iimura and Ito, 1978) as mentioned in Eqns (2) and (3) (Lindsay, 1979).



$$CdCO_3 \text{ (Octavite)} + 2H^+ = Cd^{2+} + CO_2 \text{ (g)} + H_2O \quad \log K^0 = 6.16 \quad (2)$$



$$CdS \text{ (Greenockite)} = Cd^{2+} + S^{2-} \quad \log K^0 = -27.07 \quad (3)$$

The former, Cd carbonate, is the primary form under alkali conditions (Khaokaew et al., 2011), while the latter, CdS, could be a dominant form under slightly acidic condition. The theoretical explanation based on physicochemical equation for the formation of CdS is summarized below.

Flooding paddy field shifts Eh toward a reduced state (a sharp decrease in Eh), where the sulfate ion is reduced to the sulfide (Eqns (4) and (5)).



$$H_2S \text{ (aq)} + 4H_2O = SO_4^{2-} + 10H^+ + 8e^- \quad (\log K^0 = -40.66) \quad (4)$$

Equation (4) can be rewritten by using Nernst's equation with $\log K^0$;

$$Eh = 0.301–0.0739 \text{ pH} + 0.00739 \log (SO_4^{2-}/H_2S) \quad (5)$$

H_2S is obtained from the dissociation of HS^- and S^{2-} with the following dissociation constants of K_1 and K_2.

Table 4.14 Effect of Water Management on Cadmium Content in Rice Grains (Sakurai et al., 2005)

		Water Management after Heading Time	
		Flooded	Drained
Soil*		Cd (mg kg^{-1})	
Soil A	Glasshouse	Trace	1.10
Soil B		Trace	0.68
Soil C	Field test	0.09	0.23
Soil D		0.16	0.33

*Each soil is from different Cd-contaminated areas of Japan.

$$K_1 = (H^+)(HS^-)/(H_2S) = 10^{-7.02} \quad (6)$$

$$K_2 = (H^+)(S^{2-})/(HS^-) = 10^{-12.9} \quad (7)$$

Here, a total of the water-soluble sulfides is described:

$$\Sigma H_2S = (H_2S) + (HS^-) + (S^{2-}) \quad (8)$$

Substituting the sulfide species in Eqn (8) using Eqns (6) and (7), Eqn (9) is obtained;

$$\Sigma H_2S = (H_2S)\ \{1 + K_1/(H^+) + K_1\ K_2/(H^+)^2\} \quad (9)$$

At pH 7, Eqn (9) can be reduced to Eqn (10);

$$\log\Sigma H_2S = 0.291 + \log\ (H_2S) \quad (10)$$

Finally, combining Eqns (4) and (10), Eh can be expressed by hydrogen sulfide and sulfate ion (Eqn (11)):

$$Eh = -0.215 + 0.00739\ \log\ (SO_4^{2-}/H_2S) \quad (11)$$

Assuming that dominant sulfur species in soil solution are H_2S, HS^-, S^{2-} and SO_4^{2-}, the change in the relationship between $\{(SO_4^{2-})/((SO_4^{2-})+(\Sigma H_2S))\}$ at pH 7 and Eh, is expressed by a solid line in Fig. 4.3 (Makino, 2002). The dashed line shows the relationship in a similar calculation at pH 6. On the other hand, the open circles show the measured extractable Cd with 1 M ammonium acetate from the soil in a water-submerged incubation test. The

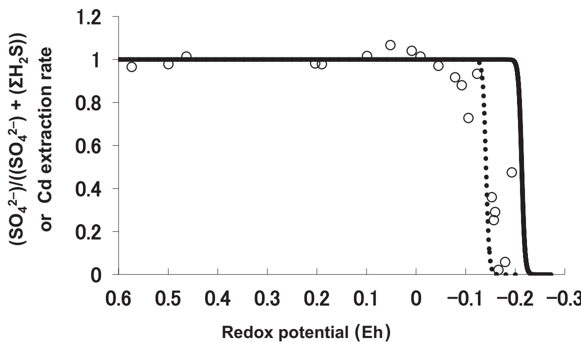


Figure 4.3 Relationships between soil Eh and rate of Cd extraction or that of sulfate residue. The lines and open circles (pH 7, … pH 6, ○ measured value) are correspondent with the $(SO_4^{2-})/\{(SO_4^{2-}) + (\Sigma H_2S)\}$ and Cd extraction rate of the vertical line in the figure. *(Modified from Makino (2002) and Iimura and Ito (1978))*.

measured Cd data closely followed the calculated lines for the sulfide formation (Fig. 4.3), indicating that the Cd extraction rate is rapidly decreased with an increase in the ratio of ΣH_2S to total S. Thus, the sulfide ion will precipitate with the Cd ion as CdS, whose solubility product is very small and hardly soluble in water (Eqn (3)).

Flooding from tillering to head formation during rice growth would be the most effective period to decrease the Cd content in rice grains. It is highly recommended to keep flooding the paddy fields as late as possible toward harvest time. However, the later the flooding, the more difficult it is for machine operation of harvest, so that we have to find a balance between lowering bioavailable Cd and the difficulty in operating machinery. Arao et al. (2009) investigated the effects of water management in rice paddy on levels of Cd and As in Japanese rice grains. Their results indicated that flooding treatment after heading was more effective than flooding treatment before heading in reducing rice grain Cd without a concomitant increase in total As levels.

5.3. Low Cd-Accumulating Rice Cultivars

5.3.1. Genotypic Variation in Grain Cd Concentration in Rice

Selection and breeding of low Cd-accumulating cultivars is the most cost-effective and environmentally friendly method for reducing the risk of contamination from Cd in food (Grant et al., 2008). Natural variations in the concentrations of Cd among cultivars have been well documented in staple crops including rice. Figure 4.4 shows the genotypic variation in grain Cd concentration in 35 rice cultivars grown in two types of Cd-polluted paddy soils (Arao and Ae, 2003; Arao and Ishikawa, 2006). Cadmium concentrations in brown rice ranged from 0.13 to 4.31 mg kg^{-1} in Fluvisols and 0.79–7.65 mg kg^{-1} in Andosols. The ranking of rice cultivars was maintained across the soils, suggesting that Cd concentration of rice grains could be controlled by genetic factors rather than environmental conditions. Generally, Cd concentrations are higher in *Indica*-type rice varieties than in *Japonica* ones. The representative Japanese *Japonica* cultivars, Nipponbare, Koshihikari, and Sasanishiki, were categorized as the rice group with low grain Cd concentrations. The lowest grain Cd concentrations were found in two varieties, LAC23 and HU-LO-TAO. These rice varieties can be used as good materials to develop varieties with lower Cd levels than those in the varieties currently under cultivation. *Indica* rice variety, IR-8, which led to the green revolution in the Asia in 1960s, was categorized as the highest group in grain Cd concentrations. Milyang 23 and Habataki were produced from the common ancestor, IR-8, and high Cd concentrations of these *Indica*

varieties must be inherited from IR-8. These high Cd-accumulating rice varieties can be used as the "cleaning plants" of Cd-contaminated paddy-field soil (see Section 5.5). Thus, large differences in Cd accumulation among rice cultivars enable us to develop phytotechnologies, such as breeding of low Cd-accumulating varieties and phytoextraction of Cd by using high Cd-accumulating varieties for reducing the Cd levels in rice grains.

5.3.2. Physiological and Genetic Mechanisms

Understanding of the physiological and genetic aspects underlying Cd transport in rice is important to control Cd transfer into grains. The level of Cd in rice grains may be influenced by any of several physiological processes: 1) root Cd uptake, 2) sequestration of Cd into root vacuoles, 3) transfer from roots to shoots via the xylem, 4) transfer from xylem to phloem, and 5) phloem transport into grains. Uraguchi et al. (2009) characterized the physiological properties involved in the differences in shoot and grain Cd accumulation between the low Cd-accumulating variety Sasanishiki and high Cd-accumulating variety Habataki. The activity of root Cd uptake was higher for Sasanishiki than for Habataki. However, Cd levels of xylem sap were well correlated with the shoot-Cd concentration in the two cultivars.

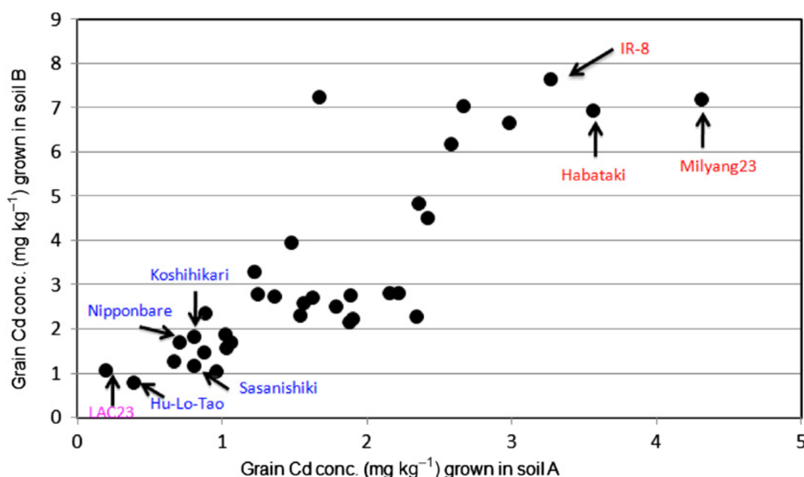


Figure 4.4 Genotypic variation in grain Cd concentration in rice. Thirty-five rice cultivars were cultivated in a container filled with two types of Cd-polluted soils under upland conditions (soil A, soil B). Koshikikari, Nipponbare, Sananishiki and Hu-Lo-Tao are *Japonica* and IR-8, Habataki and Milyang 23 are *Indica* subspecies. LAC23 is tropical *Japonica* (Javanica) variety (modified data from Arao and Ishikawa (2006)). A, Fluvisols (0.5 mg Cd kg^{-1} of dry soil); B, Andosols (5.1 mg Cd kg^{-1} of dry soil). For color version of this figure, the reader is referred to the online version of this book.

A positive and strong correlation between Cd concentrations in the xylem sap and subsequent shoot-Cd accumulation was also observed in a world rice core collection consisting of 69 accessions, which covers the genetic diversity of almost 32,000 accessions of cultivated rice (Fig. 4.5). These findings suggest that root-to-shoot Cd translocation via the xylem is the major and common physiological process determining shoot-Cd accumulation among rice cultivars.

Rice-phloem sap can be collected using cut stylets of the brown plant hopper (Kawabe et al., 1980). Using this method, Cd levels in the phloem sap were measured and it was found that more than 90% of Cd present in grains is translocated via phloem (Tanaka et al., 2007). Moreover, Cd concentration of the phloem sap of LAC23, the variety with lowest Cd accumulation in grains, was significantly lower than that of Koshihikari, the Japanese elite variety, despite similar levels of Cd in xylem sap in these cultivars (Kato et al., 2010). Thus, differences in grain Cd concentrations in rice cultivars may be in part explained by a different ability of phloem to transport Cd to grains.

It is necessary to understand the genetic aspects of Cd accumulation in order to devise a breeding plan for reducing Cd levels in rice grains. Quantitative trait loci (QTL) analysis is a powerful tool for understanding the genetic control underlying agronomic and physiological traits in

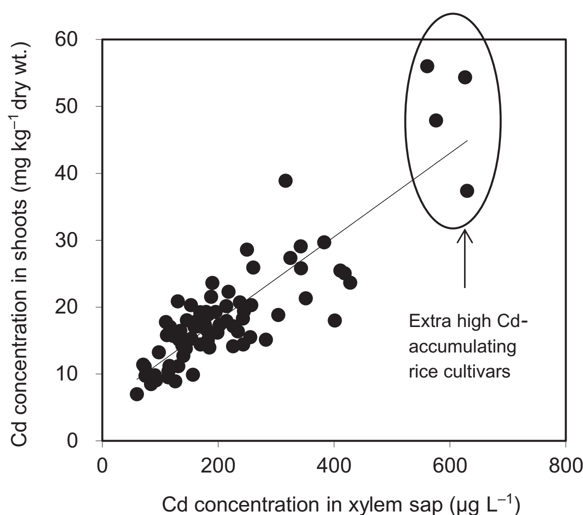


Figure 4.5 Relationship between Cd concentration in shoots and that of xylem sap in diverse rice germplasms (Uraguchi et al., 2009 with permission).

rice (Yamamoto et al., 2009). Using backcross inbred lines and advanced-backcross progenies derived from a cross between the low-Cd cultivar Sasanishiki and the high-Cd cultivar Habataki, Ishikawa et al. (2010) reported a major-effect QTL (named as qGCd7) controlling Cd concentration in rice grains without affecting concentrations of essential trace metals (Cu, Fe, Mn, and Zn), and it is located on the short-arm chromosome 7. Moreover, this QTL had no significant effect on important rice agronomic traits, such as grain yield, grain weight, and days to heading. Using other mapping populations derived from crosses between low-Cd Japanese rice cultivars and high-Cd *Indica* ones, the QTL with a major effect related to Cd-translocating ability from roots to shoots at the seedling stage has also been detected on the short arm of chromosome 7 (Tezuka et al., 2010; Ueno et al., 2009). It also has been revealed that OsHMA3, a P1B-type ATPase, is a gene that controls root-to-shoot Cd translocation (Miyadate et al., 2011; Ueno et al., 2010). Functional analyses of the OsHMA3 gene in yeast showed that low-Cd cultivars contain a functional version of this gene, which is involved in Cd storage in root vacuoles. The high-Cd cultivars have lost this function; consequently, a much higher amount of Cd was loaded into the xylem. Overexpression of the functional OsHMA3 gene from the low-Cd cultivar drastically decreased Cd accumulation, not only in shoots but also grains in rice. Thus, this gene can be used to develop the phytotechnologies for controlling Cd accumulation in rice.

5.3.3. Breeding of Low Cd-Accumulating Cultivars

Although Japanese rice cultivars are categorized as the low-Cd group and possess the functional OsHMA3 gene, some Cd-contaminated areas in Japan produce rice grains that exceed the maximum allowable limit of Cd. Thus, a breeding program has been initiated to produce rice varieties that have lower grain Cd concentration than the elite cultivars currently grown in Japan (Yamaguchi, 2006). LAC23, the tropical *Japonica* rice variety, was selected as a donor of the low-Cd trait because this variety has lower grain Cd concentration than other Japanese rice cultivars. LAC23 is not a practical variety in Japan because of late heading, long culms, long grains, and low yields. So crossing was undertaken with the Japanese rice cultivar Fukuhibiki, which has a good plant shape and offers stable high yields. This way, one could develop lines with low Cd concentrations but also with improved cultivation characteristics. By analysis across three to five self-fertilized generations (F3–F5), five promising lines were selected which, in comparison with Fukuhibiki and the elite cultivar Hitomebore, had 40–50% lower Cd

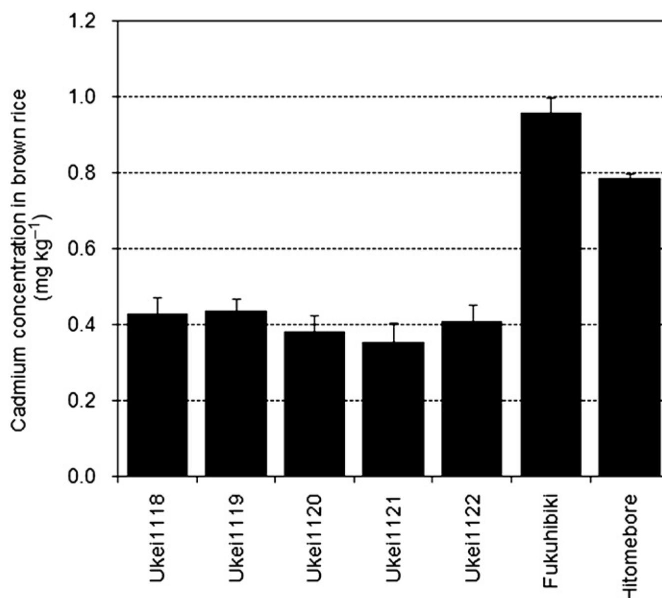


Figure 4.6 Cadmium concentration in brown rice of newly developed lines. Five promising lines (named as Ukei1118-Ukei1122) were developed from a cross between LAC23 and Fukuhibiki at the National Agricultural Research Center for Tohoku region in Japan. Hitomebore is one of the popular cultivars in Japan.

concentrations in brown rice (Fig. 4.6), headed sooner than LAC23, and became comparatively shorter in plant height (Plate 4.2). These five lines were assigned the local numbers Ukei1118 through Ukei1122 based on the place where they were raised (National Agricultural Research Center for Tohoku Region, Daisen City, Akita Prefecture, Japan). For other trace metal concentrations such as Cu, Fe, Mn, and Zn, newly developed lines were nearly equal to those of Fukuhibiki and Hitomebore. Thus, it was possible to develop lines in which only the concentrations of Cd were reduced in the brown rice. However, further improvement should be done to incorporate high grain yield and good taste into promising lines. To develop practical low-Cd cultivars efficiently, attempts are being made to identify the QTL for the low-Cd trait controlled by LAC23 allele and to develop the DNA marker linked to the QTL for the screening process.

5.4. Soil Dressing

Soil dressing is simple and is one of the most widely used techniques for heavily contaminated sites (Vangronsveld and Cunningham, 1998). This method has been adopted as a primary counter measure for Cd contamination in

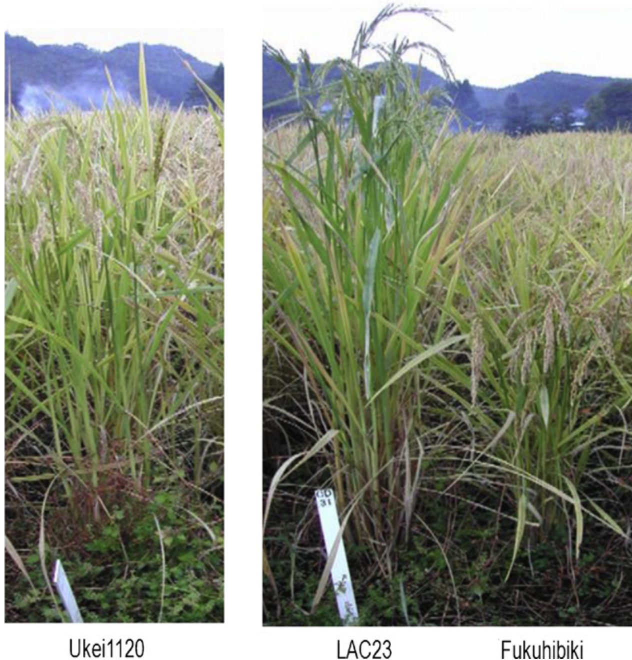


Plate 4.2 Plant shapes of the low-Cd line (Ukei1120) and parental cultivars (LAC23 and Fukuhibiki). Ukei1120 (one of the newly developed low-Cd lines) ripens sooner than LAC23 and has shorter culm length. For color version of this figure, the reader is referred to the online version of this book.

agricultural soils under the Agricultural Land Soil Pollution Prevention Law in Japan. Local managers, who are responsible for contamination prevention, prefer this technique over other countermeasures because of its low risk of failure, its predictable time frame, and because it leaves the site in a relatively pristine condition. There are several methods to amend the polluted soils by soil dressing (Yamada, 2007).

5.4.1. Simple Soil Dressing

Unpolluted soils are placed on the top of the polluted soil (Fig. 4.7). Since the paddy fields amended by this method are raised by 20–30 cm, preparation of agricultural canals and agricultural roads and rezoning of paddy fields are needed with the application of this method.

5.4.2. Soil Removal Followed by New Soil Dressing

Polluted surface soils are removed and discarded outside of paddy fields. Then, the infertile subsurface soils are covered with unpolluted soil. The

depth of polluted soil removal is determined based on the degree of soil pollution and plant root elongation.

5.4.3. In situ *Placement of Polluted Soils*

First, the polluted surface soil is removed; then the subsoil is also temporarily removed to secure the place to bury the polluted surface soil (Fig. 4.8).

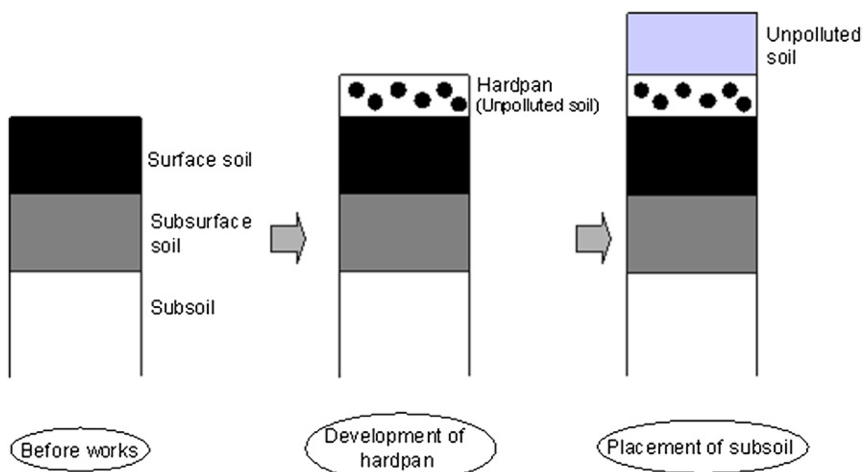


Figure 4.7 Simple soil dressing. For color version of this figure, the reader is referred to the online version of this book. *(Modified from Yamada (2007)).*

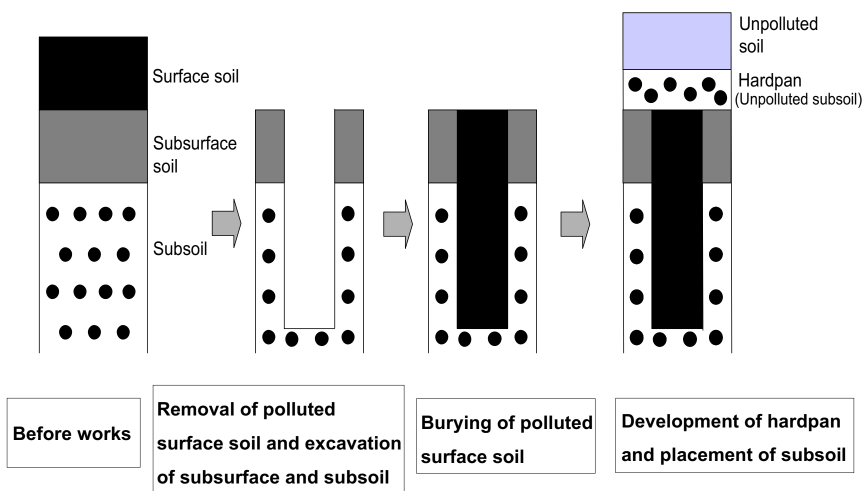


Figure 4.8 *In situ* placement of polluted soils (Yamada, 2007 with permission). For color version of this figure, the reader is referred to the online version of this book.

The polluted surface soil is then buried into subsoil layer. After that, the part of removed subsoil is returned on top of the buried surface soil. This is followed by placement of new unpolluted surface soil on the top of the returned subsoil. However, it is difficult to apply this method to paddy fields where the subsoil layer soil is also polluted and/or the water table is high. This method is applied to paddy fields where the subsoil is not polluted.

According to several follow-up surveys, soil dressing is an effective and reliable practice to decrease the Cd content in rice grains, when the newly added unpolluted soil layer is 20–30 cm thick. However, this practice is costly and becomes increasingly difficult for implementation because of the scarcity of suitable uncontaminated soils. Moreover, this method only postpones the problem to a later date and in authors opinion is not the preferred option.

5.5. Phytoremediation

5.5.1. Necessary Conditions for Phytoextraction

Phytoextraction using hyperaccumulator plants has been proposed as a promising, environmentally friendly, low-cost technology for decreasing the heavy metal content of contaminated soils and has emerged as an alternative to the engineering-based methods (Ebbs et al., 1997; McGrath et al., 2002; Robinson et al., 2006). Hyperaccumulator plants can accumulate pollutants at high concentrations in their shoots and can grow in soils containing high concentrations of metals (Ebbs et al., 1997). Chaney et al. (2004) reported that some ecotypes of *Thlaspi caerulescens* in southern France showed high potential as a phytoextraction technology with low cost for soil Cd remediation. However, *T. caerulescens* may not be suitable for many large-scale phytoextraction projects because the plants are small and grow slowly, making them difficult to harvest mechanically (Ebbs et al., 1997). Cadmium-uptake efficiency of *T. caerulescens* in soils with relatively low levels of Cd pollution may be possible but it may not be effective in soils with more severe pollution (Brown et al., 1995). In addition, culturing these hyperaccumulator species could be hampered by their susceptibility to certain diseases. For example, McGrath et al. (2000) reported that several *Thlaspi* species are infected by diseases whose development was favored by prevailing humid and warm weather conditions. Because the typical weather conditions of the Asian Monsoon summer are humid and warm, it may be difficult to introduce these species into the Asian Monsoon's paddy fields contaminated with low concentrations of Cd. To maximize the efficiency of phytoextraction, it is important to select a phytoextraction plant with high Cd-accumulating

ability that is also compatible with mechanized cultivation techniques and local weather conditions. Such a plant may yield more immediate practical results than selection based solely on high tolerance to Cd.

Several phytoextraction studies have tested nonhyperaccumulator high-biomass plants such as Indian mustard (*Brassica juncea* L.) (Ebbs et al., 1997; Nanda Kumar et al., 1995), tobacco (*Nicotiana tabacum* L.) (Mench et al., 1989), industrial hemp (*Cannabis sativa* L.) (Linger et al., 2002), flax (*Linum usitatissimum* L.) (Angelova et al., 2004), vetiver grass (*Vetiveria zizanioides*) (Chen et al., 2000), poplar (*Populus* spp.) (Laureysens et al., 2005), and willow (*Salix* spp.) (Hammer et al., 2003). These plants can be cultivated in agricultural fields in Japan. However, rice is the biggest crop in Japan, and its cultivation system is well established and highly mechanized. The use of agricultural species adapted to growing conditions of paddy fields may, therefore, be a better alternative.

5.5.2. Plant Selection for Phytoextraction

Rice, soybean, and maize (*Zea mays* L.) are the major summer crops grown in paddy fields and in upland fields (fields under aerobic soil conditions) that have been converted from paddies in Japan. However, the study of phytoextraction using rice and soybean has not yet been examined.

Rice (cv. Nipponbare and Milyang 23), soybean (cv. Enrei and Suzuyutaka), and maize (cv. Gold Dent) were grown on one Andosol and two Fluvisols with a low concentration of Cd pollution ranging from 0.83 to 4.29 mg Cd kg^{-1}, during 60 days in a greenhouse (Murakami et al., 2007). Shoot-Cd uptake was as follows: Gold Dent < Enrei and Nipponbare < Suzuyutaka and Milyang 23 (Fig. 4.9). Several soil-Cd fractions including exchangeable, inorganically bound, and organically bound decreased after harvesting of Milyang 23 (Fig. 4.10). Milyang 23 accumulated 10–15% of the total soil Cd in its shoot. These values were much higher than those reported for *B. juncea* (0.09%) and *T. caerulescens* (0.06%) grown on soil containing 40 mg kg^{-1} of total Cd for 6 weeks (Ebbs et al., 1997). The Milyang 23 rice is, thus, promising for phytoextraction of Cd from paddy soils with low pollution of Cd under aerobic soil conditions.

5.5.3. Phytoextraction by High Cd-accumulating Rice

Soybean is the major summer crop grown in Japanese upland rice fields. The Codex Alimentarius Commission set maximum levels for Cd in wheat, potato (*Solanum tuberosum* L.), many vegetables (Codex, 2005), and polished rice (Codex, 2006). The commission discontinued work on developing

a maximum level for Cd in soybeans, which it considered was not a major contributor to Cd intake (Codex, 2004). However, soybean, via tofu, natto, and soy sauce, is the main source of dietary intake of Cd in Japan (Arao et al., 2003). Thus, decreasing the Cd content of soybean seeds is extremely important. In an earlier study, Murakami et al. (2007) selected "Milyang 23" rice as a promising cultivar for phytoextraction of Cd in paddy soils with low-to-moderate pollution. However, its effect on the Cd content of subsequently grown soybean seeds has not been reported.

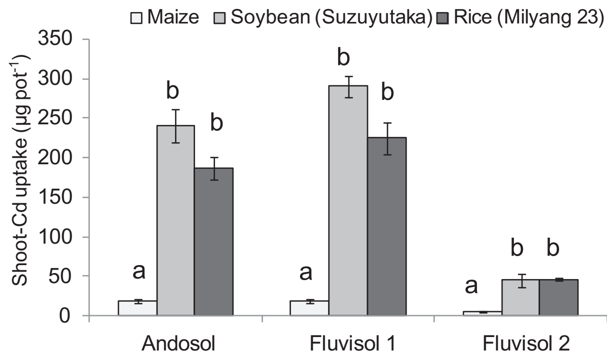


Figure 4.9 Shoot-Cd uptake by maize, soybean, and rice. Error bars represent the standard error ($n = 4$). Means in the each soil followed by the same letter are not significantly different at $p < 0.05$ based on Bonferroni's multiple-comparison test. *(Modified from Murakami et al. (2007)).*

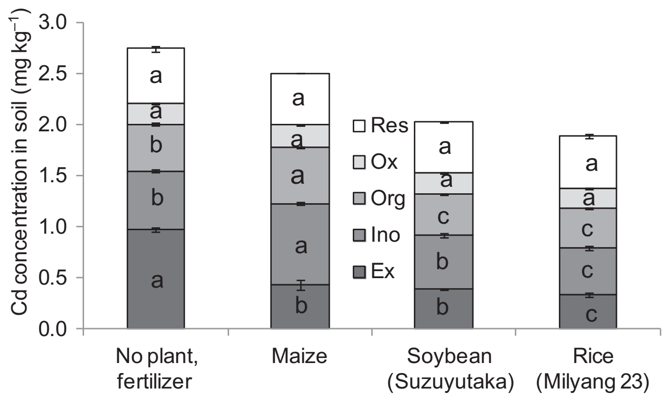


Figure 4.10 Cadmium concentrations in five fractions of Fluvisols, which were remedied by three kinds of Cd accumulator plants. Ex, exchangeable fraction; Inorg, inorganically bound fraction; Org, organically bound fraction; Ox, oxide-occluded fraction; Res, residual fraction. Error bars represent the standard error ($n = 4$). Means in the each Cd fraction followed by the same letter are not significantly different at $p < 0.05$ based on Bonferroni's multiple-comparison test. *(Modified from Murakami et al. (2007)).*

To evaluate the effect of phytoextraction by rice on the seed Cd content of soybean grown subsequently, Murakami et al. (2008) grew Milyang 23, a high Cd-accumulating rice cultivar, followed by soybeans in three paddy soils contaminated with moderate Cd concentrations (2.50–4.27 mg Cd kg^{-1}). The rice accumulated 7–14% of the total soil Cd in its shoots, and decreased several Cd fractions in soil by 8–42% and the total soil Cd by 10–19% (Fig. 4.11). Indian mustard (*Brassica juncea* (L.)) and the hyperaccumulator *T. caerulescens* accumulated 0.09 and 0.06% of the total soil Cd (40 mg kg^{-1}) when grown for 6 weeks in pots (Ebbs et al., 1997). *Nicotiana rustica* L. accumulated 6% and *N. tabacum* L. accumulated 20% of the total soil Cd (5.44 mg kg^{-1}) when grown for 8 weeks in containers (Mench et al., 1989). Thus, Milyang 23 has the potential to phytoextract soil Cd with a similar efficiency as those *Nicotiana* species. The soybean seed Cd contents were 24–46% less than those grown on control soils (nonphytoextracted). Phytoextraction by Milyang 23 rice is, thus, a promising remediation method for reducing seed-Cd contents of soybeans grown on paddy soils under aerobic soil conditions.

Previous research has shown that the Cd concentration in rice shoots grown under flooded (reducing) soil conditions may be low because Cd solubility under these conditions is lower than under oxidizing conditions

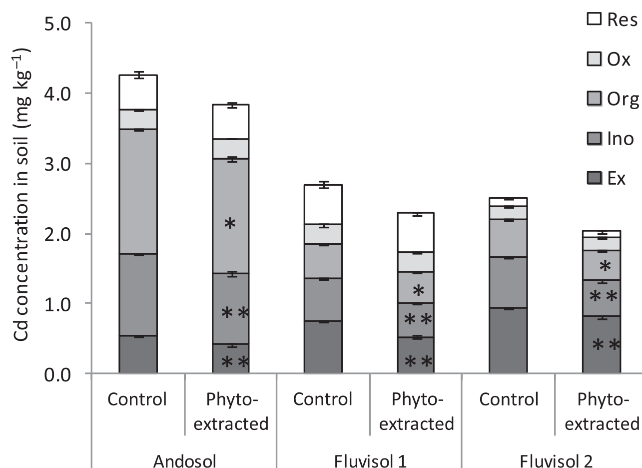


Figure 4.11 Cadmium concentrations in five fractions of control (nonphytoextracted) and phytoextracted soils (Andosol, Fluvisol 1 and Fluvisol 2) by Milyang 23. Ex, exchangeable fraction; Inorg, inorganically bound fraction; Org, organically bound fraction; Ox, oxide-occluded fraction; Res, residual fraction. Error bars represent the standard error ($n = 3$). $^{**}p < 0.01$, $^{*}p < 0.05$ (t-test). *(Modified from Murakami et al. (2008)).*

(de Livera et al., 2011; Kabata-Pendias and Pendias, 2001), as mentioned in Section 5.2. However, the dry weight (DW) of rice shoots grown under flooded soil conditions is higher than that under oxidizing soil conditions during tillering (from transplanting to 30 days before panicle initiation) (Takahashi, 1974). Because shoot-Cd uptake by rice plants equals the product of DW and the Cd concentration of the rice shoots, maximizing shoot-Cd uptake requires management practices that enhance both DW and Cd uptake by the rice shoot. Therefore, Murakami et al. (2009) undertook a field experiment in which the soils of all subplots were maintained under flooded conditions during tillering in order to maximize the DW of the rice shoots, and then drained them and kept them under oxidizing conditions until harvest to maximize Cd accumulation by the rice shoots ("without irrigation after drainage") (Fig. 4.12).

The total shoot-Cd uptake by the *Indica* Chokoukoku grown for 2 years (883 g ha^{-1}) was higher than that by the 3-year grown *Indica* Moretsu (869 g ha^{-1}), *Indica–Japonica* Milyang 23 (638 g ha^{-1}), and *Indica* IR8 (532 g ha^{-1}) (Fig. 4.13). This 2-year shoot-Cd uptake by *Indica* Chokoukoku from soil containing 1.63 mg kg^{-1} of total Cd was higher than the uptake by the hyperaccumulator *T. caerulescens* (540 g ha^{-1} after 3 years of cultivation in soil with a total Cd content of 2.8 mg kg^{-1}) (Hammer and Keller, 2003), by willow, *Salix viminalis* (170 g ha^{-1} after 5 years of cultivation in soil with a total Cd content of 2.5 mg kg^{-1}) (Hammer et al., 2003), and by poplar (*Populus*) clone Balsam Spire (57 g ha^{-1} after 2 years of cultivation in soil with a total Cd content of 0.75 mg kg^{-1}) (Laureysens et al., 2005). In contrast, Cd uptake by the residual roots of the *Indica* Chokoukoku was lower than that of the other *Indica* and *Indica–Japonica* rice cultivars

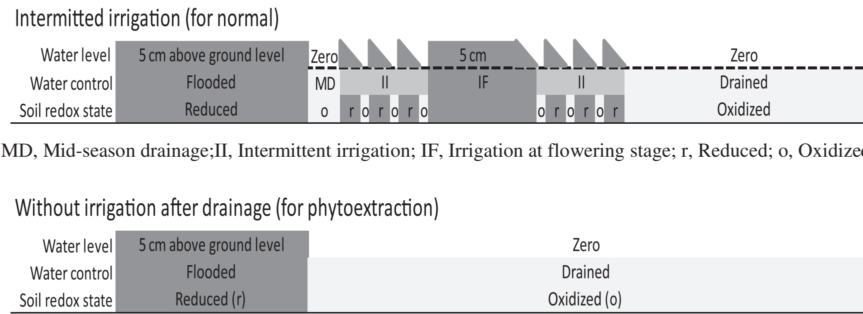


Figure 4.12 Water management during rice cultivation for normal (intermitted irrigation, upper) and for phytoextraction (without irrigation after drainage, lower). *(Modified from Murakami et al. (2009)).*

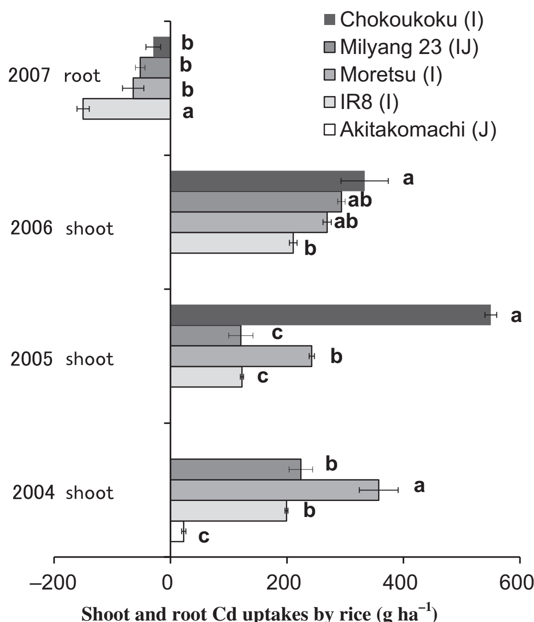


Figure 4.13 Shoot- and root-Cd uptakes by *Indica*-type rice cultivars capable of accumulating Cd at high levels and shoot-Cd uptake by *Japonica* food rice cultivar. Means in the same year (shoot or root) labeled with the same letter do not differ significantly ($p < 0.05$, Tukey–Kramer's HSD test). Error bars represent the standard error ($n = 2$). J, *Japonica*; I, *Indica*; IJ, *Indica–Japonica*. Shoots were harvested in mid-October from 2004 to 2006. Residual roots were sampled in early May in 2007. (*Modified from Murakami et al. (2009)).*

(Fig. 4.13). Cadmium in the residual roots may be released gradually into the soil as the roots are decomposed by soil organisms. Because phytoextraction involves harvesting of plant shoots that have taken up toxic elements from the soil and removing harvestable material from contaminated fields, plants such as the *Indica* Chokoukoku, with high shoot-Cd uptake and low root-Cd uptake, are ideal for phytoextraction. The shoot DWs of the four *Indica* and *Indica–Japonica* rice cultivars did not decrease, even after two or three continuous cultivations without irrigation after drainage, indicating that growth damage from continuous cultivation and the presence of toxic metals in the soil did not occur. This characteristic of rice is also useful for phytoextraction.

The exchangeable, inorganically bound, organically bound, and total soil-Cd concentrations were lowest in the *Indica* Chokoukoku subplot, despite the fact that this cultivar was grown for only 2 years (Fig. 4.14). This suggests that this cultivar can take up Cd more efficiently than the other rice cultivars from the more resistant (inorganically and organically bound)

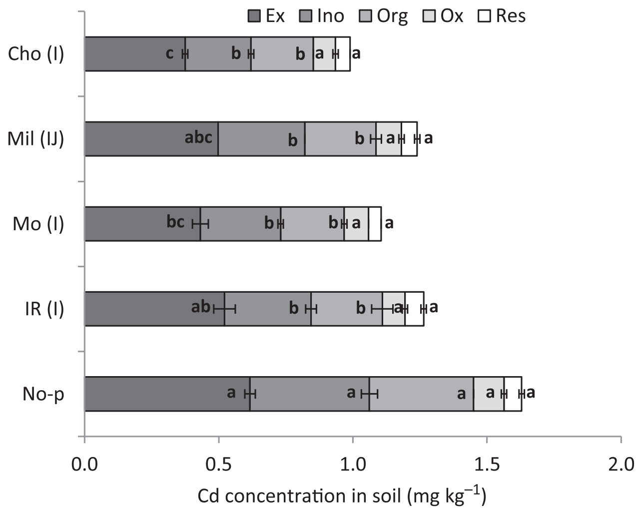


Figure 4.14 Soil-Cd concentrations in the five fractions for each subplot, sampled before plowing in 2007. Ex, exchangeable fraction; Inorg, inorganically bound fraction; Org, organically bound fraction; Ox, oxide-occluded fraction; Res, residual fraction. Error bars represent the standard error ($n = 2$). Means in the same fraction that are followed by the same letter are not significantly different ($p < 0.05$, Tukey–Kramer's HSD test). No-p, no plant (control); IR, IR8; Mo, Moretsu; Mil, Milyang 23; Cho, Chokoukoku. I, *Indica*; IJ, *Indica–Japonica. (Modified from Murakami et al. (2009)).*

fractions, as well as from the more bioavailable (exchangeable) fraction. This uptake capability equaled that of the hyperaccumulator *T. caerulescens* when grown in pots (Hammer and Keller, 2002). The Cd uptake by the residual roots of the *Indica* Chokoukoku (29.5 g ha^{-1}) corresponded to only 0.02 mg kg^{-1} of soil Cd. Even allowing for the return of this root Cd to the soil by microbial decomposition, the total soil-Cd concentration in the *Indica* Chokoukoku subplot was 38% less than the mean value in the subplots with no plants (a reduction from 1.63–1.01 mg kg^{-1}). This reduction in total soil-Cd concentration by the 2-year grown *Indica* Chokoukoku was higher than the reduction by 3-year grown hyperaccumulator *T. caerulescens* (by 15% of total soil Cd, assuming that this plant took up Cd from soil to a depth of 15 cm and with a bulk density of 0.85 Mg m^{-3}) (Hammer and Keller, 2003).

The *Japonica* food rice cultivar Yumesayaka grown after phytoextraction by the four *Indica* and *Indica–Japonica* rice cultivars and in the subplots without phytoextraction showed normal growth (Fig. 4.15). The average of the grain yields of *Japonica* Yumesayaka grown in the four subplots after phytoextraction and in the no plant subplot (5.1 Mg ha^{-1}) was similar to that of

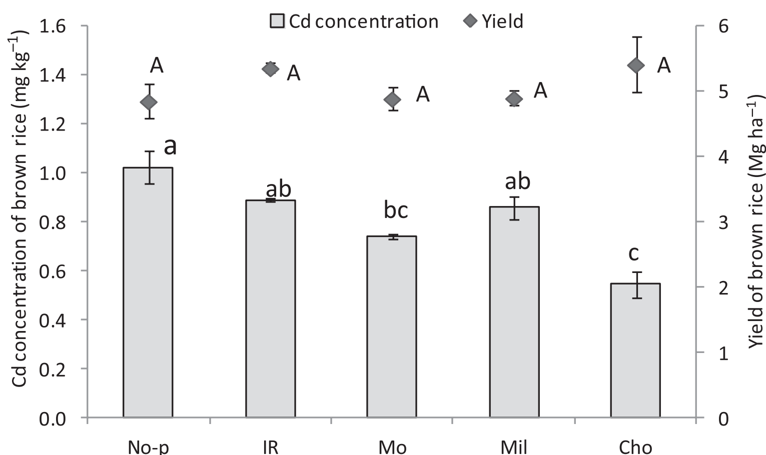


Figure 4.15 Cadmium concentration in rice grain and grain yield of a *Japonica* food cultivar (Yumesayaka) grown after phytoremediation with Indica rice cultivars capable of accumulating Cd at high levels. Error bars represent the standard error ($n = 2$). Means in the each item that are followed by the same letter are not significantly different ($p < 0.05$, Tukey's multiple-comparison test). No-p, no plant (control); IR, IR8; Mo, Moretsu; Mil, Milyang 23; Cho, Chokoukoku. *(Modified from Murakami et al. (2009)).*

Japonica food rice cultivars in Japan in 2007 (5.2 Mg ha^{-1}) (MAFF, 2008). The grain-Cd concentrations of *Japonica* Yumesayaka grown after 2 years of phytoextraction with the *Indica* Chokoukoku were reduced by 47% (to 0.54 mg kg^{-1}) compared to those of the same rice cultivar grown without phytoextraction (1.02 mg kg^{-1}) (Fig. 4.15).

Phytoextraction with the *Indica* rice Chokoukoku grown for 2 years without irrigation after drainage removed 883 g Cd ha^{-1}, reduced the total soil-Cd content by 38%, and reduced the grain-Cd content in subsequently grown *Japonica* food rice by 47% without decreasing yield. The results suggest that phytoextraction with *Indica* Chokoukoku can remove Cd from paddy fields polluted with low-to-moderate levels of Cd and reduce the grain-Cd concentration of *Japonica* food rice cultivars to below the Codex standard within a reasonable time frame. This approach will help reduce the risk of Cd pollution of rice from paddy fields.

Recently, phytoextraction has been criticized by several researchers because of the long period required for restoration, the difficulty of producing a high-biomass crop of the desired species, and the lack of knowledge of agronomic practices and management for phytoextraction (McGrath et al., 2006; Robinson et al., 2006). The research results of Murakami et al. (2009) should help to dispel these criticisms. The DW of, and Cd uptake by, the

Indica rice Chokoukoku were higher than those in the hyperaccumulator *T. caerulescens* (Hammer and Keller, 2003). Paddy rice can be cultivated continuously (De Datta, 1981), and its cultivation system is well integrated and highly mechanized. The *Indica* rice Chokoukoku was managed by agricultural techniques familiar to farmers who grow *Japonica* food rice; it is, therefore, well suited to planting on a wide scale. The 2-year phytoextraction using *Indica* Chokoukoku without irrigation after drainage reduced the total soil-Cd concentration by 38%, and it reduced the Cd concentration in the grain of subsequently grown *Japonica* food rice by 47% without decreasing yield (Murakami et al., 2009). However, the grain-Cd concentration of the *Japonica* food rice was still above the Codex Alimentarius Commission's international standard for the Cd content of rice grain (0.4 mg kg^{-1}) (Codex, 2006). Although this study showed the shoot-Cd uptake by the *Indica* IR8 was lower than that by the *Indica* Chokoukoku, 3-year phytoextraction by *Indica* IR8 on a paddy field reduced the 0.1 mol L^{-1} HCl-extractable Cd concentration in soil from 0.48 to 0.33 mg kg^{-1} and the Cd concentration in the grain of subsequently grown *Japonica* food rice to 0.11 mg kg^{-1} (Honma et al., 2009). Even if the rate of reduction of soil-Cd concentration by phytoextraction with *Indica* Chokoukoku were to become half of that in the first 2 years, an additional 2 years of phytoextraction by Chokoukoku would reduce the grain-Cd concentration of *Japonica* food rice Yumesayaka to below 0.4 mg kg^{-1}.

These results suggest that phytoextraction with the *Indica* rice cultivar Chokoukoku can remove Cd from paddy fields polluted with Cd at low-to-moderate levels and can reduce the grain-Cd concentration of the *Japonica* food rice cultivar Yumesayaka to below the Codex standard within a reasonable time frame. However, a potential hazard is in advertent use of the phytoextractor grain as a food for humans and domestic animals. For example, large numbers of people were poisoned in Iraq in the early 1970s when mercury-treated grain meant for seed was eaten in home-made bread; poisoning also occurred in the USA in 1969 when treated grain was fed to hogs, whose meat was subsequently eaten (Bakir et al., 1973; Curley et al., 1971). Phytoextraction by *Indica* rice cultivars capable of accumulating Cd at high levels will be applicable to the remediation of paddy fields in Monsoon Asia that have low-to-moderate levels of Cd pollution, provided that careful attention is paid to disposal of the high-Cd rice. Use of the phytoextraction techniques described here will help reduce the risk of Cd pollution of rice from paddy fields.

5.6. Soil Washing

Soil washing is conventionally performed ex situ using appropriate equipments, in which extracting reagents are used to remove hazardous metals from soil into aqueous solution (Elliott and Herzig, 1999). The *in situ* soil washing is usually called "soil flushing"; therefore, the word "soil washing" is consistently used in this section to avoid confusion. The soil-washing techniques offer a great advantage of high Cd-removal efficiency for contaminated soils. However, this technique has been considered to be difficult to apply directly to agricultural land because wastewater drained during the process of soil washing might pollute surrounding environments such as agricultural canals, neighboring agricultural fields, and groundwater. However, paddy fields possess an impervious hardpan just below the subsurface layer, which hinders vertical movement of water. The washed solution stays in the surface soil and does not penetrate into subsoil layers and groundwater. So, an *in situ* technology of soil washing should be utilized fully to take advantage of such unique characteristics of the paddy field.

The *in situ* soil-washing method of paddy fields has to meet the following criteria (Makino et al., 2006, 2007):

1. Use of washing chemicals with high efficiency of Cd removal but a minimal adverse impact on the paddy field and its surrounding environment.
2. Cost-effective and environmentally sound in operation of the system.
3. Soil fertility of the paddy field and its crop growth are not greatly affected by the washing treatment or can be easily corrected by the application of agricultural materials.
4. The effect of washing can last for a reasonably long period.

Makino and his team (Makino et al., 2006, 2007) have developed a new soil-washing practice combined with on-site wastewater treatment that completely satisfies the abovementioned four requirements, which is discussed in the following sections.

5.6.1. Selection of Washing Chemicals

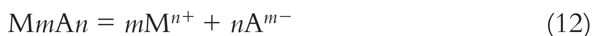
Chelating agents, neutral salts, and strong acids have been used for soil washing to solubilize metals (Davis, 2000). In particular, ethylenediamine tetraacetic acid (EDTA) has been commonly used due to its efficiency of Cd removal from contaminated soils (Abumaizar and Smith, 1999; Nakashima and Ono, 1979; Zeng et al., 2005). EDTA, however, is a persistent chemical and stays for a long time in the environment (Tandy et al., 2004). Some

scientists, therefore, have used more biodegradable chelating agents instead of EDTA (Chang et al., 2005; Hong et al., 2002; Kantar and Honeyman, 2006; Mulligan et al., 1999; Tandy et al., 2004). In case biodegradable agents are used, however, the cost becomes relatively higher than the non-/less-degradable counterparts.

Makino et al. (2006) noticed that calcium chloride ($CaCl_2$) is one of most appropriate soil-washing chemicals for Cd-contaminated paddy soils on the basis of Cd extraction efficiency, cost-effectiveness, and relatively low environmental impacts. The high efficiency of $CaCl_2$ in the extraction of soil Cd was mainly attributable to the high selectivity of Ca for soil adsorption sites compared with monovalent cations, the concurrent lowering of the solution pH due to hydrolysis of exchangeable Al, and the formation of Cd–Cl complexes. Makino et al. (2006) also mentioned that hydrochloric acid (HCl), nitric acid (HNO_3), and EDTA-2Na extracted more soil Cd than neutral salts (Figs 4.16 and 4.17). However, EDTA-2Na is difficult to use for practical purposes, because of its persistent nature in the environment and relatively high cost. Both strong acids cause serious soil acidification, which is a problem if the soils possess a low pH-buffering capacity.

Iron (III) chloride ($FeCl_3$) extracted nearly as much Cd as HCl, HNO_3, and EDTA-2Na from the Nagano (Fluvaquents) and Toyama (Epiaquepts) soils and more Cd from the Hyogo soil (Fluvaquents) (Fig. 4.16) (Makino et al., 2006). Iron is a major soil constituent and is less environmentally harmful than either of the other chemicals. In addition, $FeCl_3$ is less expensive and easier to handle than both HCl and EDTA-2Na, so that $FeCl_3$ was selected as a promising washing chemical. The Cd extraction capacity was compared with other metal salts to elucidate the mechanism of Cd extraction by $FeCl_3$. The proportion of total soil Cd extracted by the washing chemicals (i.e. the Cd extraction efficiency) increased in the following order: Mn salts ≤ Zn salts << ferric Fe salts in all three soils, with efficiencies ranging from 4 to 41%, 8 to 44%, and 24 to 66%, respectively. The amount of Cd extracted was negatively correlated with the extraction pH, suggesting that extraction pH plays an important role in determining the Cd-extraction efficiency.

When metal salts are added to soils, the dissociated metal cations may form hydroxide precipitates with the release of protons (H^+) according to the following equations (hydrolysis):



$$\mathrm{M}m\mathrm{A}n = m\mathrm{M}^{n+} + n\mathrm{A}^{m-} \qquad (12)$$

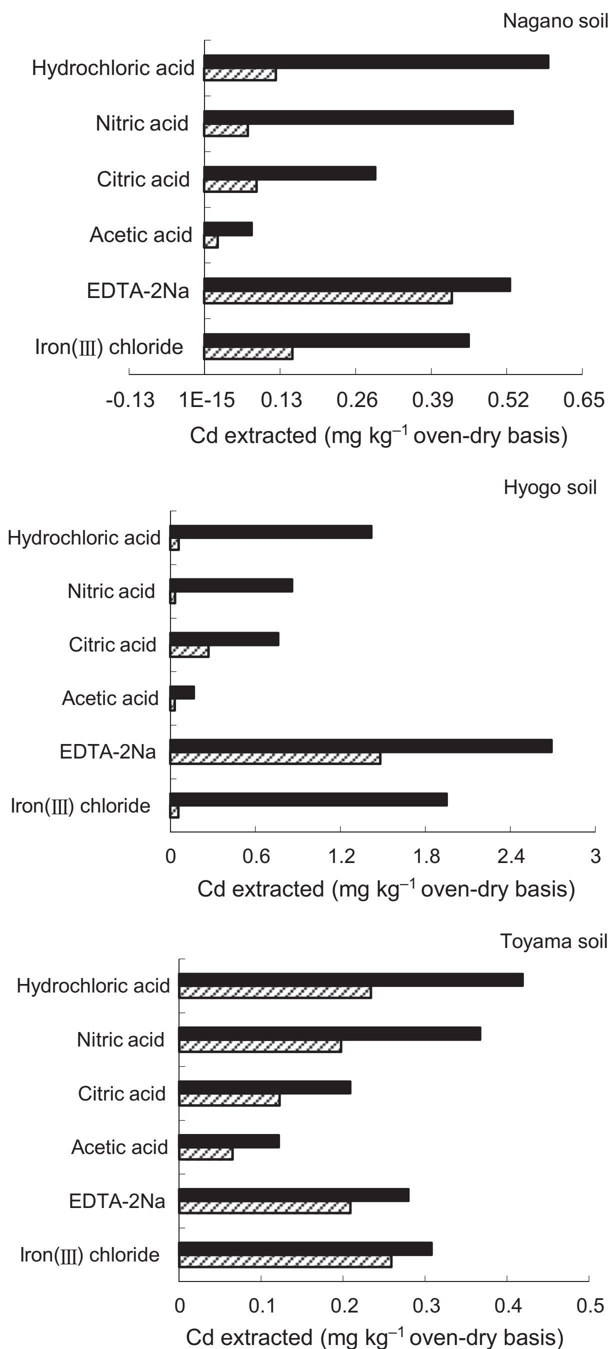


Figure 4.16 Effect of various chemicals (other than neutral salts) on the efficiency of soil Cd extraction; concentration of chemicals used for the Cd extraction (0.02 mol_c L^{-1} (▨) and 0.1 mol_c L^{-1} (■)). (Makino et al. (2008) with permission).

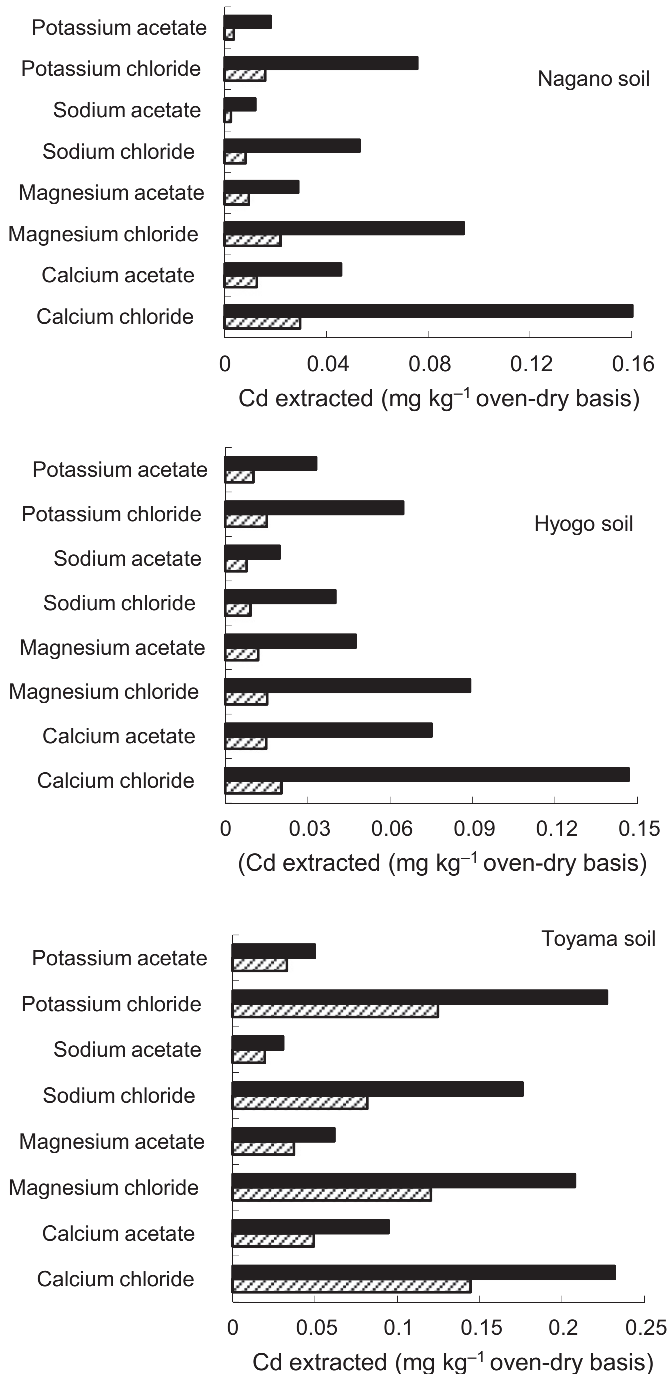
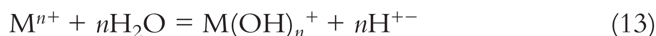


Figure 4.17 Effect of various neutral salts on the efficiency of Cd extraction from three soils; concentration of the neutral salts used for the Cd extraction (0.02 $mol_c\ L^{-1}$ (▨) and 0.1 $mol_c\ L^{-1}$ (■)). (Makino et al. (2008) with permission).



$$M^{n+} + nH_2O = M(OH)_n{}^{+} + nH^{+-} \quad (13)$$

$$K^{o}m = [M(OH)_n][H^+]^n/[M^{n+}][H_2O]^n \quad (14)$$

where MmAn denotes the metal salt, M, the metal cation (Fe, Zn, or Mn), and A, the anion (Cl^-, NO_3^-, or SO_4^{2-}); m and n represent the charge numbers of the anion and cation, respectively; K°m denotes the equilibrium constants (expressed in terms of activities) for metal M^{n+} in Eqn (13), which correspond to 2.88×10^{-4}, 3.31×10^{-13}, and 6.46×10^{-16} for Fe^{3+}, Zn^{2+}, and Mn^{2+}, respectively (Lindsay, 1979).

The precipitation of the metal hydroxide (hydrolysis of the metal ion) generates H^+ at a rate that depends on K°m, and these protons may decrease the extraction pH (Eqns (12)–(14)). Figure 4.18 illustrates the theoretical relationships between pH and activity of metal ions in the metal hydrolysis reactions at the equilibrium with soil iron (calculated using Eqn (14) and the K°m values). The pH of ferric hydroxide is around 2 (Fig. 4.18), which is much lower than the original pH of the three soils.

Thus, the Fe hydrolysis is associated with a greater decrease in soil pH compared to the other two metals. This indicates that a driving force of the Cd extraction by $FeCl_3$ is proton release, which results in a sharp decrease in soil pH. In another study, Cd was highly mobile under the oxidizing and acidic conditions seen in these soils (Kabata-Pendias, 2000). Heavy-metal solubilization was greatly enhanced by acidification and, at pH 1.3, reached more than 80% of the total Cd content of the soil (Dube and Galvez-Cloutier, 2005). Results obtained in the study endorse the effectiveness of iron salts as the washing chemical to remove soil Cd.

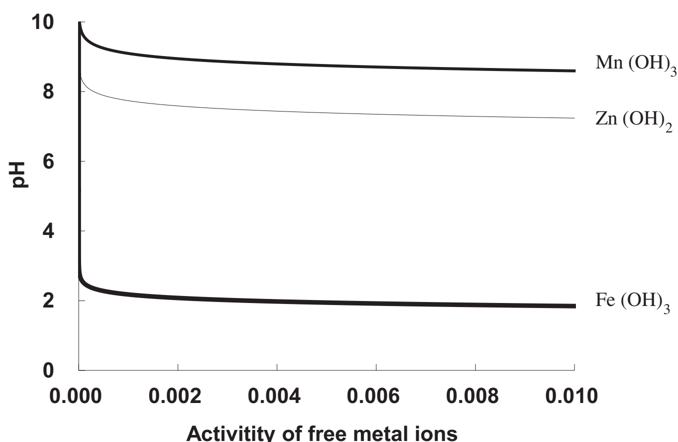


Figure 4.18 Diagram of pH and metal activity to precipitate metal hydroxides. (Makino et al. (2008) with permission).

The Cd-extraction efficiency of metal chlorides was greater than that of the corresponding metal sulfates and nitrates in all soils. Extraction efficiency decreased in the following order: chlorides > nitrates ≈ sulfates, with values ranging from 41 to 75%, 14 to 63%, and 26 to 62%, respectively, in the Nagano soil. The results were similar for the other two soils. To examine the factors that resulted in the difference in the extraction efficiency between the metal salts, Makino et al. (2008) estimated the relative abundance of dissolved Cd species in 100 mmol L^{-1} iron salt solution by the Visual MINTEQ software (Gustafsson, 2004). Figure 4.19 indicates that Cd–Cl complexes such as $CdCl^+$ and $CdCl_2$ (aq) accounted for 80% of the total dissolved Cd in the Nagano soil at 100 mM_c $FeCl_3$, versus values of 33% for $Fe_2(SO_4)_3$ and 9% for $Fe(NO_3)_3$. Similar trends were observed for the other metal salts and soils. Cadmium has a high capacity to form complexes with anions such as Cl^-, SO_4^{2-}, CO_3^{2-}, PO_4^{3-}, organic acids, and fulvic acid (Kunhikrishnan et al., 2012; Traina, 1999). Doner (1978) reported that Cd was leached more rapidly in the presence of Cl^- than in the presence of ClO_4^-. Sakurai and Huang (1996) showed that the rate of desorption of Cd from a montmorillonite was greater with KCl than with KNO_3. Smolders and McLaughlin (1996) suggested that high concentrations of Cl^- in saline soils might increase plant uptake of Cd either by enhancing mass transport of Cd or by enhancing uptake of the $CdCl^+$ complex by plant roots. Accordingly, the formation of stable Cd–Cl complexes

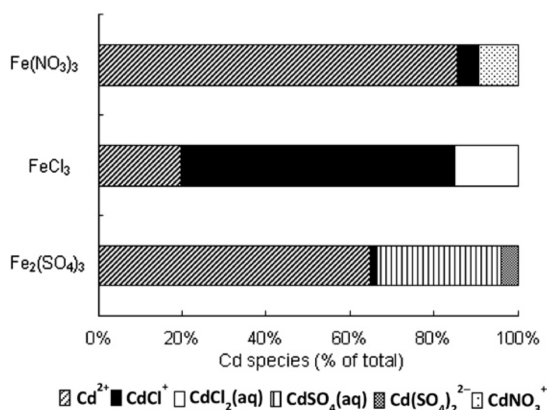


Figure 4.19 Relative abundance of various Cd species in the extracts of the Nagano soil in the presence of the three iron compounds. The Cd species were calculated using the Visual MINTEQ software (Gustafsson, 2004) based on the dataset of cations, anions, pH and dissolved organic carbon values obtained for the extracts. (Makino et al. (2008) with permission).

could inhibit resorption of the extracted Cd onto adsorption sites on the surface of the soil particles. This inhibition mechanism will improve the efficacy of extraction with $FeCl_3$ compared to that with $Fe_2(SO_4)_3$ and $Fe(NO_3)_3$, because the proportion of Cd complexes to the total dissolved Cd concentration is high in the extracts with chloride salts.

5.6.2. On-site Soil Washing (Soil Flushing) in Paddy Fields

The soil-washing procedure developed by Makino et al. (2007) consisted of three steps: (1) chemical washing with appropriate chemical solutions, such as $CaCl_2$ and $FeCl_3$ to extract Cd from soils, (2) followed by water washing to eliminate the remaining chemicals, and (3) on-site treatment of the wastewater by a portable purification apparatus with a chelating material (Fig. 4.20). In a field study, a part of the paddy field was bound with plastic boards, which were partially buried on the edges of the paddy field so that the upper two-thirds of each board remained above the ground surface. This boundary provided containment for additional water and chemicals in the paddy field.

The flushing chemical was applied to the bounded experimental field, followed by addition of agricultural water, creating a soil-solution ratio of 1:1.5–1:2. The soil suspension was mixed by a tilling machine until it turned into slurry. It is important to mix the soil suspension thoroughly enough because the structure of soil clods was maintained and the diffusion of washing chemical into the clods was likely a rate-controlling factor for the extraction

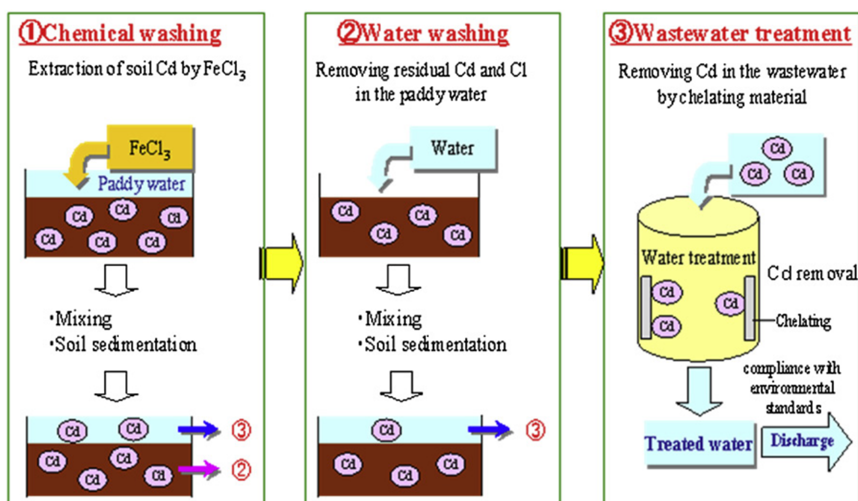


Figure 4.20 Conceptual diagram of on-site soil washing. For color version of this figure, the reader is referred to the online version of this book.

of soil Cd. The soil suspension was allowed to rest after the mixing, and then the Cd-containing supernatant of the slurry was drained off as wastewater and sent to the wastewater treatment system (Makino et al., 2007).

The Cd concentrations in the treated wastewater were below the Japanese environmental quality standard (0.01 mg Cd L^{-1}), demonstrating that the *in situ* treatment system could treat the wastewater as expected. The Cl concentration was <500 mg L^{-1} after water washes; this concentration is the threshold value for healthy rice crops.

The concentration of exchangeable Cd was significantly decreased and little changed after $CaCl_2$ and $FeCl_3$ washing, respectively, but the weakly acid-soluble Cd form decreased substantially in the $FeCl_3$ washing. Although the exchangeable Cd increased with decreasing soil pH caused by the washing treatment, adjusting the pH to the initial pH by the addition of lime could decrease the exchangeable Cd concentration and maintain it at this level after the washing.

The soil pH values were significantly decreased after the washing treatment. Although EC increased, it did not reach a level that would affect growth of rice plants. Exchangeable Mg and K decreased owing to the soil washing. The Mg and K deficiencies were corrected by the application of fertilizers to the washed soil, restoring the Mg and K concentration in soil during the growth period. Total carbon and total N concentrations changed little. Although the extraction pH became very acidic with an application of $FeCl_3$, the amount of soil Al released was <1% of the total soil Al, indicating that the *in situ* soil treatment is unlikely to cause serious soil damage such as clay mineral destruction.

Soil washing considerably decreased the Cd concentrations in the rice grain. The reduction rates of unpolished rice after $CaCl_2$ and $FeCl_3$ washings were around 40 and 80%, respectively. These results proved the efficiency and effectiveness of the soil-washing method for remediation of Cd-contaminated paddy fields.

5.7. Integrated Risk Management

A number of challenging issues need to be taken into consideration when devising strategies to manage Cd contamination in rice ecosystem. These include the following:

1. *Multisource of Cd contamination*: Cd reaches rice ecosystems through various sources that include Cd-containing P fertilizers and organic amendments, drainage from mine tailings, and domestic and industrial wastewater.

2. *Complexity of Cd contamination*: the severity and long-term persistence of Cd contamination in rice ecosystems are influenced by factors such as site hydrogeology, redox conditions, the flooding period, water use, and chemical form and speciation of Cd.
3. *Changes in chemical speciation*: Cd undergoes several biogeochemical transformation processes, especially under alternate wetting and drying conditions prevalent under rice cropping, thereby resulting in the release of Cd species which differ in their biogeochemical reactions, bioavailability, and biotoxicity.
4. *Magnitude of Cd contamination resulting from excessive use of irrigation water*: Lowland rice consumes large quantities of water, resulting in a high uptake of Cd in the presence of Cd-rich wastewater irrigation. Similarly, high uptake of As has been found to occur with the use of As-rich irrigation water in rice cropping in Bangladesh and India (Mahimairaja et al., 2005).

It is, therefore, important to formulate integrated risk-management strategies involving source avoidance, source reduction, and remediation of soil and water (Fig. 4.21). Source avoidance refers to avoiding the Cd-contaminated sources such as fertilizer, organic manure, irrigation water, mine tailings, and Cd-contaminated sites for rice cultivation. For example, Cd-free P fertilizers such as DAP can be used to supply both N and P for rice crops. Another strategy is source reduction, which refers to removing or stopping the source of Cd contamination and subsequent uptake by rice plants. Source reduction can easily be achieved when the contamination source is of anthropogenic origin such as mine sites or similar point sources. Unlike in the case of As contamination, in most regions, Cd contamination of rice ecosystems is largely of anthropogenic origin, and source reduction may be a feasible option to manage Cd contamination.

Remediation of contaminated soil and water resources requires both short-term and long-term solutions for the Cd problem. Depending on the efficiency and cost-effectiveness of the system, a combination of technologies may be required. The potential technologies for remediation of Cd-contaminated soil and water resources in relation to rice cultivation are presented in Fig. 4.21. For example, in the case of soil, a number of technologies including soil dressing followed by soil washing, immobilization of Cd using liming materials, and phytoremediation are available to manage Cd contamination. In the case of irrigation water, immobilization of Cd following by filtration can be used to remove Cd (i.e. Cd stripping). More sophisticated stripping methods, which may require a series



Figure 4.21 An integrated approach to manage Cd in rice ecosystem.

of filtering–sorptive (precipitation) setups, are necessary in order to cope with the enormous volume of irrigation water required for rice cultivation. Cultural practices to manage Cd accumulation in rice grains include cultivation of low Cd-accumulating rice varieties and flood management after heading. Hence, a successful remediation scheme for Cd-contaminated rice ecosystems should aim for an integrated approach involving the possible combination of physical, chemical, and/or biological mechanisms.

It is essential that the integration of remediation technologies should enhance efficiency, both technologically and economically, resulting in a reduction in the time required for achieving targeted levels of Cd in the

rice grain. For example, phytoremediation is a promising new technology, which is relatively inexpensive, and proven effective in large-scale remediation of both soil and water resources. Further, it would also add "green" value (esthetic) to the environment. Integrating physical, chemical, and/or bioremedial measures with phytoremediation could enhance higher uptake of Cd by sacrificial plants, thereby achieving the removal of Cd from contaminated rice fields.



6. SUMMARY AND FUTURE RESEARCH NEEDS

Cadmium (Cd) is one of the major toxic heavy metals reaching the food chain. In rice soils, Cd is derived mainly from the application of Cd-containing P fertilizers and biosolids. Contamination also results from mine tailings and acid-mine drainage. Cadmium is accumulated in plants more readily than most other metals and can be translocated into edible parts before any signs of phytotoxicity. Rice is one of the most important crops grown for human consumption, and Cd accumulation in rice grains poses a potential health risk. The enrichment of Cd in paddy rice grain tends to occur during soil oxidation, which accompanies preharvest drainage of the flooded paddy.

Several studies about Cd-contaminated soils are available but the guidelines established by individual countries worldwide to control the pollution of agricultural soils are not consistent and standardized. Scientific evidence from site-specific research, particularly long-term field trials involving all types of key conditions and factors, are necessary to understand the bioavailability of Cd in various soil types and to provide reliable parameters for health-based risk assessments. In particular, the collection of reliable databases on Cd concentrations in different conditions of soils, climates, rice cultivars, etc. must be given utmost importance. From these databases, a variety of useful information and methodologies can be developed toward achieving the ultimate goal of providing safe and high-quality rice, especially in the case of lowland soils.

Unlike upland soils, paddy soils are flattened evenly for water control under flooding and huge amounts of water are irrigated during rice cultivation. The irrigation of contaminated water and the utilization of contaminated soils are considered to be the most important routes of Cd accumulation in paddy soil and rice plants. The best solution for mitigating Cd contamination in paddy soils and the rice plant is to remove the sources of Cd in the environment and to prevent Cd flow into paddy soils. Hence,

further research needs to be done to determine the effectiveness in suppressing Cd availability when released from the sources, which include mining and industrial wastes and others. A number of soil remediation techniques for Cd-contaminated soils have been developed but some of these techniques are not efficient in terms of time, cost, and environmental compatibility. In order to select the best and most practical technique for remediation of Cd-contaminated rice paddy soils, more investigations are needed.

The biogeochemistry of Cd in rice ecosystems is complex and mostly determined by its chemical speciation resulting from chemical and biological transformations. The chemistry of soil and water (i.e. pH and Eh) plays a major role in Cd dynamics in paddy soils, which undergo changes in redox reactions during a growing season.

Risk management of Cd-contaminated paddy soils and the associated flooded water is an important issue and a great challenge. Its success is necessary to minimize Cd accumulation in paddy rice grains that reach the food chain. A number of physical, chemical, and biological technologies involving immobilization, filtration, and phytoremediation have been developed to remediate Cd-contaminated paddy soils and the associated water. Conventional physical and chemical remedial measures usually are expensive but may prove highly effective. Field testing of some of these technologies has shown them to be successful in reducing Cd accumulation in rice grains. Low Cd-accumulating rice varieties can be used to minimize Cd reaching the food chain. Phytoremediation, which is relatively inexpensive, has been proven effective in the remediation of metal(loid)s-contaminated sites, including those with Cd. Nonedible, Cd-hyperaccumulating crops, like ornamental and fuel crops, may be suitable for phytoremediation through which the entry of Cd into the food chain could largely be avoided.

Remediation of Cd-contaminated rice soils and Cd stripping from irrigation waters require an integrated approach involving a combination of physical, chemical, and biological technologies for successful and effective management of Cd-contaminated rice ecosystems. Future research is, therefore, needed along the following lines:

- Elucidation of soil and water environmental factors (e.g. pH and Eh) that govern transformations of Cd both in upland and lowland rice ecosystems.
- Examination of solid-phase and solution-phase speciation of Cd in soil and water using advanced spectroscopic-based techniques.
- Identification of biochemical mechanisms involved in the accumulation of Cd in paddy rice grains.

- Rhizosphere processes underpinning effective phytoremediation technologies for Cd removal from paddy soils.
- *In situ* immobilization techniques in paddy soils using inexpensive contaminant-free industrial byproducts high in $FeCl_3$.
- Highly effective and expensive stripping methods for the removal of Cd in water supplies destined for irrigation.

ACKNOWLEDGMENTS

The senior author thanks CRC CARE for providing funding (No 2-3-09-07/08) to undertake research on landfill site remediation. Drs Makino, Ishikawa and Murakami are grateful for the grant from the Ministry of Agriculture, Forestry and Fisheries of Japan (Research project for ensuring food safety from farm to table AC-1310, -1320); part of the review was derived from the abovementioned projects. The Postdoctoral fellowship program (PJ008650042012) with Dr Won-Il Kim at National Academy of Agricultural Science, Rural Development Administration, Republic of Korea, supported Dr Kunhikrishnan's contribution.

REFERENCES

Abumaizar, R.J., Smith, E.H., 1999. Heavy metal contaminants removal by soil washing. J. Hazard. Mater. 70, 71–86.

Adriano, D.C., 1986. Trace Elements in the Terrestrial Environment. Springer-Verlag, New York.

Adriano, D.C., 2001. Trace Elements in Terrestrial Environments: Biogeochemistry, Bioavailability and Risks of Metals, second ed. Springer, New York.

Ahnstrom, Z.S., Parker, D.R., 1999. Development and assessment of a sequential extraction procedure for the fractionation of soil cadmium. Soil Sci. Soc. Am. J. 63, 1650–1658.

Alloway, B.J., 1990. Cadmium. In: Alloway, B.J. (Ed.), Heavy Metals in Soils, John Wiley and Sons Inc., New York, pp. 100–124.

Alloway, B.J., 1995. Heavy Metals in Soils, second ed. Blackie and Son Ltd., Glasgow 25–34.

Almas, A.R., Lombnaes, P., Sogn, T.A., Mulder, J., 2006. Speciation of Cd and Zn in contaminated soils assessed by DGT-DIFS, and WHAM/Model VI in relation to uptake by spinach and ryegrass. Chemosphere 62, 1647–1655.

Álvarez-Ayuso, E., García-Sánchez, A., 2003a. Palygorskite as a feasible amendment to stabilize heavy metal polluted soils. Environ. Pollut. 125, 337–344.

Álvarez-Ayuso, E., García-Sánchez, A., 2003b. Sepiolite as a feasible soil additive for the immobilization of cadmium and zinc. Sci. Total Environ. 305, 1–12.

Ando, J., 1987. Thermal Phosphate. In: Nielsson, F.T. (Ed.), Manual of Fertilizer Processing, Marcel Dekker, New York, pp. 93–124.

Angelova, V., Ivanova, R., Delibaltova, V., Ivanov, K., 2004. Bio-accumulation and distribution of heavy metals in fibre crops (flax, cotton and hemp). Ind. Crop Prod. 19, 197–205.

Antoniadis, V., Alloway, B.J., 2002. The role of dissolved organic carbon in the mobility of Cd, Ni and Zn in sewage sludge-amended soils. Environ. Pollut 17, 515–521.

Arain, M.B., Kazi, T.G., Jamali, M.K., Afridi, H.I., Jalbani, N., Baig, J.A., 2008. Speciation of heavy metals in sediment by conventional, ultrasound and microwave assisted single extraction: a comparison with modified sequential extraction procedure. J. Hazard. Mater. 154, 998–1006.

Arao, T., Ae, N., 2003. Genotypic variations in cadmium levels of rice grain. Soil Sci. Plant Nutr. 49, 473–479.

Arao, T., Ishikawa, S., 2006. Genotypic differences in cadmium concentration and distribution of soybean and rice. JARQ Jpn. Agric. Res. Q. 40, 21–30.

Arao, T., Ae, N., Sugiyama, M., Takahashi, M., 2003. Genotypic differences in cadmium uptake and distribution in soybeans. Plant Soil 251, 247–253.

Arao, T., Kawasaki, A., Baba, K., Mori, S., Matsumoto, S., 2009. Effects of water management on cadmium and arsenic accumulation and dimethylarsinic acid concentrations in Japanese rice. Environ. Sci. Technol. 43, 9361–9367.

Arias, M., Barral, M.T., Mejuto, J.C., 2002. Enhancement of copper and cadmium adsorption on kaolin by the presence of humic acids. Chemosphere 48, 1081–1088.

Asami, T., 1972. The pollution of paddy soils by cadmium, zinc, lead and copper in the dust, fume, and waste water from Nisso Aizu smelter. Jpn. J. Soil Sci. Plant Nutr. 43, 339–343 (in Japanese).

Asami, T., 1974. Environmental pollution by cadmium and zinc discharged from a braun tube factory. Scientific Reports of the Faculty of Agriculture, Ibaraki University 22, 9–23 (in Japanese).

Asami, T., Homma, S., Kubota, M., 1984. Soil pollution by lead, antimony and cadmium around a factory manufacturing mainly lead-acid storage battery. Man. Environ. 10, 3–8 (in Japanese).

Ashworth, D.J., Alloway, B.J., 2008. Influence of dissolved organic matter on the solubility of heavy metals in sewage-sludge-amended soils. Commun. Soil Sci. Plant Anal. 39, 538–550.

Bakir, F., Damluji, S.F., Aminzaki, L., Murtadha, M., Khalidi, A., Alrawi, N.Y., Tikriti, S., Dhahir, H.I., Clarkson, T.W., Smith, J.C., Doherty, R.A., 1973. Methylmercury poisoning in Iraq. Science 181, 230–241.

Barbera, R., Farre, R., Mesado, D., 1993. Oral intake of cadmium, cobalt, copper, iron, lead, nickel, manganese and zinc in the university student's diet. Nahrung 3, 241–245.

Basta, N.T., Sloan, J.J., 1999. Bioavailability of heavy metals in strongly acidic soils treated with exceptional quality biosolids. J. Environ. Qual. 28, 633–638.

Basta, N.T., Tabatabai, M.A., 1992. Effect of cropping systems on adsorption of metals by soils. II. Effect of pH. Soil Sci. 153, 195–204.

Basta, N.T., Gradwohl, R., Snethen, K.L., Schroder, J.L., 2001. Chemical immobilisation of lead, zinc and cadmium in smelter-contaminated soils using biosolids and rock phosphate. J. Environ. Qual. 30, 1222–1230.

Berrow, M.L., Reaves, G.L., 1984. Background levels of trace elements in soils. Proceedings International Conference Environmental Contamination, CEC Consultants Ltd., London, pp. 333–340.

Bhattacharya, A., Routh, J., Jacks, G., Bhattacharya, P., Morth, M., 2006. Environmental assessment of abandoned mine tailings in Adak, Vasterbotten District (Northern Sweden). Appl. Geochem. 21, 1760–1780.

Bingham, F.T., Page, A.L., Mitchell, G.A., Strong, J.E., 1979. Effects of liming an acid soil amended with sewage sludge enriched with Cd, Cu, Ni, and Zn on yield and Cd content of wheat-grain. J. Environ. Qual. 8, 202–207.

Black, A., McLaren, R.G., Reichman, S.M., Speir, T.W., Condron, L.M., 2011. Evaluation of soil metal bioavailability estimates using two plant species (L. perenne and T. aestivum) grown in a range of agricultural soils treated with biosolids and metal salts. Environ. Pollut. 159, 1523–1535.

Bolan, N.S., Duraisamy, D., 2003. Role of soil amendments on the immobilization and bioavailability of metals in soils. Aust. J. Soil Res. 41, 533–555.

Bolan, N.S., Naidu, R., Khan, M.A.R., Tillman, R.W., Syers, J.K., 1999a. The effects of anion sorption on sorption and leaching of cadmium. Aust. J. Soil Res. 37, 445–460.

Bolan, N.S., Naidu, R., Syers, J.K., Tillman, R.W., 1999b. Surface charge and solute interactions in soils. Adv. Agron. 67, 88–141.

Bolan, N.S., Adriano, D.C., Naidu, R., 2003a. Role of phosphorus in (im)mobilization and bioavailability of heavy metals in the soil-plant system. Rev. Environ. Contam. Toxicol. 177, 1–44.

Bolan, N.S., Adriano, D.C., Duraisamy, A., Mani, P., 2003b. Immobilization and phytoavailability of cadmium in variable charge soils: III. Effect of biosolid addition. Plant Soil 256, 231–241.
Bolan, N.S., Adriano, D.C., Mani, P., Duraisamy, A., Arulmozhiselvan, S., 2003c. Immobilization and phytoavailability of cadmium in variable charge soils: II. Effect of lime addition. Plant Soil 250, 187–198.
Bolan, N.S., Adriano, D.C., Mani, P., Duraisamy, A., Arulmozhiselvan, S., 2003d. Immobilization and phytoavailability of cadmium in variable charge soils: I. Effect of phosphate addition. Plant Soil 250, 83–94.
Bolan, N.S., Adriano, D.C., Kunhikrishnan, A., James, T., McDowell, R., Senesi, N., 2011. Dissolved organic carbon: biogeochemistry, dynamics and environmental significance in soils. Adv. Agron. 110, 1–75.
Bolland, M.D.A., Posner, A.M., Quirk, J.P., 1977. Zinc adsorption by goethite in the absence and presence of phosphate. Aust. J. Soil Res. 15, 279–286.
Bowie, S.H.U., Thornton, I., 1984. Environmental Geochemistry and Health. Reidel, Dordrecht 140.
Brallier, S., Harrison, R.B., Henry, C.L., Dongsen, X., 1996. Liming effects on availability of Cd, Cu, Ni and Zn in a soil amended with sewage sludge 16 years previously. Water Air Soil Pollut. 86, 195–206.
Bramley, R.G.V., 1990. Cadmium in New Zealand agriculture. N. Z. J. Agric. Res. 33, 505–519.
Brown, S.L., Chaney, R.L., Angle, J.S., Baker, A.J.M., 1995. Zinc and cadmiun uptake by hyperaccumulator Thlaspi caerulescens and metal tolerant Silene vulgaris grown on sludge amended soils. Environ. Sci. Technol. 29, 1581–1585.
Brown, S.L., Chaney, R.L., Angle, J.S., 1997. Subsurface liming and metal movement in soils amended with lime-stabilized biosolids. J. Environ. Qual. 26, 724–732.
Brown, S.L., Chaney, R.L., Angle, J.S., Ryan, J.A., 1998. The phytoavailability of cadmium to lettuce in long-term biosolid amended soil. J. Environ. Qual. 27, 1071–1078.
Calmano, W., Hong, J., Forstner, U., 1993. Binding and mobilization of heavy metals in contaminated sediments affected by pH and redox potential. Water Sci. Technol. 28, 223–235.
Camobreco, V.J., Richards, B.K., Steenhuis, T.S., Peverly, J.H., McBride, M.B., 1996. Movement of heavy metals through undisturbed and homogenized soil columns. Soil Sci. 161, 740–750.
Campbell, P.G.C., 1995. Interactions between trace metals and aquatic organisms: a critique of the free-ion activity model. In: Tessier, A., Turner, D.R. (Eds.), Metal Speciation and Bioavailability in Aquatic Systems, John Wiley and Sons, New York, pp. 45–102.
Candelaria, L.M., Chang, A.C., 1997. Cadmium activities, solution speciation, nitrate and sewage sludge-treated soil systems. Soil Sci. 162, 722–732.
Cattani, I., Romani, M., Boccelli, R., 2008. Effect of cultivation practices on cadmium concentration in rice grain. Agron. Sustain. Dev. 28, 265–271.
Chandler, R.F., Colo, B., 1979. Rice in the Tropics: A Guide to the Development of National Programs. Westview Press.
Chaney, R.L., Hornick, S.B., 1977. Accumulation and effects of cadmium on crops. Edited Proceedings of the First International Cadmium Conference, Metals Bulletin Ltd., San Francisco, pp. 125–140.
Chaney, W.R., Strickland, R.C., Lamoreaux, R.J., 1977. Phytotoxicity of cadmium inhibited by lime. Plant Soil 47, 275–278.
Chaney, R.L., Reeves, P.G., Ryan, J.A., Simmons, R.W., Welch, R.M., Angle, J.S., 2004. An improved understanding of soil Cd risk to humans and low cost methods to phytoextract Cd from contaminated soils to prevent soil Cd risks. Biometals 17, 549–553.
Chang, A.C., Granato, T.C., Page, A.L., 1992. A methodology for establishing phytotoxicity criteria for chromium, copper, nickel, and zinc in agricultural land application of municipal sewage sludges. J. Environ. Qual. 21, 521–536.

Chang, S.H., Wang, K.S., Kuo, C.Y., Chang, C.Y., Chou, C.T., 2005. Remediation of metal-contaminated soil by an integrated soil washing-electrolysis process. Soil Sediment Contam. 14, 559–569.
Chen, L., Dick, W.A., Streeter, J.G., Hoitink, H.A.J., 1996. Ryegrass utilization of nutrients released from composted biosolids and cow manure. Compost Sci. Util. 4, 73–83.
Chen, H.M., Zheng, C.R., Tu, C., Shen, Z.G., 2000. Chemical methods and phytoremediation of soil contaminated with heavy metals. Chemosphere 41, 229–234.
Chien, S.H., Carmona, G., Prochnow, L.I., Austin, E.R., 2003. A comparison of cadmium availability from granulated and bulk-blended phosphate with potassium fertilizers. J. Environ. Qual. 32, 1911–1914.
Chien, S.H., Prochnow, L.I., Cantarella, H., 2009. Recent developments of fertilizer production and use to improve nutrient efficiency and minimize environmental impacts. Adv. Agron. 102, 267–322.
Chon, H.T., Cho, C.H., Kim, K.W., Moon, H.S., 1996. The occurrence and dispersion of potentially toxic elements in areas covered with black shales and slates in Korea. Appl. Geochem. 11, 69–76.
Chowdhury, B.A., Chandra, R.K., 1987. Biological and health implications of toxic heavy metal and essential trace element interaction. Progr. Ed. Nutr. Sci. 11, 55–113.
Chuan, M.C., Shu, G.Y., Liu, J.C., 1996. Solubility of heavy metals in a contaminated soil: effects of redox potential and pH. Water Air Soil Pollut. 90, 543–556.
Codex, 2004. Report of the 36th Session of the Codex Committee on Food Additives and Contaminants. Rep. No. ALINORM 04/27/12. Codex Alimentarius Commission, Rome.
Codex, 2005. Report of the 28th Session of the Codex Alimentarius Commission. Rep. No. ALINORM 05/28/41. Codex Alimentarius Commission, Rome.
Codex, 2006. Report of the 29th Session of the Codex Alimentarius Commission. Rep. No. ALINORM 06/29/41. Codex Alimentarius Commission, Rome.
Concas, A., Ardau, C., Cristini, A., Zuddas, P., Cao, G., 2006. Mobility of heavy metals from tailings to stream waters in a mining activity contaminated site. Chemosphere 63, 244–253.
Conrad, R., Frenzel, P., 2002. Flooded Soils. In: Britton, G. (Ed.), Encyclopedia of Environmental Microbiology, John Wiley and Sons, Inc, New York, pp. 1316–1333.
Curley, A., Sedlak, V.A., Girling, E.F., Hawk, R.E., Barthel, W.F., Pierce, P.E., Likosky, W.H., 1971. Organic mercury identified as cause of poisoning in humans and hogs. Science 172, 65–67.
Dabeka, R.W., McKenzie, A.D., 1995. Survey of lead, cadmium fluoride, nickel and cobalt in food composites and estimation of dietary intakes of these elements by Canadians in 1986–1988. J. AOAC Int. 78, 897–909.
Davis, A.P., 2000. Chemical and engineering aspects of heavy metal-contaminated soils. Revista. Inter. Contam. Ambi 16, 169–174.
Davis, A.P., Bhatnagar, V., 1995. Adsorption of cadmium and humic acid onto hematite. Chemosphere 30, 243–256.
De Datta, S.K., 1981. Principles and Practices of Rice Production. Wiley, Singapore.
de Livera, J., McLaughlin, M.J., Hettiarachchi, G.M., Kirby, J.K., Beak, D.G., 2011. Cadmium solubility in paddy soils: effects of soil oxidation, metal sulfides and competitive ions. Sci. Total Environ. 409, 1489–1497.
del Castilho, P., Chandron, W.J., Salomons, W., 1993. Influence of cattle manure slurry application on the solubility of cadmium, copper, and zinc in a manured acidic loamy sand soil. J. Environ. Qual. 22, 279–689.
Dinel, H., Pare, T., Schnitzer, M., Pelzer, N., 2000. Direct land application of cement kiln dust- and lime-sanitized biosolids: extractability of trace metals and organic matter quality. Geoderma 96, 307–320.

Doner, H.E., 1978. Chloride as a factor in mobilities of Ni(II), Cu(II), and Cd(II) in soil. Soil Sci. Soc. Am. J. 42, 882–885.
Dube, J.S., Galvez-Cloutier, R., 2005. Applications of data on the mobility of heavy metals in contaminated soil to the definition of site-specific remediation criteria. J. Environ. Eng. Sci. 4, 399–411.
Dunbar, K.R., 2004. Uptake and Partitioning of Cd in Two Cultivars of Potato (*Solanum Tuberosum* L.). Ph.D. thesis, University of Adelaide, School of Earth and Environmental Sciences, Adelaide, Australia, 123 pp.
Ebbs, S.D., Lasat, M.M., Brady, D.J., Cornish, J., Gordon, R., Kochian, L.V., 1997. Phytoextraction of cadmium and zinc from a contaminated soil. J. Environ. Qual. 26, 1424–1430.
Elliott, H.A., Herzig, L.M., 1999. Oxalate extraction of Pb and Zn from polluted soils: solubility limitations. J. Soil Contam. 8, 105–116.
Esmaeily, A. 2002. Dewatering, Metal Removal, Pathogen Elimination, and Organic Matter Reduction in Biosolids Using Electrokinetic Phenomena. Masters Thesis. Montreal, QC: Concordia University.
Evanylo, G.K., 2009. Agricultural Land Application of Biosolids in Virginia: Managing Biosolids for Agricultural Use. Virginia Cooperative Extension Publication, 452–303.
FAO/WHO Expert Committee, 1972. Evaluation of certain food additives and contaminants, mercury, lead and cadmium. Sixteenth Report of the Joint FAO/WHO Expert Committee of Food Additives, WHO Tech. Rep. Ser., vol. 505. pp. 16–24.
Foth, H.D., 1978. Fundamentals of Soil Science, fourth ed. Wiley, New York.
Fotovat, A., Naidu, R., 1997. Ion exchange resin and MINTEQA2 speciation of Zn and Cu in alkaline sodic and acidic soil extracts. Aust. J. Soil Res. 35, 711–726.
Frenkel, H., Vulkan, R., Mingelgrin, U., Ben-Asher, J., 1997. Transport of sludgeborne copper and zinc under saturated conditions. In: Iskander, I.K. (Ed.), Extended Abstracts, Fourth International Conference on the Biogeochemistry of Trace Elements, Berkeley CA, p. 149.
Friberg, L., 1984. Cadmium and the kidney. Environ. Health Perspect. 54, 1–11.
Friberg, L., Elinder, C.G., Kjellstrom, T., Nordberg, G.F., 1985. Cadmium and Health: A Toxicological and Epidemiological Appraisal. CRC Press, Boca Raton.
Fujimoto, T., Yamashita, K., 1976. Investigations of the heavy metal pollution of paddy fields in Tohoku district. Bull. Tohoku Natl. Agric. Exp. Stn. 54, 75–89 (in Japanese).
Gambrell, R.P., 1994. Trace and toxic metals in wetlands: a review. J. Environ. Qual. 23, 883–891.
Gambrell, R.P., Patrick, W.H., 1988. The influence of redox potential on the environmental chemistry of contaminants in soils and sediments. In: Hook, D. (Ed.), The Ecology and Management of Wetlands, Timber Press, Portland, pp. 319–333.
Garin, M.A.P., Cappellen, V., Charlet, L., 2003. Aqueous cadmium uptake by calcite: a stirred flow-through reactor study. Geochim. Cosmochim. Acta 67, 2763–2774.
Girling, C.A., Peterson, P.J., 1981. The significance of the Cd species in uptake and metabolism of Cd in crop plants. J. Plant Nutr. 3, 707–720.
Gonzalez, R.X., Sartain, J.B., Miller, W.L., 1992. Cadmium availability and extractability from sewage-sludge as affected by waste phosphatic clay. J. Environ. Qual. 21, 272–275.
Gove, L., Cooke, C.M., Nicholson, F.A., Beck, A.J., 2001. Movement of water and heavy metals (Zn, Cu, Pb and Ni) through sand and sandy loam amended with biosolids under steady-state hydrological conditions. Bioresour. Technol. 78, 171–179.
Grant, C.A., Clarke, J.M., Duguid, S., Chaney, R.L., 2008. Selection and breeding of plant cultivars to minimize cadmium accumulation. Sci. Total Environ. 390, 301–310.
Gray, C.W., McLaren, R.G., Roberts, A.H.C., Condron, L.M., 1999a. The effect of long-term phosphatic fertiliser applications on the amounts and forms of cadmium in soils under pasture in New Zealand. Nutr. Cycl. Agroecosyst 54, 267–277.

Gray, C.W., McLaren, R.G., Roberts, A.H.C., Condron, L.M., 1999b. Effect of soil pH on cadmium phytoavailability in some New Zealand soils. N. Z. J. Crop Hort 27, 169–179.
Grzebisz, W., Kocialkowski, W.Z., Chudzinski, B., 1997. Copper geochemistry and availability in cultivated soils contaminated by a copper smelter. J. Geochem. Explor 58, 301–307.
Gustafsson, J.P., 2004. Department of Land and Water Resources Engineering. Visual MINTEQ,Version 2.30 KTH, Stockholm.
Haldar, M., Mandal, L.N., 1979. Influence of soil moisture regimes and organic matter application on the extractable Zn and Cu content in rice soils. Plant Soil 53, 203–213.
Hammer, D., Keller, C., 2002. Changes in the rhizosphere of metal-accumulating plants evidenced by chemical extractants. J. Environ. Qual. 31, 1561–1569.
Hammer, D., Keller, C., 2003. Phytoextraction of Cd and Zn with Thlaspi caerulescens in field trials. Soil Use Manage. 19, 144–149.
Hammer, D., Kayser, A., Keller, C., 2003. Phytoextraction of Cd and Zn with Salix viminalis in field trials. Soil Use Manage. 19, 187–192.
Han, C., Wu, L., Tan, W., Zhong, D., Huang, Y., Luo, Y., Christie, P., 2011. Cadmium distribution in rice plants grown in three different soils after application of pig manure with added cadmium. Environ. Geochem. Health10.1007/s10653-011-9442-y.
Harter, R.D.R., Naidu, R., 1995. Role of metal-organic complexation in metal sorption by soils. Adv. Agron. 55, 219–264.
Hassan, M.J., Zhu, Z., Ahmad, B., Mahmood, Q., 2006. Influence of Cd toxicity on rice genotypes as affected by Zn, sulfur and nitrogen fertilizers. Caspian J. Environ. Sci. 4, 1–8.
Havlin, J.L., Tisdale, S.L., Nelson, W.L., Beaton, J.D., 1999. Soil Fertility and Fertilizers: An Introduction to Nutrient Management, sixth ed.. Prentice Hall, Upper Saddle River, NJ.
Haynes, R.J., Murtaza, G., Naidu, R., 2009. Inorganic and organic constituents and contaminants of biosolids: Implications for land application. Adv. Agron. 104, 165–267.
He, Q.B., Singh, B.R., 1994. Plant availability of cadmium in soils. 2. Factors related to the extractability and plant uptake of cadmium in cultivated soils. Acta Agric. Scand. 43, 142–150.
He, Z.L., Yanga, X.E., Stoffellab, P.J., 2005. Trace elements in agroecosystems and impacts on the environment. J. Trace Elem. Med. Bio. 19, 125–140.
He, J., Zhu, C., Ren, Y., Yan, Y., Jiang, D., 2006. Genotypic variation in grain Cd concentration of lowland rice. J. Plant Nutr. Soil Sci. 169, 711–716.
Helyar, K.R., Munns, D.N., Burau, R.G., 1976. Adsorption of phosphate by gibbsite. II. Formation of a surface complex involving divalent cations. J. Soil Sci. 27, 315–323.
Herawati, N., Suzuki, S., Hayashi, K., Rivai, I.F., Koyama, H., 2000. Cadmium, copper, and zinc levels in rice and soil of Japan, Indonesia, and China by soil type. Bull. Environ. Contam. Toxicol. 64, 33–39.
Hettiarachchi, G.M., Scheckel, K.G., Ryan, J.A., Sutton, S.R., Newville, M., 2006. XANES and XRF Investigations of metal binding mechanisms in biosolids. J. Environ. Qual. 35, 342–351.
Higurashi, N., Mastumoto, N., Miyoshi, H., 1976. Factors affecting cadmium absorption of rice in the paddy field comparatively less polluted with cadmium. Bull. Chiba Agric. Exp. Stn. 17, 150–159 (in Japanese).
Hodgson, J.F., Tiller, K.J., Martha, F., 1964. The role of hydrolysis in the reaction of heavy metals with soil-forming materials. Soil Sci. Soc. Am. Proc. 28, 42–46.
Hong, K.J., Tokunaga, S., Kajiuchi, T., 2002. Evaluation of remediation process with plant-derived biosurfactant for recovery of heavy metals from contaminated soils. Chemosphere 49, 379–387.
Hong, C.O., Chung, D.Y., Ha, B.Y., Kim, P.J., 2005. Reversed effects of phosphate fertilizer in reducing phytoavailability of cadmium in mine tailing affected soil. Korean J. Environ. Agric. 24, 210–214.

Hong, C.O., Lee, D.K., Chung, D.Y., Kim, P.J., 2007. Liming effects on cadmium stabilization in upland soil affected by gold mining activity. Arch. Environ. Contam. Toxicol. 52, 496–502.

Hong, C.O., Lee, D.K., Kim, P.J., 2008. Feasibility of phosphate fertilizer to immobilize cadmium in a field. Chemosphere 70, 2009–2015.

Hong, C.O., Gutierrez, J., Yun, S.W., Lee, Y.B., Yu, C., Kim, P.J., 2009. Heavy metal contamination of arable soil and corn plant in the vicinity of a zinc smelting factory and stabilization by liming. Arch. Environ. Contam. Toxicol. 56, 190–200.

Hong, C.O., Kim, S.Y., Gutierrez, J., Owens, V.N., Kim, P.J., 2010a. Comparison of oyster shell and calcium hydroxide as liming materials for immobilizing cadmium in upland soil. Biol. Fertil. Soils 46, 491–498.

Hong, C.O., Chung, D.Y., Lee, D.K., Kim, P.J., 2010b. Comparison of phosphate materials for immobilizing cadmium in soil. Arch. Environ. Contam. Toxicol 58, 268–274.

Honma, T., Ohba, H., Kaneko, A., Hoshino, T., Murakami, M., Ohyama, T., 2009. Phytoremediation of cadmium by rice in low-level of Cd contaminated paddy field. Jpn. J. Soil Sci. Plant Nutr. 80 166–122.

Hooda, P.S., Alloway, B.J., 1996. The effect of liming on heavy metal concentrations in wheat, carrots and spinach grown on previously sludge-applied soils. J. Agric. Sci. 127, 289–294.

Huang, P.M., Adriano, D.C., Logan, T.J., Checkai, R.T., 1988. Soil Chemistry and Ecosystem Health. SSSA Special Publication 52. Soil Science Society of America, Madison, WI.

Hyun, H., Chang, A.C., Parker, D.R., Page, A.L., 1998. Cadmium solubility and phytoavailability in sludge-treated soil: effects of soil organic matter. J. Environ. Qual. 27, 329–334.

Iimura, K., Ito, H., 1978. Behavior and balance of contaminant heavy metals in paddy soils – Studies on heavy metal pollution in paddy soils (Part 2). Bull. Hokuriku Natl. Agri. Exp. Stn. 21, 95–145 (in Japanese).

Ikeda, M., Zhang, Z.W., Moon, C.S., Imai, Y., Watanabe, T., Shimbo, S., Ma, W.C., Lee, C.C., Guo, Y.L., 1996. Background exposure of general population to cadmium and lead in Tainan City, Taiwan. Arch. Environ. Contam. Toxicol. 30, 121–126.

Ikeda, M., Zhang, Z.W., Higashikawa, K., Watanabe, T., Shimbo, S., Moon, C.S., Nakatsuka, H., Matsuda-Inoguchi, N., 1999. Background exposure of general women populations in Japan to cadmium in the environment and possible health effects. Toxicol. Lett. 108, 161–166.

Ikeda, M., Zhang, Z.W., Shimbo, S., Watanabe, T., Nakatsuka, H., Moon, C.S., Matsuda-Inoguchi, N., Higashikawa, K., 2000. Urban population exposure to lead and cadmium in east and Southeast Asia. Sci. Total Environ. 249, 373–384.

Iretskaya, S.N., Chien, S.H., Menon, R.G., 1998. Effect of acidulation of high cadmium containing phosphate rocks on cadmium uptake by upland rice. Plant Soil 201, 183–188.

Ishikawa, S., Abe, T., Kuramata, M., Yamaguchi, M., Ando, T., Yamamoto, T., Yano, M., 2010. A major quantitative trait locus for increasing cadmium-specific concentration in rice grain is located on the short arm of chromosome 7. J. Exp. Bot. 61, 923–934.

Iu, K.L., Pulford, I.D., Duncan, H.J., 1981. Influence of waterlogging and lime or organic matter additions on the distribution of trace metals in an acid soil: I. Manganese and iron. Plant Soil 59, 317–326.

Jamil, H., Theng, L.P., Jusoh, K., Razali, A.M., Ali, F.B., Ismail, B.S., 2011. Speciation of heavy metals in paddy soils from selected areas in Kedah and Penang, Malaysia. Afr. J. Biotechnol. 10, 13505–13513.

Järup, L., Berglund, M., Elinder, C.G., Nordberg, G., Vahter, M., 1998. Health effects of cadmium exposure – a review of the literature and a risk estimate. Scand. J. Environ. Health 24, 1–51.

Jiaka, L.T., Yu, H., Feng, W.Q., Qin, Y.S., Zhao, J., Liao, M.L., Wang, C.Q., Tu, S.H., 2009. Effects of different phosphate and potassium fertilizers on yields and cadmium uptake by paddy rice. Southwest China J. Agric. Sci. 22, 990–995.

Jinadasa, K.B.P.N., Milham, P.J., Hawkins, C.A., Cornish, P.S., Williams, P.A., Kaldor, C.J., Conroy, J.P., 1997. Survey of cadmium levels in vegetables and soils of greater Sydney, Australia. J. Environ. Qual. 26, 924–933.

John, M.K., Van Laerhoven, C.J., 1976. Effects of sewage sludge composition, application rate, and lime regime on plant availability of heavy-metals. J. Environ. Qual. 5, 246–251.

Jung, G.B., Kim, W.I., Lee, J.S., Shin, J.D., Yun, S.G., 2004. Studies on loading capacity of agricultural soils for heavy metal in Korea. Annu. Rep. Agric. Environ. Res. Natl. Acad. Agric. Sci. RDA, Republic Korea, 16–37 (in Korean with English summary).

Kabata-Pendias, A., 2000. Trace Elements in Soils and Plants, third ed.. CRC Press Inc., Florida.

Kabata-Pendias, A., Pendias, H., 2001. Trace Elements in Soils and Plants. CRC Press, Boca Raton, FL.

Kaihura, B.S., Kullaya, I.K., Kilasara, M., Aune, J.B., Singh, B.R., Lal, R., 1999. Soil quality effects of accelerated erosion and management systems in three eco-regions of Tanzania. Soil Till. Res. 53, 59–70.

Kantar, C., Honeyman, B.D., 2006. Citric acid enhanced remediation of soils contaminated with uranium by soil flushing and soil washing. J. Environ. Eng-ASCE 132, 247–255.

Karaca, A., Naseby, D.C., Lynch, J.M., 2002. Effect of cadmium contamination with sewage sludge and phosphate fertiliser amendments on soil enzyme activities, microbial structure and available cadmium. Biol. Fertil. Soils 35, 428–434.

Kashem, M.A., Singh, B.R., 2001. Metal availability in contaminated soils: I. Effects of flooding and organic matter on changes in Eh, pH and solubility of Cd, Ni and Zn. Nutr. Cycl. Agroecosyst. 61, 247–255.

Kashem, M.A., Singh, B.R., 2004. Transformations in solid phase species of metals as affected by flooding and organic matter. Commun. Soil Sci. Plant Anal. 35, 1435–1456.

Kato, M., Ishikawa, S., Inagaki, K., Chiba, K., Hayashi, H., Yanagisawa, S., Yoneyama, T., 2010. Possible chemical forms of cadmium and varietal differences in the cadmium concentrations in the phloem sap of rice plants (*Oryza sativa* L.). Soil Sci. Plant Nutr. 56, 839–847.

Kawabe, S., Fukumorita, T., Chino, M., 1980. Collection of rice phloem sap from stylets of homopterous insects severed by YAG laser. Plant Cell. Physiol. 21, 1319–1327.

Kawada, T., Suzuki, S., 1998. A review on the cadmium content of rice, daily cadmium intake, and accumulation in the kidneys. J. Occup. Health 40, 264–269.

Kazi, T.G., Jamali, M.K., Kazi, G.H., Arain, M.B., Afridi, H.I., Siddiqui, A., 2005. Evaluating the mobility of toxic metals in untreated industrial wastewater sludge using a BCR sequential extraction procedure and a leaching test. Anal. Bioanal. Chem. 383, 297–304.

Khairiah, J., Habibah, H.J., Anizan, I., Maimon, A., Aminah, A., Ismail, B.S., 2009. Content of heavy metals in soil collected from selected paddy cultivation areas in Kedah and Perlis, Malaysia. J. Appl. Sci. Res. 5, 2179–2188.

Khaniki, G.R.J., Zazoli, M.A., 2005. Cadmium and lead contents in rice (*Oryza sativa*) in the north of Iran. Int. J. Agr. Biol. 7, 1026–1029.

Khaokaew, S., Chaney, R.L., Landrot, G., Ginder-Vogel, M., Sparks, D.L., 2011. Speciation and release kinetics of cadmium in an alkaline paddy soil under various flooding periods and draining conditions. Environ. Sci. Technol. 45, 4249–4255.

Kibria, M.G., Osman, K.T., Ahammad, M.J., Alamgir, M., 2011. Effects of farm yard manure and lime on cadmium uptake by rice grown in two contaminated soils of Chittagong. J. Agric. Sci. Technol. 5, 352–358.

Kim, J.H., 1989. Geochemistry and genesis of the Guryongsan (Ogcheon) uraniferous black slates. J. Korean Inst. Min. Geol. 22, 35–63.

Kim, K.W., Thornton, I., 1993. Influence of Ordovician uraniferous black shales on the trace element composition of soils and food crops, Korea. Appl. Geochem. Suppl. 2, 249–255.

Kim, J.Y., Kim, K.Y., Ahn, J.S., Ko, I., Lee, C.H., 2005. Investigation and risk assessment modeling of as and other heavy metals contamination around five abandoned metal mines in Korea. Environ. Geochem. Health 27, 193–203.

Kirkham, M.B., 2006. Cadmium in plants on polluted soils: effects of soil factors, hyperaccumulation, and amendments. Geoderma 137, 19–32.
Knox, A.S., Seaman, J.C., Mench, M.J., Vangronsveld, J., 2001. Remediation of metal- and radionuclides-contaminated soils by in situ stabilization techniques. In: Iskandar, I.K. (Ed.), Environmental Restoration of Metals-contaminated Soils, CRC Press, Boca Raton, FL, USA, pp. 21–60.
Kögel-Knabner, I., Amelung, W., Cao, Z., Fiedler, S., Frenzel, P., Jahn, R., Kalbitz, K., Kölbl, A., Schloter, M., 2010. Biogeochemistry of paddy soils. Geoderma 157, 1–14.
Kreutzer, K., 1995. Effects of forest liming on soil processes. Plant Soil 168–169, 447–470.
Krishnamurti, G.S.R., Naidu, R., 2002. Solid-solution speciation and phytoavailability of copper and zinc in soils. Environ. Sci. Technol. 36, 2645–2651.
Krishnamurti, G.S.R., Huang, P.M., van Rees, K.C.J., 1996. Studies on soil rhizosphere: speciation and availability of cadmium. Chem. Spec. Bioavailab. 8, 23–28.
Kukier, U., Chaney, R.L., 2002. Growing rice grain with controlled Cd concentrations. J. Plant Nutr. 25, 1793–1820.
Kumpiene, J., Lagerkvist, A., Maurice, C., 2007. Stabilization of Pb- and Cu-contaminated soil using coal fly ash and peat. Environ. Pollut. 145, 365–373.
Kunhikrishnan, A., Bolan, N.S., Müller, K., Laurenson, S., Naidu, R., Kim, W.I., 2012. The influence of wastewater irrigation on the transformation and bioavailability of heavy metal(loid)s in soil. Adv. Agron. 115, 215–297.
Kuo, S., 1986. Concurrent adsorption of phosphate and zinc, cadmium, or calcium by a hydrous ferric oxide. Soil Sci. Soc. Am. J. 50, 1412–1419.
Lackovic, K., Angove, M.J., Wells, J.D., Johnson, B.B., 2003. Modeling the adsorption of Cd(II) onto Muloorina illite and related clay minerals. J. Colloid Interface Sci. 257, 31–40.
Lai, C.H., Chen, C.Y., Wei, B.L., Yeh, S.H., 2002. Cadmium adsorption on goethite-coated sand in the presence of humic acid. Water Res. 36, 4943–4950.
Lamy, I., Bourgeois, S., Bermond, A., 1993. Soil cadmium mobility as a consequence of sewage sludge disposal. J. Environ. Qual. 22, 731–737.
Langlands, J.P., Donald, G.E., Bowles, J.E., 1988. Cadmium concentrations in liver, kidney and muscle in Australian sheep and cattle. Aust. J. Exp. Agric. 28, 291–297.
Laureysens, I., De Temmerman, L., Hastir, T., Van Gysel, M., Ceulemans, R., 2005. Clonal variation in heavy metal accumulation and biomass production in a poplar coppice culture. II. Vertical distribution and phytoextraction potential. Environ. Pollut. 133, 541–551.
Lavres Jr., J., Reis, A.R., Nogueira, T.A.R., Cabral, C.P., Malavolta, E., 2011. Phosphorus uptake by upland rice from superphosphate fertilizers produced with sulfuric acid treatments of Brazilian phosphate rocks. Commun. Soil Sci. Plant Anal. 42, 1390–1403.
Ledgard, S.F., Lieffering, M., McDevitt, J., Boyes, M., Kemp, R., 2010. A greenhouse gas footprint study for exported New Zealand lamb. Rep. Prepared Meat Ind. Assoc. (Ballance Agri-Nutrients, Landcorp and MAF).
Lee, J., Rounce, J.R., Mackay, A.D., Grace, N.D., 1996. Accumulation of cadmium with time in Romney sheep grazing ryegrass-white clover pasture: effect of cadmium from pasture and soil intake. Aust. J. Agric. Sci. 47, 877–894.
Lee, J.S., Chon, H.T., Kim, K.W., 1998. Migration and dispersion of trace elements in the rock–soil–plant system in areas underlain by black shales and slates of the Okchon Zone, Korea. J. Geochem. Explor 65, 61–78.
Lee, C.G., Chon, H.T., Jung, M.C., 2001. Heavy metal contamination in the vicinity of the Daduk Au–Ag–Pb–Zn mine in Korea. Appl. Geochem. 16, 1377–1386.
Lee, T.M., Lai, H.Y., Chen, Z.S., 2004. Effect of chemical amendments on the concentration of cadmium and lead in long-term contaminated soils. Chemosphere 57, 1459–1471.

Levi-Minzi, R., Petruzzelli, G., 1984. The influence of phosphate fertilizers on Cd solubility in soil. Water Air Soil Pollut. 23, 423–429.
Li, Z.B., Ryan, J.A., Chen, J.L., Al-Abed, S.R., 2001. Adsorption of cadmium on biosolids-amended soils. J. Environ. Qual. 30, 903–911.
Li, P., Wang, X.X., Zhang, T.L., Zhou, D.M., He, Y.Q., 2008. Effects of several amendments on rice growth and uptake of copper and cadmium from a contaminated soil. J. Environ. Sci. 20, 449–455.
Li, Ping, Wang, X.X., Zhang, T.L., Zhou, D.M., He, Y.Q., 2009a. Distribution and accumulation of copper and cadmium in soil–rice system as affected by soil amendments. Water Air Soil Pollut. 196, 29–40.
Li, S., Liu, R., Wang, H., Shan, H., 2009b. Accumulations of cadmium, zinc, and copper by rice plants grown on soils amended with composted pig manure. Commun. Soil Sci. Plant Anal. 40, 1889–1905.
Lim, T.T., Tay, J.H., Teh, C.I., 2002. Contamination time effect on lead and cadmium fractionation in a tropical coastal clay. J. Environ. Qual. 31, 806–812.
Lin, 2002. Mapping soil lead and remediation needs in contaminated soils. Environ. Geochem. Health 24, 23–33.
Lin, H.T., Wong, S.S., Li, G.C., 2004. Heavy metal content of rice and shellfish in Taiwan. J. Food Drug Anal. 12, 167–174.
Lindsay, W.L., 1979. Chemical Equilibria in Soils. Wiley-Interscience, New York.
Linger, P., Mussig, J., Fischer, H., Kobert, J., 2002. Industrial hemp (*Cannabis sativa* L.) growing on heavy metal contaminated soil: fibre quality and phytoremediation potential. Ind. Crop Prod. 16, 33–42.
Liu, J., Li, K., Xu, J., Liang, J., Lu, X., Yang, J., Zhu, Q., 2003. Interaction of Cd and five mineral nutrients for uptake and accumulation in different rice cultivars and genotypes. Field Crop Res. 83, 271–281.
Liu, H.J., Zhang, J.L., Christie, P., Zhan, F.S., 2007. Influence of external zinc and phosphorus supply on Cd uptake by rice (*Oryza sativa* L.) seedlings with root surface iron plaque. Plant Soil 300, 105–115.
Liu, Z.B., Ji, X.H., Tian, F.X., Peng, H., Wu, J.M., Shi, L.H., 2011. Effects and mechanism of alkaline wastes application and zinc fertilizer addition on Cd bioavailability in contaminated soil. Chin. J. Environ. Sci. 32, 1164–1170 (Article in Chinese).
Logan, T.J., Lindsay, B.J., Goins, L.E., Ryan, J.A., 1997. Field assessment of sludge metal bioavailability to crops: sludge rate response. J. Environ. Qual. 26, 534–550.
Loganathan, P., Hedley, M.J., 1997. Downward movement of cadmium and phosphorus from phosphatic fertilisers in a pasture soil in New Zealand. Environ. Pollut. 95, 319–324.
Loganathan, P., Mackay, A.D., Lee, J., Hedley, M.J., 1995. Cadmium distribution in hill pastures as influenced by 20 years of phosphate fertiliser application and sheep grazing. Aust. J. Soil Res. 33, 859–871.
Loganathan, P., Hedley, M.J., Gregg, P.E.H., Currie, L.D., 1996. Effect of phosphate fertiliser type on the accumulation and plant availability of cadmium in grassland soils. Nutr. Cycl. Agroecosyst. 46, 169–179.
Loganathan, P., Louie, K., Lee, J., Hedley, M.J., Roberts, A.H.C., Longhurst, R.D., 1999. A model to predict kidney and liver cadmium concentration in grazing animals. N. Z. J. Agric. Res. 42, 423–432.
Loganathan, P., Hedley, M.J., Grace, N.D., Lee, J., Cronin, S.J., Bolan, N.S., Zanders, J.M., 2003. Fertiliser contaminants in New Zealand grazed pasture with special reference to cadmium and fluorine: a review. Aust. J. Soil Res. 41, 501–532.
Loganathan, P., Hedley, M.J., Grace, N.D., 2008. Pasture soils contaminated with fertilizer-derived cadmium and fluoride: livestock effects. Rev. Environ. Contam. Toxicol. 192, 29–66.
Loganathan, P., Vigneswaran, S., Kandasamy, J., Naidu, R., 2012. Cadmium sorption and desorption in soils: a review. Crit. Rev. Environ. Sci. Technol. 42, 489–533.

Longhurst, R.D., Roberts, A.H.C., Waller, J.E., 2004. Concentrations of arsenic, cadmium, copper, lead, and zinc in New Zealand pastoral soils and herbage. N. Z. J. Ag. Res. 47, 23–32.
Luo, Y., Wu, L., Liu, L., Han, C., Li, Z., 2009. Heavy metal contamination and remediation in Asian agricultural land. Proceedings of MARCO Symposium/Workshop-challenges for Agro-environmental Research in Monsoon Asia, Tsukuba, Japan.
Ma, L.Q., Dong, Y., 2004. Effects of incubation on solubility and mobility of trace metals in two contaminated soils. Environ. Pollut. 130, 301–307.
Ma, L.Q., Rao, G.N., 1997. Effects of phosphate rock on sequential chemical extraction of lead in contaminated soils. J. Environ. Qual. 26, 788–794.
MacDonald, A.M., Fordyce, F.M., Shand, P., Ó Dochartaigh, B.E., 2005. Using geological and geochemical information to estimate the potential distribution of trace elements in Scottish groundwater. Br. Geological Survey Groundwater Programme Commissioned Report CR/05/238N.
MAFF, 2008. Ministry of Agriculture Forestry and Fisheries of Japan, Monthly Statistics of Agriculture, Forestry and Fisheries. Japan, Tokyo.
Mahimairaja, S., Bolan, N.S., Adriano, D., Robinson, B., 2005. Arsenic contamination and its risk management in complex environmental settings. Adv. Agron. 86, 123–189.
Mahler, R.J., Bingham, F.T., Page, A.L., 1978. Cadmium-enriched sewage sludge application to acid and calcareous soils – effect on yield and cadmium uptake by lettuce and chard. J. Environ. Qual. 7, 274–281.
Maier, N.A., McLaughlin, M.J., Heap, M., Butt, M., Smart, M.K., Williams, C.M.J., 1997. Effect of current-season application of calcitic lime on soil pH, yield and cadmium concentration in potato (*Solanum tuberosum* L) tubers. Nutr. Cycl. Agroecosyst 47, 29–40.
Makino, T., 2002. The influence of oxidation-reduction on forms of heavy metals in soils. Jpn. J. Soil Sci. Plant Nutr. 73, 803–811 (in Japanese).
Makino, T., Sugahara, K., Sakurai, Y., Takano, H., Kamiya, T., Sasaki, K., Itou, T., Sekiya, N., 2006. Remediation of cadmium contamination in paddy soils by washing with chemicals: selection of washing chemicals. Environ. Pollut. 144, 2–10.
Makino, T., Kamiya, T., Takano, H., Itou, T., Sekiya, N., Sasaki, K., Maejima, Y., Sugahara, K., 2007. Remediation of cadmium-contaminated paddy soils by washing with calcium chloride – Verification of on-site washing. Environ. Pollut. 147, 112–119.
Makino, T., Takano, H., Kamiya, T., Itou, T., Sekiya, N., Inahara, M., Sakurai, Y., 2008. Restoration of cadmium-contaminated paddy soils by washing with ferric chloride: Cd extraction mechanism and bench-scale verification. Chemosphere 70, 1035–1043.
Mandjiny, S., Matis, K.A., Fedoroff, M., Jeanjean, J., Rouchaud, J.C., Toulhoat, N., Potocek, V., Maireles-Torres, P., Jones, D., 1998. Calcium hydroxyapatites: evaluation of sorption properties for cadmium ions in aqueous solution. J. Mater. Sci. 33, 5433–5439.
Mann, S.S., Rate, A.W., Gilkes, R.J., 2002. Cadmium accumulation in agricultural soils in Western Australia. Water Air Soil Pollut. 141, 281–297.
Martínez, C.E., McBride, M.B., 2001. Cd, Cu, Pb, and Zn coprecipitates in Fe oxide formed at different pH: aging effects on metal solubility and extractability by citrate. Environ. Toxicol. Chem. 20, 122–126.
Masironi, R., Koirtyohann, S.R., Pierce, J.O., 1977. Zinc, copper, cadmium in the polished and unpolished rice. Sci. Total Environ. 7, 23–43.
Masui, M., Kanamaru, N., Takesako, H., Takesako, H., Miyakoda, H., Nanba, I., Takahashi, H., 1971. Annual surveys on correlation between the degree of cadmium contamination of paddy field rice grain and the number of dry-paddyfield days in the cadmium contaminated area in Tama region of Tokyo. Bull. Toukyou-to Agr. Exp. Stn. 5, 1–5 (in Japanese).
Matsuzaki, T., Okamoto, T., Yabuki, S., 1987. The behavior of high contents of cadmium in paddy field and its influence to paddy rice. Bull. Agri. Res. Inst. Kanagawa Prefect 129, 50–57 (in Japanese).
McBride, M.B., 1980. Chemisorption of Cd2þ on calcite surfaces. Soil Sci. Soc. Am. J. 44, 26–28.

McBride, M.B., Richards, B.K., Steenhuis, T., Spiers, G., 1999. Long-term leaching of trace elements in a heavily sludge-amended silty clay loam soil. Soil Sci. 164, 613–623.
McGowen, S.L., Basta, N.T., Brown, G.O., 2001. Use of diammonium phosphate to reduce heavy metal solubility and transport in smelter-contaminated soil. J. Environ. Qual. 30, 493–500.
McGrath, S.P., Dunhum, S.J., Correll, R.L., 2000. Potential for phytoextraction of zinc and cadmium from soils using hyperaccumulator plants. In: Terry, N., Banuelos, G. (Eds.), "Phytoremediation of Contaminated Soil and Water, Lewis publishers, Boca Raton, FL, pp. 109–128.
McGrath, S.P., Zhao, F.J., Lombi, E., 2002. Phytoremediation of metals, metalloids, and radionuclides. Adv. Agron. 75, 1–56.
McGrath, S.P., Lombi, E., Gray, C.W., Caille, N., Dunham, S.J., Zhao, F.J., 2006. Field evaluation of Cd and Zn phytoextraction potential by the hyperaccumulators Thlaspi caerulescens and Arabidopsis halleri. Environ. Pollut. 141, 115–125.
McLaughlin, M.J., Tiller, K.G., Naidu, R., Stevens, D.P., 1996. Review: the behaviour and environmental impact of contaminants in fertilizers. Aust. J. Soil Res. 34, 1–54.
McLaughlin, M.J., Simpson, P.G., Fleming, N., Stevens, D.P., Cozens, G., Smart, M.K., 1997. Effect of fertiliser type on cadmium and fluorine concentrations in clover herbage. Aust. J. Exp. Agric. 37, 1019–1026.
Mench, M., Tancogne, J., Gomez, A., Juste, C., 1989. Cadmium bioavailability to *Nicotiana tabacum* L., *Nicotiana rustica* L., and *Zea mays* L. grown in soil amended or not amended with cadmium nitrate. Biol. Fertil. Soils 8, 48–53.
Ministry of Health and Welfare, the Government of Japan, 2000. Nutritional Status in Japan 1998. Dai-ichi Shuppan Press, Tokyo 73–75.
Miyadate, H., Adachi, S., Hiraizumi, A., Tezuka, K., Nakazawa, N., Kawamoto, T., Katou, K., Komada, I., Sakurai, K., Takahishi, H., Satoh-Nagasawa, N., Watanabe, A., Fujimura, T., Akagi, H., 2011. OsHMA3, a P1B-type of ATPase affects root-to-shoot cadmium translocation in rice by mediating efflux into vacuoles. New Phytol. 189, 190–199.
Moon, C.S., Zhang, Z.W., Watanabe, T., Shimbo, S., Ismail, N.H., Hashim, J.H., Ikeda, M., 1996. Non-occupational exposure of Malay women in Kuala Lumpur, Malaysia, to cadmium and lead. Biomarkers 1, 81–85.
Moon, C.S., Zhang, Z.W., Shimbo, S., Watanabe, T., Moon, D.H., Lee, C.U., Lee, B.K., Ahn, K.D., Lee, S.H., Ikeda, M., 1998. Evaluation of urinary cadmium and lead as markers of background exposure of middle-aged women in Korea. Int. Arch. Occup. Environ. Health 71, 251–256.
Mortvedt, J.J., 1996. Heavy metal contaminants in inorganic and organic fertilizers. Fert. Res. 43, 55–61.
Mousavi, S.M., Bahmanyar, M.A., Pirdashti, H., 2010. Lead and cadmium availability and uptake by rice plant in response to different biosolids and inorganic fertilizers. Am. J. Agric. Biol. Sci. 5, 25–31.
Mulligan, C.N., Yong, R.N., Gibbs, B.F., 1999. Removal of heavy metals from contaminated soil and sediments using the biosurfactant surfactin. J. Soil Contam. 8, 231–254.
Murakami, M., Ae, N., Ishikawa, S., 2007. Phytoextraction of cadmium by rice (*Oryza sativa* L.), soybean (*Glycine max* (L.) Merr.), and maize (*Zea mays* L.). Environ. Pollut. 145, 96–103.
Murakami, M., Ae, N., Ishikawa, S., Ibaraki, T., Ito, M., 2008. Phytoextraction by a high-Cd-accumulating rice: reduction of Cd content of soybean seeds. Environ. Sci. Technol. 42, 6167–6172.
Murakami, M., Nakagawa, F., Ae, N., Ito, M., Arao, T., 2009. Phytoextraction by rice capable of accumulating Cd at high levels: reduction of Cd content of rice grain. Environ. Sci. Technol. 43, 5878–5883.

Naidu, R., Bolan, N.S., 2008. Contaminant chemistry in soils: key concepts and bioavailability. In: Naidu, R. (Ed.), Chemical Bioavailability in Terrestrial Environment, Elsevier, Amsterdam, The Netherlands, pp. 9–38.

Naidu, R., Bolan, N.S., Kookana, R.S., Tiller, K.G., 1994. Ionic-strength and pH effects on the adsorption of cadmium and the surface charge of soils. Euro. J. Soil Sci. 45, 419–429.

Naidu, R., Kookana, R.S., Sumner, M.E., Harter, R.D., Tiller, K.G., 1997. Cadmium sorption and transport in variable charge soils: a review. J. Environ. Qual. 26, 602–617.

Naidu, R., Bolan, N.S., Megharaj, M., Juhasz, A.L., Gupta, S., Clothier, B., Schulin, R., 2008. Chemical bioavailability in terrestrial environments. In: Naidu, R. (Ed.), Chemical Bioavailability in Terrestrial Environment, Elsevier, Amsterdam, The Netherlands, pp. 1–6.

Nakashima, S., Ono, S., 1979. Counter plants of paddy soils contaminated by cadmium and other heavy metals in Tsushima Island. Bull. Nagasaki. Agri. Exp. Sta 7, 337–385 (in Japanese).

Nanda Kumar, P.B.A., Dushenkov, V., Motto, H., Raskin, I., 1995. Phytoextraction: the use of plants to remove heavy metals from soils. Environ. Sci. Technol. 29, 1232–1238.

Narteh, L.T., Sahrawat, K.L., 1999. Influence of flooding on electrochemical and chemical properties of West African soils. Geoderma 87, 179–207.

NIAST (National Institute of Agricultural Science and Technology, Korea)., 1997. Survey of heavy metals contamination degree of arable soil located in mining area. Annu. Rep. (Department Agric. Environment), 237–243 (in Korean).

Nogawa, K., Kido, M., 1996. Itai-itai Disease and Health Effects of Cadmium. In: Chang, L.W. (Ed.), Toxicology of Metals, CRC Lewis Publishers, NY, pp. 353–370.

Nogawa, K., Yamada, Y., Honda, R., Ishizaki, M., Tsuritani, I., Kawano, S., Kato, T., 1983. The relationship between Itai-itai disease among inhabitants of the Jinzu River basin and cadmium in rice. Toxicol. Lett. 17, 263–266.

Ogawa, T., Kobayashi, E., Okubo, Y., Suwazono, Y., Kido, T., Nogawa, K., 2004. Relationship among prevalence of patients with Itai-itai disease, prevalence of abnormal urinary findings, and cadmium concentrations in rice of individual hamlets in the Jinzu River basin, Toyama prefecture of Japan. Int. J. Environ. Health Res. 14, 243–252.

Ok, Y.S., Oh, S.E., Ahmad, M., Hyun, S., Kim, K.R., Moon, D.H., Lee, S.S., Lim, K.J., Jeon, W.T., Yang, J.E., 2010. Effects of natural and calcined oyster shells on Cd and Pb immobilization in contaminated soils. Environ. Earth Sci. 61, 1301–1308.

Ok, Y.S., Kim, S.C., Kim, D.K., Skousen, J.G., Lee, J.S., Cheong, Y.W., Kim, S.J., Yang, J.E., 2011. Ameliorants to immobilize Cd in rice paddy soils contaminated by abandoned metal mines in Korea. Environ. Geochem. Health 33, 23–30.

Oliver, D.P., Tiller, K.G., Conyers, M.K., Slattery, W.J., Alston, A.M., Merry, R.H., 1996. Effectiveness of liming to minimise uptake of cadmium by wheat and barley grain grown in the field. Aust. J. Agric. Res. 47, 1181–1193.

Onyatta, J.O., Huang, P.M., 1999. Chemical speciation and bioavailability index of cadmium for selected tropical soils in Kenya. Geoderma 91, 87–101.

Papademetriou, M.K., 2000. Rice production in the Asia-Pacific region: issues and perspectives. In: Papademetriou, M.K., Dent, F.J., Herath, E.M. (Eds.), Bridging the Rice Yield Gap in the Asia-pacific Region, Food and agriculture organization of the United Nations regional office for Asia and the Pacific, Bangkok, Thailand, pp. 4–25.

Park, J.H., Lamb, D., Paneerselvam, P., Choppala, G., Bolan, N.S., Chung, J.W., 2011. Role of organic amendments on enhanced bioremediation of heavy metal(loid) contaminated soils. J. Hazard. Mater. 185, 549–574.

Pearson, M.S., Maenpaa, K., Pierzynski, G.M., Lydy, M.J., 2000. Effects of soil amendments on the bioavailability of lead, zinc, and cadmium to earthworms. J. Environ. Qual. 29, 1611–1617.

Peterson, P.J., Alloway, B.J., 1979. Cadmium in soils and vegetation. In: Webb, M. (Ed.), The Chemistry, Biochemistry and Biology of Cadmium, Vol. 2 Elsevier North Holland Biomedical Press, Amsterdam, New York, Oxford, pp. 45–92.
Petterson, D.S., Masters, H.G., Speijers, E.J., Williams, D.E., Edwards, J.R., 1991. Accumulation of cadmium in the sheep. 26-13-26-14 In: Momcilovic, B. (Ed.), Trace Elements in Man and Animals-7, Yugoslavia, IMI, Zagreb.
Pichtel, J., Bradway, D.J., 2008. Conventional crops and organic amendments for Pb, Cd and Zn treatment at a severely contaminated site. Bioresour. Technol. 99, 1242–1251.
Pickering, W.F., 1983. Extraction of copper, lead, zinc or cadmium ions sorbed on calcium carbonate. Water Air Soil Pollut. 20, 299–309.
Ponnamperuma, F.N., 1972. The chemistry of submerged soils. Adv. Agron. 24, 29–96.
Pourrut, B., Lopareva-Pohu, A., Pruvot, C., Garçon, G., Verdin, A., Waterlot, C., Bidar, G., Shirali, P., Douay, F., 2011. Assessment of fly ash-aided phytostabilisation of highly contaminated soils after an 8-year field trial. Part 2. Influence on plants. Sci. Total Environ. 409, 4504–4510.
Prieto, M., Cubillas, P., Fernandez-Gonzalez, A., 2003. Uptake of dissolved Cd by biogenic and abiogenic aragonite: a comparison with sorption onto calcite. Geochim. Cosmochim. Acta 67, 3859–3869.
Qiao, X.L., Luo, Y.M., Christie, P., Wong, M.H., 2003. Chemical speciation and extractability of Zn, Cu and Cd in two contrasting biosolids-amended clay soils. Chemosphere 50, 823–929.
Ram, N., Veerloo, M., 1985. Effect of various organic materials on the mobility of heavy metals in soil. Environ. Pollut. B 10, 241–248.
Ramachandran, V., Bhujal, B.M., D'Souza, T.J., 1998. Influence of rock phosphates with and without vegetable compost on the yield, phosphorus and cadmium contents of rice (*Oryza sativa*) grown on an ultisol. Fresenius Environ. Bull. 7, 551–556.
Rauret, G., 1998. Extraction procedures for the determination of heavy metals in contaminated soil and sediment. Talanta 46, 449–455.
Rayment, G.E., 1988. Cadmium in Queensland's primary industries. In: Simpson, J., Curnow, W.J. (Eds.), Cadmium Accumulations in Australian Agriculture, Bureau of Rural Resources, Canberra, ACT, pp. 151–160.
Richards, B.K., Steenhuis, T.S., Peverly, J.H., McBride, M.B., 2000. Effect of sludge processing mode, soil texture and soil pH on metal mobility in undisturbed soil columns under accelerated loading. Environ. Pollut. 109, 327–346.
Riffaldi, R., Levi-Minzi, R., Saviozzi, A., Tropea, M., 1983. Sorption and release of cadmium by some sewage sludges. J. Environ. Qual. 12, 253–256.
Roberts, A.H.C., Longhurst, R.D., 2002. Cadmium cycling in sheep-grazed hill-country pastures. N. Z. J. Agric. Res. 45, 103–112.
Roberts, A.H.C., Longhurst, R.D., Brown, M.W., 1994. Cadmium status of soils, plant and grazing animals in New Zealand. N. Z. J. Agric. Res. 37, 119–129.
Robinson, B., Schulin, R., Nowack, B., Roulier, S., Menon, M., Clothier, B., Green, S., Mills, T., 2006. Phytoremediation for the management of metal flux in contaminated sites. For. Snow Landsc. Res. 80, 221–234.
Rogan, N., Serafimovski, T., Dolenec, M., Tasev, G., Dolenec, T., 2009. Heavy metal contamination of paddy soils and rice (*Oryza sativa* L.) from Koc ˇani field (Macedonia). Environ. Geochem. Health 31, 439–451.
Römkens, P.F.A.M., Guo, H.Y., Chu, C.L., Liu, T.S., Chiang, C.F., Koopmans, G.F., 2009. Prediction of cadmium uptake by brown rice and derivation of soil–plant transfer models to improve soil protection guidelines. Environ. Pollut. 157, 2435–2444.
Rothbaum, H.P., Goguel, R.L., Johnson, A.E., Mattingly, G.E.G., 1986. Cadmium accumulation in soils from long continued applications of superphosphate. J. Soil Sci. 37, 99–107.

Rys, G.J., 2011. A national cadmium management strategy for New Zealand agriculture. http://www.massey.ac.nz/~flrc/workshops/11/Manuscripts/Rys_2011.pdf

Sakurai, K., Huang, P.M., 1996. Influence of potassium chloride on desorption of cadmium sorbed on hydroxyaluminosilicate-montmorillonite complex. Soil Sci. Plant Nutr. 42, 475–481.

Sakurai, Y., Sugahara, K., Makino, T., 2005. Development of technology for suppressions of cadmium absorption by crops in arable soils. Kenkyuseika 434, 8–14 (in Japanese).

Santillan-Medrano, J., Jurinak, J.J., 1975. The chemistry of lead and cadmium in soil: solid phase formation. Soil Sci. Soc. Am. Proc. 39, 851–856.

Sapunar-Postruznik, J., Bazulic, D., Kubala, H., Balin, L., 1996. Estimation of dietary intake of lead and cadmium in the general population of the Republic of Croatia. Sci. Total Environ. 177, 31–35.

Sauerbeck, D., 1992. Conditions controlling the bioavailability of trace elements and heavy metals derived from phosphate fertilizers in soils. Proceedings of the 4th International Imphos Conference on Phosphorus, Life and Environment, Institute Mondial du Phosphate, Casablanca, pp. 419–448.

Sauve, S., Norvell, W.A., McBride, M., Hendershot, W., 2000. Speciation and complexation of cadmium in extracted soil solutions. Environ. Sci. Technol. 34, 291–296.

Schaecke, W., Tanneberg, H., Schilling, G., 2002. Behavior of heavy metals from sewage sludge in a Chernozem of the dry belt in Saxony-Anhalt/Germany. J. Plant Nutr. Soil Sci. 165, 609–617.

Schipper, L.A., Sparling, G.P., Fisk, L.M., Dodd, M.B., Power, I.L., Littler, R.A., 2011. Rates of accumulation of cadmium and uranium in a New Zealand hill farm soil as a result of long-term use of phosphate fertilizer. Agr. Ecosyst. Environ. 144, 95–101.

Schrey, P., Wittsiepe, J., Budde, U., Heinzow, B., Idel, H., Wilhelm, M., 2000. Dietary intake of lead, cadmium, copper and zinc by children from the North Sea island Amrum. Int. J. Hyg. Environ. Health 203, 1–9.

Seaman, J.C., Arey, J.S., Bertsch, P.M., 2001. Immobilization of nickel and other metals in contaminated sediments by hydroxyapatite addition. J. Environ. Qual. 30, 460–469.

Senesi, N., Loffredo, E., 1999. The chemistry of soil organic matter. In: Sparks, D.L. (Ed.), Soil Physical Chemistry, second ed. CRC Press, Boca Raton, pp. 239–370.

Senesi, N., Plaza, C., 2007. Role of humification processes in recycling organic wastes of various nature and sources as organic amendments. Clean 35, 26–41.

Shimbo, S., Zhang, Z.W., Watanabe, T., Nakatsuka, H., Matsuda-Inoguchi, N., Higashikawa, K., Ikeda, M., 2001. Cadmium and lead contents in rice and other cereal products in Japan in 1998–2000. Sci. Total Environ. 281, 165–175.

Shirvani, M., Kalbasi, M., Shariatmadari, H., Nourbakhsh, F., Najafi, B., 2006. Sorption-desorption of cadmium in aqueous palygorskite, sepiolite, and calcite suspensions: isotherm hysteresis. Chemosphere 65, 2178–2184.

Shuman, L.M., 1976. Zinc adsorption isotherms for soil clays with and without iron oxides removed. Soil Sci. Soc. Am. J. 40, 349–352.

Shuman, L.M., 1985. Fractionation method for soil microelements. Soil Sci. 140, 11–22.

Silveira, M.L., Alleoni, L.R.F., O'Connor, G.A., Chang, A.C., 2006. Heavy metal sequential extraction methods – a modification for tropical soils. Chemosphere 64, 1929–1938.

Simmons, R.W., Pongsakul, P., Saiyasitpanich, D., Klinphoklap, S., 2005. Elevated levels of cadmium and zinc in paddy soils and elevated levels of cadmium in rice grain downstream of a zinc mineralized area in Thailand: implications for public health. Environ. Geochem. Health 27, 501–511.

Simmons, R.W., Noble, A.D., Pongsakul, P., Sukreeyapongse, O., Chinabut, N., 2008. Analysis of field-moist Cd contaminated paddy soils during rice grain fill allows reliable prediction of grain Cd levels. Plant Soil 302, 125–137.

Singh, B.R., Myhr, K., 1998. Cadmium uptake by barley as affected by Cd sources and pH levels. Geoderma 84, 185–194.
Singh, B.R., Narwal, R.P., Jeng, A.S., Almas, A., 1995. Crop uptake and extractability of cadmium in soils naturally high in metals at different pH levels. Commun. Soil Sci. Plant Anal. 26, 2123–2142.
Smolders, E., McLaughlin, M.J., 1996. Chloride increases cadmium uptake in Swiss chard in a resin-buffered nutrient solution. Soil Sci. Soc. Am. J. 60, 1443–1447.
Solly, S.R.B., Revfeim, K.J.A., Finch, G.C., 1981. Concentrations of cadmium, copper, selenium, zinc and lead in tissues of New Zealand cattle, pigs and sheep. N. Z. J. Sci. 24, 81–87.
Soon, Y.K., 1981. Solubility and sorption of cadmium in soils amended with sewage sludge. J. Soil Sci. 32, 85–95.
Sparks, D.L., 2003. Environmental Soil Chemistry, second ed.. Academic Press, San Diego.
Sparrow, L.A., Salardini, A.A., Bishop, A.C., 1993. Field studies of cadmium in potatoes (*Solanum tuberosum* L). 1. Effects of lime and phosphorus on cv Russet Burbank. Aust. J. Agric. Res. 44, 845–853.
Sposito, G., 1994. Chemical Equilibria and Kinetics in Soils. Oxford University Press, London 125–150.
Stacey, S., Merrington, G., McLaughlin, M.J., 2001. The effect of aging biosolids on the availability of cadmium and zinc in soil. Euro. J. Soil Sci. 52, 313–321.
Stipp, S.L., Hochella Jr., M.F., Parks, G.A., Leckie, J.O., 1992. Cd^{2+} uptake by calcite, solid-state diffusion, and the formation of solid solution: interface processes observed with near-surface sensitive techniques (XPS, LEED, and AES). Geochim. Cosmochim. Acta 56, 1941–1954.
Street, J.J., Sabey, B.R., Lindsay, W.L., 1978. Influence of pH, phosphorus, cadmium, sewage sludge, and incubation time on the solubility and plant uptake of cadmium. J. Environ. Qual. 7, 286–290.
Syers, J.K., MacKay, A.D., Brown, M.W., Currie, L.D., 1986. Chemical and physical characteristics of phosphate rock materials of ranging reactivity. J. Sci. Food Agric. 37, 1057–1064.
Szomolányi, A., Lehoczky, E., 2002. Study on the Cd uptake by lettuce plants in liming experiment. Proceedings of the 7th Hungarian Congress on Plant Physiology, pp. 123–124.
Takahashi, E., 1974. Effects of soil moisture on the uptake of silica by rice seedlings. J. Sci. Soil Manure 45, 591–596.
Tanaka, K., Fujimaki, S., Fujiwara, T., Yoneyama, T., Hayashi, H., 2007. Quantitative estimation of the contribution of the phloem in cadmium transport to grains in rice plants (*Oryza sativa* L.). Soil Sci. Plant Nutr. 53, 72–77.
Tandy, S., Bossart, K., Mueller, R., Ritschel, J., Hauser, L., Schulin, R., Nowack, B., 2004. Extraction of heavy metals from soils using biodegradable chelating agents. Environ. Sci. Technol. 38, 937–944.
Tang, C., Barton, L., Raphael, C., 1998. Pasture legume species differ in their capacity to acidify soil. Aust. J. Agric. Res. 49, 53–58.
Tessier, A., Campbell, P.G.C., Bisson, M., 1979. Sequential extraction procedure for the speciation of particulate trace metals. Anal. Chem. 5, 844–851.
Tezuka, K., Miyadate, H., Katou, K., Kodama, I., Matsumoto, S., Kawakoto, T., Masaki, S., Satoh, H., Yamaguchi, M., Sakurai, K., Takahashi, H., Satoh-Nagasawa, M., Watanabe, A., Fujimura, T., Akagi, H., 2010. A single recessive gene controls cadmium translocation in the cadmium hyperaccumulating rice cultivar Cho-Ko-Koku. Theor. Appl. Genet. 120, 1175–1182.
Tiller, K.G., 1988. Heavy metals in soils and their environmental significance. Adv. Soil Sci. 9, 113–142.

Traina, S.J., 1999. The environmental chemistry of cadmium. In: McLaughlin, M.J., Singh, B.R. (Eds.), Cadmium in Soils and Plants, Kluwer Academic Publishers, Dordrecht, pp. 11–37.

Turekian, K.K., Wedepohl, K.H., 1961. Distribution of the elements in some major units of the earth's crust. Geol. Soc. Am. Bull. 72, 175–192.

Tyler, G., Olsson, T., 2001. Plant uptake of major and minor mineral elements as influenced by soil acidity and liming. Plant Soil 230, 307–321.

Ueno, D., Koyama, E., Kono, I., Ando, T., Yano, M., Ma, J.F., 2009. Identification of a novel major quantitative trait locus controlling distribution of Cd between roots and shoots in rice. Plant Cell. Physiol. 50, 2223–2233.

Ueno, D., Yamaji, N., Kono, I., Huang, C.F., Ando, T., Yano, M., Ma, J.F., 2010. Gene limiting cadmium accumulation in rice. Proc. Natl. Acad. Sci. U S A 107, 16500–16505.

Uraguchi, S., Mori, S., Kuramata, M., Kawasaki, A., Arao, T., Ishikawa, S., 2009. Root-to-shoot Cd translocation via the xylem is the major process determining shoot and grain cadmium accumulation in rice. J. Exp. Bot. 60, 2677–2688.

Van Cauwenbergh, V., Bosscher, D., Robberecht, H., Deelstr, H., 2000. Daily dietary cadmium intake in Belgium using duplicate portion sampling. Eur. Food Res. Technol. 212, 13–16.

Vangronsveld, J., Cunningham, S.D., 1998. Introduction to the concepts. In: Vangronsveld, J., Cunningham, S.D. (Eds.), Metal Contaminated Soils: In-situ Inactivation and Phytorestoration, Springer Verlag, Berlin, pp. 219–225.

Vega, F.A., Covelo, E.F., Andrade, M.L., 2006. Competitive sorption and desorption of heavy metals in mine soils: influence of mine soil characteristics. J. Colloid Interf. Sci. 298, 582–592.

Vine, J.D., Tourtelot, E.B., 1970. Geochemistry of black shale deposit – a summary report. Econ. Geol. 65, 253–272.

Wang, G.Q., Koopmans, G.F., Song, J., Temminghoff, E.J.M., Luo, Y.M., Zhao, Q.G., Japenga, J., 2007. Mobilization of heavy metals from contaminated paddy soil by EDDS, EDTA, and elemental sulfur. Environ. Geochem. Health 29, 221–235.

Watanabe, T., Nakatsuka, H., Ikeda, M., 1989. Cadmium and lead in rice available in various areas of Asia. Sci. Total Environ. 80, 175–184.

Watanabe, T., Shimbo, S., Moon, C.S., Zhang, Z.W., Ikeda, M., 1996. Cadmium contents in rice samples from various areas in the world. Sci. Total Environ. 184, 191–196.

Watanabe, T., Zhang, Z.W., Qu, J.B., Xu, G.F., Song, L.H., Wang, J.J., Shimbo, S., Nakatsuka, H., Higashikawa, K., Ikeda, M., 1998. Urban–rural comparison on cadmium exposure among general populations in Shandong Province, China. Sci. Total Environ. 217, 1–8.

Watanabe, T., Zhang, Z.W., Moon, C.S., Shimbo, S., Nakatsuka, H., Matsuda- Inoguchi, N., Higashikawa, K., Ikeda, M., 2000a. Cadmium exposure of women in general populations in Japan during 1991–1997 compared with 1977–1981. Int. Arch. Occup. Environ. Health 73, 26–34.

Watanabe, T., Zhang, Z.W., Qu, J.B., Gao, W.P., Jian, Z.K., Shimbo, S., Nakatsuka, H., Matsuda-Inoguchi, N., Higashikawa, K., Ikeda, M., 2000b. Background lead and cadmium exposure of adult women in Xian City and two farming villages in Shaanxi Province, China. Sci. Total Environ. 347, 1–13.

Weber, J.H., Allard, T., Tipping, E., Benedetti, M.F., 2006. Modeling iron binding to organic matter. Environ. Sci. Technol. 40, 7488–7493.

Weggler-Beaton, K., McLaughlin, M.J., Graham, R.D., 2000. Salinity increases cadmium uptake by wheat and Swiss chard from soil amended with biosolids. Aust. J. Soil Res. 38, 37–45.

Wilhelm, M., Lombeck, I., Kouros, B., Wuthe, J., Ohnesorge, F.K., 1995. Duplicate study on the dietary intake of some metals/metalloids by German children. Part II: aluminium, cadmium and lead. Zbl. Hyg. Umveltmed 197, 357–369 (in German).

Wilhelm, M., Wittsiepe, J., Schrey, P., Budde, U., Idel, H., 2002. Dietary intake of cadmium by children and adults from Germany using duplicate portion sampling. Sci. Total Environ. 285, 11–19.

Wilkinson, J.M., Hill, J., Livesey, C.T., 2001. Accumulation of potentially toxic elements by sheep grazed on grassland given repeated applications of sewage sludge. Anim. Sci. 72, 179–190.

Williams, C.H., David, D.J., 1973. The effect of superphosphate on the cadmium content of soils and plants. Aust. J. Soil Res. 11, 43–56.

Williams, C.H., David, D.J., 1976. The accumulation in soil of cadmium residues from phosphate fertilizers and their effect on the cadmium content of plants. Soil Sci. 121, 86–93.

Xiong, L.M., 1995. Influence of phosphate on cadmium adsorption by soils. Fert. Res. 40, 31–40.

Xu, Y., Schwartz, F.W., Traina, S.J., 1994. Sorption of Zn^{2+} and Cd^{2+} on hydroxyapatite surfaces. Environ. Sci. Technol. 28, 1472–1480.

Yamada, N., 2007. Leading edge technologies for remedying heavy metal-contaminated agricultural soils. 2. Remediation of heavy metal-contaminated soils by soil dressing, and sustainability of the remediation effects. Jpn. J. Soil Sci. Plant Nutr. 78, 411–416 (in Japanese).

Yamaguchi, M., 2006. Breeding of rice varieties with low or high cadmium. Res. J. Food Agric. 29, 11–14 (in Japanese).

Yamamoto, T., Yonemaru, J., Yano, M., 2009. Towards the understanding of complex traits in rice: substantially or superficially? DNA Res. 16, 141–154.

Yang, Q.W., Lan, C.Y., Wang, H.B., Zhuang, P., Shu, W.S., 2006. Cadmium in soil–rice system and health risk associated with the use of untreated mining wastewater for irrigation in Lechang, China. Agr. Water Manage. 84, 147–152.

Yap, D.W., Adezrian, J., Khairiah, J., Ismail, B.S., Ahmad-Mahir, R., 2009. The uptake of heavy metals by paddy plants (Oryza sativa) in Kota Marudu, Sabah, Malaysia American-Eurasian. J. Agric. Environ. Sci. 6, 16–19.

Yassen, A.A., Nadia, B.M., Zaghloul, M.S., 2007. Role of some organic residues as tools for reducing heavy metals hazards in plant. W. J. Agri. Sci. 3, 204–207.

Yoo, I.S., Lee, J.S., Soh, C.T., 1992. Study on heavy metals in soil and agricultural products along Mangyeong river system. J. Korean Public Health Assoc. 18, 77–87.

Ysart, G., Miller, P., Crews, H., Robb, P., Baxter, M., De L'Argy, C., Lofthouse, S., Sargent, C., Harrison, N., 1999. Dietary exposure estimates of 30 metals and other elements from the UK Total Diet Study. Food Addit. Contam. A 16, 391–403.

Yu, H., Wang, J., Fang, W., Yuan, J., Yang, Z., 2006. Cd accumulation in different rice cultivars and screening for pollution-safe cultivars of rice. Sci. Total Environ. 370, 302–309.

Yuan, G., Lavkulich, L.M., 1997. Sorption behavior of copper, zinc, and cadmium in response to simulated changes in soil properties. Commun. Soil Sci. Plant Anal. 28, 571–587.

Zachara, J.M., Resch, C.T., Smith, S.C., 1994. Influence of humic substances on Co_2þ sorption by a surface mineral separate and its mineralogic components. Geochim. Cosmochim. Acta 58, 553–566.

Zarcinas, B.A., Pongsakul, P., McLaughlin, M.J., Cozens, G., 2004. Heavy metals in soils and crops in Southeast Asia. 1. Peninsular Malaysia. Environ. Geochem. Health 26, 343–357.

Zazoli, M.A., Bazerafshan, E., Hazrati, A., Tavakkoli, A., 2006. Determination and estimation of cadmium intake from Tarom rice. J. Appl. Sci. Environ. Manage. 10, 147–150.

Zeng, Q.R., Sauve, S., Allen, H.E., Hendershot, W.H., 2005. Recycling EDTA solutions used to remediate metal-polluted soils. Environ. Pollut. 133, 225–231.

Zhai, L., Liao, X., Chen, T., Yan, X., Xie, H., Wu, B., Wang, L., 2008. Regional assessment of cadmium pollution in agricultural lands and the potential health risk related to intensive mining activities: a case study in Chenzhou City. Chinese. J. Environ. Sci. 20, 696–703.

Zhang, Z.W., Moon, C.S., Watanabe, T., Shimbo, S., He, F.S., Wu, Y.Q., Zhou, S.F., Su, D.M., Qu, J.B., Ikeda, M., 1997. Background exposure of urban populations to lead and cadmiu: comparison between China and Japan. Int. Arch. Occup. Environ. Health 69, 273–281.

Zhang, Z.W., Subida, R.D., Agetano, M.G., Nakatsuka, H., Inoguchi, N., Watanabe, T., Shimbo, S., Higashikawa, K., Ikeda, M., 1998. Non-occupational exposure of adult women in Manila, Philippines, to lead and cadmium. Sci. Total Environ. 215, 157–165.

Zhang, Z.W., Shimbo, S., Watanabe, T., Srianujata, S., Bangjong, O., Chitchumroonchokchai, C., Nakatsuka, H., Matsuda-Inoguchi, N., Higashikawa, K., Ikeda, M., 1999. Non-occupational lead and cadmium exposure of adult women in Bangkok, Thailand. Sci. Total Environ. 226, 65–74.

Zheng, S., Zhang, M., 2011. Effect of moisture regime on the redistribution of heavy metals in paddy soil. J. Environ. Sci. 23, 434–443.

Zhou, L.X., Wong, J.W.C., 2001. Effect of dissolved organic matter from sludge and sludge compost on soil copper sorption. J. Environ. Qual. 30, 878–883.

Zhu, Q.H., Huang, D.Y., Zhu, G.X., Ge, T.D., Liu, G.S., Zhu, H.H., Liu, S.L., Zhang, X.N., 2010. Sepiolite is recommended for the remediation of Cd-contaminated paddy soil. Acta Agr. Scand. B-S P 60, 110–116.

Zubillaga, M.S., Lavado, R.S., 2008. Accumulation and movement of four potentially toxic elements in soils throughout five years, during and after biosolid application. Am. J. Environ. Sci. 4, 576–582.



CHAPTER FIVE

Transport and Retention of Heavy Metal in Soils: Competitive Sorption

H. M. Selim
School of Plant, Environmental and Soil Science, Louisiana State University, Baton Rouge, Louisiana, USA

Contents

Abstract

Appreciable amounts of various heavy metals (e.g. As, Cu, Ni, and Zn) are found in surface soils of lands as a result of accidental spills or industrial waste and sewage sludge applications. Such conditions often create environmental risks and potential contamination of soil, surface and groundwater resources. Competitive adsorption and desorption processes of heavy metals by the soil matrix have significant importance on their fate and mobility in soils. In this contribution, equilibrium and kinetic models governing competitive heavy-metal sorption and transport in soils were presented. Several examples were discussed to illustrate the impact of competing ions on the reactivities and mobility of heavy metals in the soil–water environment. The examples exhibited that competition among various heavy-metal species for available adsorption sites on soil matrix surfaces often results in the enhancement of the mobility of contaminants in the soil environment. Competitive sorption based on equilibrium Freundlich and Langmuir models were derived in order to account for competitive sorption of cations and anions in soils. Competitive models of the multiple reaction type including the two-site nonlinear equilibrium-kinetic models,

Advances in Agronomy, Volume 119
ISSN 0065-2113, http://dx.doi.org/10.1016/B978-0-12-407247-3.00005-6

the concurrent- and consecutive multireaction models were modified to describe kinetic adsorption–desorption of heavy metals behavior in soil. It was shown that equilibrium Langmuir and kinetic second-order models can be extended to simulate the competitive sorption and transport in soils. A drawback of Freundlich and Langmuir approaches is that their associated parameters are specific for each soil. Moreover, since predictions of the transport of heavy metals were sometime inadequate, improved competitive modeling approaches are needed. On the other hand, geochemical models, which are based on ion exchange and surface complexation concepts, are frequently utilized to quantify competitive behavior of several chemical species under a wide range of environmental conditions. However, further research is also needed since geochemical models are incapable of describing kinetic sorption–desorption of heavy metal ions in competitive systems.

1. INTRODUCTION

Heavy metals are commonly considered as potential pollutants in the soil and groundwater environments. Primary sources of heavy-metal contamination include mining, smelting, and various industrial as well as anthropogenic factors. Moreover, industrial waste and sewage sludge disposed on land often contain appreciable amounts of heavy metals, thus creating a risk for croplands, as well as animals and humans. It has been observed that that most reported incidents of soil contamination, the source of pollutants, include an array of heavy metal species rather than a single heavy metal ion. It is also recognized that the fate and transport of heavy metals is significantly impacted by the various interactions in a multicomponent or multiple ion systems. In fact, a prerequisite in describing the fate of heavy metals in multicomponent system is the identification of dominant mechanisms governing their competitive sorption behavior. Such information is essential in order to predict the reactivity and potential mobility of multiple heavy metals in the soils and aquifers.

Predicting the risk of heavy-metal mobilization in contaminated soils and the potential for leaching into groundwater requires a quantitative description of heavy metals behavior in the soil–water environment. Thus, comprehensive modeling of heavy-metal adsorption–desorption and transport of heavy-metal elements in soils and aquifers is a challenging task. During the past several years, the development of empirical equilibrium and kinetic models and surface-complexation models and the application of these models to soils and sediment have resulted in variable degrees of success.

In this contribution, we discuss heavy metals behavior (sorption–desorption) and transport in soils and aquifers. Competitive retention of

heavy metals for available sites on matrix surfaces and subsequent impact on their transport in the vadose zone is discussed. Examples of competitive adsorption–desorption behavior for several heavy metals are presented. Several approaches of modeling for the prediction of competitive behavior during transport are presented with emphasis on kinetic of nonequilibrium models.



2. TRANSPORT

Chemical species present in the soil solution are susceptible to transport through porous media subject to the water flow constraints in the soil system or geological media. At any given point within the soil, the total amount of solute χ (μg /cm^{-3}) for a species i may be represented by

$$\chi_i = \theta C_i + \rho S_i \tag{1}$$

where S is the amount of solute retained by the soil (μg g^{-1} soil), C is the solute concentration in solution (μg mL^{-1}), θ is the soil moisture content (cm^3 cm^{-3}) and ϱ is the soil bulk density (g cm^{-3}). The rate of change of χ for the i-th species with time is subject to the law of mass conservation such that (omitting the subscript i)

$$\frac{\partial(\theta C + \rho S)}{\partial t} = -\,div\,J - Q \tag{2}$$

or

$$\frac{\partial(\theta C + \rho S)}{\partial t} = -\left(\frac{\partial J_x}{\partial x} + \frac{\partial J_y}{\partial y} + \frac{\partial J_z}{\partial z}\right) - Q \tag{3}$$

where t is the time (h) and J_x, J_y, and J_z represent the flux or rate of movement of solute species i in the x, y, and z (μg cm^{-2} h), respectively. The term Q represents the sink (Q positive) or source which accounts for the rate of solute removal (or addition) irreversibly from the bulk solution (μg cm^{-3} h). If we restrict our analysis to one-dimensional flow in the z-direction, the flux J_z, or simply J, in the soil may be given by

$$J = -\theta(D_m + D_L)\frac{\partial C}{\partial z} + qC \tag{4a}$$

where D_m is the molecular diffusion coefficient (cm^2 h^{-1}), D_L is the longitudinal dispersion coefficient (cm^2 h^{-1}), and q is the Darcy's flux (cm h^{-1}). Therefore, the primary mechanisms for solute movement are

due to diffusion plus dispersion and by mass flow or convection with water as the water moves through the soil. The molecular diffusion mechanism is due to the random thermal motion of molecules in solution and is an active process regardless of whether or not there is net water flow in the soil. The result of diffusion process is the well-known Fick's law of diffusion, where solute flux is proportional to the concentration gradient.

The longitudinal dispersion term of Eqn (4a) is due to the mechanical or hydrodynamic dispersion phenomena, which are due to the nonuniform flow velocity distribution during fluid flow in porous media. Nonuniform velocity distribution through the pores in soils or geological media is a result of variations in pore diameters along the flow path, fluctuation of the flow path due to tortuosity effect, and the variation in velocity from the center of a pore (maximum value) to zero at the solid surface interface (Poiseuille's law). The effect of dispersion is that of solute spreading, which is a tendency opposite to that of piston flow. Dispersion is effective only during fluid flow, i.e. for a static water condition or when water flow is near zero, molecular diffusion is the dominant process for solute transport in soils. For multidimensional flow, longitudinal dispersion coefficient (D_L) and transverse dispersion coefficients (D_T) are needed to describe the dispersion mechanism. Longitudinal dispersion refers to that in the direction of water flow and that for the transverse directions for dispersion perpendicular to the direction of flow.

Apparent dispersion D is often introduced to simplify the flux Eqn (4b) such that

$$J = -\theta D \frac{\partial C}{\partial z} + qC \tag{4b}$$

where D now refers to the combined influence of diffusion and hydrodynamic dispersion for dissolved chemicals in porous media. Incorporation of flux (Eqn (5)) into the conservation of mass (Eqn (3)) yields the following generalized form for solute transport in soils in one dimension:

$$\frac{\partial \theta C}{\partial t} + \rho \frac{\partial S}{\partial t} = \frac{\partial}{\partial z} \theta D \frac{\partial C}{\partial z} - \frac{\partial qC}{\partial z} - Q \tag{5}$$

The above equation is commonly known as the convective–dispersive equation (CDE) for solute transport, which is valid for soils under transient and unsaturated soil–water flow conditions. For conditions where steady

water flow is dominant, D and θ are constants, i.e. for uniform θ in the soil, we have the simplified form of the convection–dispersion equation as,

$$\frac{\partial C}{\partial t}+\frac{\rho}{\theta}\frac{\partial S}{\partial t}=D\frac{\partial^2 C}{\partial_z^2}-v\frac{\partial C}{\partial z}-\frac{Q}{\theta} \tag{6}$$

where v (cm h^{-1}) is commonly referred to as the pore-water velocity and is given by ($q\ \theta^{-1}$).

Solutions of the above convection–dispersive Eqns (6) or (7) yield the concentration distribution of the amount of solute in soil solution C and that retained by the soil matrix S with time and depth in the soil profile. In order to arrive at such a solution, the appropriate initial and boundary conditions must be specified. Several boundary conditions are identified with the problem of solute transport in porous media. The simplest is that of a first-order-type boundary condition such that a solute pulse input is described such that

$$C=C_s,\ \ z=0,\ \ t<T \tag{7}$$

$$C=0,\ \ z=0,\ \ t\geq T \tag{8}$$

where C_s (μg cm^{-3}) is the concentration of the solute species in the input pulse. The input pulse application is for a duration T which was then followed by a pulse input which is free of such a solute. Such a boundary condition was used by Lapidus and Amundson (1952). The more precise third-type boundary condition at the soil surface was considered by Brenner (1962) in his classical work, where advection plus dispersion across the interface was considered. A continuous solute flux at the surface can be expressed as

$$vC_s=-D\frac{\partial C}{\partial z}+vC,\ \ z=0,\ \ t>0 \tag{9}$$

and a flux-type pulse input as

$$vC_s=-D\frac{\partial C}{\partial z}+vC,\ \ z=0,\ \ t<T \tag{10}$$

$$0=-D\frac{\partial C}{\partial\ z}+vC,\ \ z=0,\ \ t\geq T \tag{11}$$

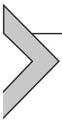
The boundary conditions at some depth L in the soil profile is often expressed as,

$$\frac{\partial C}{\partial z}=0,\ \ z=L,\ \ t\geq 0 \tag{12}$$

which is used to deal with solute effluent from soils having finite lengths. However, it is often convenient to solve the dispersion–convection equation where a semi-infinite rather than a finite length (L) of the soil is assumed. Under such circumstances, the appropriate condition for a semi-infinite medium is

$$\frac{\partial C}{\partial z}=0,\ \ z\rightarrow\infty,\ \ t\geq 0 \tag{13}$$

Analytical solutions to the convection–dispersion equation subject to the appropriate boundary and initial conditions are available for a number of situations, whereas the majority of the solute transport problems must be solved using numerical approximation methods. In general, whenever the form of the retention reaction is a linear one, a closed-form solution is obtainable. A number of closed-form solutions are available in soil physics and chemical engineering literature. However, as we discuss in this contribution, retention mechanisms for most reactive chemicals are strongly nonlinear and kinetic and analytical solutions are not available. As a result, a number of numerical models based on finite-difference or finite-element approximations are commonly used to account for multireaction and multicomponent solute transport in soils.



3. RETENTION MODELS

The form of heavy-metal reactions in the soil system must be identified if prediction of their fate in the soil is sought. In general, heavy metals retention processes in soils have been quantified by scientists using several approaches. One approach represents equilibrium reactions and the second represents kinetic or time-dependent type reactions. Equilibrium models are those where heavy metal reaction is assumed to be fast or instantaneous in nature. Under such conditions, "apparent equilibrium" may be observed in a relatively short reaction time. Langmuir and Freundlich models are perhaps the most commonly used equilibrium models for the description of fertilizer chemicals such as phosphorus and for several heavy metals. These

equilibrium models include the linear and Freundlich (nonlinear) and the one- and two-site Langmuir type. Kinetic models represent slow reactions where the amount of solute sorption or transformation is a function of contact time. Most common is the first-order kinetic reversible reaction for describing time-dependent adsorption/desorption in soils. Others include linear irreversible and nonlinear reversible kinetic models. Recently, combination of equilibrium and kinetic type (two-site) models, and consecutive and concurrent multireaction type models has been proposed. A list of retention models is given in Tables 5.1 and 5.2.

3.1. First-Order and Freundlich Models

The first-order kinetic approach is perhaps one of the earliest single form of reactions used to describe the sorption versus time for several dissolved chemicals in soils This may be written as

$$\frac{\partial S}{\partial t} = k_{\mathrm{f}} \left(\frac{\theta}{\rho} \right) C - k_{\mathrm{b}} S \tag{14}$$

where the parameters k_{f} and k_{b} represent the forward and backward rates of reactions (h^{-1}) for the retention mechanism, respectively. The first-order reaction was first incorporated into the classical convection–dispersion

Table 5.1 Equilibrium and Kinetic Retention Models

Model	**Formulation**
Linear equilibrium	$S = K_{\mathrm{d}} \cdot C$
Freundlich equilibrium	$S = K_{\mathrm{F}} \cdot C^{b}$
Langmuir equilibrium	$S/S_{\max} = K_{\mathrm{L}} \cdot C/[1 + K_{\mathrm{L}} \cdot C]$
First-order kinetic	$\partial S/\partial t = k_{\mathrm{f}} (\theta/\rho) C - k_{\mathrm{b}} S$
Freundlich kinetic	$\partial S/\partial t k_{\mathrm{f}} (\theta/\rho) C^{b} - k_{\mathrm{b}} S$
Langmuir kinetic	$\rho (\partial S/\partial t) = k_{\mathrm{f}} \theta (S_{\max} - S) C - k_{\mathrm{b}} \rho S$
Irreversible (sink/source)	$\partial S/\partial t = k_{\mathrm{s}} (\theta/\rho) (C - C_{\mathrm{p}})$
Pseudo-first-order kinetic	$\partial S/\partial t = \kappa (S_{\mathrm{eq}} - S)$
Pseudo-second-order kinetic	$\partial S/\partial t = \omega (S_{\mathrm{eq}} - S)^{2}$
Second-order irreversible	$\partial S/\partial t = k_{\mathrm{s}} (\theta/\rho) C (S_{\max} - S)$
Kinetic power model	$\partial S/\partial t = K (\theta/\rho) C^{n} S^{m}$
Mass transfer	$\partial S/\partial t = K (\theta/\rho) (C - C^{*})$

equation by Lapidus and Amundson (1952) to describe solute retention during transport under steady-state water flow conditions. Integration of Eqn (14) subject to initial conditions of $C = C_i$ and $S = 0$ at $t = 0$, for several C_i values, yields a system of linear sorption isotherms. That is, for any reaction time, t, a linear relation between S and C is obtained.

Linear isotherms are not often encountered except for selected cations and heavy metals at low concentrations. Isotherms which exhibit nonlinear or curve linear retention behavior is commonly observed for several reactive

Table 5.2 Competitive Retention Models

Model	Formulation
Freundlich equilibrium model	$S_i = K_i C_i \left(\sum_{j=1}^{l} \alpha_{i,j} C_j \right)^{n_i - 1}$
Freundlich kinetic model	$\frac{\partial (S_1)_i}{\partial t} = k_{1,i} \frac{\theta}{\rho} C_i \left(\sum_{j=1}^{l} \alpha_{i,j} C_j \right)^{n_i - 1} - k_{2,i} (S_1)_i$
Langmuir equilibrium model	$\frac{S_i}{S_{\max}} = \frac{K_i C_i}{1 + \sum_j K_j C_j}$
Langmuir kinetic model	$\frac{\partial S_i}{\partial t} = (\lambda_f)_i \frac{\theta}{\rho} C_i \left(S_{\max} - \sum_{i=1}^{l} S_j \right) - (\lambda_b)_i S_i$
Vanselow ion exchange	${}^{v}K_{ij} = \left(\frac{(a_i^*)^{\nu j}}{(a_j^*)^{\nu i}} \right) \left(\frac{(\zeta_j)^{\nu j}}{(\zeta_j)^{\nu i}} \right)$
Gaines and Thomas ion exchange	${}^{G}K_{ij} = \frac{(\gamma_j)^{\nu i}}{(\gamma_i)^{\nu j}} \left(\frac{s_i}{C_i} \right)^{\nu j} \left(\frac{s_j}{C_j} \right)^{\nu i}$
Rothmund–Kornfeld ion exchange	$\frac{(s_i)^{\nu j}}{(s_j)^{\nu i}} = {}^{R}K_{ij} \left[\frac{(c_i)^{\nu j}}{(c_j)^{\nu i}} \right]^{n}$
Elovich ion exchange	$\frac{\partial S_i}{\partial t} = a\, e^{-BS_i}$
Factional power model	$S_i = \kappa t^{\beta}$
Parabolic diffusion model	$\frac{S_i}{(S_{eq})_i} = \frac{4}{\sqrt{\pi}} \sqrt{\frac{D_m t}{r^2}} - \frac{D_m t}{r^2}$

chemicals as depicted by the isotherms for nickel, arsenic, and copper are shown in Figs 5.1–5.3, respectively (Liao and Selim, 2010; Selim and Ma, 2001; Zhang and Selim, 2005). To describe such nonlinear behavior, the first-order model of Eqn (14) is extended to include nonlinear kinetic such that,

$$\frac{\partial S}{\partial t} = k_f \left(\frac{\theta}{\rho}\right) C^b - k_b S \tag{15}$$

where b is a dimensionless parameter commonly less than unity and represents the order of the nonlinear or concentration-dependent reaction and illustrate the extent of heterogeneity of the retention processes. This nonlinear reaction (Eqn (15)) is fully reversible where the magnitudes of the rate coefficients dictate the extent of kinetic behavior of retention of the solute from the soil solution. For small values of k_f and k_b, the rate of retention is slow and strong kinetic dependence is anticipated. In contrast, for large values of k_f and k_b, the retention reaction is a rapid one and should approach quasi-equilibrium in a relatively short time. In fact, at large times, when the rate of retention approaches zero, Eqn (15) yields

$$S = K_F C^b \text{ where } K_F = \left(\frac{\theta k_f}{\rho k_b}\right) \tag{16}$$

Equation (16) is analogous to the Freundlich equilibrium equation where K_F is the solute partitioning coefficient ($cm^3\ g^{-1}$). Therefore, one

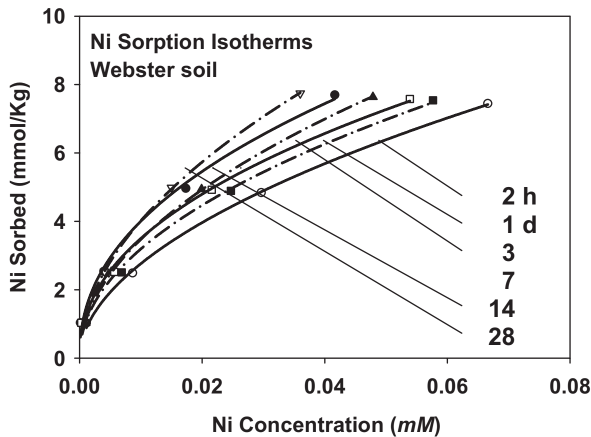


Figure 5.1 Adsorption isotherms for Ni on Webster soil at different retention times. The solid curves are based on the Freundlich equation.

may regard the parameter K_F as the ratio of the rate coefficients for sorption (forward reaction) to that for desorption or release (backward reaction).

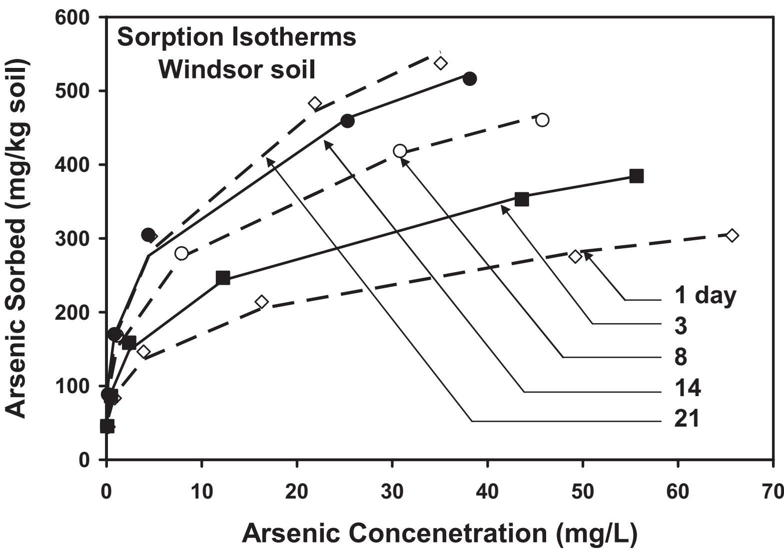


Figure 5.2 Adsorption isotherms for arsenic on Windsor soil at different retention times.

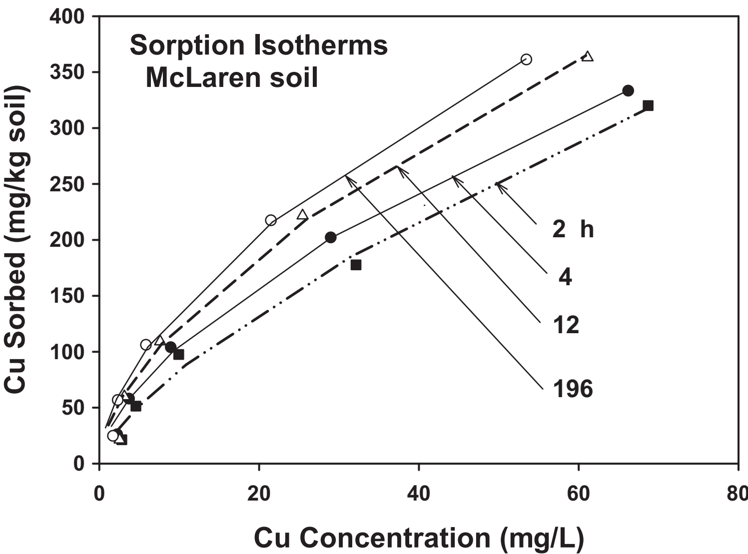


Figure 5.3 Adsorption isotherms for copper on McLaren soil at different retention times.

The parameter b is a measure of the extent of the heterogeneity of sorption sites of the soil matrix. In other words, sorption sites have different affinities for heavy-metal retention by matrix surfaces, where sorption by the highest energy sites takes place preferentially at the lowest solution concentrations. For the simple case where $b = 1$, we have the linear form

$$S = K_d C \quad \text{where } K_d = \left(\frac{\theta k_f}{\rho k_b} \right) \tag{17}$$

where the parameter K_d is the solute distribution coefficient ($cm^3\ g^{-1}$) and of similar form to the Freundlich parameter K_f. There are numerous examples of cations and heavy metals retention, which were described successfully by use of the linear or the Freundlich equation (Buchter et al., 1989; Sparks, 1989). The lack of nonlinear or concentration-dependent behavior of sorption patterns as indicated by the linear case of Eqn (17) is indicative of the lack of heterogeneity of sorption-site energies. For this special case, sorption-site energies for linear sorption processes of heavy metals are regarded as relatively homogenous.

3.2. Second-Order and Langmuir Models

An alternative to the above first- and n-th order models is that of the second-order kinetic approach. Such an approach is commonly referred to as the Langmuir kinetic and has been used for predictions of several reactive solutes including heavy metals in several soils (Selim and Amacher, 1997). Based on the second-order formulation, it is assumed that the retention mechanisms are site-specific where the rate of reaction is a function of the solute concentration present in the soil-solution phase (C) and the amount of available or unoccupied sites φ ($\mu g\ g^{-1}$ soil), by the reversible process



$$C + \phi \underset{k_b}{\overset{k_f}{\rightleftarrows}} S \tag{18}$$

where k_f to k_b are the associated rate coefficients and S is the total amount of solute retained by the soil matrix. As a result, the rate of solute retention may be expressed as

$$\rho \frac{\partial S}{\partial t} = k_f\, \theta_\phi C - k_b \rho S \quad \text{or} \quad \rho \frac{\partial S}{\partial t} = k_f\, \theta\, (S_T - S) C - k_b \rho S \tag{19}$$

where S_T represents the total amount of total sorption sites. As the sites become occupied by the retained solute, the amount of vacant sites approaches zero $(\phi \rightarrow 0)$ and the amount of solute retained by the soil approaches that of the total capacity of sites, i.e. $S \rightarrow S_T$. Vacant-specific sites are not strictly vacant. They are assumed occupied by hydrogen, hydroxyl or by other specifically sorbed species. An example of the capability of this kinetic approach in describing the retention of heavy metals in soils is illustrated in Figs 5.4 and 5.5. Copper adsorption over time in a McLaren soil was well described by the model over a wide range of input Cu concentrations (Fig. 5.4). Model predictions for adsorption as well as desorption for two initial Cu concentrations are illustrated in Fig. 5.5.

The above formulation (Eqn (19)) yields the commonly known Langmuir equilibrium model for adsorption on solid surfaces. For large times (as $t \rightarrow \infty$), i.e. when the reaction achieves local equilibrium, the rate of retention becomes

$$k_f\, \theta_\phi C - k_b \rho S = 0, \quad \text{or} \quad \frac{S}{\phi C} = \left(\frac{\theta}{\rho}\right) \frac{k_f}{k_b} = \omega \tag{20}$$

Upon further rearrangement, the second-order formulation, at equilibrium, obeys the widely recognized Langmuir isotherm equation

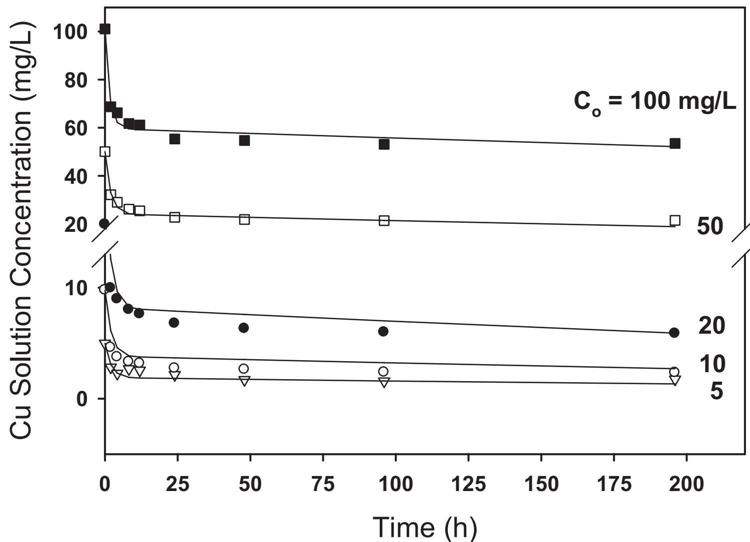


Figure 5.4 Experimental results of Cu in soil solution for McLaren soil versus time for several initial Cu concentrations (C_o's). The solid curves are the second-order model.

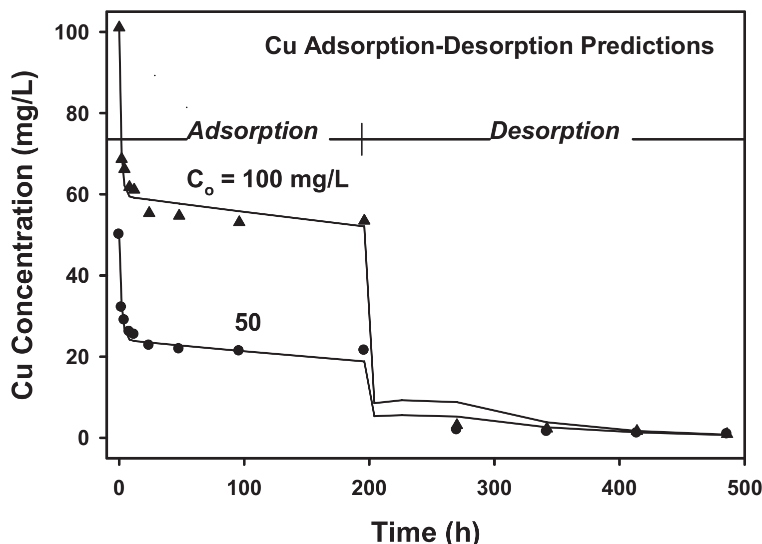
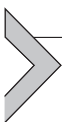


Figure 5.5 Experimental results of Cu in soil solution for McLaren soil versus time during adsorption and desorption for initial concentration $C_o = 50$ and 100 mg L^{-1}. The solid curves are the second-order model.

$$\frac{S}{S_T} = \frac{K_L C}{1 + K_L C} \tag{21}$$

where the parameter K_L is now equivalent to ω of Eqn (20) and represents Langmuir equilibrium constant. Langmuir formulation is often expressed in a similar form to Eqn (21) where the total amount sorbed S_T is replaced by maximum sorbed amount S_{max}.



4. COMPETITIVE RETENTION MODELS

It is generally accepted that competing ions strongly affect heavy-metal retention and release in soils. Industrial waste and sewage sludge disposed on land often contain appreciable amounts of heavy metal such as Cu, Zn, Cd and Ni, and thus create a risk for croplands, as well as animals and humans. Several competitive models of the equilibrium and kinetic type have been developed to describe the reactivities and mobility in a multiple ion systems. An example of metal ion competition is presented in the traditional manner as isotherms and is given in Figs 5.6 and 7 (Liao and Selim, 2009). These isotherms were described using the Freundlich model. The extent of nonlinearity of Ni and Cd isotherms are depicted by the dimensionless parameter *b* and was

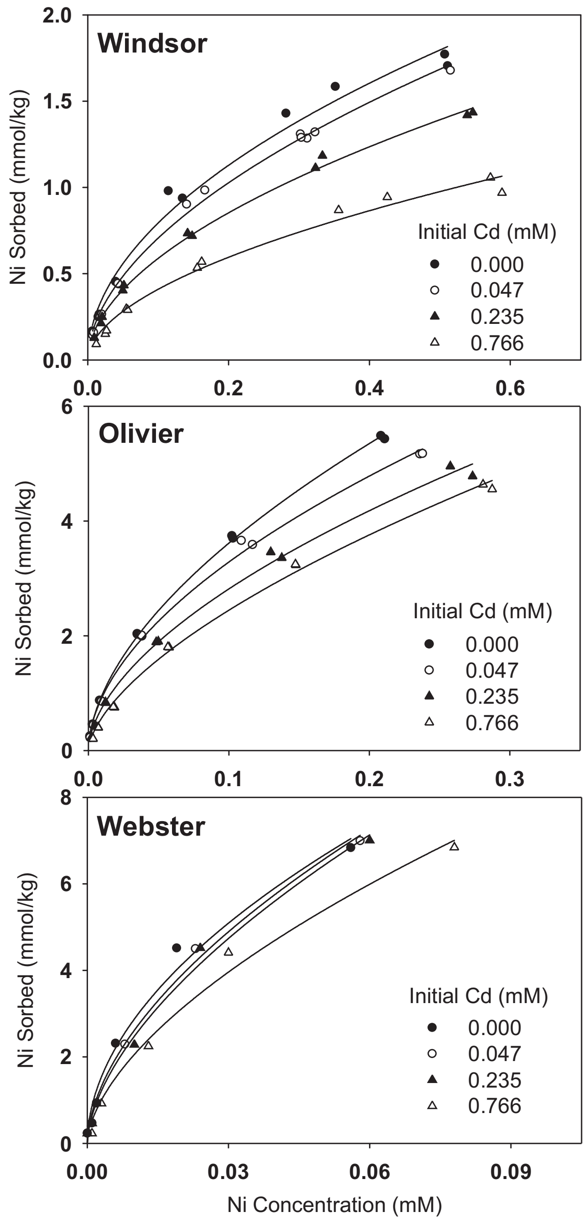


Figure 5.6 Competitive adsorption isotherms for Ni in the presence of different concentrations of Cd. Solid curves are Freundlich model calculations.

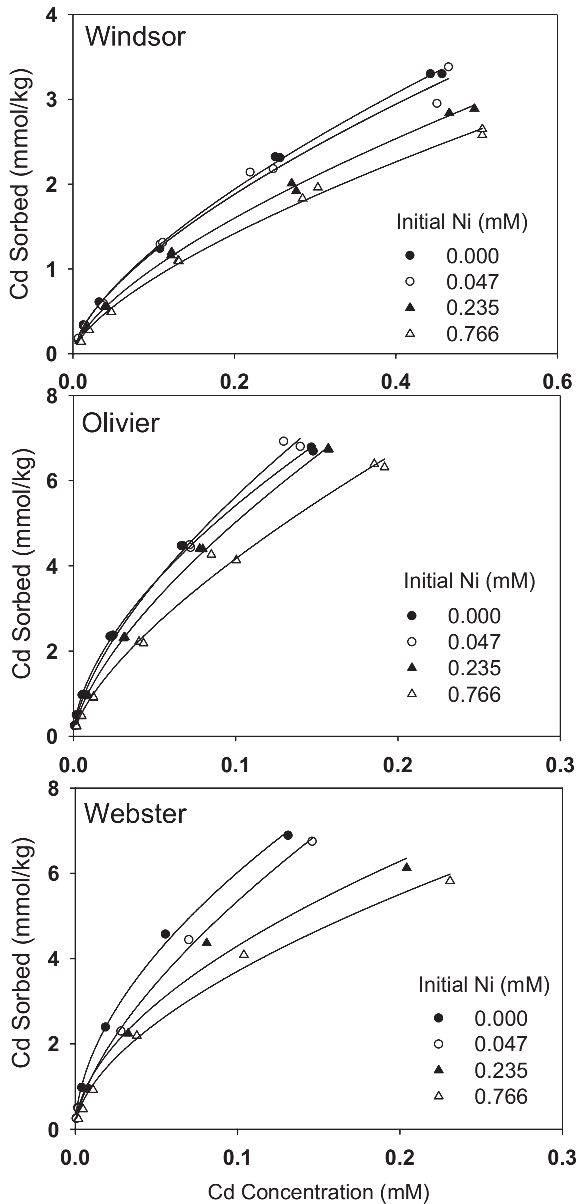


Figure 5.7 Competitive adsorption isotherms for Cd in the presence of different concentrations of Ni. Solid curves are Freundlich model calculations.

not influenced by input concentration of the competing ion. For Windsor and Olivier, Ni adsorption decreased significantly over the entire range of concentrations of the competing ion (Cd). However, Cd adsorption was less affected by the competing Ni ions for both soils. For the neutral Webster soil, Ni was not appreciably affected by the presence of Cd, especially at low Ni concentrations. This may be due to the fact that for a single-component system, Ni adsorption was much stronger than Cd for Webster soil. Another explanation of the competitive Ni sorption behavior is perhaps due to Ni–LDH precipitates which may be considered irreversible form on soils and minerals (Voegelin and Kretzschmar, 2005). This process may lead to significant long-term stabilization of the metal within the soil profile (Ford et al., 1999).

4.1. Sheindorf–Rebhun–Sheintuch Model

The Sheindorf–Rebhun–Sheintuch (SRS) equation has been developed to describe competitive or multicomponent sorption where it is assumed that the single-component sorption follows the Freundlich equation (Sheindorf et al., 1981). The derivation of SRS equation was based on the assumption of an exponential distribution of adsorption energies for each component. Specifically, the SRS model was developed to describe competitive equilibrium sorption for multicomponent systems where the sorption isotherms of single component follow the Freundlich equation. A general form of the SRS equation can be written as

$$S_i = K_i C_i \left(\sum_{j=1}^{l} \alpha_{i,j} C_j \right)^{n_i - 1} \tag{22}$$

where the subscripts i and j denote the metal components i and j, l is the total number of components, and $\alpha_{i,j}$ is the dimensionless competition coefficient for the adsorption of component i in the presence of component j. The parameters K_i and n_i are the Freundlich parameters representing a single-component system i as described in Eqn (1) above. By definition, $\alpha_{i,j}$ equals 1 when $i = j$. If there is no competition, i.e. $\alpha_{i,j} = 0$ for all $j \neq i$, Eqn (2) yields a single-species Freundlich equation for component i identical to Eqn (1). The estimated α_{Ni-Cd} for Ni adsorption, in the presence of Cd, was larger than 1 for Windsor and Olivier soils, indicating noticeable decrease of Ni in the presence of Cd. In contrast, α_{Ni-Cd} for Ni adsorption on Webster soil was <1, which is indicative of small influence of competing Cd ions. These results are in agreement with the competitive sorption reported by Antoniadis and

Tsadilas (2007). Such small α_{Ni-Cd} implies that Ni adsorption in Webster soil was least affected in a competitive Ni–Cd system in comparison to the other two soils. Moreover, the estimated α_{Cd-Ni} for Cd adsorption was 0.61 for Windsor and 0.82 for Olivier, whereas the competitive coefficient of Cd/Ni was 4.00 for Webster Soil. Although the SRS equation may be regarded as a multicomponent model and does not imply certain reaction mechanisms, differences of competitive sorption between the neutral and the two acidic soils were illustrated based on the SRS models' competitive selectivity parameters. In fact, Roy et al. (1986) suggested that the SRS parameters could be used to describe the degree of the competition under specific experimental conditions. Calculated results using the estimated α_{Ni-Cd} are given in Figs 5.8 and 9 and illustrate the capability of the SRS model in describing experimental data for competitive adsorption of Ni and Cd (Liao and Selim, 2009). An *F*-test indicated that there was no statistical difference between our experimental results and SRS model calculations (at the 95% confidence level). Based on these calculations, the SRS model was capable of quantifying competitive adsorption for Ni and Cd. However, for both Ni and Cd, the SRS model deviated considerably from experimental data for high concentrations of the competing ions. This finding is consistent with the application of SRS made earlier by Gutierrez and Fuentes (1993) and illustrates the need for model improvement to better describe competitive adsorption of heavy metals over the entire range of concentrations.

The suitability of the multicomponent SRS equation for describing the competitive adsorption isotherms of trace elements on soil and soil minerals have been investigated by several researchers. A general procedure of applying the SRS equation is first to obtain the Freundlich distribution coefficient K_F and reaction exponent b or n by fitting the single-component isotherms to Freundlich equation, followed by estimating the competition coefficients $\alpha_{i,j}$ through fitting the experimental isotherms of binary and ternary mixtures to the SRS equation (Roy et al., 1986). Although the SRS equation does not imply specific reaction mechanisms, the competition coefficients $\alpha_{i,j}$ in the equation can be used to evaluate the relative selectivity of the sorbent to the heavy metal species. It is demonstrated that SRS equation with competition coefficients estimated through nonlinear least-squares optimization successfully described the experimental competitive adsorption isotherms of Ni and Cd on three different soils (Liao and Selim, 2009). Gutierrez and Fuentes (1993) employed the SRS equation to represent the competitive adsorption of Sr, Cs and Co in Ca-montmorillonite suspensions. They found that the SRS competition coefficients $\alpha_{i,j}$ obtained from experiment

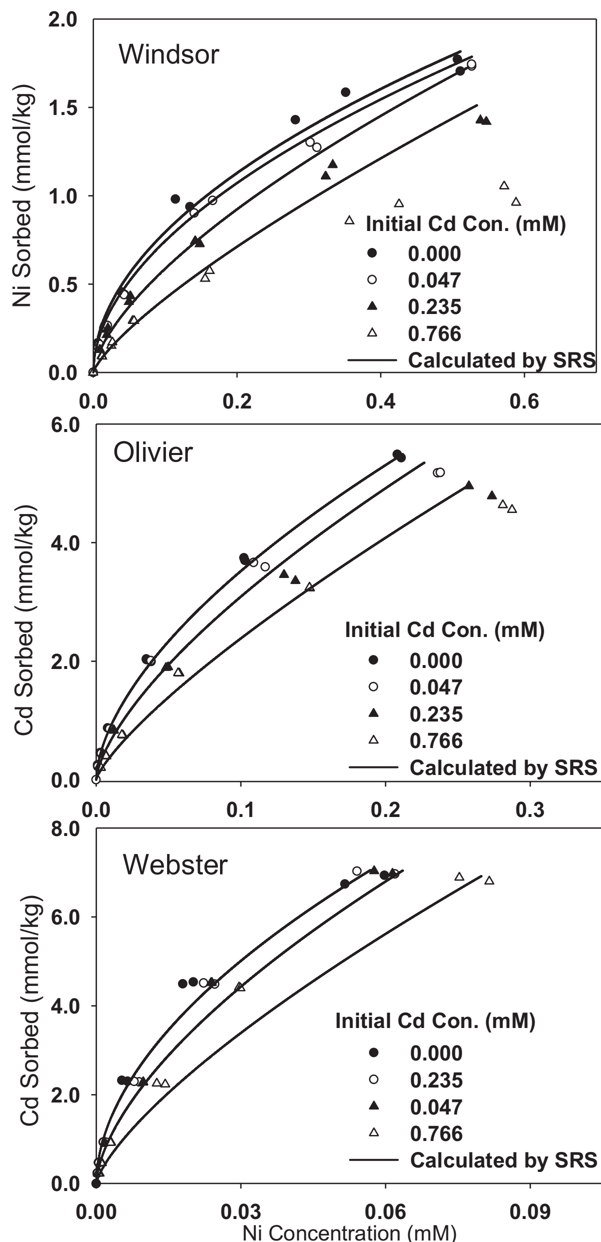


Figure 5.8 Competitive adsorption isotherms for Ni in the presence of different concentrations of Cd. Solid curves are SRS model calculations.

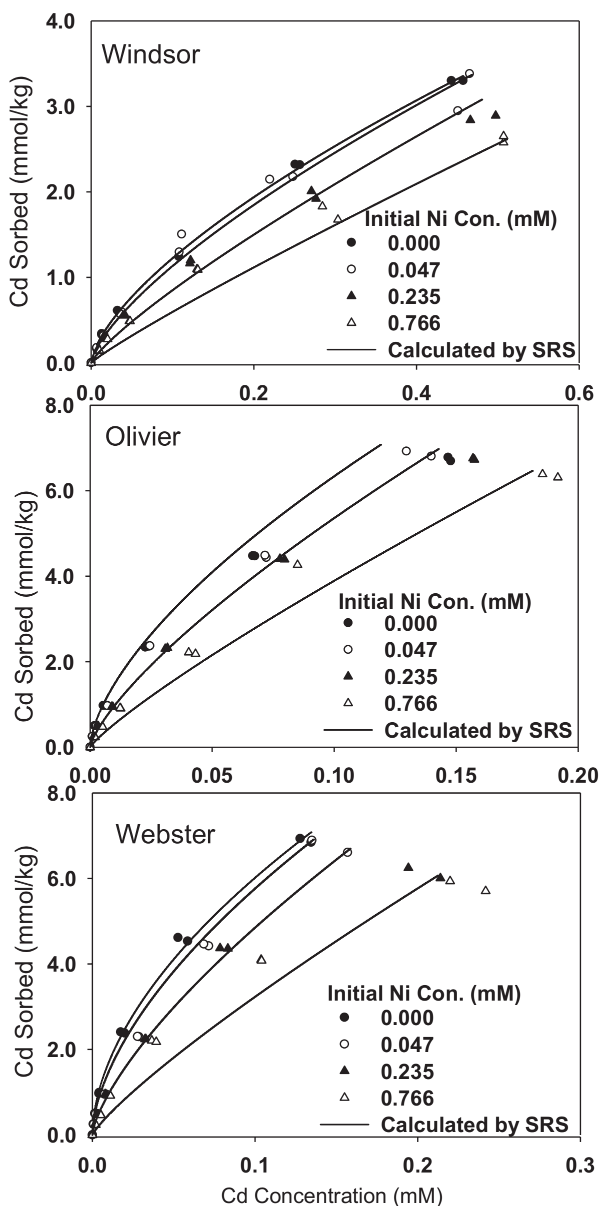


Figure 5.9 Competitive adsorption isotherms for Cd in the presence of different concentrations of Ni. Solid curves are SRS model calculations.

data of binary mixtures successfully predicted the competitive adsorption of ternary mixture Sr–Cs–Co. Similarly, Bibak (1997) found that values of SRS competitive coefficients obtained from binary sorption experiments successfully predicted sorption data of the ternary solute mixture Cu–Ni–Zn. The SRS equation was successfully used to describe for competitive sorption of Cd, Ni, and Zn on a clay soil by Antoniadis and Tsadilas (2007). In addition, SRS equation was also used by Wu et al. (2002) in representing the competitive adsorption of molybdate, sulfate, selenate, and selenite on γ-Al_2O_3 surface where relative affinity coefficient was used instead of competitive coefficients. The relative affinity coefficients were calculated as the ratios of the proton coefficients of competing anions. The simulation result showed that the sorption affinity of anions on γ-Al_2O_3 surface decreased in the order of $MoO_4^{2-} > SeO_3^{2-} > SeO_4^{2-} > SO_4^{2-}$.

4.2. Competitive Multireaction Model

The kinetic (time-dependent) sorption models of the Freundlich type given were developed to simulate the sorption of solutes during their transport in soils and aquifers (Selim, 1992). Zhang and Selim (2007) extended the equilibrium Freundlich approach to account for kinetic competitive or multiple-component systems. Specifically, the model accounts for equilibrium and kinetic adsorption in a way similar to the SRS equation described above. This model represents a modification of the multireaction model which accounts for equilibrium and kinetic retention of the reversible and irreversible types (see Fig. 5.10). MRM accounts for linear as well as nonlinear reaction processes of equilibrium and/or kinetic (reversible and irreversible) type. The model with reversible as well as irreversible sorption of the concurrent and consecutive type is shown in Fig. 5.10. Here S_e represents the amount retained on equilibrium sites (mg kg^{-1}); S_k represent the

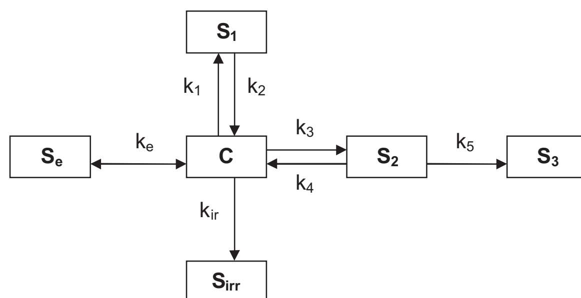


Figure 5.10 Schematics of the multireaction model (MRM).

amount retained on reversible kinetic sites (mg kg^{-1}); S_{irr} represents the amount retained on consecutive irreversible sites (mg kg^{-1}); and S_3 represents the amount retained on concurrent irreversible sites (mg kg^{-1}).

The retention reactions associated with the MRM are expressed as

$$S_e = K_e \left(\frac{\theta}{\rho}\right) C^b \tag{23}$$

$$\frac{\partial S_1}{\partial t} = k_1 \left(\frac{\theta}{\rho}\right) C^n - k_2 S_1 \tag{24}$$

$$\frac{\partial S_2}{\partial t} = \left[k_3 \left(\frac{\theta}{\rho}\right) C^m - k_4 S_2\right] - k_s S_2 \tag{25}$$

$$\frac{\partial S_s}{\partial t} = k_s S_2 \tag{26}$$

$$S_{irr} = k_{irr} \left(\frac{\theta}{\rho}\right) C \tag{27}$$

where t is the reaction time (h); ϱ is the soil bulk density (g cm^{-3}); θ is the water content (cm^3 cm^{-3}); b is the reaction order; C is the concentration in solution (mg L^{-1}). K_e is the dimensionless equilibrium constant (cm^3 g^{-1}); k_1 and k_2 (h^{-1}) are the forward and backward rate coefficients associated with S_1, respectively, and n is the reaction order; k_3 and k_4 (h^{-1}) are the forward and backward rate coefficients associated with S_2, respectively, and m is the reaction order; k_5 (h^{-1}) is the irreversible rate coefficient; and k_{irr} (h^{-1}) is the rate coefficient associated with S_{irr}. In the above equations, we assumed $n = m$ since there is no method for estimating n and/or m independently. Zhang and Selim (2007) modified MRM to account for competitive Freundlich-type retention such that,

$$(S_e)_i = K_{e,i} C_i \left(\sum_{j=1}^{l} \alpha_{i,j} C_j\right)^{n_i - 1} \tag{28}$$

$$\frac{\partial (S_1)_i}{\partial t} = k_{1,i} \frac{\theta}{\rho} C_i \left(\sum_{j=1}^{l} \alpha_{i,j} C_j\right)^{n_i - 1} - k_{2,i} (S_1)_i \tag{29}$$

$$\frac{\partial (S_2)_i}{\partial t} = k_{3,i}\frac{\theta}{\rho}C_i\left(\sum_{j=1}^{l}\alpha_{i,j}C_j\right)^{n_i-1} - (k_{4,i}+k_{s,i})(S_2)_i \tag{30}$$

$$\frac{\partial (S_s)_i}{\partial t} = k_{s,i}(S_s)_i \tag{31}$$

$$\frac{\partial (S_{\text{irr}})_i}{\partial t} = k_{\text{irr},i}\frac{\theta}{\rho}C_i \tag{32}$$

When competition is ignored, i.e. $\alpha_{i,j}$ for all $j \neq i$, Eqn. (29) yields a single species n-th-order kinetic sorption. Examples of the capability of this approach to describe the transport of the competitive arsenate and phosphate behavior in soil columns are given in Figs 5.11 and 12 (Zhang and Selim, 2007). Here As(V) and P BTCs exhibited extensive asymmetry where non-equilibrium conditions appear dominant as indicated by the drop in As(V) and P concentrations in response to flow interruption (or stop flow). These simulations demonstrate that competitive retention for arsenate and phosphate over time was successfully predicted using this kinetic approach where model coefficients were based on single-component kinetic batch results.

4.3. Competitive Langmuir Model

The Langmuir equation can be extended to account for competitive sorption of multiple heavy metals in multicomponent systems. In the multicomponent Langmuir approach, one assumes that there is only one set of sorption sites for all competing ions. Furthermore, the model also assumes that the presence of competing ions does not affect the sorption affinity of other ions. Because of these overly simplified assumptions, the modeling ability of the model is rather limited. It should be noted that with the assumption of fixed amount of reaction sites, the surface-complexation model described in this chapter gives Langmuir type of adsorption isotherms under constant pH and ionic strength. The time-dependent sorption of competing ions, the multicomponent second-order kinetic equation was proposed in the form of

$$\frac{\partial S_i}{\partial t} = (\lambda_{\text{f}})_i\frac{\theta}{\rho}C_i\left(S_{\max} - \sum_{i=1}^{l}S_j\right) - (\lambda_{\text{b}})_i S_i \tag{33}$$

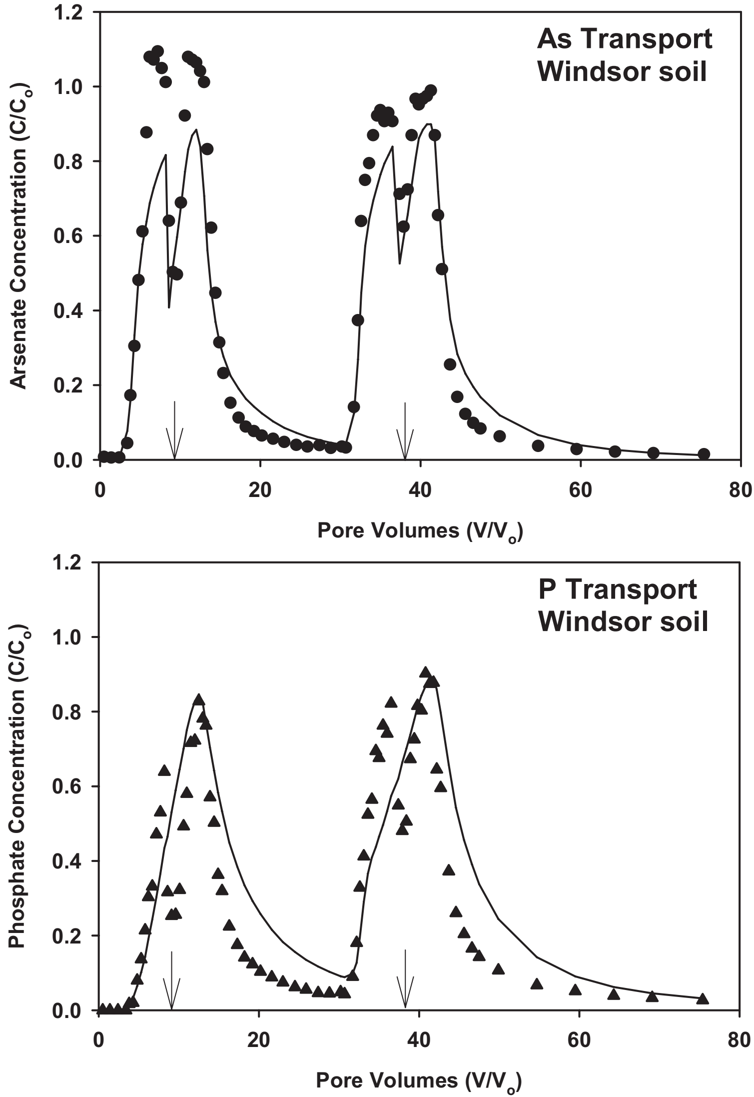


Figure 5.11 Experimental As(V) and P breakthrough curves (BTCs) in Windsor soil. Solid curves are simulations using the competitive multireaction model (CMRM). Arrows indicate when stop flow occurred.

Under equilibrium condition, Eqn (32) yields

$$(K_L)_i = (\lambda_f)_i \frac{(\lambda_f)_i \theta}{(\lambda_b)_i \rho} \tag{34}$$

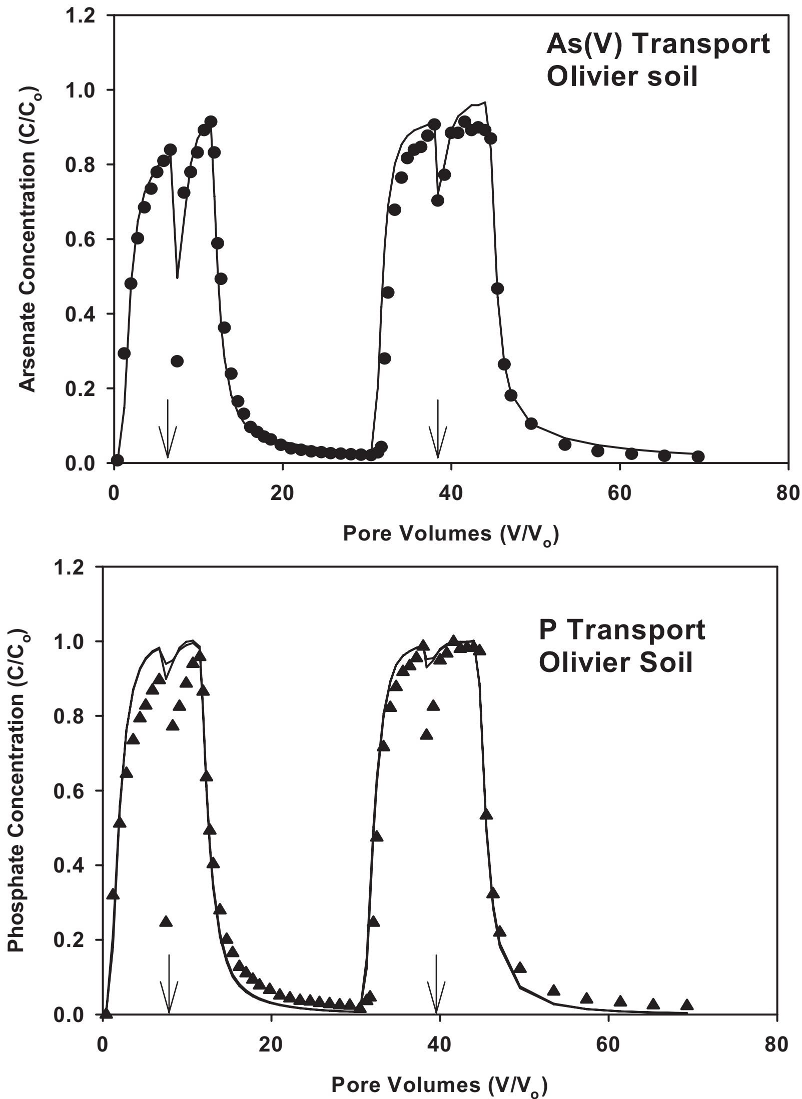


Figure 5.12 Experimental As(V) and P breakthrough curves (BTCs) in Olivier soil. Solid curves are simulations using the CMRM. Arrows indicate when stop flow occurred.

Moreover, for the case where one assumes negligible competition among the various ions, Eqn (32), upon omitting the subscript *i*, is reduced to the second-order formulation discussed earlier.

4.4. Ion-Exchange Models

Ion exchange is considered an instantaneous process representing (nonspecific) sorption mechanisms and as a fully reversible reaction between heavy

metal ions in the soil solution and those retained on charged surfaces of the soil matrix. In a standard mass action formulation, the exchange reaction for two competing ions i and j, having valencies v_i and v_j, respectively, may be written as

$$^{T}K_{ij} = \frac{\left(a_i^*\right)^{\nu j}}{\left(a_j^*\right)^{\nu i}} \tag{35}$$

where $^{T}K_{ij}$ denotes the thermodynamic equilibrium constant and a and $a^\star$ (omitting the subscripts) are the ion activity in soil solution and on the exchanger surfaces, respectively. Based on Eqn (33), one can denote the parameter $^{v}K_{ij}$ as

$$^{v}K_{ij} = \frac{^{T}K_{ij}}{\left(\frac{\left(\zeta_j\right)^{\nu j}}{\left(\zeta_j\right)^{\nu i}}\right)} \tag{36}$$

where $^{v}K_{ij}$ is the Vanselow selectivity coefficient and ζ is the activity coefficient on the soil surface. It is recognized that in soils, ion exchange involves a wide range of thermodynamically different sites. As a result, a common practice is to ignore the activity coefficients of the adsorbed phase (ζ) in general. In addition, the much simpler Gaines and Thomas (1953) selectivity coefficient $^{G}K_{ij}$ may be used, where

$$^{G}K_{ij} = \frac{\left(\gamma_j\right)^{\nu i}}{\left(\gamma_i\right)^{\nu j}}\left(\frac{s_i}{C_i}\right)^{\nu j}\left(\frac{s_j}{C_j}\right)^{\nu i} \tag{37}$$

This formulation is more conveniently incorporated into the dispersion–convection transport (Eqn (7)). In Eqn (36), γ_i and γ_j are the dimensionless solution-phase activity coefficients where $a_i = \gamma_i C_i$. In addition, the terms s_i and s_j are dimensionless, representing the solid-phase concentrations expressed in terms of equivalent fraction, $s_i = S_i/\Omega$. Here the term Ω is the cation exchange (or adsorption) capacity of the soil (mmol$_c$ kg^{-1} soil) and S_j is the concentration of adsorbed-phase (mmol$_c$ kg^{-1} soil). Although Ω is often assumed as invariant, it is recognized that Ω has been observed to be dependent on soil pH and the counter ions present in the soil. Moreover, there are several other ways to express the adsorbed-phase concentration on a fractional basis including that of a molar rather than an equivalent.

Several studies indicated that the affinity of heavy metals to soil matrix surfaces increase with decreasing heavy metal fraction on exchanger surfaces (Abd-Elfattah and Wada, 1981; Harmsen, 1977; Hinz and Selim, 1994; Selim et al., 1992). Using an empirical selectivity coefficient, it was shown that Zn affinity increased up to two orders of magnitude for low Zn surface coverage in a Ca background solution (Abd-Elfattah and Wada, 1981). Mansell et al. (1988) successfully relaxed the assumption of constant affinities and allowed the selectivity coefficients to vary with the amount adsorbed amount on the exchange surfaces. The Rothmund–Kornfeld incorporates variable selectivity based on the amount of adsorbed or exchanger composition. The approach is empirical and provides a simple equation that incorporated the characteristic shape of binary exchange isotherms as a function of equivalent fraction of the amount sorbed as well as the total solution concentration in solution. Bond and Phillips (1990) and Harmsen (1977) expressed the Rothmund–Kornfeld as

$$\frac{(s_i)^{vj}}{(s_j)^{vi}} = {}^{R}K_{ij}\left[\frac{(c_i)^{vj}}{(c_j)^{vi}}\right]^n \tag{38}$$

where n is the dimensionless empirical parameter associated with the ion pair i–j and ${}^{R}K_{ij}$ is the Rothmund–Kornfeld selectivity coefficient. The above equation is best known as a simple form of the Freundlich equation which applies to ion exchange processes. As pointed out by Harmsen (1977), the Freundlich equation may be considered as an approximation of the Rothmund–Kornfeld equation valid for $s_i << s_j$ and $c_i << c_j$, where

$$s_i = {}^{R}K_{ij}(c_i)^n \tag{39}$$

This equilibrium Rothmund–Kornfeld ion-exchange equation was used by Hinz and Selim (1994) to describe the exchange isotherm of Zn–Ca and Cd–Ca as well as the breakthrough curve of Zn and Cd in uniformly packed columns of Windsor and Olivier soils. They concluded that the Rothmund–Kornfeld ion-exchange equation well described binary ion exchange isotherms but overestimated the extent of retardation during Zn and Cd transport in soils. Examples of experimental and simulated ion isotherms and breakthrough curves are illustrated in Figs 5.13 and 5.14.

Numerous studies indicated that ion exchange is a kinetic process in which equilibrium was not instantaneously reached. Observed kinetic or time-dependent ion-exchange behavior is most likely a result of the transport of initially sorbed ions from exchange sites to the bulk solution

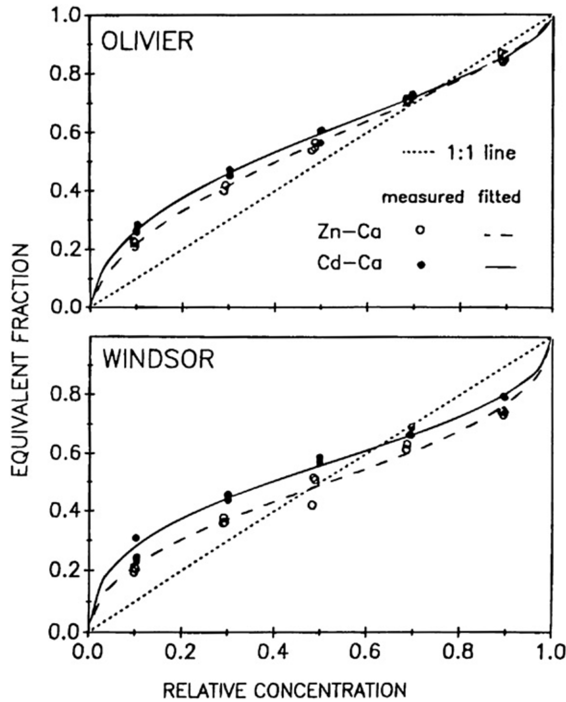


Figure 5.13 Ion exchange isotherms of Cd–Ca and Zn–Ca for Olivier and Windsor soils (relative concentration, C/C) versus the sorbed fraction (s). Solid and dashed curves are fitted using the Rothmund–Kornfeld model.

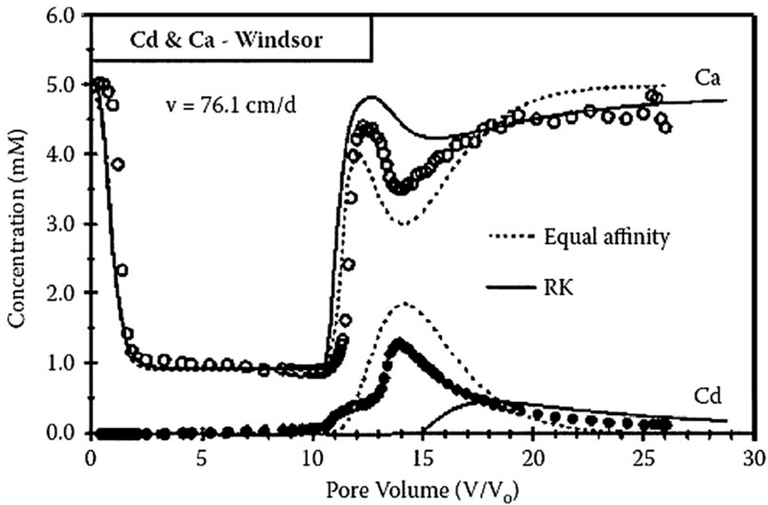


Figure 5.14 Cadmium (Cd) and calcium (Ca) breakthrough curves in Windsor soil at variable ionic strengths. Predictions were based on equal affinity (K_{ij} = 1) and the Rothmund–Kornfeld (RK) equation.

and the reverse process of the transport of replacing ion from bulk solution to exchange sites. Specifically, the rate of ion exchange is dependent on the following processes: (i) diffusion of ions in the aqueous solution; (ii) film diffusion at the solid/liquid interface; (iii) intraparticle diffusion in micropores and along pore wall surfaces; and (iv) interparticle diffusion inside solid particles (Sparks, 1989). Due to the complexity of the kinetic processes, over past three decades, several kinetic rate formulations have been proposed. Such formulations have been applied to describe sorption–desorption kinetic results for heavy metal ions. The pseudo first-order or mass action model is perhaps the most commonly used approach where one assumes the kinetic rate is function of the concentration gradient on the exchange surfaces. For the exchangeable amount S (omitting the subscript i), the rate equation can be expressed as (Selim et al., 1992);

$$\frac{\partial S}{\partial t} = \alpha \left(S_{eq} - S \right) \tag{40}$$

where α is an apparent rate coefficient (d^{-1}) for the kinetic-type sites. For large values of α, S approaches S_{eq} in a relatively short time and equilibrium is rapidly achieved. In contrast, for small α, kinetic behavior should be dominant for extended period of time. Expressions similar to the above model have been used to describe mass transfer between mobile and immobile water in porous media (Coats and Smith, 1964) as well as chemical kinetics (Parker and Jardine, 1986). To simulate the transport of Cd in different soils, Selim et al. (1992) developed a multicomponent transport model which incorporates the kinetics of ion exchange and specific sorption in the advection–dispersion equation. Based on the assumption of mass transfer or diffusion as rate-limiting step, a first-order mass-transfer equation with an apparent rate coefficient was incorporated into the transport equation. The simulation results in Fig. 5.15 demonstrate that the model with kinetic ion exchange adequately predicted Cd breakthrough curves for Eustis soil. The simulations shown also demonstrate the effect of the value of the apparent rate coefficient α on Cd predictions.

Other kinetic expressions have also been employed to describe the kinetic exchange of ions in mineral and soils. The parabolic diffusion model is based on the assumption of diffusion controlled rate-limited process in media with homogeneous particle size. The parabolic diffusion equation was derived from the Fick's second law of diffusion in radial coordinate system.

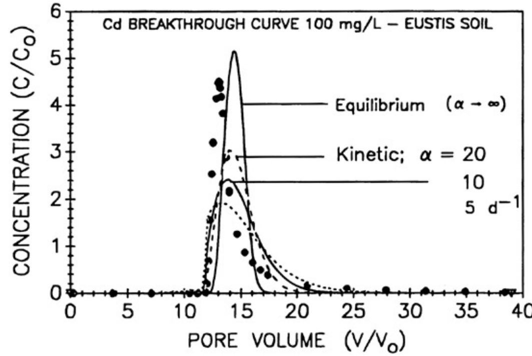


Figure 5.15 Measured (closed circles) and predicted breakthrough curves (BTCs) for Cd in Eustis soil. Curves are predictions using an equilibrium model and a kinetic ion-exchange model with different rate coefficients α.

$$\frac{S_i}{\left(S_{eq}\right)_i} = \frac{4}{\sqrt{\pi}}\sqrt{\frac{D_m t}{r^2}\frac{D_m t}{r^2}} \tag{41}$$

where r is the average radius of soil or mineral particle, and D_{m} is the molecular diffusion constant. The Elovich model is anther empirical kinetic retention model which may be expressed as D_{m} is molecular diffusion coefficient. The Elovich model is anther empirical kinetic retention model which may be expressed as

$$\frac{\partial S_i}{\partial t} = a\ e^{-BS_i} \tag{42}$$

where a is the initial adsorption rate and B is the empirical constant. Jardine and Sparks (1984) have compared the first-order, parabolic diffusion, and Elovich approaches described above to describe the kinetic exchange of K–Ca in clay minerals and soils. They found that the pseudo first-order model provided the best overall goodness-of-fit of the experimental results. Recently, a fractional power approach was introduced by Serrano et al. (2005) having of the form

$$S = \kappa t^{\beta} \tag{43}$$

where κ and β are the empirical constants. They compared the overall sorption kinetics of Pb and Cd for single and binary systems. Their results showed that the simultaneous presence of the competing metal did not affect the estimated apparent sorption rate, which indicated that the rate-limiting process of the sorption of heavy metal ions were not impacted by the competing ions.

4.5. Surface-Complexation Models

Surface-complexation models have been used to describe an array of equilibrium-type chemical reactions including proton dissociation, metal cation and anion adsorption reactions on oxides, and clays, organic ligands adsorption and competitive adsorption reactions on oxide and oxide-like surfaces. Application and theoretical aspects of surface-complexation models are extensively reviewed by Goldberg (1992) and Sparks (2003). Surface-complexation models are chemical models based on molecular description of the electric double layer using equilibrium-derived adsorption data.

Surface complexes can exist as inner-sphere surface complexes or outer-sphere surface complexes. Inner-sphere surface complexes are strong complexes involving either ionic or covalent bonding without water molecules between the adsorbing ion and the surface functional group. Outer-sphere surface complexes are less-stable complexes involving electrostatic bonding with at least one water molecule between the adsorbing ion and the surface functional group. A list of the mass action equations complexation and the associated with equilibrium reaction coefficients are given by Goldberg (1992) and Zhang and Selim (2012).

Surface-complexation models, in combination with ion exchange models, have been used with various degrees of success to describe competitive sorption and transport of heavy metals in soils (Bradbury and Baeyens, 2005; Serrano et al., 2009; Voegelin et al., 2001). For example, Serrano et al. (2009) demonstrated the capability of surface complexation modeling in describing competitive sorption of Pb and Cd over a range of pH and metal concentrations for three acid soils. Voegelin et al. (2001) incorporated the CDE (Eqn (6)) into surface-complexation modeling in order to predict competitive sorption of Cd, Zn and Ni during transport in soils. Based on Voegelin et al. (2001), their study indicates that heavy metal adsorption in acidic soils was perhaps reversible where time-dependent reactivities were negligible. An example of their experimental and model calculations for Ca, Zn and Ca breakthrough curves are illustrated in Fig. 5.16.

A major drawback of surface-complexation models is that they are limited to describing equilibrium type reactions and do not account for kinetic sorption–desorption processes in soils. In the heterogeneous soils with a variety of sorbents having different reactivities, time-dependent sorption is often observed. Kinetics or nonequilibrium sorption may

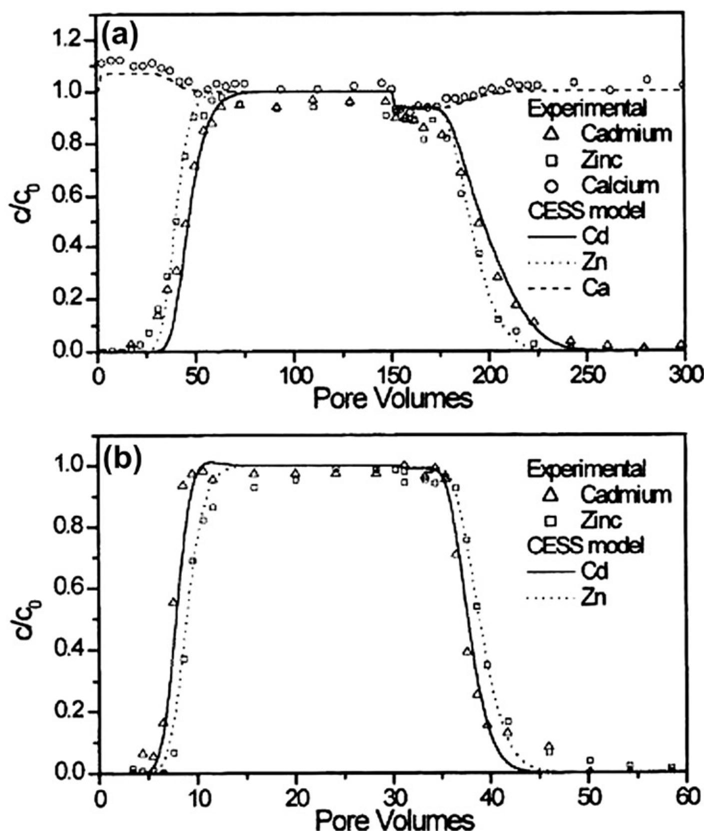
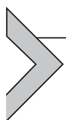


Figure 5.16 Breakthrough curves of Cd and Zn applied pulse in a $CaCl_2$ background electrolyte solution of 10^{-3} M (a) and 10^{-2} M (b). Curves model calculations. *(Reproduced with permission from Voegelin et al. (2001)).*

arise due to the heterogeneity of sorption sites of matrix surfaces. In fact, various types of surface complexes (e.g. inner-sphere, outer-sphere, monodentate, bidentate, mononuclear, binuclear) with contrasting sorption affinities can be formed on mineral surfaces at various surface coverage of metals and metalloids. This heterogeneity of sorption sites may contribute to observed adsorption kinetics where sorption takes place preferentially on high-affinity sites and followed subsequently by slow sorption on sites of low-sorption affinity. Furthermore, diffusion of ions to reaction sites within the soil matrix was proposed as an explanation to the time-dependent adsorption by many researchers (e.g. Fuller et al., 1993; Raven et al., 1998).



5. SUMMARY

In this contribution, the framework covering the basics of heavy metals transport in soils is presented. The processes that govern their retention in soils are discussed in the order of their complexity. Commonly used single retention models of the equilibrium type are discussed along with various kinetic-type approaches. Retention models of the multiple reaction type including the two-site equilibrium-kinetic models, the concurrent- and consecutive multireaction models, and the second-order approach have been subsequently presented. Several examples are presented for the purpose of illustrating the impact of competing ions on the reactivities and mobility of heavy metals in the soil–water environment. Examples presented here demonstrate the influence of ligands competition for adsorption sites on mineral surfaces. Furthermore, we demonstrated that the equilibrium Freundlich and Langmuir approaches can be extended to account for competitive retention when multiple heavy metals are present in the soil–water system. Such models may be further modified to describe the frequently observed time-dependent behavior of heavy metals in soils. A major drawback of the Freundlich and Langmuir approaches is that these models are empirically based and their associated parameters are specific for each soil. Geochemical models based on ion exchange and surface complexation are subsequently discussed. Although such models require a large number of input parameters, they have been shown to be capable of quantifying the competitive behavior of several chemical species and under a wide range of chemical conditions. Geochemical models are not capable of describing time-dependent sorption in competitive systems, however. Therefore, further research is needed to characterize physical and chemical mechanisms of kinetic sorption involved in soils.

REFERENCES

Abd-Elfattah, A., Wada, K., 1981. Adsorption of lead, copper, zinc, cobalt, and calcium by soils that differ in cation-exchange materials. J. Soil Sci. 32, 271–283.

Antoniadis, V., Tsadilas, C.D., 2007. Sorption of cadmium, nickel, and zinc in mono- and multi-metal systems. Appl. Geochem. 22, 2375–2380.

Bibak, A., 1997. Competitive sorption of copper, nickel, and zinc by an oxisol. Commun. Soil Sci. Plant Anal. 28, 927–937.

Bond, W.J., Phillips, I.R., 1990. Approximate solution for cation transport during unsteady, unsaturated soil water flow. Water Resour. Res. 26, 2195–2205.

Bradbury, M.H., Baeyens, B., 2005. Experimental measurements and modeling of sorption competition on montmorillonite. Geochim. Cosmochim. Acta 69, 4187–4197.

Brenner, H., 1962. The diffusion model of longitudinal mixing in beds of finite length: Numerical values. Chem. Eng. Sci. 17, 220–243.

Buchter, B., Davidoff, B., Amacher, M.C., Hinz, C., Iskandar, I.K., Selim, H.M., 1989. Correlation of Freundlich K_d and n retention parameters with soils and elements. Soil Sci. 148, 370–379.
Coats, K.H., Smith, B.D., 1964. Dead-end pore volume and dispersion in porous media. Soc. Pet. Eng. 4, 73–84.
Ford, R.G., Scheinost, A.C., Scheckel, K.G., Sparks, D., 1999. The link between clay mineral weathering and the stabilization of Ni surface precipitates. Environ. Sci. Technol. 33, 3140–3144.
Fuller, C.C., Davis, J.A., Waychunas, G.A., 1993. Surface chemistry of ferrihydrite: part 2. Kinetics of arsenate adsorption and coprecipitation. Geochim. Cosmochim. Acta 57, 2271–2282.
Gaines, G.L., Thomas, H.C., 1953. Adsorption studies on clay minerals. II. A formulation of the thermodynamics of exchange adsorption. J. Chem. Phys. 21, 714–718.
Goldberg, S., 1992. Use of surface complexation models in soil chemical systems. Adv. Agron. 47, 233–329.
Gutierrez, M., Fuentes, H.R., 1993. Modeling adsorption in multicomponent systems using a Freundlich-type isotherm. J. Contam. Hydrol. 14, 247–260.
Harmsen, K., 1977. Behavior of Heavy Metals in Soils. Centre for Agriculture Publishing and Documentation, Wageningen, The Netherlands.
Hinz, C., Selim, H.M., 1994. Transport of zinc and cadmium in soils—experimental-evidence and modeling approaches. Soil Sci. Soc. Am. J. 58, 1316–1327.
Jardine, P.M., Sparks, D.L., 1984. Potassium-calcium exchange in a multireactive soil system. I. Kinetics. Soil Sci. Soc. Am. J. 48, 39–45.
Lapidus, L., Amundson, N.L., 1952. Mathematics for adsorption in beds. VI. The effect of longitudinal diffusion in ion exchange and chromatographic column. J. Phys. Chem. 56, 984–988.
Liao, L., Selim, H.M., 2009. Competitive sorption of nickel and cadmium in different soils. Soil Sci. 174, 549–555.
Liao, Lixia, Selim, H.M., 2010. Reactivity of nickel in soils: evidence of retention kinetics. J. Environ. Qual. 39, 1290–1297.
Mansell, R.S., Bloom, S.A., Selim, H.M., Rhue, R.D., 1988. Simulated transport of multiple cations in soil using variable selectivity coefficients. Soil Sci. Soc. Am. J. 52, 1533–1540.
Parker, J.C., Jardine, P.M., 1986. Effect of heterogeneous adsorption behavior on ion transport. Water Resour. Res. 22, 1334–1340.
Raven, K.P., Jain, A., Loeppert, R.H., 1998. Arsenite and arsenate adsorption on ferrihydrite: kinetics, equilibrium, and adsorption envelopes. Environ. Sci. Technol. 32, 344–349.
Roy, W.R., Hassett, J.J., Griffin, R.A., 1986. Competitive coefficient for the adsorption of arsenate, molybdate, and phosphate mixture by soils. Soil Sci. Soc. Am. J. 50, 1176–1182.
Selim, H.M., 1992. Modeling the transport and retention of inorganics in soils. Adv. Agron. 47, 331–384.
Selim, H.M., Amacher, M.C., 1997. Reactivity and Transport of Heavy Metals in Soils. CRC, Boca Raton, FL 240 pp.
Selim, H.M., Buchter, B., Hinz, C., Ma, L., 1992. Modeling the transport and retention of cadmium in soils: multireaction and multicomponent approaches. Soil Sci. Soc. Am. J. 56, 1004–1015.
Selim, H.M., Ma, L., 2001. Modeling nonlinear kinetic behavior of copper adsorption–desorption in soil. Soil Sci. Soc. Am. Spec. Publ. 56, 189–212.
Serrano, S., Garrido, F., Campbell, C.G., Garcia-Gonzalez, M.T., 2005. Competitive sorption of cadmium and lead in acid soils of Central Spain. Geoderma 124, 91–104.

Serrano, S., O'Day, P.A., Vlassopoulos, D., Teresa Garcia-Gonzalez, M., Garrido, F., 2009. A surface complexation and ion exchange model of Pb and Cd competitive sorption on natural soils. Geochim. Cosmochim. Acta 73, 543–558.
Sheindorf, C., Rebhun, M., Sheintuch, M., 1981. A Freundlich-type multicomponent isotherm. J. Colloid Interface Sci. 79, 136–142.
Sparks, D.L., 2003. Environmental Soil Chemistry, second ed.. Academic Press, San Diego, CA.
Sparks, D.L., 1989. Kinetics of Soil Chemical Processes. Academic Press, San Diego, CA.
Voegelin, A., Kretzschmar, R., 2005. Formation and dissolution of single and mixed Zn and Ni precipitates in soil: evidence from column experiments and extended X-ray absorption fine structure spectroscopy. Environ. Sci. Technol. 39, 5311–5318.
Voegelin, A., Vulava, V.M., Kretzschmar, R., 2001. Reaction-based model describing competitive sorption and transport of Cd, Zn, and Ni in an acidic soil. Environ. Sci. Technol. 35, 1651–1657.
Wu, C.-H., Kuo, C.-Y., Lin, C.-F., Lo, S.-L., 2002. Modeling competitive adsorption of molybdate, sulfate, selenate, and selenite using a Freundlich-type multi-component isotherm. Chemosphere 47, 283–292.
Zhang, H., Selim, H.M., 2005. Kinetics of arsenate adsorption–desorption in soils. Environ. Sci. Technol. 39, 6101–6108.
Zhang, H., Selim, H.M., 2007. Modeling competitive arsenate–phosphate retention and transport in soils: a multi-component multi-reaction approach. Soil Sci. Soc. Am. J. 71, 1267–1277.
Zhang, H., Selim, H.M., 2012. Equilibrium and kinetic modeling of competitive heavy metal sorption and transport in soils. In: Selim, H.M. (Ed.), Competitive Sorption and Transport of Trace Elements in Soils and Geological Media, CRC/Taylor ad Francis, Boca Raton, FL, pp. 42–74.



CHAPTER SIX

Clean Coal Technology Combustion Products: Properties, Agricultural and Environmental Applications, and Risk Management

Balaji Seshadri[*,†,#], **Nanthi S. Bolan**[*,†], **Ravi Naidu**[*,†], **Hailong Wang**[‡], **Kenneth Sajwan**[§]

[*]Centre for Environmental Risk Assessment and Remediation (CERAR), University of South Australia, South Australia, Australia
[†]Cooperative Research Centre for Contaminants Assessment and Remediation of the Environment (CRC CARE), University of South Australia, South Australia, Australia
[‡]School of Environmental and Resource Sciences, Zhejiang A & F University, Hangzhou, Zhejiang, China
[§]Department of Natural Science, Savannah State University, Savannah, GA, USA
[#]Corresponding author: Balaji.Seshadri@unisa.edu.au

Contents

Advances in Agronomy, Volume 119
ISSN 0065-2113, http://dx.doi.org/10.1016/B978-0-12-407247-3.00006-8

Abstract

Coal combustion products (CCPs), as the name suggests, are residues derived from the burning of coal in power generation industries. Traditionally, they have been dumped in large piles and/or ash-ponds mostly around the power stations. The CCPs are generally ash materials, mostly made of fine particles but some are also generated as coarse particles. Generation of these products poses serious threats to air, water and soil, and consequently to living organisms. The extent of the environmental effects caused by CCPs depends on (1) the coal source, (2) the combustion technology used and (3) the collection and segregation of the residues. Over the past two decades, there have been progressive research on the quality of power generation in terms of economic viability and environmental safety, and the effective usage of the waste products generated as a result of the power generation. This resulted in the emergence of clean coal technologies (CCTs), which aim at minimal environmental impacts, especially in curbing air pollution and ensuring more beneficial residues compared to conventional methods of combustion. In the global perspective, CCTs also reduce emission of several pollutants, decrease waste generation and increase the amount of energy gained per unit amount of coal combustion. This chapter will focus on the recent developments in CCTs and the applications of CCPs arising from those technologies, particularly agricultural and environmental applications. This chapter outlines the coal economy, their importance in power generation, latest technologies in the coal-fired power stations addressing emission control, the properties of CCPs generated, applications of CCPs and threats posed by the products. Each section will start with the products of conventional combustion technology (e.g. fly ash) and will later cover the applications pertaining to the products from CCTs (e.g. fluidized bed combustion ash). Future research should aim to focus more on the biological implications of CCPs addition to soil, long-term trials and a repository on ash information.

"The scientific utilization, by liquefaction, pulverization and other processes, of our vast and magnificent deposits of coal, constitutes a national object of prime importance."

Sir Winston Leonard Spencer Churchill, 1928

1. INTRODUCTION

1.1. Coal as an Energy Source

Coal is the altered remains of prehistoric vegetation that originally accumulated in swamps and peat bogs, which is composed mainly of carbon (50–98%), hydrogen (3–13%) and oxygen, and smaller amounts of nitrogen (N), sulfur (S), and traces of other elements including phosphorus (Geoscience Australia (GA), 2010; World Coal Association (WCA), 2005). Coal also contains moisture and when coal is burnt, residual ash materials made of inorganic matter are formed. In addition, up to one-tenth of coal's mass has no fuel value, which apparently ends up as ash. Based on the quality of coal

as determined by coal's physical and chemical properties, it can be classified as low-rank (lignite and sub-bituminous coals) and high-rank coals (bituminous, anthracite and graphite). Low-rank coals are typically softer, friable materials with a dull and earthy appearance in comparison with harder and stronger high-rank coals with black translucent appearance (WCA, 2005). Besides, Ramage (1997) categorized the volatile matter, moisture, carbon (C) and ash contents in the various ranks of coals (Fig. 6.1). The carbon content is known for the coal's fuel value and the high-rank coals consisted of high carbon contents ranging from 77 to 96% per dry mass of coal (WCA, 2005).

Irrespective of the C content present in various types of coals, their importance as the chief energy source for electricity production is inevitable in most of the developed and developing countries. This is due to their abundance and economic availability. Coal is present in all the continents and recoverable reserves of coal can be found in around 70 countries, which at current production levels are estimated to last for 119 years (WCA, 2010). China is the largest coal producer, followed by United States and India (Fig. 6.2). Coal remains the backbone of economy in many successful industrial nations like United States, Japan, China, India, Australia, and South Africa, with coal power plants contributing over 50% to the energy

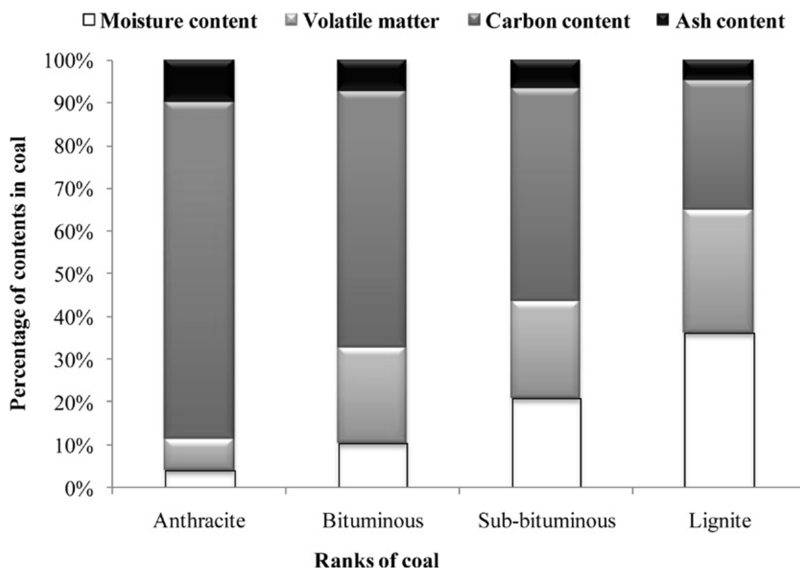


Figure 6.1 Ranks of coal and their distinctive physical and chemical characteristics (Ramage, 1997).

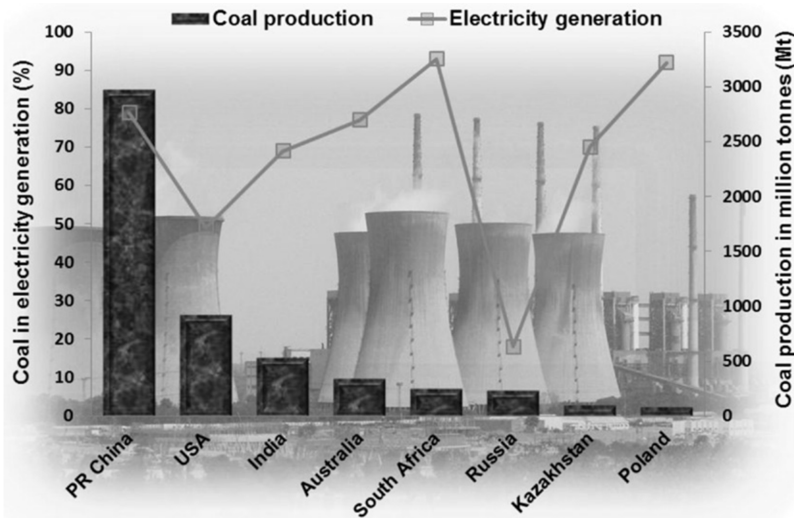


Figure 6.2 Coal production and consumption statistics among selected top coal producers (WCA, 2010).

needs of some of these countries (IEA, 2008). For example, in the United States, where coal is mined in 27 states, over 90% of the coal used is for generating electricity, with coal-fired power plants contributing up to 45% of the country's energy needs (US EIA, 2011). According to WCA (2010), South Africa (93%) and Poland (92%) are the largest consumers of coal, used especially for electricity generation (Fig. 6.2). Nevertheless, the global coal consumption is expected to increase at an average rate of 1.7% per year until 2020 and the share of coal in world's primary energy demand will remain stable at about 27% until 2020. In developing countries, coal consumption will increase at a rate of about 3% per year until 2020 (WCA, 2005, 2010) and much of the global coal consumption growth takes place in China and India (Knights and Hood, 2009; Van der Zwaan, 2004; WCA, 2010).

With a current share of 41%, coal is the largest contributor to power production worldwide and this trend has been predicted to progress in the next two decades (Knights and Hood, 2009). Both coal production and consumption has resulted in the pollution of air, land, and water resources, causing severe impairment to the environmental health and consequently human wellbeing (Gautam et al., 2012; Hendryx and Ahern, 2008; Table 6.1). Although advanced technologies are being practiced to curtail the environmental pollution in mine sites, the technological developments addressing

Table 6.1 Environmental Impact of Coal Production and Consumption

Environmental Impacts	Coal Production	Coal Consumption
Air	Dust and noise	Greenhouse gases
Land	Soil erosion and acid mine drainage	Accumulation of hazardous residues (ash materials)
Water	Acid mine drainage and movement of nutrients and heavy metals to ground water.	Leaching and surface runoff of heavy metals from ash-ponds.
Biological health	Impairs local biodiversity	Public health and safety concerns, especially respiratory issues.

the environmental issues (emission control and waste reduction) pertaining to the utilization of coal for electricity generation is still evolving in terms of pollution abatement.

1.2. Clean Coal Combustion Technologies

The burning of coal for electricity generation not only results in hazardous emissions but also produces residues called coal combustion products (CCPs). Traditionally, the CCPs have been dumped in large piles and/or ash-ponds mostly around the power stations. The CCPs are generally ash materials, made of fine particles and they are also generated as coarse particles. The generation of these products poses serious threats to air, water, and soil, and consequently to living organisms. The extent of the environmental effects caused by CCPs depends on

1. the coal source,
2. the combustion technology used and
3. the collection and segregation of the residues.

The two main residues that emerge out of coal combustion in power stations are fly ash (FA) and bottom ash (BA). In the past four decades, the power stations have been targeting on technologies that minimizes the effects of coal combustion in terms of limiting atmospheric pollution and reducing residues generated (Beer, 2000). The anticipation of restriction on the CO_2 emissions has forced the coal-dependent power stations in Organization for Economic Co-operation and Development (OECD) countries to improve the thermodynamic efficiency of the combustion technology used (Beer, 2000). Since carbon is the main coal constituent, the emissions related to carbon were highly significant and accentuated by most of the environmental agencies globally, for their contribution to greenhouse gas (GHG)

Table 6.2 Emission of Greenhouse Gases (GHGs) based on Various Sectors

Sector	Mt CO_2e	% Emission
Electricity and heat	10,318.6	26.9
Manufacturing and construction	4467.5	11.6
Transportation	4836.0	12.6
Other fossil fuel combustion	3527.4	9.2
Fugitive emissions	1579.0	4.1
Industrial processes	1369.4	3.6
Agriculture	5729.3	14.9
Land use change and forestry	5165.9	13.5
Waste	1360.5	3.5
Total	**38,353.6**	

World Resources Institute (WRI), 2011

emissions (Table 6.2). Hence, there have been a number of technologies aimed at reducing carbon-related atmospheric emission, such as postcombustion capture, oxyfuel combustion, and precombustion capture. The first two technologies are carried out by amine scrubbing, which separates CO_2 and the precombustion capture that removes 85% of CO_2, where hydrogen gas alone serves as a combustion fuel after the process (Gupta et al., 2003; IEA, 2002). Apart from the discharge of carbon-associated release of pollutants, the coal-fired power industries also emit other harmful gases such as sulfur oxides (SO_x) and nitrogen oxides (NO_x). All these technologies come under clean coal technologies (CCTs) and are mainly practiced to mitigate air pollution (Beer, 2007), although there are changes in the nature of the CCPs produced as a result of the adaptation of CCTs (Table 6.3). For example, the CCPs emerging from some technologies pertaining to NO_x reductions contain large ammonia content (Butalia and Wolfe, 2001); similarly technologies designed to remove SO_x during coal combustion can lead to S-rich byproducts (Wang et al., 2006). These byproducts can be used as a major source of plant nutrients (Wang et al., 1995, 2006).

In the global perspective, CCTs reduce emission of several pollutants, decrease waste generation and increase the amount of energy gained per unit amount of coal combustion. These technologies include various chemical and physical treatments applied pre- or postcombustion (Table 6.3). They may be broadly grouped into processes relating either to combustion efficiency, pollution control (especially, control and reduction of NO_x, SO_2, mercury and particulate matter) or carbon sequestration (Beer, 2007; Franco and Diaz, 2009; Longwell et al., 1995). There are two major categories in NO_x reduction technologies: (1) combustion modifications and

Table 6.3 List of Advancements in CCTs, their Benefits and Byproducts Generated

CCTs	Description	Benefits	Byproducts	References
Low-NO_x burners (LNB)	Provides internal staged combustion, thus reducing peak flame temperatures and oxygen availability	• Low operating cost • Compatible with other technologies • Moderate NO_x removal (30–50%)	Ammonia- and carbon-rich FA	Melick et al., 2005
Overfire air (OFA)	Staged combustion, creating fuel-rich and fuel-lean zones	• Low operating cost • No capital equipment required • Moderate NO_x removal (30–60%)	Ammonia-rich FA	Beer, 2000
Selective catalytic reduction (SCR)	Catalyst located in flue gas stream promotes reaction of NH_3 with NO_x	• High NO_x removal (70–90%)	Ammonia-rich FA	Franco and Diaz, 2009
Selective noncatalytic reduction (SNCR)—urea injection	Injection of urea into furnace to react with NO_x to form nitrogen and water	• Low capital coat • Relatively simple system • Moderate NO_x removal: Nontoxic chemical (25–50%)	Ammoniarich FA	Franco and Diaz, 2009
Selective non catalytic reduction (SNCR)—ammonia injection	Injection of ammonia into furnace to react with NO_x to form nitrogen and water	• Low operating cost • Moderate NO_x removal • (25–50%)	Ammonia-rich FA	Franco and Diaz, 2009
Fluidized bed combustion (FBC)	Injection of air into a bed of inert ash and crushed limestone	• Low cost for scrubber installation	FBC ash	Wang et al., 2006
Flue gas desulphurization (FGD)	A wet scrubbing process which uses limestone slurry as an absorbent	• High SO_x removal (90–95%)	FGD gypsum	Srivastava, 2000

(2) postcombustion processes. The most common combustion modification processes are as follows:

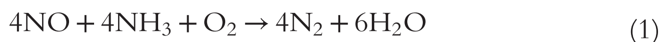
1. **Low-NO_x burners (LNBs)** are designed to burn in a lower maximum flame temperature and a reduced oxygen concentration by controlled mixing of fuel and air, resulting in staged combustion (Magel et al., 1996), ensuring lower thermal and fuel NO_x production. The main disadvantage of the LNBs is generation of high carbon combustion wastes (ash) as a result of the lower flame temperature employed during combustion, which makes the marketing of the ash undesirable (Melick et al., 2005).
2. **Overfire air (OFA)** technology involves the injection of air into the furnace above the normal combustion zone and this approach is generally used in conjunction with operating the burners at a lower than normal air-to-fuel ratio, which reduces NO_x formation. The OFA process is frequently used in association with LNBs. The use of oxygen in the OFA reduces loss of ignition (LOI), thereby ensuring low carbon ash (Bool and Kobayashi, 2003).
3. **Reburning** process reduces NO_x by injecting 10–25% of the coal in a separate reburn zone, where the fuel-rich conditions lead to the reduction of NO_x formed in the normal combustion zone. The OFA technology is also employed above the reburn zone to complete the combustion. Hence, there are three zones in the furnace for this reburning technology: (1) *a combustion zone* with an approximately normal air-to-fuel ratio; (2) *a reburn zone*, where added fuel results in a fuel-rich condition; and (3) *a burnout zone*, where OFA leads to completion of combustion (Moyeda, 2004).

4. **Flue gas recirculation (FGR)** is used to modify the conditions in the combustion zone (lowering the temperature and reducing the oxygen concentration) which consequently decreases the formation of NO_x. In FGR, the flue gas is recirculated to the furnace in the combustion zone and also used as a carrier to inject fuel into a reburn zone to increase penetration and mixing. Baltasar et al. (1997) observed marked decrease of NO_x emissions in FGR technology without significant effects on the flame stability.

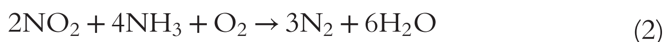
The postcombustion processes include addition of reactive substances or catalysts to convert the already formed NO_x into molecular nitrogen or nitrates and the most prominent treatment processes are the following:

1. **Selective catalytic reduction (SCR)** reduces NO_x in the presence of a catalyst and an injection reagent (vaporized ammonia—NH_3). The coal is burned along with the catalyst and NH_3 in a catalyst vessel

installed downstream of the furnace at 570–750 °F, to produce nitrogen and water vapor. The catalyst plays an important role in chemisorption of NH_3 onto its active sites. In this process, the N is released as an inert dinitrogen gas and the reactions involved in SCR process are as follows (US EPA, 1997):



$$4NO + 4NH_3 + O_2 \rightarrow 4N_2 + 6H_2O \quad (1)$$



$$2NO_2 + 4NH_3 + O_2 \rightarrow 3N_2 + 6H_2O \quad (2)$$

2. **Selective noncatalytic reduction (SNCR)** uses a reducing agent (typically NH_3 or urea), which is injected into the furnace above the combustion zone, where it reacts with NO_x similar to SCR. The even distribution of the reducing agent in the furnace and sufficient residence time in the appropriate temperature range are the critical factors for SNCR technology (Wu, 2002).

Both SCR and SNCR processes can be used in conjunction with each other as a hybrid process and also with LNBs for synergistic benefits. The disadvantage of these methods is the production of NH_3-rich ash, due to high levels of NH_3 slip as part of the operational impacts, resulting in low commercial value of the ash (Wu, 2002).

Sulfur dioxide (SO_2) is another major pollutant emitted in large quantities from the burning of coal with high sulfur content. More than 95% of sulfur is converted to SO_2 from coal combustion (Franco and Diaz, 2009). Along with NO_x, SO_2 is capable of producing acid rain. Widespread occurrence of acid precipitation and dry deposition results in industrial emissions of SO_x and NO_x (Longhurst, 1991). These gases are transformed in the atmosphere as sulfuric and nitric acids (Table 6.4); transported over long distances and deposited on vegetation, soils, surface water, and building materials. While the majority of NO_x emissions are local/natural origin, SO_x emissions are often transboundary in nature (Bolan et al., 2007). The average annual ratio of sulfuric acid to nitric acid is about 2:1 in North America but nitric acid is becoming progressively more important because of the installation of flue gas desulphurization (FGD) systems in coal-fired power stations (Dick et al., 2000).

Similar to NO_x removal, SO_2 can also be removed using both combustion modifications and postcombustion technologies. The most prominent combustion modification process for SO_2 removal is the fluidized bed combustion (FBC), where the coal is burnt in a bed of inert ash and crushed limestone. The bed is held in suspension by injecting air through a perforated

Table 6.4 Transformation of Sulphur Dioxide and Nitric Oxide in Atmosphere

Process	Transformation Equation	H^+ ($mol_c\ mol^{-1}$)
Oxidation of sulfur dioxide	$2SO_2 + O_2 \rightarrow SO_3$ (3)	0
Hydrolysis of sulfur trioxide	$SO_3 + H_2O \rightarrow H_2SO_4 \rightarrow SO_4 + 2H^+$ (4)	+2
Photochemical oxidation of nitric oxide	$O_3 + NO \rightarrow N_2O + O_2$ (5)	0
Hydrolysis of nitrogen dioxide	$2NO_2 + H_2O \rightarrow HNO_3 + HNO_2 \rightarrow NO_3 + H^+$ (6)	+1

floor. The limestone reacts with the released SO_2 to form calcium sulfate (Eqns (8) and (9)). The use of lower (between 1449 and 1598 °F) FBC technology compared to the conventional coal-fired furnaces (2552–2912 °F) results in optimum S capture, thereby minimizing the usage of limestone and also reducing NO_x formation (Terman et al., 1978). Therefore, these boilers possess potential in coal-fired power plants for meeting air quality standards without the usage of highly expensive SO_2 scrubbers. The conversion of limestone into calcium sulfate is described by the following equations (Wang et al., 2006):



$$CaCO_3 \rightarrow CaO + CO_2 \tag{7}$$



$$CaO + SO_2 \rightarrow CaSO_3 \tag{8}$$



$$2CaSO_3 + O_2 \rightarrow 2CaSO_4 \tag{9}$$

The FBC ash is formed as a mixture of conventional coal combustion ash (either bed or fly ash), the SO_2 reaction product (primarily anhydrite, $CaSO_4$) and unspent sorbent (Stehouwer et al., 1999; Wang et al., 2006). Hence, the FBC ash is highly alkaline and has the potential to be used as liming material and S fertilizer.

In United States, the SO_2 reduction is largely carried out using the postcombustion technology, namely, FGD. The advantage of this system is that it can be installed to any existing conventional coal-fired power station and has the capability of removing up to 95% or more SO_2 in

flue gases (Franco and Diaz, 2009; Srivastava, 2000). The reagents that are used as sorbents to scrub flue gases include limestone ($CaCO_3$), lime (CaO) or caustic soda (NaOH). Generally, FGD processes are classified as wet or dry scrubbers. A wet FGD process is the commonly used, which produces slurry waste, which is a saleable byproduct. However, the dry FGD technology produces solid waste which is easily disposable compared to the former process. The value-added CCPs emerging from FGD process are termed as FGD gypsum (Shahandeh and Sumner, 1991; Sumner, 2007).

Although the development of combustion systems in electricity generation had been discussed widely since the peak industrial revolution era (mid 1900s), the CCTs have started emerging only during the 1970s which is called as Environmental Era (Beer, 2000). After the initial attention on satisfying the demands of CO_2 mitigation, the focus shifted toward reducing the emission of nitrogen (NO_x) and sulfur (SO_x) oxides, which also contribute to acid rain and climate change. The CCPs generated from NO_x technologies are commercially undesirable because of NH_3- and carbon-rich ashes. However, they can be used as plastic fillers after chemical processing, which can act as an alternative for the usage of chemical fillers such as calcium carbonate or aluminosilicate (Huang et al., 2003). Hence, the products from SO_2 reduction processes such as FGD and FBC will be broadly discussed in this review.

1.3. Production and Global Market Demand of CCPs

In general, the use of CCPs as a soil amendment has been an ongoing area of investigation by the Ash Development Association of Australia (ADAA, 2008) since the mid-1990s and also by several other organizations globally, with major contributions from American Coal Ash Association (ACAA). Currently, CCPs are used extensively in the construction sector as cement and concrete replacements, including brick making. For example, in supplying the power requirements for Australian households, around 14.6 Mt (million tonnes) of CCPs are produced annually, of which about 1.787 Mt is utilized in the construction industry primarily as a partial cement replacement. Only about 0.5 Mt is used for noncementitious applications, which include agriculture and environment (ADAA, 2009). Similarly, utilization of CCPs (Fig. 6.3) as a percentage of total generated in different countries amounts to around 85% in West Germany, 73% in Denmark, 60% in France and UK, 50% in Poland, 44% in US, 33% in Canada, 31% in Australia, 97.2% in Japan, 58% in China, and 13% in India (ADAA, 2009; CIRCA, 2010; JCOAL, 2010; Kalyoncu, 2001; Sinha and

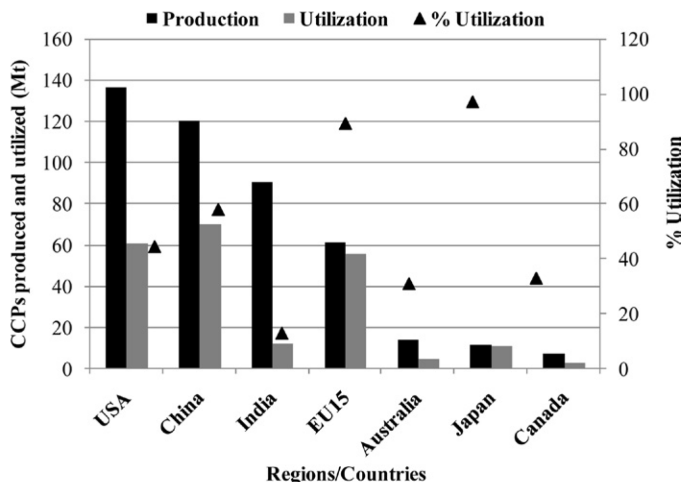


Figure 6.3 Production and utilization of CCPs in selected regions (Dhadse et al., 2008).

Basu, 1998; Wang and Wu, 2004). However, there is a potential for greater utilization of these CCPs in agriculture and environmental applications worldwide (Table 6.5).

In agriculture, CCPs are primarily used as an amendment to improve the physical and chemical properties of soil, as a source of liming material to ameliorate soil acidity and as a nutrient source to supply calcium and sulfur (Wang et al., 2006). In the construction industry, they are used mainly as a source of concrete, roofing material and road surface sealing (Bilodeau and Malhotra, 2000). Increasingly, CCPs are being used in the remediation of contaminated environments including control of acid mine drainage (AMD), mitigating phosphorus leaching in farm lands and immobilization of toxic metals in mine sites and agricultural soils (McDowell et al., 2008; Pathan, 2003; Stout et al., 1998). Moreover, the byproducts (FBC ash and FGD gypsum) emerging from CCTs can address coal industry's own perils such as AMD at the mine site.

1.4. Current Usage and Scope of CCPs

International research into the use of CCPs as a soil amendment has grown markedly over the past few decades, focusing mainly on the feasibility of using these products in agriculture and some environmental applications. Although there have been reviews on the beneficial utilization of CCPs (e.g. Adriano et al., 1980; Basu et al., 2009; El-Mogazi et al., 1988; Yunusa et al., 2006), these reviews cover mostly the agricultural

Table 6.5 Extent of CCPs Usage in Developed Countries by Various Sectors (in million tonnes)

CCPs Production and Utilization	USA	EU15	Canada	Australia
Total production	130.18	57.15	1.62	14.08
Concrete/concrete products/grout	11.67	1.11	0.00	0.01
Blended cement/raw feed for clinker	4.13	0.64	0.05	1.90
Flowable fill	0.20	–	–	0.04
Structural fills/embankments	9.12	0.51	0.00	0.10
Road base/sub-base	0.96	0.93	0.05	0.32
Soil modification/stabilization	0.97	0.55	–	0.01
Snow and ice control	0.59	–	–	–
Blasting grit/roofing granules	1.36	0.60	–	–
Mining applications	12.72	0.01	–	0.08
Gypsum panel products	7.66	1.13	0.00	0.00
Waste stabilization/solidification	3.41	0.02	–	0.01
Agriculture	0.51	0.01	–	0.00
Aggregate	0.59	–	–	0.01
Miscellaneous/other	1.44	0.39	0.00	0.00
CCPs utilized	55.34	5.90	0.10	2.48

ADAA, 2009; CIRCA, 2010; ECOBA, 2008.

applications of conventional CCPs such as fly ash. Research on the potential applications of the byproducts emerging from CCTs has been rising for the past two decades and needed better compilation of the latest advancements both on the technologies used and beneficial utilization of various byproducts generated. This chapter will discuss the CCTs pertaining to SO_2 emissions and the potential benefits of the resultant CCPs (FBC ash and FGD gypsum) in the soil environment (Fig. 6.4) focusing on the following:

- Soil amendment (liming material and nutrient source)
- Nutrient (phosphorus) retention and bioavailability
- Heavy-metal immobilization
- Mitigating AMD and acid-sulfate soils
- Carbon sequestration.

This comprehensive review will be a significant resource for aspiring researchers and environmental regulators to take up the new challenges posed by these CCTs and to manage CCPs for beneficial agricultural and environmental applications. The term CCPs used in this entire review will indicate CCPs from both conventional (e.g. FA) and contemporary CCTs (e.g. FBC and FGD).

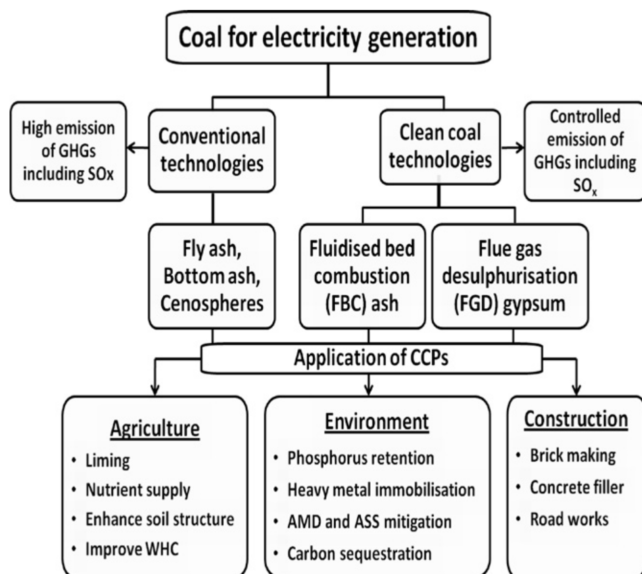


Figure 6.4 Production of CCPs by different technologies and their various applications.

2. PHYSICAL AND CHEMICAL PROPERTIES OF CCPS

The physical and chemical properties of CCPs which determine their agricultural and environmental applications depend upon a number of factors, including the type of coal burnt, the boiler conditions, the type and efficiency of the emission controls (Adriano et al., 1980; Basu et al., 2009). Certain characteristics have a propensity to be similar in most ashes. Chemically, CCPs are mainly silicoaluminate glasses, with the presence of other mineral materials such as calcium (Ca), magnesium (Mg) and iron (Fe) (ADAA, 2007). According to the American Society for Testing and Materials (ASTM), there are two classes (C and F) of CCPs; class F is produced from the combustion of bituminous coal and class C from sub-bituminous and lignite coals (Manz, 1999). In Australia, the majority of CCPs produced is categorized as Class F—being mainly silica and alumina (80–85%) and <10% CaO. Class F CCPs are highly pozzolanic and reacts with various cementitious materials. The other type of CCPs produced in countries such as India is the Class C CCPs, which generally contains more than 20% lime (CaO). Hence, they do not require an activator for cementing. Alkali and sulfate (SO_4) contents are generally higher in Class C type. Furnace BA can comprise 10–20% of the total CCPs produced and range in grain size from fine sand to coarse lumps. They have chemical compositions similar to FA.

The characteristics of CCPs produced by CCTs (FBC and FGD) differ both physically and chemically from conventional FA, mainly because of the additives and modifications in the combustion technology (Fu, 2010; Li et al., 2006).

2.1. Physical Properties

The main physical characteristics of combustion residues include particle size, particle shape or morphology, hardness and density. These properties are a function of the particle size of the feed coal, and the type of combustion and particulate control devices used (Kim, 2002). About 50% of CCPs are glassy spheres, which are mainly composed of silt-sized materials having a diameter from 0.01 to 100 μm (Gupta et al., 2012; Singh and Siddiqui, 2003). The importance of these particles on chemical reactivity is described under "Chemical Properties" (Section 2.2).

When compared with mineral soils, CCPs possess lower values of bulk density, hydraulic conductivity, and specific gravity. Among the CCPs, FA has the lowest bulk density (Table 6.6). Finer particles of FA have larger surface areas, which allows for deposition/absorption of volatile elements on the surface of the CCPs during the combustion process (Goodarzi et al., 2008). The extent of the surface area also determines the water-holding capacity (WHC) and other surface reaction properties (e.g. adsorption) of CCPs. Aitken et al. (1984) found that the surface area alone cannot explain the high WHC. The variation in the proportion of particles with porosity among the ashes may also influence the WHC. Both crystalline (mullite) and amorphous (glass) phases have been identified by X-ray diffraction in FA (Mattigod et al., 1990). The texture is fine for FA and is coarse for the CCT-derived CCPs. The FBC appears dark gray in color which may be attributed to the scrubbing of NO_x and SO_x. The particle size ranges from 0.01 to 740 μm in the order of FA > FBC > FGD. Bulk density and moisture content are high in FBC. Ash content is low in FBC and FGD compared to their conventional counterpart (Table 6.6).

2.2. Chemical Properties

The chemical properties of CCPs will largely be determined by the metal oxides (Si, Al, Fe, Ca, Mg, Na, K) that are surface adsorbed during particle formation and the primary minerals that include quartz, mullite, hematite, clays, and feldspars. The electron dispersion spectroscopy (EDS) studies conducted by Kutchko and Kim (2006) in an FA sample lists out the predominant elements as Si, Al, Fe, and Ca. They observed lesser amounts of other

Table 6.6 Physical Characteristics of CCPs

Physical Properties	FA	FBC	FGD
Texture	Fine	Fine to coarse granules	Coarse granules
Color	White	Dark gray	White
Particle size (μm)	0.01–100	0.2–200	1–740
Bulk density (kg m^{-3})	960–1600	1520–1680	780–1250
Moisture content (wt%)	7.8–9	21.5–27.5	8–10
Volatile matter (wt%)	4.7	33.1	19.6
Ash content (wt%)	79.5	9.1	6.7
Reference	Asokan, 2003	Wang et al., 2006	Baligar et al., 2011

elements such as K, Mg, Na, and S. The general association included aluminosilicates, calcium sulphates, calcium oxides and iron oxides. In the case of FBC and FGD, the Ca- and S-based compounds may be predominantly generated due to the Ca-based additives and stripping of S from the coal.

The maximum temperature and the rate of cooling influence the morphology and composition of CCPs (Kim, 2002). The trace elements present in CCPs include As, B, Ba, Cd, Cu, Hg, Mn, Mo, Ni, Pb, Sb, Se, V and Zn (McDowell, 2005; Punshon et al., 2001; Sajwan et al., 2007; Stehouwer et al., 1999; Wang et al., 1995; Table 6.7). The partitioning of these elements is primarily determined by volatilization and condensation processes involved in the combustion of coal. Natusch and Wallace (1974) observed that 5–30% of toxic elements, especially Cd, Cu and Pb, are leachable. Radionuclides of uranium (U) and thorium (Th) series were reported in FA (Tadmore, 1986). Majority of FA are not significantly enriched in radioactive elements or in associated radioactivity compared to common soils or rocks (Zielinski and Finkelman, 1997).

Three groups of solid chemical components have been identified in FA (Adriano et al., 1980; Terman et al., 1978; Table 6.8), which also determines the physical properties of CCPs generated. The CCPs are also composed of two types of silt-sized glassy spheres, (1) some of the spheres are hollow, termed as cenospheres, and (2) spheres filled with smaller spheres named as plerospheres (Ghosal and Self, 1995; Sreenivas et al., 2011). During the combustion and subsequent cooling process, many different metal oxides can precipitate and concentrate on the surfaces of these spheres. Hence, these oxides control the chemical properties of the CCPs generated. They may also affect the physicochemical properties of some CCPs, especially the pozzalonic (cementitious) reactivity (Stewart and Tyson, 1997).

Table 6.7 Selected References on Nutrient and Trace Metal Concentrations in CCPs

	Nutrients (g kg^{-1})						Trace Elements (mg kg^{-1})						
CCPs	**P**	**S**	**Al**	**Ca**	**Fe**	**B**	**As**	**Cd**	**Cr**	**Hg**	**Pb**	**Se**	**References**
FA	–	–	–	–	–	1.69	7.0	0.1	38	1.3	15	2.9	McDowell (2005)
	0.956–1.002	–	110–130	5.3–5.7	82–100	–	116–129	2.8–3.5	155–169	0.27–0.45	60–63	12–17	Punshon et al. (2003)
	1.388–1.432	1.26–1.3	75–117	13–14	41–73	0.01–0.02	112–125	3.0–5.0	97–155	0.22–0.31	247–263	8.4–11	Adriano et al. (2002)
	0.2315	2.738	4.136	8.43	13.51	0.29	–	2.8	26.8	–	2.5	–	Sajwan et al. (2007)
FBC	–	28	13.0	300	55.0	–	–	<2	50.0	–	85.0	–	Karapanagioti and Atalay (2001)
	0.875	62.0	18.0	254	36.0	1.36	6.5	<0.1	<0.1	–	<2.0	<3.0	Wang et al. (1995)
	0.1	86.4	27.5	244	20.8	0.21	46.7	3.5	17.5	–	28.0	2.3	Stehouwer et al. (1999)
	0.2	38	0.1	391	5.0	1.32	8.1	0.2	33	–	88.0	3.3	Wright et al. (1998)
FGD	0.573	85	25.5	146	85	0.35	107	<0.2	51	–	15	–	Ahn et al. (2001)
	–	67.1	19.6	260	16.5	0.19	118	<0.1	123	–	139	<6.0	Chen et al. (2005)
	–	–	–	193	51	0.04	68.9	0.35	13.7	0.03	17.1	29.2	Punshon et al. (2001)
	0.2	52.1	39.3	175	51.7	0.17	75.0	1.9	36.9	–	16	5.6	Stehouwer et al. (1999)
	0.2	182	8.0	201	0.1	0.13	6.3	0.7	15.0	–	100	2.3	Wright et al. (1998)
	–	205.4	3.3	269.1	–	–	1.08	<0.1	9.70	0.65	4.08	0.84	Wang et al. (2006)

Table 6.8 Groups of Solid Components in FA

Groups	Components	Properties
Group I	Oxides of Si, Al, Fe and Ti	Low water reactivity, possess surface charge
Group II	Metals and metalloids	Adsorption to oxides
Group III	Oxides of Ca, Mg, K, Na, Ba, SO_3, Gypsum	High water reactivity

Adriano et al., 1980; Terman et al., 1978.

The chemical compositions of most CCPs vary according to their parent coal materials. In the case of FBC and FGD materials, the major difference comes from the Ca-based additives during/postcombustion, and hence higher amounts of Ca and S can be observed (Table 6.7), compared to conventional CCPs (FA). The Ca concentrations ranged from 146 to 391 g kg^{-1} for FBC and FGD, compared to <30 g kg^{-1} for FA. Similarly, S concentration reached up to 105 g kg^{-1} in FGD, indicating the amount of S scrubbed by the CCTs. The behavior of volatile elements such as Se and Hg is highly dependent upon the burning conditions within the boiler and the sorbents used for capturing S (Punshon et al., 2003). During the combustion and subsequent cooling process, many different metal oxides can precipitate and concentrate on the surfaces of CCPs. The abovementioned physical and chemical properties have driven the coal industries and environment researchers explore the possible applications of CCPs as part of the sustainable utilization strategies of these resources.

3. APPLICATIONS OF CCPS

In most developed countries, the CCPs are used extensively in the construction industry as supplementary cementitious materials and moderately as agricultural supplements and in environmental restoration. In the construction industry, they are used mainly as a source of concrete, roofing material and road surface sealing (Chugh et al., 2006). In Australasia, about 85% of the current "beneficial use" of FA is for partial cement replacement (10–20%) to enhance the properties of concrete and other building materials. The cement and concrete industry through their channel members are continuously building up significant market for the beneficial use of certain CCPs, especially FA (ADAA, 2009). In the construction industry, FA can provide certain material advantages such as greater workability, higher strength, and increased longevity in the finished concrete product. Fly ash is also used as a partial substitute for sand, or gravel in structural fill, or as a substitute for portland

cement in waste stabilization (Ahmaruzzaman, 2010; Andini et al., 2010). BA can be used to offset sand and gravel in applications such as structural fill, road base, and concrete (Arenas et al., 2011; Chindaprasirt et al., 2009). Among the CCPs arising from CCTs, FBC does not meet ASTM C618 standards that endorse conventional civil engineering and concrete applications (Fu, 2010). But FGDs are known to be useful in construction industry as plasterboards and also as retarder for Portland cement (Harben, 1999).

In agriculture, CCPs are used primarily as an amendment to improve the physical and chemical properties of soil, as a source of liming material to ameliorate soil acidity and as a nutrient source to supply Ca and S (Heidrich, 2003; Korcak, 1995; Wang et al., 1999a, 1999b). The idea of utilizing CCPs in agriculture has originally arisen as a result of their role as a nutrient supplement to crops in soils, that are low in nutrients such as Se, Mo, Cu, Zn, or B (Adriano et al., 1980; Aitken et al., 1984; Gupta et al., 2012; Page et al., 1979). Most CCPs contain K, Ca, Mg, S and P, which can act as good nutrient source to crops (Adriano et al., 1980; Cervelli et al., 1987; Kalra et al., 1998; Martens et al., 1970; Page et al., 1979; Pathan et al., 2002; Sikka and Kansal, 1994; Singh et al., 1997). The addition of CCPs generally increases plant growth and nutrient uptake (Aitken et al., 1984; Ciravolo and Adriano, 1979; Stout et al., 2003).

3.1. Agricultural Applications

The use of CCPs in agriculture not only offers potential physical (structural) and chemical (nutrient) benefits to degraded soils but also provides broader environmental benefits through resource reuse, as an alternative to the unsustainable practice of land filling. Much of the literature regarding the beneficial use of CCPs in agriculture describes application rates at levels of 5–20%. Application rates are typically modified according to the soil type and their physical or chemical characteristics (Adriano et al., 2002; Elrashidi et al., 1999). Between 1981 and 2010, the use of CCPs in agriculture was widely studied (Baligar et al., 2011; Bhumbla et al., 1991; Kumar and Singh, 2003; Stevens and Dunn, 2004), where the potential of CCPs as liming agent, source of plant nutrients, and soil modifier has been exploited. The uptake or enrichment of various nutrients and toxic trace elements (Table 6.9) in soil after FA amendment has been investigated, and crop produce has been found safe for consumption (Sen et al., 1997). However, comprehensive studies on the implications of contemporary CCPs are limited.

The agricultural use of CCPs depends on not only the nature of the parent coal used for power generation but also the combustion technology (e.g. FBC) and additives used (e.g. lime). The criterion for usage of

Table 6.9 Selected References on CCP-Induced Mobilization of Nutrients and Heavy Metals in Soils

Nutrients	CCPs	Key Finding	Reference
Nutrients			
Nitrogen	FA	Addition of FA to alkaline-treated wastewater sludge decreased the rate of mineralization of organic nitrogen in the sludge, thereby increased the residual value of sludge as a nitrogen source	Topaç et al., 2008
	FA	Integrated use of FA, bluegreen biological fertilizer and nitrogen fertilizer improved growth, yield and mineral composition of the rice plants besides reducing the high demand of nitrogen fertilizers.	Tripathi et al. (2008)
	FA	FA is an important source of alkalinity in the upper 0–5 cm of lignite-containing lake sediments that enhanced plant growth and led to enrichment of the sediment with nitrogen from organic matter derived from plant material	Chabbi and Rumpel (2004)
	FA	FA is low in nitrogen but increased the mineralization of organic N. Organic-matter-rich soils or nitrogen-fixing plants with an apparent heavy-metal tolerance can be helpful as the early colonizers of FA dumps and nearby areas.	Gupta et al. (2002)
	Class C FA	Co-applications of FA and animal manure products stabilized manure P, thereby widened its effective N:P ratio, allowing land application rates needed to fulfill plant N requirements without causing water quality impairments.	Dao (1999)

	FA	FA is low in N; cocomposting FA with biosolid increases the supply of N	Alva et al. (1999)
	FA and BA	Although applications of CCPs had little influence on the fertilizer N, application of bed ash caused substantial decreases in the total N content of water-extracted soil through the mobilization of organic N and losses of N in the forms of amino sugars, amino acids, and hydrolyzable NH_4^+ could account largely for losses of total N in bed ash-amended soils, resulting from an increase in soil pH.	Stuczynski et al. (1998)
	FGD gypsum	Application of FGD gypsum with N fertilizer promotes the uptake of N by corn in S-responsive soils, thereby decreasing the amount of N required for high-yield corn production and reducing the degradation of water quality associated with oversupply of N.	Chen et al. (2005)
	FA	Enhanced N release from cow dung when vermicomposted in the presence of FA.	Bhattacharya and Chattopadhyay (2004)
Phosphorus	FA	In a greenhouse experiment, fresh cattle manure mixed with Ca amendments inhibited P uptake by barley and decreased extractable ortho P concentrations in soils. Chemical and biological reactions in plant–soil systems led to the apparent dissolution or desorption of ortho P from fresh manure mixed with FA and composted manure-co-amendment mixtures.	Whalen (2002)
	FA	Co-applications of FA and animal manure products stabilized manure P, thereby allowing land application rates needed to fulfill plant N requirements without causing water quality impairments.	Dao (1999)
	FA	Treatment of drainage water with coal slag prevents phosphorus loss from tile-drained land	McDowell et al. (2008)

Continued

Table 6.9 Selected References on CCP-Induced Mobilization of Nutrients and Heavy Metals in Soils—cont'd

Nutrients	CCPs	Key Finding	Reference
	FA	Sand amended with FA as filter media in bioretention cells increased phosphorus removal	Zhang et al. (2008)
	FA	Application of FA to rice cultivation increased available phosphorus resulting from high content of P (786 mg kg^{-1}) in the applied FA	Lee et al. (2007)
	FA and phosphogypsum	The mixture significantly reduced water-soluble phosphate (W–P) in the surface soils by shifting from W–P and iron bound-P (Fe–P) to calcium-bound P (Ca–P) and aluminum-bound P (Al–P) during rice cultivation, thereby reducing P loss from paddy soils.	Lee et al. (2007)
	FA	Addition of FA to pasture soil increased the mineralization of organic P.	McDowell et al. (2008)
	FGD gypsum	Treatment of high P soils with FGD gypsum decreases water-extractable P by conversion to soil IP fractions that are stable with time, does not decrease plant production, and suggests that the potential for P export in surface runoff may be reduced for several years.	Stout et al. (2003)
	FA	The FA amendment retarded NO_3^-, NH_4^+, and P leaching in sandy soils and may therefore be a useful tool for improvement of nutrient management in sandy soils.	Pathan et al. (2002)
	FA	Immediate and long-term decreases in P desorption occurred in the incubation study at all ash rates when greater than 500 mg P kg^{-1} were added but FA had little effect on P desorption at P rates <50 mg P kg^{-1}.	O'Reilly and Sims (1995)

	FA	P mobilization enhanced by organic acids and microbial activity in swine manure amended with fly ash; B was highly soluble at the highest application rate and was detrimental to plant growth.	Vincini et al. (1994)
	FBC	Increased P loss—solubilization of organic P due to an increase in soil pH resulting from free CaO content	McDowell (2004)
Sulfur, Calcium, Potassium, Magnesium Sodium	FBC	Water-soluble S is upto 50% with slow dissolution of remaining S; most of K is in the soluble form; dissolution of gypsum and portlandite in FBC increased soluble Ca concentration, <50% of the Na salts in FBC were water extractable.	Wang et al. (1995)
	FA	Released Mg at rates comparable to most Mg fertilizers.	Hill and Lamp (1980)
	FBC	Leachate Mg and S concentrations increased as $MgSO_4$ ion pair.	Stehouwer et al. (1999)
	FGD	Ca, Mg and S mobility increased with increasing depths of FGD application in soil. 90% of leachate S was present as SO_4–S.	Stehouwer et al. (1999)
	FA	Boron is highly leachable (17–64%) from alkaline FA with, but not completely pH dependent.	Jankowski et al. (2006)
	FA	Soluble calcium increased gradually over time under field conditions and increased sharply under alternate wet–dry conditions in a lignite-mine spoil.	Seoane and Leiros (2001)
Heavy metals			
Zinc, iron, manganese	FA	Bacterial activity in FA-amended soil increased mobility of Zn, Fe and Mn initially, but slowly decreased as the incubation period increased.	Tiwari et al. (2008)
Cadmium, antimony	FA	Increased the water-extractable fractions of Cd and As.	Fernández-Turiel et al. (1994)

Continued

Table 6.9 Selected References on CCP-Induced Mobilization of Nutrients and Heavy Metals in Soils—cont'd

Nutrients	CCPs	Key Finding	Reference
Copper and zinc	FA	Sequential fractionation indicated 2.6% of Cu and 3.4% of Zn in FA was water soluble.	Soco and Kalembkiewicz (2007a)
Chromium	FA	Under extreme environmental conditions (oxidizable or reducible), FA increases Cr mobility from 8.2 to 52.4% Cr.	Soco and Kalembkiewicz (2007b)
Arsenic	FA	Phosphate in FA displaced As, thereby increasing its mobility.	Qafoku et al. (1999)
Molybdenum, selenium	FA	Increased Mo and Se availability in soil at elevated pH.	Carlson and Adriano (1993)
Aluminum, iron, zinc, manganese	FBC	Reduction in leachate concentrations, which are phytotoxic in acidic conditions.	Stehouwer et al. (1999)
Chromium, copper, lead, zinc	FBC	Reduced mobility at high pH.	Riehl et al. (2010)

CCPs in agriculture has often been assessed in relation to its effects on: (1) improvements in soil quality; (2) crop yield and development; (3) uptake and accumulation of nutrient and non-nutrient elements; and (4) toxicity levels of trace elements (El Mogazi et al. 1988; Manoharan et al., 2010a, 2010b; Yunusa et al., 2006).

3.1.1. Effect on Soil Structure and Quality

Effect of CCPs on soil quality, which determines the soil health, manifests into soil productivity and has far reaching effects on the soil ecosystem. While the health of soil depends on inorganic and organic matter content, processes like erosion, salinization and chemical contamination have a direct bearing on groundwater contamination, land use and management practices (Acton and Gregorich, 1995; Lerner and Harris, 2009; Qiao et al., 2011). The CCPs contain trace elements, which can readily percolate down from conventionally used earth-lined lagoons and pollute groundwater whose solubility is <10% (Bhattacharyya et al., 2009; Haynes, 2009; Rohriman, 1971; Rout, 2011; Stropnik et al., 1991).

Most CCPs induce overall beneficial effects on soil physicochemical and biological properties if applied judiciously. In the presence of Ca–Si minerals with a pozzolanic nature (zeolite formation), along with the moisture of the soil, CCPs bring about improvements in various physicochemical properties such as porosity, WHC and the available water in the soil (Fulekar and Dave, 1986; Pratt et al., 2007) (Table 6). Generally, the moisture content and bulk density of FBC are highest among the CCPs, which help in limiting the percentage of CCPs application in soil. In most cases, the CCPs possess higher silt content than soil, and the infiltration rate of sandy soils or mine spoil is drastically checked because of the increase in silt (Furr et al., 1977; Korcak, 1995; Pathan et al., 2003; Wang et al., 1995), whereas in the clay-rich type of soils, the reverse is the case, with better water movement and workability, apart from decreased plasticity or crack formation after drying (Brooks et al., 2011; Kolias et al., 2005; Wilkinson et al., 2010).

As CCPs possess most of the essential plant nutrients other than nitrogen and humus (Menon et al., 1990; Pathan et al., 2002), applying it to the soil naturally improves its fertility by enriching it with the essential elements, thereby resulting in increased crop yields. The organic amendments cocomposted with FA also help in improving the humus and microbial activities of the amended soil or mine spoil, besides adjusting the pH by the way of decomposition and N demineralization (Adriano et al., 1982; Gupta et al., 2003; Sims et al., 1993; Topaç et al., 2008; Wong, 1995), controlling the

availability of metals to the plant by chelation, and releasing nutrients during vegetation (Logan and Traina, 1993; McDowell et al., 2008).

Since CCPs contain many silt-sized particles, their addition at high rates to soils high in sand or clay can change the soil texture (Pathan et al., 2002). When ash was added to five soils with sandy textures, the bulk density increased, while ash addition to three soils with clayey textures decreased bulk density. This difference could be due to the structural changes in soil after incorporation of CCPs and the consequent changes in pore space. In a microcosm leaching experiment involving earthworms conducted by Riehl et al. (2010), two different types of FBC ashes—(1) silico aluminous (SiAl) and (2) sulpho-calcic (SCa)—were applied to a calcareous soil and found decreased structural stability of soil amended with FBCs compared to the control (structural stability: control soil > SCa amended soil > SiAl amended soil). They argued that earthworms may have affected the structural stability of the soil aggregates. They also attributed the role of organominerals in water adsorption, where both clay and silt contents play a major role in changing the soil's structural stability, hence contributing to soil erosion and nutrient losses to runoff and leaching (Binet and Le Bayon, 1999).

The addition of CCPs has also been found to increase the WHC of soils. For example, Campbell et al. (1983) demonstrated that addition of 10% FA to fine (0.2–0.5 mm) and coarse (1.4–2.0 mm) sand fractions increased the available water content in the sands by 7.2% and 13.5%, respectively. Among the Australian CCPs (11 of 13 tested), the ash materials were found to have >40% available water (Aitken et al., 1984). Improvements in available water in FA-amended soils have also been reported by other researchers (Pathan et al., 2002; Salter et al., 1971; Summers et al., 1998). It is unclear whether the increases in WHC also result in increases in plant available water. This could be due to other growth limiting effects of the FA, such as B toxicity or high-soluble salts. The yields of carrot (*Daucus carota*), beetroot (*Beta vulgaris*), radish (*Raphanus sativus*), and bean (*Phaseolus vulgaris*) showed no improvement in response to the application of FA to a sandy loam soil, even though the WHC had increased (Salter et al., 1971). These improvements in physical and chemical nature of soil, coupled with positive effect on soil microorganisms, make the degraded soils productive. Thus, the use of CCPs for reclaiming threatened soils provides an economical way of disposal (Jala and Goyal, 2006).

The ADAA and University of Western Australia have already demonstrated substantial improvement in water retention and pasture growth in sandy soils. Some of the findings have highlighted the ability of FA to improve water retention in soils with low moisture-holding capacity (i.e. sandy soils) to over 30% compared to untreated soils. Furthermore, FA

provided increased plant growth without the need for additional fertilizers (ADAA, 2009). The addition of FGD to soil has also provided several structural benefits including improvement in WHC. Greater aggregate stability and less soil compaction have enabled FGD to retain more water, and thereby minimize water erosion and runoff (Korcak, 1998; Norton and Zhang, 1998). The Ca in FGD has great ability to enhance flocculation/aggregation of soil particles, particularly clay, and keep soils friable, enhance water penetration, and allow roots to penetrate hard/compact soil layers (Clark et al., 2001; Ritchey et al., 2000; US EPA, 2008).

It is reported that FBC ash could be used to mitigate soil-water repellency problem (Wang et al., 2006). In both field and laboratory conditions, Wang (1996) tested the effectiveness of using FBC ash to ameliorate water repellency in a New Zealand peat soil, where severe water repellency is a common problem in dry summer and autumn periods. It was found that normal liming and S fertilizer rates of FBC ash application had negligible effect on water repellency and water infiltration into dry peat soils. However, a high rate (up to 19,185 kg ha^{-1}) of surface dressed FBC applied to a peat soil under pasture can reduce the water repellency of the surface soil and increase the rate of water infiltration (Fig. 6.5). This was attributed to the high alkalinity of the applied FBC ash, which modified the hydrophobic nature of the peat soil by removing fatty acids from the soil particle surface (Wang, 1996).

3.1.2. Nutrient Source

A number of studies have examined the value of CCPs as a nutrient source. The major nutrient elements in CCPs include Si, Al, Fe, Ca and S, together

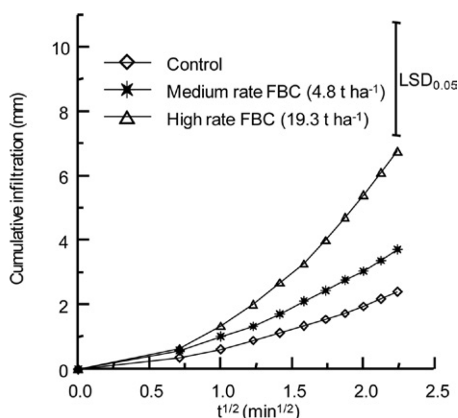


Figure 6.5 Field evaluation of the effect of slaked FBC treatment on water infiltration into a water-repellent peat soil. *(Adapted from Wang (1996)).*

with lesser amounts of Na, Mg, B, Sr and K (Table 6.6). For example, FBC and FGD ashes have Ca and Mg contents ranging from 13% to 39% and from 0.1% to 16%, respectively depending on whether the sorbent used is calcite or dolomite (Baligar et al., 2011; Korcak, 1998; Wang et al., 2006). Due to the presence of unspent sorbent, FBC is usually highly alkaline (pH_{water} 10.5–12.5) with significant neutralization potential. It has been reported that the best agricultural use of FBC ash is as a liming source to overcome the problems associated with soil acidity (Stout et al., 1998, 2000; Terman et al., 1978; Wang et al. 1995, 2006). The S content of FBC and FGD is also relatively high, being mainly in the form of $CaSO_4$ (anhydrite) (Wang et al., 2006). Therefore, these two CCPs are major sources of both Ca and S for plant nutrition in addition to their relatively high liming value (Wang et al., 1995). Compared with Ca and S, the amounts of N, P and K are negligible in most CCPs. The micronutrient content in CCPs is low except for boron (B) that ranges from 36 to 1360 mg kg^{-1} (Table 6.8). Boron is an essential mineral nutrient for all vascular plants. The functions of B are primarily extracellular, which relates to lignification and xylem differentiation. Some of the CCPs such as FBC also contain small amounts of selenium (Se, 0.16–5.6 mg kg^{-1}) which is an essential nutrient for animals but not plants.

The presence of S in FBC and FGD ashes as anhydrite ($CaSO_4$) or gypsum ($CaSO_4 \cdot 2H_2O$) after hydration make these CCPs the major source of S in S-deficient soils. Gypsum, including industrial byproducts such as phosphogypsum, has been successfully used as an S fertilizer to increase the yields of winter wheat, rice and pasture. Terman et al. (1978) demonstrated that FBC ash is an effective S source for growing corn and peanuts. Approximately 50% of S in slaked FBC ash is present as sparingly soluble ettringite, which can act as a slow-release S fertilizer (Wang, 1996). Therefore, slaked FBC ash shows potential to be used as a basal S fertilizer in soils prone to severe leaching, which are common in some high rainfall areas of New Zealand and in soils with low anion retention capacities. For example, results from a field study in the peat soil indicated that ettringite-S in slaked FBC ash was less affected by leaching loss than gypsum and resulted in longer-term pasture yield S responses to FBC ash treatments (Wang, 1996). This was supported by herbage S analysis where, 8 months after application, herbage S contents in the high rates of FBC ash treatments (about 6 and 26 ton ha^{-1}) were significantly higher than the control. Hill and Lamp (1980) demonstrated that in Australian soils, FA released magnesium (Mg) at rates comparable with established Mg fertilizers. The S-rich FGD can also control the mobility of Ca and Mg in soil profile by raising the pH. In addressing the S deficiencies in agricultural soil, Chen et al. (2005)

demonstrated that alfalfa yields can be increased up to 40% on the application of FGD and they observed minimal positive yield effects for soybean.

In Australian soils, FA released Mg at rates comparable with established Mg fertilizers. The Mg in FA was more soluble than that in the established fertilizers. It released significant amounts of Mg over a wide range of pH. It contained both a water-soluble, and a citrate-soluble fraction (Hill and Lamp, 1980). The strong correlation between pH correction and nutrient availability in the soil suggests that in CCPs, most elements are associated with the mineral phase as carbonates and oxides. One can therefore expect that interaction between the predominantly inorganic CCPs and organic matter may further enhance their beneficial effects on plant growth in problem soils (Baligar et al., 2011; Dou et al., 2003; Molliner and Street, 1982; Page et al., 1979; Power and Dick, 2000).

Generally, the CCPs does not seem to be an optimal source of phosphorus as it was found inferior to monocalcium phosphate (MCP), which are used as soluble P fertilizers (Martens et al., 1970), but some FA are high in P (Pathan et al., 2002; Seshadri et al., 2010). However, FBC can be used in the conversion of highly soluble MCP ($Ca(H_2PO_4)_2{\cdot}H_2O$) in single superphosphate (SSP) to less-soluble dicalcium phosphate (DCP, $CaHPO_4{\cdot}2H_2O$), thereby reducing P leaching (Wang et al., 1995). The MCP is the main P component in superphosphate fertilizers and on hydrolysis in the presence of FBC as calcium hydroxide ($Ca(OH)_2$), they precipitate DCP (less soluble), releasing orthophosphoric acid (Eqn (10)). This slow-release DCP can be used as effective P fertilizers in minimizing P losses, thereby maximizing P uptake by plants (Wang et al., 2006).



$$Ca(H_2PO_4)_2 + Ca(OH)_2 \rightarrow CaHPO_4 \cdot 2H_2O + H_3PO_4 \tag{10}$$

Although, higher B availability limits the use of CCPs in crop production (Aitken and Bell, 1985; Page et al., 1979), the problem can be overcome by proper weathering of the CCPs, which reduces B availability to below toxic level. Increased Se accumulation in plant tissues with increased FA application warrants close monitoring and use of appropriate quantity of weathered FA depending upon the end use of the produced biomass (Furr et al., 1977; Straughan et al., 1978).

3.1.3. Liming Material

One most beneficial property of certain types of CCPs is their liming potential. The liming potential of CCPs is derived primarily from CaO, MgO and other alkaline metal oxides. In a study of 23 ashes from across the United States, Furr et al. (1977) found that ash pH ranged from 4.2 to 11.8 and fresh unweathered

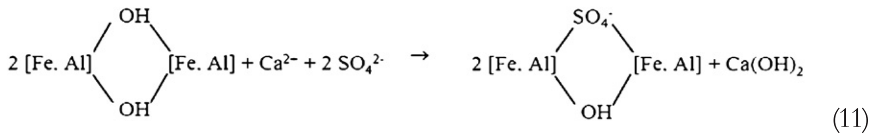
FA can have pH values higher than 9 but it is rare to find pH values higher than 8.5 for weathered FA (Adriano et al., 1980; Elrashidi et al., 1999).

Most CCPs are high in Ca and Mg oxides and have a significant acid neutralizing capacity. The basic property of CCPs measured to quantify the effect on soil pH is the calcium carbonate equivalence (CCE) of the materials. The neutralizing effect of pure $CaCO_3$ is 100% and that of CCPs usually ranges from 20% to 60% (Wang et al., 2006). Therefore, if a CCP has a CCE of 50%, twice as much CCP as $CaCO_3$ is needed to neutralize the same amount of soil acidity. The CCPs with neutralizing capacities of up to 10% CCE have been reported, but CCE values of l–6% are more common (Aitken et al., 1984; Reichert and Norton, 1994). Thus, more than 20 ton of most FA would be required to replace 1 ton of ground limestone. This indicates that CCPs may not be effective in raising a low pH, highly buffered system due to the large amount of ash needed. However, they can be more effective in poorly buffered, coarse textured systems, such as coal refuse. Water-soluble Ca content was found to be the best indicator of ash potential to produce alkalinity (Theis and Wirth, 1977). A long-term study on the environmental benefits for CCPs utilization in Australian agricultural and horticultural systems reveals that when FA is considered as a liming agent in terms of agricultural applications, the levels of cadmium, mercury and lead is well under the permissible limit under Fertilizer Act, 1985 (Heidrich, 2003). Lime in FA readily reacts with acidic components in soil and releases nutrients such as S, B and Mo in the form and amount beneficial to crop plants (Elseewi et al., 1978; Phung et al., 1978). In the case of FGD, $CaCO_3$ component is poorly soluble in soil and effective only on surface incorporation as they are not readily leached, but $CaSO_4$ present in FGD can effectively leach to subsurface and increase the Ca supply, thereby producing the neutralization effect (Clark et al., 2001). The best liming agent among the CCPs is FBC (CCE ranging from 31% to 105%), which is often utilized as a liming source to overcome the problems associated with soil acidity (Korcak, 1985, 1995; Marsh and Grove, 1992; Stehouwer et al., 1999; Stout et al., 1998; Wang et al., 1995, 2006).

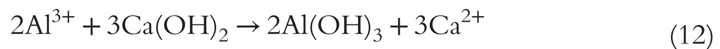
Korcak and Kemper (1993) investigated the long-term effects of FBC applied at disposal levels on soil chemical properties. In 1980, FBC was applied as a soil "cap" about 50 mm thick within the rows of an established, young apple orchard at rates up to 112 ton ha^{-1}. Eleven years after application, soil profile pH was significantly elevated by the FBC treatment to a depth of 660 mm. They suggested that horticultural utilization of FBC at relatively high rates of application may be a practical consideration

for disposing of FBC. Adriano et al. (2002) also found that high rates of FA application benefited turf grass growth and better groundwater quality. In orchard settings, FBC can be surface applied and remain in place for long periods. Results from their original apple study showed overall good growth and productivity of the trees.

Laboratory and field experiments on the use of FGD as liming material to a virgin clay in Germany, proved to enhance seedling growth in wild rye grass and poplar trees, respectively (Narra, 2009). The higher Ca activity of FGD gypsum induces the complexation of Al with sulfate which increases the exchangeable Ca. Also, the heavy-metal accumulation for FGD-amended soil was found to be less than lime application. Although FGD gypsum does not mitigate soil acidity in the same way as commercial limestone, they induce "self-liming effect"; increases Ca content in the subsurface soil; and precipitation, displacement and leaching of Al from the soil surface (Wang et al., 2006). The "self-liming effect" is based on the adsorbed SO_4^{2-} displacing OH^- from hydrous oxide surfaces, followed by hydrolysis and precipitation of exchangeable Al as in Eqns (11) and (12).



(11)



$$2Al^{3+} + 3Ca(OH)_2 \rightarrow 2Al(OH)_3 + 3Ca^{2+} \quad (12)$$

In a laboratory leaching study, Wang et al. (1999a) applied lime, FBC ash and FGD gypsum in the top 50 mm of repacked columns of a variable charge allophanic soil in New Zealand. The FBC treatment ameliorated both top and sub-surface soil acidity through liming and the "self-liming effect," respectively. The values of soil solution pH of the top and subsurface layers of the allophanic soil in the FBC treatment were significantly ($P < 0.01$) higher than those in the control treatment. Consequently, phytotoxic monomeric Al concentrations in soil solution of the FBC treatment were significantly ($P < 0.01$) reduced. Although FGD treatment had a similar "self-liming effect" on the subsurface of the allophanic soil, it had no significant effect on the topsoil acidity. In contrast, the lime treatment only reduced the topsoil acidity (Fig. 6.6). In a pot experiment, Wang et al. (1999b) found that the FBC and FGD treatments (top 50 mm soil incorporated) significantly improved alfalfa (*Medicago sativa*. L) root penetration into the subsurface of

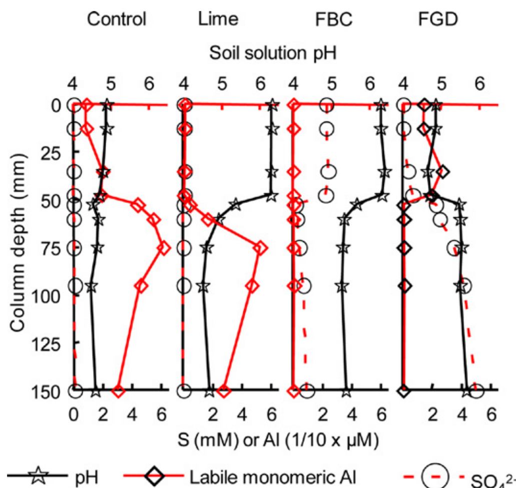


Figure 6.6 Concentrations of labile monomeric Al, sulfate, and pH in soil solutions from sections sampled from leached columns of a variable charged allophanic soil, after lime, FBC and FGD were incorporated into the top 50 mm layer. (*Adapted from Wang et al. (1999a)*). For color version of this figure, the reader is referred to the online version of this book.

the allophonic soil ($P < 0.05$), whereas the lime treatment had no effect on root elongation in the acidic subsurface of the soil (Fig. 6.7). In these experiments, no "self-liming effect" was observed in the subsurface of an ultisol, which is dominated by permanently charged clay minerals (Wang et al., 1999a, 1999b). This indicates that soil mineralogy may influence the effectiveness of "self-liming effect" induced by FBC and FGD materials.

3.1.4. Value-Added CCPs

Adriano et al. (1980) recommended mixing alkaline FA with highly carbonaceous acidic material to make compost for soil treatment. Interestingly, with several essential plant nutrients, CCPs are devoid of the much important humus and nitrogen (Baligar et al., 2011; Menon et al., 1990), which can be supplemented by organic amendments (Adriano et al., 1980; Baligar et al., 2011; Clark et al., 2001; Dou et al., 2003). Similarly, although most of CCPs contain insignificant amount of nitrogen, application of CCPs with organic amendments such as biosolids has been shown to increase the mobilization of N by inducing the mineralization of organic N (Stuczynski et al., 1998). An appreciable change in the soil physicochemical properties, rising of pH and increased rice crop yield was obtained by mixed application of FA and paper factory sludge and farmyard manure (Hill and Lamp, 1980; Molliner and Street, 1982).

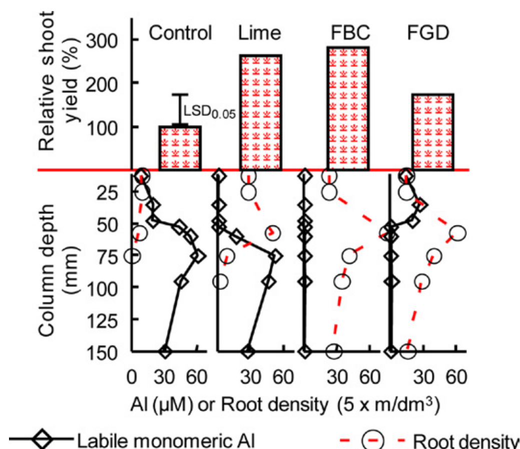


Figure 6.7 Aluminum toxicity and alfalfa growth in pots of a variable-charged allophanic soil, after lime, FBC and FGD were incorporated into the top 50 mm layer. *(Adapted from Wang et al. (1999b))*. For color version of this figure, the reader is referred to the online version of this book.

Use of swine manure with FA increased the availability of Ca and Mg by balancing the ratio between monovalent and bivalent cations ($Na^+ + K^+/Ca^{2+} + Mg^{2+}$), which otherwise proves detrimental to the soil (Giardini, 1991). Calcium readily replaces Na at clay exchange sites to enhance soil flocculation and stability. Vincini et al. (1994) observed that P mobilization was enhanced by production of organic acids and an increase in microbial activity, when FA was amended with swine manure. Zhang et al. (2004) found that co-application of FGD with organic waste reduced the availability of P, from the water-soluble to the bicarbonate extractable, which retained its availability for plant uptake, while reducing the likelihood of environmental losses through leaching.

Sajwan et al. (1995) mixed FA with sewage sludge (SS) at various ratios (SS:FA mixtures of 4:1, 4:2, 4:3, and 4:4) to *Sorghum vulgaris* var. and *Sudanese hitche* ("sorgrass") and found increase in biomass at rates of 50–100 ton acre^{-1} of all ratios of SS:FA mixtures. Schumann and Sumner (1999) used nutrient availability data and linear programming to formulate mixtures of CCPs and biosolids (sewage sludge and animal manure) to successfully avoid CCPs-related issues such as B toxicity, excessive As levels and overliming, and derive environmentally safe CCP formulations. Knox et al. (2006), and Ebanks et al. (2010) and Sajwan et al. (2011) reported that application of 1% FGD either weathered or unweathered to acid soils (pH < 5.5) was beneficial for corn biomass production. However, beyond 1% FGD application, detrimental effects on corn growth were observed

due to high levels of B, As, and Se levels in plant tissues. The combination of FGD and organic materials (e.g. animal manures, biosolids, yard wastes, municipal solid wastes) for land reclamation not only supplies nutrients like N, P, Ca, Si and B but also helps to improve soil structure, WHC and detoxification of Al by chelation (Brown et al., 1998; Power and Dick, 2000). The FGD materials are also used as sterilizing agents for composting some of the organic materials, while enriching the final product with minerals (Baligar et al., 2011).

3.2. Environmental Applications

Coal combustion byproducts are used as an amendment for coal refuse piles and nonagricultural lands, especially for reclaiming mined areas (Stehouwer and Sutton, 1992). Australia has been quite efficient in controlling the GHG emission through sustainable use of available resources in all aspects of industrialization. For example, since 1975, some 16 MT of GHGs have been replaced indirectly by the effective use of FA concrete in Australia (ADAA, 2007). CCPs are used for various environmental application that include the following:

- Phosphorus retention
- Heavy metal immobilization
- AMD mitigation and mine site reclamation
- Carbon sequestration.

3.2.1. Phosphorous Retention

Loss of P through leaching and surface runoff, especially in sandy soils, is a major environmental issue in many places including Australia, resulting in the eutrophication of surface waters (Pierzynski et al., 2005; Sharpley and Moyer, 2000). For example, concentrations of P in runoff from agricultural catchments in southern Australia are high and well above national and international limits (Cox et al., 2005). They argue that P loss is a serious problem in most parts of Australia due to its unique soil (sandy texture) and climatic (xeric; i.e. strong seasonal wetting and drying cycles) conditions. Cheung and Venkitachalam (2000) reported that coarse, sandy soil such as those found in Perth (Western Australia) exhibit low attenuation capabilities for P during effluent infiltration.

Lime and gypsum are often used as the preferred amendment to reduce P loss from agricultural catchments (Murphy and Stevens, 2010) and in South Australia, gypsum is the widely used amendment (Cox et al., 2005) based on: (1) a proven history of yield improvement when applied to some

soils (e.g. Sumner, 2007), (2) being a good source of Ca because of the relatively high solubility of gypsum (compared with liming agents; Bolan et al., 1991), and (3) its ready availability and relative cheapness in South Australia which gives it a potentially cost-effective advantage. Previous work by Stout et al. (1998) indicated that FGD gypsum may be successful in reducing P solubility (through enhancing Ca–P precipitation).

Various CCP sources including FA and BA have shown potential as soil amendments to decrease soil inorganic P solubility (Stout et al., 1998). In New Zealand soils, McDowell (2004) assessed the effectiveness of FA in decreasing P loss from grassland. He observed increased P losses when soil pH was raised with the application of CCPs. However, McDowell (2005) concluded that CCPs could be useful as a supplement or alternative to lime in cropping soils where the pH is commonly maintained at a higher level and may, in these soils, prove beneficial in mitigating P loss. There are limited studies on the direct effects of CCPs on manure applied P in soils that showed potential effects on P immobilization and utilization (Dao, 1999; Dou et al., 2003; Elrashidi et al., 1999).

Apart from FGD and FA, FBC has also been tested in a number of studies to reduce solubility and mobility of P in soils with high P concentration and in P-rich organic wastes (Codling et al., 2002; Dou et al., 2003). Calcium in FBC acts as a P immobilizing agent by reacting with soluble P to form insoluble Ca–P at neutral and alkaline conditions (Lindsay, 1979; Wang et al., 2006). In a packed column leaching study involving dairy manure, Elrashidi et al. (1999) reported that P in leachate in FBC-treated column was reduced by more than 80% compared with the control treatment containing dairy manure only. In a laboratory incubation and extraction study, Dou et al. (2003) found that FBC applied at a rate of 400 g kg^{-1} reduced readily soluble P by 50–60% in P-rich manures including dairy, swine and broiler litter. The CCPs also help in the transformation of P, applied as chemical fertilizers in the soil system (CFRI, 2000; Dou et al., 2003; Johnson et al., 2011; Pierzynski et al., 1990; Seshadri et al., 2010; Seshadri, 2011), leading to prolonged residual effects of CCPs application (Fig. 6.8).

Stout et al. (1998) reported that FBC has consistently reduced concentrations of water-soluble P in a number of soils with high concentration of soluble P. They found that amendment with FBC resulted in a shift from readily available resin P and less available NaOH-extractable Fe- and Al-bound P fractions to HCl-extractable Ca-bound P. They suggest that the neutralizing capacity of FBC is the primary factor in shifting a sizable portion of the soil P to the Ca-bound P fraction. However, considering the high

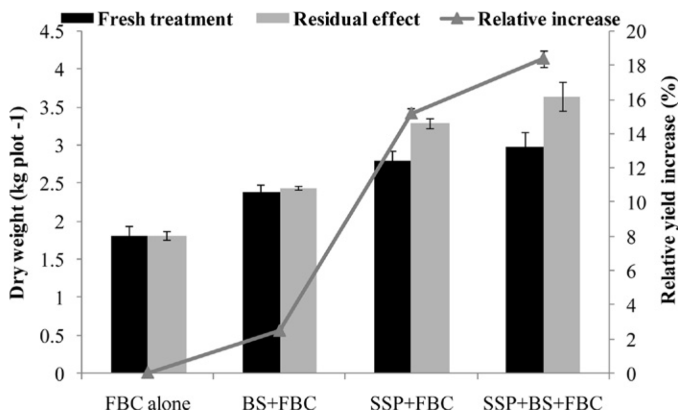


Figure 6.8 Effect of FBC on the sunflower yields in the second cropping. *(Adapted from Seshadri (2011)).*

treatment rates (10 g kg^{-1} or higher, about 22 ton ha^{-1}) required to significantly reduce readily available P in soils, Codling et al. (2002) suggested that FBC may not be suitable for field application to sequester P in high P soils.

Seshadri et al. (2009) compared the effects of various sources of CCPs including FA, FBC and FGD ashes on P sorption in a variable-charge soil. The increase in P sorption with the addition of CCPs has been attributed to an increase in soil pH and an increase in the concentration of aluminum (Al), Iron (Fe) and Ca in soil solution resulting in the formation of insoluble Al–P, Fe–P and Ca–P (McDowell, 2004). The decrease in P sorption with increasing levels of FGD gypsum was attributed to the decrease in soil pH (Fig. 6.9). Bolan et al. (2007) examined P leaching as affected by various liming materials including FBC, which decreased both bioavailable P as measured by Olsen P and leaching of P.

However, McDowell (2004) observed increased P losses in New Zealand pasture soils when soil pH was raised with the application of FBC ash which has been attributed to the solubilization of organic P due to free CaO in this ash byproduct. He consequently concluded that CCPs could be useful as a supplement or alternative to lime in cropping soils, where the pH is commonly maintained at a higher level and may, in these soils, prove beneficial in mitigating P loss (McDowell, 2005).

There are very limited field studies on the application of CCPs to mitigate P-related issues in soil (Johnson et al., 2011; Seshadri, 2011; Stout et al., 2000). For example, Stout et al. (2000) reported that FBC and FGD reduced dissolved P in runoff by 20% and 43%, respectively, when incorporated in

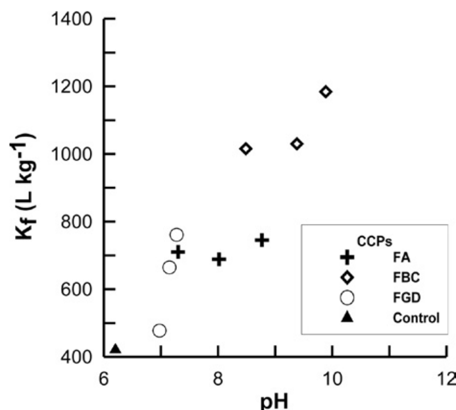


Figure 6.9 Effect of CCPs on K_f value as affected by pH of CCPs amended soil. *(Adapted from Seshadri et al. (2009)).*

the surface 5 cm of an acidic (pH = 6.0) soil at 20 g kg^{-1}. More field studies have to be conducted to determine the effects of various types of CCPs in soils with high P loss, and optimize the composition and application rates of the soil amendments. Seshadri (2011) conducted field experiment in a municipal landfill site, which examined the effect of FBC on P treated as SSP and/or biosolids (BS). The residual effect in the second crop showed the beneficial outcome of the FBC addition as the biomass yields of the plants increased for SSP + FBC- and SSP + BS + FBC-treated plots, which may be attributed to the mobilization of previously retained nutrients as the FBC amended soil ages (Fig. 6.8). The relative yield increase indicated higher bioavailability in the second cropping period and is an indication of long-term effects of FBC application.

3.2.2. Immobilization of Heavy Metals

The uptake and accumulation of trace and heavy metals in grain crops depend on several factors such as pH, OC, CEC, microorganisms, concentration of metals and their form of occurrence, their mobility to the root and transport from root surface to root interior, and their translocation from root to shoot (Ram et al., 2006). The remediation measures required to clean up heavy-metal-contaminated sites is often complex that their implementation becomes economically unsustainable. The value of CCPs as a viable option in immobilizing heavy metals in contaminated soils has been examined in many studies. For example, Ciccu et al. (2001) conducted a study using soils from Italian mine site

contaminated severely with heavy metals and showed decreased levels of heavy metals in percolating water from FA mixed soil, indicating that FA in such soils can lead to immobilization of heavy-metal ions. Some studies have demonstrated the successful immobilization of metals, especially Pb, by P-containing materials and also CCPs, due to the precipitation of pyromorphite-type minerals (Brown et al., 2005; Bertocchi et al., 2006; Cao et al., 2004; Chen et al., 2003; Majumdar and Singh, 2007; McGowen et al., 2001; Melamed et al., 2003; Wang et al., 2008). In a research conducted by Riehl et al. (2010) on a sandy loam, FBC was added to study the difference in physicochemical properties of the soil. They observed an increase in soil pH and also enhanced retention of Cr, Cu, Pb and Zn in the soil.

Soil amendments such as Fe oxides, organic matter, and alkaline materials can reduce metal mobility and availability in soil by adsorption, complexation, (co)precipitation or a combination thereof, and help to restore soil properties (Basta et al., 2005; Park et al., 2011). Iron oxides (FeO_x) have a high sorptive capacity for metals (Brown et al., 2005; Chen et al., 2000; Lombi et al., 2002). Some CCPs that are rich in Fe oxides can be used to overcome problems related to metal solubility (Iyer and Scott, 2001; Misra et al., 1996; Xenidis et al., 2002). Application of CCPs increases the surface area available for element adsorption, improves the physical properties of soil (Gorman et al., 2000), neutralizes the pH of acidic soils and renders most cationic metals less mobile (Ciccu et al., 2003). These authors have demonstrated that relatively small additions of CCPs can drastically reduce the heavy-metal contents of the soil leachates. They attributed this effect to the alkaline nature of the materials used and to the coexistence of constituents potentially capable of absorbing heavy metals.

As mentioned earlier, the CCPs are rich in aluminosilicate elements, which is a prerequisite for zeolite production. Fly ash has been found to be capable of forming a zeolite layer on its surface on contact with water (Sahu, 1999; Wang et al., 2003). Sahu (1999) explained that zeolite layer may form two exchangeable sites to accommodate (1) micronutrients (Fe, Co, Cr, Cu, I, Mn, Se, Zn, and Mo) and (2) macronutrients (Ca, Mg, P, K, Na, S, Cl), which can make CCPs a potential nutrient pump. Although the interaction of elements (adsorption, desorption, and exchange) in soil are being pH dependent, the nutrient pump may be energized selectively for nutrient transfer, thereby supporting rapid growth of plants in the FA-amended soils (Sahu, 1999). Furthermore, during the ash–water interaction, oxyhydroxide

of iron (goethite) is formed and acts as a major scavenger of trace metals. The oxyhydroxide flocculates, either as coating or as discrete grains, and thus immobilize heavy metals, leading to their reduced availability (Leekie et al., 1980; Panuccio et al., 2008).

Kumpiene et al. (2007) demonstrated reduced leaching of Cu and Pb from contaminated soil using FA and peat as soil amendments. They observed that the amendments reduced the exchangeable metal forms, likely because of the formation of new mineral Cu- and Pb-bearing phases and the enhanced metal sorption due to increased amount of sorptive sites. They also observed reduced metal uptake by plants and reduced soil toxicity to microorganisms. This was attributed to the rise of soil pH and the lowered metal mobility due to FA additions. Stehouwer (1995) observed that FBC reduced leachate concentrations of Al, Fe, Mn and Zn that are frequently phytotoxic in acid soils (Table 9). Decreased solubility and mobility of these metals would also improve surface and drainage water quality.

However, the presence of heavy metals in the CCPs may be a concern if applied at higher application rates than current usage of up to 20% w/w (Korcak, 1995). Among the CCPs, FGD has the lowest concentration of heavy metals (Punshon et al., 2001) and can be readily applied for soil remediation and agricultural purposes.

3.2.3. AMD and Mine Site Rehabilitation

The use of CCPs in the presence of an organic material may allow revegetation of mine sites even without a topsoil cap. Addition of a topsoil cap is generally the major expense in reclamation of disturbed lands. Abandoned ash basins have been successfully revegetated with trees without the need for topsoil (Carlson and Adriano, 1993; Cheung et al., 2000; Chaudhary et al., 2011; Chu, 2009; Pillman and Jusaitis, 1997). The common properties of spoils and refuse that restrict plant growth and limit their productivity are (i) acidity, (ii) compaction near the surface and (iii) course texture. In the case of steep-slope terrain, these problems are compounded by erosion, runoff and difficulty in operation machinery. Application of CCPs could remedy some of these problems as most CCPs are alkaline in nature and could neutralize acidity.

Projects conducted by ADAA evaluated the co-utilization of CCPs and organic amendments such as municipal biosolids in disturbed land reclamation and found that the CCPs helped in modifying soil pH and texture; biosolids served as an N source for plant establishment and growth

(ADAA, 2009). As with CCPs, biosolids addition should be accompanied by the maintenance of a suitable pH to keep trace elements in the desired concentration ranges. Application of CCPs could decrease particle size and neutralize acidity if applied in large quantities. This could result in the beneficial reuse of ash and in improved reclamation results (Stewart and Tyson, 1997).

The use of FA in reclamation of coal refuse has been the subject of several experiments (Adams et al., 1972; Jastrow et al., 1981; Singh et al., 2011; Stewart and Tyson, 1997), but has not become a widespread practice in the United States, primarily due to regulatory constraints and the lack of ash sources within many mining districts. The extremely acidic nature of mined lands, resulting from oxidation of Fe and sulphites, often requires basic material additions to bring pH up to the range where plants can grow and trace element availability is controlled. Consequently, the use of CCPs (especially, FBC), which are highly alkaline, can assist in moderating pH to the desired levels thereby reducing trace element availability in acidic soils (Haering and Daniels, 1991; Riehl et al., 2010).

Because of the alkaline nature of many CCPs, a number of studies have examined their effect on modifying soil chemistry, primarily pH. Successful modification of soil pH has been demonstrated with a wide range of CCPs. Agricultural applications in most situations will probably be based on soil pH modification (Korcak and Kemper, 1993). The quantity of CCPs required to reclaim such areas depends on the pH and age (state of weathering) of the product and also pH of the land to be reclaimed. Hence, CCPs serve as an alternative to lime for reclaiming the acidic mine spoils (Carlson and Adriano, 1993; Haering and Daniels, 1991; Ram and Masto, 2010; Wang et al., 2006).

Investigated the efficacy of FBC as an amendment for acidic mine spoils and the potential for adverse environmental impacts from salts and trace elements when FBC was applied at high rates needed for mine spoil reclamation. In their eight-month column leaching and greenhouse study, they found that FBC (60% CCE) was effective in neutralizing acid conditions in the mine spoils when added to spoil at 30–60 g kg^{-1} spoil weight. This solves not only the AMD problem but also disposal difficulties of FBC. They concluded that FBC is very suitable for mine spoil amendment if the amendment is limited to amounts that will not cause excessively high pH, or, phytotoxic salt concentrations. Kost et al. (2005) suggested that the fine particle size and the mineral composition

(CaO, $Ca(OH)_2$, $CaCO_3$ and $CaSO_4$) of FGD can be beneficial in neutralizing soil acidity.

3.2.4. Carbon Sequestration

The carbon intensity of world energy use during 2000–2030 is expected to decrease by about 25%, due to the deployment of efficient and clean fossil fuel combustion technologies, CO_2 sequestration and use of more renewable energy source. ADAA (2007) predicted that by 2030, 72% of global coal-based power generation will be using advanced technologies. But energy-related emissions of CO_2 had almost doubled in the past decade, due to the growth of population and the consequent energy demand in the developing countries (ADAA, 2007).

Gases in the earth's lower atmosphere that may contribute to global warming include CO_2, SO_2, CH_4, NO_x and chlorofluorocarbons (CFCs). The major GHG in Australia's inventory is CO_2, with a share of 73.5% (404.6 Mt), followed by methane (CH_4) which comprises 19.7% (108.5 Mt) and the remaining gases make up 6.7%. These include nitrous oxide (N_2O), perfluorocarbons, hydrofluorocarbons, and sulfur hexafluoride (SF_6). Emission of CO_2 in Australia from various sources has been charted in Fig. 6.10, where energy production tops the chart, followed by agriculture and transports. Global annual emissions based on the various sectors also follow similar trends (Fig. 6.10). In terms of fossil-fuel-related emissions, China leads the emission of CO_2 with around 7000 MT, followed by USA, India and Russia (Fig. 6.11). Although Australia emits less CO_2 (<1000 MT), their per capita C emission is the highest (>5 MT), followed by USA and Canada (Fig. 6.11). Hence, serious measures have to be taken to limit the emission of this GHG in these countries. Also, the rising economies such as India

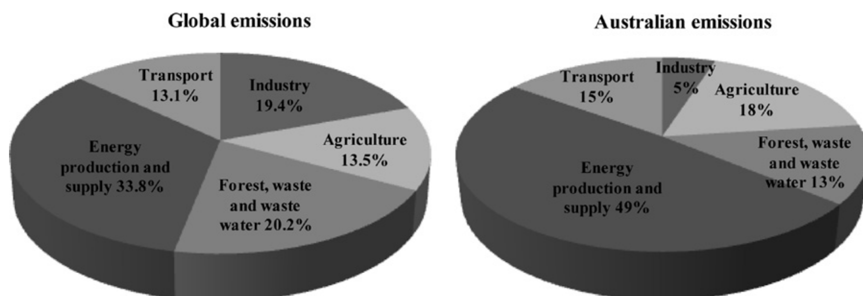


Figure 6.10 Contribution to total net CO_2 emissions for World vs Australia by various sectors. *Boden et al. (2011) and NGGI (2007)*

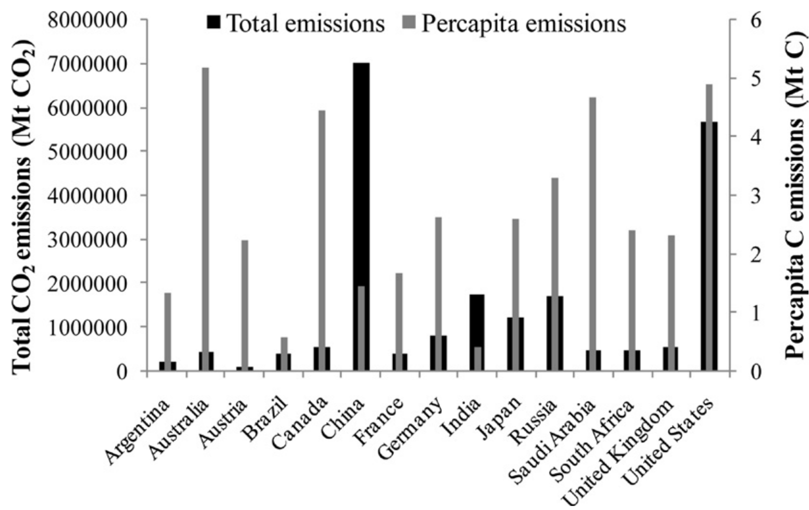


Figure 6.11 Global CO_2 emissions from fossil fuels (solid, liquid and gas) vs Per capita C emissions for selected countries. *Boden et al. (2011)*.

and China are also increasing their emissions through rapid industrial and infrastructural activities.

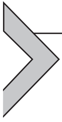
The best approach to mitigate rising CO_2 concentrations and one that is designed to complement the development of energy-efficient technologies is the enhanced storage or sequestration of C in terrestrial ecosystems (e.g. Paustian et al., 1998; Reichle et al., 1999). One aspect of the terrestrial sequestration approach envisions the use of soil and vegetation functioning as long-term storage pools for atmosphere-derived C. To accomplish this, increased sequestration of C can be conceptually achieved by enhancing the natural biological processes that assimilate CO_2 (i.e. increased productivity of lands) and then allocating the assimilated C to plant tissues and/or pools of soil organic matter, resistant to microbial decomposition (Chen et al., 2009; Ussiri and Lal, 2005). Although a key objective in C management research is to enhance the natural capacity of plants and soils to sequester C, the functionality of C storage in terrestrial ecosystems as a whole is a poorly understood process. Many facets of terrestrial C sequestration have been explored, including the use of forest ecosystems, grasslands and agricultural applications (Conant et al., 2001; Denef et al., 2009; Ge et al., 2012; Post and Kwon, 2000; Richter et al., 1994).

Scientists from Tennessee Valley Authority (TVA), USA are working on carbon sequestration using CCPs as a sequestering medium for CO_2

with subsequent conversion of CO_2 into algal biomass for production of methane and other carbon-containing products. The ADAA (2007) focuses on increasing user awareness of the benefits arising through the effective utilization of this valuable mineral byproduct, which if realized, has benefits for industry, the environment and the community as a whole. Highlighting this aspect of the environment, since 1975, about 16 MT of GHGs has been replaced indirectly by the effective use of FA concrete.

The majority of Australian agricultural soils are hard setting due to their poor aggregation or structure and extremely low organic carbon (Chittleborough, 1992; Oades, 1993). Application of CCPs including FA is likely to increase carbon sequestration by promoting formation of humus and physically protecting existing organic carbon from decomposition (Amonette et al., 2003; Palumbo et al., 2004). Alkalinity of CCPs and the Fe oxides contents stabilize tyrosinase enzymes that catalyze oxidative polymerization reactions of humification (humus formation), for which Class F FA is particularly effective (Amonette et al., 2003). The preponderance of nanometer-sized pores, such as plerospheres, physically protects any organic matter that is sorbed onto mineral surfaces from microbial decomposition of humus that liberates carbon dioxide (Palumbo et al., 2004).

Hence, the potential for C sequestration in soils is by indirect improvements on soil properties, thereby facilitating plant growth and C assimilation. Ussiri and Lal (2005) suggested that FGD has the potential for influencing C sequestration in soils. This potential can further be enhanced when these products are supplemented with organic amendments such as mulch, agriculture residues and biosolids (Haering et al., 2000). The direct application of CCPs in mitigating CO_2 emissions is by adsorption at source by CCPs, as they can potentially serve as CO_2 sorbents, forming mineral carbonates and thereby sequestering CO_2 emitted from power plants (Nyambura et al., 2011; Sun et al., 2012). Montes-Hernandez et al. (2009) demonstrated that CO_2 can be adsorbed through the carbonation of carbonate minerals present in CCPs. They found that 1 ton of FA could sequester up to 26 kg of CO_2 (38.18 ton of FA per ton of CO_2 sequestered). This confirms the possibility to use this alkaline residue for CO_2 mitigation. Previously, Fauth et al. (2002) tried contemporary CCPs (FBC and FGD) for sequestering CO_2 by aqueous carbonation and found them as a potential technology for controlling industrial emissions.



4. RISK MANAGEMENT OF CCPS IN THE ENVIRONMENT

Extensive environmental and health impacts studies have been carried out on FA, which contains trace and heavy metals. They can readily percolate down from conventionally used earth-lined ash lagoons and pollute groundwater. Effect of FA on groundwater is a function of physical and chemical characteristics of ash and hydrogeologic and climatic conditions of the disposal site (Ciccu et al., 2003; Goetz, 1983; Kopsick and Angino, 1981; Kumpiene et al., 2007). Weathered FA deposits cause more groundwater contamination because of the presence of higher levels of soluble salts. In unweathered ash, although there is generally a higher release of soluble salts initially, it declines rapidly with time (Hjelmar, 1990; Jones and Lewis, 1960; Kopsick and Angino, 1981; Mattigod et al., 1990; Theis et al., 1978).

FA, particularly when it has been dry collected and handled, contains moderate-to-high levels of soluble salts, primarily sulphates and borates. Dissolution of these salts into soil solution can generate high levels of salts, which can suppress plant growth or actually kill salt-sensitive seedlings and/or established vegetation (Adriano et al., 2002). This behavior is referred to as phytotoxicity, and generally decreases drastically once the ash-bound salts are leached away by rainfall. The soluble salt content of CCPs or CCPs-treated soil is measured by an assessment of the electrical conductance over a water extract. Under strongly acidic conditions (<pH 5.0), ash-bound heavy metals such as Al, Mn, Zn and Cu can also come into solution and become phytotoxic (Daniels et al., 2002). Therefore, application of CCPs mainly depends on the pH of the amended soil (Seshadri, 2011; Fig. 6.9). For example, when the soil pH raises above 8.5 after amending with CCPs, fertilizer P applied to soil can be retained and precipitated in the soil. Similarly, when pH falls below 6.5, mobilization of some of the heavy metals (native or CCPs-derived) may take place and can result in toxic effects to plants. Under such a scenario, phytomining can be a potential option for the environmental management of CCPs in soil. At optimal pH (6–7), the use of CCPs in soil encourages agricultural applications, especially in terms of effective phosphorus management (Figs 6.8 and 6.12).

Very little is known regarding the effects of CCPs amendment on soil biological properties (Schutter and Fuhrmann, 2001). Few studies have been conducted on the size, activity and nature of the microbial community on

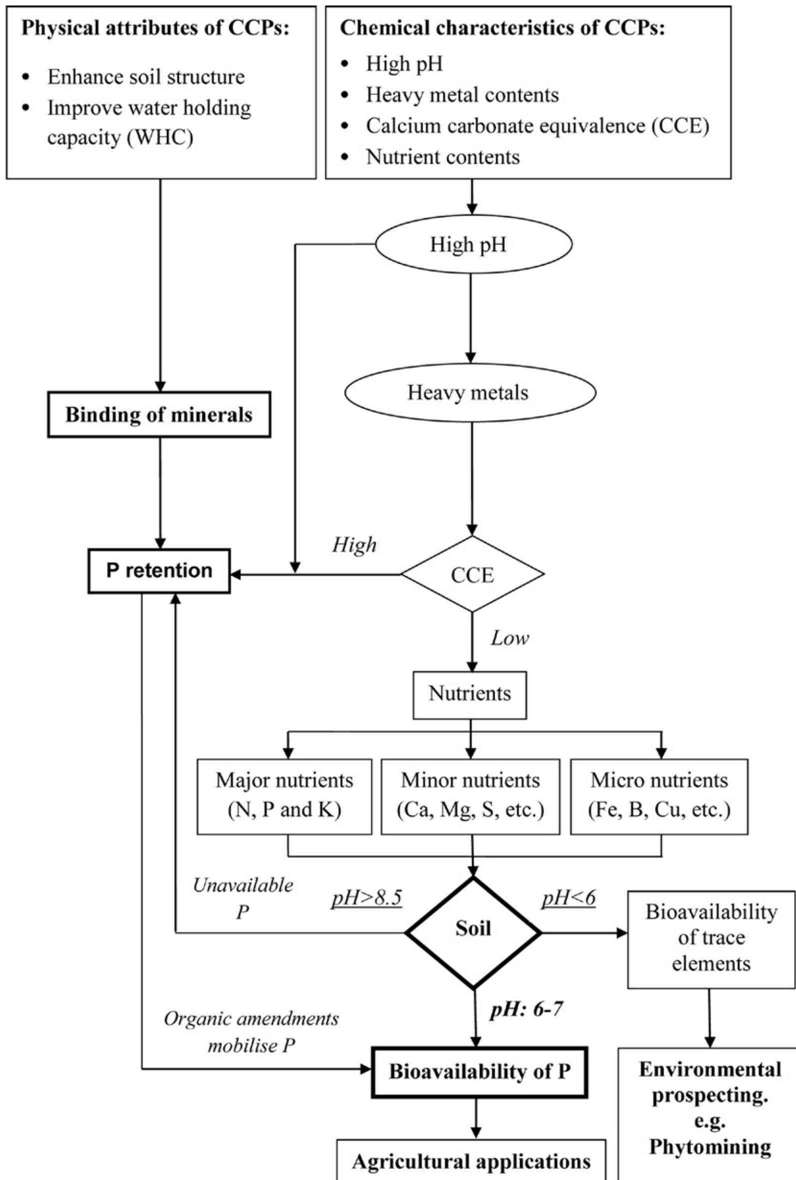


Figure 6.12 Schematic representation on pH-based risk management approaches in the utilization of CCPs.

ash disposal sites. All of the factors discussed above (viz. high pH, salinity, toxicities of B and other elements, poor physical conditions) can limit colonization of microorganisms as well as plants in the ash (Carlson and Adriano, 1993). Even so, by far, the most limiting factors for microbial activity are often a lack of substrate C as an energy source for heterotrophic microorganisms and the lack of an adequate N supply (Klubek et al., 1992).

Several short-term laboratory incubation studies found that addition of unweathered FA to sandy soils severely inhibited microbial respiration, enzyme activity and soil nitrogen cycling processes such as nitrification and N mineralization (Cervelli et al., 1987; Garau et al., 1991; Gupta et al., 2012; Pitchel and Hayes, 1990; Topaç et al., 2008; Wong and Wong, 1986). Adriano et al. (2002) reported that at higher levels of FA, some heavy metals might become more active and hinder microbial activity. These metals form complexes, which undergo transformation, influenced by various factors like pH, moisture, cation exchange and microbial activity (Milovsky and Kononov, 1992).

Generally, the FA particles are small enough to escape emission control devices and easily get suspended in the air. Repeated exposure to FA can cause irritation in eyes, skin, nose, throat and respiratory tract and result in As poisoning (Belkin et al., 1999; Carlson and Adriano, 1993; Davison et al., 1974; Finkelman et al., 2000; Natusch and Wallace, 1974). Fine ash particles formed during coal combustion in power stations, if not collected in the air pollution control devices are emitted into the atmosphere. The fine ash particles can remain airborne for long periods and can result in deleterious health effects when inhaled and deposited in the lungs (Buhre et al., 2005).

Harrison and Yin (2000) conducted epidemiological studies on FA particulate matter exposure and consistently demonstrated adverse effects on human health, the mechanism of effect was unclear. Depending on their toxicity, chemical properties and concentration in the air, FA particles may pose an inhalation hazard to exposed workers. When FA particles are inhaled and deposited in the lung, they can impose health risks by leaching genotoxic compounds, and through the alteration of immunological mechanisms. Studies have indicated that exposure to high concentrations of fine particulate matter may not be the sole contributor to these adverse effects, but that particle toxicology could also play an important role (Harrison and Yin, 2000). The emissions of fine ash particles and trace (toxic) elements from coal combustion are closely associated because of the relative enrichment in trace elements of these fine particles (Lighty et al., 2000). Although the fine particles are enriched in trace elements, their composition is not determined by these elements. Coal composition is shown to

be an important parameter affecting the amount and composition of the submicron ash particles (Buhre et al., 2005).

Toxic heavy metals from CCPs are likely to be leached under acidic conditions. These metals can be easily taken up by humans through drinking water supplies, causing severe health problems:

- Lead—brain, kidney, and nervous system damage
- Cadmium—high blood pressure, liver damage, cancer
- Mercury—deterioration of the nervous system
- Arsenic—carcinogenic

Arsenic is classified as a Class A human carcinogen (US EPA), and is at the top of the most hazardous substances list (ATSDR, 1997). Viriyavejakul and Watanasak (2003) evaluated carcinogenic risks of As present in CCPs and observed that As levels are within the acceptable limits. They also related the potential human health risk with the distance from the contaminated site and concluded that health risk decreased with the distance away from the site.

In vitro studies show that CCPs independent of type of coal combustion, origin or precipitation are capable of exerting cytotoxicity in a number of conventional tests using either animal lung cells, human red blood cells or cell lines such as hamster ovary cells (Borm, 1997). Dogra et al. (1995) demonstrated that inhaling CCPs may result in an impairment of the local immune response of the lungs without an associated effect on the systemic immunity. They have shown that phagocytosis and adherence of alveolar macrophages, as well as the appearance of antibody forming cells in lymph nodes were moderately but significantly affected by in vivo exposure to both FA and silica (Dogra et al., 1995).

In general, CCPs are less toxic than crystalline silica (when used as positive control) but significantly more toxic than negative controls (TiO_2, latex beads, methacrylate polymers). McDonald et al. (2001) observed strong association between silicosis and lung cancer in silica-exposed cohorts, demanding a careful evaluation of the health effects of CCPs containing considerable amount of silica.



5. CONCLUSIONS AND RESEARCH PRIORITIES

Most human activities affect environment, by either degradation or pollution. With the ever-increasing population, the limitations in energy consumption and the demand for CCTs, most countries are targeting efficient technologies to enhance their energy utilization capabilities. The

emission control laws have further motivated the countries to adopt effective measures to tackle the polluting sources. The waste products generated from the combustion technologies also pose threat to the environment. Hence, the contemporary combustion technologies not only focused on emission of harmful gases but also have the potential to restore the degraded environment.

With the number of issues related to soil quality, agriculture and environment, these CCPs have proved to be potential remediators of environmental problems such as soil acidity, mobility of nutrients and heavy metals, and so on. The availability of CCPs at cheaper costs make them a viable option for replacing the usage of their traditional counterparts such as lime and gypsum as they possess similar chemical properties such as high pH and high Ca contents, which is desirable for controlling the mobility of some nutrients (e.g. phosphorus) and heavy metals in soil (e.g. lead). More research on the CCPs emerging from the modern technologies is need of the hour and the potential avenues are briefed below.

The primary advantage of utilizing CCPs is their capability to increase soil pH and provide structural benefits to soil, thereby holding more moisture and nutrients. Some CCPs also supply certain nutrients such as phosphorus, boron, selenium, calcium and sulfur, which are essential for plant growth. The same CCPs also have the potential to deposit undesirable quantities of certain nutrients such as lead, chromium and arsenic if judicious application rates are not followed. It is desirable that the application rates must be optimized for each and every CCPs source so as to cover the diverse range of chemical composition of various CCPs produced from different parent coals. Also, there is a threat of accumulation of heavy metals over a period of repeated application, which requires long-term monitoring studies. The problem of accumulation of toxic metals can be addressed by removal of these undesirable methods through sequential leaching techniques.

Although the CCPs are effective in supplying inorganic nutrients, they are poor in organic matter. This deficiency is addressed by amending CCPs with organic materials such as poultry manure, biosolids, sewage sludge, and so on, because organic materials are important for soil health, providing both structural and chemical benefits. Hence, value-addition of CCPs with these materials can bring up fertilizer-like products with high commercial value. Moreover, FGD's pure nature even helps to sterilize organic materials before using as crop manure. Cocomposting of organic materials with CCPs will increase the quality of the value-added CCPs.

Future research should focus more on the implications of CCPs in improving the biological properties of soil, which requires long-term toxicological studies. The use of molecular biology tools as indicators of health of an organism should be employed. A database similar to NCBI (National Center for Biotechnology Information) should be created, which should cover the aspects such as geology and morphology of parent coal materials; types of combustion technologies used in specific power stations; chemical composition indicating the hazardous levels; and physical characteristics of CCPs generated worldwide. This will serve as a repository for future researchers and environmental land managers. Long-term monitoring studies on the behavior of nutrients and heavy metals are lacking, which is essential to understand the accumulation characteristics. The studies should be conducted at different geochemical, mineralogical and hydrological settings to explore the carbon sequestration potential of CCPs in soil.

REFERENCES

Acton, D.F., Gregorich, L.J., 1995. The Health of our Soils: Toward Sustainable Agriculture in Canada. Centre for Land and Biological Resources Research, Research Branch Agriculture and Agri-Food, Canada Publications 1906/E.

ADAA, 2007. Coal combustions products – assessment criteria for use in agricultural applications. Reference Data Sheet No. 8, April 2007. Ash Development Association of Australia. pp. 1–2.

ADAA, 2008. Annual Membership survey results. January–December 2008. Ash Development Association of Australia. pp. 1–2.

ADAA, 2009. Australian experience with fly ash in concrete: applications and opportunities. Fly ash Technical Note No.8, November 2009. Ash Development Association of Australia. pp. 1–3.

Adams, L.M., Capp, J.P., Gillmore, D.W., 1972. Coal mine spoil and refuse bank reclamation with power plant fly ash. Compost. Sci. 13, 20–26.

Adriano, D.C., Page, A.L., Elseewi, A.A., Chang, A.C., Straughan, I., 1980. Utilization and disposal of fly ash and other coal residues in terrestrial ecosystems: a review. J. Environ. Qual. 9, 333–344.

Adriano, D.C., Page, A.L., Elseewi, A.A., Chang, A.C., 1982. Cadmium availability to sudangrass grown on soils amended with sewage sludge and fly ash. J. Environ. Qual. 11, 197–203.

Adriano, D.C., Weber, J., Bolan, N.S., Paramasivam, S., Koo, Bon-Jun, Sajwan, K.S., 2002. Effects of higher rates of coal fly ash on soil, turfgrass, and groundwater quality. Water Air Soil Pollut. 139, 365–385.

ATSDR – Agency for Toxic Substances and Diseases Registry, 1997. List of Top 20 Hazardous Substances. http://www.heritageresearch.com/Top20HazSub.htm.

Ahmaruzzaman, M., 2010. A review on the utilization of fly ash. Prog. Energ. Conserv. Sci. 36 (3), 327–363.

Ahn, C., Mitsch, W.J., Wolfe, W.E., 2001. Effects of recycled FGD liner on water quality and macrophytes of constructed wetlands: a mesocosm experiment. Water Res. 35, 633–642.

Aitken, R.L., Campbell, D.J., Bell, L.C., 1984. Properties of Australian fly ashes relevant to their agronomic utilization. Aust. J. Soil Res. 22, 443–453.

Aitken, R.L., Bell, L.C., 1985. Plant uptake and phytotoxicity of boron in Australian fly ashes. Plant Soil 84, 245–257.

Alva, K., Paramasivam, S., Prakash, O., Sajwan, K.S., Ornes, W.H., Van Clief, D., 1999. Effects of fly ash and sewage sludge amendments on transport of metals in different soils. In: Sajwan, K.S., Alva, A.K., Keefer, R.F. (Eds.), Biogeochemistry of Trace Elements in Coal and Coal Combustion By-products, Kluwer Academic/Plenum Publishers, New York, pp. 207–222.

Amonette, J.E., Kim, J., Russell, C.K., Palumbo, A.V., Daniels, W.L., 2003. Fly ash catalyzes carbon sequestration. Proceedings Second Annual Conference on Carbon Sequestration, Alexandria, Virginia.

Andini, S., Cioffi, R., Colangelo, F., Ferone, C., Montagnaro, C., Santoro, L., 2010. Characterization of geopolymer materials containing MSWI fly ash and coal fly ash. Adv. Sci. Technol. 69, 123–128.

Arenas, C.G., Marrero, M., Leiva, C., Soli-Guzman, J., Arenas, L.F.V., 2011. High fire resistance in blocks containing coal combustion flyashes and bottomash. Waste Manag. 31 (8), 1783–1789.

Asokan, P., 2003. Application of Coal Combustion Residues in Hazardous Waste Management. Second Annual Progress Report. Indian Institute of Technology, Bombay, India.

Baligar, V.C., Clark, R.B., Korcak, R.F., Wright, R.J., 2011. Flue gas desulphurization product use on agricultural land. Adv. Agron. 111, 51–86.

Baltasar, J., Carvalho, M.G., Coelho, P., Costa, M., 1997. Fluegas recirculation in a gas-fired laboratory furnace: measurements and modeling. Fuel 76 (10), 919–929.

Basta, N.T., Rayan, J.A., Chaney, R.L., 2005. Trace element chemistry in residual-treated soil: key concepts and metal bioavailability. J. Environ. Qual. 34, 49–63.

Basu, M., Pande, M., Bhadoria, P.B.S., Mahapatra, S.C., 2009. Potential fly-ash utilisation in agriculture: a global review. Progr. Nat. Sci. 19, 1173–1186.

Beer, J.M., 2000. Combustion technology developments in power generation in response to environmental challenges. Progr. Energ. Combust. Sci. 26 (4), 301–327.

Beer, J.M., 2007. High efficiency electric power generation: the environmental role. Progr. Energ. Combust. Sci. 33 (2), 107–134.

Belkin, H.E., Finkelman, R.B., Zhang, B.S., 1999. Arsenic poisoning caused by residential coal combustion in Guizhou Province, China. Pan-Asia-Pacific Conference on Fluoride and Arsenic Research, Shenyang.

Bertocchi, A.F., Ghiani, M., Peretti, R., Zucca, A., 2006. Red mud and fly ash for remediation of mine sites contaminated with As, Cd, Cu, Pb and Zn. J. Hazard. Mater. 134, 112–119.

Bhattacharya, S.S., Chattopadhyay, G.N., 2004. Transformation of nitrogen during vermicomposting of fly ash. Waste Manag. Res. 22, 488–491.

Bhattacharyya, S., Donahoe, R.J., Patel, D., 2009. Experimental study of chemical treatment of coal flyash to reduce the mobility of priority trace elements. Fuel 88 (7), 1173–1184.

Bhumbla, D.K., Singh, R.N., Keeker, R.F., 1991. Water quality from surface mined land reclaimed with fly ash. Proceedings of the 9th Ash Use Symposium. American Coal Ash Association, vol. 57. Academic Press, Orlando, Florida, pp. 1–22.

Bilodeau, A., Malhotra, V.M., 2000. High volume fly ash system: concrete solution for sustainable development. ACI Mater. J. 97 (1), 41–48.

Binet, F., Le Bayon, R.C., 1999. Space-time dynamics in situ of earthworm casts under temperate cultivated soils. Soil Biol. Biochem. 31, 85–93.

Boden, T., Marland, G., Andres, B., 2011. Carbon Dioxide Emissions from Fossil-fuel Consumption and Cement Manufacture. Carbon dioxide Information Analysis Centre, Oak Ridge Tennessee. http://cdiac.ornl.gov/ftp/ndp030/nation.1751_2008.ems.

Bolan, N.S., Syers, J.K., Sumner, M.E., 1991. Evaluation of the dissolution of various sources of gypsum in aqueous solutions and in soil. J. Sci. Food. Agric. 57, 527–541.

Bolan, N.S., Naidu, R., Wang, H., 2007. Utilization of coal combustion products (CCPs) for environmental remediation. In: Zhu (Ed.), Biogeochemistry of Trace Elements: Environmental Protection, Remediation and Human Health, Tsinghua University Press, Beijing, pp. 352–353.

Bool, L., Kobayashi, H., 2003. NOx Reduction from a 44 MW Wall-fired Boiler Using Oxygen Enhanced Combustion. Clear water conference, Tonawanda, New York. pp. 1–6.

Borm, P.J.A., 1997. Toxicity and occupational health hazards of coal fly ash (CFA). A review of data and comparison to coal mine dust. Ann. Occup. Hyg. 41, 659–676.

Brooks, R., Udoeyo, F.F., Takalapelli, K.V., 2011. Geotechnical properties of problem soils stabilized with fly ash and limestone dust in Philadelphia. J. Mater. Civ. Eng. 23, 711–717.

Brown, S., Angle, J.S., Jacobs, L., 1998. Beneficial Co-utilization of Agricultural, Municipal and Industrial By-products. Kluwer Academic Publishers, Boston, MA.

Brown, S., Christensen, B., Lombi, E., McLaughlin, M., McGrath, S., Colpaert, J., Vangronsveld, J., 2005. An inter-laboratory study to test the ability of amendments to reduce the availability of Cd, Pb, and Zn *in situ*. Environ. Pollut. 138, 34–45.

Buhre, B.J.P., Hinkley, J.T., Gupta, R.P., Wall, T.F., Nelson, P.F., 2005. Submicron ash formation from coal combustion. Fuel 84, 1206–1214.

Butalia, T.S., Wolfe, W.E., 2001. Utilization of Coal Combustion Products in Ohio for Construction and Repair of Highways. Beneficial Use of Recycled Materials in Transportation Applications Conference. Arlington, Virginia. pp. 803–812.

Campbell, D.J., Fox, W.E., Aitken, R.L., Bell, L.C., 1983. Physical characteristics of sands amended with fly ash. Aust. J. Soil Res. 21, 147–154.

Cao, R.X., Ma, L.Q., Rhue, D.R., Appel, C.S., 2004. Mechanisms of lead, copper, and zinc retention by phosphate rock. Environ. Pollut. 131, 435–444.

Carlson, C.L., Adriano, D.C., 1993. Environmental impacts of coal combustion residues. J. Environ. Qual. 22, 227–247.

Cervelli, S., Petruzelli, G., Perna, A., 1987. Fly ashes as an amendment in cultivated soils. I. Effect on mineralization and nitrification. Water Air Soil Pollut. 33, 331–338.

CFRI (Central Fuel Research Institute), 2000. Bulk scale utilization of coal ash in agriculture and for reclamation of waste/degraded lands of Murshidabad District in West Bengal. CFRI, Dhanbad, Jharkhand. CFRI Report No. TR/CFRI/3.04/1999–2000.

Chabbi, A., Rumpel, C., 2004. Chemical composition of organic matter in extremely acid, lignite-containing lake sediments impacted by flyash contamination. J. Environ. Qual. 33, 628–636.

Chaudhary, S.K., Rai, U.N., Mishra, K., Huang, H.G., Yang, X.E., Inouhe, M., Gupta, D.K., 2011. Growth and metal accumulation potential of *Vigna radiata* L. grown under fly ash amendments. Ecol. Eng. 37 (10), 1583–1588.

Chen, H.M., Zheng, C.R., Tu, C., Shen, Z.G., 2000. Chemical methods and phytoremediation of soil contaminated with heavy metals. Chemosphere 41, 229–234.

Chen, M., Ma, L.Q., Singh, S.P., Cao, R.X., Melamed, R., 2003. Field demonstration of in situ immobilization of soil Pb using P amendments. Adv. Environ. Res. 8, 93–102.

Chen, L., Dick, W.A., Nelson, S., 2005. Flue gas desulfurization products as sulfur sources for alfalfa and soybean. Agron. J. 97, 265–271.

Chen, S., Lin, G., Huang, J., Jenerette, G.D., 2009. Dependence of carbon sequestration on the differential responses of ecosystem photosynthesis and respiration to rain pulses in a semiarid steppe. Global Change Biol. 15 (10), 2450–2461.

Cheung, K.C., Venkitachalam, T.H., 2000. Improving phosphate removal of sand infiltration system using alkaline fly ash. Chemosphere 41, 243–249.

Cheung, K.C., Wong, G.P.K., Zhang, Z.Q., Wong, J.W.C., Wong, M.H., 2000. Revegetation of lagoon ash using the legume species *Acacia auriculiformis* and *Leuceana leucocephala*. Environ. Pollut. 109 (1), 75–82.

Chindaprasirt, P., Jaturapitakkul, C., Chalee, W., Rattanasak, U., 2009. Comparative study on the characteristics of fly ash and bottomash geopolymers. Waste Manag. 29 (2), 539–543.

Chittleborough, D.J., 1992. Formation and pedology of duplex soils. Aust. J. Exp. Agric. 32, 815–825.

Chu, L.M., 2009. Natural revegetation of coal fly ash in a highly saline disposal lagoon in Hong Kong. Appl. Veg. Sci. 11 (3), 297–306.

Chugh, Y., Patwardhan, A., Munish, S., Botha, F., 2006. Development of construction materials using sulfite-rich scrubber sludge and fly ash. Fuel 85, 2323–2329.

Ciccu, R., Ghiani, Peretti, R., Serci, A., Zucca, A., 2001. Heavy Metal Immobilisation Using Fly Ash in Soils Contaminated by Mine Activity. International Ash Utilisation Symposium, www.flyash.info.

Ciccu, R., Ghiani, M., Serci, A., Fadda, S., Peretti, R., Zucca, A., 2003. Heavy metal immobilization in the mining-contaminated soils using various industrial wastes. Miner. Eng. 16, 187–192.

Ciravolo, T.G., Adriano, D.C., 1979. Utilisation of coal ash by crops under green house conditions. In: Wali, M. (Ed.), Ecology and Coal Resources Development, Pergamon Press, New York, p. 958.

CIRCA, 2010. Fly ash Update #1.Canadian Industries Recycling Coal Ash, November 2010. http://www.circainfo.ca/PDF/Fly%20Ash%20Update%201%20-%20Nov%202010.pdf (accessed 20.03.12.).

Clark, R.B., Ritchey, K.D., Baligar, V.C., 2001. Benefits and constraints for use of FGD products on agricultural land. Fuel 80, 821–828.

Codling, E.E., Mulchi, C.L., Chaney, R.L., 2002. Biomass yield and phosphorus availability to wheat grown on high phosphorus soils amended with phosphate inactivating residues. III. Fluidized bed coal combustion ash. Comm. Soil Sci. Plant Anal. 33, 1085.

Conant, R.T., Paustian, K., Elliott, E.T., 2001. Grassland management and conversion into grassland: effects on soil carbon. Ecol. Appl. 11, 343–355.

Cox, J.W., Varcoe, J., Chittleborough, D.J., Leeuwen, J.V., 2005. Using gypsum to reduce phosphorus in runoff from subcatchments in South Australia. J. Environ. Qual. 34, 2118–2128.

Daniels, L.W., Stewart, B., Haering, K., Zipper, C., 2002. The Potential for Beneficial Reuse of Coal Fly Ash in Southwest Virginia Mining Environments. Virginia Cooperative Extension, http://www.ext.vt.edu/pubs/mines/460-134/460-134.html#L4 460–434.

Dao, T.H., 1999. Co-amendments to modify phosphorus extractability and nitrogen:phosphorus ratio in stockpiled and composted feedlot manure. J. Environ. Qual. 28, 1114–1121.

Davison, R., Natusch, D., Wallace, J., 1974. Trace elements in fly ash: dependence of concentration on particle size. Environ. Sci. Technol. 8, 1107–1113.

Denef, K., Roobroeck, D., Wadu, M., Lootens, P., Boeckx, P., 2009. Microbial community composition and rhizodeposit-carbon assimilation in differently managed temperate grassland soils. Soil Biol. Biochem. 41 (1), 144–153.

Dhadse, S., Kumari, P., Bhagia, L.J., 2008. Fly ash characterization, utilization and government initiatives in India – a review. J. Sci. Ind. Res. 67, 11–18.

Dick, W.A., Stehouwer, R., Bingam, J.M., Wolfe, W.E., Hao, Y., Adriano, D.C., Beeghly, J.H., Haefner, R.J., 2000. Beneficial uses of flue gas desulphurisation by-products: examples and case studies of land application. In: Power, J.F., Dick, W.A. (Eds.), Land Application of Agricultural, Industrial and Municipal By-products, Soil Science Society of America, Madison, Wisconsin, pp. 505–536.

Dogra, S., Khanna, A.K., Kaw, J.L., 1995. Alterations in the pulmonary and systemic immune response in rats exposed to coal fly ash. Immunopharmacology 29, 103–109.

Dou, Z., Zhang, G.Y., Stout, W.L., Toth, J.D., Ferguson, J.D., 2003. Efficacy of alum and coal combustion by-products in stabilizing manure phosphorus. J. Environ. Qual. 32, 1490–1497.

Ebanks, S., Paramasivam, S., Alva, A., Sajwan, K., 2010. Effect of flue gas desulfurization wastes on corn plants. 19th World Congress of Soil Science 1–7 August, 2010, Brisbane, Australia.

ECOBA, 2008. Statistics on Production and Utilisation of CCPs in Europe (EU15). European Coal Combustion Products Association. www.ecoba.org.

El-Mogazi, D., Lisk, J.D., Weinstein, L.H., 1988. A review of physical, chemical and biological properties of fly ash and effects on agricultural ecosystems. Sci. Total Environ. 74, 1–37.

Elrashidi, M.A., Baligar, V.C., Korcak, R.F., Persaud, N., Ritchey, K.D., 1999. Chemical composition of leachate of dairy manure mixed with fluidized bed combustion residue. J. Environ. Qual. 28, 1243–1251.

Elseewi, A.A., Binghman, F.T., Page, A.L., 1978. Growth and mineral composition of lettuce and swiss chard grown on flyash amended soils. In: Adriano, D.C., Brisbin, I.L. (Eds.), Environmental Chemistry and Cycling Processes, p. 568 Conf. 760429, U.S. Department of Commerce, Springfield, Virginia.

Fauth, D.J., Soong, Y., White, C.M., 2002. Carbon Sequestration Utilising Industrial Solid Residues. Preprints Symposium, American Chemical Society, Division Fuel Chemistry pp. 37–38.

Fernández-Turiel, J.L., deCalvalho, W., Cabanas, M., Querol, X., López-Soler, A., 1994. Mobility of heavy metals from coal fly ash. Environ. Geol. 23, 264–270.

Finkelman, R.B., Belkin, H.E., Zhang, B.S., Centeno, J.A., 2000. Arsenic poisoning caused by residential coal combustion. Proceedings of the 31st International Geological Congress, Guizhou Province, China.

Franco, A., Diaz, A.R., 2009. The future challenges for “clean coal technologies”: joining efficiency increase and pollutant emission control. Energy 34 (3), 348–354.

Fulekar, M.H., Dave, J.N., 1986. Disposal of fly ash – an environmental problem. Int. J. Environ. Stud. 26, 191–215.

Furr, A.K., Parkinson, T.F., Hinrich, R.A., van Campen, R.A., Bache, D.R., Gutenmann, W.H., St. John, L.E., Pakkala, I.S., Lisk, D.J., 1977. National survey of elements and radioactivity in fly ashes. Sci. Technol. 11, 1194–1201.

Fu, J., 2010. Challenges to Increased Use of Coal Combustion Products in China. Thesis submitted to Linkoping University.

GA – Geoscience Australia, 2010. Coal Resources. Commonwealth of Australia. Australian Government website. http://www.ga.gov.au/energy/coal-resources.html (accessed 20.06.11.).

Garau, M.A., Dalmau, I.L., Felipo, M.T., 1991. Nitrogen mineralization in soil amended with sewage sludge and fly ash. Biol. Fertil. Soils 12, 199–201.

Gautam, S., Patra, A.K., Prusty, B.K., 2012. Opencast mines: a subject to major concern for human health. Int. Res. J. Geol. Min. 2 (2), 25–31.

Ge, T., Yuan, H., Zhu, H., Wu, X., Nie, C., Liu, C., Tong, C., Wu, J., Brookes, P., 2012. Biological carbon assimilation and dynamics in a flooded rice-soil system. Soil Biol. Biochem. 48, 39–46.

Ghosal, S., Self, S.A., 1995. Particle size-density relation and cenosphere content of coal fly ash. Fuel 74 (4), 522–529.

Giardini, L., 1991. Agronomic aspects of manure management. J. Agric. Eng. 12, 679–689.

Goetz, L., 1983. Radiochemical techniques applied to laboratory studies of water leaching of heavy metals from coal fly ash. Water Sci. Technol. 15, 25–47.

Goodarzi, F., Huggins, F.E., Sanei, H., 2008. Assessment of elements, speciation of As, Cr, Ni and emitted Hg for a Canadian power plant burning bituminous coal. Int. J. Coal Geol. 74, 1–12.

Gorman, J.M., Sencindiver, J.C., Horvath, D.J., Singh, R.N., Keefer, R.F., 2000. Erodibility of fly ash used as a topsoil substitute in mineland reclamation. J. Environ. Qual. 29, 805–811.

Gupta, D.K., Rai, U.N., Tripathi, R.D., Inouhe, M., 2002. Impacts of fly-ash on soil and plant responses. Plant Res. 115, 401–409.
Gupta, M., Koyle, I., Thambimuthu, K., 2003. CO_2 capture technologies and opportunities in Canada. Strawman document for CO_2 capture and storage (CC&S) Technology road map. 1st Canadian CC&S Technology Roadmap Workshop.18–19 September 2003. Calgary, Alberta, Canada.
Gupta, A.K., Singh, R.P., Ibrahim, M.K., Lee, B.K., 2012. Fly ash for agriculture: implications for soil properties, nutrients, heavy metals, plant growth and pest control. Sustain. Agric. Rev. 8, 269–286.
Haering, K.C., Daniels, W.L., 1991. Fly ash: characteristics and use in mineland reclamation. A literature review. Virginia Coal Energ. J. 3, 33–46.
Haering, K.C., Daniels, W.L., Feagley, S.E., 2000. Reclaiming mined lands with biosolids, manures, and papermill sludges. Chapter 24. In: Barnhisel, R.E., Daniels, W.L., Darmody, R.G. (Eds.), Reclamation of Drastically Disturbed Lands, second ed. American Society of Agronomy, Madison, Wisconsin.
Harben, P.W., 1999. The Industrial Minerals Handbook, third ed.. Industrial Minerals Information Ltd, London.
Harrison, R.M., Yin, J., 2000. Particulate matter in the atmosphere: which particle properties are important for its effects on health? Sci. Total Environ. 249, 85–101.
Haynes, R.J., 2009. Reclamation and revegetation of flyash disposal sites – challenges and research needs. J. Environ. Manage. 90 (1), 43–53.
Heidrich, C., 2003. Ash Utilization – an Australian Perspective. International Ash Utilization Symposium. Centre for Applied Energy Research, University of Kentucky.
Hendryx, M., Ahern, M.M., 2008. Relations between health indicators and residential proximity to coal mining in West Virginia. Am. J. Public Health 98 (4), 669–671.
Hill, M.J., Lamp, C.A., 1980. Use of pulverised fuel ash from Victorian brown coal as a source of nutrients for a pasture species. Aust. J. Exp. Agric. Anim. Husb. 20, 377–384.
Hjelmar, O., 1990. Leachate from land disposal of coal fly ash. Waste Manag. Res. 8, 429–449.
Huang, X., Hwang, J.Y., Gillis, J.M., 2003. Processed low NO_x fly ash as a filler in plastics. J. Miner. Mater. Characterization and Engineering 2 (1), 11–31.
IEA International Energy Agency, 2002. Solutions for 21st Century – Zero Emissions Technologies for Fossil Fuels. International Energy Agency, 2002.
IEA – International Energy Agency, 2008. World Energy Outlook. International Energy Agency, Paris.
Iyer, R.S., Scott, J.A., 2001. Power station fly ash – a review of value-added utilization outside of the construction industry. Resour. Conserv. Recycl. 31, 217–228.
Jala, S., Goyal, D., 2006. Fly ash as a soil ameliorant for improving crop production – a review. Bioresour. Technol. 97, 1136–1147.
Jankowski, J., Ward, C.R., French, D., Groves, S., 2006. Mobility of trace elements from selected Australian fly ashes and its potential impact on aquatic ecosystems. Fuel 85, 243–256.
Jastrow, J.D., Zimmennan, C.A., Dvorak, A.J., Hinchman, R.R., 1981. Plant growth and trace element uptake on acidic coal refuse amended with lime or fly ash. J. Environ. Qual. 10, 154–160.
JCOAL, 2010. Status of Coal Ash Production. Retrieved on April 12, 2012, from JCOAL. http://www.jcoal.or.jp/coaltech_en/coalash/ash01e.html.
Johnson, K.N., Allen, A.L., Kleinman, P.J.A., Hashem, F.M., Sharpley, A.N., Stout, W.L., 2011. Effect of coal combustion by-products on phosphorus runoff from a coastal plain soil. Comm. Soil Sci. Plant Anal. 42, 778–789.
Jones, L.H., Lewis, A.V., 1960. Weathering of fly ash. Nature 185, 404–405.
Kalra, N., Jain, M.C., Joshi, H.C., Choudhary, R., Harit, R.C., Vatsa, B.K., Sharma, S.K., Kumar, V., 1998. Flyash as a soil conditioner and fertilizer. Bioresour. Technol. 64, 163–167.

Kalyoncu, R.S., 2001. Coal combustion products – production and uses. Proceedings of 18th Pittsburgh International Coal Conference, p. 16 New Castle, Australia.
Karapanagioti, H.K., Atalay, A.S., 2001. Laboratory evaluation of ash materials as acid disturbed land amendments. Global Nest Int. J. 3 (1), 11–21.
Kim, A.G., 2002. Physical and chemical characteristics of CUB. In: Vories, K.C., Throgmorton, D. (Eds.), Proceedings of Coal Combustion By-products and Western Coal Mines, US Department of Interior, Office of Surface Mining Coal Research Center, Southern Illinois University at Carbondale, p. 18.
Klubek, B., Carlson, C.L., Oliver, J., Adriano, D.C., 1992. Characterization of microbial abundance and activity from three coal ash basins. Soil Biol. Biochem. 24, 1119–1125.
Knights, P., Hood, M., 2009. Coal and the Commonwealth – The Greatness of an Australian Resource. The University of Queensland, Brisbane, Australia 1–192.
Knox, A.S., Knox, J.D., Adriano, D.C., Sajwan, K.S., 2006. Influence of coal combustion flue gas desulfurization waste on elements uptake by maize. In: Sajwan, K.S., Twardowska, I., Punshon, T., Alva, A.K. (Eds.), Coal Combustion Byproducts and Environmental Issues, Springer Publishers, New York, pp. 184–189.
Kolias, S., Rogopoulou, V.K., Karahalios, A., 2005. Stabilisation of clayey soils with high calcium flyash and cement. Cement Concr. Compos. 27 (2), 301–313.
Kopsick, D.A., Angino, E.E., 1981. Effect of leachate solutions from fly and bottom ash on groundwater quality. J. Hydrol. 54, 341–356.
Kost, D.A., Bigham, J.M., Stehouwer, R.C., Beeghly, J.H., Fowler, R., Traina, S.J., Wolfe, W.E., Dick, W.A., 2005. Chemical and physical properties of dry flue gas desulfurization products. J. Environ. Qual. 34, 676–685.
Korcak, R.F., 1985. Effect of coal combustion waste used as lime substitutes on nutrition of apples on three soils. Plant Soil 85, 437–441.
Korcak, R.F., Kemper, W.D., 1993. Long-term effects of gypsiferous coal combustion ash applied at disposal levels on soil chemical properties. Plant Soil 154, 29–32.
Korcak, R.F., 1995. Utilization of coal combustion by-products in agriculture and horticulture. In: Karlen, D.L., Wright, R.J., Kemper, W.O. (Eds.), Agriculture Utilization of Urban and Industrial By-products, ASA Special Publication No 58. ASA, CSSA, SSSA, Madison, Wisconsin, pp. 107–130.
Korcak, R.F., 1998. Agricultural uses of municipal, animal, and industrial byproducts. In: Wright, R.J., Kemper, W.D., Milner, P.D., Power, J.F., Korcak, R.F. (Eds.), Conservation Research Report No. 44, US Department of Agriculture, Agricultural Research Service, Beltsville, M.D.
Kumar, D., Singh, B., 2003. The use of coal fly ash as in sodic soil reclamation. Land Degrad. Dev. 14, 285–299.
Kumpiene, J., Lagerkvist, A., Maurice, C., 2007. Stabilization of Pb- and Cu-contaminated soil using coal fly ash and peat. Environ. Pollut. 145, 365–373.
Kutchko, B.G., Kim, A.G., 2006. Fly ash characterization by SEM-EDS. Fuel 85, 2537–2544.
Lerner, D.N., Harris, B., 2009. The relationship between land use and groundwater resources and quality. Land Use Pol. 26 (1), 265–273.
Lee, C.H., Lee, Y.B., Lee, H., Kim, P.J., 2007. Reducing phosphorus release from paddy soils by a fly ash–gypsum mixture. Bioresour. Technol. 98, 1980–1984.
Leekie, J.O., Benjamin, M.M., Kaufman, H.A., Atman, S., 1980. Adsorption/Co-precipitation of Trace Elements from Water with Iron Oxy-hydroxides. Electric Power Research Institute, Palo Alto, California.
Li, Y., Liu, C., Luan, Z., Peng, X., Zhu, C., Chen, Z., Zhang, Z., Fan, J., Jia, Z., 2006. Phosphate removal from aqueous solutions using raw and activated red mud and fly ash. J. Hazard. Mater. 137 (1), 374–383.
Lighty, J.S., Veranth, J.M., Sarofim, A.F., 2000. Combustion aerosols: factors governing their size and composition and implications to human health. J. Air Waste Manag. Assoc. 50 (9), 1565–1618.

Lindsay, W.L., 1979. Chemical Equilibria in Soils. John Wilsey and Sons, New York.
Logan, T.J., Traina, S.J., 1993. Trace metals in agricultural soils. In: Allen, H.E. (Ed.), Metals in Groundwater, Lewis Publishers, Chelsea, Michigan, pp. 309–347.
Lombi, E., Zhao, J., Zhang, G., Sun, B., Fitz, W., Zhang, H., McGrath, S.P., 2002. *In situ* fixation of metals in soils using bauxite residue: chemical assessment. Environ. Pollut. 118, 435–443.
Longhurst, J.W., 1991. Acid Deposition: Origins, Impacts and Abatement Strategies. Springer, Berlin 353.
Longwell, J., Rubin, E.S., Wilson, J., 1995. Coal: energy for the future. Progr. Energ. Combust. Sci. 21, 269–360.
Magel, H.C., Schnell, U., Hein, K.R.G., 1996. Simulation of detailed chemistry in a turbulent combustor flow. Symp. Combust. 26 (1), 67–74.
Majumdar, K., Singh, N., 2007. Effect of soil amendments on sorption and mobility of metribuzin in soils. Chemosphere 66, 630–637.
Manoharan, V., Yunusa, I.A.M., Loganathan, L.R., Burchett, M.D., Murray, B.R., Skilbeck, G.C., Eamus, D., 2010a. Boron contents and solubility in Australian fly ashes and its uptake by canola (*Brassica napus* L.) from the ash-amended soils. Aust. J. Soil Res. 48, 480–487.
Manoharan, V., Yunusa, I.A.M., Loganathan, P., Lawrie, R., Skilbeck, G.C., Burchett, M.D., Murray, B.R., Eamus, D., 2010b. Assessments of class F fly ashes for amelioration of soil acidity and their influence on growth and uptake of Mo and Se by canola. Fuel 89, 3498–3504.
Manz, O.E., 1999. Coal fly ash – a retrospective and future look. Fuel 78, 133–136.
Marsh, B.H., Grove, J.H., 1992. Plant and soil composition as affected by an alternative lime source containing sulphate. Soil Sci. Soc. Am. J. 56, 1831.
Martens, D.C., Schnappinger, M.G., Doran, J.W., Milford, F.R., 1970. Fly ash as a fertilizer. Proceedings of 2nd Ash Utilization Symposium, U.S. Department of Interior Bureau Mines Information Circle 8488, Pittsburgh. Pennsylvania, pp. 310–326.
Mattigod, S.V., Rai, D., Early, L.E., Ainsworth, C.C., 1990. Geochemical factors controlling the mobilization of inorganic constituents from fossil fuel combustion residues: I. Review of the major elements. J. Environ. Qual. 19, 188–201.
McDonald, A.D., McDonald, J.C., Rando, R.J., Hughes, J.M., Cohort, W.H., 2001. Mortality study of North American industrial sand workers. I. Mortality from lung cancer, silicosis and other causes. Ann. Occup. Hyg. 45, 193–199.
McDowell, R.W., 2004. The effectiveness of Industrial by-products to stop phosphorus loss from a pallic soil. Aust. J. Soil Res. 42, 755–761.
McDowell, R.W., 2005. The effectiveness of coal fly-ash to decrease phosphorus loss from grassland soils. Aust. J. Soil Res. 43, 853–860.
McDowell, R.W., Condron, L.M., Stewart, I., 2008. An examination of potential extraction methods to assess plant-available organic phosphorus in soil. Biol. Fertil. Soils 44, 707–716.
McGowen, S.L., Basta, N.T., Brown, G.O., 2001. Use of diammonium phosphate to reduce heavy metal solubility and transport in smelter-contaminated soil. J. Environ. Qual. 30, 493–500.
Melamed, R., Cao, X., Chen, M., Ma, L.Q., 2003. Field assessment of lead immobilization in a contaminated soil after phosphate application. Sci. Total Environ. 305, 117–127.
Melick, T., Sommer, T., Conrads, H., 2005. Real-time monitoring of unburned carbon on utility fly ash. World of Coal Ash/DOE UBC Conference 2005.
Menon, M.P., Ghuman, G.S., James, J., Chandra, K., Adriano, D.C., 1990. Physico-chemical characterization of water extracts of different coal fly ashes and fly ash-amended composts. Water Air Soil Pollut. 50, 343–353.
Milovsky, A.V., Kononov, O.V., 1992. Mineralogy. In: Savostin, P. (Ed.), Zpflanzenernaehr Bodent, vol. 1132. Mir Publishers, Moscow, pp. 37–45.

Misra, M., Yang, K., Mehta, R.K., 1996. Application of fly ash in the agglomeration of reactive mine tailings. J. Hazard. Mater. 51, 181–192.
Molliner, A.M., Street, J.J., 1982. Effect of fly ash and lime on growth and composition of corn (*Zea mays* L.) on acid sandy soils. Soil Crop Sci. Soc. Fla. 41, 217–220.
Montes-Hernandez, G., Perez-Lopez, R., Renard, F., Nieto, J.M., Charlet, L., 2009. Mineral sequestration of CO_2 by aqueous carbonation of coal combustion fly-ash. J. Hazard. Mater. 161 (2), 1347–1354.
Moyeda, D., 2004. Reburn Technology Application Guidelines. DOE NETL Conference on Reburning for NOx Control. Morgantown, West Virginia. 18 May 2004.
Murphy, P.N.C., Stevens, R.J., 2010. Lime and gypsum as source measures to decrease phosphorus loss from soils to water. Water Air Soil Pollut. 212, 101–111.
Narra, S., 2009. Flue gas desulphurization gypsum as a soil amendment in the growth of wild rye and poplar (Hybrid 275 and Weser 6) clones in Lusatia, Germany. Int. J. Agric. Res. 4, 297–309.
Natusch, D.F.S., Wallace, J.R., 1974. Urban aerosol toxicity: the influence of particle size. Science 186, 695–699.
NGGI – National greenhouse gas inventory, 2007. National Greenhouse Gas Inventory – Kyoto Protocol Accounting Framework. Department of Climate Change and Energy Efficiency. Australian Government. http://ageis.climatechange.gov.au/NGGI.aspx (accessed 12.03.12.).
Norton, L.D., Zhang, X.C., 1998. Substances that enhance the physical properties of soil. In: Wallace, A., Terry, R.E., Dekker, M. (Eds.), Handbook of Soil Conditioners, New York.
Nyambura, M.G., Mugera, G.W., Felicia, P.L., Gathura, N.P., 2011. Carbonation of brine impacted fractionated coal fly ash: implications for CO_2 sequestration. J. Environ. Manage. 92 (3), 655–664.
Oades, J.M., 1993. The role of biology in the formation, stabilization and degradation of soil structure. Geoderma 56, 377–400.
O'Reilly, S.E., Sims, J.T., 1995. Phosphorus adsorption and desorption in a sandy soil amended with high rates of coal flyash. Commun. Soil Sci. Plant Anal. 26, 2983–2993.
Page, A.L., Elseewi, A.A., Straughan, I., 1979. Physical and chemical properties of fly ash from coal-fired power plants with references to environmental impacts. Residue Rev. 71, 83–120.
Palumbo, A.V., McCarthy, J.F., Amonette, J.E., Fisher, L.S., Wullschleger, S.D., Daniels, W.L., 2004. Prospects for enhancing carbon sequestration and reclamation of degraded lands with fossil-fuel combustion by-products. Adv. Environ. Res. 8 (3–4), 425–438.
Panuccio, M.R., Crea, F., Sorgona, A., Cacco, G., 2008. Adsorption of nutrients and cadmium by different minerals: experimental studies and modeling. J. Environ. Manage. 88, 890–898.
Park, J.H., Lamb, D., Paneerselvam, P., Choppala, G., Bolan, N.S., Chung, J.W., 2011. Role of organic amendments on enhanced bioremediation of heavy metal(loid) contaminated soils. J. Hazard. Mater. 185, 549–574.
Pathan, S.M., Aylmore, L.A.G., Colmer, T.D., 2002. Reduced leaching of nitrate, ammonium and phosphorus in a sandy soil by fly ash amendment. Aust. J. Soil Res. 40, 1201–1211.
Pathan, S.M., 2003. Fly Ash Amendment of Sandy Soils to Improve Water and Nutrient Source in Turf Grass. PhD Thesis. University of Western Australia: Agricultural and Plant Sciences.
Pathan, S.M., Aylmore, L.A.G., Colmer, T.D., 2003. Properties of several fly ash materials in relation to use as soil amendments. J. Environ. Qual. 32, 687–693.
Paustian, K., Cole, C.V., Sauerbeck, D., Sampson, N., 1998. CO_2 mitigation by agriculture: an overview. Clim. Change 40, 135–162.
Phung, H.T., Lund, I.J., Page, A.L., 1978. Potential use of flyash as a liming material. In: Adriano, D.C., Brisbin, I.L. (Eds.), Environmental Chemistry and Cycling Processes, p. 504 Conf. 760429, U.S. Department of Energy.

Pierzynski, G.M., Logan, T.J., Traina, S.J., Bigham, J.M., 1990. Phosphorus chemistry and mineralogy in excessively fertilized soils: quantitative analysis of phosphorus rich particles. Soil Sci. Soc. Am. J. 54, 1576–1583.

Pierzynski, G.M., McDowell, R.W., Sims, J.T., 2005. Chemistry, cycling, and potential movement of inorganic phosphorus in soils. In: Sims, J.T., Sharpley, A.N. (Eds.), Phosphorus: Agriculture and the Environment, ASA, CSSA, and SSSA, Madison, Wisconsin, pp. 53–86.

Pillman, A., Jusaitis, M., 1997. Revegetation of waste fly ash lagoons II. Seedling transplants and plant nutrition. Waste Manag. Res. 15 (4), 359–370.

Pitchel, J.R., Hayes, J.M., 1990. Influence of fly ash on soil microbial activity and populations. J. Environ. Qual. 19, 593–597.

Post, W.M., Kwon, K.C., 2000. Soil carbon sequestration and land-use change: processes and potential. Global Change Biol. 6, 317–327.

Power, J.F., Dick, W.A., 2000. Land Application of Agricultural, Industrial, and Municipal By-products. Soil Science Society of America, Madison, Wisconsin Book Series No. 6.

Pratt, C., Shilton, A., Pratt, S., Havercamp, R.G., Bolan, N.S., 2007. Phosphorus removal mechanisms in active slag filters treating waste stabilization pond effluent. Environ. Sci. Technol. 41, 3296–3301.

Punshon, T., Adriano, D.C., Weber, J.T., 2001. Effect of flue gas desulfurization residue on plant establishment and soil and leachate quality. J. Environ. Qual. 30, 1071–1080.

Punshon, T., Seaman, J.C., Sajwan, K.S., 2003. The production and use of coal combustion products. In: Sajwan, K.S., Alva, A.K., Keefer, R.F. (Eds.), Chemistry of Trace Elements in Fly Ash, Kluwer Academic/Plenum Publishers, New York, pp. 1–11.

Qafoku, N.P., Kukier, U., Sumner, M.E., Miller, W.P., Radcliffe, D.E., 1999. Arsenate displacement from fly ash in amended soils. Water Air Soil Pollut. 114, 185–198.

Qiao, M., Cai, C., Huang, Y., Liu, Y., Lin, A., Zheng, Y., 2011. Characterization of soil heavy metal contamination and potential health risk in metropolitan region of northern China. Environ. Monit. Assess. 172, 353–365.

Ram, L.C., Srivastava, N.K., Tripathi, R.C., Jha, S.K., Sinha, A.K., Singh, G., Manoharan, V., 2006. Management of mine spoils for crop productivity with lignite fly ash and biological amendments. J. Environ. Manage. 79, 173–187.

Ram, L.C., Masto, R.E., 2010. An appraisal of the potential use of fly ash for reclaiming coal mine spoil. J. Environ. Manage. 91 (3), 603–617.

Ramage, J., 1997. Energy: A Guidebook, second ed. Oxford University Press, New York 55.

Reichle, D., Joughton, J., Kane, B., Kemann, J., 1999. Developing an emerging technology road map for carbon capture and sequestration. Carbon Sequestration Research and Development. USDOE Office of Science, Washington, DC; DOE/SC/FE-1.

Reichert, J.M., Norton, L.D., 1994. Fluidised bed bottom-ash effects on infiltration and erosion of swelling soils. Soil Sci. Soc. Am. J. 58, 1483–1488.

Richter, D.D., Markewitz, D., Wells, C.G., 1994. Soil chemical change during three decades in an old-field loblolly pine (*Pinus taeda* L.) ecosystem. Ecology 75, 1463–1473.

Riehl, A., Elsass, F., Duplay, J., Huber, F., Trautmann, M., 2010. Changes in soil properties in a fluvisol (calcaric) amended with coal fly ash. Geoderma 155, 67–74.

Ritchey, K.D., Clark, R.B., Elrashidi, M.A., Baligar, V.C., 2000. Properties and examples of beneficial use of gypsumlike by-products. In: Power, J.F., Dick, W.A. (Eds.), Land Application of Agricultural, Industrial, and Municipal By-products, Soil Science Society of America, Madison, Wisconsin, pp. 537–565.

Rohriman, F.A., 1971. Analysing the effect of flyash on water pollution. Power 115, 76–77.

Rout, J.R., 2011. Study of the Settling Characteristics of Fly Ash-water Slurry and Designing of a Settling Pond. BTech thesis. National Institute of Technology, Rourkela, India.

Sahu, K.C., 1999. Characterization and utilisation of fly ash. Proceedings of the National Seminar on Fly Ash Utilisation, February 26–27, 1999, NML Jamshedpur, India.

Sajwan, K.S., Ornes, W.H., Youngblood, T., 1995. The effect of fly ash/sewage sludge mixtures and application rates on biomass production. J. Environ. Sci. Health 30, 1327–1337.
Sajwan, K.S., Paramasivam, S., Alva, A.K., 2007. Effects of different rates of fly ash and sewage sludge mixture amendments on cation availability and their leachability. J. Environ. Sci. Health 42, 1155–1160.
Sajwan, K.S., Beckley, C., Price, J., Alva, A.K., Sahi, S.V., Knox, A., 2011. Performance of corn plant growth under weatherd and un-weatherd flue gas desulfurization waste. Proceedings 11th International Conference on the Biogeochemistry of Trace elements, Florence, Italy, pp. 83–84.
Salter, P.J., Webb, D.S., Williams, J.B., 1971. Effects of pulverized fuel ash on the moisture characteristics of coarse-textured soils and on crop yields. J. Agric. Sci. 77, 56–60.
Schumann, A.W., Sumner, M.E., 1999. Plant nutrient availability from mixtures of fly ashes and biosolids. J. Environ. Qual. 28, 1651–1657.
Schutter, M.E., Fuhrmann, J.J., 2001. Soil microbial community responses to fly ash amendment as revealed by analyses of whole soils and bacterial isolates. Soil. Biol. Biochem. 33, 1947–1958.
Sen, P.K., Saxena, A.K., Bhowmick, S., 1997. In: Raju (Ed.), Ground Water Contamination Around Ash Ponds and Ash Disposal System, Narosa, New Delhi, pp. 326–342.
Seoane, S., Leiros, M.C., 2001. Acidification neutralization processes in a lignite mine spoil amended with fly ash or limestone. J. Environ. Qual. 30, 1420–1431.
Seshadri, B., Wickremaratne, C., Bolan, N.S., Brodie, K., Naidu, R., 2009. Enhancing phosphorus retention capacity of soils using coal combustion products. Clean up 2009 Conference. September 2009. Adelaide, Australia.
Seshadri, B., Wickremaratne, C., Bolan, N.S., Brodie, K., Naidu, R., 2010. Sorption and bioavailability of phosphorus in soils as affected by coal combustion products. 19th World Congress of Soil Science. 1–7 August, 2010. Brisbane, Australia.
Seshadri, B., 2011. Influence of Coal Combustion Products on the Transformation and Bioavailability of Phosphorus in Soils. PhD thesis. University of South Australia. Australia.
Shahandeh, H., Sumner, M.E., 1991. Establishment of vegetation on by-product gypsum materials. J. Environ. Qual. 22 (1), 57–61.
Sharpley, A.N., Moyer, B., 2000. Phosphorus forms in manure and compost and their release during simulated rainfall. J. Environ. Qual. 29, 508–514.
Sikka, R., Kansal, B.D., 1994. Characterization of thermal power-plant fly ash for agronomic purposes and to identify pollution hazards. Bioresour. Technol. 50, 269–273.
Sims, J.T., Vasilas, B.L., Ghodrati, M., 1993. Effect of coal fly ash and composted sewage sludge on emergence and easy growth of cover crops. Commun. Soil Sci. Plant Anal. 24, 503–512.
Singh, S.N., Kulshreshtha, K., Ahmad, K.J., 1997. Impact of fly ash soil amendment on seed germination, seedling growth and metal composition of *Viciafaba.* L. Ecol. Eng. 9, 203–208.
Singh, L.P., Siddiqui, Z.A., 2003. Effects of fly ash and *Helminthosporium oryzae* on growth and yield of three cultiver of rice. Bioresour. Technol. 86, 73–78.
Singh, S., Ram, L.C., Masto, R.E., Verma, S.K., 2011. A comparative evolution of minerals and trace elements in the ashes from lignite, coal refuse and biomass fired power plants. Int. J. Coal Geol. 87 (2), 112–120.
Sinha, K.S., Basu, K., 1998. Mounting flyash problems in growing coal based power stations-few pragmatic approaches towards a solution. In: Verma, C.V.J., Lal, P.K., Kumar, V., Lal, R., Krishnamurthy, R. (Eds.), Proceedings of International Conference on Flyash Disposal and Utilization, vol. ICentral Board of Irrigation and Power, New Delhi, India, pp. 15–27.
Soco, E., Kalembkiewicz, J., 2007a. Investigations of sequential leaching behaviour of Cu and Zn from coal fly ash and their mobility in environmental conditions. J. Hazard. Mater. 145, 482–487.

Soco, E., Kalembkiewicz, J., 2007b. Investigations on Cr mobility from coal fly ash. Fuel 88, 1513–1519.

Sreenivas, V.N., Karthik, D., Kumar, A.V., Sidharth, V.D., Sundaram, T.M., Sarkar, S., Sabarish, N.B., 2011. Determination of complex permittivity of fly ash for potential electronic applications. Appl. Mech. Mater. 110, 4292–4296.

Srivastava, R.K., 2000. Controlling SO_2 Emissions: A Review of Technologies, U.S. Environmental Protection Agency – EPA/600/R-00/093, November 2000.

Stehouwer, R.C, Sutton, P., 1992. Treatment of acid mine spoil with dry FGD byproducts: Leachate quality and plant growth. Abandoned Mine Lands Conference. August 23–26, 1992. Chicago.

Stehouwer, R.C., Dick, W.A., Sutton, P., 1999. Acidic soil amendment with a magnesium-containing fluidized bed combustion by-product. Agron. J. 91, 24–32.

Stevens, G., Dunn, D., 2004. Fly ash as a liming material for cotton. J. Environ. Qual. 33, 343–348.

Stewart, B., Tyson, S.S., 1997. Potential Use of Coal Combustion By-product (CCB) in the Eastern Coal Region: Site Characteristics. American Coal Ash Association.

Stout, W.L., Sharpley, A.N., Pionke, H.B., 1998. Reducing soil phosphorus solubility with coal combustion by-products. J. Environ. Qual. 27, 111–118.

Stout, W.L., Sharpley, A.N., Landa, J., 2000. Effectiveness of coal combustion by-products in controlling phosphorus export from soils. J. Environ. Qual. 29, 1239–1244.

Stout, W.L., Sharpley, A.N., Weaver, S.R., 2003. Effect of amending high phosphorus soils with flue-gas desulfurization gypsum on plant uptake and soil fractions of phosphorus. Nutr. Cycl. Agroecosys. 67, 21–29.

Straughan, I., Elseewi, A.A., Page, A.L., 1978. Mobilization of selected trace elements in residues from coal combustion with special reference to fly-ash. In: Hemphill, D.D. (Ed.), Trace Substances in Environmental Health – XII. A Symposium, University of Missouri, Columbia, pp. 389–402.

Stropnik, B., Tamse, M., Ramsak, R., Roser, A.D., Stegnar, P., 1991. The Effects of Coal Mining and Energy Production in the Salek Valley, Slovenia, on Surface Water Bodies. 4th International Mine Water Congress. Slovenia, Yugoslovia, September 1991.

Stuczynski, T.I., McCarthy, G.W., Wright, R.J., 1998. Impact of coal combustion product amendments on soil quality: I. Mobilization of soil organic nitrogen. Soil Sci. 163, 952–959.

Summers, R.M., Clarke, M., Pope, T., O'Dea, T., 1998. Western Australian flyash on sandy soils for clover production. Commun. Soil Sci. Plant Anal. 29, 2757–2767.

Sumner, M.E., 2007. Soil chemical responses to FGD gypsum and their impact on crop yields. Presented at the workshop on agricultural and industrial uses of FGD Gypsum. October 2007, Atlanta, USA. http://library.acaa-usa.org/3-Soil_Chemical_Responses_to_FGD_Gypsym_and_Their_Impact_on_Crop_Yields.pdf.

Sun, Y., Parikh, V., Zhang, L., 2012. Sequestration of carbon dioxide by indirect mineralization using Victorian brown coal fly ash. J. Hazard. Mater. 209, 458–466.

Tadmore, J., 1986. Radioactivity from coal-fired power plants: a review. J. Environ. Radioact. 4, 177–244.

Terman, G.L., Kilmer, V.J., Hunt, C.M., Buchanan, W., 1978. Fluidised bed boiler waste as a source of nutrients and lime. J. Environ. Qual. 7, 147–151.

Theis, T.L., Westrick, J.D., Hsu, C.L., Marley, J.J., 1978. Field investigation of trace metals in groundwater from fly ash disposal. J. Water Pollut. Control Fed. 50, 2457–2469.

Tiwari, S., Kumari, B., Singh, S.N., 2008. Evaluation of metal mobility/immobility in flyash induced by bacterial strains isolated from the rhizospheric zone of *Typhalatifolia* growing on fly ash dumps. Bioresour. Technol. 99, 1305–1310.

Topaç, F.O., Başkaya, H.S., Alkan, U., 2008. The effects of fly ash incorporation on some available nutrient contents of wastewater sludges. Bioresour. Technol. 99 (5), 1057–1065.

Tripathi, R.D., Dwivedi, S., Shukla, M.K., Mishra, S., Srivastava, S., Singh, R., Rai, U.N., Gupta, D.K., 2008. Role of blue green algae biofertilizer in ameliorating the nitrogen demand and fly-ash stress to the growth and yield of rice (*Oryza sativa* L.) plants. Chemosphere 70, 1919–1929.

US EPA. (1997). Performance of selective catalytic reduction on coal-fired steam generating units. Acid Rain Program. U.S. Environment Protection Agency (June 1997). http://www.epa.gov/airmarkt/progsregs/arp/docs/scrfinal.pdf.

US EPA, 2008. Agricultural uses for flue gas desulfurization (FGD) gypsum. U.S. Environmental Protection Agency. EPA530-F08-009 (March 2008). http://www.epa.gov/osw

Ussiri, D.A.N., Lal, R., 2005. Carbon sequestration in reclaimed minesoils. Crit. Rev. Plant Sci. 24 (3), 151–165.

US EIA, 2011. Electricity in the US. Electric Power Annual, 2010. United States Energy Information Administration. http://www.eia.gov/electricity/monthly/current_year/february2011.pdf. (accessed 22.02.11.).

Van der Zwaan, B.C.C., 2004. Will coal depart or dominate global power production during the 21st century? Workshop 'Clean Coal Power Technologies and Investment Risks'. November 2004. ECN, Amsterdam.

Vincini, M., Carini, F., Silva, S., 1994. Use of alkaline fly ash as an amendment for swine manure. Bioresour. Technol. 49, 213–222.

Viriyavejakul, S., Watanasak, M., 2003. Assessment of human health risk associated with arsenic in fly ash from Mae Moh lignite power plant. Thammasat Int. J. Sci. Technol. 8 (3), 20–28.

Wang, H., Hedley, M.J., Bolan, N.S., 1995. Chemical properties of fluidised bed boiler ash relevant to its use as a liming material and fertiliser. N. Z. J. Agric. Res. 38, 249–256.

Wang, H., 1996. Potential Uses of Fluidized Bed Boiler Ash (FBA) as a Liming Material, Soil Conditioner and Sulphur Fertilizer. PhD Thesis, Massey University, Palmerston North, New Zealand, 1996.

Wang, H., Hedley, M.J., Bolan, N.S., Horne, D.J., 1999a. The influence of surface incorporated lime and gypsiferous by-products on surface and subsurface soil acidity. I. Soil solution chemistry. Aust. J. Soil Res. 37, 165–180.

Wang, H., Hedley, M.J., Bolan, N.S., Horne, D.J., 1999b. The influence of surface incorporated lime and gypsiferous by-products on surface and subsurface soil acidity. II. Root growth and agronomic implications. Aust. J. Soil Res. 37, 181–190.

Wang, F., Wu, Z., 2004. Hand Book for Coal Ash Utilization, second ed.. China electricity publish press.

Wang, D.J., Zhang, Y.H., Dong, A.G., Tang, Y., Wang, Y.J., Xia, J.C., Ren, N., 2003. Conversion of fly ash cenosphere to hollow microspheres with zeolite/mullite composite shells. Adv. Funct. Mater. 13 (7), 563–567.

Wang, H., Bolan, N.S., Hedley, M.J., Horne, D.J., 2006. Potential uses of fluidized bed boiler ash (FBA) as a liming materials, soil conditioner and sulfur fertilizer. In: Sajwan, K.S., Twardowska, I., Punshon, T., Alva, A.K. (Eds.), Coal Combustion Byproducts and Environmental Issues, Springer Publishers, New York, pp. 202–215.

WCA – World Coal Association, 2005. The Coal Resource – A Comprehensive Overview of Coal. WCA publications, World Coal Association, pp. 1–48.

WCA – World Coal Association, 2010. Coal Statistics. September 2010. World coal Association website http://www.worldcoal.org/resources/coal-statistics/. (accessed 20.06.11.).

Whalen, J., 2002. Calcium co-amendments modify extractable orthophosphate levels in freshand composted cattle manure. Water Air Soil Pollut. 141, 105–124.

Wilkinson, A., Haque, A., Kodikara, J., 2010. Stabilisation of Clayey Soils with Industrial Byproducts: Part A. Ground Improvement (Proceedings of the ICE). vol. 163, 149–163.

Wong, M.H., Wong, J.W.C., 1986. Germination and seedling growth of vegetable crops in fly ash amended soils. Agr. Ecosyst. Environ. 26, 25–35.

Wong, J.W.C., 1995. The production of artificial soil mix from coal fly ash and sewage sludge. Environ. Technol. 16, 741–751.
WRI – World Resources Institute, 2011. Global Greenhouse Gas Emissions by Country, Economic Sector, and Gas. Climate Analysis Indicators Tool (CAIT) Version 9.0. World Resources Institute, Washington, DChttp://cait.wri.org/cait.php?page=sectors (accessed 17.04.12.).
Wright, R.J., Codling, E.E., Stuczynski, T., Siddaramappa, R., 1998. Influence of soil applied coal combustion by-products on growth and elemental composition of annual rye grass. Environ. Geochem. Health 20, 11–18.
Wu, Z., 2002. NO_x Control for Pulverized Coal Fired Power Stations. IEA Coal Research, London.
Xenidis, A., Mylona, E., Paspaliaris, I., 2002. Potential use of lignite fly ash for the control of acid generation from sulphidic wastes. Waste Manag. 22, 631–641.
Yunusa, I.A.M., Eamus, D., DeSilva, D.L., Murray, B.R., Burchett, M.D., Skilbeck, G.C., Heidrich, C., 2006. Fly-ash: an exploitable resource for management of Australian agricultural soils. Fuel 85, 2337–2344.
Zhang, G.Y., Dou, Z., Toth, J.D., Ferguson, J., 2004. Use of fly ash as environmental and agronomic amendments. Environ. Geochem. Health 26, 129–134.
Zhang, W., Brown, G.O., Storm, D.E., Zhang, H., 2008. Fly-ash-amended sand as filter media in bioretention cells to improve phosphorus removal. Water Environ. Res. 80 (6), 507–516.
Zielinski, R.A., Finkelman, R.B., 1997. Radioactive elements in coal and fly ash: abundance, forms, and environmental significance: U.S. Geological Survey Fact Sheet. pp. 163–197.



CHAPTER SEVEN

An Assessment of the Variation of Manure Nitrogen Efficiency throughout Europe and an Appraisal of Means to Increase Manure-N Efficiency

J. Webb[*,1], Peter Sørensen[†], Gerard Velthof[‡], Barbara Amon[§], Miriam Pinto[¶], Lena Rodhe[**], Eva Salomon[**], Nicholas Hutchings[†], Piotr Burczyk[††], Joanne Reid[*]

*Ricard-AEA, Didcot, UK
†University of Aarhus, Dept. of Agroecology, Tjele, Denmark
‡Alterra, Wageningen, The Netherlands
§Leibniz Institute for Agricultural Engineering, Department of Technology Assessment and Substance Cycles Max-Eyth-Allee 100, D-14469 Potsdam, Germany
¶NEIKER, Derio (Bizkaia), Spain
**Swedish Institute of Agricultural and Environmental Engineering (JTI), Uppsala, Sweden
††Institute of Technology and Life Sciences (ITP), Westpomeranian Research Centre in Szczecin, Szczecin, Poland
[1]Corresponding author: E-mail: j.webb@Ricardo-aeat.com

Contents

Advances in Agronomy, Volume 119
ISSN 0065-2113, http://dx.doi.org/10.1016/B978-0-12-407247-3.00007-X

Abstract

Using the nitrogen (N) in organic manures more effectively reduces losses to the environment. A requirement to take allowance of the N conserved by reduced ammonia (NH_3)-emission techniques would increase manure-N efficiency by up to 15%. Covering manure stores and land application of slurry by injection beneath the soil surface and by rapid incorporation of both slurries and solid manures into uncropped soil reduce NH_3 emissions. Injection of cattle slurry also reduces N immobilization compared with application methods, which mix the slurry with soil and increases manure-N efficiency by *ca* 10–15%. In growing cereals, NH_3 emissions can be reduced by band spreading within the canopy. Anaerobic digestion of slurry may also increase manure-N availability in the season of application by 10–20%, compared with undigested slurry. Slurry acidification may increase manure-N efficiency by 35–65% by reducing total NH_3 losses by 70% compared with unacidified slurry stored without cover and not incorporated after spreading.

To fully utilize the fertilizer value of manure-N, uptake over more than 1 year needs to be accounted for. This is particularly important for solid manures which provide less-available N in the season after application than slurries but release more N to crops in subsequent years. Using manure-N as a sole N source may limit overall manure-N efficiency. Applying manures at reduced rates over a larger crop area, using N fertilizer at times when crop recovery of manure-N may be limited, may give the greatest overall manure-N efficiency.



1. INTRODUCTION

Organic manures applied to agricultural land arise mainly from livestock production as liquid manures (slurries), litter-based solid manures (FYM) and poultry manures and from other sources such as treated sewage sludges (commonly called biosolids), composts, digestate from the anaerobic digestion (AD) of energy crops, and industrial "wastes" such as paper crumble and food industry by-products. These are valuable sources of most major plant nutrients and organic matter (OM). Careful recycling to land allows their nutrient value to be used to enhance crop growth and maintain or improve soil fertility, reducing the environmental and economic costs associated with the use of inorganic fertilizers.

Traditionally, organic manures, along with deposits of excreta during grazing, legumes and green manures, were the main inputs of crop nutrients added to those already in the soil. With the availability of inexpensive mineral-N fertilizers, manures came to be regarded as sources of phosphorus (P) and potassium (K), rather than nitrogen (N), as variations in the quantity and quality of N present, combined with large variations in losses to the atmosphere, meant that the availability of manure-N was difficult to predict. Oenema et al. (2007) indicated that in 2000, total N excretion by livestock in the EU member states (MS) (EU-27) was around 10.4 million tonnes and that only around 50% of the N excreted in livestock was recycled as a plant nutrient.

Manures can present a considerable environmental risk if their N content is not used effectively (see Butterbach-Bahl et al., 2011; Dise et al., 2011; Grizzetti et al., 2011; Moldanová et al., 2011; Velthof et al., 2011; for a full accounts of the environmental threats posed by N in Europe). In particular, large amounts of N may enter the wider environment following the application of manures to land. Nitrate (NO_3^-) enters ground and surface waters (Grizzetti et al., 2011), increasing eutrophication and reducing drinking water quality. Ammonia (NH_3), when deposited to terrestrial and aquatic ecosystems, increases N eutrophication and soil acidification (Butterbach-Bahl et al., 2011; Dise et al., 2011). Nitrous oxide (N_2O) contributes to global warming

(Bouwman, 1990) and breakdown of stratospheric ozone (Crutzen, 1981). Only emissions of dinitrogen (N_2) have no direct impact on the environment, though the N lost by such emissions must be replaced, for example, via the addition of fertilizer, which has associated off-farm environmental costs.

Reduction of N pollution from agriculture has been a focus of environmental policy since the 1990s, both at European and international level (Oenema et al., 2011). The EU Nitrates Directive 91/676 (EEC, 1991) requires MS to introduce measures to reduce NO_3^- losses to ground and surface waters from agricultural sources. The 1999 Gothenburg Protocol sets targets to reduce emissions of atmospheric pollutants including NH_3 and NO_x. The National Emissions Ceilings (NEC) Directive places limits on the amount of NH_3 that may be emitted by each MS. Under the Kyoto protocol on Climate Change, signatories committed themselves to greenhouse gas (GHG) emission reduction targets, including N_2O. Subsequently, numerous initiatives have been initiated. For example, the United Kingdom has set a national target of an overall 80% reduction in GHG emissions by 2050 and the agriculture sector is committed to playing its part in contributing to this goal. Denmark (DK) has set a target of 20% reduction by 2020.

The Nitrates Directive was the first Europe-wide legislation targeting nutrient loss, so has had the greatest impact on agricultural practices. The objectives of the Nitrates Directive are to reduce water pollution caused or induced by NO_3^- from agricultural sources and to prevent further such pollution through a number of steps to be fulfilled by MS, i.e.

- Monitor water quality (with regard to NO_3^- concentration and trophic status);
- Designate nitrate vulnerable zones (NVZ) or apply measures to the whole country;
- Establish a Code of Good Agricultural Practices (CGAP) (obligatory within NVZ/voluntary implementation outside NVZ);
- Establish action programs (AP), a set of measures to prevent and reduce NO_3^- pollution (these may be obligatory within NVZ or be applied to the whole country).

Annexes II and III of the Nitrates Directive set out a list of measures, which must be included in the CGAPs (Annex II) and the AP (Annex II and III). In particular, the CGAPs and the AP must contain provisions relating to manure storage capacity, restrictions on application of fertilizers and manure and tuning of the amount of N applied to crops to the demand for N of that crop and the N supply from the soil and all external sources, including fertilization (i.e. balanced N fertilization).

In NVZs (which could be the whole country), the permissible amount of total N in livestock manures applied to land each year, including by the animals themselves, must not exceed 170 kg ha^{-1} yr^{-1}, and may be required to be less than this amount in order to reduce the risk of polluting water-courses. The Nitrates Directive allows for the possibility of a derogation with respect to the maximum amount of 170 kg N ha^{-1} yr^{-1} for livestock manure, provided it is demonstrated that the objectives of the Directive can still be achieved and that the derogation is based on objective criteria such as long growing seasons, crops with large N uptake, high net precipitation or soils with a high denitrification capacity. In addition to the requirements of the Nitrates Directive, it may be necessary to limit organic-manure applications on some fields, in order to avoid excessive enrichment of soil P levels. In NVZs, it is mandatory to follow the restrictions on the application of organic manures and mineral fertilizers included in the AP.

There is a synergy between direct measures to reduce N pollution and the adoption of measures which increase the agronomic efficiency of manure applications. Reducing N pollution is likely to conserve more manure-N in the soil making it potentially available for crop uptake. Losses of N, such as those of NH_3, are highly variable and reducing those losses will make the manure-N content both greater and easier to predict. Initiatives to increase the proportion of manure-N taken up by crops will leave smaller residues of N after harvest which may subsequently be lost as NO_3^- or N_2O. This introduces a virtuous cycle in which confidence in the N fertilizer value of manure is increased thus incentivizing a commensurate reduction in the use of mineral-N fertilizer. Finally, as the perception of manure as a valuable source of N gains credit, more attention may then be given to reducing the risks of manure-N being lost to the environment.

In this chapter, we assessed the various estimates of manure-N efficiency made by each MS when assessing the need for subsequent inputs of fertilizer-N. Crop utilization over more than one season was also taken into account. The objectives of this review were to identify the most effective measures and practices to improve manure-N efficiency with reference to how these methods might be utilized or adjusted with respect to differences in:

- Manure type: solid versus liquid manures; different types of livestock;
- Type of rotation/crop to which manure is applied: permanent vs annual; autumn- vs spring-sown;
- Time of application;
- Soil type;
- Climate;

- Method of application;
- Manure treatment prior to application.

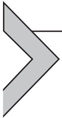
Moreover, recommendations for the most effective and practical means of increasing manure-N efficiency throughout the EU are provided.

The review is subsequently divided among three sections:

(1) In the first section, we report and discuss different approaches to the definition of manure-N efficiency among EU MS. This includes a summary of the extent to which differences in these factors lead to significant differences in the availability of manure-N for both crop uptake and NO_3^- leaching among the MS and regions of the EU, together with an explanation of the reasons behind any differences reported.

(2) The second section is a systematic review of recent literature to identify the most effective measures and practices to improve manure-N efficiency.

(3) The final section is a brief discussion of our findings and conclusions and recommendations for increasing the efficiency with which manure-N may be used by crops.



2. THE AVAILABILITY OF MANURE-N TO CROPS

Nitrogen is present in manures in both mineral and organic forms. Consequently, the characteristics of manure can be expressed in a number of ways:

Mineral-N in manures consists mainly of ammonium (NH_4^+) ions and NH_3 in solution, which together are commonly referred to as total ammoniacal N (TAN). After aerobic decomposition, manures can also contain mineral-N as NO_3^-.

Organic N is principally complex molecules derived from recalcitrant components excreted in feces or present in litter (Van Faassen and Van Dijk, 1987), together with some simpler organic compounds such as allantoin excreted in the urine (Whitehead et al., 1989). Organic-N becomes available for crop uptake after mineralization over a period of months to years. This also needs to be taken into account (Schröder et al., 2007), to fully assess the agronomic potential of organic manures.

Until the mid-1990s, the uptake of organic N by plants was assumed to be negligible. However, the capacity to utilize organic N is widespread among plants and many agricultural species readily take up organic N (Näsholm et al., 2000, 2001; Okamoto et al., 2003; Yamagata and Ae, 1996). Unfortunately, there is little quantitative information on the importance

of organic N utilization by crops (Gärdenäs et al., 2011) and climate and hydrology have a large influence on plant utilization of organic and inorganic N (Gärdenäs et al., 2011). Organic N uptake is more important in cool and wet than in hot and dry environments (Schmidt and Stewart, 1999; Warren, 2006). Agricultural soils usually display concentrations of inorganic N in the mM range, but with concentrations of individual organic N compounds in the low micromolar range, suggesting plant-N nutrition should be dominated by inorganic N in these systems (Gärdenäs et al., 2011). Only plant uptake of simple organic compounds like amino acids has been shown, and these compounds are also quickly mineralized in soil. Thus, while direct uptake of organic manure-N by crops cannot be discounted, it appears that the majority of manure-N taken up by plants is in the mineral form.

Available nitrogen is the N regarded as potentially available for uptake by the crop grown in the season of manure application. This is often considered to equate to the *mineral-N* together with uric acid-N, albeit the available N often includes other easily mineralizable organic N. The uric acid content of poultry manure is counted as available N as it is rapidly hydrolyzed in soil to urea (Kirchmann, 1991).

Crop-available N is the proportion of N available for crop uptake and is dependent on N losses (NH_3, N_2O, NO and NO_3^- leaching and surface runoff) following application to land (Fig. 7.1). Crop-available N is influenced by manure application technique (e.g. implementation of NH_3

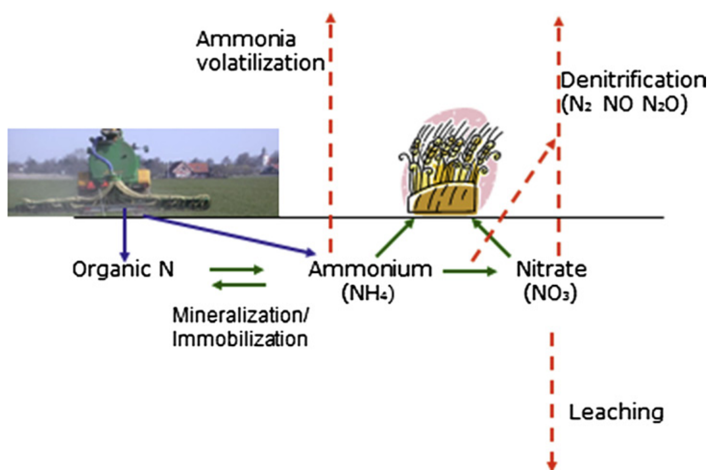


Figure 7.1 The most important N transformations and losses after application of animal manure to soil. For color version of this figure, the reader is referred to the online version of this book.

Table 7.1 Average and Range of Composition Values for Different Types of Manure Reported from 15 EU Countries and Switzerland (Menzi, 2002)

		DM	OM	N	NH_4–N
		kg t^{-1} or kg m^{-3}			
Liquid manure/slurry					
Cattle	Average	6.7	5.7	4.0	2.3
	Range	1.5–12.3	1.0–7.5	2.0–7.0	1.0–4.9
Pigs	Average	5.2	3.8	4.8	3.4
	Range	1.5–9.2	0.5–6.4	1.2–8.2	1.9–6.1
Poultry	Average	17.0	12.2	11.2	5.3
	Range	1.00–30.0	2.00–19.8	2–18	1.9–7.8
Solid manure					
Cattle	Average	22.3		4.8	1.3
	Range	16–43		2.0–7.7	0.5–2.5
Pigs	Average	23.8		6.8	2.4
	Range	20–30		4.0–9.0	0.7–6.0
Laying hens	Average	40.6		23.6	10.9
	Range	22–55		5.1–25	37–60
Broilers	Average	60.3		24.5	8.0
	Range	45–85		21.8–40	2.0–15

DM = dry matter.
OM = organic matter.
NH_4–N = ammonium N.

abatement techniques), time of application, weather conditions, soil type, and so on. The efficiency of use of organic N is dependent on the rate of mineralization, which depends on the nature of the manure OM, and soil conditions such as temperature and moisture.

Slurries and poultry manures have relatively large proportions of mineral-N (typically in the range of 35–80% of total N) compared with FYM which usually has a much smaller proportion of N in mineral form (10–45% of total N; Menzi, 2002). Table 7.1 summarizes the results of Menzi (2002) presenting the means and ranges of manure analyses to illustrate the variation in estimates of manure composition reported in European countries.

2.1. Concepts of Manure-N Efficiency

Nitrogen use efficiency (NUE) can be applied at different scales, i.e. plant scale, animal scale, field scale and farm scale. At the farm scale, NUE is the overall efficiency with which N is used in the entire farm system to produce outputs. With respect to crop production, NUE is also referred to as recovery fraction, apparent recovery fraction, agronomic efficiency, and partial

Table 7.2 Terms Used to Describe the Efficiency with which Manure-N may be Used by Crops

Term	Definition	Description
Available-N	The mineral and easily mineralized fraction of manure-N.	The N in manures potentially available for crop uptake in the season the manure is applied.
Crop-available N	The proportion of available-N actually available for crop uptake.	The available-N remaining after losses of NH_3, NO_3^-, etc. following application to land.
NFRV	Nitrogen fertilizer replacement value	The amount of N fertilizer that can be replaced by a given amount of manure-N.
Manure-N efficiency	The proportion of manure-N that can be recovered by crop roots over more than one season. This is not the same as the crop recovery of manure-N or NUE of manure-N	Crop-available N plus the part of mineralized manure-N that is crop-available during the following 5–10 seasons.

factor productivity (Dobermann, 2005). When explicitly considering the efficiency of use of manure-N by crops, a number of terms are commonly used (Table 7.2). The N fertilizer replacement value (NFRV) is the amount of mineral-N fertilizer that would produce the same crop-N or dry-matter yield as the manure-N available to the crop during the season, in which the manure is applied. NFRV can be calculated as $NUE_{manure}/NUE_{mineral\ fertilizer}$. This definition of manure-N efficiency regards manure-N relative to mineral fertilizer-N since crops are usually only considered to respond to fertilizer-N in the season in which the mineral fertilizer is applied.

In principle, based on extrapolation from long-term experiments, mineralization of manure-N can continue for *ca* 100 years. However, accounting over 100 years is not practical. Studies have generally reported agronomically significant mineralization for up to 10 years. We therefore express manure-N efficiency as the proportion of manure-N that can be recovered by crop roots over 5–10 seasons.

In order to make our definition of manure-N efficiency clear, which is not the same as manure-N use efficiency, we provide the following example.

The NUE of mineral-N applied to a barley crop can be about 60% in the season of application. Residual NUE is small, 1–7% of the fertilizer-N applied

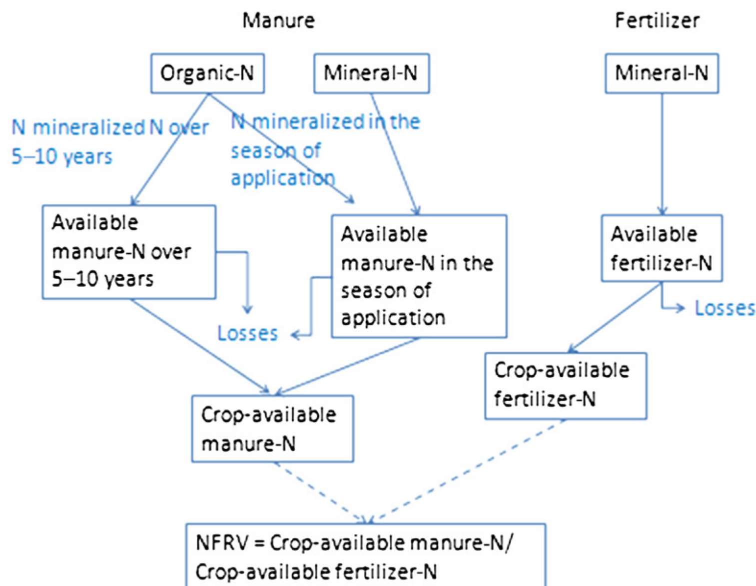


Figure 7.2 Concepts of manure-N efficiency. For color version of this figure, the reader is referred to the online version of this book.

in year 1 was reported to be taken up by subsequent crops by Sieling et al. (2006). If the NUE of manure-N is 30% when applied to the same crop in the season of application then the NFRV is 50%. If we then add an NFRV of the total residual effects of 10% over the following 5–10 seasons, then we have a manure-N efficiency of 60%, according to our definition.

These concepts are illustrated in Fig. 7.2 below.

For this chapter, the efficiency with which the N in manure applied to land may be utilized by crops was assessed, so that manure can be properly taken into account when assessing the need for supplementary inputs of fertilizer-N. Crop utilization over more than one season needs to be taken into account. Henceforth, we will refer to manure-N efficiency using the terms defined in Table 7.2.

2.2. Availability of Manure-N to Crops

Oenema et al. (2007) reported that around 50% of the N in livestock excreta deposited in and around buildings and collected as manure in the EU-27 was lost to the environment. The greatest of these losses (38%) was as NH_3 emissions, with around 19% lost from buildings and stores and another 19% of the N excreted in housed livestock systems emitted as NH_3 following the

application of the manure to land. Other losses were via emissions of nitric oxide (NO), N_2O and N_2 (7%) and 4% via leaching and runoff. The results indicate that around 52% of the N excreted in livestock was recycled as a potential plant nutrient. Differences between MS in mean N losses (mainly as NH_3) from manure stores were particularly large (range 19.5–35%). Since losses of manure-N are dominated by losses of NH_3, it would appear as the most-effective means of increasing manure-N efficiency will be by reducing these emissions. While our definition of manure-N efficiency takes manure ex storage as a starting point, and reduction of storage loss will have little effect on manure-N efficiency as we have defined it, it is still worth giving some consideration to reducing losses of N from livestock buildings and manure stores as such measures will have potential to increase NUE at the farm scale.

2.2.1. Short-Term Crop Availability of Manure-N

A significant N turnover takes place immediately after manure application, with mineralization and immobilization occurring simultaneously; net N mineralization is the difference (Jansson, 1958; Sørensen, 2001). During the initial days, immobilization is normally greater than mineralization and the initial N immobilization is significantly influenced by the concentration of decomposable organic compounds such as volatile fatty acids in the manure (e.g. Kirchmann and Lundvall, 1993). Part of the immobilized N is remineralized within some weeks, whereas a part of it is stabilized in soil (Sørensen and Amato, 2002). After 8–12 weeks, net mineralization of slurry N is often close to zero, but both positive and negative net mineralization can be observed depending on slurry composition and soil type (Bechini and Marino, 2009). The net mineralization is influenced by the time of decomposition, soil temperature and by the C/N_{org} ratio (Burger and Venterea, 2008; Chadwick et al., 2000).

Nitrogen availability, therefore, depends on manure composition. Short-term N release from organic fertilizers varies greatly from 0% (some compost) to nearly 100% (urine) (Whitehead and Raistrick, 1990). The most important indicators to be used for predicting the short-term availability of manure-N are the mineral-N content as NH_4–N or NO_3–N, the C/N ratio (especially of the decomposable organic fraction), and stability of the organic substances (Webb et al., 2012 and references therein).

Recommended manure application rates are based, in some MS, solely on the total N (or total P) content of a given manure. More usually, the NH_4^+–N in manure is considered to be the fraction of manure-N available for crop uptake in the season of application (Olesen et al., 2004). The C/N and NH_4^+/organic N ratios of applied manures have also been used

as potential predictors of crop-available N because these properties influence N immobilization and mineralization (Beauchamp and Paul, 1989). Short-term (growing season of application) programs that calculate manure application rates generally assume that 100% of the NH_4^+–N, and some percentage (0–50%) of the organic N, become available for plant uptake during the growing season of application (Thompson et al., 1997). However, there are few data available to support these assumptions, or to discriminate among specific manure, soil, and climate conditions. Such data are particularly scarce for central and southern Europe. The application of manures in those regions to soils, which are potentially warmer and drier in spring might affect crop N uptake from manures due to lesser mobility of NH_4^+ ions in drier soils or through impacts on mineralization of labile organic N.

The parameters that determine manure-N availability, and the dynamics of organic manure-N mineralization, will be affected by different factors: moisture; temperature; livestock type and diet or different processes that can be used for manure treatment (e.g. slurry separation, Bertora et al., 2008; Sørensen and Thomsen, 2005; composting, Raviv et al., 2004). Composting reduces the mineral-N content and increases the stability of the OM (Castellanos and Pratt, 1981; Kirchmann and Witter, 1989; Munoz et al., 2008; Sommer, 2001), whereas AD increases NH_4^+–N content as well as the stability of OM, but decreases the C/N ratio considerably, resulting in a product with a large proportion of directly available N (Gutser et al., 2005). The range in the proportions of crop available N is illustrated below in Table 7.3 (Chambers et al., 1999—who refer to readily available N). This readily available N ranges from 70% (some slurries) to 10% for "old" cattle manure but more than 90% of N has been found as mineral-N in separated pig slurry (Sørensen and Thomsen, 2005).

Several studies have reported the mineralization rate of organic manure-N during the first year. When data on N availability in the first year are reviewed, it can be observed that the mineralization rate is quite different depending on the country and on the study conditions.

It is difficult to measure mineralization of organic-N (Reeves, 2007), and hence any reported variation in measured rates may also be related to experimental methods. However, since temperature and soil-water content affect most of the soil biological processes that give rise to mineralization several authors have established how the mineralization rate is affected by these parameters (Burger and Venterea, 2008; Chadwick et al., 2000). These studies show a lesser mineralization rate for lower temperature and lower moisture (Table 7.4) and agree with the findings of Van Kessel and Reeves (2002) who, after studying 107 dairy slurries, reported a highly variable range in their N mineralization

Table 7.3 Default Manure Analysis, Fresh Weight Basis (Chambers et al., 1999). Analysis based on Samples of around 20 for Beef Slurry to 250 for Cattle FYM

Manure Type	DM %	Total, N kg t^{-1}	RAN,* kg t^{-1}	RAN*, % of total N
Cattle FYM, fresh	25.0	6.0	1.5	25
Cattle FYM, old	25.0	6.0	0.6	10
Pig FYM, fresh	25.0	7.0	1.8	25
Pig FYM, old	25.0	7.0	0.7	10
Layer manure	30.0	15.0	7.5	50
Broiler/turkey litter	60.0	29.0	11.6	40
Dairy slurry	6.0	3.0	1.5	50
Beef slurry	6.0	2.3	1.2	50
Pig slurry	4.0	4.0	2.4	60
Separated slurry, strainer box	1.5	2.1	1.5	70
Separated slurry, weeping wall	3.0	2.0	1.4	70
Mechanically separated slurry	4.0	3.0	1.5	50
Separated slurry solids	15.0	5.0	1.0	20
Liquid undigested sewage sludge	5.0	1.8	0.6	30
Liquid digested sewage sludge	4.0	2.0	1.2	60
Undigested sludge	25.0	7.5	1.5	20
Digested sludge cake	25.0	7.5	1.1	15

*Readily available N, NH_4–N plus uric acid.

Table 7.4 Mineralized ^{15}N Recovered from Various Labeled Dairy Manure Components over all Temperatures at Day 168. All Values are % of Applied ^{15}N (From Cusick et al., 2006).

Temperature (°C)	Urine	Feces	Bedding	All
11	44	13	15	24
18	60	18	24	30
25	63	26	25	36
$P_t > F$	0.054	0.003	<0.001	0.088
LSD, 0.05	16.2	5.7	3.5	10.4

characteristics, from a net mineralization of 55% to a net immobilization of 29% of the organic-N. Chadwick et al. (2000) found that only 2% of the organic N in one sample of dairy slurry with a C:organic-N ratio of 15 was mineralized within 199 days of application, whereas 19% was mineralized from another sample of dairy slurry with a C:organic-N ratio of 10. Nevertheless, this wide range of mineralization values is consistent with the known effects of environmental conditions on mineralization rate. Generally, organic materials with an organic-C:organic-N ratio >15 will immobilize N, and those with ratios <15 will release N (Chadwick et al., 2000; Petersen and Sørensen, 2008b). The prediction of manure-N mineralization is further complicated as some studies indicate that mineralization and immobilization processes do not respond similarly to temperatures (Andersen and Jensen, 2001).

With the aim of optimizing manure utilization, assessing the correct dosage and coupling it with crop requirements, several authors have developed models to simulate the N release during the year, e.g. MANNER (Chambers et al., 1999). These models consider different factors in order to estimate N availability. The simple model of Beauchamp and Paul (1989) for predicting manure-N availability in the field divides the manure-N content into NH_4^+–N and organic N. Others have developed mathematic equations of N availability that calculate the relationship between N release and time as a polynomial (cubic) (Azeez and Van Averbeke, 2010). Azeez and Van Averbeke (2010) described the following release phases:

- Initial rapid N release at 0–30 days;
- Phase of constant release, 40–55 days;
- Decline phase in N release, 70–90 days;
- Sharp decrease in N release at 120 days.

However, other studies indicate that there often is an initial immobilization phase (e.g. Gutser et al., 2005; Kirchmann and Lundvall, 1993; Sørensen and Amato, 2002).

In conclusion, we can state that the short-term N availability varies greatly depending on:

- Livestock type, feeding, production system and application techniques;
- C:organic-N ratio; organic materials with a C:organic-N ratio >15 will immobilize N, and those with C:organic-N ratios < 15 will release N within 2–4 months of decomposition;
- Climate; less mineralization at lower soil temperatures and moisture contents.

The values recorded in the papers reviewed fit well with those reported by Gutser et al. (2005) that can be seen in Fig. 7.3.

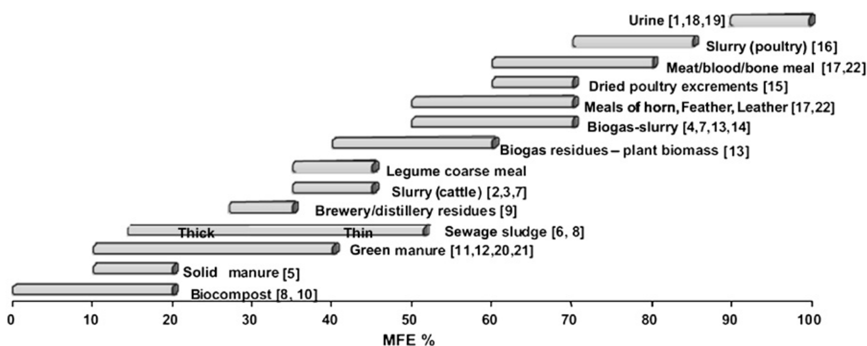


Figure 7.3 Mineral fertilizer equivalents for several organic fertilizers in the year of application (Fig. 5 in Gutser et al. (2005)).

2.2.2. Longer Term Mineralization of Organic-N

2.2.2.1. Longer Term Mineralization of a Single Application of Manure

Organic manures may give rise to residual N effects after the year of their application (e.g. Daudén et al., 2004; Schröder et al., 2005). The residual effects are relatively small in the years after application and they are difficult to measure. To study the availability and fate of manure-N in subsequent years ^{15}N-labeled manures, obtained by feeding animals on labeled diets, have been used. This approach also enables comparison of the fate of different components in animal manure (bedding, feces, urine). In the year of application, there are great differences in N availability between the sources like urine, feces and mineral-N (Jensen et al., 1999). However, in the years after application plant uptake of labeled N in various crops is relatively small and consistent irrespective of original N source (Table 7.5). The crop recovery of manure-N in the second year is typically 3–6% and in the third year 1–2% of total N. The crop recovery of labeled fertilizer-N is only slightly less (Table 7.5). Despite this, the residual effect of more recalcitrant manures with a high proportion of organic N will be greater as more total N must be applied with recalcitrant manures than with manures with a large proportion of mineral-N or mineral fertilizers to obtain the same yield. So even though the % release rate is very similar, the residual effect increases with increasing amounts of organic N in manures. The studies with ^{15}N-labeled manures show that there is a fast decline in relative decomposition rate (RDR) as the crop recovery of labeled N in the third year is only 30–50% of the crop recovery in the second year (Table 7.5).

Table 7.5 Crop Recovery of ^{15}N Added with Animal Manures in the Second and Third Year after Application, % of Total N Applied

^{15}N-Labeled Component	Manure Type	Second Year ^{15}N Recovery in Crop	Third Year ^{15}N Recovery in Crop	Reference
Bedding straw	Fresh solid	3.3 (2.9)	1.2 (1.2)	*
Ruminant feces	Fresh solid	4.1 (2.9)	1.5 (1.2)	*
	Feces	5.7 (4.7)	–	†
	Slurry	3 (3)	–	‡
	Slurry	3.3 (2.1)	1.5 (1.1)	§
Pig feces	Slurry	4.2 (1.7)	–	‖
Cattle feces + urine	Semisolid	4–8 (–)	1–3 (–)	¶
Ruminant urine	Fresh solid	3.6 (2.9)	1.3 (1.2)	*
	Slurry	3 (3)	–	‡
	Slurry	2.6 (2.1)	1.3 (1.1)	§
Pig urine	Pig slurry	2.5 (1.1)	–	‖
Poultry excreta	Fresh excreta	4–6 (3–4)	1–2	#
Ammonium-N	Pig slurry	3 (2)	1–2 (1)	**
	Cattle slurry	2.6–2.9 (1.9)	1.1–1.7 (1.1)	††

Numbers in parentheses indicate the recovery of labeled N from a parallel reference treatment with ^{15}N-labeled mineral fertilizer.
*Jensen et al., 1999.
†Sørensen et al., 1994.
‡Thomsen et al., 1997.
§Bosshard et al., 2009.
‖Sørensen and Thomsen, 2005.
¶Cusick et al., 2006.
#Thomsen, 2004.
**Sørensen and Amato, 2002.
††Sørensen, 2004.

The crop recovery of labeled manure-N cannot be directly converted into residual effects estimated by traditional methods like N recovery by difference in N uptake, but in some cases, a good accordance between ^{15}N recovery and apparent recovery has been found (Cusick et al., 2006). Cusick et al. (2006) estimated second-year availabilities after a single application of semisolid cattle manure using the N-fertilizer equivalence, difference, and relative effectiveness methods to be 12, 8, and 4% of total manure-N applications, respectively. Estimates of third-year availability by these methods were 3, 1, and 5%, respectively. Because residual N effects are relatively small, published models generally account for manure-N mineralization during only the first 3 or 4 years following application (Berntsen et al. 2007; Mallory and Griffin, 2007; Schröder et al., 2005) with mineralization during subsequent years assumed to be negligible.

In order to estimate the mineralization of organic manure-N, Anon (2001) "stripped" cattle and pig FYM, cattle and pig slurry, layer manure and broiler litter of their NH_4^+–N content by cycles of wetting and drying over a period of 8 weeks. The treated manures, containing only residual organic-N, were then applied to loamy sand and sandy loam soils in field experiments at two sites over 6 years with a perennial ryegrass test crop. The organic N release data from both sites were not significantly different ($P > 0.05$) and were pooled in order to derive "generic" functions for modeling purposes. Comparison of 95% confidence intervals for the slope of each organic-N release relationship showed that the data fell into two broad groups, with pig slurry and poultry manure having a greater rate of organic-N release (0.022 × cumulative day degrees (CDD)) than cattle/pig FYM and cattle slurry (0.0076 × CDD). Thus, in total, around 50% of the organic-N in pig slurry and poultry manure might ultimately be mineralized and potentially available for crop N uptake but only around 17% of cattle or pig FYM up to 2300 CDD, which in these experiments was reached in the second season after manure accumulation.

2.2.2.2. The Cumulative Effects of Repeated Manure Applications

Long-term experiments show that although annual release of organic N is very small, cumulatively these small contributions could have a large impact on the total N availability in a long-term period (Berntsen et al. 2007; Mallory et al., 2010; Schröder, 2005).

In the 2 years following application of ^{15}N-labeled cattle slurry applied by Sørensen (2004) to a sandy loam in replicated micro plots, N uptake in barley in the year after application was 2–4 kg N ha^{-1} greater on the slurry-treated plots compared with the mineral-N treatment, and N uptake with the cover crop was 3–5 kg N ha^{-1} greater on the slurry-treated plots. However, none of these differences were statistically significant ($P < 0.05$). In the second year after application, there were also no significant differences in N uptake. Sørensen (2004) concluded that while a significant proportion of NH_4^+–N in cattle slurry is immobilized shortly after application to soil, the fertilizer value of the slurry may be slightly less or equal to the TAN content when gaseous N losses are avoided due to mineralization of organic N in the slurry. The immobilized N is only slowly released and contributes little to the residual effects in the first years.

The residual effects of 4 years repeated cattle slurry applications on grassland were studied by Schröder et al. (2007) who reported that dry matter (DM) yields and N offtake of cut grassland responded positively

($P < 0.05$) to both current manure applications and applications in previous years, whereas mineral fertilizer-N increased yields only in the year of application. They found NFRV of injected cattle slurry of 51–53% in the first year and they calculated an NFRV of approximately 70% after 7–10 yearly applications. Nitrogen offtake could be reasonably well predicted with a simple N model, adopting an annual RDR of the organic N in manure of 0.10–0.33 year^{-1} during the year of application and 0.10 year^{-1} in the following years, albeit keeping RDR at 0.10 year^{-1} for subsequent years is not in accordance with other results such as those presented in Table 7.5 above. In contrast, it took two to four decades of yearly applications to raise the NFRV of surface-applied FYM to a similar level from an initial value of 31%.

Cela et al. (2011) evaluated the residual effects of pig slurry applied for 6 years to continuous maize. The residual effects of six consecutive pig slurry applications on wheat-N uptake ranged from 3 to 4% of the total N input. The authors compared these uptakes with the 2–5% in the year after slurry application reported by Sørensen (2004) and Schröder et al. (2007) in northern Europe. Cela et al. (2011) found that mineralization of the organic N applied in pig slurry, at rates compliant with the Nitrates Directive, contributed with further residual N effects and would allow farmers to reduce N fertilization of a subsequent wheat crop by around 30 kg N ha^{-1}. This large residual effect could be due to greater proportions of residual mineral-N remaining in soil under dry Mediterranean conditions.

Hence, the accumulated effect of repeated manure application should be accounted for in fertilizer planning (Schröder et al., 2007). Bosshard et al. (2009) showed that the previous field management, including previous manuring history, has insignificant influence on the availability of N in a new manure application.

Generally, the residual effect is greatest for manures containing a large proportion of organic N. As the mineralization of N in soil takes place during most of the year, the residual effect is greatest in crops with a long growing season (Sørensen and Amato, 2002); vice versa, losses of N are greater in crops with short growing season.

2.2.3. Implications of Longer Term Mineralization for Manure-N Efficiency

Although long-term N fertilization affects soil organic N reserves, N mineralization potential, and crop response to applied N, little information is available on the influence of short-term N fertilizer management on soil organic N availability and crop response (Glendining et al., 1997). This is a

concern because it is a common practice for farmers to repeatedly apply manure to the same fields. To accurately assess the total plant availability of manure nutrients and to ensure balanced fertilization, it is necessary to account for the nutrients remaining in soil from previous manure applications. The amount of residual N that will be released during following years will increase the risk of excess N application if not accounted for when deciding on N fertilizer application rates. The long-term, as well as short-term, mineralization is affected by different parameters such as temperature, moisture, type of livestock manure, timing (Beckwith et al., 2002) and mineral-N fertilizer use. Thus, the long-term effects of organic fertilizers through the slow release of N have to be considered to enable optimization of fertilizer use. Given the long manuring history of most agricultural systems, a re-evaluation of the fertilizer value of manure appears justified (Schröder et al., 2005). The results also imply that the long-term consequences of reduced N application rates may be underestimated if manuring histories are insufficiently taken into account. This was also the conclusion of Shepherd (1993).

A number of simple models have been described to estimate the residual effects of manure-N (e.g. Klausner et al., 1994; Petersen and Sørensen, 2008a; Schröder et al., 2007). In Table 7.6 an example of model-estimated residual N effects under North European conditions is given. This model is based on mineralization rates of residual organic N that diminish over the years after application.

We conclude that:

- While residual N effects are relatively small, even in the year after application, the accumulated effect of repeated manure application can be significant and should be accounted for in fertilizer planning.
- The N availability over the long term will be affected by the multiple parameters of manure type and composition, environmental parameters (moisture and temperature), application technique and timing.

Table 7.6 Residual Nitrogen Effects of a Single and Repeated Manure Applications Given as Mineral Fertilizer Replacement Values (% of Annual Total N Application)

	Repeated Manure Applications		
Manure Type	**1 year**	**2 years**	**10 years**
Cattle slurry	3–5%	5–7%	9–14%
Pig slurry	2–3%	3–5%	6–8%
Solid manure	5–8%	7–13%	12–24%

Model calculation from Petersen and Sørensen (2008a).

- In the years following the season of application, the recovery of N is greater for more recalcitrant compounds than for readily available components such as urine, due to the slower release of N that enables crop recovery in later seasons.
- Most authors reported only small percentages of N availability for successive years, most of them being around 2–3% of extra N available per year, reaching average values from 50 to 80% for the total N availability in a 6–10 year period.

2.3. Factors Affecting the Plant Availability of Manure-N

The availability of manure-N is influenced both by the chemical composition of the manure and by N losses that occur before and after application in the field. The chemical composition of the manure is influenced by livestock species, feed composition, additions to the manure such as bedding material, chemical transformations during storage (including losses of N in buildings and storage) and with some manure management systems, the partitioning of urine and feces into solid and liquid manure fractions. Chemical composition can also be influenced by manure treatment.

2.3.1. Effects of Feeding

The N content of manure is related to the N content in the diet. Matching the N input in the diet to the animal's requirements is an effective option to reduce N excretion. Feed composition influences the balance between excreted urine and feces N and also the availability of manure-N. Important factors are the protein and fiber composition of the feed (Canh et al., 1998; Paul et al., 1998; Sørensen and Fernández, 2003; Sørensen et al., 2003a). Most of the urine N is urea while most of the feces N is in the organic form.

Different feeding is reflected in the chemical composition of manure including the C/N ratio. A high correlation between C/N ratio and NFRV of slurries from differently fed cattle and pigs has been found (Fig. 7.4).

Velthof et al. (2005) analyzed the effects of pig diets on emissions from stored slurry and slurry applied to the field. From the tested diets, decreasing the protein content had the largest potential to simultaneously decrease NH_3 and CH_4 emissions during manure storage and N_2O emission from soil. It was concluded that an integral assessment of the environmental and agricultural impact of handling and application of pig manure as a result of diet manipulation provides opportunities for farmers to maximize the value of manures as fertilizer and soil conditioner and to minimize N and C emissions to the environment.

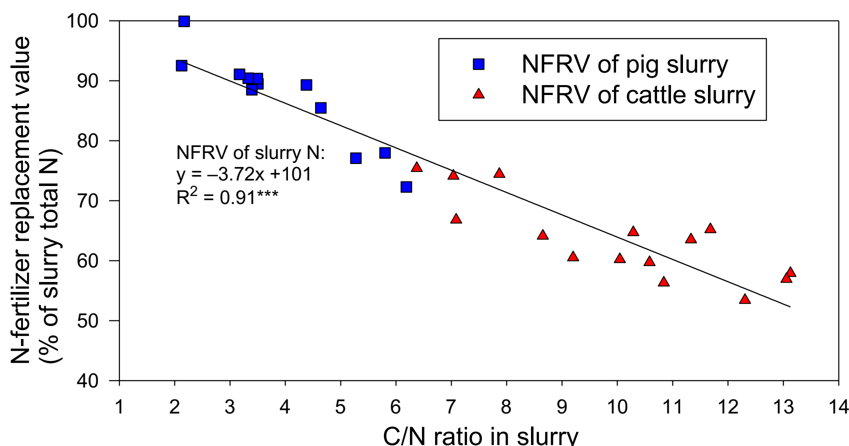


Figure 7.4 Relationship between C/N ratio in slurry from differently fed cattle and pigs and corresponding NFRV measured after simulated slurry injection before sowing a barley crop. *(Data from Sørensen et al. (2003a) and Sørensen and Fernández (2003))*. For color version of this figure, the reader is referred to the online version of this book.

2.3.2. Nitrogen Loss from Buildings Housing Livestock and the Influence of Bedding Material

Gaseous losses from livestock buildings occur by NH_3 volatilization, nitrification and denitrification (Webb et al., in press), mainly in the form of NH_3. These losses mainly derive from TAN in manure, and by reducing the amount of TAN in the excreta and manure, the relative N availability is also reduced. The EMEP/CORINAIR emission inventory guidebook gives default estimates of N emissions from livestock buildings of 12% from buildings housing cattle and 17% from buildings housing pigs. Actual emissions will depend on the building type and manure management, and greater losses can be expected under conditions with higher temperatures.

Measures to reduce emissions of NH_3 from livestock buildings have been the subject of several reviews (Ndegwa et al., 2008; Philippe et al., 2011; Sommer et al., 2006a; Webb et al., 2005) and will only be summarized here.

The immediate source of NH_3 following N excretion by livestock is urea excreted in the urine. Urea is rapidly hydrolyzed by the enzyme urease to ammonium carbonate ($(NH_4)_2CO_3$) and NH_4^+ ions provide the main source of NH_3. Urease is widespread in soils and feces and, in consequence, hydrolysis of urea is usually complete within a few days (Whitehead and Raistrick, 1990). An alternative to cleaning soiled floors is to separate urine and feces (Ndegwa et al., 2008). One of the most important factors

controlling NH_3 emissions is the total area of soiled surfaces (Sommer et al., 2006a and references therein). Hence, reducing the total soiled area, either by reducing the area where the animals excrete or by cleaning the floor soiled by excreta, will reduce total emissions.

2.3.2.1. Cattle

Techniques for reducing NH_3 emissions from naturally-ventilated buildings include grooved flooring, the frequent removal of manure and manure cooling (Sommer et al., 2006a). If the floor is smooth, scraping may reduce emission by up to 30% but to the detriment of animal welfare (Sommer et al., 2006a). It is also possible to reduce emissions from buildings by reducing the area available to the animals and, hence, reduce the floor area contaminated by excreta (Camp et al., 2009). This may have an adverse impact on animal welfare.

In buildings where cattle are housed on straw, increases in the amounts of straw used for bedding may reduce NH_3 emissions from the building (Gilhespy et al., 2006). This approach has the advantage that by immobilizing TAN in the straw, there will be no subsequent increase in NH_3 emissions from the storage or spreading of the manure, unless the manure composts during storage.

2.3.2.2. Pigs

In general, NH_3 emissions from pig housing will be reduced if the surface area of the exposed slurry or manures is reduced and/or it is frequently removed and placed in covered storage outside the building (UNECE, 2000). Ndegwa et al. (2008) concluded that all of the urine–feces segregation methods they evaluated and reviewed can reduce NH_3 emissions from livestock buildings by about 50% compared with conventional manure handling systems. Compared with a fully slatted floor system, a partly slatted floor system produces less emission of NH_3 (Philippe et al., 2011). Cast iron, metal or plastic slats can reduce NH_3 emissions by 10–40% compared with concrete slats (Philippe et al., 2011) although plastic slats are not considered appropriate for heavy pigs (<100 kg). Philippe et al. (2011) considered greater emissions from bedded systems are partly explained by the larger space allowance for the livestock which also enhances the bacterial processes in the litter.

2.3.2.3. Poultry

Emissions from poultry buildings may be greatly reduced if the DM of the manure or litter is 60% or more. This inhibits hydrolysis of uric acid to

urea and, hence, keeps the N in a stable form which will not emit NH_3. Keeping the litter (e.g. sawdust) on the floors of buildings housing broiler chickens as dry as possible, by minimizing spillage of water (e.g. by installing drinking nipples), thus helps to minimize NH_3 emissions (Elwinger and Svensson, 1996).

In buildings housing laying hens, NH_3 emissions can also be greatly reduced by drying the manure on the belts fitted beneath the cages, which remove manure (Groot Koerkamp, 1994). Some reduction is also possible by frequently removing the droppings using belts. Emissions from poultry buildings may be greatly reduced if the DM of the manure is 60% or more. For housing with forced ventilation, chemical or biological scrubbing of the exhaust air can substantially reduce NH_3 and airborne particle emissions.

2.3.2.4. Bedding Material

Addition of straw, or other bedding material with a large C/N ratio, to livestock housing will increase the amount of degradable C and induce immobilization of mineral-N, transforming inorganic- to organic-N (Kirchmann and Witter, 1989), thus reducing the N availability of manure-N (Kirchmann, 1985; Van Faassen and Van Dijk, 1987). During storage of farmyard manure, the reverse process may occur and some UK studies (Chadwick, 2005; Sagoo et al., 2006; Williams et al., 2003), which carried out a mass balance of total and organic-N at the beginning and end of a storage period, indicated net mineralization of up to 0.30 of the initial organic N content of the heap.

2.3.3. Nitrogen Loss during Manure Storage

During storage of both liquid and solid manures, significant N losses occur mainly from the TAN pool in the form of NH_3 emission. Under North European conditions, Sommer et al. (2006b) estimated yearly losses of 6–30% of total N from uncovered slurry stores. However, losses can be reduced by more than 80% by coverage of the slurry store to 1–3% loss of total N (Sommer et al. 2006b). During the period, slurry is held in livestock buildings and manure stores, a significant part of the organic N is mineralized to TAN. The mineralization of organic N in stored slurry can vary from 10 to 80% and is influenced by livestock species, feeding, storage temperature and time (Sommer et al., 2006b; Sørensen, 1998; Sørensen et al., 2003a). About 90% of the urine organic-N has been reported to be converted to NH_4^+ during anaerobic storage (Sørensen et al. 2003a). This assessment is based on measurements under laboratory conditions and

storage for about 20 weeks at 10–15 °C. This gives about a 30% mineralization of cattle feces N and a 40% mineralization of pig feces N during manure management (including TAN in excreted feces) (Petersen and Sørensen, 2008a; Sørensen, 1998; Sørensen and Fernández, 2003; Sørensen et al., 2003a).

Total N losses of up to 50% from stored solid pig manure and 30% from stored solid cattle manure have been reported (Chadwick, 2005; Petersen and Sørensen, 2008b; Petersen et al., 1998), but on average losses are less: 15% for cattle FYM and 31% from pig FYM (Webb et al., 2012). Hansen et al. (2008) assessed an average N emission of 15% of total N from uncovered solid cattle manure, 10% from uncovered cattle deep litter, and 40% from solid pig manure during more than 100 days storage under North European conditions. The losses can be significantly reduced by covering and/or compaction of manure heaps (Chadwick, 2005; Sommer, 2001). During the storage of solid manures, losses may also occur by leaching on unsealed surfaces (Petersen et al., 1998), or by surface runoff (Martins and Dewes, 1992), in addition to the gaseous emissions. The losses will be larger if the areas involved are not covered or roofed since rainfall will aggravate the problem. Ensuring that there are adequate facilities to intercept leaching/runoff from livestock housing/manure storage and return the dirty water to the manure management system (e.g. to a slurry tank) will increase the N fertilizer efficiency and reduce aquatic pollution.

If solid manures (FYM, deep litter) are composted, increasing the straw content of the manure increases the N immobilization and may also result in reduced NH_3 emission during composting (Kirchmann, 1985). During storage of slurry and solid manure under anaerobic conditions, bedding straw causes no N immobilization but after application to soil, the straw causes significant immobilization and a reduced N availability (van Faasen and van Dijk, 1987; Kirchmann and Witter, 1989; Sørensen, 1998).

By reducing storage losses, the manure contains a greater concentration of N and the N availability is also greater (Sommer, 2001). This aspect is not considered in detail as the emphasis in this review was on identifying the most appropriate methods for the application of manures and any suitable treatments for improving the agronomic value of the manures.

Despite the turnover of N during storage of slurry under anaerobic conditions in livestock buildings and manure stores, the time spent in storage appears to have no detectable effect on the plant availability of N, provided losses are insignificant (Sørensen, 1998). This is possibly because a significant

proportion of the readily decomposed organic N is rapidly mineralized in both storage and in the soil.

2.3.4. Manure Management and Treatment

Slurry composition is not ideal with regard to optimizing its potential as a fertilizer and making the best use of techniques to reduce emissions. In particular, the high DM and C content pose several problems during storage, and during and after slurry application (Table 7.7).

The fibrous OM in slurry tends to produce a crust on the slurry surface and/or sediment on the bottom of the slurry tank. As a result, slurry must be homogenized prior to application to achieve an even distribution of nutrients. Homogenization of high DM slurry is energy-consuming and increases NH_3 emissions. Thus, the need for slurry homogenization should be reduced as far as possible, which is only possible if the slurry DM content is reduced. However, producing low-DM slurries would normally mean that a greater volume of slurry is produced. The increased energy needed to spread the larger volume needs to be compared with the extra energy for homogenization of high-DM slurries.

There are potential conflicts in the management of slurry storage which need to be addressed. The first is that natural crusting is suggested

Table 7.7 Problems Arising from Slurry High-DM and -Carbon Content

Area	Problem
Storage	• Crust formation and consequent sedimentation of solids* • Increased energy consumption for pumping and mixing • Emission of NH_3,* N_2O, CH_4, and odor
Spreading, the process of manure application	• NH_3 and N_2O losses after application • Greater effort for even and reduced emission application • Crop damage due to scorching by slurry in warm climates
Fertilization, the effect of manure-N as a crop nutrient	• Less effective than mineral fertilizer • Effect less predictable than from mineral fertilizer • N immobilization in the soil • Denitrification and subsequent N_2O emissions

*Crusting will reduce NH_3 emissions during storage but can make it difficult to empty the store.

as a means to conserve N by reducing NH_3 emissions (Misselbrook et al., 2005; Smith et al., 2007). No studies have been carried out to assess the overall impacts of allowing stored slurry to crust. This is likely to be a net reduction in NH_3 emissions providing the crust does not become too thick making it difficult to disperse and likely to impair the effectiveness of reduced NH_3 emission slurry spreaders. Yet while crusting is a proven means of reducing NH_3 emissions during storage, it has disadvantages and these could be overcome by using a manufactured cover, which can also be more effective in reducing NH_3 emissions (Sommer et al., 1993), albeit more costly. A straw cover can also generate N_2O emissions (Sommer et al., 2000). The second conflict is more difficult to reconcile, in some countries at least. There are advantages to having slurry of low DM (and with a certain concentration of N to be attractive as a fertilizer). However, covering stores to reduce NH_3 emissions will stop rainfall entering the store and hence may give rise to higher DM slurry. There may well be a significant regional difference here. For example, in the UK, rain falling on a slurry store over winter can double the volume (Laws et al., 2003). But in warmer countries, covers may reduce evaporation giving rise to slurry with a reduced DM content compared with slurry stored without a cover. This relationship between covering slurry stores and the impact on DM is one that is likely to vary among regions within the EU.

Low-DM slurry has advantages when it comes to its use as a fertilizer. The aim should be to make optimum use of slurry N and making slurry N as predictable as possible (i.e. a consistent NFRV). This means that slurry should have a low-DM content and be stored under an artificial cover. Slurry dilution (by rainfall or water addition) is not the best means to reduce DM content, except perhaps in dry or hot regions, as it increases slurry volume and hence, more storage capacity is required, more volume to be transported, more pressure on soil structure and greater risk of polluting surface waters by runoff.

Slurry contains easily degradable C that serves as a nutrient source to microbes. During slurry storage, a continuous degradation of OM can be observed (Sommer et al., 2007). Degradation intensity is strongly dependent on slurry-DM quality. As conditions in the slurry are anaerobic, degradation of OM must always occur via anaerobic pathways. This means that CH_4 and CO_2 are formed as end products of the degradation process.

The N availability to plants is difficult to calculate with high-DM slurry. The narrower the C/N ratio, and the greater the NH_4–N content,

the more N is available to plants immediately after slurry application. With a wide C/N ratio, part of the slurry N is immobilized in the soil N pool and becomes available only at a later and non-predictable stage. The C/N ratio of manures tends to increase as the feed protein is reduced. This is a very effective measure for reducing N losses from the whole system, but may make it more difficult to predict N release from manures as a smaller proportion is likely to be available in the season of application.

It is thus useful to reduce slurry DM and C content at an early stage of manure management (Fig. 7.5). There may be concerns that applying slurry with a reduced DM and C content will have an adverse effect on soil structure and fertility (less adding OM) in the long-term. However,

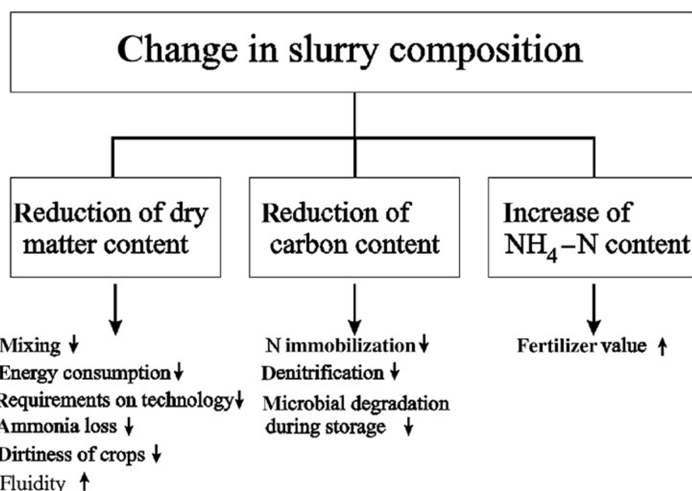


Figure 7.5 Changes in slurry composition to be achieved by successful manure treatment.

the amounts of C added to soil in slurries are much less than those added in litter-based manures and any effect is likely to be very small. The OM left after a reduction of manure C is in more stable compounds and contributes more to the long-term carbon retention in soil (Thomsen et al., in press).

There are various techniques of manure treatment that can be classified as physical, chemical or biological (Fig. 7.6).

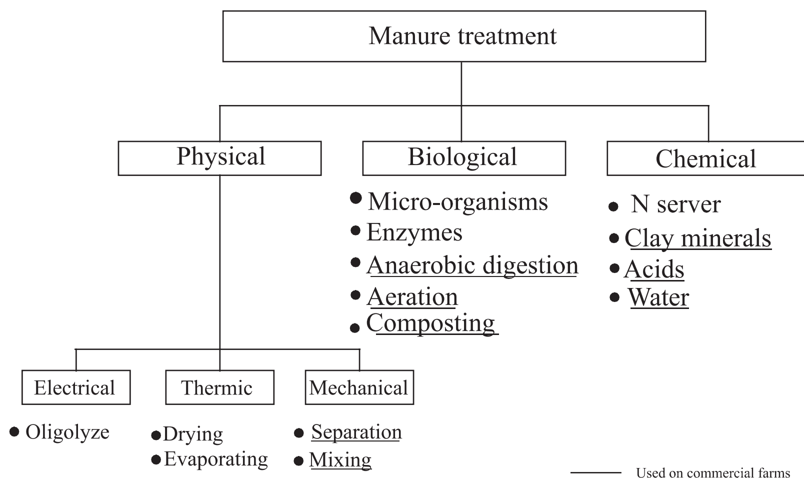


Figure 7.6 Classification of manure treatments as physical, chemical or biological way of treatment.

Possible slurry treatments are listed in Table 7.8 below with an outline of how they might change manure-N efficiency.

Other possible manure treatments, AD, manure composting, slurry separation and slurry acidification are considered in more detail in the following section.

2.3.5. Influence of the Length of Growing Season

The length of the growing season influences the manure-N that is available to the first crop due to the continued mineralization of organic manure-N (Olesen et al., 2004). For crops with a long growing season, a greater availability of manure-N is expected. Studies with ^{15}N-labeled manures have shown an uptake of 1.5–6.0% of the labeled manure-N in ryegrass cover crops following the spring barley crop to which the ^{15}N-labeled manures were applied (Olesen et al., 2004). Based on this, Petersen and Sørensen (2008a) estimated the additional mineral fertilizer replacement value in crops with a growing season which extends into the autumn, such as beets, maize and grassland, to be equivalent to 2–5% of the total manure-N applied, depending on the proportion of organic N in the manure (North European conditions).

2.3.6. Timing of Manure Applications

The optimum time of manure application is usually in spring and summer when the crops are taking up nutrients. The greatest barrier for using the

Table 7.8 Slurry Treatments and their Potential Impacts on Manure-N Efficiency

Treatment	Impact on Manure-N Efficiency
AD	Increases TAN concentration and reduces DM content leading to a manure with potentially increased manure-N efficiency in the season of application. The increased pH can lead to increased NH_3 emissions during storage and after spreading.
Manure composting	Reduces TAN concentration and likely to reduce manure-N efficiency in the season of application
Slurry separation	The liquid fraction has a more consistent TAN concentration than untreated slurry making it easier to estimate the NFRV and adjust mineral-N fertilizer applications accordingly, but the opposite is true for the solid fraction
Slurry acidification	Reduces emissions of NH_3 during storage and following slurry application to land thereby increasing the amount of crop available N
Slurry aeration	Aeration introduces oxygen into the slurry in order to allow aerobic microbes to develop. OM is oxidized to CO_2 and H_2O. Odorous compounds are degraded. The slurry-DM content decreases. Thus, less mixing is needed and handling properties of slurry are improved. Slurry aeration results in an increase in NH_3 emissions and in energy consumption. The potential for N_2O emissions is likely to increase as well.
Slurry dilution	Reduces the DM concentration making it easier for the slurry to infiltrate the soil potentially reducing emissions of NH_3 and thereby increasing the amount of crop available N (Mkhabela et al., 2009). However, a significant effect is only achieved if the water-to-slurry-ratio is at least 2:1. This would result in a dramatic increase in slurry volume that has to be stored and applied.
Use of additives	Chemical–physical additives are meant to adsorb NH_4–N and thus reduce NH_3 emissions (Ndegwa et al., 2008 and references cited therein) and can potentially increase the amount of crop available N. Enzyme-based additives are intended to increase biological degradation of OM. The mode of action and composition of commercial additives are in many cases not known and further research is needed.

Continued

Table 7.8 Slurry Treatments and their Potential Impacts on Manure-N Efficiency—cont'd

Treatment	Impact on Manure-N Efficiency
Slurry mixing	Slurry mixing is the most commonly applied manure treatment technology. Slurry is homogenized prior to application in order to achieve an even distribution of nutrients. Mixing slurry will lead to a more consistent material being applied to land making it easier to estimate the NFRV and adjust mineral-N fertilizer applications accordingly.

optimal timing of application is often the required manure storage capacity. Significant investment is needed to achieve a storage capacity of, e.g. 9–12 months. In areas with high precipitation and heavy soils, it is also problematic to use the heavy application machinery in spring. The advantage of spring application is greatest in areas with high rainfall during the autumn and winter period.

2.3.7. NH_3 Loss after Application

Large emissions of NH_3 have been measured following surface application of livestock manures to land (e.g. Pain et al., 1989), with around 50% of the total NH_3 loss occurring within 4–12 h after slurry application (Pain et al., 1989). NH_3 emission is from the TAN fraction of manure-N (Søgaard et al., 2002). The rate of NH_3 volatilization from slurry applied to soil increases with increasing temperature and wind speed (Table 7.9). After surface application, the emission of NH_3 per unit area also increases with increasing slurry DM content (Søgaard et al., 2002). This may be due to the effect of the slurry solids on the interception of slurry by stubble or crop leaves, or due to a reduction in the rate of infiltration of the slurry water into the soil. The loss of TAN as NH_3 after manure application reduces the amount of available manure-N. Thus, NH_3 emissions not only have negative environmental impacts but are also a loss of a valuable plant nutrient that, in consequence, has to be bought as mineral fertilizer.

In addition to the direct reduction of emissions following manure application, the use of reduced NH_3-emission application techniques will conserve much of any NH_3 saved through emission mitigation measures applied during housing and storage (Webb et al., 2005). Since these application techniques also reduce the overlapping/spatially uneven applications that are at risk with broadcast spreading, they reduce the chance of

Table 7.9 Factors Influencing NH_3 Emissions after Manure Application (Søgaard et al., 2002)

Factor	NH_3 Emissions Decrease with…
Weather	Low wind speed, low temperature, light rainfall
Slurry composition	Low DM, low pH
Application technique	Low trajectory application in crop canopy or with immediate incorporation or injection

NO_3^- leaching due to localized overfertilization. Timing of application, reduction in slurry DM content and low trajectory application techniques (band spreading) in growing crops have been proposed as ways to reduce NH_3 emissions following manure application.

Different techniques are available, such as deep injection, shallow injection, incorporation of slurry by plowing or by rotary harrow, and application of slurry by band spreaders. Special injectors have been developed for injection into grassland and for tillage land, respectively. Generally, the greatest reductions in NH_3 emission are obtained when slurry is immediately incorporated by plowing (Webb et al., 2010) or injected deeply (Huijsmans et al., submitted for publication). Applying slurry using the trailing hose (TH) or trailing shoe (TS) techniques on bare soil only gives a small reduction in NH_3 emission; the largest NH_3-emission reduction application by TH is obtained from applications under the canopies of growing crops (Sommer and Hutchings, 2001). NH_3 emission from slurry applied by different methods is described in the ALFAM model (Søgaard et al., 2002). This model predicts the NH_3 emission from field-applied pig and cattle slurry, as a function of the weather (temperature and wind speed) and the application technique used.

The more effective NH_3 abatement techniques, such as injection or immediate incorporation into soil, are usually more effective in increasing N uptake than the less-effective NH_3 abatement techniques such as the TH (e.g. Mattila et al., 2003). Increased manure-N efficiency has also been reported following rapid incorporation of solid manures (e.g. Maidl et al., 1999). But in other cases, little or no effect on crop yield could be seen after shallow injection in open slots compared with TH on grassland (Rodhe and Etana, 2005; Smith et al., 2000). Generally, the reduction in NH_3 emission is related to how effectively and quickly the manure is covered with soil. At injection, the slots created for the slurry must have the volume to hold the slurry applied. This means that there must be a balance between rate and slot space. Deep injection (more than 20 cm depth) will ensure that

the slurry is placed beneath the soil surface, but the design of the injector tine will also influence how well the slurry is covered by the soil (Hansen et al., 2003). Improved management of application method, by using the TS instead of splash plate, and timing, by applying slurry in April rather than June, increased NFRV of cattle slurry applied to grassland in a study in Ireland (Lalor et al., 2011) (Fig. 7.7).

The method of FYM treatment also influences the change in manure composition, especially in the NH_4–N content. During the composting process part of the NH_4–N not lost during composting is transformed to more stable, organic-N forms that are less subject to gaseous losses. Anaerobic stacking tends to inhibit both nitrification and immobilization of NH_4–N. NH_3 emissions during and after FYM spreading are strongly influenced by the NH_4–N content. Emissions after spreading have also to be included in the measurements in order to calculate the net total of emissions from composted and anaerobically stacked FYM. Webb et al. (2004) measured NH_3 emissions following the application of conventionally stored and anaerobically stacked FYM but did not find any differences in emissions following surface application. Moreover, NH_3 emissions from both types of manure were reduced by around 90% by immediate incorporation and by 60% by incorporation within 4 h of application.

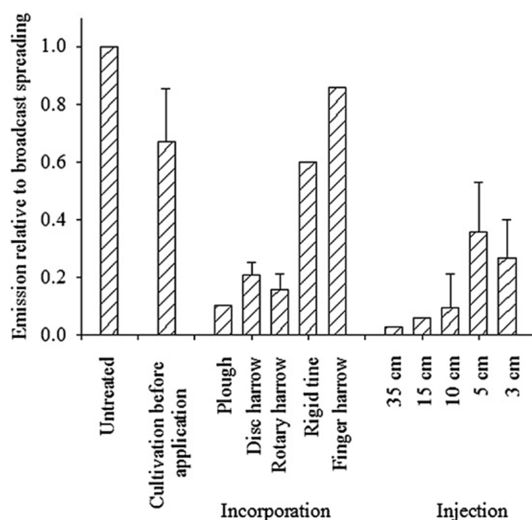


Figure 7.7 Reduction in NH_3 emission due to application technique related to NH_3 losses from animal slurry broadcast onto soil or a plant covered soil (Sommer and Hutchings, 2001).

2.3.8. Denitrification Losses after Application

Denitrification losses in the form of N_2O and N_2 are usually increased after manure application as compared with equivalent application of mineral-N fertilizers (Velthof et al., 2003). Such N losses also imply a reduction in manure-N availability. Denitrification is promoted under conditions with decreased oxygen concentration in the soil in the presence of NO_3^-. Microbial decomposition of organic compounds in manure consumes oxygen and low levels of oxygen occur temporarily in soil (Hernandez-Ramirez et al. 2009). Nitrous oxide emission also occurs by nitrification of NH_4 in soil (Skiba et al., 1993). Denitrification losses are extremely variable in space and time, and prediction of the losses from manure-N is difficult.

The losses are influenced by, e.g. soil type, soil-moisture conditions and by the distribution of manure in soil. Losses can be large, e.g. by deep injection in heavy soils when conditions are wet after application (Thompson et al., 1987). Manure also contains available C, which may stimulate denitrification (Paul and Beauchamp, 1989). In a study of Velthof and Mosquera (2011), shallow injection of slurry increased average emissions of N_2O in comparison with surface application on both grassland and maize land.

Petersen and Sørensen (2008a) used the SIMDEN model (http://xwww.agrsci.dk/media/webdav/filer/jpm/ostof/simden_ver_2_0_uk) to calculate average extra N losses equivalent to 3% of total slurry N after surface application and 5% of total N after shallow injection. This calculation is an average for soil types found in DK, and in areas with clay soils denitrification losses can be greater.

2.3.9. NO_3^- Leaching after Application

Timing manure applications to reduce the risk of NO_3^- leaching is a well-documented approach to conserving the available-N in manures and increasing manure-N efficiency. For example, the impact of different times of application was clearly illustrated by Webb et al. (2001) for UK conditions (Fig. 7.8).

The losses illustrated in Fig. 7.8 are those occurring in the season of manure application; NO_3^- losses will be even greater if losses in subsequent winters are taken into consideration (e.g. Thomsen, 2005). Hence, although appropriate timing of manure applications is a very effective means of reducing NO_3^- leaching in the season of application, it will not decrease losses in subsequent winters. To reduce long-term NO_3^- losses from manures, it is necessary to use crops with a long growing season or to include cover crops taking up N mineralized in autumn.

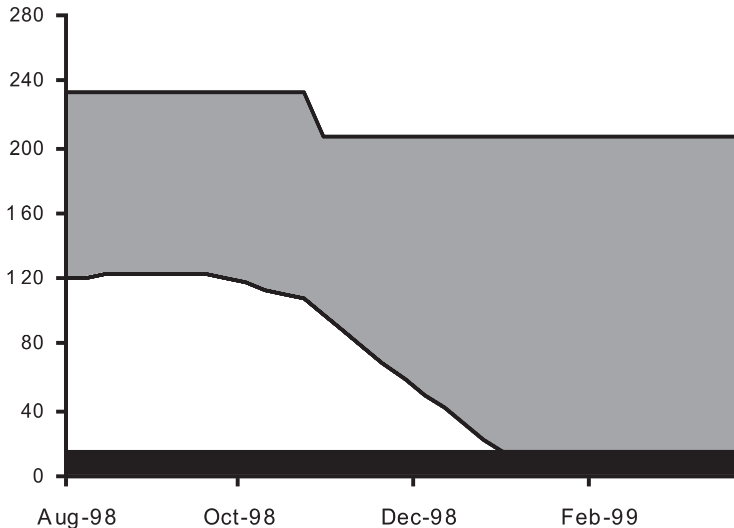


Figure 7.8 The proportion of N lost by NO_3^- leaching from application of broiler manure to a CL soil in Eastern England at times of application between early August and late March in a year of average hydrologically effective rainfall for the location. The white area of the graph represents the manure-N lost by leaching. The black area represents NH_3–N emissions and the gray area, the manure-N remaining in the soil. The units of the *y*-axis are kg N ha^{-1} (Webb et al., 2001).

Manure-N loss by leaching also has a direct relation to manure-N availability. Autumn applications of manure cause increased NO_3^- leaching in areas with moderate or high precipitation during autumn and winter (Webb and Archer, 1993; and references therein). Soil texture has an influence on NO_3^- losses with the greatest losses on sandy soils, but even on heavy soils NO_3^- losses can be significant (Webb and Archer, 1993; and references therein).

Schröder et al. (2010) showed that the N surplus (i.e. the difference between total N input and harvested N) was a better predictor of NO_3^- leaching from grasslands on sandy soil than total N input from mineral fertilizer and slurry. The effective N surplus, based on the difference between the summed inputs of the plant-available N and harvested N, proved to be the best indicator of leaching.

2.3.10. Soil-Type Effects and Effects of/Interactions with Manure Distribution in Soil

Jarvis and Aarts (2000) reported for grassland that the transfer of manure-N to soil with an efficiency of up to 93% was technically attainable by means of reduced-emission application techniques and optimum timing of manure

application. They also reported that on sandy soils, N could be taken up by crops with an efficiency of 77%. Hence, the potential for manure-N efficiency by crops, the product of the efficiency with which manure-N could be transferred to soil and the efficiency with which soil N could be recovered by crops, was 72% on sandy soils. Those workers reported that the average achieved was just 42%. This estimate of potential efficiency, being based on results from sandy soils, may be considered at the upper end of the range across all soil types. Webb et al. (1998) reported recovery of fertilizer-N to be greater on sandy soils (70%) than on clay soils (60%, Bloom et al., 1988) or shallow soils developed over chalk 55% (Grylls et al., 1997).

A number of laboratory experiments have indicated that net mineralization of manure-N is related to soil texture and that net mineralization decreases with increasing soil clay and silt content (Sørensen and Jensen, 1995). However, when slurry is placed concentrated in soil, e.g. by injection, net N immobilization is reduced and the plant availability increased, especially in more finely textured soils (Sørensen and Jensen, 1995, 1998) indicating that the effects of soil texture may be offset when manure is not dispersed throughout the soil. This effect of slurry distribution seems to be more significant with cattle than with pig slurry (Sørensen and Amato, 2002), probably because pig slurry better infiltrates the soil due to typically lesser DM (Anon, 2001). These effects were observed in small plot and pot experiments but they seem to be supported by measurements of fertilizer values in on-farm field experiments (Pedersen, 2001), as the observed increase in fertilizer value by injection of cattle slurry compared with incorporation by harrowing is greater than can be justified by the reduction in NH_3 emission.

It has been suggested that injection and incorporation of manures could increase crop N uptake not only by reducing NH_3 volatilization but also by introducing manure-N to the soil closer to the roots (Mattila, 2006). The extent of this effect will depend on crop type and method, e.g. sod injection in grassland will give less heterogeneous distribution of N. This could be particularly important when slurry is injected into soils that have developed a soil moisture deficit and hence, downward movement of surface applied slurry is constrained. However, any effect of placement could also be due to improved uptake of manure-P rather than manure-N.

2.3.11. Use of Specific Manure Analysis of Ammonium-N and/or Total N

The proportion of manure-N available to crops, both in the season of application and in subsequent years, needs to be accurately estimated in order

to correctly determine the amount of fertilizer-N needed for optimum crop growth, and to avoid excess applications of crop-available N. Increased farmer confidence in, and knowledge of, manure-N content is essential in changing attitudes from manure disposal to one of nutrient management. Typically, farmers are encouraged to use average values for nutrients published in handbooks (Jarvis and Menzi, 2005). However, official manure standards are currently inadequate, see Section 2.2.

An improvement would be to develop a methodology to predict manure-N efficiency and how it is influenced by different livestock production and manure handling systems. Specific check points could be ex-animal, ex-building, ex-storage and before spreading.

Due to variability within manure stores, representative sampling is crucial but also difficult, especially for solid manures (Webb et al., 2004). Slurries can normally be mixed in the store before taking a sample and, for analysis of NH_4^+–N, mixing is not that important if the surface layer is avoided. To get representative samples from solid manure, it is necessary to take large number of subsamples and carefully mix these. Analysis of NH_4^+–N in manure usually gives a good measure of the first year N availability. The variation in manure composition for a given farm is much less with time than the variation among farms. Hence, manure-N use may be improved even by infrequent analyses of manure samples. Meters are available for on-farm use estimating the plant-available N content of manures and can be used on subsamples of slurry prior to application: these tests take approximately 10 min to complete and some meters are reliable at estimating NH_4^+–N contents of slurries (Reeves, 2007; Williams et al., 1999). Near-infrared reflection spectroscopy (NIRS) has been shown to be a more accurate and rapid method to measure total and NH_4^+–N contents of manures (Reeves, 2007). However, NIRS instruments are still too expensive for on-farm measurement, but can be used for fast laboratory analyses (Sørensen et al., 2007). Hydrometers can be used because there is a good relationship between DM and nutrient contents. Significant progress has also been made in quantifying nutrient contents in-line on slurry tankers. Methods to measure plant-available N in organic N have been tested (e.g. Velthof et al., 1998), but the uncertainty of these methods is considerable and therefore, they are not widely applied.

We conclude that, for cattle and pig slurries, good estimates of first-season available N may be obtained by measuring manure NH_4^+. For poultry manure, it is important to take into account the content of uric acid.

2.4. Manure-N Efficiency Rates Currently Used in the EU 27

A review was carried out of how each MS takes account of manure-N efficiency in their AP and reports regional differences in manure-N efficiency rates. We also assessed the extent of differences in the availability of manure-N for both crop uptake and NO_3^- leaching among the MS and explored the reasons behind any reported differences in order to obtain a comprehensive overview of the current manure-N efficiency rates applied throughout the EU.

None of the MS presents a specific reference to, or definition of, manure-N efficiency in their AP or CGAP. The most commonly used term is "available N": the percentage (%) available N may be considered equivalent to the efficiency of manure-N in the season of application and this is the definition we use in Table 7.2. Values of the proportions of manure-N considered available to crops in the season after manure application are reported in Table 7.10 below.

While there are some differences among MS in estimates of the proportions of N available for crop uptake in any given type of manure, there is reasonable agreement in the ranking of manures, with N availability decreasing in the order pig slurry > cattle slurry > poultry manure > FYM.

Broadly similar estimates of the relative availability of different types of manure are to be expected since manures will be similar wherever the livestock are raised. Litter-based FYM will tend to have a smaller proportion of available N due to high gaseous N emissions and/or some of the TAN being immobilized in high C/N ratio litter. Hence, the widespread practice of allowing application of FYM in autumn, due to the small proportion of TAN and hence, lesser (but not insignificant) capacity for NO_3^- leaching compared with slurry.

Although many MS require manures to be applied by methods which reduce emissions, few actually report that they allow for a greater manure-N efficiency from incorporated than from broadcast manure (Italy, Netherlands, UK).

Insofar, as soil type was reported to be taken into account, it was in relation to the impact of soil type on NO_3^- leaching rather than on crop uptake of manure-N. Several MS allow application of FYM throughout the autumn but application of slurries and poultry manure is almost always forbidden during at least some autumn months. Very few countries report regional differences within the MS, although some countries use modeling systems which take account of regional and local factors (France, Romania).

Table 7.10 Reported Values of Crop Available % of Total-N (= Manure-N Efficiency). These Values are Used throughout the MS, not just within NVZs

	Cattle		Pigs		Layer		Broiler	Sheep
MS	**Slurry**	**Solid**	**Slurry**	**Solid**	**Slurry**	**Solid**		
AT	50	5/15	65	5/15	60	30	30	NR
BE (Flan)	60	30	60	30	60	30	30	30
BE (Wall)	NR	NR	NR	NR	NR	NR	NR	NR
BG	20–35	20	40–45	20	40–50	40–50	40–50	NR
CY	NR	NR	NR	NR	NR	NR	NR	NR
CZ	60	40	60	40	60	40	40	40
DK[*]	70	65[†]	75	65[†]	70	65	65[†]	65[†]
EE	50	25	50	25	50	25	25	25
FI	NR	NR	NR	NR	NR	NR	NR	NR
FR[‡]	Low C/N	High C/N	Low C/N	High C/N	Low C/N	Low C/N	Low C/N	High C/N
DE	50	25–30	60	25–30	60	30	60	NR
GR	20–35	10	25–45	10	20–30	20–30	20–30	10
HU	NR	NR	NR	NR	NR	NR	NR	NR
IE	40	30	50	50	50	50	50	NR
IT[§]	24–62	24–62	28–73	28–73	32–84	32–84	32–84	NR
LV	50	25	50	25	30	25	25	NR
LT		35[‖]		35[‖]			35[‖]	35[‖]
LU	25–50	30–50	30–60	30–50	NR	50	50	NR
MT	NR	NR	NR	NR	NR	NR	NR	NR
NL	60	40	60–70	55	60/70	55	55	NR
PL	50–60	30	50–60	30	50–60	30	30	30
PT	55–75	30–60	50–80	40–60	50–70	40–60	40–60	40–60
RO[¶]	50	30	50	30	NR	30	50	NR
SK	50	30	50	30	30	50	50	NR
SI	50	30	50	30	30	50	50	NR
ES[#]	NR	NR	NR	NR	NR	NR	NR	NR
SE	40–50[**]	36–41[**]	57	47	NR	48	47/57[††]	38
GB	20/35[‡‡]	10	25/50[‡‡]	10	NR	20/35[‡‡]	20/30[‡‡]	10
GB NI		30	50	30			30	

NR, not reported.
[*] Also includes residual-N effects in the following years after application.
[†] 45% for deep litter.
[‡] In the AP of France, manure-N availability is not expressed with respect only to the N content of the manure but with respect to the carbon-to-nitrogen (C/N) ratio in the manure.
[§] Availabilities are presented as a matrix according to soil type and time of application.
[‖] First year only. Total over 3 years = 70%.
[¶] There are no figures available to indicate how manure-N uptake is changed by these factors as the calculations are performed using actual soil and climate conditions for all the soil polygons included in NVZs.
[#] Different values are used in different regions.
[**] Depending on class of animal.
[††] Deep litter/other.
[‡‡] Autumn/spring application.

There does not appear to be any systematic variation in the reported manure-N efficiency across the EU that can be related to climate. Default national estimates of crop-available N do not differ consistently between the cooler northern MS and the warmer Mediterranean MS or between the wetter maritime MS and those MS with a continental climate. There may be two reasons for this. The first is that by far, the most significant driver for differences in crop N availability is the time of manure application in relation to the period of over-winter soil drainage and hence NO_3^- leaching: manures applied in autumn often lose much or all of their crop-available N by leaching while those applied in spring will not (Webb and Archer, 1993 and references cited therein). Many MS have closed periods for the application of those manures which contain large proportions of crop-available N (slurries and poultry manure). Hence, in those MS, slurries and poultry manures are only applied in spring, i.e. during or just prior to the start of the growing season. This restriction of the time of spreading will mean that slurry and poultry manure applications will tend to be made under similar climatic conditions, irrespective of geographic location. This will tend to eliminate differences that might otherwise be reported due to differences in the amounts of available N lost over winter by leaching or runoff due to differences in the amount of overwinter rainfall.

Estimates of manure-N efficiency are mainly based on field measurements either supplemented by literature review or developed by modeling. Some MS have derived values from the literature of comparable countries. In Sweden, it is possible either to use standard values of the manure-N efficiency or use analyzed TAN content of the manure. Clearly, some countries have carried out considerable research to assess the agronomic values of different types of manure. However, among such countries, differences in the estimates of crop-available N may be due less to differences in research findings and more to do with differences in the beginning and end of closed periods for manure application. For example, the United Kingdom publishes clear differences in the available N according to the time of manure application, in particular between manures applied in spring and in autumn (Anon, 2010). DK and The Netherlands, two countries where considerable study has been made of the agronomic value of manure, make no such distinction. This is because autumn applications of slurry are no longer allowed in those countries.

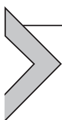
Hence, current NVZ rules are leading to a degree of harmonization across the EU in the timing of manure application and in the proportions of N available for crop uptake. The major differences among MS are in the lengths of the closed periods and the extent to which closed periods differ for grass and arable crops. Figure 7.9 presents the duration of closed



Figure 7.9 Closed periods in the MS. T = tillage land (maroon bars), G = grassland (dark green). Where a single bar (light green) is presented, there is a single closed period for tillage and grassland. The closed period for grassland in Spain is related to grass growth and not to the calendar. For SE, there are also restrictions on manure application from 1 August to 31 October in defined areas (mostly at the coast), where spreading is only allowed to growing crops or before sowing of winter rape. For interpretation of the references to color in this figure legend, the reader is referred to the online version of this book.

periods by grouping countries according to climate by ordering them on a north-south/west-east basis. Insofar, as any geographical trends exist, Fig. 7.9 suggests countries with the coldest winters end their closed periods latest, although the late ends of the closed periods in Italy and Malta contradict this suggestion. There is also a suggestion that countries with maritime climates have closed periods that begin earliest. The closed periods for Ireland and Northern Ireland appear to contradict this conclusion, but land use in those countries is dominated by grassland and the closed periods for those two countries are similar to that applied in the United Kingdom for grassland on soils other than light soils. However, current closed periods are not necessarily the most appropriate to reduce N leaching and in several MS closed periods are under review by the MS in discussion with the Commission.

A further difficulty in accounting for the source of differences is that some countries derive region or site-specific assessments of crop-available N from models, e.g. DEXEL in France (Manneville, 2006) (albeit the use of the DEXEL model is not obligatory), and ROMPEIL in Romania (Audsley et al., 2006).



3. REVIEW OF RECENT WORK EVALUATING METHODS TO INCREASE MANURE-N AVAILABILITY/REDUCE LOSSES

3.1. Treatment before Application

3.1.1. Anaerobic Digestion

During AD of manures, OM is converted into biogas and part of the organic N is mineralized to NH_4^+–N, thereby increasing the amount of NH_4–N and the NH_4–N:total-N ratio in slurry (Rubæk et al., 1996). As a result, the digested manure contains about 50% less C and DM, while the pH is increased by about 0.5–1.0 units (Sommer and Husted, 1995). The easily decomposable compounds such as volatile fatty acids that cause N immobilization after the application of slurry to soil are decomposed during the treatment (Kirchmann and Lundvall, 1993). Kirchmann and Lundvall (1993) studied the relationship between N immobilization and volatile fatty acids in soil after application of pig and cattle slurry. They found N immobilization in soil from digested to be only half that of undigested slurry, due to less easily-decomposable C in the digested slurry. Therefore, there is potential for greater N availability after digestion if NH_3 losses are prevented.

AD of livestock manures is mainly implemented for energy production reasons (Chantigny et al., 2009; Defra, 2011). Methane produced in an agricultural biogas plant is collected and transformed to electricity and heat in a combined heat and power coupling. AD not only reduces CH_4 emissions from manure stores, but consumption of fossil fuels, as well. Both processes reduce anthropogenic GHG emissions (Clemens et al., 2006). Improvement of manure quality is a "by-product" of AD.

Since both the NH_4–N content and pH in digested slurry are higher than in untreated slurry, the potential for NH_3 emissions during slurry storage is enhanced. However, due to the reduced DM content, digested slurry can infiltrate more rapidly into the soil which reduces NH_3 emissions after slurry application. Nevertheless, the increases in pH and TAN concentration increase the risk of NH_3 emission following application to land and the greatest utilization is obtained by direct injection or immediate incorporation of the digested manure.

AD significantly increased apparent N recovery (ANR) of cattle slurry compared with undigested in 1 year out of the two in which the treatments were applied, but by an average of 6% (Schröder et al., 2007). Chantigny et al. (2007) carried out replicated field experiments applying raw, digested

and separated pig slurry by means of the TS to grassland on sandy loam and loam soils. Even though the differences were not always statistically significant, crop-N uptake tended to be greater with treated than with raw pig slurry. The authors hypothesized that the greater crop-N uptake with the treated than with the raw pig slurry was partly due to the reduction in NH_3 losses. In addition, the proportion of N as TAN tends to be increased by AD. However, the reduced C content of the treated pig slurry may also have resulted in a greater N availability compared with raw pig slurry as described above (Kirchmann and Lundvall, 1993).

Wulf et al. (2002) applied beef cattle slurry anaerobically digested with biowaste (household) in replicated field experiments to grass on a poorly drained Stagno-gleyic Luvisol. Emissions of NH_3 from digested slurry were significantly less ($P < 0.05$) than from untreated slurry. The reduction of NH_3 emissions was considered due to the reduced DM content and faster infiltration of the substrate. This confirms experiments conducted by Rubaek et al. (1996) who reported NH_3 emissions of approximately 35% of TAN after TH application of digested slurry compared with 45% from untreated slurry. Nevertheless, this reduction of NH_3 losses seemed to be limited to warm and dry weather because in the same study, when infiltration was generally impeded due to high soil moisture content, no reduction of NH_3 emissions could be observed.

Pedersen (2001) reported the results of a large number of field experiments. The digested slurries used in these experiments consisted of mixtures of pig and cattle slurries codigested with other organic wastes. Pig slurry, cattle slurry, and digested slurry all gave an average MFRV in winter wheat of 57% of total manure-N for injected cattle slurry, 74% for injected pig slurry, and 82% for injected digested slurry. The MFRV for the digested slurry was only 64% after surface application. Even though the digested slurry infiltrated soil due to a lower DM content, hence reducing the potential for NH_3 volatilization, the higher pH can still result in a significant NH_3 volatilization after surface application.

De Boer (2008) carried out a replicated pot experiment using a sandy soil and a ryegrass test crop in which five co-digested pig slurries (CS) were compared with their raw source slurries. The five co-products came from the food-processing industry. Crop recovery of N from surface-applied pig slurry was reported to increase by around 10% as a result of digestion. The NFRV increased from 75% for undigested pig slurry to 95% for the digested slurry. The author concluded this could have been due to less NH_3 emission from digested slurry, greater available-N or a mixture of both.

The reduced content of organic N in the digested slurry also means that the potential long-term NO_3^- leaching losses from mineralized N can be reduced and that the residual fertilizer-N effects in the years after application are less (Schröder et al., 2007).

These studies indicate that in the season of application, the NFRV of N from surface-applied pig slurry may increase by around 10–20% as a result of digestion, but is significantly influenced by NH_3 emission. The results generally show a positive relationship between crop recovery and the mineral-N to total-N ratio of digestate. The reduced C content of digestate may also give greater N availability because the breakdown of labile slurry C during digestion may reduce soil N immobilization following digestate application. In planning N-fertilizer application, the greater N availability of the digested manure in the first year should be taken into account or there may be increased leaching losses, due to an excess of plant-available N.

3.1.2. Slurry Separation

During slurry separation, solids are mechanically separated from slurry. This results in two fractions: a liquid slurry fraction with low-DM content and a solid fraction that can be stored in heaps. Slurry separation is mainly used as a tool when there is a need to export/transport slurry P or OM over longer distances, e.g. to and from central/large biogas plants. Slurry P and OM are concentrated in the solid fraction. Emissions of NH_3 during the separation process are small as separation takes very little time and slurry is in the separator during that time. The greatest NH_3 emissions arising from slurry separation have been reported to be during the storage of the solid fraction (Amon et al., 2006).

The DM content in the liquid fraction is reduced by 40–45%. The C content is reduced by 45–50% (Amon, 1995). The effort needed for reduced emission application techniques is reduced as the liquid fraction of separated slurry is less viscous and flows more easily through spreading hoses. Separated slurry has a narrow C/N ratio, which reduces the potential for N immobilization in the soil. Nitrogen availability is more predictable and can be better calculated in order to match nutrient requirements of plants to fertilization. Significant N losses have been observed after storage of solid fractions from slurry separation (Petersen and Sørensen, 2008b), and proper management of the solid fraction containing 10–20% of the slurry N is important to maintain a high overall N utilization. Prediction of the plant availability of N in the solid fraction is also more difficult (Petersen and Sørensen, 2008b).

Sørensen and Thomsen (2005) studied the effects of separation of pig slurry on N utilization by spring barley and winter wheat and N loss using ^{15}N-labeled slurry applied to PVC cylinders inserted into a loamy sand soil. Nitrogen recovery was greater from the liquid fraction than from unseparated slurry in both wheat and barley. However, N recovery was similar when the uptake by the separated fractions was totaled in comparison with whole slurry at 82% NFRV for weighted separated slurry with 81% for whole slurry to spring barley in 2001, and 66–69 and 69% for winter wheat in 2002. They concluded that overall slurry separation does not appear to provide any consistent increase in manure-N efficiency when the manure fractions are applied to the same crop as the unseparated slurry. But NUE can be improved after separation by using the liquid in the winter crop by surface application in spring and using the solid residue on other areas where it can be incorporated in spring.

Bhandral et al. (2009) carried out a field study to estimate the impacts of cattle slurry separation on crop N uptake by grass together with NH_3 and N_2O emissions. Separated cattle slurry was applied to grass on a silty to sandy loam soil using mechanically assisted infiltration (MAI), which was carried out by manually banding the slurry over aeration slots. The effect of MAI on N uptake was inconclusive in this study despite substantially reduced NH_3 losses, probably due to the generally low-crop N recovery. Multi-year trials are needed to assess the long-term economic and environmental benefits of applying manure using improved infiltration strategies that reduce losses and accumulation of N and P.

Mattila et al. (2003) found that recovery from separated slurry was significantly greater only in 1 year of a 3-year field experiment ($P < 0.009$). Separation may increase N recovery compared with surface application of untreated slurry but the effect is uncertain and depends more on climate and soil conditions. Dosch and Gutser (1996) measured the effects of the mechanical separation of cattle slurry and application by surface broadcast or injection in field and pot experiments on a clay-loam soil. NH_3 emissions were reduced, and N availability increased when separated slurry was applied by broadcasting. However, there were no differences in NH_3 emissions when separated and unseparated slurry were applied by TH. Due to a reduced C content, the separated slurry led to less-N immobilization and consequently, a better utilization of the applied NH_4–N during the first vegetation period.

One possible way of treatment is that livestock slurry is separated in a solid and liquid fraction and that the mineral concentrate, which results from reverse osmosis of the liquid fraction, is used as a mineral fertilizer (Velthof et al., 2011). The mineral concentrate is a product containing N

and K and has only small concentrations of OM and P, while about 90% of the total N is NH_4^+. The mineral concentrate can be used as a liquid mineral-N and K fertilizer and the solid fraction primarily as source of P and OM, but it also contains available N.

3.1.3. Slurry Acidification

NH_3 volatilization significantly increases with increasing manure pH. Hence, acidification of slurry with sulfuric or nitric acid significantly reduces NH_3 volatilization by 50–70% during housing, storage and after application (Kai et al. 2008). As a result, the content of plant-available N in acidified manure is increased following slurry application, relative to untreated slurry, which leads to greater plant availability of N (Stevens and Laughlin, 1997; Stevens et al., 1989). Wulf et al. (2002) also reported emissions after acidification of cattle slurry were significantly less ($P < 0.05$) compared with untreated slurry. However, adding nitric acid to slurry increases N_2O emissions, both during storage (Oenema and Velthof, 1993) and after application to the field (Velthof and Oenema, 1993).

A system with acidification of slurry in buildings is now used in DK, where slurry pH is reduced to about pH 5.5 by adding sulfuric acid. The system has been documented to reduce NH_3 volatilization from housing, storage and application of pig slurry by about 70% (Kai et al., 2008). Kai et al. (2008) calculated that this could result in 32% more slurry N being available to the crop when comparing systems without coverage of the stored slurry. NH_3-emission reduction of about 50% is reported by similar acidification of cattle slurry. Kai et al. (2008) calculated that NH_3 emission is reduced from 15 to 4.8% of total N from buildings and from 9 to 1% from storage by acidification of pig slurry to pH 5.5 under Danish conditions. That means that the acidified pig slurry contains 26% more total N than untreated slurry after storage. This calculation is for uncovered storage. Under conditions with covered storage, it can be calculated that acidified pig slurry contains about 15% more N than untreated slurry based on Kai et al. (2008).

Sørensen and Eriksen (2009) measured the effects of slurry acidification with sulfuric acid combined with aeration on the turnover and plant availability of N in small plots. Slurry was applied by simulated incorporation before spring barley and simulated TH in winter wheat. Acidified cattle and pig slurry were applied. The pig slurry was obtained from a farm where half is acidified. Acidified slurry was aerated for 6 h or 4 d. Treatments also included an untreated control and acidified slurry without aeration. Neither acidification nor aeration had any significant effect on N dynamics in soil.

The NFRV of untreated pig slurry applied by surface-banding to winter wheat was equivalent to 74% of total N while the NFRV of the acidified pig slurry was 101–103%. The NFRV of cattle slurry was 39% for the untreated and 63–66% for the acidified slurry applied to winter wheat. Thus, acidification resulted in an NFRV that was about 25% points greater for the surface-banded slurry. This is equivalent to an increase in NFRV of 35–65% after surface-banding of acidified slurry compared with untreated slurry. A similar increase of NFRV after surface application of acidified pig slurry to wheat was found by Kai et al. (2008). In barley, the NFRV was 93% for the untreated pig slurry and about 100% for the acidified pig slurry (90% for on-farm acidified), and the NFRV of cattle slurry was 59% for untreated and 61–68% for the acidified cattle slurries. Thus, after the application of slurry to a barley crop by incorporation, there were only non-significant, positive effects of acidification on N utilization in the field, indicating that NH_3 volatilization was low with all slurry treatments.

About 50–100 in-house acidification units are now installed on farms in DK, but due to the costs, it is mainly expected to be used in areas with severe restrictions on NH_3 emission from livestock, and only by establishment of new livestock buildings. A slurry tanker with controlled addition of sulfuric acid to slurry during application is now also marketed in DK (Nyord, 2011).

In contrast to acidification with nitric acid, which has been shown to increase emissions of N_2O, a set of measurements from DK showed no increase (Sørensen pers. comm.) when acidification was by sulfuric acid.

We conclude that when pig slurry is acidified in livestock buildings, it may contain 15–25% more total N than untreated slurry after storage, the increase being greater for uncovered storage. Acidification can increase NFRV by about 35–65% for surface-banded slurry. Due to the large costs, acidification is mainly of use in areas with severe restrictions on NH_3 emission from livestock.

3.1.4. Manure Composting

During storage of solid manures, composting processes occur spontaneously, to varying degrees, depending on manure porosity and moisture content, and on the extent to which air can gain access (Parkinson et al., 2004). The composting process can be further promoted by forced aeration or by frequent turning of manure piles. During composting of manures, OM is decomposed and this includes organic-N compounds. Manure temperature increases temporarily up to about 70 °C if the manure is sufficiently aerated. Composting of livestock manures prior to application to land may be

used to reduce the viability of weed seeds, produce a less-odorous material, control the spread of pathogens, minimize the production of phytotoxic substances, improve storage and handling, reduce unpleasant odors, especially in the case of poultry manures (Tiquia and Tam, 2000) and reduce the mass thereby reducing transport and application costs.

During composting, N transformations such as mineralization, NH_3 volatilization, nitrification, and denitrification may be increased. NH_3 volatilization and denitrification may lead to significant losses of N (Bernal et al., 1996; Martins and Dewes, 1992), in particular as NH_3–N (Kirchmann, 1985). Composting often results in greater NH_3 emissions than conventional stacking (Tam and Tiquia, 1999). Such losses will affect the agronomic value of the composted product. Gaseous N losses during composting of animal manure range from 21 to 77% (Martins and Dewes, 1992; Rao Bhamidimarri and Pandey, 1996). Nitrogen losses depend on several factors such as aeration, moisture content, and temperature (Bishop and Godfrey, 1983). The C/N ratio of the initial composting material has also been reported to affect losses of N during composting (Bishop and Godfrey, 1983; de Bertoldi et al., 1980, 1985; Witter and Lopez-Real, 1988). A very narrow C/N ratio can lead to a large loss of N through NH_3 volatilization (de Bertoldi et al., 1985; Tam and Tiquia, 1999), especially if the compost piles are aerated mechanically or turned manually. de Bertoldi et al. (1985) reported that the N loss was greater with turning (18% N loss) than with forced aeration (5% N loss). Such losses of N would decrease the nutrient value of the mature compost material.

Tam and Tiquia (1999) reported total N in the compost mass (concentration × mass of the pile) decreased from 31 to 13 kg during composting. This loss was around 59% of the initial N mass of the piles and was comparable with losses reported on composting of livestock manure of 21 ± 77% by Martins and Dewes (1992) and Rao Bhamidimarri and Pandey (1996). Tam and Tiquia (1999) attributed losses of N largely to NH_3 volatilization.

Since composting changes the nature of the manure, it can affect the usefulness of manure as a fertilizer. After composting, the plant availability of the remaining manure-N is significantly reduced as a result of an increased stability of organic N in the manure and of the loss of mineral-N during composting (Kirchmann and Witter, 1989; Munoz et al., 2008; Sommer, 2001). While there may be less immobilization of any mineral-N applied to soil, due to the breakdown of labile C compounds during composting, the mineralization of organic N in soil is reduced by composting.

After removal from livestock buildings, FYM can be stacked anaerobically, which will reduce NH_3 emissions compared with conventional storage (Chadwick, 2005). Exclusively anaerobic storage may also reduce N_2O emissions as there can be no denitrification if the manure is never allowed to aerate and nitrification is prevented (Chadwick, 2005 and papers cited therein). However, the anaerobic storage of manure which has earlier been allowed to aerate risks increasing N_2O emissions. There is also the issue of CH_4 emissions that will increase during anaerobic storage. However, when expressed in terms of CO_2 equivalents, the increases in emission of CH_4 tend to be outweighed by the decreases in emission of N_2O (Chadwick, 2005).

It is very difficult to find the very best option for FYM storage. Especially, when other factors that are important (e.g. in organic farming: humic substances; aerobic turnover desired…) are taken into account. In practice, this discussion might be more or less-academic as it seems to be unlikely that farmers will have the time and money to guarantee a good composting process with sufficient oxygen supply and sufficiently frequent turning of the manure. Hence, piling manure into heaps which are anaerobic may be the most practical option and lead to the greatest conservation of N.

There are two general "fertilizing philosophies" that must be distinguished and that lead to different approaches to applying nutrients:

(1) Fertilizing the crop that is currently growing = "conventional fertilizing," including the application of mineral fertilizer; N must be applied as closely to crop demand as possible. Application as TAN is desirable.

(2) Fertilizing the soil rather than the crop; common in organic farming. Here, the aim is to improve soil quality and soil fertility. Crops recover nutrients from soil reserves rather than from direct fertilization. A continuous coverage of the soil with crops is required to minimize N leaching; N application must not necessarily be readily available.

One routinely cited environmental advantage of composting organic manures before application to soil is that the reduced N mineralization rates in soil may decrease the potential for NO_3^- leaching by delaying the conversion of organic-N to NO_3^-–N. However, the low mineralization rate may be both an environmental and an agronomic shortcoming. The lack of control over the timing of subsequent mineralization may mean that mineral-N becomes available at times of the year when there is little plant uptake and hence, in the longer term, may contribute to NO_3^- leaching.

Thomsen (2001) labeled manures with ^{15}N separately in the feces, urine and straw components. Half of each manure was composted, the other half stored anaerobically by preventing any oxygen supply. The manures were

applied to a loamy sand soil in field microplots which were sown to winter wheat. When adjusted for N losses during storage, the first-year ^{15}N recovery in winter wheat was equivalent to 8% of N initially present before the anaerobic storage and to only 4% of initial N before composting.

Composting may increase the N concentration of the original material as C losses are often greater than those of N. However, composting also transforms N into stable forms whose plant availability is reduced. Evanylo et al. (2008) cited earlier workers who had previously ascribed poor yield response to compost to inadequate N mineralization. The organic N eventually mineralized to contribute significantly to the pool of soil N available to be leached or, in this case, assimilated by a winter cover crop. On the other hand, spreading manure with a large C/N ratio as compost instead of as uncomposted manure can be preferable when uncomposted solid manure can cause substantial N immobilization. One example is horse manure with a large proportion of litter.

These results indicate the asynchrony between timing of compost N mineralization and crop-nutrient requirement, due to delayed N mineralization of stabilized N, may reduce crop yields compared with other forms of N. The lack of control over the timing of subsequent mineralization may mean that compost-N becomes available at times of the year when there is little plant uptake and hence, in the longer term, may contribute to NO_3^- leaching. Fertilizing with composted FYM should go hand-in-hand with a whole-year coverage of the soil with crops. Periods with bare soil should be limited to a minimum. We, therefore, suggest that composted FYM should be applied in systems that aim at a coverage of the soil by crops during the whole year. FYM will not serve as an optimum fertilizer in cropping systems with some period of bare soil during the year. In colder regions, where the rate of mineralization over winter is negligible, application of FYM to such cropping systems might be an option provided it is incorporated to minimize the risk of runoff. The application and use of compost including its advantages and disadvantages must be seen in the context of whole production systems.

An effective option for improving the use of N in solid manures may be to use them for AD (codigestion with slurry). The digestate may then be stored and applied as a slurry using covered storage and direct injection. Solid manures are already widely used in Danish commercial digesters (codigestion with slurry in liquid flow-digesters), but on a relatively small scale. Both deep litter and solid fractions from slurry separation are used. They increase the energy production per digester volume (Møller et al., 2007).

3.2. Method of Manure Application

3.2.1. Slurry Injection

Injection of slurry has been reported in a number of papers to increase ANR compared with broadcast surface application by an average of 11% when no damage was caused to the crop by injection. Mattila et al. (2003) carried out replicated field experiments on clay loam (CL), fine sand and peat soils growing grass leys. On the CL soil, ANR of injected cattle slurry was greater than from broadcast or TH in 1995 and 1996. Injection significantly increased N recovery on clay and sandy soils but not on peat. Schils and Kok (2003) applied cattle slurry by injection or splash plate to grass paddocks on sandy soil of high OM in field experiments at two sites and injection was found to increase ANR by an average of 15%. Neither of those studies reported the NFRV of the cattle slurry. Schröder et al. (2007) found that injection into permanent grass increased ANR of cattle slurry significantly each year and by an average of 11% in a replicated field experiment on a loamy sand soil. The average NFRV of injected digested slurry was 58% in the first year while the NFRVs of undigested slurry in the first year, averaged 51–53% after injection. However, in cases where the injection tools damage grass swards, this may counteract the greater amount of NH_4–N left after spreading. Little or no effect on yield or ANR was reported for injection in grassland by Rahman et al. (2001) or Rodhe and Etana (2005). In a two-year study, the yield decrease related to crop damage averaged 2–8%, with greater yield reduction after spring use compared with after the first cut (Rodhe and Halling, 2010).

Petersen and Sørensen (2008a) reviewed experiments with injection of slurry into bare soil, most of these were reported in Danish. The average first-year NFRV after injection and after TH application followed by incorporation by harrow within 6 h was about 75 and 70%, respectively, for pig slurry and 65 and 50%, respectively, for cattle slurry. In a 3-year field experiment, Sørensen et al. (2003b) found more significant effects of injection on slurry N utilization in spring barley (Table 7.11). They also found more significant effects of injection of cattle slurry than of pig slurry on ANR. These results also suggested that there are other beneficial effects of slurry injection than reduced NH_3 loss, probably due to reduced N immobilization in soil, especially after cattle slurry injection.

3.2.2. Trailing Shoe

The TS was designed primarily for use on grassland although it may also be used on bare soil, and has been tested at a range of times of application

Table 7.11 Nitrogen Fertilizing Value of Pig and Cattle Slurry after Incorporation (within a Few Hours) or Injection to a Spring Barley Crop. Average of 3-Years Repeated Field Experiments on a Sandy Loam Soil at Askov Experimental Station 1999–2001 All Slurry Treatments Received 100 kg NH_4–N ha^{-1}. (Data from Sørensen et al. (2003b))

Fertilizer/Manure	Grain Yield (ton ha^{-1}, 15% Moisture)	N in Grain + Straw (kg N ha^{-1})	NFRV (% of Total N).
Cattle slurry incorporated (roto-till)	4.26	81	41
Cattle slurry injected	5.14	109	68
Pig slurry incorporated (roto-till)	4.63	90	63
Pig slurry injected	5.13	103	79
NPK fertilizer (100 kg N ha^{-1})	5.19	104	100
LSD ($P < 0.95$)	0.200	9.0	4.8

throughout the growing season. As well as demonstrating the effectiveness of the TS in reducing NH_3 emissions and increasing N uptake by grass, these studies have provided evidence of how manure-N efficiency can change throughout the season. Lalor et al. (2011) applied cattle slurry to grass on a well-drained sandy loam to loam soil by TS in a replicated field experiment. The NFRV was strongly influenced by the month, in which manure was applied, increasing from 0.30 to 0.40 when applied in April but from 0.14 to 0.24 when applied in June. Replicated field experiments, in which cattle slurry was applied to grassland by TS on a silty to sandy loam soil. Bittman et al. (2007) also found that later cuts did not use N as efficiently as the first cut. This was considered due to less crop growth (possibly more root growth in autumn) and perhaps, more NH_3 volatilization under warmer conditions and greater denitrification in autumn compared with spring or because of immobilization associated with root death. The results support the conclusion that better utilization can be achieved by applying N in diminishing amounts over the growing season (Bittman et al., 2005). Godden et al. (2007) applied cattle slurry by TS in an arable rotation on a silt loam soil in replicated field experiments. They also reported that recovery decreased with increasing N addition regardless of the form of N applied and concluded that it is better to use moderate rates of manure-N and top up crop N requirement with mineral fertilizer. Bittman et al. (1999) applied

cattle slurry by TS and surface application to grassland on silt loam and a CL soils in replicated field experiments. Over the entire study, application of slurry by TS increased ANR by around 15% compared with application by splash plate.

Hoekstra et al. (2010) simulated broadcast and TS to grassland using ^{15}N-labeled slurry NH_4^+ fraction to follow the fate of slurry N in the soil–plant system in field studies. Cumulative ^{15}N recovery was significantly affected by application method, with application by TS increasing slurry-N recovery by an average of 13% compared with broadcast application (BC).

3.2.3. Trailing Hose

Mattila et al. (2003) reported that N recovery from slurry applied by TH did not differ from BC in any year. This may have been, at least in part, due to the dry conditions in the three summers over which the work was carried out (1995–1997).

By application of slurry on cereal crops, NH_3 volatilization is reduced by use of TH compared with BC and the difference increases with increasing crop height (Sommer and Hutchings, 2001). Thus, the N recovery from slurry is also expected to be greater when using TH in growing crops, and field experiments has shown higher N utilization when using TH in winter wheat (Pedersen, 2001). However, application on bare soil by TH has little effect on N losses.

3.2.4. Rapid Incorporation

Yagüe and Quílez (2009) applied pig slurry to wheat grown on a silt loam soil in a field experiment at two rates of surface application, 30 and 60 t ha^{-1}, by splash plate or incorporation together with an unmanured control. Following the 60 t ha^{-1} treatment (but not the 30 t ha^{-1}), soil NH_4–N was measured to 60 cm 4 days after application and found to be +100 kg ha^{-1} greater following incorporation than surface application, equivalent to manure-N recoveries of 96 and 47%, respectively. But wheat yield and N uptake were independent of application method. This was considered due to both treatments supplying adequate N for crop needs.

Mattila (2006) carried out replicated field experiments, in which incorporation was by means of harrowing pig slurry to 5 cm on CL. The ANR by spring barley was greater for incorporated slurry than for surface-applied. Mattila (2006) pointed out that the location of manure within a soil profile will influence N recovery. Mineral-N applied to 8 cm was more available than

manure incorporated to 0–5 cm depth. This was attributed more to greater availability of moisture below the surface rather than a purely physical effect.

Sørensen (2004) simulated the effects of incorporation and injection on the immobilization, remineralization and residual effects of cattle slurry N in subsequent crops compared with mineral fertilizer-N by means of microplots. Application of cattle slurry by injection increased crop uptake of manure-N compared with incorporating the slurry by mixing. Sørensen and Jensen (1998) used ^{15}N-labeled manure to study the turnover and utilization of ruminant manure-N from simulated incorporation and injection using PVC cylinders. Their results were consistent with results from Sørensen and Jensen (1995), who had found plant uptake of N after simulated injection to be *ca* 17% greater than after incorporation of cattle slurry into soil, and Sørensen and Jensen (1995) also found a strong interaction with soil type with a greater increase of N uptake in a loam than in a sand soil.

The alternation of applications of N between manure- and fertilizer-N yielded the same amount of grass as a larger rate of manure-N application despite a 24% smaller application of total-N, and yielded 2 Mg ha^{-1} more than the larger rate of fertilizer-N application despite similar rates of mineral-N (Bittman et al., 2007). The authors considered that the relatively high efficiency obtained by alternating applications of manure- and fertilizer-N (equal to that of the high rate of fertilizer-N which supplied *ca* 10% more mineral-N) may have been due to release of organic N, improved status of other nutrients (P, K and sulfur) and improved soil water-holding capacity due to increased soil OM. They concluded that by alternating manure and mineral fertilizer, 18% more grass containing more crude protein could be grown at the same rate of N compared with using manure alone. Hence, alternating between manure and fertilizer may improve productivity per unit land area without decreasing the rate of N recovery per unit of herbage produced.

3.2.5. Uptake of Reduced Emission Techniques by Farmers

The question remains, given such encouraging results from experimental studies, to what extent can reduced NH_3 emission techniques be adopted by commercial farmers to increase manure-N efficiency?

In DK, more than 80% of manure-N is applied as a liquid, and more than 96% of pig manure in DK is as slurry. In Table 7.12, typical NFRVs of pig slurry in the year of application and residual effects in the following 10 years are estimated for the most common crops on pig farms which are winter wheat, spring and winter barley and winter oilseed rape.

Table 7.12 Utilization of Manure-N in a Typical Crop Rotation on Pig Farms in DK with Pig Slurry (Petersen and Sørensen, 2008a).

Crop	Application Time	Manure Application Method	Estimated NFRV 1 year (% of Total N)	Estimated Residual N Effect (within 10 years) (% of Total N)
Winter wheat	Mar–May	TH on crop	65	7
Winter wheat second year	Mar–May	TH on crop	65	7
Spring barley	Mar–April	Direct injection*	75	7
Winter barley	Mar–May	TH on crop	65	7
Winter oilseed rape	August	Direct injection in August	65	7
	Mar–April	TH on crop	65	7

Loamy Sand – Sandy Loam Soils with 10 – 20% Clay. Annual Precipitation: 600 – 800 mm. NFRV: Mineral Fertilizer Replacement Value.
Average TAN in pig slurry in DK: 78% of total N (Hansen et al., 2008).
Typical application rate: 25–30 t ha^{-1}.
*Direct injection (7 – 12 cm depth) is mandatory in Denmark on fodder grass and before sowing a new crop.

In Table 7.13, typical NFRV of cattle slurry in the year of application and residual effects in the following 10 years are estimated for the most common crops on dairy farms: clover grass; silage maize; spring barley.

The use of direct injection before spring sowing is widely used by farmers on a voluntary basis in DK and it gives the greatest first-year utilization of slurry N. From 2011, it has become mandatory in DK to use injection before sowing a new crop and also for slurry application on fodder grass (alternatively slurry must be acidified and applied by TH). However, on pig farms, winter cereals are used widely and here, TH application works well, especially with pig slurry. It should be noted that direct injection can be difficult to apply on heavy textured soils. Injection is also problematic on steep-sloping areas. The example of DK confirms that the application of slurry by reduced NH_3-emission techniques can be used on commercial farms to increase manure-N efficiency compared with BC.

There has been a large increase in the uptake of reduced-NH_3 emission machines by UK farmers since *ca* 2007 (Webb et al., 2010). The main

Table 7.13 Utilization of Manure-N in a Typical Crop Rotation on Cattle Farms in DK with Cattle Slurry (Petersen and Sørensen, 2008a).

Crop	Application Time	Manure Application Method	Estimated NFRV 1 year (% of Total N)	Estimated Residual N Effect (within 10 years) (% of Total N)
Spring barley	Mar–April	Direct injection*	65	13
Clover grass 1 yr	Mar–Aug	Open slot injection	53	13
Clover grass 2 yr	Mar–Aug	Open slot injection	53	13
Spring barley	Mar–April	Direct injection*	65	13
Silage maize	Mar–May	Direct injection*	68	13

Sandy soils: 5–10% clay. Annual precipitation: 600–900 mm. NFRV: nitrogen fertilizer replacement value.
Average TAN in cattle slurry in DK: 58% of total N (Hansen et al., 2008).
Typical application rate: 25–40 t ha^{-1}.
*Direct injection (7 – 12 cm depth) is mandatory in Denmark on fodder grass and before sowing a new crop.

reasons given by farmers for the change in practice are the savings in N fertilizer, especially with recent increases in N prices, and odor reduction (especially on pig farms) in specific locations. It is not always clear whether savings in fertilizer are entirely due to the machine or could have been achieved by more considered use of surface spreading. Shallow injectors are popular for use on grassland unless conditions are such that there is poor soil penetration (especially very heavy or stony soils) or soils that are too wet. TSs overcome some of these problems. However, many farmers and contractors were not able to use the machine to apply all the slurry produced on their farm and often used the splash plate for a proportion. This was due to difficult soil conditions (too wet or too dry at times of the year, stony or steeply sloping land, some slurry too thick or containing stones, etc., inaccessibility of some fields) and time constraints. In general, the capital cost of ownership is too great for individual farmers and most use contractors for manure application.

3.3. Moderating Application Rates of Manures in Order to Increase Overall NUE

Shepherd and Harrison (2000) demonstrated how pig slurry (a manure with a large potential for NO_3^- leaching) can successfully be integrated into cereal rotations. By adopting a strategy of late-winter or -spring applications

and making appropriate N-fertilizer reductions, manure management systems that apply "high risk" manures (pig slurry, poultry manures) to a field only every 2–3 years can result in NO_3–N losses of a similar level to those from fields receiving only inorganic fertilizer at recommended levels. Manure application rates were targeted at a loading of 210 kgha^{-1} total N in line with then current NVZ application limits. The seven-year average NO_3–N concentrations were 22.8 mg L^{-1} for broiler litter applied three times in 7 years and 21.3 mg L^{-1} for the inorganically fertilized control. Average NO_3–N concentrations were the same as the control (11.9 and 11.7 mg L^{-1}, respectively) from five applications of FYM/slurry in 7 years. This is a positive message for farmers and policy makers.

In contrast, annual applications of manure increased NO_3^- leaching, even when the rules on application timing and rate were followed. Average concentrations of NO_3–N over 7 years were 29.6, 32.5 and 21.3 mg L^{-1} for annual FYM, annual broiler litter and control, respectively. It is thought that annual FYM, generally considered a "low-risk" manure, increased the labile-N pool such that soil-N supply increased. Annual FYM on the heavier soil did not increase losses, however. Annual pig-slurry applications increased average NO_3–N concentrations from 11.7 to 17.1 mg L^{-1} on an alluvial-silt soil.

Thus, having just enough land available for spreading manure from an animal unit is not sufficient. Intensive manure use also leads to other potential problems such as soil nutrient build-up.

The results of Shepherd and Harrison (2000) demonstrated that fertilizer-N inputs can be reduced significantly after manures with no loss of yield. The drive to save input costs as fertilizer prices have risen in recent years, may well be a strong driver in convincing farmers of this message.

3.4. Grazing

Nitrogen excreted as urine and dung during grazing has also to be considered in the Nitrates Directive. The N excreted during grazing is distributed heterogeneously and urine patches contain large amounts of N, which may result in large local N losses (Hutchings et al., 2007). However, at the field scale, NH_3 emissions during grazing are generally considered to be small (e.g. Webb and Misselbrook, 2004); extended grazing is considered to be an option to reduce NH_3 emissions (Webb et al., 2005). Losses of N may also take place as a result of denitrification (Bussink and

Oenema, 1996; Oenema et al., 1997; Van Groenigen et al., 2005). Treading and trampling by grazing animals also contribute to denitrifying activity because of soil compaction (Brůček et al., 2009). NO_3^- leaching losses in grazed grassland are usually related to urine (and dung) patches, especially following grazing in autumn (Hack ten Broeke and der Putten, 1997) as excreta will be deposited only a short time before the onset of over-winter drainage and there will be little recovery of the N by the grass. Because of this heterogeneous distribution and large N losses from NO_3^- leaching (Cuttle et al., 1992), the N efficiency of N excreted during grazing may be less than the N efficiency of properly applied manure (Williams et al., 1989). Adjustment of the grazing regimes strongly affects N leaching losses. However, it also affects the amounts of N excreted and stored in house and in manure storage systems, and hence, the N emissions from these compartments of the farming system. To avoid exchanging emissions during grazing for emissions from managed manure, systems should be optimized to take into account the environmental and agricultural (economic) aspects of the whole farming system.



4. DISCUSSION

4.1. Improvements Arising from the Adoption of Reduced NH_3-Emission Techniques

Slurry injection has been shown to significantly increase ANR by crops by up to around 15% compared with surface application, with greater effects for cattle than for pig slurry. In the season of manure application, uptake of available manure-N from cattle slurry applied by injection has been reported to be as great as from a similar amount of NH_4^+–N applied as fertilizer. Similar application rates of mineral-N application of cattle slurry to grassland by TS can give ANR by crops from manure application equivalent to that obtained by fertilizer-N at a range of application rates, timings, or seasons. Work has shown that reduced NH_3-emission techniques can be adopted by commercial farmers to increase manure-N efficiency.

4.2. Slurry Separation

Separation has been shown to increase N uptake due to a reduction of N immobilization by using the liquid as a top dressing to a winter crop and using the solid residue on other areas where it can be incorporated in spring. However, if the liquid and solid manure fractions are both applied

to the same crop, overall utilization of N may be no greater than from the unseparated slurry. This is due to greater emissions from the solid fraction balancing the reduction in emissions from the liquid fraction.

4.3. Anaerobic Digestion

After AD treatment of livestock manure the proportion of available N is increased and the concentration of decomposable C is decreased, potentially increasing plant availability in the season of application. However, residual N affects are decreased as less organic N is applied to the soil. AD also increases manure pH and decreases the DM concentrations having opposing effects on potential NH_3 loss. Thus, the effects of AD on NH_3 loss and crop N availability depends on the specific application conditions. The decomposition of manure C during digestion may reduce soil N immobilization, thereby increasing plant N uptake. Hence providing the potential for greater emissions of NH_3 is controlled, either through the use of reduced NH_3-emission application techniques or by ensuring the digested slurry is applied to soils with good surface structure and a soil moisture deficit to ensure rapid infiltration, AD provides another option for increasing manure-N efficiency. Since in many EU countries AD is being adopted to provide renewable energy and to reduce emissions of GHG (e.g. Defra, 2011) there is a potential synergy here between the two objectives of GHG mitigation and tightening the agricultural N cycle.

4.4. Timing of Manure Application

Manure-N applied in diminishing amounts over the growing season has been shown to increase manure-N efficiency since manure-N applied early in the year, e.g. to grassland for first cut, is used more efficiently than manure-N applied for later cuts. In order to maximize ANR by crops there could be advantage in preferentially applying livestock manures to crops whose active growing period coincides best with the time of active mineralization of manure-N, e.g. maize, potatoes and sugarbeet. However, rates of N application will need to be carefully matched with crop N requirement as large leaching losses are observed after maize cropping in some MS.

4.5. Interaction between Manure-N Efficiency and Soil Type

This review indicates that there is greater plant uptake of manure-N after simulated injection than after incorporation of cattle slurry into soil, and a strong interaction with soil type. Mixing manure with soil immobilizes crop available N, to a much greater extent than when manure is introduced

to the soil in discrete bands. This effect is greatest in clay and silt soils. Hence, although incorporation, if carried out quickly enough after manure application, has greater potential to reduce NH_3 emissions than injection, any additional conservation of NH_3–N may not lead to additional crop N uptake. In order therefore to increase manure-N efficiency it may be advisable to promote the use of cattle slurry injection on arable soils in preference to rapid incorporation. Such effects have not been observed for pig slurry (Sørensen and Amato, 2002).

Studies of fertilizer-N uptake by crops have indicated greater recovery of N on sandy than on heavier soils. Such differences have also been reported for net N mineralization and crop recovery of manure-N. On the other hand, there can be greater long-term residual effects on heavier soils. These differences among soils should be included in guidance for manure-N utilization.

4.6. Long-Term N Uptake

It is difficult to measure residual N effects of livestock manure, since these effects are often relatively small and overshadowed by normal variability in field experiments. Nevertheless, there is evidence of continued uptake of manure-N in the seasons following manure application. This uptake needs to be accounted for when assessing manure-N efficiency and determining fertilizer-N requirements of crops in rotations to which livestock manures are applied regularly. For example Petersen and Sørensen (2008a) estimated residual effects equivalent to 2–8% of total manure-N in the year after application and 6–24% after 10 years.

4.7. Moderating Application Rates of Manures in Order to Increase Overall NUE

Manure use impacts on other environmental and sustainability issues as well as NO_3^- leaching. The imbalance in NPK between manure inputs and crop removals means that regular manure use will elevate P and K levels in the soil if crops are not supplied with other N sources. While there is no environmental disbenefit of high soil K levels, excessive P levels are associated with increased risk of P loss to water. A move to maximum P loadings, rather than N, and supplementation with mineral-N fertilizer would reduce this risk (Shepherd and Harrison, 2000). Given the relatively small P requirement by crops, this would increase the land area required for manure application, reinforcing the argument for not applying manures every year. Such arguments for integrating manure use across farming systems were also advanced by Schröder (2005).

5. CONCLUSIONS

The methods used to increase the efficiency of N use after manure application can be based on the following underlying principles:

- Applying manure-N in amounts and at times of the year that match the uptake ability of the crop.
- Reducing losses of NH_3 by reducing the area of manure that is exposed to the atmosphere or the length of time it is exposed.
- Reducing losses of N_2 or N_2O by avoiding the application of manure to soils when conditions would encourage denitrification and by avoiding manure application techniques that would strongly enhance denitrification losses.

The review of how each Member State (MS) takes account of manure-N efficiency in their Action Plan (AP) found reasonable agreement in the estimates of the proportions of N available for crop uptake in any given type of manure, with N availability decreasing in the order pig slurry > cattle slurry > poultry manure > FYM. Although many Member State (MS) require manures to be applied by methods which reduce emissions, few actually report greater manure-N efficiency from incorporated than from broadcast manure. Soil type was taken into account in relation to the impact of soil type on NO_3^- leaching rather than on crop uptake of manure-N. There does not appear to be any systematic variation in the reported manure-N efficiency across the EU that can be related to climate. The adoption of closed periods for manure spreading will tend to eliminate differences that might otherwise be reported due to differences in the amounts of available N lost over winter by leaching or runoff due to differences in the amount of overwinter rainfall.

The review of literature indicates that a number of measures can be implemented to increase manure-N efficiency:

- Apply manures by techniques that reduce NH_3 emissions and therefore, conserve more manure-N in the soil. For example, uptake of N from the mineral-N fraction of slurry can be as great as from equivalent amounts of fertilizer-N when the slurry is applied by injection machinery in spring. Acidification of slurry is a very effective means of conserving N at all stages of manure management, albeit it may be an expensive option.
- In order to fully utilize the fertilizer value of organic-, as well as mineral manure-N, there is a need to account for manure-N availability over more than 1 year.

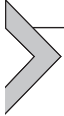
- More efficient use may be made of manure-N by appropriate timing of manure applications and applying moderate rates of manure-N. Manure application in spring, shortly before the period of crop-nutrient uptake, enables the greatest potential recovery of manure-N. Late season applications, e.g. for late summer and early autumn grass, are less efficient. Application techniques should enable manure application to growing crops during the growing period. In crop rotations that use intercrops and/or aim at a constant covering of the soil, autumn applications can also be efficient. In farming systems, where N input from manures is less than N uptake by crops, the best option is to integrate manure application with application of fertilizer-N to give the greatest overall efficiency of manure-N use.
- AD of livestock manure increases the proportion of available-N and reduces the potential for N immobilization in soil. AD slurry must be applied with reduced emission techniques to avoid elevated NH_3 losses during application.

There is no simple technique or approach that can be guaranteed to increase manure-N efficiency. If N efficiency is only improved in one stage of the livestock production cycle, N may leak at another stage and overall N emissions may not decrease. Management options which decrease the amount of external N needed to produce a crop or animal product will decrease N emissions. While reduced NH_3-emission techniques, especially injection and the Trailing Shoe, can increase manure-N efficiency, a carefully integrated strategy is needed which takes account of differences in manure-N uptake among crops and according to the timing of manure application. Minimizing the overall impact of N use in agriculture requires the maximum usage of manure-N in order to reduce the need for fertilizer-N and to reduce the emissions arising from both its manufacture and application. However, attempting to supply all of a crop's requirement for N by manure may limit the overall N fertilizer replacement value (NFRV), both in the year of application and subsequently. Several studies have shown that limiting overall manure application rates in order to apply manures over a larger crop area, together with limited use of N fertilizer at times of the year when apparent N recovery by crops of manure may be limited, may give a greater NFRV than concentrating purely on means to conserve manure-N. Such an approach has also been shown to be an effective means of reducing NO_3^- leaching. By using such an approach, accumulation of P in soil can also be avoided. Such a strategy will differ from region to region within the EU and also within farming systems. In many parts of the EU, livestock farming is already so concentrated that unless manures are exported long distances the most appropriate means of

fertilizing crops is predominantly with manure. Nevertheless, in regions and localities where mixed farming still exists, either in the form of farms which raise crops and livestock or where livestock and other farms are intermingled, further specialization of farms or localities may counter initiatives to increase manure-N efficiency at the EU level if further concentration of livestock is not avoided. Livestock and crop-production systems must be integrated in terms of manure reuse. Schröder (2005) concluded that an integration of farm types within the landscape should be given priority over specialized farming.

ACKNOWLEDGMENTS

This chapter was prepared from work carried out as part of EU project ENV.B.1/ETU/2010/0008 "Study on variation of manure-N efficiency throughout Europe." This study was purchased by EU DG Environments and is their property. The opinions, conclusions and recommendations in this chapter are those of the authors and do not necessarily reflect the views of the Commission.



GLOSSARY

Abbreviation and full name of each EU member state referred to.

Abbreviation	EU Member State
AT	Austria
BE (Flan)	Belgium (Flanders)
BE (Wall)	Belgium (Wallonia)
BG	Bulgaria
CY	Cyprus
CZ	Czech Republic
DK	Denmark
EE	Estonia
FI	Finland
FR	France
DE	Germany
GR	Greece
HU	Hungary
IE	Ireland
IT	Italy
LV	Latvia
LT	Lithuania
LU	Luxemburg

Abbreviation	EU Member State
MT	Malta
NL	Netherlands
PL	Poland
PT	Portugal
RO	Romania
SK	Slovakia
SI	Slovenia
ES	Spain
SE	Sweden
GB	Great Britain
GB NI	Great Britain (Northern Ireland)

REFERENCES

Amon, B., 1995. Prozeßsteuerung der Flüssigmistseparierung mit einem Preßschneckenseparator. Landtechnische Berichte aus Praxis und Forschung, Bayerisches Staatsministerium für Ernährung, Landwirtschaft und Forsten, Gelbes Heft 55, Dissertation, TU München Weihenstephan.

Amon, B., Kryvoruchko, V., Moitzi, G., Amon, T., 2006. Greenhouse gas and ammonia emission abatement by slurry treatment. Int. Congr. Ser. 1293, 315–318.

Andersen, M.K., Jensen, L.S., 2001. Low soil temperature effects on short-term gross N mineralisation–immobilisation turnover after incorporation of a green manure. Soil Biol. Biochem. 33, 511–521.

Anon, 2001. Defra Project NT2001, Mineralisation of Organic Nitrogen from Farm Manure Applications. http://randd.defra.gov.uk/Document.aspx?Document=NT2106_355_FRP.doc.

Anon, 2010. Fertilizer Manual (RB209), eighth ed. TSO, Norwich, UK. 249 pp. www.tso.co.uk.

Audsley, E., Pearn, K.R., Simota, C., Cojocaru, G., Koutsidou, E., Rounsevell, M.D.A., Trnka, M., Alexandrov, V., 2006. What can scenario modelling tell us about future European scale agricultural land use, and what not? Environ. Sci. Policy 9, 148–162.

Azeez, J.O., Van Averbeke, W., 2010. Nitrogen mineralization potential of three animal manures applied on a sandy clay loam soil. Bioresour. Technol. 101, 5645–5651.

Beauchamp, E.G., Paul, J.W., 1989. A simple model to predict manure N availability to crops in the field. In: Hansen, J.A.A., Henriksen, K. (Eds.), Nitrogen in Organic Wastes Applied to Soils, Academic Press, New York, pp. 140–149.

Bechini, L., Marino, P., 2009. Short-term nitrogen fertilizing value of liquid dairy manures is mainly due to ammonium. Soil Sci. Soc. Am. J. 73, 2159–2169.

Beckwith, P., Lewis, P.J., Chalmers, A.G., Froment, M.A., Smith, K.A., 2002. Successive annual applications of organic manures for cut grass: short-term observations on utilization of manure nitrogen. Grass Forage Sci. 57, 191–202.

Bernal, M., Navarro, A.F., Roig, A., Cegarra, J., Garcia, D., 1996. Carbon and nitrogen transformation during composting of sweet sorghum bagasse. Biol. Fertil. Soils 22, 141–148.

Berntsen, J., Petersen, B.M., Sørensen, P., Olesen, J.E., 2007. Simulating residual effects of animal manures using ^{15}N isotopes. Plant Soil 290, 173–187.

Bertora, C., Alluvione, F., Zavattaro, L., van Groenigen, J.W., Velthof, G.L., Grignani, C., 2008. Pig slurry treatment modifies slurry composition, N_2O, and CO_2 emissions after soil incorporation. Soil Biol. Biochem. 40, 1999–2006.

Bhandral, R., Bittman, S., Kowalenko, G., Buckley, K., Chantigny, M.H., Hunt, D.E., Bounaix, F., Friesen, A., 2009. Enhancing soil infiltration reduces gaseous emissions and improves N uptake from applied dairy slurry. J. Environ. Qual. 38, 1–11.
Bishop, P.L., Godfrey, C., 1983. Nitrogen variations during sludge composting. BioCycle 24, 34–39.
Bittman, S., Kowalenko, C.G., Forge, T., Hunt, D.E., Bounaix, F., Patni, N., 2007. Agronomic effects of multi-year surface-banding of dairy slurry on grass. Bioresour. Technol. 98, 3249–3258.
Bittman, S., Kowalenko, S.G., Hunt, D.E., Schmidt, O., 1999. Surface-banded and broadcast dairy manure effects on Tall Fescue yield and nitrogen uptake. Agron. J. 91, 826–833.
Bittman, S., van Vliet, L.J.P., Kowalenko, C.G., McGinn, S., Hunt, D.E., Bounaix, F., 2005. Surface-banding liquid manure over aeration slots: a new low-disturbance method for reducing ammonia emissions and improving yield of perennial grasses. Agron. J. 97, 1304–1313.
Bloom, T.M., Sylvester-Bradley, R., Vaidyanathan, L.V., Murray, A.W.A., 1988. Apparent recovery of fertilizer nitrogen by winter wheat. In: Jenkinson, D.S., Smith, K.A. (Eds.), Nitrogen Efficiency in Agricultural Soils, Elsevier Applied Science, London, pp. 27–37.
Bosshard, C., Sørensen, P., Frossard, E., Dubois, D., Mäder, P., Nanzer, S., Oberson, A., 2009. Nitrogen use efficiency of animal manure and mineral fertiliser applied to long-term organic and conventional cropping systems. Nutr. Cycl. Agroecosyst. 83, 271–287.
Bouwman, A.F., 1990. Exchange of greenhouse gases between terrestrial ecosystems and the atmosphere. In: Bouwman, A.F. (Ed.), Soils and the Greenhouse Effect, Wiley and Sons, Chichester, pp. 61–227.
Brůček, P., Šimek, M., Hynšt, J., 2009. Long-term animal impact modifies potential production of N_2O from pasture soil. Biol. Fertil. Soils 46, 27–36.
Burger, M., Venterea, R., 2008. Nitrogen immobilization and mineralization kinetics of cattle, hog, and Turkey manure applied to soil. Soil Sci. Soc. Am. J. 72, 1570–1579.
Bussink, D.W., Oenema, O., 1996. Ammonia volatilization from dairy farming systems in temperate areas; a review. Nutr. Cycl. Agroecosyst. 51, 19–33.
Butterbach-Bahl, K., Gundersen, P., Ambus, P., Augustin, J., Beier, C., Boeckx, P., Dannenman, N., Gimeno, B.S., Kiese, R., Kitzler, B., Ibrom, A., Rees, R.M., Smith, K.A., Stevens, C., Vesala, T., Zechmeister-Boltenstern, S., 2011. Nitrogen processes in terrestrial ecosystems. In: Sutton, M.A., Howard, C.M., Erisman, J.W., Billen, G., Bleeker, A., Grennfelt, P., van Grinsven, H., Grizzetti, B. (Eds.), The European Nitrogen Assessment, Cambridge University Press, UK, pp. 99–125.
Camp, V., Gilhespy, S.L., Misselbrook, T.H., Chadwick, D.R., 2009. Relationship between cattle stocking density and NH_3 emissions from cattle housing. Bulg. J. Ecol. Sci. Ecol. Future 8, 25–27.
Canh, T.T., Aarnink, A.J.A., Schutte, J.B., Sutton, A., Langhout, D.J., Verstegen, M.W.A., 1998. Dietary protein affects nitrogen excretion and ammonia emission from slurry of growing-finishing pigs. Livest. Prod. Sci. 56, 181–191.
Castellanos, J.Z., Pratt, P.F., 1981. Mineralization of manure nitrogen – correlation with laboratory indexes. Soil Sci. Soc. Am. J. 44, 354–357.
Cela, S., Santiveri, F., Lloveras, J., 2011. Residual effects of pig slurry and mineral nitrogen fertilizer on irrigated wheat. Eur. J. Agron. 34, 257–262.
Chadwick, D.R., 2005. Emissions of ammonia, nitrous oxide and methane from cattle manure heaps: effect of compaction and covering. Atmos. Environ. 39, 787–799.
Chadwick, D.R., John, F., Pain, B.F., Chambers, B.J., Williams, J., 2000. Plant uptake of nitrogen from the organic nitrogen fraction of animal manures: a laboratory experiment. J. Agric. Sci. (Camb.) 134, 159–168.
Chambers, B.J., Lord, E.I., Nicholson, F.A., Smith, K.A., 1999. Predicting nitrogen availability and losses following arable land application of manures: MANNER. Soil Use Manage. 15, 137–143.

Chantigny, M.H., Angers, D.A., Rochette, P., Belanger, G., Masse, D., Cote, D., 2007. Gaseous nitrogen emissions and forage nitrogen uptake on soils fertilized with raw and treated swine manure. J. Environ. Qual. 36, 1864–1872.
Chantigny, M.H., MacDonald, J.D., Beaupré, C., Rochette, P., Angers, D.A., Massé, D., Parent, L.-E., 2009. Ammonia volatilization following surface application of raw and treated liquid swine manure. Nutr. Cycl. Agroecosyst. 85, 275–286.
Clemens, J., Trimborn, M., Weiland, P., Amon, B., 2006. Mitigation of greenhouse gas emissions by anaerobic digestion of cattle slurry. Agric. Ecosyst. Environ. 112, 171–177.
Crutzen, P.J., 1981. Atmospheric chemical process of the oxides of nitrogen, including nitrous oxide. In: Delwiche, J. (Ed.), Denitrification, Nitrification and Nitrous Oxide, Wiley, New York, pp. 17–44.
Cusick, P.R., Kelling, K.A., Powell, J.M., Muñoz, G.R., 2006. Estimates of residual dairy manure nitrogen availability using various techniques. J. Environ. Qual. 35, 2170–2177.
Cuttle, S.P., Hallard, M., Daniel, G., Scurlock, R.V., 1992. Nitrate leaching from sheep-grazed grass/clover and fertilized grass pastures. J. Agric. Sci. (Camb.) 119, 335–343.
Daudén, A., Quílez, D., Martínez, C., 2004. Residual effects of pig slurry applied to a Mediterranean soil on yield and N uptake of a subsequent wheat crop. Soil Use Manage. 20, 56–162.
de Bertoldi, M., Citernesi, U., Gricelli, M., 1980. Bulking agents in sludge composting. Compost Sci. Land Util. 21, 32–35.
de Bertoldi, M., Vallini, G., Pera, A., 1985. Technological aspects of composting including modeling and microbiology. In: Gasser, J.K.R. (Ed.), Composting of Agricultural and Other Wastes, Elsevier Applied Science Publishers, New York, USA, pp. 27–41.
De Boer, H.C., 2008. Co-digestion of animal slurry can increase short-term nitrogen recovery by crops. J. Environ. Qual. 37, 1968–1973.
Defra, 2011. Anaerobic Digestion Strategy and Action Plan. A Commitment to Increasing Energy from Waste through Anaerobic Digestion. Defra, London 52 pp.
Dise, N.B., Ashmore, M., Belyazid, S., Bleeker, A., Bobbink, R., de Vries, W., Erisman, J.W., Spranger, T., Stevens, C.J., van den Berg, L., 2011. Nitrogen as a threat to European terrestrial biodiversity. In: Sutton, M.A., Howard, C.M., Erisman, J.W., Billen, G., Bleeker, A., Grennfelt, P., van Grinsven, H., Grizzetti, B. (Eds.), The European Nitrogen Assessment, Cambridge University Press, UK, pp. 463–494.
Dobermann, A., 2005. IFA International Workshop on Enhanced-Efficiency Fertilizers Frankfurt, Germany, 28–30 June 2005 Nitrogen Use efficiency – State of the Art.
Dosch, P., Gutser, R., 1996. Reducing N losses (NH_3, N_2O, N_2) and immobilization from slurry through optimized application techniques. Fertil. Res. 43, 165–171.
EEC, 1991. Protection of water against pollution by nitrates from agriculture. EEC/91/976, Official Journal No L375, 31.12.1991. Brussels.
Elwinger, K., Svensson, L., 1996. Effect of dietary protein content, litter and drinker type on ammonia emission from broiler houses. J. Agric. Eng. Res. 64, 197–208.
Evanylo, G., Sherony, C., Spargo, J., Starner, D., Brosius, M., Haering, K., 2008. Soil and water environmental effects of fertilizer-, manure-, and compost-based fertility practices in an organic vegetable cropping system. Agric. Ecosyst. Environ. 127, 50–58.
Gärdenäs, A.I., Ågren, G.I., Bird, J.A., Clarholm, M., Hallin, S., Ineson, P., Kätterer, T., Knicker, H., Nilsson, S.I., Näsholm, T., Ogle, S., Paustian, K., Persson, T., Stendahl, J., 2011. Knowledge gaps in soil carbon and nitrogen interactions—from molecular to global scale. Soil Biol. Biochem. 43, 702–717.
Gilhespy, S., Webb, J., Retter, A., Chadwick, D., 2006. Dependence of ammonia emissions from cattle housing on the time spent inside. J. Environ. Qual. 35, 1659–1667.
Glendining, M.J., Poulton, P.R., Powlson, D.S., Jenkinson, D.S., 1997. Fate of ^{15}N-labelled fertilizer applied to spring barley grown on soils of contrasting nutrient status. Plant Soil 195, 83–98.

Godden, B., Destain, J.P., Luxen, P., 2007. Efficiency and recovery of different cattle manure applied on arable crops in rotation. In: De Neve, S., Salomez, J., Den Bossche, A.Van, Haneklaus, S.,Van Cleemput, O., Hofman, G., Schnug, E. (Eds.), Mineral versus Organic Fertilizers: Conflict or Synergism, pp. 229–234 Proceedings of the 16th International CIEC Symposium.

Grizzetti, B., Bouraoui, F., Billen, G., van Grinsven, H., Cardoso, A.C., Thieu, V., Garnier, J., Curtis, C., Howarth, R., Johnes, P., 2011. Nitrogen as a threat to European water quality. In: Sutton, M.A., Howard, C.M., Erisman, J.W., Billen, G., Bleeker, A., Grennfelt, P., van Grinsven, H., Grizzetti, B. (Eds.), The European Nitrogen Assessment, Cambridge University Press, UK, pp. 379–404.

Groot Koerkamp, P.W.G., 1994. Review on emissions of ammonia from housing systems for laying hens in relation to sources, processes, building design and manure handling. J. Agric. Eng. Res. 59, 73–87.

Grylls, J.P., Webb, J., Dyer, C.J., 1997. Seasonal variation in response of winter wheat and winter barley to nitrogen fertilizer and apparent efficiency of recovery of fertilizer nitrogen on chalk soils in southern England. J. Agric. Sci. (Camb.) 128, 251–262.

Gutser, R., Ebertseder, Th., Weber, A., Schram, M., Schmidhalter, U., 2005. Short-term and residual availability of nitrogen after long-term application of organic fertilizers on arable land. J. Plant Nutr. Soil Sci. 168, 439–444.

Hack ten Broeke, M.J.D., der Putten, A.H.J., 1997. Nitrate leaching affected by management options with respect to urine-affected areas and groundwater levels for grazed grassland. Agric. Ecosyst. Environ. 66, 197–210.

Hansen, M.N., Sommer, S.G., Hutchings, N.J., Sørensen, P., 2008. Emission factors for calculation of ammonia volatilization by storage and application of animal manure (in Danish with English summary). Emissionsfaktorer til beregning af ammoniakfordampning ved lagring og udbringning af husdyrgødning. DJF Husdyrbrug Nr 84 Aarhus University, Denmark.

Hansen, M.N., Sommer, S.G., Madsen, P., 2003. Reduction of ammonia emission by shallow slurry injection: injection efficiency and additional energy demand. J. Environ. Qual. 32, 1099–1104.

Hernandez-Ramirez, G., Brouder, S.M., Smith, D.R., Van Scoyo, G.E., Michalski, G., 2009. Nitrous oxide production in an Eastern corn belt soil: sources and redox range. Soil Sci. Soc. Am. J. 73, 1182–1191.

Hoekstra, N.J., Lalor, S.T.J., Richards, K.G., O'Hea, N., Lanigan, G.J., Dyckmans, J., Schulte, R.P.O., Schmidt, O., 2010. Slurry $^{15}NH_4$–N recovery in herbage and soil: effects of application method and timing. Plant Soil 330, 357–368.

Huijsmans, J.F.M., Bussink, D.W., Groenestein, C.M., Velthof, G.L., Vermeulen, G.J. Ammonia emission factors for field-applied manure, fertilisers and grazing in the Netherlands. Atmos. Environ. submitted for publication.

Hutchings, N.J., Olesen, J.E., Petersen, B.M., Berntsen, J., 2007. Modelling spatial heterogeneity in grazed grassland and its effects on nitrogen cycling and greenhouse gas emissions. Agric. Ecosyst. Environ. 121, 153–163.

Jansson, S.L., 1958. Tracer Studies on Nitrogen Transformations in Soil with Special Attention to Mineralisation—Immobilization Relationships. Royal Agricultural College of Sweden, Uppsala (SE) 361.

Jarvis, S.C., Aarts, H.P.M., 2000. Nutrient management from a farming systems perspective. In: Søgaard, K., Ohlsson, C., Hutchings, N.J., Kristensen, T., Sehested, J. (Eds.), Grassland Farming: Balancing Environmental and Economic Demands, pp. 363–373. Proceedings of the 18th General Meeting of the European Grassland Federation, Aalborg, Denmark.

Jarvis, S.C., Menzi, H., 2005. Optimising best practice for N management in livestock systems: meeting production and environmental targets. In: Lüscher, A., Jeangros, B., Kessler,

W., Huguenin, O., Lobsiger, M., Milar, N., Suter, D. (Eds.), Land Use Systems in Grassland Dominated Regions, Proc. 20th General Meeting of the EGF, Luzern, Switzerland, 21–24 June 2004.

Jensen, B., Sørensen, P., Thomsen, I.K., Jensen, E.S., Christensen, B.T., 1999. Availability of nitrogen in ^{15}N-labeled ruminant manure components to successively grown crops. Soil Sci. Soc. Am. J. 63, 416–426.

Kai, P., Pedersen, P., Jensen, J.E., Hansen, M.N., Sommer, S.G., 2008. A whole-farm assessment of the efficacy of slurry acidification in reducing ammonia emissions. Eur. J. Agron. 28, 148–154.

Kirchmann, H., 1985. Losses, plant uptake and utilization of manure nitrogen during a production cycle. Acta Agr. Scand. B-sp 24.

Kirchmann, H., 1991. Carbonic and nitrogen mineralization of fresh, aerobic and anaerobic animal manures during incubation with soil. Swed. J. Agr. Res. 21, 165–173.

Kirchmann, H., Lundvall, A., 1993. Relationship between N immobilization and volatile fatty acids in soil after application of pig and cattle slurry. Biol. Fertil. Soils 15, 161–164.

Kirchmann, H., Witter, E., 1989. Ammonia volatilization during aerobic and anaerobic manure decomposition. Plant Soil 115, 35–41.

Klausner, S.D., Kanneganti, V.R., Bouldin, D.R., 1994. An approach for estimating a decay series for organic nitrogen in animal manure. Agron. J. 86, 897–903.

Lalor, S.T.J., Schröder, J.J., Lantinga, E.A., Oenema, O., Kirwan, L., Schulte, R.P.O., 2011. Nitrogen fertilizer replacement value of cattle slurry in grassland as affected by method and timing of application. J. Environ. Qual. 40, 362–373.

Laws, J.A., Pain, B.F., Webb, J., Forrester, A., 2003. Added Benefits in Adopting Techniques to Abate Ammonia Emissions on UK Farms. British Grassland Society, Seventh Research Conference, Aberystwyth 1–3 September 2003.

Maidl, F.-X., Sticksel, E., Valta, R., 1999. Investigations for improved slurry utilization in maize. 1. Report: utilization of nitrogen in slurry by maize (silage and grain) using different application techniques. Pflanzenbauwissenschaften 3, S.9–S.16 (In German, with English abstract and table headings).

Mallory, E.B., Griffin, T.S., 2007. Impacts of soil amendment history on nitrogen availability from manure and fertilizer. Soil Sci. Soc. Am. J. 71, 964–973.

Mallory, E.B., Griffin, T.S., Porter, G.A., 2010. Seasonal nitrogen availability from current and past applications of manure. Nutr. Cycl. Agroecosyst. 88, 351–360.

Manneville, V., 2006. Dexel, diagnostic environnemental de l'exploitation d'élevage. Méthode et référentiel. Institut de l'Elevage, 2-84148-211-1 Collection méthode et outils.

Martins, O., Dewes, T., 1992. Loss of nitrogenous compounds during composting of animal wastes. Bioresour. Technol. 42, 103–111.

Mattila, P.K., 2006. Spring barley yield and nitrogen recovery after application of peat manure and pig slurry. Agri. Food Sci. Finland 15, 124–137.

Mattila, P.K., Joki-Tokola, E., Tanni, R., 2003. Effect of treatment and application technique of cattle slurry on its utilization by leys: II. Recovery of nitrogen and composition of herbage yield. Nutr. Cycl. Agroecosyst. 65, 231–242.

Menzi, H., 2002. Manure management in Europe. In: Venglovsky, J., Greserova, G. (Eds.), 10th FAO Ramiran Conference on Recycling of Organic Residues in Agriculture, University of Veterinary Medicine, Kosice, Slovakia, pp. 93–102.

Misselbrook, T.H., Brookman, S.K.E., Smith, K.A., Cumby, T., Williams, A.G., McCrory, D.F., 2005. Crusting of stored dairy slurry to abate ammonia emissions: pilot-scale studies. J. Environ. Qual. 34, 411–419.

Mkhabela, M.S., Gordon, R., Burton, D., Smith, E., Madani, A., 2009. The impact of management practices and meteorological conditions on ammonia and nitrous oxide emissions following application of hog slurry to forage grass in Nova Scotia. Agric. Ecosyst. Environ. 130, 41–49.

Moldanová, J., Grennfelt, P., Jonsson, A., Simpson, D., Spranger, T., Aas, W., Munthe, J., Rabl, A., 2011. Nitrogen as a threat to European air quality. In: Sutton, M.A., Howard, C.M., Erisman, J.W., Billen, G., Bleeker, A., Grennfelt, P., van Grinsven, H., Grizzetti, B. (Eds.), The European Nitrogen Assessment, Cambridge University Press, UK, pp. 99–125.

Møller, H.B., Nielsen, A.M., Nakakubo, R., Olsen, H.J., 2007. Process performance of biogas digesters incorporating pre-separated manure. Livest. Sci. 112, 217–223.

Munoz, G.R., Kelling, K.A., Rylant, K.E., Zhu, J., 2008. Field evaluation of nitrogen availability from fresh and composted manure. J. Environ. Qual. 37, 944–955.

Näsholm, T., Huss-Danell, K., Högberg, P., 2000. Uptake of organic nitrogen in the field by four agriculturally important plant species. Ecology 81, 1155–1161.

Näsholm, T., Huss-Danell, K., Högberg, P., 2001. Uptake of glycine by field grown wheat. New Phytol. 150, 59–63.

Ndegwa, P.M., Hristov, A.N., Arogo, J., Sheffield, R.E., 2008. A review of ammonia emission mitigation techniques for concentrated animal feeding operations. Biosystems Eng. 100, 453–469.

Nyord, T., 2011. Virkningen af forsuring af gylle under udbringning (SyreN). Sammendrag Af Indlæg Plantekongres, Faculty of Agricultural Sciences, Aarhus University and Videncentret for Landbrug, Aarhus, Denmark, pp. 71–72.

Oenema, O., Bleeker, A., Braathen, N.A., Budňácková, M., Bull, K., Čermák, P., Geupel, M., Hicks, K., Hoft, R., Kozlova, N., Leip, A., Spranger, T., Valli, L., Velthof, G., Winiwarter, W., 2011. Nitrogen in current European policies. In: Sutton, M.A., Howard, C.M., Erisman, J.W., Billen, G., Bleeker, A., Grennfelt, P., van Grinsven, H., Grizzetti, B. (Eds.), The European Nitrogen Assessment, Cambridge University Press, UK, pp. 62–81.

Oenema, O., Oudendag, D., Velthof, G.L., 2007. Nutrient losses from manure management in the European Union. Livestock Sci. 112, 261–272.

Oenema, O., Velthof, G.L., 1993. Denitrification in nitric-acid-treated cattle slurry during storage. Neth. J. Agr. Sci. 41, 63–80.

Oenema, O., Velthof, G.L., Yamulki, S., Jarvis, S.C., 1997. Nitrous oxide emissions from grazed grassland. Soil Use Manage. 13, 288–295.

Okamoto, M., Okada, K., Watanabe, T., Ae, N., 2003. Growth responses of cereal crops to organic nitrogen in the field. Soil Sci. Plant Nutr. 49, 445–452.

Olesen, J.E., Sørensen, P., Thomsen, I.K., Eriksen, J., Thomsen, A.G., Berntsen, J., 2004. Integrated nitrogen input systems in Denmark. In: Mosier, A.R. (Ed.), Agriculture and the Nitrogen Cycle, Island Press, Washington, DC, pp. 129–140.

Pain, B.F., Phillips, V.R., Clarkson, C.R., Klarenbeek, J.V., 1989. Loss of nitrogen through NH_3 volatilisation during and following application of pig or cattle slurry to grassland. J. Sci. Food Agr. 47, 1–12.

Parkinson, R., Gibbs, P., Burchett, S., Misselbrook, T., 2004. Effect of turning regime and seasonal weather conditions on nitrogen and phosphorus losses during aerobic composting of cattle manure. Biores. Technol. 91, 171–178.

Paul, J.W., Beauchamp, E.G., 1989. Effect of carbon constituents in manure on denitrification in soil. Can. J. Soil Sci. 69, 49–61.

Paul, J.P., Dinn, N.E., Kannangara, T., Fisher, L.J., 1998. Protein content in dairy cattle diets affects ammonia losses and fertilizer nitrogen value. J. Environ. Qual. 27, 528–534.

Pedersen, C.Å., 2001. Oversigt over Landsforsøgene. Landsudvalget for Planteavl, Aarhus, Denmark (in Danish).

Petersen, J., Sørensen, P., 2008a. Loss of nitrogen and carbon during storage of the fibrous fraction of separated pig slurry and influence on nitrogen availability. J. Agric. Sci. (Camb.) 146, 403–413.

Petersen, J., Sørensen, P., 2008b. Fertilizer value of nitrogen in animal manures – basis for determination of a legal substitution rate (in Danish with English summary). DJF Rapport Markbrug Nr 138. 111 pp Gødningsvirkning Af Kvælstof I Husdyrgødning – Grundlag for Fastlæggelse Af Substitutionskrav. Aarhus University, Denmark.

Petersen, S.O., Lind, A.M., Sommer, S.G., 1998. Nitrogen and organic matter losses during storage of cattle and pig manure. J. Agric. Sci. (Camb.) 130, 69–79.

Philippe, F.-X., Cabaraux, J.F., Nicks, B., 2011. Ammonia emissions from pig houses: influencing factors and mitigation techniques. Agric. Ecosyst. Environ. 141, 245–260.

Rahman, S., Chen, Y., Zhang, Q., Tessier, S., Baidoo, S., 2001. Performance of a liquid manure injector in a soil bin and on established forages. Can. Biosyst. Eng. 43, 2.33–2.40.

Rao Bhamidimarri, S.M., Pandey, S.P., 1996. Aerobic thermophilic composting of piggery solid wastes. Water Sci. Technol. 33, 89–94.

Raviv, M., Medina, S., Krasnovsky, A., Ziada, H., 2004. Organic matter and nitrogen conservation in manure compost for organic agriculture. Compost Sci. Util. 12, 6–10.

Reeves III, J.B., 2007. The present status of "quick tests" for on-farm analysis with emphasis on manures and soil: what is available and what is lacking. Livestock Sci. 112, 224–231.

Rodhe, L., Etana, A., 2005. Performance of slurry injectors compared with band spreading on three Swedish soils with ley. Biosyst. Eng. 92, 107–118.

Rodhe, L., Halling, M.A., 2010. Grassland yield response to knife/tine slurry injection equipment – benefit or crop damage?. In: Cláudia, S.C., dos Santos Cordovil, M., Ferreira, L. (Eds.), Proceedings of the 14th Ramiran International Conference 12–15 September 2010, Ref No: 0141, Instituto Superior de Agronomia, Universidade Técnica de Lisboa, Portugal, 978-972-8669-47-8.

Rubaek, H., Henriksen, K., Petersen, J., Rasmussen, B., Sommer, S.G., 1996. Effects of application technique and anaerobic digestion on gaseous nitrogen loss from animal slurry applied to ryegrass (Lolium perenne). J. Agric. Sci. (Camb.) 126, 481–492.

Sagoo, E., Williams, J.R., Chambers, B.J., Chadwick, D.R., 2006. Defra Project WA0716, Management Techniques to Minimise Ammonia Emissions from Solid Manures. Final report to Defra, London ADAS Gleadthorpe Research Centre, Mansfield, Notts NG20 9PF, pp. 35.

Schils, R.L.M., Kok, I., 2003. Effects of cattle slurry manure management on grass yield. Neth. J. Agric. Sci. 51, 41–65.

Schmidt, S.K., Stewart, G.R., 1999. Glycine metabolism by plant roots and its occurrence in Australian plant communities. Aust. J. Plant Physiol. 26, 253–264.

Schröder, J., 2005. Revisiting the agronomic benefits of manure: a correct assessment and exploitation of its fertilizer value spares the environment. Bioresour. Technol. 96, 253–261.

Schröder, J.J., Assinck, F.B.T., Uenk, D., Velthof, G.L., 2010. Nitrate loss from grassland on sandy soils, as affected by soil properties and the rate and nature of the N-input. Grass Forage Sci. 65, 49–57.

Schröder, J.J., Jansen, A.G., Hilhorst, G.J., 2005. Long-term nitrogen supply from cattle slurry. Soil Use Manage. 21, 196–204.

Schröder, J.J., Uenk, D., Hilhorst, G.J., 2007. Long-term nitrogen fertilizer replacement value of cattle manures applied to cut grassland. Plant Soil 299, 83–99.

Shepherd, M.A., 1993. Measurements of soil mineral nitrogen to predict the response of winter wheat to fertilizer nitrogen after applications of organic manures or after ploughed-out grass. J. Agric. Sci. (Camb.) 121, 223–231.

Shepherd, M.A., Harrison, R., 2000. Managing organic manures—is the closed nitrogen cycle achievable? Asp. Appl. Biol. 62, 119–124.

Sieling, K., Brase, T., Svib, V., 2006. Residual effects of different N fertilizer treatments on growth, N uptake and yield of oilseed rape, wheat and barley. Eur. J. Agron. 25, 40–48.

Skiba, U., Smith, K.A., Fowler, D., 1993. Nitrification and denitrification as sources of nitric oxide and nitrous oxide in a sandy soil. Soil Biol. Biochem. 25, 1527–1536.

Smith, K., Cumby, T., Lapworth, J., Misselbrook, T., Williams, J., 2007. Natural crusting of slurry storage as an abatement measure for ammonia emissions on dairy farms. Biosystems Eng. 97, 464–471.

Smith, K.A., Jackson, D.R., Misselbrook, T.H., Pain, B.F., Johnson, R.A., 2000. Reduction of ammonia emission by slurry application techniques. J. Agr. Eng. Res. 77, 277–287.
Søgaard, H.T., Sommer, S.G., Hutchings, N.J., Huijsmans, J.F.M., Bussink, D.W., Nicholson, F., 2002. Ammonia volatilization from field-applied animal slurry—the ALFAM model. Atmos. Environ. 36, 3309–3319.
Sommer, S.G., 2001. Effect of composting on nutrient loss and nitrogen availability of cattle deep litter. Eur. J. Agron. 14, 123–133.
Sommer, S.G., Christensen, B.T., Nielson, N.E., Schjørring, J.K., 1993. Ammonia volatilization during storage of cattle and pig slurry: effect of surface cover. J. Agric. Sci. (Camb.) 121, 63–71.
Sommer, S.G., Husted, S., 1995. The chemical buffer system in raw and digested animal slurry. J. Agric. Sci. (Camb.) 124, 45–53.
Sommer, S.G., Hutchings, N.J., 2001. Ammonia emission from field applied manure and its reduction—invited paper. Eur. J. Agron. 15, 1–15.
Sommer, S.G., Jensen, B.-E., Hutchings, N., Lundgård, N.H., Grønkjær, A., Birkmose, T.S., Petersen, P., Jensen, H.B., 2006b. Emissionskoefficienter til brug ved beregning af ammoniakfordampning fra stalde. (In Danish). DJF-rapport, Husdyrbrug Nr 70. 45 pp.
Sommer, S.G., Petersen, S.O., Søgaard, H.T., 2000. Greenhouse gas emission from stored livestock slurry. J. Environ. Qual. 29, 744–751.
Sommer, S.G., Petersen, S.O., Sørensen, P., Poulsen, H.D., Møller, H.B., 2007. Methane and carbon dioxide emissions and nitrogen turnover during liquid manure storage. Nutr. Cycl. Agroecosyst. 78, 27–36.
Sommer, S.G., Zhang, G.Q., Bannink, A., Chadwick, D., Misselbrook, T., Harrison, R., Hutchings, N.J., Menzi, H., Monteney, G.J., Ni, J.Q., Oenema, O., Webb, J., 2006a. Algorithms determining ammonia emission from buildings housing cattle and pigs and from manure stores. Adv. Agron. 89, 261–335.
Sørensen, P., 1998. Effects of storage time and straw content of cattle slurry on the mineralization of nitrogen and carbon in soil. Biol. Fertil. Soils 27, 85–91.
Sørensen, P., 2001. Short-term nitrogen transformations in soil amended with animal manure. Soil Biol. Biochem. 33, 1211–1216.
Sørensen, P., 2004. Immobilization, remineralization and residual effects in subsequent crops of dairy cattle slurry nitrogen compared to mineral fertilizer nitrogen. Plant Soil 267, 285–296.
Sørensen, P., Amato, M., 2002. Remineralization and residual effects of N after application of pig slurry to soil. Eur. J. Agron. 16, 81–95.
Sørensen, P., Eriksen, J., 2009. Effects of slurry acidification with sulphuric acid combined with aeration on the turnover and plant availability of nitrogen. Agric. Ecosyst. Environ. 131, 240–246.
Sørensen, P., Fernández, J.A., 2003. Dietary effects on the composition of pig slurry and on the plant utilization of pig slurry nitrogen. J. Agric. Sci. (Camb.) 140, 343–355.
Sørensen, P., Jensen, E.S., 1995. Mineralization–immobilization and plant uptake of nitrogen as influenced by the spatial distribution of cattle slurry in soils of different texture. Plant Soil 173, 283–291.
Sørensen, P., Jensen, E.S., 1998. The use of ^{15}N labelling to study the turnover and utilization of ruminant manure N. Biol. Fertil. Soils 28, 56–63.
Sørensen, P., Jensen, E.S., Nielsen, N.E., 1994. The fate of ^{15}N-labelled organic nitrogen in sheep manure applied to soils of different texture under field conditions. Plant Soil 162, 39–47.
Sørensen, L.K., Sørensen, P., Birkmose, T.S., 2007. Application of reflectance near infrared spectroscopy for animal slurry analyses. Soil Sci. Soc. Am. J. 71, 1398–1405.
Sørensen, P., Thomsen, I.K., 2005. Separation of pig slurry and plant utilization and loss of nitrogen-^{15}-labeled slurry nitrogen. Soil Sci. Soc. Am. J. 69, 1644–1651.

Sørensen, P., Vinther, F.P., Petersen, S.O., Petersen, J., Lund, I., 2003b. Høj udnyttelse af gyllens kvælstof ved direkte nedfældning. Grøn Viden, Markbrug no 281. pp. 1–6. (In Danish).
Sørensen, P., Weisbjerg, M.R., Lund, P., 2003a. Dietary effects on the composition and plant utilization of nitrogen in dairy cattle manure. J. Agric. Sci. (Camb.) 141, 79–91.
Stevens, R.J., Laughlin, R.J., 1997. The impact of cattle slurries and their management on ammonia and nitrous oxide emissions from grassland. In: Jarvis, S.C., Pain, B.F. (Eds.), Gaseous Nitrogen Emissions from Grasslands, CAB International, Wallingford UK, pp. 233–256.
Stevens, R.J., Laughlin, R.J., Frost, J.P., 1989. Effect of acidification with sulphuric acid on the volatilization of ammonia from cow and pig slurries. J. Agric. Sci. (Camb.) 113, 389–395.
Tam, N.F.Y., Tiquia, S.M., 1999. Nitrogen transformation during co-composting of spent pig manure, sawdust litter and sludge under forced-aerated system. Environ. Technol. 20, 259–267.
Thomsen, I.K., 2001. Recovery of nitrogen from composted and anaerobically stored manure labelled with ^{15}N. Eur. J. Agron. 15, 31–41.
Thomsen, I.K., 2004. Nitrogen use efficiency of ^{15}N-labeled poultry manure. Soil Sci. Soc. Am. J. 68, 538–544.
Thomsen, I.K., 2005. Crop N utilization and leaching losses as affected by time and method of application of farmyard manure. Eur. J. Agron. 22, 1–9.
Thomsen, I.K., Kjellerup, V., Jensen, B., 1997. Crop uptake and leaching of ^{15}N applied in ruminant slurry with selectively labelled faeces and urine fractions. Plant Soil 197, 233–239.
Thomsen, I.K., Olesen, J.E., Møller, H.B., Sørensen, P., Christensen, B.T., Carbon dynamics and stabilization in soil after anaerobic digestion of dairy cattle feed and faeces. Soil Biol. Biochem. in press.
Thompson, R.B., Morse, D., Kelling, K.A., Lanyon, L.E., 1997. Computer programs that calculate manure application rates. J. Prod. Agric. 10, 58–69.
Thompson, R.B., Ryden, J.C., Lockyer, D.R., 1987. Fate of nitrogen in cattle slurry following surface application or injection to grassland. J. Soil Sci. 38, 689–700.
Tiquia, S.M., Tam, N.F.Y., 2000. Fate of nitrogen during composting of chicken litter. Environ. Pollut. 110, 535–541.
UNECE (United Nations Economic Commission for Europe), 2000. Protocol to Abate Acidification, Eutrophication and Ground-level Ozone, The 1999 Gothenburg Protocol to Abate Acidification, Eutrophication and Ground-level Ozone. http://www.unece.org/env/lrtap/multi_h1.htm.
Van Faassen, H.G.F., Van Dijk, H., 1987. Manure as a source of nitrogen and phosphorus in soils. In: Van Meer, H.G., Unwin, R.J., Van Dijk, T.A., Eunik, G.C. (Eds.), Animal Manure on Grassland and Fodder Crops, Fertilizer or Waste? vol. 30. Martinus Nijhoff, The Hague, pp. 27–45.
Van Kessel, J.S., Reeves III, J.B., 2002. Nitrogen mineralization potential of dairy manures and its relationship to composition. Biol. Fertil. Soils 36, 118–123.
Velthof, G., Barot, S., Bloem, J., Butterbach-Bahl, K., de Vries, W., Kros, J., Lavelle, P., Olesen, J.E., Oenema, O., 2011. Nitrogen as a threat to European soil quality. In: Sutton, M.A., Howard, C.M., Erisman, J.W., Billen, G., Bleeker, A., Grennfelt, P., van Grinsven, H., Grizzetti, B. (Eds.), The European Nitrogen Assessment, Cambridge University Press, UK, pp. 495–512.
Velthof, G.L., Kuikman, P.J., Oenema, O., 2003. Nitrous oxide emission from animal manures applied to soil under controlled conditions. Biol. Fertil. Soils 37, 221–230.
Velthof, G.L., Mosquera, J., 2011. The impact of manure application technique on nitrous oxide emission from agricultural soils. Agric. Ecosyst. Environ. 140, 298–308.
Velthof, G.L., Nelemans, J.A., Oenema, O., Kuikman, P.J., 2005. Gaseous nitrogen and carbon losses from pig manure derived from different diets. J. Environ. Qual. 34, 698–706.

Velthof, G.L., Oenema, O., 1993. Nitrous oxide flux from nitric-acid-treated cattle slurry applied to grassland under semi-controlled conditions. Neth. J. Agric. Sci. 41, 81–93.

Velthof, G.L., van Beusichem, M.L., Raijmaker, M.W.F., Janssen, B.H., 1998. Relationship between availability indices and plant uptake of nitrogen and phosphorus from organic products. Plant Soil 200, 215–226.

Warren, C.R., 2006. Potential organic and inorganic N uptake by six eucalyptus species. Funct. Plant Biol. 33, 653–660.

Webb, J., Archer, J.R., 1993. Pollution of soils and watercourses by wastes from livestock production systems. In: Ap Dewi, I., Axford, R.F.E., Marai, I.F.M., Omed, H. (Eds.), Pollution in Livestock Production Sytems, CAB International, Oxford, pp. 189–204.

Webb, J., Chadwick, D., Ellis, S., 2004. Emissions of ammonia and nitrous oxide following incorporation into the soil of farmyard manures stored at different densities. Nutr. Cycl. Agroecosyst. 70, 67–76.

Webb, J., Henderson, D., Anthony, S.G., 2001. Optimising livestock manure applications to reduce nitrate and ammonia pollution: scenario analysis using the MANNER model. Soil Use Manage. 17, 188–194.

Webb, J., Menzi, H., Pain, B.F., Misselbrook, T.H., Dammgen, U., Hendriks, H., Dohler, H., 2005. Managing ammonia emissions from livestock production in Europe. Environ. Pollut. 135, 399–406.

Webb, J., Pain, B., Bittman, S., Morgan, J., 2010. The impacts of manure application methods on emissions of ammonia, nitrous oxide and on crop response—a review. Agric. Ecosyst. Environ. 137, 39–46.

Webb, J., Seeney, F.M., Sylvester-Bradley, R., 1998. The response to fertilizer nitrogen of cereals grown on sandy soils. J. Agric. Sci. (Camb.) 130, 271–286.

Webb, J., Sommer, S.G. Kupper, T., Groenestein, K., Hutchings, N.J., Eurich-Menden, B., Rodhe, L., Misselbrook, T.H., Amon, B., 2012. Gaseous emissions during the management of solid manures. A review. Sust. Agric. Rev. 8, 67–107.

Whitehead, D.C., Lockyer, D.R., Raistrick, N., 1989. Volatilization of ammonia from urea applied to soil: influence of hippuric acid and other constituents of livestock urine. Soil Biol. Biochem. 21, 803–808.

Whitehead, D.C., Raistrick, N., 1990. Ammonia volatilization from five nitrogen compounds used as fertilizers following surface application to soils. J. Soil Sci. 41, 387–394.

Williams, J.R., Chambers, B.J., Chadwick, D.R., Balsdon, S.L., 2003. Defra Project WA0632, Ammonia Fluxes within Solid and Liquid Manure Management Systems. Final Report to Defra, London. ADAS Gleadthorpe Research Centre, Mansfield, Notts NG20 9PF, pp. 33.

Williams, P.H., Hedley, M.J., Gregg, P.E.H., 1989. Uptake of potassium and nitrogen by pasture from urine-affected soil. N. Z. J. Agric. Res. 32, 415–421.

Williams, J.R., Hurst, C.L., Chambers, B.J., Brookman, S., Chadwick, D., 1999. Rapid methods for the analysis of readily available nitrogen in manures. BGS Occasional Symposium No. 33. In: Corrall, A.J. (Ed.), Accounting for Nutrients – A Challenge for Grassland Farmers in the 21st Century, British Grassland Society, Reading, UK, pp. 171–172.

Witter, E., Lopez-Real, J., 1988. Nitrogen losses during the composting of sewage sludges, and the effectiveness of clay soil, zeolite, and compost in adsorbing the volatilized ammonia. Biol. Waste. 23, 279–294.

Wulf, S., Maeting, M., Bergmann, S., Clemens, J., 2002. Simultaneous measurement of NH_3, N_2O and CH_4 to assess efficiency of trace gas emission abatement after slurry application. Phyton (Austria) Spec. Issue: "Nitrogen Emissions" 41 (3), 131–142.

Yagüe, M.R., Quílez, D., 2009. Direct and residual response of wheat to swine slurry application method. Nutr. Cycl. Agroecosyst. 86, 161–174.

Yamagata, M., Ae, N., 1996. Nitrogen uptake response of crops to organic nitrogen. Soil Sci. Plant Nutr. 42, 389–394.

INDEX

Note: Page numbers followed by "*f*" indicate figures and "*t*" indicate tables.

D

G

H

I

J

K

L

M

N

O

P

Q

R

S

T

U

V

W

X

COLOR PLATE

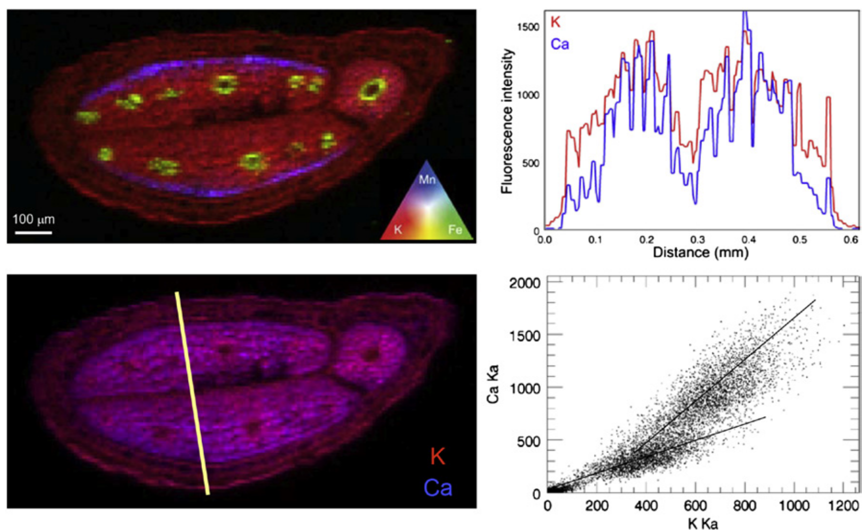


Figure 1.5 Tricolor (RGB) image of K, Fe, and Mn with color triangle and bicolor (RB) image of K and Ca in the *Noccaea* seed; "line-out" spectra for K Kα and Ca Kα showing the trend in their distribution between seed coat (testa) and embryo (denoted by line); correlation plot for counts in K Kα and Ca Kα channels of the bicolor image showing two distinct clouds of points with different [Ca]/[K] ratios in each population (population-segmentation method indicates the populations belong to the seed coat and embryo, respectively).

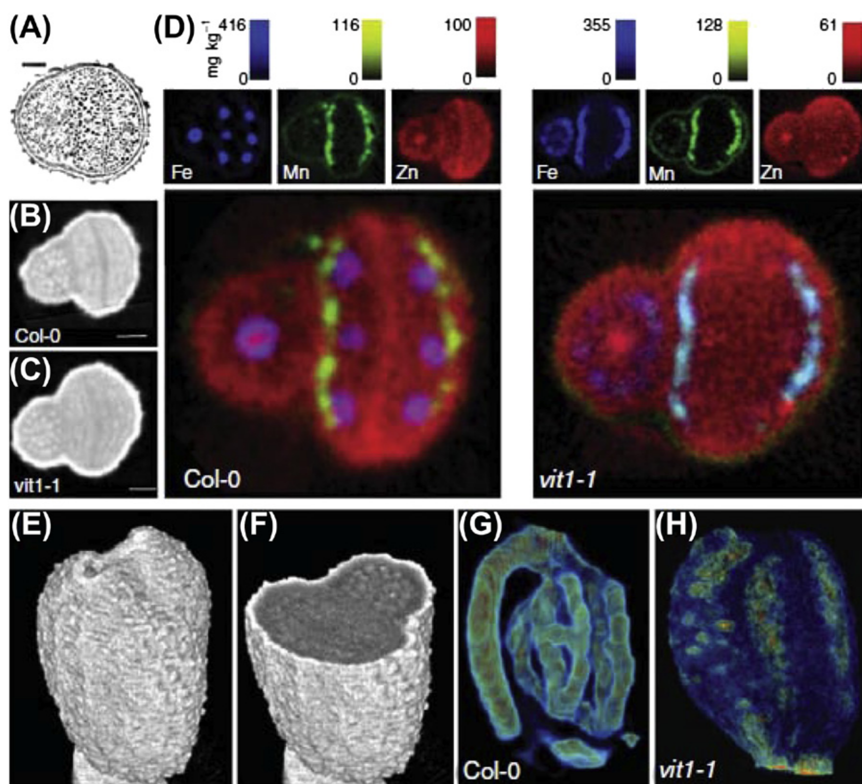


Figure 1.6 fCMT of *Arabidopsis* seed. (A) Light micrograph cross-section of a mature seed. (B, C) Total X-ray absorption tomographic slices of Columbia-0 (wild-type) and vit1-1 mutant seeds. (D) µXRF tomographic slices and composite images of Fe (blue), Mn (green) and Zn (red) K α fluorescence lines from Columbia-0 and vit1-1. (E, F) Three-dimensional rendering of total X-ray absorption of a wild-type *Arabidopsis* seed. (G, H) Three-dimensional rendering of Fe K α fluorescence in Columbia-0 and vit1-1, respectively. *(Reprinted with permission from Kim et al. (2006)).*

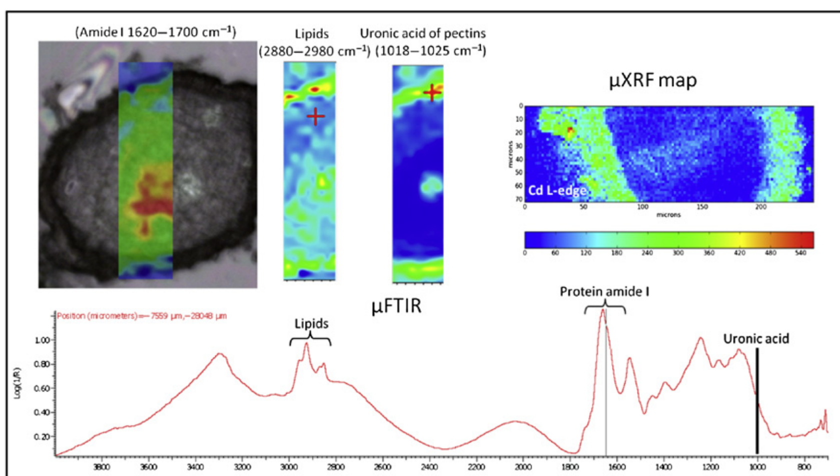


Figure 1.8 SR-µFTIR chemical distribution of lipids, protein and pectin from a root apex of sunflower plants exposed to Cd. The maps were acquired in transmission mode and the sample thickness was 10 µm. The infrared spectrum was obtained from the apical meristem of the sample. The µXRF map from the Cd L-edge shows the localization of Cd in the root surface.

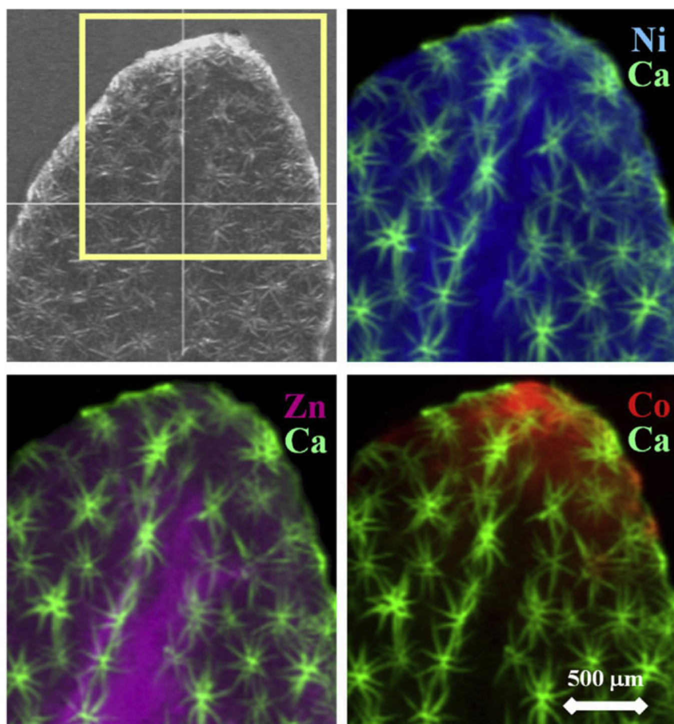


Figure 1.9 µXRF images of the nickel (Ni), cobalt (Co), and zinc (Zn) distributions in a hydrated *Alyssum murale* leaf. Leaf trichomes are depicted in the Ca channel. The optical microscope image shows the leaf region selected for SXRF imaging. *(Reprinted with permission from Tappero et al. (2007)).*

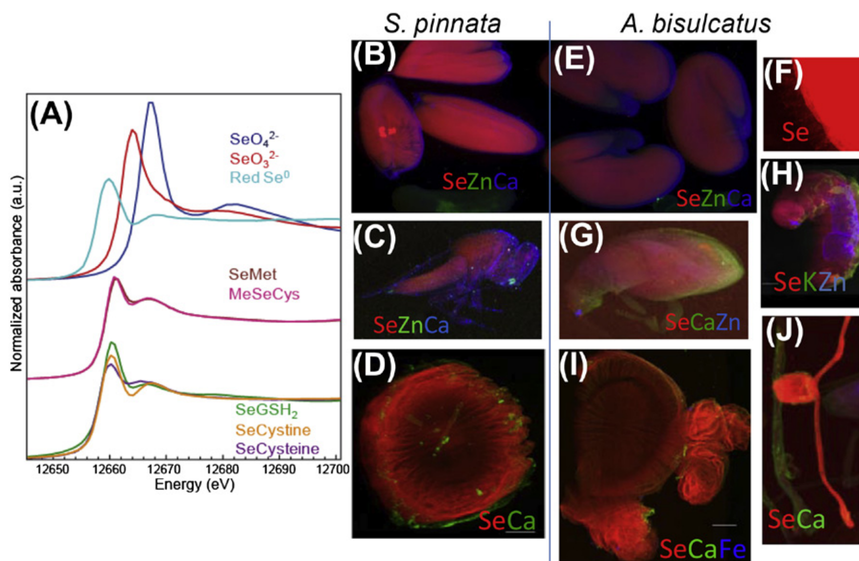


Figure 1.10 (A) Se K-edge XANES spectra from different selenocompounds. SeMet: Selenomethionine; MeSeCys: methyl-selenocysteine; $SeGSH_2$: Selenodiglutathione. (B–J) m X-ray fluorescence maps of Se (in red) and other elements in two hyperaccumulator plant species and their Se-resistant ecological partners. B: *S. pinnata* seed, including one with frass left behind by seed wasp larva; C: adult seed wasp from *S. pinnata* ; D: root cross-section of *S. pinnata* colonized by fungus; E: *A. bisulcatus* seeds; F: seed coat fungus growing on *A. bisulcatus* seed; G: seed weevil from *A. bisulcatus* seed; H: *Apamea sordens* moth larva found feeding on *A. bisulcatus* leaves; I,J: root of *A. bisulcatus* with root nodules containing *Rhizobia* bacteria.

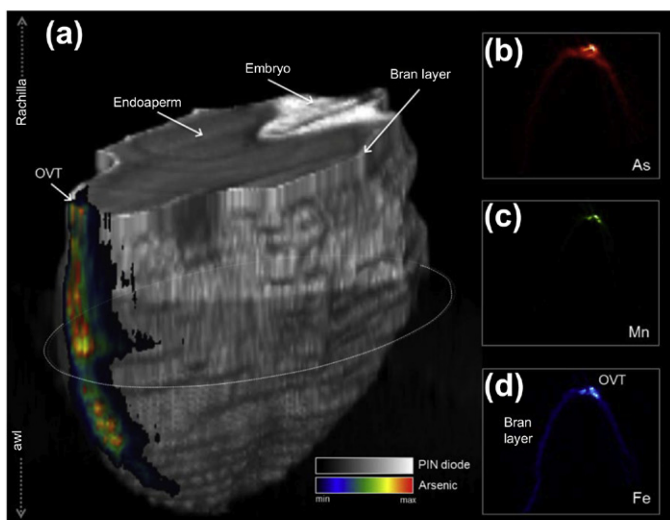
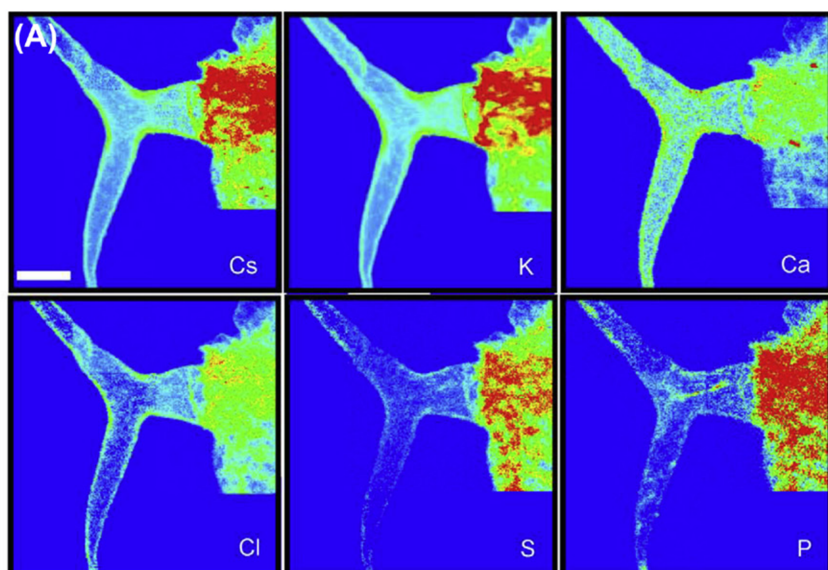
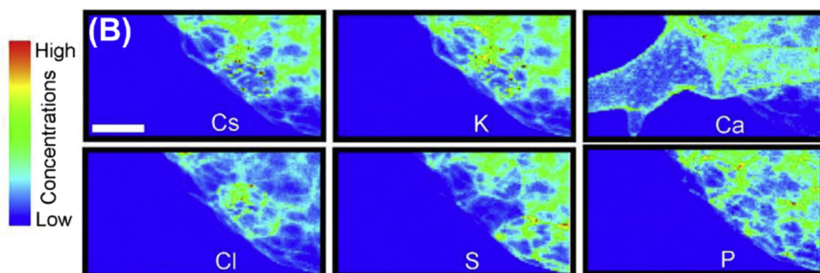
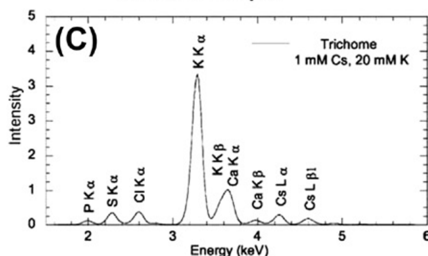


Figure 1.12 Three-dimensional rendering of total X-ray absorption (gray-scale color bar) and arsenic (As) (rainbow color bar) fluorescence of an immature rice grain pulsed with 133 μM arsenite (a). (b–d) Individual tomograms of As, manganese (Mn) and iron (Fe) in the ovular vascular trace. *(Redrawn with permission from Carey et al. (2011b)).*







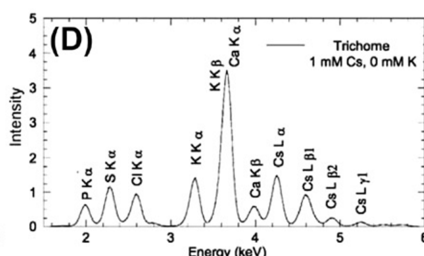


Figure 1.13 False-color elemental μXRF maps of trichomes recorded on plants treated for 4 days with 1 mM Cs, 20 mM K (A), and with 1 mM Cs, 0 mM K (B), and X-ray fluorescence spectra (arbitrary units) collected on the basis of the trichome treated for 4 days with 1 mM Cs, 20 mM K (C) and 1 mM Cs, 0 mM K (D). *(Reprinted with permission from Isaure et al. (2006b)).*

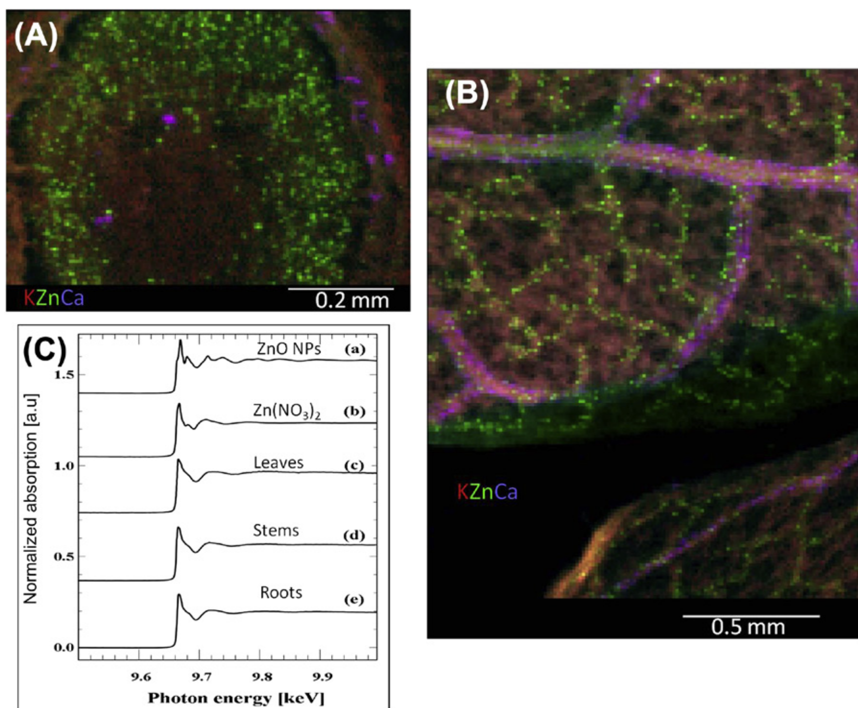


Figure 1.14 Tricolor micro-XRF images from mesquite tissues exposed to ZnO NPs. (A) Mesquite root thin sections (30 μm thickness). (B) Freeze-dried leaves. (C) XANES spectra from mesquite tissues and the ZnO NPs reference. *(Reprinted and adapted with permission from Hernandez Viezcas et al. (2011)).*

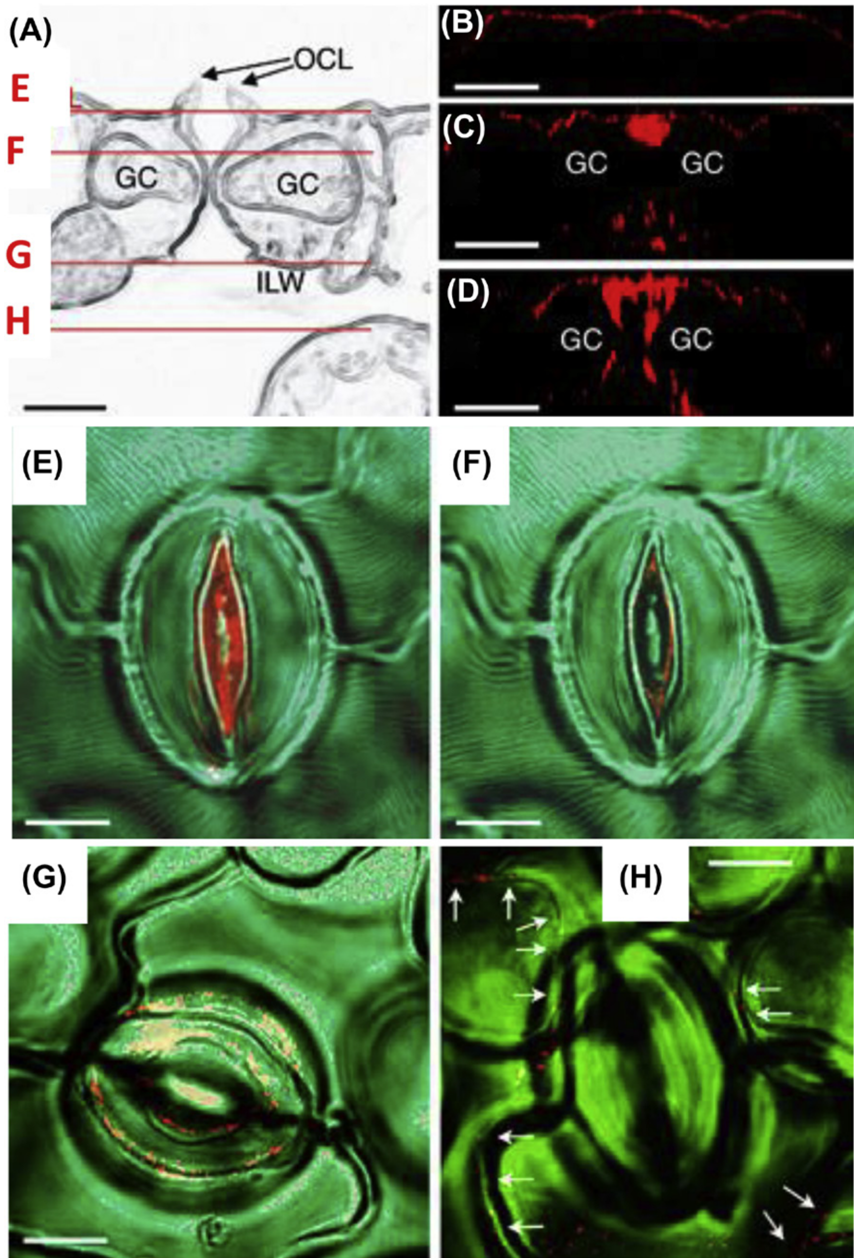


Figure 1.15 (A) Vertical section of *Vicia faba* stomata. Red lines indicate the approximate position of the respective image planes of Fig. 1.1 E–H. GC, guard cell; OCL, outer cuticular ledges; ILW, inner lateral guard cell wall. The CLSM images (B–H) show the distribution of fluorescent particles of 43 nm diameter in *V. faba* leaves in optical vertical sections (B – D) and in optical paradermal sections in different depths below the leaf surface (E–H). Fluorescence is detectable on the cuticle, between the pair of guard cells and below in the substomatal cavity. The focal planes in (E–H) are in depths of 3.6, 14.5, 41 and 63 mm below the leaf surface, respectively. Bars ¼ 10 mm. *(Modified after Eichert et al. (2008)).*